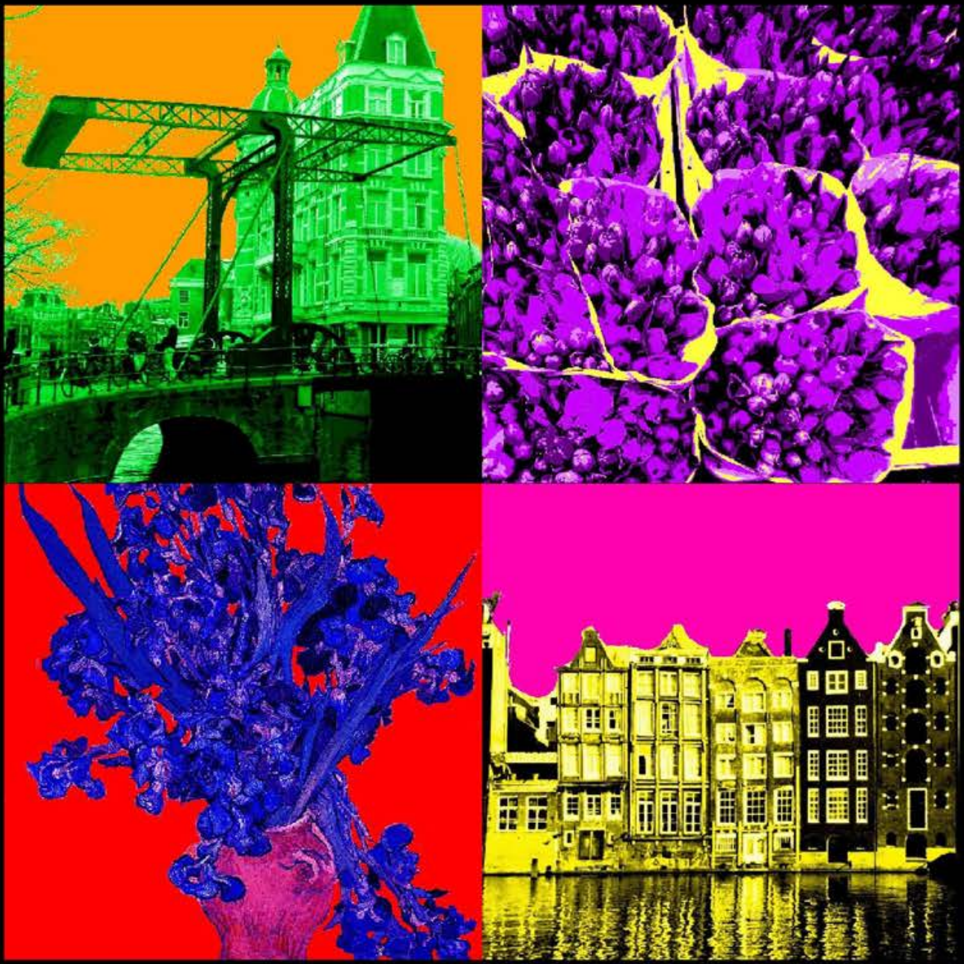

EORS 2012
AMSTERDAM

EUROPEAN ORTHOPAEDIC RESEARCH SOCIETY
20th ANNUAL MEETING

TRANSACTIONS VOL. 20

EUROPEAN ORTHOPAEDIC
RESEARCH SOCIETY

EORS 2012 Programme

Also available for Smartphones & Tablets

Scan QR code & Download the free App!

For iPhone & iPad

For Android

Or search for **ConPass** App in iTunes / Google Play!

Full content available offline!

Data traffic only necessary for initial download.

Thus read, search or share the conference content w/o roaming fees or while on the plane.

Free Wifi available on-site for initial download.

ConPass App

EORS 2012
runs in ConPass

EORS 2012 Transactions only available digital

Download pdf at: **www.eors.info/eors_DOCS/EORS2012.pdf**
Or scan QR-code

Table of Content:

Sponsors

Word of Welcome

Dear colleagues and friends,

Welcome to the 20th Anniversary Annual Meeting of EORS 2012! It is a great pleasure to invite you to join this jubilee summit of Orthopaedic Research in Europe with your abstracts, discussions, networking activities and collegial spirit. We are sure you will share our excitement about an inspiring programme. One theme will be the translational research between orthopaedics and dentistry, as EORS is proud to stage its 2012 meeting at the fantastic facilities and with the full support of ACTA, the Amsterdam Centre for Dentistry.

We hope you will enjoy the rich content, high quality and broad range of topics represented by:

- 9 Workshops
- 3 Presidential Guest Lectures
- 13 Invited Lectures
- 150 Oral presentations
- 185 Poster presentations

We extend a special welcome to our colleagues from France, “Friendship Country” of this year’s conference, a new EORS initiative to showcase the research landscape of one country and seed new networks. There are also a number of initiatives for young investigators to connect with experienced researchers or to steer the discussions as session moderators. A new Young Investigator Award, both for orals and posters shall achknowledge and stimulate the young research talents.
Building on the two decade history of successful EORS meetings, EORS 2012 will look into an exciting future!

Bernd Grimm & Edward Valstar

Conference Chairs

Dear colleagues and friends,

On behalf of the Executive Committee of EORS, I am proud to announce that EORS 2012 annual meeting is being launched. Drs. Grimm and Valstar have deployed intensive activity and succeeded in preparing an innovative format of a classical meeting, to host the Orthopaedic research community all around Europe in Amsterdam this September 2012.

A renewed EORS welcomes scientists and clinicians that look across Europe for a platform to present, discuss, interact, and therefore network with other scientists and specialists devoted to musculoskeletal science. Amsterdam has always represented this open mind in Europe, and will be not only the 20th Anniversary of the Society, but also the preamble of new opportunities, like the Combined Orthopaedic Research Societies Meeting to be hosted by EORS in 2013. To learn more and to be involved, we will be pleased to welcome you at the 2012 EORS Annual Meeting in Amsterdam.

Enrique Gomez-Barrena

President EORS

EORS 2012 Committees

EORS 2012 Conference Chairs

Bernd Grimm	*Atrium Medical Center, Heerlen, NL*
Edward Valstar	*Leiden University Medical Center, Leiden, NL*

Representative Host Institute

Jenneke Klein Nulend	*ACTA, VU University & University of Amsterdam, NL*

Organzing Committee

Leendert Blankevoort	*Academisch Medisch Centrum Amsterdam, NL*
Pieter Buma	*Radboud University, Nijmegen, NL*
Wouter Dhert	*University Medical Center Utrecht, NL*
Bernd Grimm	*Atrium Medical Center, Heerlen, NL*
Ide Heyligers	*Atrium Medical Center, Heerlen, NL*
Rob Nelissen	*Leiden University Medical Center, Leiden, NL*
Jenneke Klein Nulend	*ACTA, VU University & University of Amsterdam, NL*
Barend van Royen	*VU University, Amsterdam, NL*
Edward Valstar	*Leiden University Medical Center, Leiden, NL*
Harrie Weinans	*Erasmus Medical Center, Rotterdam, NL*

Scientific Committee

Chris Arts	*Maastricht University Medical Center, Maastricht*
Nicola Baldini	*Istituto Ortopedico Rizzoli, Bologna, Italy,*
Ashley Blom	*University of Bristol, Bristol, UK*
Sjoerd Bulstra	*University Medical Center Groningen, NL*
Denitsa Docheva	*Ludwig Maximilians University, Munich, Germany*
Richie Gill	*University of Bath, Bath, UK*
Enrique Gómez Barrena	*Universidad Autónoma de Madrid, Spain*
Florelle Gindraux	*CHU de Besançon, France – Coordinator Friendship Country France*
Markus Heller	*Charite, Berlin, Germany*
Geoff Richards	*AO Foundation, Davos, Switzerland*
Jos Van der Sloten	*Katholieke Universiteit Leuven, Belgium*
Theo Smit	*VU University Amsterdam, NL*
Robert Streicher	*ETH Zürich, Switzerland*
Klemens Trieb	*Klinikum Wels – Grieskirchen, Wels, Austia*
Gabrielle Tuijthof	*Academisch Medisch Centrum Amsterdam, NL*
Gianluca Vadala	*University of Rome, Rome, Italy – Coordinator Young Investigators Initiatives*
Jan Verhaar	*Erasmus Medical Center, Rotterdam, NL*

Additional Reviewers

Wouter van Hemert	*Atrium Medical Center, Heerlen, NL*
Holger Jahr	*Delft University of Technology, Delft, NL*
Rachel Senden	*Atrium Medical Center, Heerlen, NL*
Amir Zadpoor	*Erasmus Medical Center, Rotterdam, NL*

EORS Executive Committee

Enrique Gómez Barrena	*President*	Klemens Trieb	*Vice-President*
Nicola Baldini	*Past President*	Edward Valstar	*Secretary*
Bernd Grimm	*Treasurer*	Ashley Blom	*Member-at-Large*
Denitsa Docheva	*Member-at-Large*	Richie Gill	*Member-at-Large*
Geoff Richards	*Member-at-Large*	Gianluca Vadala	*Member-at-Large*

Award Jury

Enrique Gómez Barrena
Denitsa Docheva
Geoff Richards

Ashley Blom
Richie Gill
Gianluca Vadalà

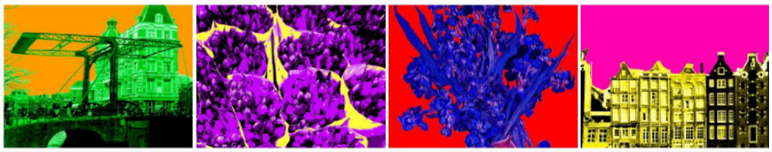

Invited Speakers

Presidential Guest Lectures	Title
Jenneke Klein Nulend *ACTA, VU University & University of Amsterdam, NL*	Translational Research between dentistry & orthopaedics
Allen Goodship *Royal Veterinary College, London, UK*	The fun of nurturing nature, and making it happen in orthopaedic translational research
Enrique Gómez Barrena *Universidad Autónoma de Madrid, Spain*	Challenges and opportunities of orthopaedic research in Europe

Invited Lectures	Title
Jos Van der Sloten *Katholieke Universiteit Leuven, Belgium*	Patient specific biomechanical modelling for patient specific implants
Astrid Bakker *ACTA, VU University and University of Amsterdam, NL*	The role of cytokines in bone formation and degeneration
Geoff Richards *AO Foundation, Davos, Switzerland*	What's new in infection research in fractue fixation
Rommel Bacabac *San Carlos University, Cebu, Philippines*	Bone cell mechanosensing: On shapes and forces
Ashley Blom *University of Bristol, UK*	Metal-on-Metal hips: New evidence from the joint registers
Richie Gill *University of Bath, UK*	Metal-on-Metal hips: The problem and what to do now?
Rob Nelissen *Leiden University Medical Center, Leiden, NL*	Improving the quality of orthopaedic implants: Role of RSA and registers
Klaas de Groot *University of Twente, Enschede, NL*	Dental research: Inspiring Orthopaedics
Martin Stoddart *AO Foundation, Davos, Switzerland*	The role of multi-axial load on mesenchymal stem cell fate
Denitsa Docheva *LM University, Munich, Germany*	Tissue engineering for tendon and ligaments
Pierre Layrolle *INSERM, Nantes, France*	Regenerating bone defects using new biomedical engineering approaches
Dirk Jan Veeger VU University Amsterdam & Delft University, NL	Will patient-specific biomechanical models optimise upper extremity surgery
Corine Visscher VU University Medical Center, Amsterdam, NL	Aspects of accuracy of orthopaedic tests in dentistry

Partners & Sponsors

GOLD LEVEL

Mobelife®
custom orthopaedics

SILVER LEVEL

stryker®

SILVER LEVEL

LifeTec Group

BIOMET®

Materialise

motek medical
improving human performance

3DS SIMULIA

zimmer

Pro-Motion
MEDICAL

EURAM

ETB

mXl
improving joint surgery

KONINKLIJKE NEDERLANDSE
AKADEMIE VAN WETENSCHAPPEN

General Information

Address:
ACTA, Academic Center for Dentistry Amsterdam
Gustav Mahler Laan 3004
1081 LA AMSTERDAM

Getting there

From the Airport:
Train to Station "Amsterdam Zuid"
(direction Utrecht or Hilversum, not Amsterdam!)
Duration: 7-8min
Frequency: each 5-10min; Ticket: 2.50EUR
Timetables: www.ns.nl
From "Amsterdam Zuid" to ACTA: 5-10min walk

From the City Center:
(e.g. Leidseplein, Amsterdam Central Train Station):
Metro Nr 51 (to station 'de Boelelaan' or 'Ziud')
Tram 5 (to station 'de Boelelaan' or 'Ziud')
Duration: 18 min; Frequency: each 5-10min; Ticket: 1.42EUR
Timetables: http://9292.nl/en
Bus 172

Hotel
CitizenM Amsterdam City
Prinses Irenestraat 30
1077 WX Amsterdam, NL
+31 20 811 7090

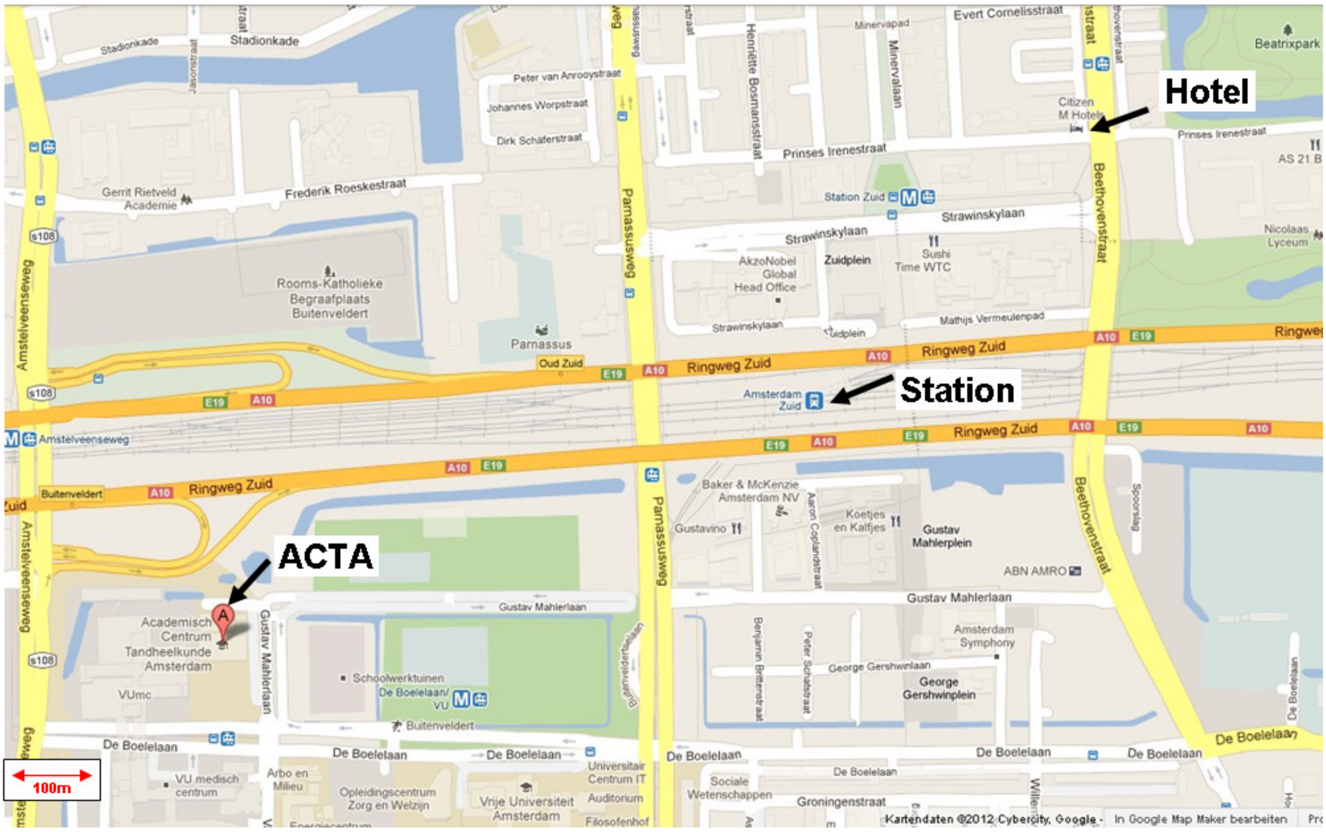

Public Transport: www.gvb.nl

Prepaid OV-chip cards carry travel credit you purchased earlier on special machines located on stations and at the entry of many supermarkets. There are 24-, 48-, 72-, 96-, etc. hour OV-chip cards for unlimited travel on all public transport. OV-chip cards are not sold onboard!

Onboard only a **1-hour OV card** can be purchased (€ 2,60)!

General Information

Dinner Cruise, Thursday 27.9

19.00h
Bus in Front of ACTA building for transfer to Rederij Lovers
19.30h
Embarking canalboats at Prins Hendrikkade opposite Nr 25.
Indonesian Buffet & drinks included on board
22.00h
Disembark the vessel at Prins Hendrikkade

Tickets at the registration desk upon registration.
Pre-registration only, only limited tickets available onsite
Bus from/to ACTA building, returns via CitizenM hotel

Registration

The registration desk is open:

Wednesday	9:00-18:00h
Thursday	7:30-18:00h
Friday	7:30-17:00h

Onsite Registration

Members	€ 450,--
Students	€ 350,--
Non-Members	€ 500,--

Lunch & Coffee Breaks

Coffee & Lunches are included in the registration fee.

Certificates of Attendance

Available at registration desk.

CME Credits

17 CME credits approved
18 NOV credits through GAIA

Internet Access

WIFI is available onsite.
Access codes are available at the registration desk.

Information for presenters

Oral

Presentations are **6min + 2min discussion**.
Please stay on time! Moderators strictly control time slots to make the programme fit the schedule.

Presentations can be uploaded at the Speakers Desk.
Please upload early to avoid delays or queues.

Poster

Posters must be **maximum A1 portrait**!
Height × Width: **84.1cm × 59.4cm**
Must **not be wider than 60cm** or covers neighbour!

Poster Mounting

From 8:00h on Thursday 27.9.
Shall be up by Poster Session 1: Thu 27.9. 12:45h
Dismounting after Poster Session 2: Fri 27.9. 13:30h

Poster Presenters

Even poster Numbers:	Session 1, Thursday
Uneven poster numbers:	Session 2, Friday

Conference Secretariat

EXCEL CONGRESSERVICE
Nieuwe Bossche Weg 9
5017 JJ Tilburg
M. +31 (0)6 549 73 987

General Information

Conference Website

www.eors2012.org

Conference App

Available for Android & Apple smartphones and tablets
Read, search, share full content and make your agenda.
Once installed works offline! Use on plane or abroad w/o roaming.

General Assembly

The General Assembly for EORS members is scheduled:
Friday 28.9. 12:00 – 12:30, Large Auditorium

Awards

EORS Awards are granted for both oral presentations & posters in 3 categories.

i) Translational Research
ii) Basic Research
iii) Young Investigator

The award ceremony takes place during during the closing session (Friday, 16:45).

Floor Plan

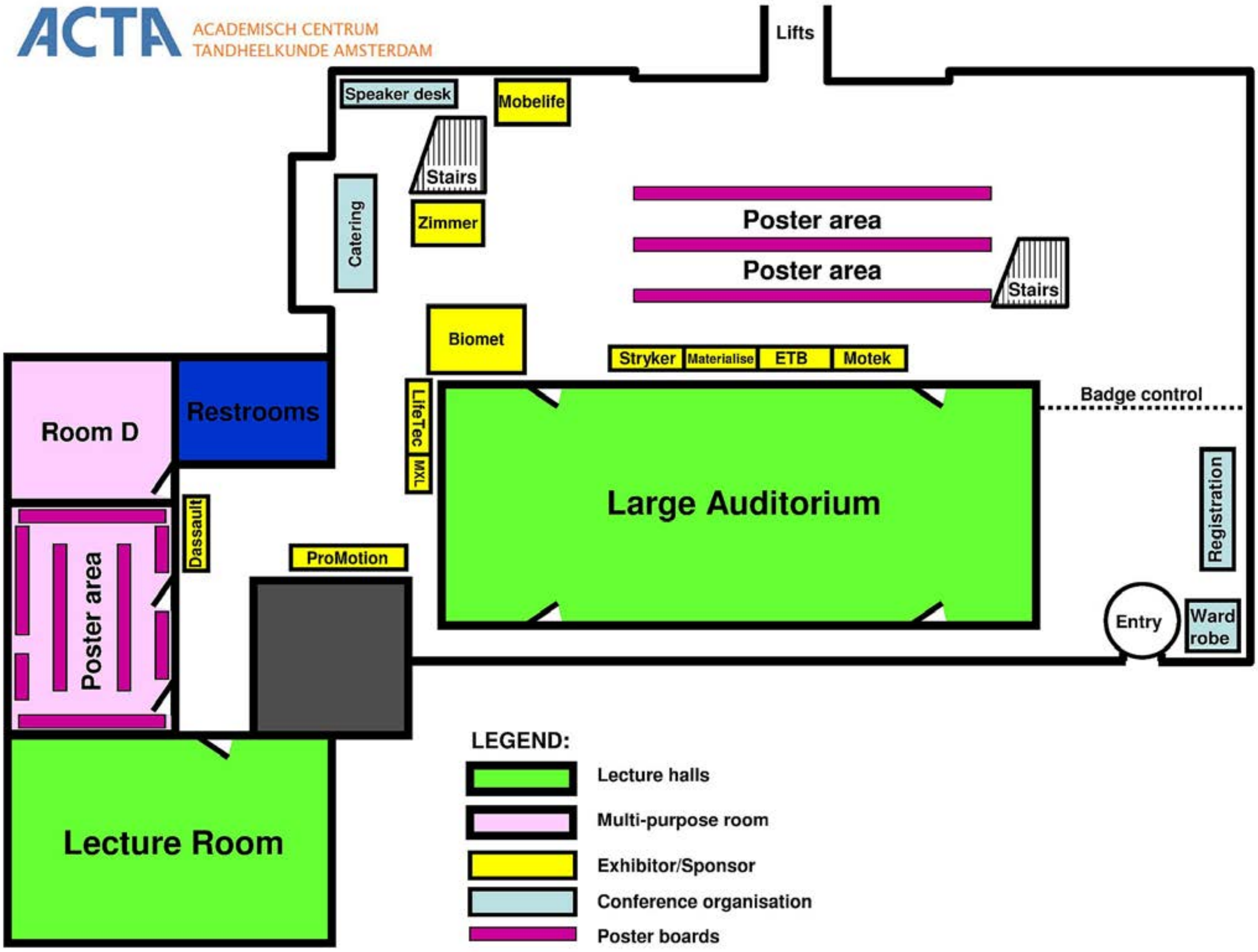

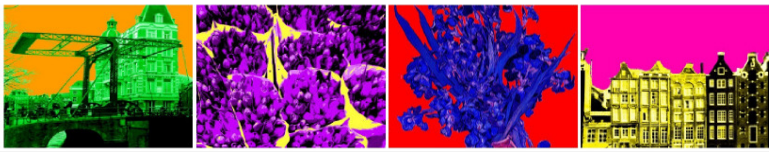

Overview

WEDNESDAY 26.9.

8:00			
5			
10			
15			
20			
25			
30			
35			
40			
45			
50			
55			
9:00	Registration	Registration	Registration
5			
10			
15			
20			
25			
30			
35			
40			
45			
50			
55			
10:00			
5			
10			
15			
20			
25			
30			
35			
40			
45			
50			
55			
11:00	**Workshop 1.1**	**Workshop 1.2**	**Workshop 1.3**
5			
10	Model-based	Obtaining	Virtual Reality in
15	RSA	public funding:	Training &
20		Advice and	Education
25		Guidance	
30			
35			
40	*Leiden*	*EURAM Ltd.*	*ACTA*
45	*University*		
50			
55			
12:00			Attention!
5			Moved to
10			13:45-15:45
15			
20			
25			
30	Room 11N-62	Room 12N-62	Simodont Room
35			
40			
45			
50			
55	*120min*	*120min*	*120min*
13:00			
5			
10			
15			
20	Lunch	Lunch	Lunch
25			
30			
35			
40	*45min*	*45min*	*45min*
13:45	**Workshop 2.1**	**Workshop 2.2**	**Workshop 2.3**
50			
55	Prosthetic Joint	Patient-specific	Gait Analysis
14:00	Infection:	modeling and	for Orthopeadics
5	What is next?	analysis	
10			
15	*Groningen*	*Charite*	*Motek*
20	*University*	*Berlin*	
25			
30			
35			
40			
45			
50			
55			
15:00			
5			
10			
15	Room 11N-62	Room 12N-62	VU University
20			Medical Center
25			
30			
35			
40	*120min*	*120min*	*120min*
15:45			
50			
55	Coffee Break	Coffee Break	Coffee Break
16:00			
5			
10	*30min*	*30min*	*30min*
16:15	**Workshop 2.1**	**Workshop 2.2**	**Workshop 2.3**
20			
25	Skeleton:	How to develop	Gait Analysis
30	Musculoskeletal	tomorrow's	for Orthopeadics
35	Biology,	implants	
40	Mechanics		
45	and Imaging		
50			
55	*Oxford*	*Materialise*	*Motek*
17:00	*University*		
5			
10			
15			
20			
25			
30			
35			
40			
45	Room 11N-62	Room 12N-62	VU University
50			Medical Center
55			
18:00			
5			
10	*120min*	*120min*	*120min*
18:15			

THURSDAY 27.9.

	Large Auditorium	Lecture Hall	
8:00	Registration	Registration	
5			
10			
15			
20			
25			
8:30	**Opening**	**Opening**	
35			
40	*15min*	*15min*	
8:45	**Session 1.A**	**Session 1.B**	
50			
55	***Biomechanics 1***	***Biomaterials 1***	
9:00			
5			
10			
15			
20			
25			
30			
35			
40			
45			
50			
55			
10:00			
5			
10	*90min*	*90min*	
10:15			
20			
25	Coffee Break	Coffee Break	
30			
35			
40	*30min*	*30min*	
10:45	**Guest Lecture**	**Guest Lecture**	
50			
55			
11:00			
5	*25min*	*25min*	
10	**Short Break**	**Short Break**	
11:15	**Session 2.A**	**Session 2.B**	
20			
25	***Infection***	***Cells & Molecular 1***	
30	***& Trauma***		
35			
40			
45			
50			
55			
12:00			
5			
10			
15			
20			
25			
30			
35			
40	*90min*	*90min*	
12:45			
50			
55			
13:00			**YI**
5			Meet-a-Mentor
10	Poster & Lunch	Poster & Lunch	
15			
20			
25			
30			
35			
40			
45			*50min*
50			
55	*75min*	*75min*	
14:00	**Session 3.A**	**Session 3.B**	
5			
10	***Spine &***	***Cells & Molecular 2***	
15	***Upper Extremity***		
20			
25			
30			
35			
40			
45			
50			
55			
15:00			
5			
10			
15			
20			
25	*90min*	*90min*	
15:30			
35	Coffee Break	Coffee Break	
40			
45	*20min*	*20min*	
15:50	**Session 4.A**	**Session 4.B**	
55			
16:00	***Metal-on-Metal***	***Tumors***	
5	***& Hip Arthroplasty***		
10			
15			
20			
25			
30			
35			
40			
45	*60min*	*60min*	
16:50	**Short Break**	**Short Break**	
55	*10min*	*10min*	
17:00	**Session 5.A**	**Session 5.B**	
5			
10	***Imaging***	***Gait & Kinematics***	
15			
20			
25			
30			
35			
40			
45			
50			
55	*60min*	*60min*	
18:00			
19:00h	**Canal Cruise & Dinner**		

FRIDAY 28.9.

	Large Auditorium	Lecture Hall
8:00	**Session 6.A**	**Session 6.B**
5		
10	***Hip Arthroplasty***	***Biomaterials 2***
15		
20		
25		
30		
35		
40		
45		
50		
55		
9:00		
5		
10		
15		
20		
25	*90min*	*90min*
9:30		
35		
40	Coffee Break	Coffee Break
45		
50		
55	*30min*	*30min*
10:00	**Guest Lecture**	**Guest Lecture**
5		
10		
15		
20	*25min*	*25min*
25	**Short Break**	**Short Break**
10:30	**Session 7.A**	**Session 7.B**
35		
40	***Clinical Outcome &***	***Stem Cells***
45	***Arthroplasty***	
50		
55		
11:00		
5		
10		
15		
20		
25		
30		
35		
40		
45		
50		
55	*90min*	*90min*
12:00	**General Assembly**	**General Assembly**
5		
10		
15		
20		
25	*30min*	*30min*
12:30		
35		
40		
45		
50	Poster & Lunch	Poster & Lunch
55		
13:00		
5		
10		
15		
20		
25	*60min*	*60min*
13:30	**Session 8.A**	**Session 8.B**
35		
40	***The Knee***	***Bone Regeneration***
45		***Tissue Engineering***
50		
55		
14:00		
5		
10		
15		
20		
25		
30		
35		
40		
45		
50		
55	*90min*	*90min*
15:00	**Coffee Break**	**Coffee Break**
5		
10	*15min*	*15min*
15:15	**Session 9.A**	**Session 9.B**
20		
25	***Biomechanics 2***	***Bone &***
30		***Miscellaneous***
35		
40		
45		
50		
55		
16:00		
5		
10	*60min*	*60min*
16:15	**Guest Lecture**	**Guest Lecture**
20		
25		
30		
35		
40	*30min*	*30min*
45	**Awards & Closing**	**Awards & Closing**
50		
55	*15min*	*15min*
17:00		
5		
10		
15		
20		
25		
30		
35		
40		
45		
50		
55		
18:00		

Wednesday September 26

11:00

Workshop 1.1	Workshop 1.2	Workshop 1.3 Attention! Moved to 13:45-15:45
Room 11N-62	Room 12N-62	Simodont Room
Model-based RSA: Technique and Clinical Applications	**Obtaining public funding for your project ideas – strategic advice and guidance on obtaining funding.**	**Virtual reality development in training & education. A bridge between dental and orthopedic surgery**
Bart Kaptein	***Nigel Lambert***	***P.R. Wesselink***
Leiden University Medical Center, NL	*Euram LTD, West Bridford Nottinghamshire, UK*	*Endodontology, Academic Centre for Dentistry Amsterdam*
In this workshop, not only the technical background of RSA and Model-based RSA will be presented, you will also learn how to setup a clinical RSA study. The results of high impact RSA studies from Leiden and Oxford will be presented. Apart from that, some alternative applications of RSA and the future of RSA in Orthopaedics will be shown. By following this workshop, you will have up-to-date knowledge about the possibilities and status of RSA in Orthopaedic research.	A workshop intended to provide attendees with a better understanding of how best to develop R&D project ideas that are well suited to attract funding from a public funding body such at the European Commission (FP7).	The Moog Simodont dental trainer provides a virtual world which confronts the student from beginning with realistic problems working on images of realistically diseased teeth. The Simodont offers a realistic feel of the drill and realistic images of the teeth allowing students to switch back and forth between clinic and Simodont and to practice complex procedures developing the required competencies . On scanned in patients students can practice to treat his patient first virtually to be well prepared for the reality. During this workshop these opportunities will be shown and practiced by the practitioners to make this virtual world accessible to orthopedic surgery.
120min	*120min*	*120min*

13:00

Lunch	**Lunch**	**Lunch**
45min	*45min*	*45min*

13:45

Workshop 2.1	Workshop 2.2	Workshop 2.3
Room 11N-62	Room 12N-62	VU Medical Center
Prosthetic Joint Infection: What is next?	**Patient-specific modeling and analysis of joint reconstructions**	**Gait Analysis for Orthopeadics: with Real-time Feedback for Gait Re-Training**
Paul Jutte & Sjoerd Bulstra	***Markus Heller***	***Frans Steenbrink***
Orthopaedic Surgery, University Medical Center Groningen	*Julius Wolff Institute, Charité, Berlin, Germany*	*New Product Development, Motek Medical, Amsterdam*
Prosthetic Joint Infection (PJI) occurs in 1-2% of all primary implants in orthopaedics. It is estimated that 10% of all costs related to imlant surgery is due to these infections. Detection is notoriously difficult as many infections are low grade. Treatment is done according to intuition rather than to evidence; in many cases the prosthesis has to be taken out followed by multiple surgeries. There are many influences in PJI: host factors, micro-organisms, surgical concepts and materials. The workshop comprises an overview of PJI, new ways of detection, new treatment algorithm, host factors and development of new strategy in biomaterials aimed at prevention and treatment.	This workshop describes a combination of modeling approaches and tools that - in combination - allow the accurate prediction of mechanical parameters that drive the clinical outcome of joint surgery. Here, the speakers will provide insight into state of the art approaches recently developed and verified within the EC funded MXL project.	GRAIL provides the full functionality of a conventional gait lab calculating all gait parameters in real- time (spatio-temporal parameters, kinematics, kinetics and muscle-activation). An off-line analysis tool with cycle navigator offers extensive data analysis.
120min	*120min*	*120min*

15:45

Coffee Break	**Coffee Break**	**Coffee Break**

16:15

Workshop 3.1	Workshop 3.2	Workshop 3.3
Room 11N-62	Room 12N-62	VU Medical Center
Skeleton: Musculoskeletal Biology, Mechanics and Imaging	**How to develop tomorrow's implants: Improve standards to fit like custom, or make customs the new standard?**	**Gait Analysis for Orthopeadics: with Real-time Feedback for Gait Re-Training**
James Edwards	***Koen Engelborghs***	***Frans Steenbrink***
Nuffield Dept. of Orthopaedics, University of Oxford, UK	*Director of Biomedical Engineering, Materialise NV.*	*New Product Development, Motek Medical, Amsterdam*
Musculoskeletal integrity is maintained through cellular interactions governed by local, systemic and environmental factors. This Review workshop will summarize i) established and emerging concepts in musculoskeletal biology, ii) how mechanical forces impact the skeletal system and are assessed experimentally, and iii) how the skeletal system can be imaged to accurately assess musculoskeletal tissues, using conventional and novel technologies in small animal models.	People come in all shapes and size, depending on gender, ethnicity, age, etc. and unfortunately designing an implant that fits well on each patient is not just a matter of scaling up the average person. During this workshop we will look at two opposite approaches to improve the fit of implants for the entire population: custom implants or improved standard implants.	GRAIL provides the full functionality of a conventional gait lab calculating all gait parameters in real- time (spatio-temporal parameters, kinematics, kinetics and muscle-activation). An off-line analysis tool with cycle navigator offers extensive data analysis. (same as Workshop 2.3)
120min	*120min*	*120min*

18:15

Thursday September 27

7:30 – 8:30 **Coffee & Registration**

8:30 – 8:45 **Large Auditorium** **Plenary Opening**
EORS 2012 Chairmen, President EORS, Dean Acta

8:45 – 10:15 **Large Auditorium** **SESSION 1A: Biomechanics 1**
Chairs: Leendert Blankevoort
Jan Nadorf

Keynote
8:45
Patient specific biomechanical modelling for patient specific implants

Jos Van der Sloten
Faculty of Engineering Science, KU Leuven, Belgium

1A.1
9:01
Bone substitute reduces significantly the secondary loss of reduction: A biomechanical study of tibial depression fractures

Stefanie Doht*, Teresa Lehnert, Sönke Frey, Kai Fehske, Hendrik Jansen, Torsten Blunk, Rainer Meffert
**Department of Trauma, Hand, Plastic and Reconstructive Surgery, Wuerzburg, Germany*

1A.2
9:09
Stem cell response to mechanical stretch is dependent on surface microtopography

Laura Saldana*, Lara Crespo, Fatima Bensiamar, Nuria Vilaboa
**La Paz University Hospital, Madrid, Spain*

1A.3
9:17
A simplified method to determine joint loading as a surrogate marker of pain/disability in a canine model of osteoarthritis, validated using force plate analyses as a gold standard

Karen Wiegant*, Herman Hazewinkel, Arie Doornebal, Angelique Barten-van Rijbroek, Simon Mastbergen, Floris Lafeber
**University Medical Center Utrecht, Utrecht, The Netherlands*

1A.4
9:25
Assessment of the mechanical properties of plantar tissue by a combined CT imaging and modelling approach

Michiel Oosterwaal*, Paul Klaver, Joris Hermus, Lodwijk van Rhijn, Kenneth Meijer
**Maastricht University Medical Centre, Maastricht, Netherlands*

1A.5
9:33
Biomechanical investigation on distal inter-locking screw breakage in tibia nails comparing angular stable and conventional fixation.

Mark Lenz*, Boyko Gueorguiev, Robert Geoff Richards, Thomas Mückley, Guenter Hofmann, Dankward Höntzsch, Markus Windolf
**AO Research Institute Davos, Davos, Switzerland*

1A.6
9:41
A patient-specific musculoskeletal mandible model using force-dependent kinematics

Michael Skipper Andersen*, Mark de Zee
**Department of Mechanical and Manifacturing Engineering, Aalborg University, Denmark*

1A.7
9:49
Standardized synthetic femur models – a biomechanical comparison

Jan Nadorf*, Eike Jakubowitz, Christian Heisel, Jörn Reinders, Robert Sonntag, Jan Philippe Kretzer
**University of Heidelberg, Heidelberg, Germany*

1A.8
9:57
TLEMsafe: a european project to improve predictability of functional recovery of patients requiring severy musculoskeletal surgery

Nico Verdonschot*, Bart Koopman, Roel Wirix-Speetjens, Soren Torholm, Thomas Feilkas, Marjolein van der Krogt
**Radboud University Nijmegen Medical Centre, Nijmegen and University of Twente, Enschede, Netherlands*

1A.9
10:05–
10:13
Measurement of fluid pressures behind an acetabular cup in vitro.

Sarah Sydney*, Samantha Wright, Irene Turner, Anthony Miles,
**University of Bath, Bath, UK*

10:15 – 10:45 **Coffee break**

🇫🇷 1st author representing EORS 2012 Friendship country France

Author Nname Presenting author

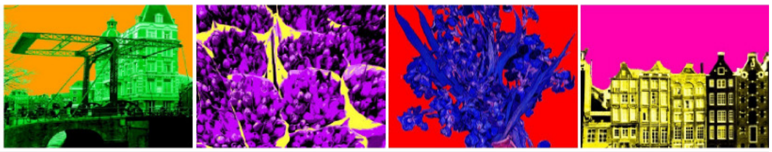

Thursday September 27

7:30 – 8:30 **Coffee & Registration**

8:30 – 8:45 **Large Auditorium** **Plenary Opening**
EORS 2012 Chairmen, Dean Acta, President EORS

8:45 – 10:15 **Lecture Room** **SESSION 1B: Biomaterials 1**
Chairs: Theo Smit
Florelle Gindraux

Keynote **The role of cytokines in bone formation and degeneration**
8:45

Astrid Bakker
Dept Oral Cell Biology, Academic Centre for Dentistry Amsterdam (ACTA), University of Amsterdam and VU University Amsterdam, NL

1B.1 **Preosteoblasts response to Ti6Al7Nb surfaces modified by plasma electrolytic oxidation**
9:01

Nicole de Groot*, Johannes van Leeuwen, Bogdan Necula, Lidy Fratila-Apachitei, Jurek Duszczyk
**Delft University of Technology, Delft, Netherlands*

1B.2 **Bacterial adherence to MWCNT/UHMWPE composites: searching new clinical applications for multi wall carbon nanotubes structures**
9:09

Gema del Prado*, Francisco Pascual, Pere Castell, Diana Molina-Manso, José Antonio Puértolas, Enrique Gómez-Barrena, Jaime Esteban Moreno
**IIS-Foundation Jiménez Díaz, Madrid, Spain*

1B.3 **Human Polyethylene Granuloma Tissues Inhibit Bone Healing In A Novel Xenograft Animal Model**
9:17

Christina Esposito*, Rema Oliver, Pat Campbell, William Walter, Chris Christou, William Walsh
**Surgical & Orthopaedic Research Laboratories, Sydney, Australia*

1B.4 **The effect of a biphasic injectable bone substitute on the interface strength in a rabbit knee prosthesis model**
9:25

Jian-Sheng Wang*, Vasilis Zampelis, Lars Lindgren, Hanna Isaksson, Magnus Tägil
**Lund University, Lund, Sweden*

1B.5 **A method to preserve tensile properties of radiation crosslinked polyethylene**
9:33

Andrew George*, Hung Ngo, Anuj Bellare
**Department of Orthopedic Surgery, Brigham and Women's Hospital, Harvard Medical School, Boston, MA, USA*

1B.6 **The Effect of Processing, Sterilization and Carrier on the Osteoinductivity of Ovine Demineralized Bone Matrix in an Ectopic Athymic Rat Model**
9:41

Nicholas Russell*, Veldran Lovric, Yan Yu, Alain Rives, Matthew Pelletier, William Walsh
**University of New South Wales, Sydney, Australia*

1B.7 **Synthetic material to replicate fibrous tissue occurring in joint replacement.**
9:49

Samantha Wright*, Sarah Sydney, Anthony Miles
**University of Bath, Bath, UK*

1B.8 **Biotribology of a vitamin E stabilised polyethylene for hip arthroplasty – influence of bearing material, surface roughness, ageing and third-body particles**
9:57

Thomas Grupp*, Melanie Holderied, Marie-Anne Mulliez, Rouven Streller, Thomas Hermle, Wilhelm Blömer
**Aesculap AG, Tuttlingen, Germany*

1B.9 **Biodegradation of magnesium implants ZX50 and WZ21 in a transepiphyseal rat model**
10:05–
10:13

Tanja Kraus*, Stefan Fischerauer, Elisabeth Martinelli, Michael Fiedler, Silvia Zoetsch, Stefan Treichler, Karin Pichler, Eva Fischerauer, Peter Uggowitzer, Annelie Weinberg
**Medical Universitiy of Graz, Graz, Austria*

10:15 – 10:45 **Coffee break**

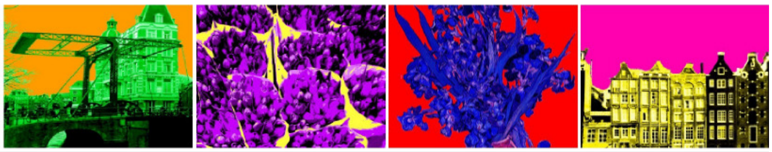

Thursday September 27

10:45 – 11:10	**Large Auditorium**	**Presidential Guest Lecture** **Translational Research between dentistry & orthopaedics** **Jenneke Klein Nulend,** *ACTA, VU University & University of Amsterdam, Netherlands*

11:15 – 12:45	**Large Auditorium**	**SESSION 2A: Infection and Trauma**	Chairs: Geoff Richards Enrico Pola

Keynote 11:15 — **What's new in infection research in fracture fixation**

Geoff Richards
AO Research Institute Davos, Davos, Switzerland

2A.1 11:31 — **The immune response to bacterial contamination of orthopaedic implant materials**

Edward Rochford*, Alexandra Poulsson, Liam O'Mahony, Mario Ziegler, Robert Geoff Richards, T. Fintan Moriarty
**AO Research Institute Davos, Davos, Switzerland*

2A.2 11:39 — **Augmented bone-implant constructs fail by shearing of the cement-screw interface: experimental and computational micromechanics**

Samuel Basler*, Juri Steiner, David Christen, Ralph Müller, Harry van Lenthe
**Institute for Biomechanics, ETH Zurich, Zurich, Switzerland*

2A.3 11:47 — **In vitro susceptibility to antibiotics in biofilms of staphylococci isolated from orthopaedic infections**

Diana Molina-Manso*, Gema del Prado, Alberto Ortiz-Pérez, Miguel Manrubia-Cobo, Enrique Gómez-Barrena, José Cordero-Ampuero, Jaime Esteban Moreno, Toribio Otero
**IIS-Foundation Jiménez Díaz, Madrid, Spain*

2A.4 11:55 — **The masquelet technique for segmental tibial defects a preclinical ovine model**

Chris Christou*, Adrian Low, Rema Oliver, William Walsh
**Surgical & Orthopaedic Research Laboratories, Sydney, Australia*

2A.5 12:03 — **3D Morphology of the Sacrum and its Impact on Treating Sacral Insufficiency Fractures. A Workflow using CT based 3D Statistical Modeling**

Daniel Wagner*, Pol M. Rommens, Takeshi Sawaguchi, Lukas Kamer, Hansrudi Noser
**AO Research Institute Davos, Davos, Switzerland*

2A.6 12:11 — **Reduction of bacterial adhesion on Ti6Al4V surfaces functionalized with siloxanes**

Miguel Angel Pacha Olivenza*, Abraham Rodríguez-Cano, Amparo María Gallardo-Moreno, José Morales-Bruque, Reyes Babiano, Pedro Cintas, María Luisa González-Martín
**Networking Research Center on Bioengineering, Biomaterials and Nanomedicine CIBER-BBN and Department of Applied Physics, Faculty of Sciences. University of Extremadura, Badajoz, Spain*

2A.7 12:19 — **Pre-vascularized 3D constructs for bone critical size defects**

Sophie Verrier*, Fabian Duttenhoefer, Lorin Benneker, Robert Geoff Richards, Mauro Alini
**AO Research Institute Davos, Davos, Switzerland*

2A.8 12:27– 12:35 — **Periprosthetic Fractures Around the Hip in a UK North West Trauma Unit**

Zuned Hakim*, Hui Chiu, Anthony Helm
** Royal Preston Hospital, Preston, UK*

12:45 – 14:00	**Lunch & Poster Session 1**	**13:00 – 13:50**	**Meet-a-Mentor Session** **Young Investigators + Experienced Seniors**

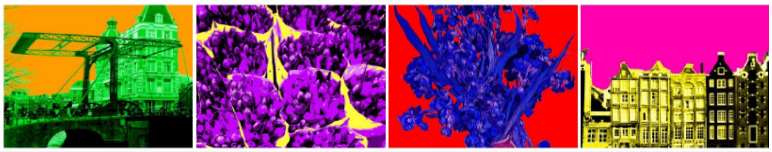

Thursday September 27

10:45 – 11:10 **Large Auditorium**

Presidential Guest Lecture
Translational Research between dentistry & orthopaedics
Jenneke Klein Nulend, _ACTA, VU University & University of Amsterdam, Netherlands_

11:15 – 12:45 **Lecture Room** **SESSION 2B: Cells & Molecular 1**

Chairs: Harrie Weinans
Agata Nyga

Keynote 11:15
Bone cell mechanosensing: On shapes and forces

Rommel Bacabac
San Carlos University, Cebu, Philippines

2B.1 11:31
BMP-2 and BMP-7: Differential Regulation of Chondrogenic Differentiation

Marjolein Caron*, Pieter Emans, Marielle Coolsen, Don Surtel, Andy Cremers, Lodwijk van Rhijn, Tim Welting
*Maastricht University Medical Center, Dept. Orthopaedic Surgery, Maastricht, Netherlands

2B.2 11:39
Macrophages response to wear particles is determined by macrophage polarization

Jukka Pajarinen*, Vesa-Petteri Kouri, Jami Mandelin, Jari Salo, Yrjö Konttinen
*Department of Medicine, Institute of Clinical Medicine, University of Helsinki, Helsinki, Finland

2B.3 11:47
Inhibition of NF-kB activation delays the onset of age-dependent spinal degeneration in a murine model of human progeria

Luigi Aurelio Nasto*, Enrico Pola, Andria Robinson, Arvydas Usas, Gwendolyn Sowa, Paul Robbins, Laura Niedernhofer, James Kang, Nam Vo
*Department of Orthopaedic Surgery, Catholic University of Rome, Rome, Italy

2B.4 11:55
Innate immune sensors enhanced macrophagic reaction after phagocytosis of wear debris in so-called “aseptic ” condition

Yasushi Naganuma*, Tomoyuki Hirayama, Yasunobu Tamaki, Yuya Takakubo, Kan Sasaki, Michiaki Takagi
*Yamagata University, Yamagata, Japan

2B.5 12:03
Modulation of osteoclast formation by cyclically-strained myotubes is mediated by IL-6

Petra Juffer*, Richard Jaspers, Jenneke Klein-Nulend, Astrid Bakker
*Department of Oral Cell Biology, Academic Centre for Dentistry Amsterdam (ACTA), University of Amsterdam and VU University Amsterdam, MOVE Research Institute Amsterdam, Netherlands

2B.6 12:11
Eicosapentanoic acid prolongs survival and attenuates inflammatory response in an experimental model of lethal trauma

Stephanos Koutsostathis*, Christos Paganias, Thomas Tsaganos, Nikitas Schizas, Evangelos Giamarellos- Bourboulis, Eleftheria Kontou, George Macheras
*KAT Hospital, Kifissia, Athens, Greece

2B.7 12:19
Elevated Lysyl hydroxylase 2b expression during experimental OA; the potential cause of persistent synovial fibrosis

Dennis Remst*, Esmeralda Blaney Davidson, Elly Vitters, Arjen Blom, Reinout Stoop, Jessica Snabel, Ruud Bank, Wim van den Berg, Peter van der Kraan
*Radboud University Nijmegen Medical Centre, Nijmegen, Netherlands

2B.8 12:27
Deleterious interaction between BMP2 and TGF-beta signaling in articular chondrocytes: Harmful role for BMP2 in OA?

Esmeralda Blaney Davidson*, Arjan van Caam, Laurie de Kroon, Elly Vitters, Wim van den Berg, Peter van der Kraan
* Radboud University Nijmegen Medical Centre, Nijmegen, Netherlands

2B.9 12:35– 12:43
The bio-mechano-reactor: design and development of a new tool for Osteoarthritis research

Thijs de Jong*, Karen Wiegant, Simon Mastbergen, Floris Lafeber
*University Medical Center Utrecht, Utrecht, Netherlands

12:45 – 14:00 **Lunch & Poster Session 1**

13:00 – 13:50 **Meet-a-Mentor Session**
Young Investigators + Experienced Seniors

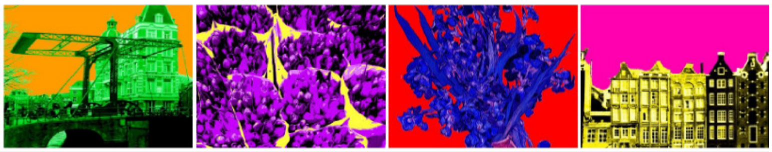

Thursday September 27

14:00 – 15:30 **Large Auditorium** **SESSION 3A: Spine & Upper Extremity** Chairs: Barend van Royen
Gianluca Vadalà

3A.1 14:00 **Lumbar Posterolateral Spinal Fusion with a Collagen/TCP Scaffold in an Ovine Model**

Ali Ismailoglu*, Frank Vizesi, Bryan Cunningham, Kenneth Mullinix, Ashley Murgatroyd, Sung-Ching Chen, Joost de Bruijn, Erik Erbe (Florence de Groot)
**NuVasive, San Diego, CA, USA*

3A.2 14:08 **Biological effects of clinically relevant CoCr nanoparticles on the cells of the Dura Mater. Phenotypic analysis of the porcine model and establishment of the phagocytotic potential of each type of dural cells**

Iraklis Papageorgiou*, Bharat Bhel, Chris Brown, Richard M. Hall, Joanne L. Tipper, John Fisher, Eileen Ingham
**Institute of Medical and Biological Engineering, Leeds University, UK*

3A.3 14:16 **How do Tamoxifene and Raloxifene effect bipedal scoliotic mice?**

Nadir Yalcin*, Ibrahim Akel, Gokhan Demirkiran, Ozgur Dede, Deniz Olgun, Ralph Marcucio, Emre Acaroglu
**Ataturk Training and Research Hospital, Ankara, Turkey*

3A.4 14:24 **Monitoring of cement injection during a verterbroplasty by time-lapsed computed tomography and micro-finite element modelling reveals the migration of high stresses concentration in the bone structure**

Vincent Stadelmann*, Ivan Zderic, Andreas Boger, Markus Windolf
**AO Research Institute Davos, Davos, Switzerland*

3A.5 14:32 **Near Infrared Spectroscopy for the Intra-operative Assessment of Human Spinal Cord Blood Perfusion**

Amir Amiri*, Lee Cheong, Terence Leung, Michael Hetreed, Michael Craggs, Casey Adrian
**Royal National Orthopaedic Hospital, London, UK*

3A.6 14:40 **With or without the long head of the biceps tendon?**

Marco Hoozemans*, Bart Burger, Dirk Jan Veeger
**Orthopaedic Outpatient Department, Medical Centre Alkmaar, Alkmaar, Netherlands*

3A.7 14:48 **Botulinum toxin injections to reduce internal rotation contractures in obstetric brachial plexus injuries**

Bouke Duijnisveld*, Rietje van Wijlen-Hempel, Simone Hogendoorn, Kees de Boer, Martijn Malessy, Jochem Nagels, Rob Nelissen
**Leiden University Medical Center, Department of Orthopaedics, Netherlands*

3A.8 14:56 **Teres major tendon transfer surgery for massive irreparable posterosuperior rotator cuff tears**

Jan Ferdinand Henseler*, Jochem Nagels, Peer van de Zwaal, Rob Nelissen
**Leiden University Medical Center, Leiden, Netherlands*

3A.9 15:04 **Fusion less 3-D correction of idiopathic scoliosis. Feasibility of concept and pilot study results.**

Chris Arts*, Rob Bogie, Alex Roth, Karlien Ceelen, Mischa Nelis, Paul Willems, Tim Welting, Lodwijk van Rhijn
**Maastricht University Medical Centre, Maastricht, Netherlands*

3A.10 15:12 **T1rho magnetic resonance imaging quantification of early lumbar intervertebral disc degeneration in healthy young adults**

Gianluca Vadalà*, Bruno Beomonte Zobel, Riccardo Del Vescovo, Sofia Battisti, Fabrizio Russo, Arijit Borthakur, Vincenzo Denaro
**Campus Bio Medico University Hospital - Department of Orthopaedic and Trauma Surgery, Rome, Italy*

3A.11 15:20 – 15:28 **Proteomic Analysis of Ligamentum Flavum from Lumbar Spinal Canal Stenosis**

Yuchiro Goda*
**Dept of Orthopedics, Institute of Health Biosciences, University of Tokushima Graduate School, Tokushima, Japan*

15:30 – 15:50 **Coffee break**

Thursday September 27

14:00 – 15:30 **Lecture Room** **SESSION 3B: Cells & Molecular 2**
Chairs: Sjoerd Bulstra
Francesca Perut

3B.1
14:00
Mechanical stimulation of tendon-derived cells and investigation of its influence on gene expression

Cvetan Popov*, Kreja Ludwika, Anita Ignatius, Matthias Schieker, Denitsa Docheva
**Ludwig-Maximilians University Munich, Munich, Germany*

3B.2
14:08
Human End-Stage Osteoarthritic Cartilage is Responsive to Transforming Growth Factor Beta and Contains a Population of Cells that Expresses SMAD2/3P and SMAD1/5/8P

Arjan van Caam*, Esmeralda Blaney Davidson, Elly Vitters, Wim van den Berg, Peter van der Kraan
**Nijmegen Centre for Molecular Life Sciences, Radboud University Nijmegen Medical Centre, Nijmegen, Netherlands*

3B.3
14:16
Heat Shock proteins 70 and 90 in osteoarthritis progression

Michiel Siebelt*, Harald Groen, Marjan Sandker, Erwin Waarsing, Nicole Kops, Christina Muller, Jan Verhaar, Marion de Jong, Willem van Eden, Holger Jahr, Harrie Weinans
**Dept. of Orthopaedic Surgery, Erasmus Medical Center, Rotterdam, Netherlands*

3B.4
14:24
Fluid flow induced osteoclast differentiation is associated with alterations in genes regulating IL-6 signaling, cell death and osteoblast differentiation

Anna Fahlgren*, Rune Madsen, Aleksey Dvorzhinskiy, Benjamin McArthur, Göran Andersson, Patrick Ross, Mathias Bostrom
**Hospital for Special Surgery, New York, USA*

3B.5
14:32
Utilization of platelet rich plasma (PRP) in orthopeadic practice: clinical and biological analysis of terapeutic effectivenes

Rocco Papalia*, Francesco Franceschi, Gianluca Vadalà, Biagio Zampogna, Sebastiano Vasta, Lorenzo Diaz Balzani, Andrea Tecame, Erika Albo, Nicola Maffulli, Vincenzo Denaro
**Campus Bio Medico University Hospital - Department of Orthopaedic and Trauma Surgery, Rome, Italy*

3B.6
14:40
Isoprostane levels are altered in rheumatoid arthritis and suppress NFκB activity to inhibit osteoclast formation

Seint Lwin*, Joshua Brooks, Lynett Danks, Karen Lundberg, Jason Morrow, Ginger Milne, James Edwards
**University of Oxford, UK*

3B.7
14:48
Synovial Wnt and WISP1 expression leads to OA-like cartilage damage by skewing of TGF-beta signaling

Martijn van den Bosch*, Arjen Blom, Peter van Lent, Henk van Beuningen, Fons van de Loo, Esmeralda Blaney Davidson, Peter van der Kraan, Wim van den Berg
**Radboud University Nijmegen Medical Centre, Nijmegen, Netherlands*

3B.8
14:56
Differences in expression profiles of osteolysis-related cytokines in tissues retrieved from aseptically failed hip and knee arthroplasties

Tereza Tomankova*, Eva Kriegova, Martin Petrek, Jiri Gallo
**Laboratory of Immunogenomics and Immunoproteomics, Faculty of Medicine and Dentistry, Palacky University Olomouc, Olomouc, Czech Republic*

3B.9
15:04
Continued cell exposure to parathyroid hormone-related peptide (1-36) decreases osteogenic and angiogenic gene expression

Timothy Hardwick*, Priya Kalia, Joanna Baawa-Ameyaw, Daniel Lozano, Joydeep Sinha, Lucy Di Silvo
**King's College Health Partnerships, London, UK*

3B.10
15:12
The BMP2-eNOS Axis Regulates Bone Development and Anabolic Effects of Statins

Megan Weivoda*, Ross Garrett, Jonathon Lowrey, Gloria Gutierrez, Gregory Mundy, James Edwards
**University of Oxford, UK*

3B.11
15:20 – 15:28
Nfat5 is involved in in vitro chondrogenic differentiation under normal and increased tonicity

Marjolein Caron*, Anna van der Windt, Pieter Emans, Lodwijk van Rhijn, Holger Jahr, Tim Welting
**Maastricht University Medical Center, Dept. Orthopaedic Surgery, Maastricht, Netherlands*

15:30 – 15:50 **Coffee break**

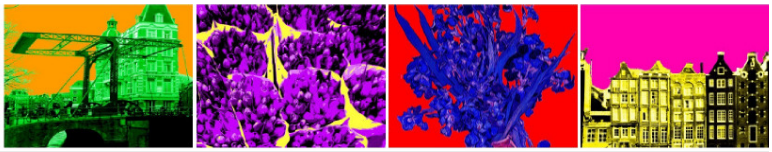

Thursday September 27

15:50 – 16:50 **Large Auditorium** **SESSION 4A: Metal on Metal & Total Hip**

Chairs: Ashley Blom
Richie Gill

Keynote **Metal-on-Metal hips: New evidence from the joint registers**
15:50

Ashley Blom
Avon Orthopaedic Centre, Southmead Hospital, Bristol, United Kingdom

Keynote **Metal-on-Metal hips: The problem and what to do now**
16:02

Richie Gill
University of Bath, Bath, UK

4A.1 **A potential mechanism of cobalt-induced inflammation found in MOM hip implants**
16:14

Agata Nyga*, Marcin Lignowski, Ferdinand Lali, Alister Hart
**Imperial College London, London, United Kingdom*

4A.2 **How important is the femoral cup thickness in hip resurfacing?**
16:22

António Ramos*, Ricardo Duarte, Carlos Relvas, José Simões
**University of Aveiro, Aveiro, Portugal*

4A.3 **Mal-positioning Alone Does Not Necessarily Lead to Increased Wear in Metal-on-Metal Hip Resurfacing**
16:30

Stephen Mellon*, George Grammatopoulos, David Murray, Harinderjit Gill, Michael Skipper Andersen
**University of Oxford, Oxford, UK*

4A.4 **Periprosthetic acetabular bone density and metal ion levels after large head metal-on-metal total hip arthroplasty, short-term results from a randomized controlled trial**
16:38 – 16:46

Wierd Zijlstra*, Hugo van der Veen, Inge van den Akker-Scheek, Mark Zee, Sjoerd Bulstra, Jos van Raay
**Martini Hospital, Groningen, Netherlands*

16:50 – 17:00 **Short break**

Thursday September 27

15:50 – 16:50 **Lecture Room** **SESSION 4B: Tumors** Chair: Nicola Baldini

---

4B.1 **JIP1-inhibition sensitises osteosarcoma to doxorubicin**
15:50

Jantine Posthuma de Boer*, Pim van Egmond, Marco Helder, Renée de Menezes, Anne-Marie Cleton-Jansen, Henk Verheul, Barend van Royen, Gert-Jan Kaspers, Victor van Beusechem
**VU University Medical Center, Amsterdam, Netherlands*

4B.2 **Tumours Outside of the Local Skeletal Environment Contribute to Generalized Bone Loss**
15:58

Seint Lwin*, Jessica Fowler, Nazanine Ruppender, Julie Sterling, Gregory Mundy, Claire Edwards, James Edwards
**University of Oxford, UK*

4B.3 **Surface proteomic analysis of osteosarcoma identifies EPHA2 as receptor for targeted drug delivery**
16:06

Jantine Posthuma de Boer*, Sander Piersma, Thang Pham, Jaco Knol, Victor van Beusechem, Gert-Jan Kaspers, Barend van Royen, Connie Jiménez, Marco Helder
**VU University Medical Center, Amsterdam, Netherlands*

4B.4 **Effects of Low Intensity Pulsed Ultrasound (LIPUS) on Cancer Cells**
16:14

Yasushi Sawai*, Hiroaki Murata, Kazutaka Koto, Takaaki Matsui, Naoyuki Horie, Motoyuki Horii, Eishi Ashihara, Taira Maekawa, Shinji Fushiki, Toshikazu Kubo
**Department of Orthopaedics, Graduate School of Medical Science, Kyoto Prefectural University of Medicine, Kyoto, Japan*

4B.5 **Autologous vaccine for dog osteosarcomas**
16:22
🇫🇷

Patrick Frayssinet*, Didier Mathon, Michel Simonet, Jean Louis Trouillet
**Urodelia, St Lys, France*

4B.6 **Effects of costunolide and dehydrocostus lactone on viability, matrix metalloproteinases and apoptosis in human soft tissue sarcoma cells**
16:30

Birgit Lohberger*, Beate Rinner, Nicole Stuendl, Olaf Kunert, Herbert Bochzelt, Andreas Leithner, Rudolf Bauer, Nadine Kretschmer
**Department of Orthopaedic Surgery, Medical University of Graz, Graz, Austria*

4B.7 **Recurrence rate and progression of chondrosarcoma correlates with heat shock protein expression**
16:38–
16:46

Klemens Trieb*, Irene Sulzbacher, Bernd Kubista
**Department of Orthopedics, Wels, Austria*

16:50 – 17:00 **Short break**

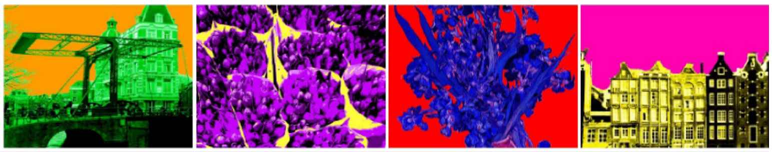

Thursday September 27

17:00 – 18:00 **Large Auditorium** **SESSION 5A: Imaging** Chair: Bart Kaptein

5A.1 17:00
Selective MR imaging of rabbit knee cartilage using a mixture which contains both positive and negative contrast agents

Masamitsu Kido*, Ikoma Kazuya, Yusuke Hara, Ken-ichi Matsuda, Mitsuhiro Kawata, Masahiro Umeda, Toshikazu Kubo
**Kyoto Prefectural University of Medicine, Kajii-cho, Kamigyo-ku, Kyoto-city, Kyoto, Japan*

5A.2 17:08
Knee angle measurements on 3D-CT are influenced by femur orientation, slice thickness and reslicing.

Rachel Senden*, Sabine Cox, Tim Boymans, Ide Heyligers, Bernd Grimm
**AHORSE Research Institute, Atrium Medical Center, Dept. Orthopaedics, Heerlen, Netherlands*

5A.3 17:16
Quantifying periprosthetic osteolysis of the hip using CT images

Francois Malan*, Edward Valstar, Charl Botha, Rob Nelissen
**Leiden University Medical Center, Leiden, Netherlands*

5A.4 17:24
Effect of Sagittal Cutting Angel for Morphology of Anterior Cruciate Ligament in MRI

Ho-Joong Jung*, Han-Jun Lee, Jae-Sung Lee
**Chung-Ang University, Seoul, Korea*

5A.5 17:32
In vitro assessment of primary human chondrocyte viability following treatment with intra-articular contrast media and local anaesthetic

James Broderick*, Joe Baker, Pauline Walsh, Kevin Mulhall
**Mater Misericordiae University Hospital, Dublin, Ireland*

5A.6 17:40
Sensitivity and specificity of ultrasound for detecting small (osteo-)chondral defects in the talus in a cadaveric study

Aimee-Claire Kok*, Juri Aaftink, Maaike Terra, Niek van Dijk, Gino Kerkhoffs, Gabrielle Tuijthoff
**Academic Medical Center, Amsterdam, Netherlands*

5A.7 17:48–17:56
Registration and Quantification of T1Rho MRI on Patients with Knee Osteoarthritis

Pieter Oomen*, Roberto Garcia van der Westen, Ellen Schmitz, Ruud Gransier, Pieter Emans, Lodwijk van Rhijn, Kenneth Meijer
**Maastricht University Medical Centre, Maastricht, Netherlands*

19:00 **Canal Cruise & Conference Dinner**

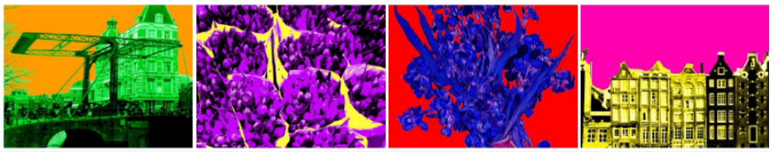

Thursday September 27

17:00 – 18:00 **Lecture Room** **SESSION 5B: Gait & Kinematics** Chair: Frans Steenbrink

---

5B.1
17:00
Decreased range of motion differentiates the incidental radiographic finding from clinical femoroacetabular impingement

Jan Van Houcke*, Christophe Pattyn, Luc Vanden Bossche, Emmanuel Audenaert
**Ghent University Hospital, Ghent, Belgium*

5B.2
17:08
Fluoroscopic assessment of femoral kinematics using a statistical shape model

Nora Baka*, Marleen de Bruijne, Theo van Walsum, Bart Kaptein, Erik Giphart, Michiel Schaap, Wiro Niessen, Boudewijn Lelieveldt
**Leiden University Medical Center, Leiden, Netherlands*

5B.3
17:16
Subject-specific kinematic modelling of clavicular and scapular movements

Bart Bolsterlee*, Frans van der Helm, Dirk Jan Veeger
**Delft University of Technology, Delft, Netherlands*

5B.4
17:24
Unicondylar Knee Arthroplasty kinematics in vitro

Thomas Heyse*, Bilal El-Zayat, Yan Chevalier, Bernardo Innocenti, Susanne Fuchs-Winkelmann, Luc Labey
**Department of Orthopaedics, University Hospital, Marburg, Germany*

5B.5
17:32
Ambulatory measurement of knee angles in the sagittal plane using inductive coil technology; a validation against 3D-motion analysis on healthy subjects.

Ruud Gransier*, Par Dunias, Pieter Emans, Chris Arts, Lodwijk van Rhijn, Kenneth Meijer
**Maastricht University Medical Centre, Maastricht, Netherlands*

5B.6
17:40
Intraoperative kinematic analysis of mobile bearing TKA using imageless navigation

Danilo Bruni*, Francesco Iacono, Mirco Lo Presti, Bharat Sharma, Giovanni Raspugli, Maurilio Marcacci
**Istituto Ortopedico Rizzoli, Bologna, Italy*

5B.7
17:48 –
17:56
The effect of shortening the walkway in clinical inertia-based gait analysis.

Rachel Senden*, Ide Heyligers, Bernd Grimm
**AHORSE Research Institute, Atrium Medical Center, Dept. Orthopaedics, Heerlen, Netherlands*

19:00 **Canal Cruise & Conference Dinner**

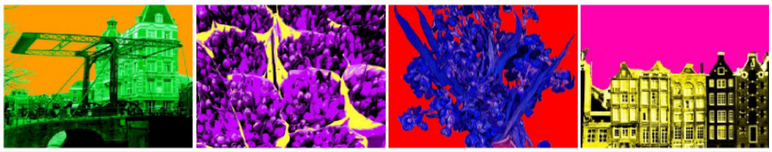

Friday September 28

8:00 – 9:30 **Large Auditorium** **SESSION 6A: Hip Arthroplasty** Chair: Ide Heyligers

---

Keynote
8:00
Improving the quality of orthopaedic implants: Role of RSA and registries

Rob Nelissen
Leiden University Medical Center, Department of Orthopaedics, Leiden, Netherlands

---

6A.1
8:16
Laser-modified CoCrMo- and Al2O3- surfaces for use in the total joint Arthroplasty - A tribological in vitro investigation

Robert Wendlandt*, Rigo Peters, Mohamad Tarabolsi, Arndt-Peter Schulz
**University Lübeck, Biomechanics, Lübeck, Germany*

6A.2
8:24
Suppression of Toll-like receptor (TLR)4, and IRAK1, 4 in macrophages after phagocytosis of lipopolysaccharide-coated titanium particles

Michiaki Takagi*, Yasunobu Tamaki, Takakubo Yuya, Hirayama Tomoyuki, Yasushi Naganuma, Sasaki Kan, Yrjö Konttinen
**Yamagata University School of Medicine Department of Orthopaedic Surgery, Yamagata-city, Yamagata, Japan*

6A.3
8:32
Evaluation of Interleukins and TNF alfa in Serum and Synovial Fluid as Markers for Aseptic Loosening of Hip Arthroplasty

Maria Angeles Cuadrado-Cenzual*, D. Varillas, P. Martin, V. Gomez, José Antonio De Pedro-Moro
**Hospital Clínico San Carlos, Madrid, Spain*

6A.4
8:40
Antibiotic loaded plaster of Paris: Wear of artificial hip joints in the presence of gypsum particles

Roman Heuberger*, Jeannine Krieg, Peter Wahl, Emanuel Gautier
**RMS Foundation, Bettlach, Switzerland*

6A.5
8:48
Restoration of large acetabular bone defects in hip arthroplasty with impaction grafting and coated porous titanium particles as a full bone substitute.

Lucas Walschot*, René Aquarius, Nico Verdonschot, Barend Schreurs, Pieter Buma
**Radboud University Nijmegen Medical Centre, Orthopaedic Research Lab, Nijmegen, Netherlands*

6A.6
8:56
Surgical reconstruction of failed hip Abductors - A new technique using Graft Jacket allograft human dermal matrix

Biyyam Madhusudhan Rao*, Taylor Lee, John Vafaye, Kamal Tamer
**St. Richard's Hospital, Western Sussex Hospitals NHS Trust, Chichester, UK*

6A.7
9:04
Statins may reduce femoral osteolysis in patients with total hip arthroplasty

Anne Lübbeke*, Guido Garavaglia, Kenneth Rothman, Alexis Bonvin, Constantinos Roussos, Pierre Hoffmeyer
**Geneva University Hospitals, Geneva, Switzerland*

6A.8
9:12
Long term results of Müller reinforcement rings in acetabular revision surgery for large bone defects.

George Macheras*, Nikitas Schizas, Christos Paganias, Anastasios Koutroufinis-Tatatsis, Panagiotis Lepetsos, Panagiotis Anastasopoulos, Stephanos Koutsostathis
**KAT Hospital, Kifissia, Athens, Greece*

6A.9
9:20–
9:28
The predictive value of radiostereometric analysis for stem survival in total hip arthroplasty. A systematic review.

Lieke de Vries*, Walter van der Weegen, Piotr Stolarczyk, Thea Sijbesma, Erik Hoffman
**Franciscus Hospital, Roosendaal, Netherlands*

9:30 – 10:00 **Coffee break**

10:00 – 10:25 **Large Auditorium**

Presidential Guest Lecture
The fun of nurturing nature, and making it happen in orthopaedic translational research
Allen Goodship, *University College London and Royal Veterinary College, London, UK*

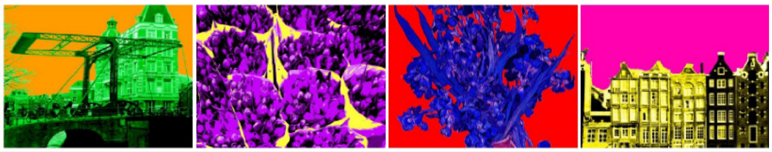

Friday September 28

8:00 – 9:30 **Lecture Room** **SESSION 6B: Biomaterials 2** Chair: Jenneke Klein Nulend

Keynote 8:00
Dental research: Inspiring Orthopaedics
Klaas de Groot
University of Twente, Enschede, Netherlands

6B.1 8:16
Hyaluronic Acid-Based Hydrogel Enhances Neuronal Survival in Mouse Organotypic Spinal Cord Slice Cultures
Nikos Schizas*, Ramiro Rojas, Brittmarie Andersson, Sujit Kootala, Jöns Hilborn, Nils Hailer
**KTH, Stockholm, Sweden*

6B.2 8:24
Bone Cell Proliferation, Differentiation, and Cytokine Production on Titanium-Nitride versus Cobalt-Chromium-Molybdenum Surface
Ruud van Hove*, Peter Nolte, Cornelis Semeins, Jenneke Klein-Nulend
**Dept of Orthopaedics, Spaarne Hospital, Hoofddorp, Netherlands*

6B.3 8:32
Developing Robocast Ceramic/Polymer Scaffolds for Bone Implants
Pedro Miranda*, Francisco Martínez-Vázquez, Fidel Perera, Antonia Pajares, Fernando Guiberteau
**Universidad de Extremadura, Badajoz, Spain*

6B.4 8:40
Comparison of cellular behavior with different bone grafting materials
Massimiliano Leigheb*, Michela Bosetti, Andrea E. Bianchi, Federico A. Grassi, Mario Cannas
**Orthopaedics and Traumatology, AOU Maggiore della Carità, University of Eastern Piedmont, Novara, Italy*

6B.5 8:48
Guided bone regeneration in critical defects using porous titanium scaffolds loaded with gelatin nanosphere-based gels for controlled release of BMP-2 and FGF-2
Johan van der Stok*, Haili Wang, Saber Amin Yavari, Amir Abbas Zadpoor, Esther Van Lieshout, Peter Patka, Jan Verhaar, Holger Jahr, Sander Leeuwenburgh, Harrie Weinans
**Erasmus University, Rotterdam, The Netherlands*

6B.6 8:56
In vivo biological fixation of selective laser melted bone scaffolds
Jan Demol*, Ana Soares, Bram Lenaerts, Steven Leuridan, Sebastian de Boodt, Hendrik Delport
**Mobelife, Leuven, Belgium*

6B.7 9:04
Bone marrow aspirate and biomaterials for osteoregeneration
Claudia Eder*, Sabrina Schildböck, Jochen Meissner, Erwin Falkner, Michael Ogon
**Orthopedic Hospital Speising, Vienna, Austria*

6B.8 9:12
Lysophosphatidic Acid (LPA)-functionalised titanium; a superior implant material for supporting human osteoblast differentiation
Julia Blackburn*, Jason Mansell, Ashley Blom, Jonathan Knapp, Charl Faul
**Musculoskeletal Research Unit, Avon Orthopaedic Centre, Bristol, UK*

6B.9 9:20– 9:20
Effect of intrarticular platelet-rich plasma (PRP) injection in osteochondritis. An experimental histological study in rabbits
Javier Cervero*, Lorena Benito José Antonio De Pedro-Moro, Francisco Collia-Martín, Antonio J. Pérez, Francisco Collia
**Hospital San Agustin, Avilés, Spain*

9:30 – 10:00 **Coffee break**

10:00 – 10:25 **Large Auditorium**
Presidential Guest Lecture
The fun of nurturing nature, and making it happen in orthopaedic translational research
Allen Goodship, *University College London and Royal Veterinary College, London, UK*

Friday September 28

10:30 – 12:00 **Large Auditorium** **SESSION 7A: Clinical Outcome & Arthroplasty** Chair: Klemens Trieb

7A.1 10:30
In vivo Measurement of the Stiffness of Regenerate Bone in Distraction Osteogenesis of the Tibia using RSA, Load Measurement and CT

Ian McCarthy*, Esther Reina Romo, Peter Calder, David Marsh
**UCL Institute of Orthopaedics and Musculoskeletal Science, London, UK*

7A.2 10:38
Physical activity monitoring in knee arthroplasty patients using a body-fixed sensor: Reference data and comparison with clinical scores.

Simon van Laarhoven*, Rachel Senden, Matthijs Lipperts, Ide Heyligers, Bernd Grimm
**AHORSE Research Institute, Atrium Medical Center, Dept. Orthopaedics, Heerlen, Netherlands*

7A.3 10:46
Total Knee Arthroplasty: do custom cutting blocks improve mechanical axis reconstruction?

Nemanja Polic*, Frederic Vauclair, Nemanja Polic, Brigitte Haeberli-Jolles
**CHUV, Lausanne, Switzerland*

7A.4 10:54
Survivorship, Patient Reported Outcome and Satisfaction Following Resurfacing and Total Hip Replacement

Alexander Aquilina*, Michael Whitehouse, Patel Sajal, Stephen Eastaugh-Waring, Ashley Blom
**Avon Orthopaedic Centre, Southmead Hospital, Bristol, UK*

7A.5 11:02
Effect of PCL Over-tightness in Cruciate Retaining Total Knee Arthroplasty

Bo Gao*, Laurent Angibaud
**Exactech, Gainesville, USA*

7A.6 11:10
A short-form of the new KSS is a valid and practical clinical outcome tool for the younger and more demanding patient

Remco Dinjens*, Rachel Senden, Ide Heyligers, Bernd Grimm
**AHORSE Research Institute, Atrium Medical Center, Dept. Orthopaedics, Heerlen, Netherlands*

7A.7 11:18
Total hip replacement can be predicted by shape variations of the hip: A nationwide prospective cohort study

Rintje Agricola*, Max Reijman, Sita Bierma-Zeinstra, Jan Verhaar, Harrie Weinans, Erwin Waarsing
**Erasmus Medical Center, Rotterdam, Nederland*

7A.8 11:26
Towards an instrument for the intraoperative assessment of the initial stability of acetabular implants

Steven Leuridan*, Leonard Pastrav, Kathleen Denis, Michiel Mulier, Wim Desmet, Jos Van der Sloten
**Department of Mechanical Engineering, Division of Biomechanics, Katholieke Universiteit Leuven, Leuven, Belgium*

7A.9 11:34
Age Related Changes in Lower Limb Segment Movement during Gait in a Healthy Population Measured by Inertial Measurement Units

Ian McCarthy*, Maureen Monda, Matt Thornton, Peter Smitham, Andrew Goldberg
**UCL Institute of Orthopaedics and Musculoskeletal Science, London, UK*

7A.10 11:42
Assessing Results After Distal Radius Fracture Treatment: A Comparison of Objective and Subjective Tools

Iris Kwok*, Frankie Leung, Grace Yuen
**Queen Mary Hospital, Hong Kong*

7A.11 11:50–11:58
Analysis of how knee flexion characteristics can be used as an outcome assessment for knee osteoarthritis

Diana Hodgins*, Ian McCarthy, Amit Mor, Avi Elbaz, Ganit Segal
**European Technology for Business Ltd, Codicote, UK*

12:00 – 12:30 **Large Auditorium** **EORS General Assembly**

12:30 – 14:00 **Lunch & Poster Session 2**

Friday September 28

10:30 – 12:00 **Lecture Room** **SESSION 7B: Stem Cells**
Chairs: Martin Stoddart
Tulyapruek Tawonsawatruk

Keynote **The role of multiaxial load on mesenchymal stem cell fate**
10:30

Martin Stoddart
AO Research Institute Davos, Davos, Switzerland

7B.1 **Critical time point for MSCs implantation in atrophic non-union.**
10:46

Tulyapruek Tawonsawatruk*, Antonello Spacido, Bruno Péault, Hamish Simpson
**The University of Edinburgh, Edinburgh, UK*

7B.2 **Intra articular infusion of autologous expanded bone marrow mesenchymal cells (MSCs) in knee osteoarthritis (OA)**
10:54

Francesc Soler*, Robert Soler, Xavier Peirau, Anna Munar, M. Alberca, A. Sanchez, J. Garcia, Lluis Orozco
**ITRT, Barcelona, Spain*

7B.3 **Regulation of players involved in the osteogenic differentiation of mesenchymal stem cells**
11:02

Serena Rubina Baglio*, Donatella Granchi, Nicola Baldini
**Istituto Ortopedico Rizzoli, Bologna, Italy*

7B.4 **To die or not to die: glucose as a determinant of the survival of human mesenchymal stem cells upon implantation**
11:10
🇫🇷

Mickael Deschepper*, Joseph Paquet, Mathieu Manassero, Karim Oudina, Laurent Emmanuel Monfoulet, Morad Bensidhoum, Delphine Logeart-Avramoglou, Herve Petite
**B2OA, paris, France*

7B.5 **Regenerative potential of human muscle stem cells in chronic inflammation**
11:18

Bouke Duijnisveld*, Anne Bigot, Karel Beenakker, Vincent Mouly, Gillian Butler-Browne, Rob Nelissen, Andrea Maier
**Leiden University Medical Center, Department of Orthopaedics, Netherlands*

7B.6 **Short (15 Minutes) BMP-2 Treatment Stimulates Osteogenic Differentiation of Human Adipose Stem Cells Seeded on Calcium Phosphate Scaffolds**
11:26

Janice Overman*, Elisabet Farré-Guasch, Marco Helder, Christiaan ten Bruggenkate, Engelbert Schulten, Jenneke Klein-Nulend
**ACTA-University of Amsterdam and VU University Amsterdam, Research Institute MOVE, Dept Oral Cell Biology, Amsterdam, Netherlands*

7B.7 **Adipose stem cells for the treatment of bone lesions in an animal model**
11:34

Alonso Moreno*, José Luis Leal, Eduardo Noboa, Cristina Abadía, Fernando de Miguel
**Hospital Universitario La Paz, Madrid, Spain*

7B.8 **Stem cells transplantation and core decompression therapies for avascular necrosis of femoral head**
11:42–
11:50

Sun Mengyao*, Fei Chang
**China-Japan Union Hospital, Jilin University, Changchun, China*

12:00 – 12:30 **Large Auditorium** **EORS General Assembly**

12:30 – 14:00 **Lunch & Poster Session 2**

Friday September 28

13:30 – 15:00 **Large Auditorium** **SESSION 8A: The Knee** Chair: Rob Nelissen

---

Keynote
13:30
Tissue engineering for tendon and ligaments

Denitsa Docheva
Ludwig Maximilians University, Munich, Germany

8A.1
13:46
A computational platform for design-phase evaluation of knee replacement

Clare Fitzpatrick*, Xiangyi (Cheryl) Liu, Srikanth Kannan, Samarth Shah, Paul Rullkoetter
**Computational Biomechanics Lab, University of Denver, Denver,USA*

8A.2
13:54
High-flexion Total Knee Arthroplasty is a safe alternative in selected patients: Similar migration during 5 year follow-up of a 4-arm randomized controlled clinical and Roentgen Stereophotogrammetric Analysis (RSA) Study

Marc Nieuwenhuijse*, Paul van der Voort, Bart Kaptein, Edward Valstar, Rob Nelissen
**Leiden University Medical Center, Leiden, Netherlands*

8A.3
14:02
Structural Tissue Changes and Prolonged Clinical Improvement by Joint Distraction in Treatment of End-stage Knee Osteoarthritis; the Two Years Follow-up

Karen Wiegant*, Peter van Roermund, Femke Intema, Sebastian Cotofana, Felix Eckstein, Simon Mastbergen, Floris Lafeber
**University Medical Center Utrecht, Utrecht, Netherlands*

8A.4
14:10
Collateral ligament strain after implantation of a total knee arthroplasty with measured resection technique

Hendrik Delport*, Luc Labey, Ronny De Corte, Bernardo Innocenti, Jos Van der Sloten, Johan Bellemans
**Department of Orthopedics,K.U.Leuven, Leuven, Belgium*

8A.5
14:18
A combined clinical and biomechanical look on early femoral component loosening in high flexion total knee arthroplasty: what about the cement-bone interface?

Sebastiaan van der Groes*, Maarten de Waal Malefijt, Nico Verdonschot
**Radboud University Nijmegen Medical Centre, Nijmegen, Netherlands*

8A.5
14:26
Intra-Articular injections for degenerative cartilage lesions of the knee: Platelet Rich Plasma VS Hyaluronic Acid

Rocco Papalia*, Francesco Franceschi, Gianluca Vadalà, Stefano Carnì, Biagio Zampogna, Lorenzo Alirio Diaz, Stefano D'adamio, Sebastiano Vasta, Nicola Maffulli, Vincenzo Denaro
**Campus Bio Medico University Hospital - Department of Orthopaedic and Trauma Surgery, Rome, Italy*

8A.6
14:34
Effect of extramedullary tibial jig pin placement on the tibial alingment in Total Knee Replacement

Priyanka Jani*, Barlas, Bagga
**Diana Princess of Wales Hospital, Grimsby, UK*

8A.7
14:42
The Effect of Insert Conformity on Total Knee Replacement Wear

Abdellatif Abdelgaied*, Claire Brockett, Feng Liu, Louise Jennings, John Fisher, Zhongmin Jin
**University of Leeds, UK*

8A.8
14:50
Sensitivity of total knee volumetric wear measurement using RSA

Emiel van IJsseldijk*, Solene Gouzy, Benoit Lebel, Bart Kaptein, Edward Valstar, Berend Stoel, Rob Nelissen, Claude Vielpeau
**Leiden University Medical Center, Leiden, Netherlands*

15:00 – 15:30 **Coffee break**

Friday September 28

13:30 – 15:00 **Lecture Room** **SESSION 8B: Bone regenerative Medicine & Tissue Engineering** Chairs: Pieter Buma
Gabrielle Tuijthof

Keynote 13:30 **Regenerating bone defects using new biomedical engineering approaches**

Pierre Layrolle
University of Nantes, Nantes, France

8B.1 13:46 **Healing of segmental femoral defect in nude rats using human bone marrow mesenchymal stem cell (hMSC) cultured on HA/TCP scaffold**

Julien Stanovici*, Philippe Rosset, Dominique Heymann, Pierre Layrolle
**University of Nantes, Nantes, France*

8B.2 13:54 **GMP-compliant ex-vivo expansion of bone marrow derived MSC**

Natalie Fekete*, Markus Rojewski, Hubert Schrezenmeier
**University of Ulm, Ulm, Germany*

8B.3 14:02 **Potential of osteoblastic differentiated Adipose Mesenchymal Stem Cells for bone tissue engineering in a porcine pre-clinical model**

Thomas Schubert*, Sébastien Lafont, Gwen Beaurin, Christian Delloye, Pierre Gianello, Denis Dufrane
**Center of Tissue and Cell Therapy, Brussels, Belgium*

8B.4 14:10 **Bioplasty for vertebral fractures: a pre-clinical study on goats using autologous modified skin fibroblasts**

Enrico Pola*, Debora Colangelo, Valentina Neri, Wanda Lattanzi, Daniele Pressato, Nicola Magarelli, Giandomenico Logroscino, Luigi Aurelio Nasto
**Department of Orthopaedic Surgery, Catholic University of Rome, Rome, Italy*

8B.5 14:18 **Effect of Tricalcium Phosphate-Disilicate Calcium Ceramics on Human Bone Marrow Mesenchymal Stem Viability, Proliferation, Adhesion and Osteoblast Differentiation**

Luis Meseguer-Olmo*, David Garcia-Bernal, Francesca Cragnolini, Isabel Martinez, Pablo Velasquez, Salvador Aznar-Cervantes, Jose Luis Cenis-Anadon, Piedad Nieves de Aza
**Arrixaca University Hospital, Murcia, Spain*

8B.6 14:26 **Coral particle size influences human mesenchymal stem cell osteogenesis but not cell survival in an ectopic mouse model**

Martina Sladkova*, Mathieu Manassero, Valentin Myrtil, Hema Savari, Madelaine Fall, Daila Thomas, Delphine Logeart-Avramoglou, Herve Petite
**University Paris 7, Paris, France*

8B.7 14:34 **The role of pericellular matrix hyaluronan in cell adhesion to polyelectrolytes**

Caterina Fotia*, Gabriela Ciapetti, Graziana Messina, Giovanni Marletta, Nicola Baldini
**Pathophysiology Lab, Istituto Ortopedico Rizzoli, Bologna, Italy*

8B.8 14:42 **Factors affecting stability of osteochondral grafts: effect of graft length, depth of defect and congruency**

Kathryn Lowery*, Serena Russell, David Shaw, Zhongmin Jin, Eileen Ingham, John Fisher
**Institute of Medical and Biological Engineering, Leeds University, UK*

8B.9 14:50–14:58 **Osteoinductive properties of platelet gels prepared by different techniques**

Francesca Perut*, Giuseppe Filardo, Erminia Mariani, Valentina Devescovi, Elizaveta Kon, Maurilio Marcacci, Andrea Facchini, Donatella Granchi, Nicola Baldini
**Laboratory for Orthopaedic Pathophysiology and Regenerative Medicine, Istituto Ortopedico Rizzoli, Bologna, Italy*

15:00 – 15:30 **Coffee break**

Friday September 28

15:15 – 16:15 **Large Auditorium** **SESSION 9A: Biomechanics 2**
Chairs: Nico Verdonschot
Mark Lenz

Keynote
15:15
Will patient-specific biomechanical models optimise upper extremity surgery

Dirk Jan Veeger
Research Institute MOVE, Faculty of Human Movement Sciences, VU University Amsterdam, and Department of Biomechanical Engineering, Delft University of Technology, Amsterdam and Delft, Netherlands

---

9A.1
15:31
An indexation algorithm for femoral shape and bmd can perform bone similarity searches and generate synthetic bones

Ilaria Palmadori*, Enrico Schileo, Christelle Boichon, Michel Rochette, Fulvia Taddei
**Istituto Ortopedico Rizzoli, Bologna, Italy*

9A.2
15:39
Biomechanical considerations in the development of a Novel Polycarbonate-Urethane Meniscal Implant

Jonathan Elsner*, Vincenzo Condello, Claudio Zorzi, Farshid Guilak, Ron Arbel, Elliott Hershman, Eran Linder-Ganz
**Active Implants Corp., Netanya, Israel*

9A.3
15:47
Is double-looped double pegged? A biomechanical study on different cerclage configurations

Mark Lenz*, Boyko Gueorguiev, Robert Geoff Richards, Thomas Mückley, Gunther Olaf Hofmann, Dankward Höntzsch, Stephan Marcel Perren, Markus Windolf
**AO Research Institute Davos, Davos, Switzerland*

9A.4
15:55
FE-based strength estimation for the prediction of femoral neck fracture

Cristina Falcinelli*, Enrico Schileo, Magda Morawska, Marco Viceconti, Fulvia Taddei
**Istituto Ortopedico Rizzoli, Bologna, Italy*

9A.5
16:03–16:11
The influence of porosity on fracture toughness of human cortical bone: An xFEM study

Silke Besdo*, Deepak Vashishth
**Institute of Continuum Mechanics, Leibniz Universitaet Hannover, Hannover, Germany*

16:15 – 16:45 **Large Auditorium**

Presidential Guest Lecture
Challenges and Opportunities of Orthopaedic Research in Europe
Enrique Gomez Barrena, *EORS president*

Round Table Debate: Future of Orthopaedic Research
Panel: Ashley Blom, Denitsa Docheva, Ide Heyligers, Geoff Richards, Gianluca Vadalà

16:45 – 17:00 **Awards Session & Closing**

---

13. Oct – 16. Oct. 2013

21st Annual Meeting EORS
+
8th Tri-Annual Meeting of the Combined Orthopaedic Research Socities
CORS 2013
Venice, Italy


CORS 2013
VENICE
8th COMBINED MEETING
OF ORTHOPAEDIC
RESEARCH SOCIETIES
13-16 OCTOBER 2013
SAN SERVOLO
VENICE, ITALY
www.cors2013.org

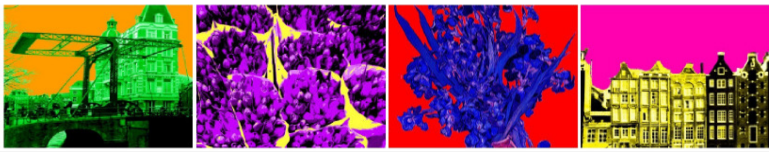

Friday September 28

15:15 – 16:15 **Lecture Room** **SESSION 9B: Bone & Miscellaneous**
Chairs: Chris Arts
Martina Sladkova

Keynote 15:15
Aspects of accuracy of orthopaedic tests in dentistry
Corine M. Visscher
VU University Medical Center, Amsterdam, Netherlands

9B.1 15:31
A curious effect in the jaw joint following bisphosphonate treatment.
Greetje Renders*, Geerling Langenbach, Carla Prins, Jenny Vermeer, Ineke Jansen, Teun de Vries, Vincent Everts
**Academic Center for Dentistry Amsterdam, Amsterdam, Netherlands*

9B.2 15:39
Biological membranes for bone repair
Laurent Obert*, Romain Laurent, Benoit de Billy, Fabienne Poulthier, Caroline Malugani, Patrick Garbuio, Florelle Gindraux
**University of Franche-Comté, CIC-BT, Besançon, France*

9B.3 15:47
The lacunar - canalicular structure of irradiated mandible studied by scanning electron microscopy
Timo Ruotsalainen*, Pekka Asikainen, Jopi Mikkonen, Arto Koistinen, Arja Kullaa
**Institute of Dentistry, Oulu, Finland*

9B.4 15:55
Evolution simulations predict variable mechanoregulated endochondral ossification process in animal populations
Hanifeh Khayyeri*, Patrick Prendergast
**Trinity Centre for Bioengineering, Trinity College Dublin, Dublin, Ireland*

9B.5 16:03–16:11
A Novel Method for Generating Crack Extension Resistance Curves in Small Bone Samples using High-Speed Videography
Orestis Katsamenis*, Thomas Jenkins, Sofia Michopoulou, Ian Sinclair, Philipp Thurner
**Bioengineering Sciences Research Group, Faculty of Engineering and the Environment, University of Southampton, UK*

16:15 – 16:45 **Large Auditorium**

Presidential Guest Lecture
Challenges and Opportunities of Orthopaedic Research in Europe
Enrique Gomez Barrena, *EORS president*

Round Table Debate: Future of Orthopaedic Research
Panel: Ashley Blom, Denitsa Docheva, Ide Heyligers, Geoff Richards, Gianluca Vadalà

16:45 – 17:00 **Awards Session & Closing**

---

13. Oct – 16. Oct. 2013

21st Annual Meeting EORS
+
8th Tri-Annual Meeting of the Combined Orthopaedic Research Socities
CORS 2013
Venice, Italy

POSTER PRESENTATIONS

PA	**Biomaterials**	**1-17**
PB	**Biomechanics**	**1-22**
PC	**Cells and Molecular**	**1-17**
PD	**Hip**	**1-29**
PE	**Knee**	**1-28**
PF	**Spine and Upper Extremity**	**1-17**
PG	**Tissue Engineering**	**1-12**
PH	**Trauma and Infection**	**1-26**
PI	**Miscellaneous**	**1-17**

POSTER PRESENTATIONS

PA Biomaterials

PA.01 **Both N- and C-terminal PTHrP peptides improve the osteogenic properties of hybrid poly-vinyl alcohol/bioactive glass scaffolds in vitro in osteoblastic cells**

Daniel Lozano*, Pablo Mortarino, Agda Aline Rocha Oliveira, Sergio Portal-Núñez, Marivalda Pereira, Sara Feldman, Pedro Esbrit

**Laboratorio de Metabolismo Mineral y Óseo (IIS-FJD) and Instituto de Salud Carlos III-RETICEF, Madrid, Spain*

PA.02 **Histological evaluation of a new calcium phospate biomaterial in sheep**

Lorena Benito*, José Antonio De Pedro-Moro, Francisco Collia-Martín, Sussette Padilla, Raúl Carrodeguas, Arcadio García de Castro, Francisco Collia

**University of Salamanca. Faculty of Medicine, Salamanca, Spain*

PA.03 **Development of Gene Activated Matrices for osteochondral regeneration in osteoarthritis**

Matteo D'Este*, Pascal Borget, Guy Daculsi, Olga Mykhaylyk, Christian Plank, Martina Anton, Mauro Alini, David Eglin

**AO Research Institute Davos, Davos, Switzerland*

PA.04 **Antibacterial properties of TI-O doped with different concentrations of silver**

R. Pérez -Tanoira*, A. Mosquera, C. Pérez-Jorge Peremarch, J. L. Endrino, MA Arenas, A. Conde, Enrique Gómez-Barrena, Jaime Esteban Moreno

**IIS-Foundation Jiménez Díaz, Madrid, Spain*

PA.05 **Combined diffusive/pvd coating solutions in modular couplings to improve in vivo life-time of orthopaedic implants**

Elia Marin*, Marco Regis, Simonetta Fusi, Alex Lanzutti, Lorenzo Fedrizzi

**University of Udine, Udine, Italy*

PA.06 **Evaluation of a new calcium phospate biomaterial by multiple fluorescence bone-labelling**

Lorena Benito*, José Antonio De Pedro-Moro, Yasmina Guadilla, Francisco Collia-Martín, Sussette Padilla, Raúl Carrodeguas, Arcadio García de Castro, Francisco Collia

**University of Salamanca. Faculty of Medicine, Salamanca, Spain*

PA.07 **Seeding of mesenchymal stromal cells on high and low porosity tricalcium phosphate scaffolds**

Arina Buizer*, Albert Veldhuizen, Sjoerd Bulstra, Roel Kuijer

**University Medical Center Groningen, Groningen, Netherlands*

PA.08 **Effect of thermal treatment on the nanostructure and mechanical properties of crosslinked Vitamin-E-blended UHMWPE**

Andrew George*, Hung Ngo, Anuj Bellare

**Department of Orthopedic Surgery, Brigham and Women's Hospital, Harvard Medical School, Boston, MA, USA*

PA.09 **Osteoinductive Potential of Different Collagen/TCP Scaffolds in Canine Intramuscular Defect**

Ali Ismailoglu*, Frank Vizesi, Huipin Yuan, Sung-Ching Chen, Joost de Bruijn, Erik Erbe (Florence de Groot)

**NuVasive, San Diego, CA, USA*

PA.10 **Parathyroid hormone-related protein (PTHrP) (1-37) or PTHrP (107-111) loading increases the osteogenic capacity of biopolymer-coated nanocrystalline hydroxyapatite (HAGlu) in vitro**

Daniel Lozano*, Mercedes Vila, Sandra Sánchez-Salcedo, Sergio Portal-Núñez, Enrique Gómez-Barrena, María Vallet-Regí, Pedro Esbrit

**Laboratorio de Metabolismo Mineral y Óseo (IIS-FJD) and Instituto de Salud Carlos III-RETICEF, Madrid, Spain*

PA.11 **Ti6Al4V after UV-C irradiation: Bactericidal and electrical surface behavior**

Miguel Angel Pacha Olivenza*, Amparo María Gallardo-Moreno, José Morales-Bruque, Juan Carlos Galván-Sierra, María Luisa González-Martín

**Networking Research Center on Bioengineering, Biomaterials & Nanomedicine CIBER-BBN and Department of Applied Physics, Faculty of Sciences. University of Extremadura, Badajoz, Spain*

PA.12 **Antibacterial effects of silver ion implantation**

R. Pérez -Tanoira*, F. Martín Julian, C. Pérez-Jorge Peremarch, A. Medrano Fernández, G. Fuentes, Enrique Gómez-Barrena, Jaime Esteban Moreno

**IIS-Foundation Jiménez Díaz, Madrid, Spain*

PA.13 **A Novel Mixing Method For The Incorporation Of Gentamicin Into Orthopaedic Bone Cement**

Davinder Bhachu*, Richard Mallett, Sanjukta Deb

**Department of Biomaterials, King's College London, UK*

PA.14 **In vivo evaluation of novel injectable hydrogel for viscosupplementation treatment**

William Walsh*, Francesco Segatti, David Mercuri, Gennyfer De Conti, Nicky Bertollo, R Da Assuncao, R. Haddad, Yan Yu, Simonetta Fusi

**University of New South Wales, Sydney, Australia*

PA.15 **A Collagen Augmented Acrylic Bone Cement**

Mohamad Hachem*, Sanjukta Deb,

**Department of Biomaterials, King's College London, UK*

PA.16 **Functionalization of silk-fibroin meshes with polypyrrole for medical purposes. Pilot study.**

*Luis Meseguer-Olmo, Salvador Aznar-Cervantes, Francesca Cragnolini, Maria Isabel Roca, Jose Gabriel Martinez, Jose Luis Cenis-Anadon, Piedad Nieves de Aza, Vicente Ortega, David Garcia-Bernal

**Arrixaca University Hospital, Murcia, Spain*

PA.17 **Incorporation of Raloxifene-impregnated Allograft around Orthopaedic Titanium Implants**

Lars Lykke Hermansen*, Mette Sørensen, Jørgen Baas, Jeppe Barckman, Joan Bechtold, Kjeld Søballe

**Orthopaedic Research Laboratory, Aarhus University Hospital, Aarhus C, Denmark*

POSTER PRESENTATIONS

PB Biomechanics

PB.01 Prediction of the elastic strain limit of the tendon using a shape-based comparative method

Alejandra Magaly Reyes Lua*, Holger Jahr, Hans van Schie, Harrie Weinans, Amir Abbas Zadpoor

**University Medical Center Rotterdam, Rotterdam, Netherlands*

PB.02 Waterjet drilling in bone: the effects of nozzle diameter and joint type on hole depth and diameter

Steven den Dunnen*, Lars Mulder, Aimee-Claire Kok, Jenny Dankelman, Gino Kerkhoffs, Gabrielle Tuijthoff

**Delft University of Technology, Delft, Netherlands*

PB.03 Investigation on Poisson's ratio of human cortical bone determined via LED-Micrometer – a feasibility study

Annette Sitzer*, Klaus Waizner, Robert Wendlandt, Heinz Handels, Imke Weyers, Christian Jürgens, Arndt-Peter Schulz

**University Hospital Schleswig-Holstein, Biomechanics Laboratory, Lübeck, Germany*

PB.04 Influence of tool geometry on drilling performance of cortical and trabecular bone

Gabrielle Tuijthof*, Christine Frühwirt, Christoph Kment

** BioMechanical Engineering, Delft University of Technology, Netherlands*

PB.05 Biomechanical evaluation of a new fixation concept for intramedullary nailing of proximal humerus fractures

Boyko Gueorguiev*, Stephan Rothstock, Martin Kloub, Damiano Schiuma, Michael Plecko

**AO Research Institute Davos, Davos, Switzerland*

PB.06 Effect of electrolyte-plasma polishing on the surface properties of titanium bone plates - an in-vitro study with a novel testing device mimicking tendon properties

Robert Wendlandt*, Christian Jürgens, Arndt-Peter Schulz

**University Lübeck, Biomechanics, Lübeck, Germany*

PB.07 The comparison of a biomechanical testing using 4 point bending in rat Tibia between specimen with and without muscle cleaning

Tulyapruek Tawonsawatruk*, Robert Wallace, Hamish Simpson

**The University of Edinburgh, Edinburgh, UK*

PB.08 Cell deformation behavior in a rabbit model of early OA

Siru Turunen*, Sang Kuy Han, Walter Herzog, Rami Korhonen

**University of Eastern Finland, Kuopio, Finland*

PB.09 Fixation of the Fitmore® stem - A biomechanical Analysis.

Jan Nadorf*, Wojciech Pepke, Marcus Streit, Volker Ewerbeck, Jörn Reinders, Robert Sonntag, Jan Philippe Kretzer

**University of Heidelberg, Heidelberg, Germany*

PB.10 Accuracy of robot spine drilling

Rumen Kastelov*, George Boiadjiev, Kamen Delchev, Kazimir Zagurski, Tony Boiadjiev

**Institute of Mechanics – Bulgarian Academy of Sciences, Sofia, Bulgaria*

PB.11 The interprosthetic gap as a risk factor for peri-prosthetic fractures of the femur. A biomechanical evaluation

Thomas Quirynen*, Olivier Segal, Jos van der Sloten, Johan Bellemans, Kristoff Corten

**Biomechanics Section, Faculty of Engineering, KU Leuven, and Orthopaedic Surgery Dept University Hospital Pellenberg, Belgium*

PB.12 Progressive failure in the femoral neck during a sideways fall

Mohamad Ridzwan*, Pal Bidyut, Unrich Hansen, Andrew Amis

**Biomechanics Group, Department of Mechanical Engineering, Imperial College, London, UK*

PB.13 Changes in Core Suture Geometry within Repaired Flexor Tendons: Investigations with a novel radiographic method

Tim Sebastian Peltz*, Peter Scougall, Sean Nicklin, Mark Gianoustos, Bertollo Nicki, William Walsh

**University of New South Wales, Surgical & Orthopaedic Research Laboratories, Prince of Wales Hospital, Sydney, Australia*

PB.14 Multi-scale Modelling of the Cement-Bone Interface

Dennis Janssen*, Daan Waanders, Kenneth Mann, Nico Verdonschot

**Radboud University Nijmegen Medical Centre, Nijmegen, Netherlands*

PB.15 A biomechanical knee model with deformable structural components to dynamically simulate TKR

Dario Bovio*, Esteban Pavan, Massimo Audrito, Carlo Frigo, Antonio Pedotti

**Politecnico di Milano, Milan, Italy*

PB.16 Active isometric abduction causes cranial translation of the humeral head in rotator cuff tear patients

Jan Ferdinand Henseler*, Pieter Bas de Witte, Jochem Nagels, Rob Nelissen, Jurriaan de Groot

**Leiden University Medical Center, Leiden, Netherlands*

PB.17 The influence of interprosthetic gap on single-plate fracture reconstruction with or without anterior strut allograft. A biomechanical evaluation

Thomas Quirynen*, Olivier Segal, Jos van der Sloten, Johan Bellemans, Kristoff Corten

**BMe - Biomechanics Section, Faculty of Engineering, KU Leuven, Belgium and Orthopaedic Surgery Department, University Hospital Pellenberg, Pellenberg, Belgium*

PB.18 Development of a micro FE model of a titanium porous implantable material

Fernando José Quevedo González*, Natalia Nuño, Iñigo Morales Martín, Carlos Atienza, Luis Portolés Griñán

**École de technologie supérieure, Montréal, Canada*

PB.19 A new osseointegratable and damageable interface element for modeling of bone-implant and bone-cement interfaces

Christiane Caouette*, Martin Bureau, Pascal-André Vendittoli, Martin Lavigne, Natalia Nuño

**École de technologie supérieure, Montréal, Canada*

PB.20 Local stresses around scapular implant in total shoulder arthroplasty: a finite element model

Ibrahim Kalouche*, Jérôme Crépin, Eva Héripré, Geneviève Guillot, Graciella Bertolino, Olivier Gagey

**Bicetre University Hospital, Paris, France*

PB.21 Shaping Patient Specific Templates for Arthroplasty to obtain High Docking Robustness

Joost Mattheijer*, Just Herder, Gabrielle Tuijthof, Rob Nelissen, Jenny Dankelman, Edward Valstar

**Delft University of Technology, Delft, Netherlands*

PB.22 Complex tibial plateau fractures - a finite element analysis of locked angle lateral plating

Dan Crisan*

**Clinica Ortopedie-Traumatologie Timisoara, Timisoara, Romania*

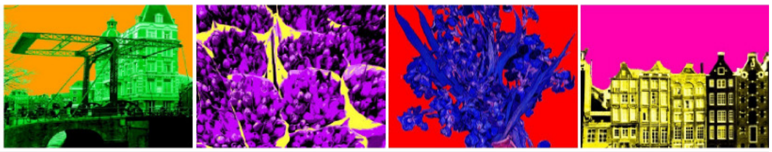

POSTER PRESENTATIONS

PC Cells and Molecular

PC.01 A 3-Dimensional osteogenic-like structure from human autologous adipose mesenchymal stem cells: Reproducibility, Genetic stability, clinical safety/efficacy.

Denis Dufrane*, Hélène Antoine-Poirel, Pierre-Louis Docquier, Najima Aouassar, Geneviève Ameye, Line Verhaeghe, Sandrine Nonckreman, Wivine Andre, Christian Delloye

**Center of Tissue and Cell Therapy / University Clinical Hospital St-Luc, Brussels, Belgium*

PC.02 Polyamine role in osteogenesis of adipose derived stem cells

*Serena Guidotti, Annalisa Facchini, Daniela Platano, Eleonora Olivotto, Giovanni Trisolino, Ermanno Martucci, Silvia Cetrullo, Flavio Flamigni, Andrea Facchini, Rosa Borzi

**Istituto Ortopedico Rizzoli, Bologna, Italy*

PC.03 Combination of Osteotomy with Autologous Chondrocyte Implantation

Atanu Bhattacharjee*, Goebel Lars, Amir Qureshi, J. H. Kuiper, Naomi Dugard, Madry Henning, J. B. Richardson

**Robert Jones & Agnes Hunt Orthopaedic Hospital, Oswestry, UK*

PC.04 Linking tendon stem/progenitor cells to tendon aging

Julia Kohler*, Cvetan Popov, Paolo Alberton, Franz Jakob, Matthias Schieker, Denitsa Docheva

**Ludwig-Maximilians University Munich, Munich, Germany*

PC.05 The stem cells therapy in longs bone non-unions

Viorel Nacu*, Pavel Ciobanu, Filip Gornea, Gheorghe Croitoru, Mihail Darciuc, Boris Topor

**SMPhU Nicolae Testemitanu, Chisinau, Rep of Moldova*

PC.06 A comparison of mesenchymal stem cell incorporation and growth in 3 dimensional scaffolds with potential for osteochondral tissue repair

Nupur Kohli*, Martyn Snow, Eustace Johnson

**School of Life & Health Sciences, Aston University, Birmingham, UK*

PC.07 Development of a chemoattractant delivery system for MSCs recruitment in the degenerated intervertebral disc.

Catarina Leite Pereira*

**AO Research Institute, Davos, Switzerland, and INEB/Instituto de Engenharia Biomedica, Porto, Portugal*

PC.08 In vitro differentiation of bone marrow derived mesenchymal stem cells

Annamalai Chandrasekaran*, Baraneedharan, Venkatachalam, Paul Solomon

**Department Of Orthopaedic Surgery, Sri Ramachandra University, Chennai, India*

PC.09 Differential Effects of Cyclooxygenase-1 and -2 specific NSAIDs on Chondrogenic Differentiation

Marjolein Caron*, Pieter Emans, Don Surtel, Andy Cremers, Daan Ophelders, Kathleen Sanen, Lodwijk van Rhijn, Tim Welting

**Maastricht University Medical Center, Dept. Orthopaedic Surgery, Maastricht, Netherlands*

PC.10 Early increase of serum angiopoietin-2 is associated with early progression to death in experimental injury.

Stephanos Koutsostathis*, Nikitas Schizas, Thomas Tsaganos, Christos Paganias, Evangelos Giamarellos- Bourboulis, Petros Prodromou, George Macheras

**KAT Hospital, Kifissia, Athens, Greece*

PC.11 Equivalent changes in gene expression in articular cartilage after physiological and excessive loading. Activation of protective TGF-beta signaling.

Wojciech Madej*, Arjan van Caam, Eric de Mulder, Peter van der Kraan, Pieter Buma

**Nijmegen Centre for Molecular Life Sciences, Radboud University Nijmegen Medical Centre, Nijmegen, Netherlands*

PC.12 Immunologic factors underlying periprosthetic osteolysis in THA

Jiri Gallo*, S. Goodman, Yrjö Konttinen, M. Raska,

**Department of Orthopaedic Surgery, Palacky University, University Hospital Olomouc, Czech Republic*

PC.13 The involvement of endoplasmic reticulum stress in FGFR3-related chondroplasias

Ryosuke Sato*

**Department of Orthopedics, Institute of Health Biosciences, University of Tokushima Graduate School, Tokushima, Japan*

PC.14 Redifferentiation of Human Articular Chondrocytes in 2D versus 3D culture

Marjolein Caron*, Pieter Emans, Marielle Coolsen, Laura Voss, Don Surtel, Lodwijk van Rhijn, Tim Welting

**Maastricht University Medical Center, Dept. Orthopaedic Surgery, Maastricht, Netherlands*

PC.15 BMP 7 in the treatment of pseudoarthroses of the foot

Gerald Pass*, Stefan Hofstätter, Klemens Trieb

**Department of Orthopedics, Wels, Austria*

PC.16 Stem cells transplantation and core decompression therapies for osteonecrosis of the femoral head (ONFH)

Fei Chang*, Bojian Liang, Sun Mengyao, Jincheng Wang, Zhongli Gao

**China-Japan Union Hospital, Jilin University, Changchun, China*

PC.17 Preconditioned myotubes showed greater cell viability after exposure to 4 hours of ischaemia. This increase in cell viability was associated with an increase in Nrf2 signalling.

Pauline Walsh*, James Broderick, Kevin Mulhall

** University College Dublin, Dublin, Ireland*

POSTER PRESENTATIONS

PD Hip

PD.01 Fast Powder Sintering: an innovative process suitable for application of Ti foam onto challenging substrates

Luca Facchini*, Francesco Bucciotti, Pierfrancesco Robotti, Eleonora Preve

**Eurocoating, Pergine Valsugana - Trento, Italy*

PD.02 A prospective randomized clinical trial with radiostereometric analysis comparing the Taperloc® and Mallory-Head Porous® uncemented femoral stem designs

Paul van der Voort*, Julius Wolkenfelt, Edward Valstar, Rob Nelissen

**Leiden University Medical Center, Leiden, Netherlands*

PD.03 Wear of vitamin-E blended polyethylene against large diameter CoCrMo metal and EBPVD chromium nitride coated femoral heads

Danielle de Villiers*, Andy Fox, Amy Kinbrum, Leona Morton, Simon Collins, Julia Shelton

**Queen Mary, University of London, UK*

PD.04 Pressures required for water jet dissection in minimally invasive hip refixation tested in interface tissue substitutes

Gert Kraaij*, Steven den Dunnen, Jenny Dankelman, Rob Nelissen, Edward Valstar

**Delft University of Technology, Delft, The Netherlands*

PD.05 The acetabular bone fissure formation in press fit hip artroplasty

Ricardo Duarte*, António Ramos, Carlos Relvas, António Completo, José Simões

**University of Aveiro, Aveiro, Portugal*

PD.06 Application and survival curve of total hip arthroplasties using national hip arthroplasty registers

Patrick Sadoghi*, Andreas Fottner, Peter Müller, Volkmar Jansson, Andreas Hölzer

**Department of Orthopaedic Surgery, Medical University of Graz, Graz, Austria*

PD.07 Analysis of the detection of femoral stem loosening

Evelyn García*, Francisco Díaz, Rafael Claramunt, Antonio Ros, José Antonio De Pedro-Moro

**Departamento de Mecánica Estructural E.T.S. de Ingenieros Industriales. Universidad Politécnica de Madrid, Madrid, Spain*

PD.08 Reconstruction of the Native Center of Rotation in Primary Total Hip Arthroplasty

Geert Meermans*, Jacco van Doorn, Janjaap Kats

**Department of Orthopaedic Surgery, Lievensberg Hospital, Bergen op Zoom, Netherlands*

PD.09 Measuring hip wound area using a time of flight (TOF) camera

David Putzer*, Michael Nogler, Helga Fritsch

**Medical University Innsbruck, Austria*

PD.10 Neck fractures in modular uncemented femoral stem in primary total hip arthroplasty

Biyyam Madhusudhan Rao*, Taylor Lee, Michael Moss

**St. Richard's Hospital, Western Sussex Hospitals NHS Trust, Chichester, UK*

PD.11 The role of the hydroxiapatite coating in the progression of osteolisis after total hip replacements. The sealing effect in the proximal femur

Manuel Ángel Sandoval García*, Iván Pérez-Coto, Ana Escandón, Daniel Hernández-Vaquero

**Hospital San Agustín, Avilés, Spain*

PD.12 Pain thresholds in hip osteoarthritis patients before a total hip replacement using quantitative sensory testing (QST).

Haili Wang*

**Orthopaedic University Hospital Heidelberg, Germany*

PD.13 The influence of cement modulus on fatigue performance of hip implants tested to ISO and ASTM standards

Amy Kinbrum*, Leona Morton, Simon Collins (Conor Lowry)

**Corin, Cirencester, UK*

PD.14 A novel coating to retard fretting and corrosion of titanium alloy against cobaltchrome total hip arthroplasty trunion interfaces

Amy Kinbrum*, Leona Morton, Simon Collins, Andy Fox, Jonathon Housden (Conor Lowry)

**Corin, Cirencester, UK*

PD.15 An increasing trend of investigating occult hip fractures with CT scans

Robert Jordan*, Edward Dickenson, Daniel Westacott, Njalalle Baraza, Srinivasan Kuntrapaka

**Birmingham Heartlands Hospital and University Hospitals Coventry & Warwickshire, UK*

PD.16 Non-Object Based Calibration of Digital Radiographs

Geert Meermans*, Jacco van Doorn, Janjaap Kats

**Department of Orthopaedic Surgery, Lievensberg Hospital, Bergen op Zoom, Netherlands*

PD.17 Taper corrosion and measurement of a retrieved metal-on-poly total hip joint device

Chenxi Li*, Sam Smith

**Smith & Nephew, London, UK*

PD.18 Periprosthetic fracture after excessive stress shielding in a fully hydroxyapatite(HA)-coated femoral revision stem

Chris Arts*, Ilknur Sanli, Jacobus Arts, Jan Geurts

**Maastricht University Medical Centre, Maastricht, Netherlands*

PD.19 Return to theatre in 30 days following hip or knee replacement – a comparison of thromboprophylaxis with enoxaparin and dabigatran

Brett Rocos*, Benedict Lankester

**Yeovil District Hospital, Yeovil, UK*

PD.20 Comparative study of Caucasian and Chinese femur shapes for evidence-based implant design

*Lara Vigneron, Joris van Deun, Emmanuel Audenaert, Vinod Kaimal, Sebastian de Boodt, Koen Engelborghs

**Materialise, Leuven, Belgium*

PD.21 Optimization of Hip Resurfacing Arthroplasty Cement Penetration: The Role of Cement Mantle Space

Paulick Mark*, John Hsih, Amir Jamali, Scott Hazelwood,

**University of California Davis Medical Center, Sacramento, CA, USA*

PD.22 Determining strain for cadaveric hip specimens when implanted with a novel Titanium foam acetabular shell

Conor Lowry*, Leona Morton, David Simpson, Simon Collins

**Corin, Cirencester, UK*

POSTER PRESENTATIONS

PD Hip

PD.23 **Hip Resurfacing Arthroplasty in Older Patients**

Geert Meermans*, Kristoff Corten, Daan Koppens, Niek Schepel, Kathleen Pittoors

**Department of Orthopaedic Surgery, Lievensberg Hospital, Bergen op Zoom, Netherlands*

PD.24 **Functional Outcome in Patients with High Body Mass Index Following Primary Total Hip Arthroplasty**

Claire Rutherford*, Elisabeth McKiernan, Zuned Hakim, Anthony Helm

**Lancashire Teaching Hospitals NHS Trust, North West, UK*

PD.25 **The Use of Preoperative DEXA Scans to Evaluate Bone Quality in Hip Resurfacing**

Geert Meermans*, Kristoff Corten, Daan Koppens, Niek Schepel, Kathleen Pittoors

**Department of Orthopaedic Surgery, Lievensberg Hospital, Bergen op Zoom, Netherlands*

PD.26 **Post operative thigh pain in patients with uncemeneted hip hemiarthroplasty – A retrospective outcome study**

Naveen Keerthi*, Ashlea Norton, Raghavendra Marappa, Haider Mamoowala, Ronan McGivney

**Fairfield Hospital, Bury, UK*

PD.27 **Ceramic Large Diameter Ball Head in Total Hip Replacement**

Bernard Masson*

**CeramTec, Paris, France*

PD.28 **The Outcome of Extensively Porous Coated Stems for Revision Total Hip Arthroplasty**

William Peace*, Henry Ho, Robert Hopper, Charles Engh

**Colorado Permanente Medical Group, Denver, CO, USA*

PD.29 **Marker wire position is an important factor in the risk of polyethlyene bearing fracture**

Elise Pegg*, Richie Gill, Hemant Pandit, Harinderjit Gill, John O'Connor, David Murray

**University of Oxford, Botnar Research Centre, UK*

PE Knee

PE.01 **Effect of implant alignment on bone resection volume during femoral intercondylar notch preparation in PS TKA**

Bo Gao*, Laurent Angibaud, Joseph Lipman, Michael Mauldin

**Exactech, Gainesville, USA*

PE.02 **Quad-Snip" or TTO for revision of septic knee arthroplasty? Prospective randomized comparison at 8 years mean follow-up"**

Danilo Bruni*, Mirco Lo Presti, Bharat Sharma, Giovanni Raspugli, Maurilio Marcacci

**Istituto Ortopedico Rizzoli, Bologna, Italy*

PE.03 **Local infiltration analgesia following total knee arthroplasty. The effect on postoperative pain and opioid consumption; a meta-analysis**

Renee Keijsers*, Michel van den Bekerom, Rogier van Delft, Manon van Lotten, Maarten Rademakers, Peter Nolte

**Spaarne Hospital, Hoofddorp, Netherlands*

PE.04 **Knee arthrodesis with a press-fit modular intramedullary nail without bone-on-bone fusion after an infected revision TKA**

Danilo Bruni*, Mirco Lo Presti, Bharat Sharma, Giovanni Raspugli, Maurilio Marcacci

**Istituto Ortopedico Rizzoli, Bologna, Italy*

PE.05 **Tantalum – Is it the final frontier for managing extreme osteolysis in Revision Knee Arthroplasty?**

Biyyam Madhusudhan Rao*, Michael Moss, John Vafaye, Kamal Tamer

**St. Richard's Hospital, Western Sussex Hospitals NHS Trust, Chichester, UK*

PE.06 **Predicting deformation and recovery of UHMWPE in total knee arthroplasty**

Said Gomaa*, Matthew Dressler

**DePuy Orthopaedics, Inc., Indiana, USA*

PE.07 **Continuous Local Infiltration Analgesia; the effect of an intra-articular catheter on pain management after TKA, a meta-analysis.**

Renee Keijsers*, Michel van den Bekerom, Rogier van Delft, Manon van Lotten, Maarten Rademakers, Peter Nolte

**Spaarne Hospital, Hoofddorp, Netherlands*

PE.08 **The Functional Flexion Axis of the Knee Corresponds to the Clinical Epicondyle Axis in Posterior-Stabilized Total Knee Arthroplasties**

Hitoshi Nochi*, Satomi Abe, Takuya Ruike, Hiroshi Kobayashi, Hiroshi Ito

**Asahikawa Medical University, Japan*

PE.09 **Effect of Implant Design on Bone Resection Volume during Intercondylar Notch Preparation in Hi-Flexion PS TKA**

Bo Gao*, Laurent Angibaud, Joseph Lipman, Michael Mauldin

**Exactech, Gainesville, USA*

PE.10 **Navigated evaluation of the position of the patella and its relationship with early clinical results after a TKA**

Danilo Bruni*, Mirco Lo Presti, Bharat Sharma, Giovanni Raspugli, Maurilio Marcacci

**Istituto Ortopedico Rizzoli, Bologna, Italy*

PE.11 **Evaluation of a patient-specific cutting block system for total knee arthroplasty using computer navigation**

Sébastien Lustig*, Scholes Corey, Samir Oussedik, Myles Coolican, David Parker

**Albert Trillat Center, Lyon, France*

PE.12 **Correlation of intraoperative navigation data and postoperative outcome measures in total knee arthroplasty**

Sébastien Lustig*, Scholes Corey, Widmer Benjamin, Myles Coolican, David Parker

**Albert Trillat Center, Lyon, France*

PE.13 **Medialised loading position may increase risk of pain after unicompartmental knee arthroplasty**

Elise Pegg*, Richie Gill*, Jonathan Walter, Stephen Mellon, Hemant Pandit, David Murray, Darryl D, Benjamin Fregly, Harinderjit Gill, ,

**University of Oxford, Botnar Research Centre, UK*

PE.14 **No clinical advantages of mobile-bearing total knee arthroplasty**

Paul van der Voort*

**Leiden University Medical Center, Leiden, Netherlands*

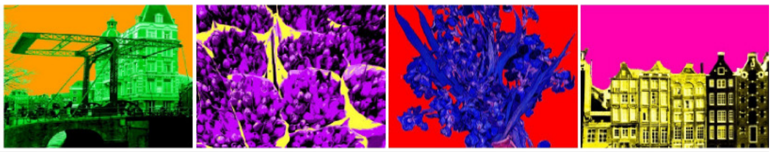

POSTER PRESENTATIONS

PE Knee

PE.15 **MRI study of tibial slope changes after medial opening wedge high tibial osteotomy**

🇫🇷 Sébastien Lustig*, Scholes Corey, Myles Coolican, David Parker

**Albert Trillat Center, Lyon, France*

PE.16 **Software analysis of femoral cartilage volume after meniscal surgery**

🇫🇷 Sébastien Lustig*, Scholes Corey, Mark Kazzi, Myles Coolican, David Parker

**Albert Trillat Center, Lyon, France*

PE.17 **In-vitro stability testing of a non-fixed meniscal implant: the effect of surgical technique and knee condition**

Jonathan Elsner*, Tara Bonner, Alex Greene, Rishi Gupta, Robert Butler, Eran Linder-Ganz, Elliott Hershman, Robb Colbrunn

**Active Implants Corp., Netanya, Israel*

PE.18 **The New Knee Society Score: evaluation of the clinimetric quality in Dutch patients.**

Remco Dinjens*, Rachel Senden, Ide Heyligers, Bernd Grimm

**AHORSE Research Institute, Atrium Medical Center, Dept. Orthopaedics, Heerlen, Netherlands*

PE.19 **Is UKA a viable option for spontaneous osteonecrosis of the knee?**

Danilo Bruni*, Mirco Lo Presti, Bharat Sharma, Giovanni Raspugli, Maurilio Marcacci

**Istituto Ortopedico Rizzoli, Bologna, Italy*

PE.20 **The financial burden of performing joint arthroplasty in obese patients**

Benjamin Bradley*, Shelley Griffiths, Kyle Stewart, Moshin Khan, Gordon Higgins

**South Devon Hospitals NHS Trust, Devon, UK*

PE.21 **The benefits of a composite design for a Novel Polycarbonate-Urethane Meniscal Implant**

Jonathan Elsner*, Gal Zur, Elliott Hershman, Farshid Guilak, Eran Linder-Ganz

**Active Implants Corp., Netanya, Israel*

PE.22 **Role of Rotating Hinge Knee in Revision Knee Arthroplasty**

Biyyam Madhusudhan Rao*, Michael Moss, Taylor Lee, John Vafaye

**St. Richard's Hospital, Western Sussex Hospitals NHS Trust, Chichester, UK*

PE.23 **Rotation of Sagittal Cutting Plane for Tibial Component in Unicompartmental Knee Arthroplasty**

Ho-Joong Jung*, Seungbum Koo, Han-Jun Lee, Jae-Sung Lee, Seung-Hwan Chang

**Chung-Ang University, Seoul, Korea*

PE.24 **The midvastus approach: a compromise between the standard approach and the minimally invasive approach in total knee arthroplasty**

Saleh Mohamed Mostafa*

**Orthopaedic Department, Suez Canal University, Egypt*

PE.25 **The effect of ischaemic preconditioning in total knee arthroplasty patients**

Pauline Walsh*, James Broderick, Kevin Mulhall

**University College Dublin, Dublin, Ireland*

PE.26 **Analysis of different stem lengths and fixation techniques in hinged total knee arthroplasty**

Susanne Fuchs-Winkelmann*, Bilal El-Zayat, Thomas Heyse, Nelson Fanciullacci, Yan Chevalier, Bernardo Innocenti

**Department of Orthopaedics, University Hospital, Marburg, Germany*

PE.27 **The influence of gender, age and ethnicity on three-dimensional patellar morphology using high resolution CT-scans**

Wesley van der Ven*, Rachel Senden, Tim Boymans, Bernd Grimm

**AHORSE Foundation, Atrium Medical Center, Dept. Orthopaedics, Heerlen, Netherlands*

PE.28 **Outcomes of total knee athroplasty in a multiethnic asian population stratified by ethnicity**

*Jiang Lei, Hamid Rahmatullah, Chong Hwei Chi, Andrew Tan Hwee Chye

**Singapore General Hospital, Singapore*

PF Spine & Upper Extremity

PF.01 **A comparison of two reconstruction techniques for chronic type III acromio-clavicular joint injury**

William Wong*, Geraint Williams, Raman Bohra, Thomas Redfern

**Leighton Hospital, Crewe, Cheshire, UK*

PF.02 **Outcome assessment of 58 basal thumb joint replacements with additional vitamin C**

Paul Zollinger*, Maarten Ellis, Halil Ünal, Wim Tuinebreijer

**Ziekenhuis Rivierenland, Tiel, Netherlands*

PF.03 **How Diameter and Cement Augmentation Technique Influence the Fixation and Motion of Pedicle Screws**

Rebecca Kueny*

**TUHH Technical University of Hamburg, Germany*

PF.04 **A novel combination technique in the treatment of lateral epicondylitis**

Benjamin Bradley*, Jonathan Kosy, Nicola Fine, Rangaraju Ramesh

**South Devon Hospitals NHS Trust, Devon, UK*

PF.05 **The Importance of Central Screw Placement in the Distal and Proximal Pole in Scaphoid Waist Fractures**

Geert Meermans*, Marc Braem, Francis van Glabbeek, Guy Hubens, Frederik Verstreken

**Department of Orthopaedic Surgery, Lievensberg Hospital, Bergen op Zoom, Netherlands*

PF.06 **Biomechanical testing of conventional vs. angular stable osteosynthesis plates with a synthetical fracture model of the osteopenic distal humerus**

Robert Wendlandt*, Klaus Waizner, Christina Rank, Felix Renken, Arndt-Peter Schulz

**University Lübeck, Biomechanics, Lübeck, Germany*

PF.07 **Effect of post operative immobilization of thumb carpo-metacarpal arthroplasty on post operative dislocations**

Priyanka Jani*, G. Packer, C. Sivaji

**Southend Hospital, Southend on Sea, UK*

POSTER PRESENTATIONS

PF Spine & Upper Extremity

PF.08 **Effect of post operative POP immobilization on incidence of dislocation in patients undergoing thumb CMC joint arthroplasty**
Priyanka Jani*, G. Packer, C. Sivaji
**Southend Hospital, Southend on Sea, UK*

PF.09 **Position and Orientation of Drill Holes in Arthroscopic and Open Tightrope Fixation for Acromioclavicular Joint Reconstruction**
Mohamad Hachem*, Timothy Hardwick, Mahesh Pimple, Adel Tavakkolizadeh, Joydeep Sinha
**Department of Biomaterials, King's College London, UK*

PF.10 **Morphological and mechanical 3D finite element modeling of the glenoid**
🇫🇷 Ibrahim Kalouche*, Jérôme Crépin, Eva Héripré, Geneviève Guillot, Olivier Gagey
**Bicetre University Hospital, Paris, France*

PF.11 **The transpedicular approach as alternative route for intervertebal disc regeneration**
Gianluca Vadalà*, Fabrizio Russo, Girish Patappa, Marianna Peroglio, Sybille Grad, Lorin Benneker, Mauro Alini, Vincenzo Denaro
**Campus Bio Medico University Hospital - Department of Orthopaedic and Trauma Surgery, Rome, Italy*

PF.12 **Biomechanical investigation of augmentation in the lumbar vertebrae**
Luca Cristofolini*, Stephen Ferguson, Nicola Brandolini, Valentina Danesi, Mateusz Juszczyk, Marco Viceconti
**University of Bologna, Engineering Faculty, Bologna, Italy*

PF.13 **Dynamic Comparison of Porcine Lumbar Specimens with Intact Discs and Disc Replacements**
Timothy Holsgrove*, Sabina Gheduzzi, Anthony Miles
**University of Bath, Bath, UK*

PF.14 **How Evidence Based are Publications in Clinical Spinal Journals?**
Amir Amiri*, Kavitha Kanesalingam, Suzie Cro, Adrian Casey
**Royal National Orthopaedic Hospital, London, UK*

PF.15 **Does bipedality effect the morphology of the lumbar vertebrae and IVDs in mice?**
Nadir Yalcin*, Ozgur Dede, Ibrahim Akel, Gokhan Demirkiran, Emre Acaroglu, Ralph Marcucio
**Ataturk Training and Research Hospital, Ankara, Turkey*

PF.16 **Does the previous whiplash affect the outcome of a second whiplash injury?**
Ravindra Thimmaiah*, A. Koshy, S. Gandham, G. Ampat
**Southport Hospital, Southport, UK*

PF.17 **Blinded Radiological Evaluation of OsteoAMP vs. rhBMP-2 in TLIF/LLIF Spine Procedures**
Jeffrey Roh*, Christopher Yeung, Justin Field (Amit Govil)
**Orthopaedics International, Seattle, WA*

PG Tissue Engineering

PG.01 **A computational study on the detection of cartilage defects by ultrasound**
Teun Koomen*, Giovanni Mores, Björn Vennema, Jan Wessels, Gabrielle Tuijthoff, Amir Abbas Zadpoor
**Delft University of Technology, Delft, Netherlands*

PG.02 **Bone Augmentation with Adipose Stem Cells and Calcium Phosphate Carriers for Human Maxillary Sinus Floor Elevation: An Ongoing Phase I Clinical Trial.**
Henk-Jan Prins*, Marco Helder, Janice Overman, Christiaan ten Bruggenkate, Engelbert Schulten, Jenneke Klein-Nulend
**Academic Center for Dentistry Amsterdam, Amsterdam, Netherlands*

PG.03 **One year results of CHONDRON, a Gel-Type Chondrocyte Transplantation technique. A Pilot Study**
Jeeshan Rahman*, Babar Kayani, Elizabeth Gillott, George Bentley, John Skinner, Jonathan Miles, Richard Carrington, Timothy Briggs, ,
**Royal National Orthopaedic Hospital, Stanmore, UK*

PG.04 **Biotribology of osteochondral allografts post-implantation**
Serena Russell*, Eileen Ingham, John Fisher
**Institute of Medical and Biological Engineering, Leeds University, UK*

PG.05 **Sustained oxygen release from PLGA microspheres**
Hilde Steg*, Arina Buizer, Albert Veldhuizen, Sjoerd Bulstra, Roel Kuijer
**University Medical Center Groningen, Groningen, Netherlands*

PG.06 **A novel acellular and viroinactivated meniscus allograft**
🇫🇷 Nathalie Tan*, Elvire Servien, Harold Couchoux, Laurence Barnouin, Robert Henri, Philippe Neyret
**TBF Tissue Engineering, Tissue Bank, Mions, France*

PG.07 **Novel Bilayered Gellan gum/Gellan gum-hydroxyapatite Scaffolds for Application in Osteochondral Tissue Engineering**
*Joaquim Oliveira, Diana Pereira, Joana Silva-Correia, Hélder Pereira, João Espregueira-Mendes, , Rui Reis
**3Bs Research Group, Guimarães, Portugal*

PG.08 **Joint Distraction in Treatment of Canine Experimentally Induced Osteoarthritis leads to Cartilage Repair accompanied by Sustained Relieve of Pain**
Karen Wiegant*, Simon Mastbergen, Femke Intema, Peter van Roermund, Herman Hazewinkel, Floris Lafeber
**University Medical Center Utrecht, Utrecht, Netherlands*

PG.09 **Variation of awl geometry in microfracture does not influence the repair of osteochondral defects in the goat talus**
Aimee-Claire Kok*, Gabrielle Tuijthof, Steven den Dunnen, Michiel Siebelt, Jasper van Tiel, Vincent Everts, Niek van Dijk, Gino Kerkhoffs
**Academic Medical Center, Amsterdam, Netherlands*

POSTER PRESENTATIONS

PG Tissue Engineering

PG.10 **Does the Secondary Structure of Collagen Determine which Regions of a Turkey Tendon Become Mineralised? An Investigation Using Raman Spectroscopy**

Kevin Buckley*, Jemma Kerns, Anthony Parker, Pavel Matousek, Allen Goodship

**Science and Technology Facilities Council, Harwell Oxford, U.K.*

PG.11 **Silk-fibroin scaffolds for meniscus cell-based tissue engineering therapy**

Hélder Pereira*

**3Bs Research Group, Guimarães, Portugal*

PG.12 **Comparison Between Tissue-Engineered and Non Tissue-Engineered Constructs in New Bone Formation**

E. Garcia-Gareta*, Jia Hua, Gordon Blunn

**Institute of Orthopaedics and Musculoskeletal Science, University College London, Stanmore, UK*

PH Trauma and Infection

PH.01 **Anterior cruciate ligament injury prevention training programs: what is the current evidence?**

Patrick Sadoghi*, Arvind von Keudell, Patrick Vavken

**Department of Orthopaedic Surgery, Medical University of Graz, Graz, Austria*

PH.02 **Treatment of stable intertrochantric fractures : A comparison between 2 hole and 4 hole Dynamic Hip Screw. A prospective Randomized Clinical Trial.**

Saeid Tabatabaei*, Darab Younesi

**Jundishapur University of Medical Sciences, Ahvaz, Iran*

PH.03 **Comparison of different techniques for flexible fixation of openbook type pelvic injuries with two leg alternate loading. A biomechanical study**

Yash Agarwal*, F. Stuby, Markus Windolf, Thomas Shiozawa, Björn Ochs, Christoph Gonser, Ulrich Stöckle, Boyko Gueorguiev

**AO Research Institute Davos, Davos, Switzerland*

PH.04 **A study to predict transverse fracture strength of long bones in an infant by development of an in-vitro animal model of immature porcine metacarpal bones and using three-point bending**

Shahbaz Malik*, Sheraz Malik, Peter Theobald, Mike Jones

**Cardiff School of Engineering, Cardiff, UK*

PH.05 **Hip fracture surgery delay and cancellation: the impact of UK best practice tariffs.**

Tarek Boutefnouchet*, Basil Budair, Qutub Qadri

**Dudley Group of Hospital NHS Trust, West Midlands, UK*

PH.06 **Short-term topical negative pressure wound therapy (NPWT) followed by polyacrylate superabsorber wound dressings yields better granulation tissue than NPWT alone**

Hans Smola*, Simon Cuhlmann, Pierre Croizat, Axel Eckstein

**Paul Hartmann AG, Heidenheim, Germany*

PH.07 **Use of low-Intensity Pulsed Ultrasound Stimulation of Delayed Unions of the Osteotomized Fibula: A Prospective Randomized Double-Blind Trial**

Sjoerd Rutten*, Jenneke Klein-Nulend, Gerard L. Guit, G. H. Robert Albers, Clara M. Korstjens, Paul I.J.M. Wuisman, Peter Nolte

**Dept of Orthopaedics, Spaarne Hospital, Hoofddorp, Netherlands*

PH.08 **Healing of distal radius fractures assessed by HR-pQCT**

J. de Jong*, Chris Arts, S. Bours, Paul Willems, P. Geusens, B. van Rietbergen, J. van den Bergh

**Maastricht University Medical Centre, Maastricht, Netherlands*

PH.09 **Distal tibial locking plates – not an easy option for surgeon or patient**

Zuned Hakim*, Amer Shoaib, Omar Alsawaf, Farhan Alvi

**Lancashire Teaching Hospitals NHS Trust, Royal Preston Hospital and Stockport NHS Foundation Trust, UK*

PH.10 **Tip-apex distance (TAD): a comparison between dynamic hip screw (DHS) and Cephalomedullary nail fixation of extracapsular fractures of the hip**

*SiehYean Kiew, Gunasekaran Kumar

**Royal Liverpool University Hospital, Liverpool, UK*

PH.11 **Mortality after fractures among elderly Japanese-American men living in Hawaii**

Satona Murakami*, Beatriz Rodriguez, James Davis

**Nagoya City University, Nagoya, Japan*

PH.12 **Open Lower Limb Fractures. Experiences from a District General Hospital**

William Carlino*, Caroline Bartolo

**Royal United Hospital, Bath, UK*

PH.13 **Myofibroblasts in posttraumatic elbow contractures**

Job Doornberg*

**Department of Orthopaedic Surgery, Academic Medical Center, University of Ámsterdam, Netherlands*

PH.14 **The Exeter Trauma Stem. Outcome Experiences from the Royal United Hospital, Bath**

William Carlino*, Mark Kemp, Joyce Muhlschlegel, Harvey Sandhu

**Royal United Hospital, Bath, UK*

PH.15 **Risk factors associated with the early failure of cannulated screws**

Robert Jordan*, Edward Dickenson, Nicholas Smith

** University Hospitals Coventry & Warwickshire, UK*

PH.16 **Procalcitonin: improvement of diagnostic and therapeutic strategies in cancer patients with febril neutropenia**

Maria Angeles Cuadrado-Cuenca*, D. Varillas, P. Martin, V. Gomez, José Antonio De Pedro-Moro

**Hospital Clínico San Carlos, Madrid, Spain*

PH.17 **Analysis on Toll-like receptor mediating signal pathway in periprosthetic infection**

Tamaki Yasunobu*, Tomoyuki Hirayama, Yuya Takakubo, Yasushi Naganuma, Kan Sasaki, Yrjö T. Konttinen, Stuart B. Goodman, Michiaki Takagi

**Yamagata University School of Medicine, Yamagata, Japan*

POSTER PRESENTATIONS

PH Trauma and Infection

PH.18 **Novel human biomarkers for the identification of infection in orthopedic revision-surgery patients**

Mathias Glehr*, Patrick Sadoghi, Joerg Friesenbichler, Gerald Gruber, Guenter Hofmann, Gerwin Bernhardt, Maximilian Zacherl, Alexander Avian, Reinhard Windhager, Andreas Leithner

**Department of Orthopaedic Surgery, Medical University of Graz, Graz, Austria*

PH.19 **Diagnostic value procalcitonin, interleukin 6 in complications of hip arthroplasty**

Maria Angeles Cuadrado-Cenzual*, Teresa Alonso, Dolores Ortega de Heredia, José Antonio De Pedro-Moro

**Hospital Clínico San Carlos, Madrid, Spain*

PH.20 **Comparable study of antibiotic release on commercially PMMA bone cements**

Johannes Stadler*, Clemens Kittinger, Michaela Lipp, Andreas Leithner, Klaus Dieter Kühn

**Medical Universitiy of Graz, Graz, Austria*

PH.21 **Diagnosing neck of femur fractures on plain radiographs- who is more accurate radiologists or orthopaedic trainees?**

Robert Jordan*, Edward Dickenson, Njalalle Baraza, Daniel Westacott, Srinivasan Kuntrapaka

**Birmingham Heartlands Hospital and University Hospitals Coventry & Warwickshire, UK*

PH.22 **Management of large bone defect – a study of 40 cases using mechanical principles of ilizarov circular fixator**

Annamalai Chandrasekaran*

**Department Of Orthopaedic Surgery, Sri Ramachandra University, Chennai, India*

PH.23 **Pantoprazole, a proton pump inhibitor, delays fracture healing in mice**

Tina Histing*, David Stenger, Claudia Scheuer, Wolfgang Metzger, Patric Garcia, Joerg Holstein, Moritz Klein, Tim Pohlemann, Michael Menger,

**Department of Trauma-, Hand and Reconstructive Surgery, University of Saarland, Homburg/Saar, Germany*

PH.24 **A new metaphyseal fracture defect model in osteoporotic rats**

Seemun Ray*, Ulrich Thormann, Alexander Langheinrich, Lutz Dürselen, Katrin Lips, Reinhard Schnettler, Volker Alt

**University of Giessen, Giessen, Germany*

PH.25 **Outcome of internal fixation in high energy bicondylar proximal tibial fractures: single for double plating**

Veenesh Selvaratnam*, Kiran Saldanha, Ravikumar V. Pydisetty

**St Helens and Knowsley NHS Trust, England*

PH.26 **Management of infected non union of tibia by ilizarov circular fixator- a study of 41 cases**

Annamalai Chandrasekaran*

**Department Of Orthopaedic Surgery, Sri Ramachandra University, Chennai, India*

PH.27 **Refixation of osteochondral fractures by ultrasound-activated, resorbable pins - an ovine in-vivo study**

H. Neumann*, A.P. Schulz, J. Gille, M. Klinger, C. Jürgens, N. Reimers, B. Kienast

**BG Trauma Center, Hamburg, Germany*

PI Miscellaneous

PI.01 **Comparison of the relative bone position between normal and flat feet using 3D CT reconstruction images of tarsal bones**

Kan Imai*, Ikoma Kazuya, Masahiro Maki, Masamitsu Kido, Ryota Takatori, Daisaku Tokunaga, Nozomu Inoue, Toshikazu Kubo,

**Department of Orthopaedics, Graduate School of Medical Science, Kyoto Prefectural University of Medicine, Kyoto, Japan*

PI.02 **Receptor activator of nuclear factor kappaB (RANK) expression is a prognostic factor in human osteosarcoma**

Klemens Trieb*, Irene Sulzbacher, Bernd Kubista

**Department of Orthopedics, Wels, Austria*

PI.03 **Prognostic factors for determining survival in patients operated for metastatic epidural spinal cord compression**

Laurens Bollen*, Sander Dijkstra

**Leiden University Medical Center, Leiden, Netherlands*

PI.01 **Asymmetric ankle osteoarthritis - long-term effects of realignment surgery on walking**

Corina Nüesch*, Cora Huber, Geert Pagenstert, Victor Valderrabano

**Orthopaedic Department, University Hospital Basel, Basel, Switzerland*

PI.05 **Changes In Foot Dimensions After Forefoot Surgery – Why Does The Shoe Still Not Fit.**

Zuned Hakim*, Priam Heire, Gerard Lattouf, Amer Shoaib

**Stockport NHS Foundation Trust, Stockport, UK*

PI.06 **Is the conservative treatment of achilles tendon ruptures in older patients ageist?**

Amer Shoaib*, Omar Alsawaf, Noel Fisher, Zuned Hakim, Omar Mirza

**Stockport NHS Foundation Trust, Stockport, UK*

PI.07 **Weil's Osteotomies Successfully Treat Morton's Neuroma - Do We Understand the Pathology?**

Amer Shoaib*, Zuned Hakim, Gerard Lattouf, Alsawaf Omar

**Stockport NHS Foundation Trust, Stockport, UK*

PI.08 **Gait analysis of the effect of postoperative rehabilitation shoes**

Zuned Hakim*, Cameron Choi, Gerard Lattouf, Amer Shoaib

**Stockport NHS Foundation Trust, Stockport, UK*

PI.09 **Mechanical factors dominate over the influence of the joint homeostasis in trauma induced experimental osteoarthritis in the goat**

Karen Wiegant*, Simon Mastbergen, Angelique Barten-van Rijbroek, Roel Custers, Laura Creemers, Daniel Saris, Floris Lafeber

**University Medical Center Utrecht, Utrecht, Netherlands*

PI.10 **Raman spectroscopy can identify molecular changes in osteoarthrotic subchondral bone**

Jemma Kerns*, Panagiotis Gikas, Kevin Buckley, Helen Birch, Ian McCarthy, Jonathan Miles, Timothy Briggs, Anthony Parker, Pavel Matousek, Allen Goodship

**UCL Institute of Orthopaedics, Royal Nacional Orthopaedic Hospital, Stanmore, U.K.*

PI.11 **Microvascular architecture of irradiated mandible**

Arja Kullaa*, Tuomo Silvast, Pekka Asikainen, Timo Ruotsalainen, Arto Koistinen

**Inst. of Dentistry, Oulu, Finland*

POSTER PRESENTATIONS

PI Miscellaneous

PI.12 **Prediction of open locking in the hypermobile jaw joint**

Jan Harm Koolstra*, Matthijs Tuijt, Frank Lobbezoo, Machiel Naeije

**ACTA, Functional Anatomy, Netherlands*

PI.13 **Assessment of Rehabilitation Programme for Joint Hypermobility Syndrome using Postural Stability as a Quantitative Outcome Measure**

Ian McCarthy*, Xiaoyang Hu, Daniella Kostic, Wang Sin Tan, Sobitha Sathiananda, Helen Cohen, Roger Wolman

**UCL Institute of Orthopaedics and Musculoskeletal Science, London, UK*

PI.14 **Central versus local coordination in the international HEALTH trial**

Paul Burgers*, Rudolf Poolman, Sarah Culgin, Thomas Einhorn, Mohit Bhandari, Peter Patka, Esther van Lieshout

**Erasmus Medical Center, Rotterdam, Netherlands*

PI.15 **Viscosity of synovial fluid determined by free oscillation rheometry**

Arne Borgwardt*

**Department of Orthopaedic Surgery, Frederiksberg University Hospital, Frederiksberg, Denmark*

PJ.16 **Giant Cell Tumours of Bone – correlation of clinical and histopathological features to outcome post-surgical treatment; a single institution experience**

Lily Li*, Panagiotis Gikas, D. Williams, J. Jagiello, E. Gilliot, W. Aston, R. Pollock, John Skinner, S. Cannon, Timothy Briggs, M.F. Amary, A.M. Flanagan

**Royal National Orthopaedic Hospital, Stanmore, UK*

PJ.17 **Raman Spectroscopy shows that Human Subchondral Bone in Osteoarthritis is Hypermineralised**

Barian Mohidin*, Panagiotis Gikas, Jemma Kerns, Helen Birch, Jonathan Miles, Timothy Briggs, Kevin Buckley, Anthony Parker, Pavel Matousek, Keen R, Allen Goodship

**UCL Institute of Orthopaedics and Musculoskeletal Science, London, UK*

21st Annual Meeting European Orthopaedic Research Society
EORS 2013
+
8th Tri-Annual Meeting Combined Orthopaedic Research Societies
CORS 2013

CORS 2013
VENICE
8th COMBINED MEETING
OF ORTHOPAEDIC
RESEARCH SOCIETIES
13-16 OCTOBER 2013
SAN SERVOLO
VENICE, ITALY
www.cors2013.org

Become an EORS Member!

Fill in and fax or email scan of paper membership form

Or submit your membership form online: www.eors.info/eors_MEMBERS.htm

EUROPEAN ORTHOPAEDIC RESEARCH SOCIETY

EUROPEAN ORTHOPAEDIC RESEARCH SOCIETY

Administrative Office:
EORS c/o Vienna Medical Academy
Alser Str. 4
1090 Vienna, Austria

www.eors.eu
Tel +43 1 405 1383-24
Fax +43 1 407 8274
Email: EORS@medacad.org

RENEWAL - EORS Membership 2012/13 for INDIVIDUAL Membership

Please amend the details shown if necessary and return, with payment (30 Euro) to
EORS Office:
Fax: 0043/1/407 82 74
Email: vr@medacad.org

Last Name:

First Name:

Academic Titel:

Position:

Background: O clinical, O biomechanics, O biology

Correspondence Address:

Dept./ Inst. /University:

Street:

City:

Zip/Postal Code:

Country:

Phone:

Fax:

Email:

Mobile:

Payment modalities for Individual Membership Fee 2012/2013:

☐ **BANK TRANSFER for Euro 30.00 to**

ERSTE BANK, Alser Str. 23, 1080 Wien
Bank code: 20 111 SWIFT: GIBAATWWXXX
Account number: 296 489 968/00 IBAN: AT37 20111 296 489

☐ **please charge my CREDIT CARD for 30 Euro**	☐ **EUROCARD/MASTERCARD**	☐ **VISA**
	EXPIRYDATE: ______/______	
	CARD NUMBER ________/________/________/________	
	Name and Signature of the cardholder:	


EUROPEAN ORTHOPAEDIC
RESEARCH SOCIETY

EUROPEAN ORTHOPAEDIC
RESEARCH SOCIETY

Risk factors associated with the early failure of cannulated screws

Robert Jordan
University Hospitals Coventry & Warwickshire, West Midlands, UK

Our study provides further evidence that patient selection is key for a successful outcome following cannulated hip screws for intracapsular fractures with screw configuration having no measurable effect on outcome.

Introduction

Current indications for cannulated hip screws in the management of intracapsular neck of femur fractures include young patients and those with undisplaced fractures. Reported re-intervention rates are high and knowledge of risk factors for failure allows for better patient selection. We aim to share our experience of cannulated hip screws and analyse the risk factors associated with early failure.

Methods

All patients undergoing cannulated hip screws for intracapsular hip fractures at our centre between November 2009 and November 2011 were retrospectively identified. Electronic records were reviewed for patient demographics. Pre and intra operative radiographs were analysed using ‘Traumacad’ for displacement, fracture angle, posterior comminution, successful reduction, and screw configuration. Early failure was defined as re-operation within 6 months and risk factors were analysed statistically using IBS SPsSS Statistics 19.0.

Results

340 patients were included in the study with 69.1% female and a mean age of 80.5 years. The median follow up period was 18.7 months; 73 patients died (21.5%) and 111 patients (32.6%) required further surgery during this period. Early failure occurred in 77 patients with the majority undergoing hemiarthoplasty (59.7%) or total hip replacement (31.2%). Age (p=0.026), females (p=0.014), initial fracture displacement (p=0.03), successful lateral reduction (p

Conclusion

There remains a distinct indication for the use of cannulated hip screws for undisplaced intracapsular fractures or in young patients. Patient selection has the biggest impact on the need for early re-intervention and should be carefully considered before surgery.

Rotation of Sagittal Cutting Plane for Tibial Component in Unicompartmental Knee Arthroplasty

Ho-Joong Jung
Chung-Ang University, Seoul, Korea

There is a total 17¡ of tibial rotation relative to the femur during range of motion This should be considered to decide the rotation of tibial component in UKA.

Introduction

Normal rotational movement of tibia relative to the femur should be considered to decide the optimal tibial component orientation in unicompartmental knee arthroplasty. We tried to evaluation for the tibial rotation relative to the anatomical axis of femur using biplanar fluoroscopy.

Materials and Methods

Ten human cadaveric lower extremities were scanned with 3D-CT and the in vitro 3-dimensional kinematics was measured using biplane fluoroscopy. The task included a passive flexion of the knee from 0° to full flexion. Imaginary sagittal tibial cutting planes in 90° of flexion were set to (1) parallel to mechanical axis(MA), (2) 2° external rotation to MA and (3) 2° internal rotation to MA . Measuring the angle between the sagittal tibial cutting plane and anatomical axis of the femur throughout the range of motion using coordinate transformation algorithm.

Results

Tibial Internal rotation magnitude was lager than external rotation of tibia from 90° .The sagittal tibial cutting plane rotate externally 4.8 ± 0.5° from 90° to 0° of knee flexion, and rotate internally 12.5 ± 0.7° from 90° to full flexion, There is no differences in magnitude of rotation according to different sagittal cutting angle.

Conclusions

There is a total 17° of tibial rotation relative to the femur during range of motion This should be considered to decide the rotation of tibial component in UKA.

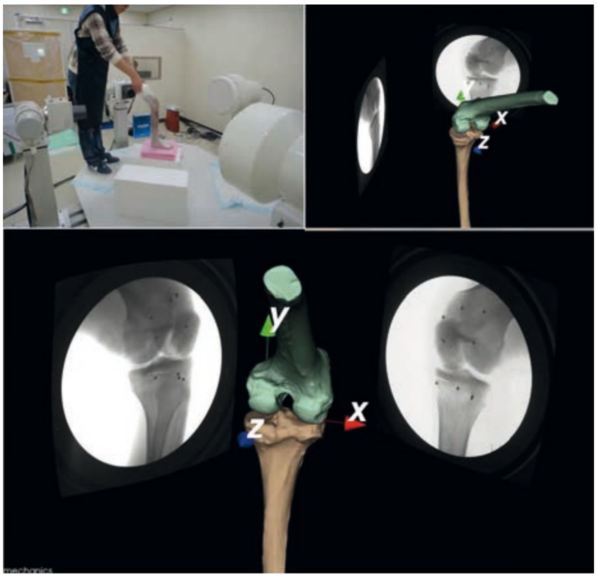

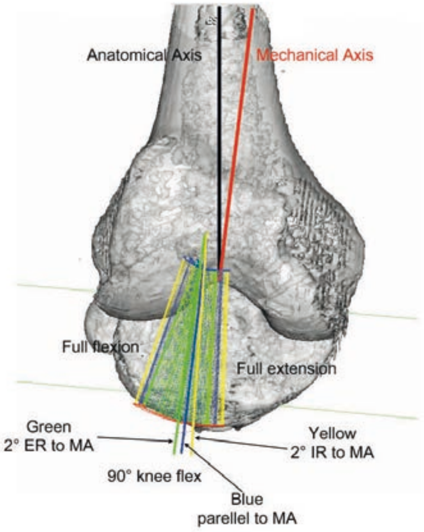

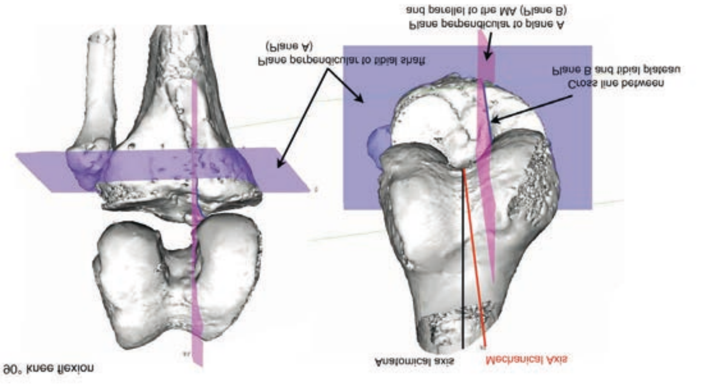

3D Matrix extraction by matching between 3D CT & Biplanar fluoroscopic data

-Explanation for Locus(Path) calculation

-Path of tibial sagittal cutting plan in whole range of motion

The Importance of Central Screw Placement in the Distal and Proximal Pole in Scaphoid Waist Fractures

Geert Meermans
Department of Orthopaedic Surgery, Lievensberg Hospital, Bergen op Zoom, The Netherlands

The purpose was to compare central and eccentric screws in fixation of scaphoid waist fractures. Biomechanical testing demonstrated that central placement of the screws in the proximal and distal pole resulted in greater stiffness compared to the proximal pole only.

Introduction

When using a percutaneous volar approach, central screw placement is complicated by the shape of the scaphoid and obstruction by the trapezium. This can be avoided by opening the scaphotrapezial joint and manipulation of the scaphoid or by using a transtrapezial approach. Alternatively, a more radial entry point on the distal pole of the scaphoid can be used, but this does not allow central placement of the screw in the distal pole. The aim of this study is to determine whether central placement of the screw in the proximal and distal pole of the scaphoid offers a biomechanical advantage over a screw that is central only in the proximal pole.

Methods

Fourteen matched pairs of cadaveric wrists were randomly assigned to a treatment group. Under fluoroscopic control, a guidewire was drilled into the scaphoid, using either a transtrapezial approach (central, group C) or a standard volar approach avoiding the trapezium (eccentric, group E). Guidewire position was measured in the coronal and sagittal plane in 3 transverse planes perpendicular to the central axis that divided the scaphoid in 4 equal parts. A transverse osteotomy was made along the scaphoid waist, followed by the insertion of the longest possible cannulated headless bone screw. Each specimen was placed into a fixture with a pneumatically driven plunger resting on the surface of the distal pole. The load was applied by using a load-controlled test protocol in a hydraulic testing machine at a rate equivalent to 10 N per second until failure. Data acquisition was done with specialized software at 25 points per second. Load at 2 mm of displacement, load at failure and mechanism of failure were recorded.

Results

Radiographic evaluation of all of the specimens confirmed placement of the screw within the central one-third of the proximal pole of the scaphoid. There was a significant difference between guidewires in group C and group E at the distal pole ($p<0.001$). All screws in group C were inside and all screws in group E were outside the central one-third of the distal pole.

The mean screw length in group C (25.57 mm standard error of the mean (SEM) 0.52; range 22-28 mm) was similar to that of group E (25.00 mm SEM 0.50; range 22-28).

The load at 2 mm of displacement and load at failure were 324.4 N SEM 73.49 and 386.4 N SEM 65.58 for group C compared with 125.7 N SEM 22.61 ($p=0.002$) and 191.4 N SEM 36.30 ($p=0.005$) for group E respectively.

Discussion

Exact central positioning of a screw in the proximal and distal pole of the scaphoid can be reliably done using a transtrapezial approach. This offers a biomechanical advantage in the internal fixation of scaphoid waist fractures, compared with central placement in the proximal pole only. Clinical efforts and techniques that facilitate placement of the screw in the central one-third of the proximal and distal pole of the scaphoid should be encouraged.

Role of Rotating Hinge Knee in Revision Knee Arthroplasty

Biyyam Madhusudhan Rao
St.Richards Hospital, Western Sussex Hospitals NHS Trust, Chichester, West Sussex, UK

Prospective study to evaluate the clinical and radiographic outcomes of a newer generation Rotating hinged total knee in a large cohort of patients of revision knee arthroplasty with major bone loss and soft tissue deficiencies.

Introduction

Historically older generation of hinged knee replacements have been known to have inferior results. The aim of this prospective study is to evaluate the clinical and radiographic outcomes of a newer generation hinged total knee in a large cohort of patients of revision knee arthroplasty with major bone loss and soft tissue deficiencies.

Methods and Materials

In this prospective study we include 108 patients undergoing Revision knee arthroplasty using modern Rotating Hinged knee (RHK) prosthesis (Zimmer Inc., Warsaw, Indiana). Indications for revision knee arthroplasty included periprosthetic infections with major bone loss (39 patients), aseptic loosening with major osteolysis (32 patients), periprosthetic fractures around knee (04 patients), failed Unicompartmental knee replacements with major bone defects (04 patients), mal-alignment of prosthesis (6 patients), unexplained painful knees (04 patients) and ligamentous instability (19 patients). To address the combined bone loss and collateral instability, we used the Rotating Hinged total knee prosthesis (Fig.1)in all 108 patients. Associated bony defects were classified according to Anderson Orthopaedic research institute (AORI) classification. We used 30 tibial and 4 femoral trabecular metal cones (Zimmer Inc., Warsaw, Indiana) in type 2 and type 3 AORI defects (Fig.2) to address the bone loss along with RHK. The mean age of patients was 76 years (range 56-92 years) with 64 men and 44 women. The mean follow up of this study is of 34 months (range 18 - 48 months).

Results

The mean Oxford scores improved from 21 to 32 (p value - 0.006) and mean American knee society scores (KSS) improved from 32 to 76 (p value 0.001). Based on KSS results we had 52% excellent results, 32% good, 14% fair and 6% poor results. The SF-36 mean physical functioning score was 46.09 points (SD - 3.34), and the SF-36 mean mental functioning score was 51.57 points (SD - 17.73). Radiographic analysis showed non progressive radiolucent lines around tibial stems and femoral stems in 2 patients but no subsidence of implant was noticed in any patient. Of these one had to be re-revised for continual pain. Complications included 4 deaths from unrelated causes, 1 above knee amputation for recurrent infection, 3 re-revisions for infections and 2 infections on long term suppressive antibiotics. There was one periprosthetic fracture around tibial stem treated conservatively and one femoral stem disengagement (Fig.3) with no untoward knee functional results.

Conclusions

With advent of modern rotating hinge devices there appears to be place for them in revision knee arthroplasty especially with major bone loss and gross ligamentous instability. The newer generation rotating hinge knee prosthesis are 95% condylar weight bearing (Zimmer Inc., Warsaw, Indiana), which appear to have better functional outcome in revision knee arthroplasties compared to the previous designs and studies. Still use of these hinge prostheses should be reserved for extreme circumstances, such as for gross instability, massive bone loss, periprosthetic fractures, and chronic dysfunction of the extensor mechanism. Use of less constrained devices is recommended whenever possible, and revision surgery should be performed as soon as failure is diagnosed to avoid massive bone loss.

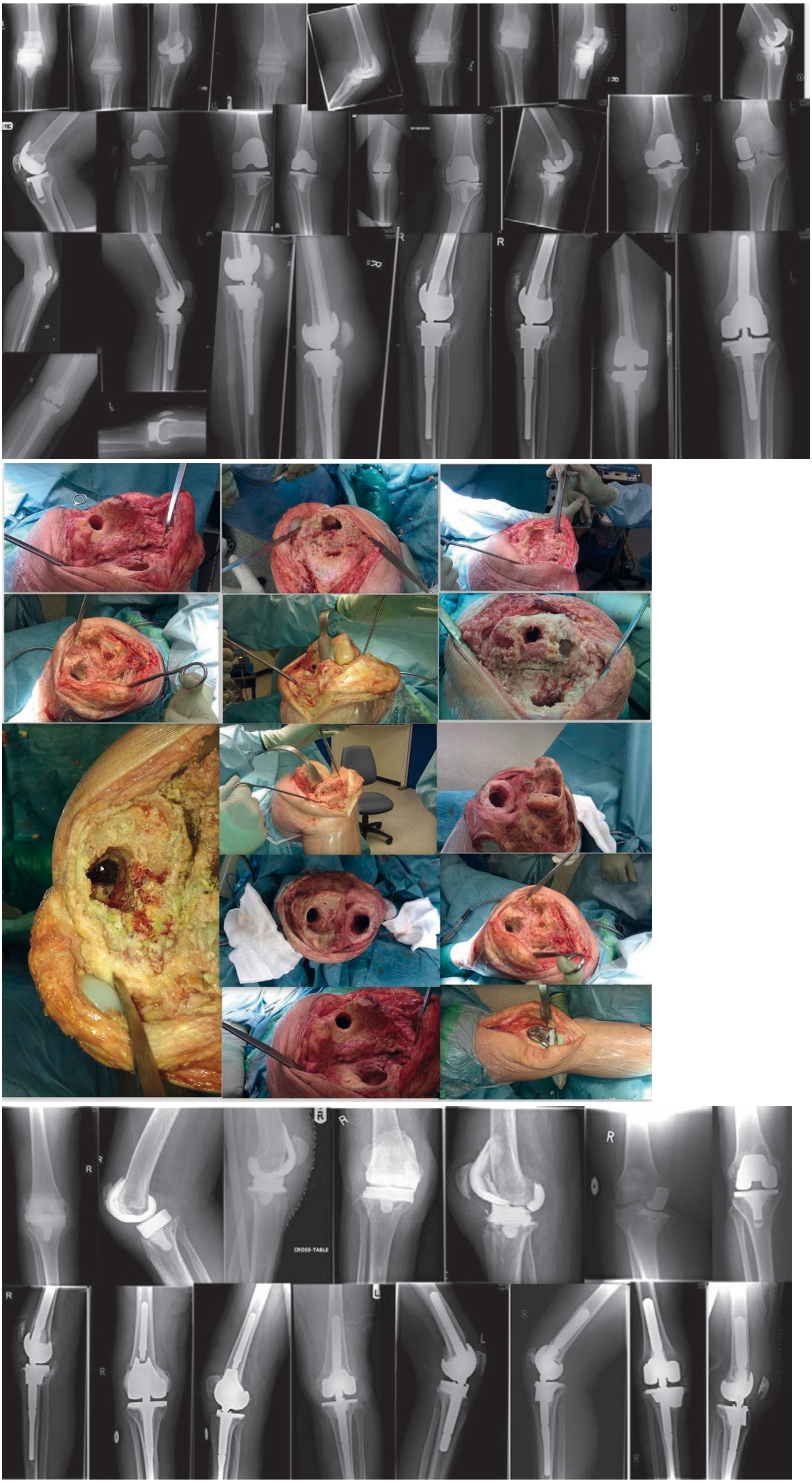

Radiographs showing preoperative and postoperative results with Rotating Hinge Knee prosthesis
-AORI type 2 and 3 defects
-Radiographs of cases with Rotating Hinge Knee prosthesis including one complication of stem disengagement

The bio-mechano-reactor: design and development of a new tool for Osteoarthritis research.

Thijs de Jong
University Medical Center Utrecht, Utrecht, The Netherlands

A new tool for osteoarthritis research, based on in-vitro bioreactors, and an isolated whole canine stifle joint, is currently being developed. A joint isolation protocol was created and validated. The concept bioreactor showed feasibility for whole joint culture.

Introduction

Osteoarthritis (OA) affects a substantial part of the adult population. Its pathophysiology is not fully understood yet. To investigate OA pathology and possible treatment modalities, in-vitro techniques including bioreactors, or in-vivo animal models are used. However, in-vitro culture conditions are often far from the in-vivo situation, and animal models accompany a ‘black box’ from the moment of initiation/intervention, to the moment of analysis.

The current project aim is to create a new tool for OA research that combines the advantages of animal models of OA, and in-vitro bioreactors. This model will be based on an isolated whole canine stifle joint, which is brought into in-vitro culture in a biomechanically stimulated environment (figure 1).

Methods

Two sets of experiments were performed, to validate the joint isolation protocol, and to assess the feasibility of whole joint culture in a custom bioreactor.

Joint isolation protocol: The hind limbs of three dogs (one male, two females, mixed breed, age 14.7±1.2 months (range 14-16 months)) were isolated. In all dogs, the left knee cartilage was immediately harvested, and provided control samples. The right stifle joint was isolated according to the protocol: the skin, the musculature and synovial tissue were removed while the menisci, cruciate- and collateral ligaments were left intact. After this, the cartilage from the right knee joints was also harvested. After three days of culture, the proteoglycan (PG) turnover in the cartilage of both joints was compared. The sterility of the isolation procedure was monitored with swab samples.

Bioreactor culture: The hind limbs of one dog (female, Beagle breed, age 31 months) were isolated. The left knee cartilage was immediately harvested, and provided control samples. The right knee was isolated as described above, and cultured for four days in the bioreactor in a non-moving setup. After culture, the PG turnover of the cartilage of both joints was compared.

Results

Isolation protocol (figure 2): No differences in PG-content (25.23±1.60 vs 23.62±0.25 mg/g_{tissue}, p=0.39), PG-release (13.47±1.37 vs 17.97±1.85 %, p=0.16), PG-synthesis (4.58±0.76 vs 4.46±0.65 nmol/h.g_{tissue}, p=0.74), and release of newly formed PGs (24.69±7.29 vs 25.79±6.06 %, p=0.73) between the experimental and control cartilage respectively were seen. The tissues intended for bioreactor culture showed no contaminations after isolation.

Bioreactor culture (figure 3): No differences in PG-content (23.86±1.63 vs 20.23±1.28 mg/g_{tissue}, p=0.11), PG-release (18.71±1.36 vs 22.21±4.10 %, p=0.51), and release of newly formed PGs (13.39±1.51 vs 21.91±3.86 %, p=0.07) between the experimental and control cartilage respectively were seen. Experimental samples that had full medium contact showed a 75% decrease in PG-synthesis (4.57±1.08 vs 18.48±2.58 nmol/h.g_{tissue} p=0.03), which was significantly higher than samples without medium contact (-90% synthesis, 1.27±0.55 vs 12.03±1.49 nmol/h.g_{tissue}, p=<0.001).

Conclusions

Joint preparation for bioreactor culture has no consequences for the cartilage PG metabolism, and the tissues intended for culture remain sterile. Whole joint culture in the bioreactor is feasible, but the cartilage metabolism is decreased, probably due to lack of medium contact. To overcome this, in the near future culture experiments will be performed wherein in-vivo movement of the stifle joint is simulated.

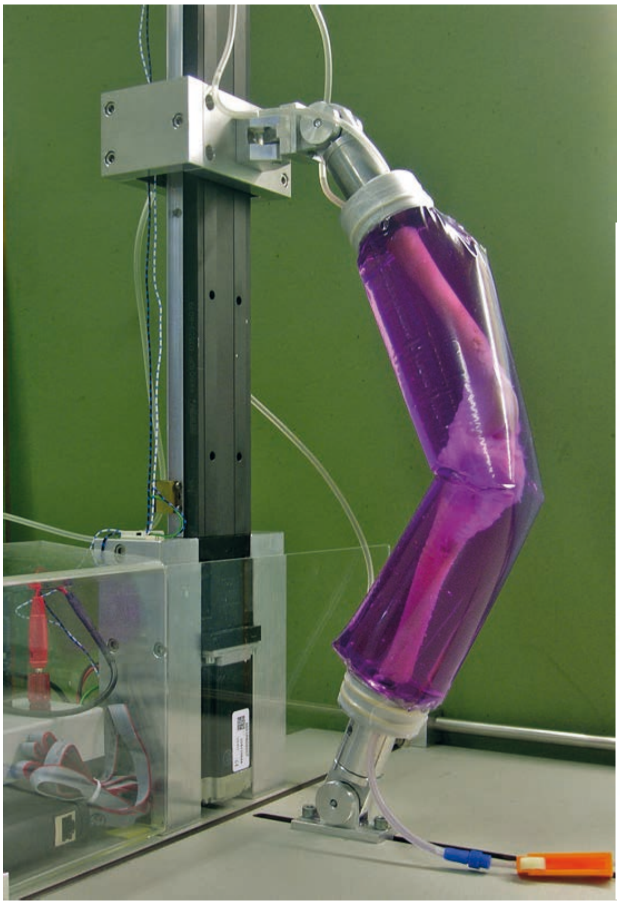

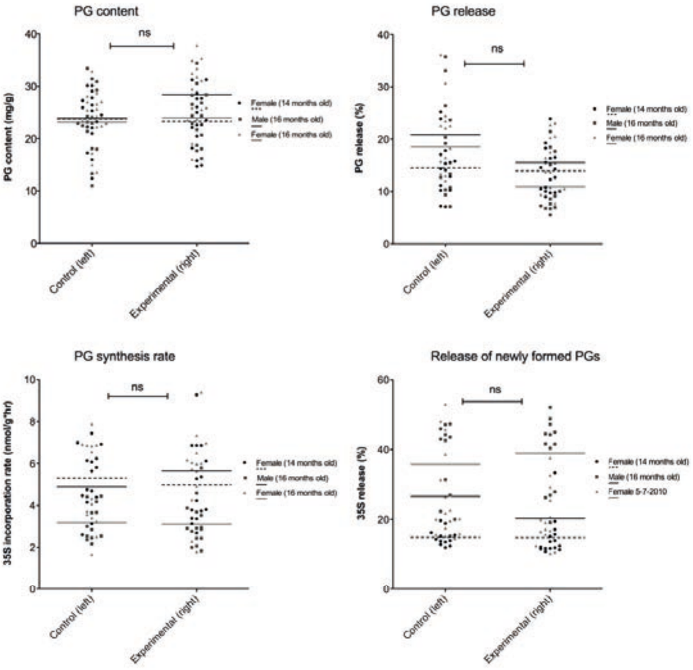

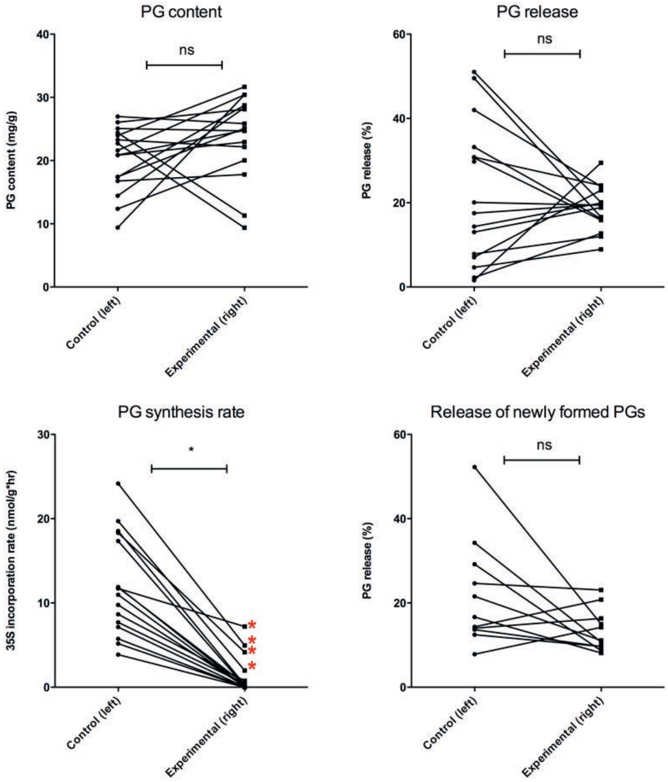

-Photograph of the bio-mechano-reactor with an isolated whole canine stifle joint incorporated.

-Proteoglycan (PG) turnover in the cartilage of an experimental joint prepared for bioreactor culture, and control samples. The bars represent the mean values for the individual dogs. ns = not significant.

-Proteoglycan (PG) turnover in the cartilage of an experimental joint cultured in the bioreactor, and control samples. PG Synthesis rate: the red asterisks indicate samples with full medium contact. ns = not significant, * = $p<0.05$.

The Exeter Trauma Stem. Outcome Experiences from the Royal United Hospital, Bath.

William Carlino
Royal United Hospital, Bath, UK

Hip fracture management is an extremely important aspect of orthopaedic trauma. The major issue highlighted by this study was the difficulty experienced in obtaining equal post operative leg lengths which can have a significant impact.

Introduction:

Hip fracture management is often regarded as 'routine', but is an extremely important aspect of orthopaedic trauma. There is widespread agreement that surgery is superior to non-operative treatment for most patients, but there remains controversy over the surgical options.

The Exeter Trauma Stem is a monoblock unipolar implant widely used for intracapsular hip fractures, but there remains only one peer reviewed publication on this prosthesis.

Method:

All patientswho had a hip fracture treated with an ETS between2008 and 2010 were retrospectively evaluated. Patient demographics andoperative detailswere collected from the patient notes and the hospital database. We assessedcement mantles using the Barrack grading system and measured leg lengths using a validated technique with digital imaging.

Results:

Complete data was obtained for 104 patients. The mean age was 81 years. Overtwo thirdsof cement mantles were Barrackgrade A or B. There were equal leg length measurements in only 10% of patients. Three patients required revision of their ETS stem to a total hip replacement for recurrent dislocation, peri-prosthetic fracture and significant acetabular wear.

Conclusions:

The major issue highlighted by this study was the difficulty experienced in seating both the trial broach and the prosthesis which is required to obtain equal post-operative leg lengths.Post-operative leg length discrepancy can result in significant functional impairment and the requirement for revision surgery.Our department now uses a modular prosthesis for hip fractures which has several stem sizes that permit an intra-operative trial and easier stem insertion. This has resulted in improved post operative leg lengths.

The comparison of a biomechanical testing using 4 point bending in rat Tibia between specimen with and without muscle cleaning

Tulyapruek Tawonsawatruk
The University of Edinburgh, Edinburgh, UK

A biomechanical testing of specimen without muscle cleaning technique can be used for evaluating in fracture healing specimen in order to avoid interfere of callus as mechanical properties of specimens without cleaning muscle were similar to specimens with muscle cleaning.

Introduction

The biomechanical properties of bone healing are important to evaluate functional outcomes of the fracture healing process. Bending tests are common methods used to evaluate the mechanical behaviour of small animal bones such as mice or rats. Proper preparation of the specimen can increase an accuracy of biomechanical testing. To test whole bones, it is recommended that soft tissues around should be cleaned properly before testing. However, cleaning the specimens might disturb callus structure and crate stress raiser (see fig.1) which interfere the mechanical property of the callus. It should be more appropriate to test bone sample without muscle cleaning. Thus, this study is aim to compare a mechanical property of rat Tibia between specimen without muscle cleaning and specimen with muscle cleaning which is a standard preparation technique using 4 point bending.

Materials and methods

12 male Wistar rats aged 3-4 months were used for this study. One rat tibia from each of 12 pairs was harvested from animals for biomechanical testing. All soft tissues including skin and muscle were dissected from only right tibia, whereas muscles at left tibia were left intact. The mechanical property of specimen with and without soft tissues cleaning was tested using 4-point bending test (Zwick Inc., Ulm, Germany). Ultimate load, stress and young's modulus from each group were compared. Paired t-test was conducted to test statistical significance. The Bland-Altman plots were used to show the difference between two techniques of specimen preparation.

Results

All specimens displayed a basic failure pattern from load-displacement graph (see fig 2). Mean ultimate load of was 105.2 N (S.E.M. =7.60, n=12) for specimen with muscle cleaning and 101.6 N (S.E.M. = 7.32, n=12) for specimen without muscle cleaning. Mean ultimate strength of was 281.50 MPa (S.E.M. = 34.98, n=12) for specimen with muscle cleaning and 288.70 MPa (S.E.M. =20.83, n=12) for specimen without muscle cleaning. Mean Young's modulus was 8.97 (S.E.M. = 1.44, n=12) for specimen with muscle cleaning and 10.05 (S.E.M. = 0.69, n=12) for specimen without muscle cleaning. No statistical differences of mechanical properties were found between specimen with muscle cleaning and specimen without muscle cleaning ($p>0.05$). The comparison points of the difference of ultimate load, ultimate strength and young's modulus were within the limits of agreement according the Bland Altman-plots (see fig.3).

Discussion

The mechanical properties including ultimate load, ultimate strength and young's modulus from specimens without cleaning muscle were similar to specimen with muscle cleaning. Therefore, a biomechanical testing of specimen without muscle cleaning technique can be used for evaluating in fracture healing specimen in order to avoid interfere of callus. The advantages of this technique are taking short time for specimen preparation and decreasing risk making the stress raiser at the callus.

References

Bak B, Jensen KS. Standardization of tibial fractures in the rat. Bone. 1992; 13(4):289-95.
Turner CH, Burr DB. Basic biomechanical measurements of bone: a tutorial. Bone. 1993 Jul-Aug; 14(4):595-608.

A) Load-displacement graph of specimen cleaned

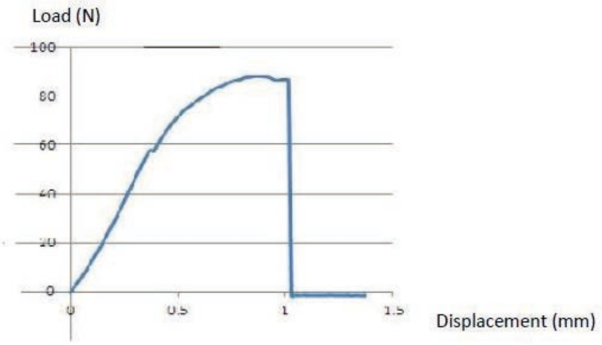

B) Load-displacement graph of specimen cleaned

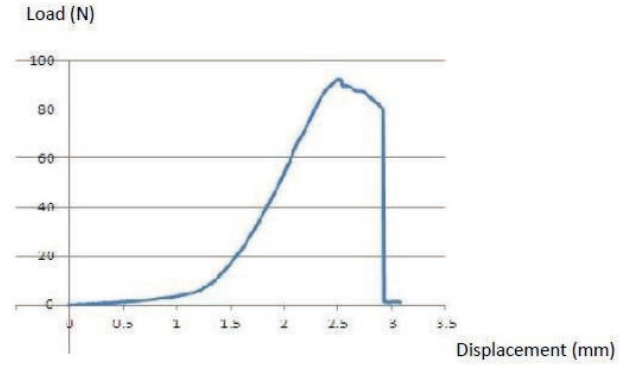

Bland-Altman Plot for Difference of Ultimate load vs average of Ultimate load

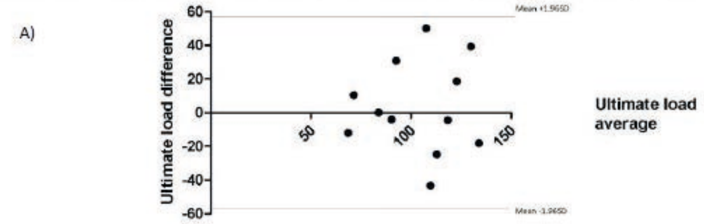

Bland-Altman of Difference of Ultimate strenght vs Average of Ultimate stress

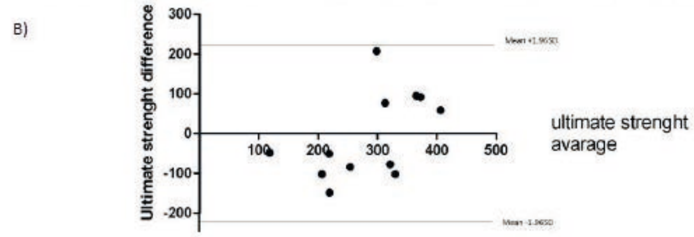

Bland-Altman of Difference of Young 's modulus vs Average Young 's modulus

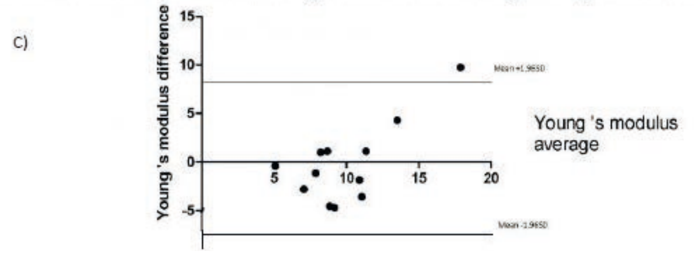

-MicroCT shows the stress raiser at the bone callus.
-Graphs compare the load-displacement from 4-point bending test of specimen with muscle cleaning (a) and without muscle cleaning.
-The bland-Altman plots demonstrate the difference of ultimate load (a), ultimate strength (b) and Young's modulus (c) between two techniques of specimen preparation.

The Effect of Insert Conformity on Total Knee Replacement Wear

Abdellatif Abdelgaied
University of Leeds

The current study showed that a potential method for increasing the expected total knee replacements lifetime may be to introduce less conforming knee replacements. In addition, the conventional UHMWPE wear was shown to be highly cross-shear ratio dependent.

Introduction:

Demand for joint replacements in young patients is increasing, and therefore there is a need to increase the lifetime of the prostheses. To fulfil in this new requirement, new replacements designs and materials are being introduced. One of the design parameters that may affect wear of total knee replacements, and hence the predicted lifetime of such prostheses, is the insert conformity [1].

Materials and Methods:

To investigate the effect of insert conformity on wear in TKRs, four different insert designs, with different conformity (see Fig.1), were tested against the same femoral geometry. The DePuy Sigma fixed femoral (DePuy International, UK) was run against custom flat, partial flat, lipped and curved inserts, with conventional UHMWPE inserts material. The Sigma curved and lipped inserts were based on a size 3 geometry with a thickness of 10mm (DePuy International, UK). The partial flat was based on the Sigma High Performance Partial Knee, while the custom flat insert was created by flattening the contact surface of the partial flat insert.The models were run under two different kinematic inputs (intermediate kinematic and high), with different cross-shear ratios [2], for three million cycles per each design and each kinematic input in a computational model.

The computational framework used in the present study was based on the contact area and an independent experimentally determined non-dimensional wear coefficient, and was validated against the experimental results, for the curved and flat inserts, elsewhere [3]. The effects of cross-shear and creep on wear predictions were also considered. The conventional UHMWPE was modelled as an elastic-plastic material, using the true stress-strain data [4], with a modulus of elasticity of 463MPa and a Poisson's ratio of 0.46 [5, 6].

Results:

The predicted average wear rates under intermediate kinematic inputs were 1.7, 1.9, 3.2 and 6 mm^3/millioncycles, for the flat, partial flat, lipped and curved inserts respectively. The corresponding predicted wear rates under high kinematics were 2.5, 2.7, 5.8 and 8.7 mm^3/millioncycles respectively (see Fig.2).

Discussion:

The results showed that, under both intermediate and high kinematics, the less conforming geometries had the lower predicted wear. The predicted wear rate for the curved insert was more than three times that for the flat insert, under the same kinematic inputs. Contrasting the predicted wear rates under different kinematics, the predicted wear rates under high kinematics were approximately 1.5 times the corresponding predicted wear rates under intermediate kinematics.

Conclusion:

The current study showed that a potential method for increasing the expected total knee replacement lifetime may be to introduce less conforming knee replacements. In addition, the conventional UHMWPE wear was shown to be highly cross-shear ratio dependent.

References:

[1] Fisher et al. 2010 Clinical Orthopaedics and Related Research 468 12-18.
[2] McEwen et al. 2005 J Biomechanics 38 357-365.
[3] Abdelgaied et al. 2011 J Biomechanics 44 1108-1116.
[4] Godest et al. 2001 J Biomechanics 35 267-275.
[5] Bartel et al. 1995 Clinical Orthopaedics and Related Research 317 76-82.
[6] Kurtz et al. 2002 J Biomechanics 23 1907-1919.

Conflict of interest statement:

J. Fisher is a consultant to DePuy International Ltd, UK, a Director and share holder of Tissue Regenix plc and BITECIC

Ltd and a Director of Medilink. C. Brockett is a consultant to DePuy International Ltd, UK.

Acknowledgments:

A. Abdelgaied is supported by The Egyptian Ministry of Higher Education &Scientific Research (Helwan University).

J. Fisher is an NIHR senior investigator.

This research work is supported by EPSRC, the Leeds Centre of Excellence in Medical Engineering, WELMEC, funded by the Wellcome Trust and EPSRC, WT088908/Z/09/Z and the Leeds Musculoskeletal Biomedical Research Unit (LMBRU), funded by NIHR.

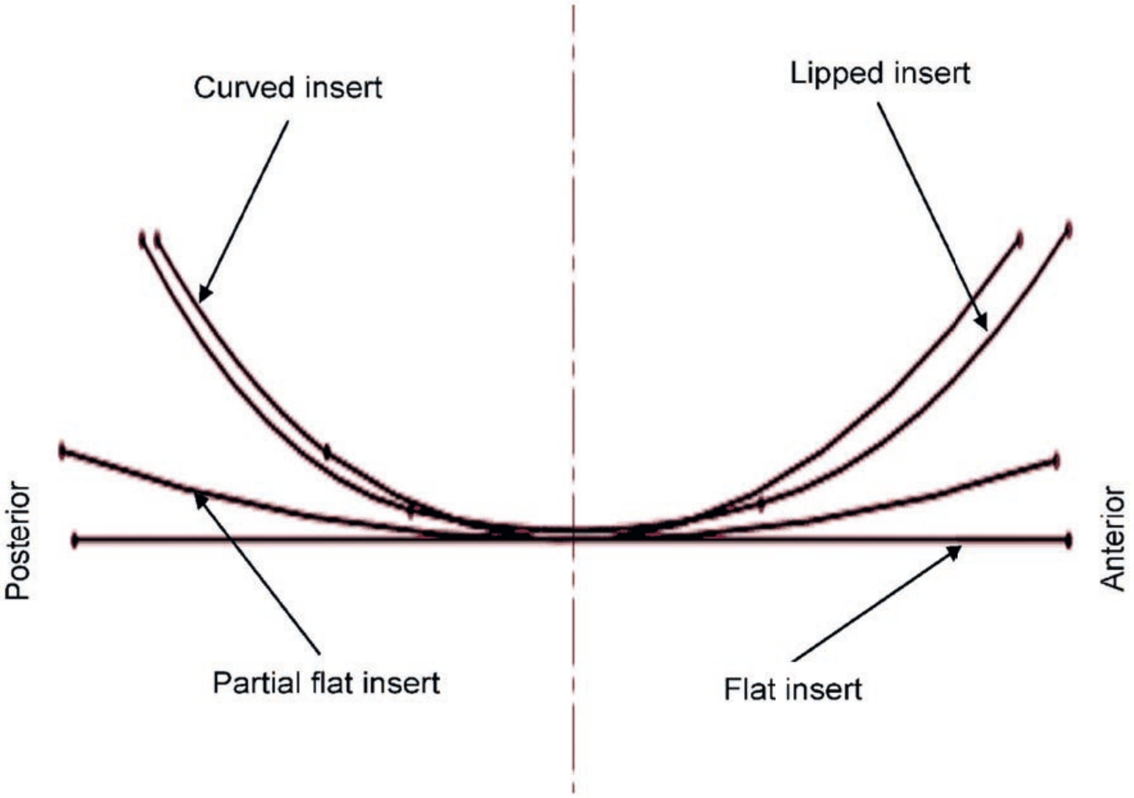

Figure 1: The curvature at the medial condyle centre, for different insert types.

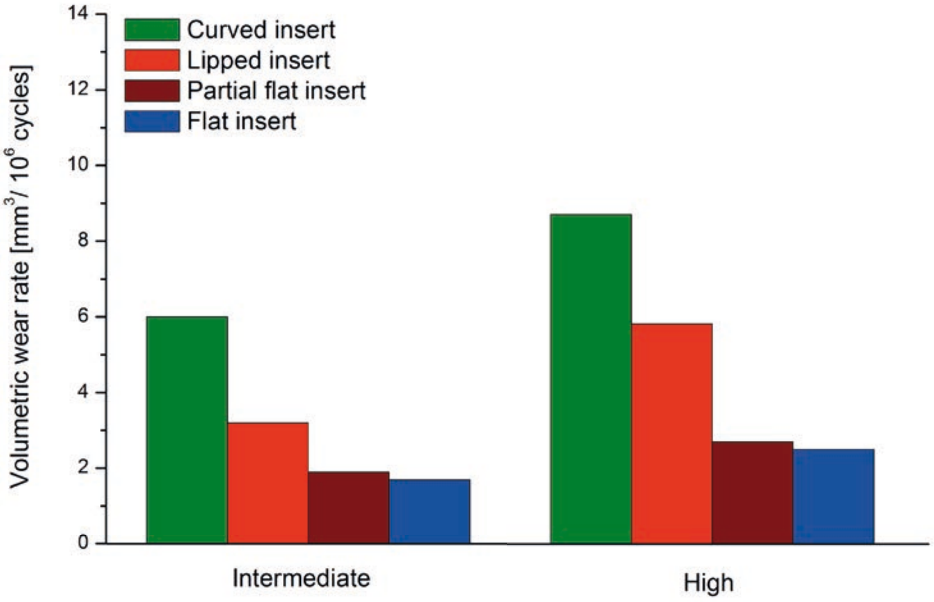

Figure 2: Predicted volumetric wear rate for different inserts, under intermediate and high kinematic inputs.

The acetabular bone fissure formation in press fit hip artroplasty

Ricardo Duarte
University of Aveiro, Aveiro, Portugal

We studied the formation of fissures in acetabular bone due to hip replacement arthroplasty using numerical finite element models. One intact model and two implanted models with and without fissures on the posterior side were analyzed and compared.

Introduction:

Due to the hip joint functions and because it is one of the most requested joints of the human body, its wear is inevitable, which eventually leads to the necessity of a total hip arthroplasty. Some clinical reports indicate that occasionally, during the surgery process, due to the excessive reaming or impact force placing the socket, a fracture near the acetabular cavity may occur. This has also been observed in vitro procedures.

We evaluated the influence of a fissure when placing the acetabular component of the hip prosthesis. Three numerical models of the hip replacement were compared concerning the principal strains around the acetabular cavity and along the fissure. One intact model and two replaced models were used, these latter with a crack induced in the posterior side of the acetabulum.

Methods:

A geometric model of an intact and replaced joint were modeled using CATIA V5v (Dassault Systems) based on in vitro models made with composite bones (Sawbones®, femur - 3404, iliac - 3405). The Lafitt® press-fit acetabular joint with 52mm diameter and a 28 mm femoral head size was used. In one of the models we made a fissure with 0,5mm thickness and 17mm on the posterior side of the acetabular cavity in the cortical bone.

In the finite element models the interfaces between the components on both models were considered as bonded, except between the femur's head and cartilage in the intact model. A friction coefficient of 0,01 for the intact model and 0,2 for the implanted model were considered in the simulations. The iliac was fixed on the wing of the illium and on the ischial tuberosity and the femur was clamped on its diaphysis. A load of 600N was applied on the pubic tubercle of both models (Table 1).

Results:

In both implanted models the maximum and minimum principal strains p1,</sub> p3</sub>) decreased comparatively to the same of the intact model; we observed a higher reduction of strains in the vicinity of the fissure region with a fissure on the posterior side.

Comparing the two implanted models, we observed that the strains p1</sub> are very similar along the acetabular cavity. Relatively to the p3 </sub>strains there are noticeable differences in the entire surface, namely on the region of the crack (figure 1).

Along the fissure edge, we observed that there is pronounced decrease of the principal strains on the fissured model, when compared with the others. We also observed that this difference decreases when approaching to the crack's end and become identical after this region (figure 2).

Discussion:

If a fissure is created when the acetabular socket is placed, it changes the strain distribution on the bone structure, manely around it. The numerical results showed that the fissure decreases the principal strains in its region, suggesting a decrease of bone density and consequently can influence the bone remodeling mechanism.

Table 1: Mechanical properties of the finite element models

Component	Young's Modulus(GPa)	Poisson's Ratio	
Cortical Bone	16,7	0,3	Natural
Cancellous Bone	0,155	0,3	
Cartilage	0,00625	0,4	
Femoral Stem	120	0,3	Prosthetic
Femoral Head	370	0,22	
Socket	120	0,3	
Insert	0,5	0,3	

Figure 1: Strain distribution in the acetabular cavity.

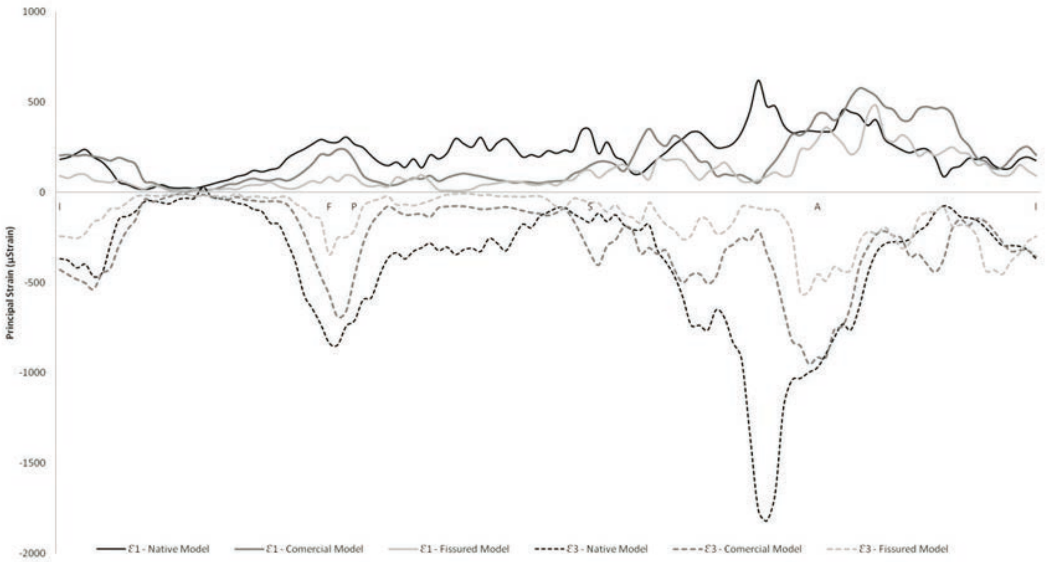

Figure 2: Strain distribution at region of the fissure edge.

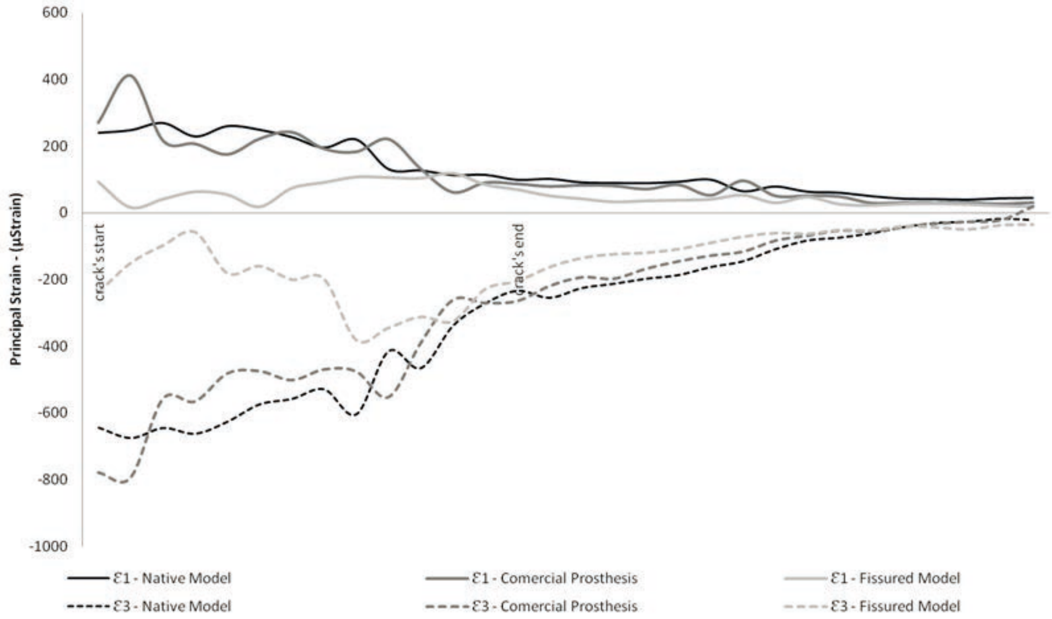

The benefits of a composite design for a Novel Polycarbonate-Urethane Meniscal Implant

Jonathan Elsner
Active Implants Corp., Netanya, Israel

A bio-stable composite synthetic meniscal implant with a dependable biomechanical performance, resembling that of the natural meniscus was developed to provide adequate response to the needs of younger and older patients without relying on tissue regeneration.

It is now recognized that the knee meniscus has an important function in distributing joint loads, thus preventing degenerative changes or osteoarthritis in knee joint. Consequently, treatment of meniscus injury has been changing from resection to repair. Sometimes, however, meniscectomy cannot be avoided, and in such cases, a synthetic meniscal implant could be beneficial in reducing pain associated with knee overloading. Artificial prostheses offered to date are based principally on tissue engineering concepts. The variability in the body response to biodegradable implants and the quality of the tissue formed still pose a problem in this respect, thus making it difficult to attain satisfying results from scaffold-type meniscal implants under intense knee loading conditions. Therefore, the goal of this study was to develop a bio-stable synthetic meniscal implant, which combines durability with a dependable biomechanical performance, resembling that of the natural meniscus. Such solution should provide adequate response to the needs of younger and older patients without need to rely on tissue regeneration.

The biomechanical function of the natural meniscus is closely linked to its distinctive microstructure, and specifically to the ability of circumferential bundles of collagen fibers, embedded within a hydrated matrix, to bear circumferential hoop stresses (Fig. 1). We thus hypothesized that a composite anisotropic structure is needed to recreate the pressure distribution of the natural meniscus (Fig. 2). Biomechanical evaluation and design optimization of the composite implant were focused on in-vitro measurements of tibial contact pressure in cadaver knees, and computational finite element(FE)analyses. The latter model was validated by comparing calculated pressures, determined from FE analysis to tibial contact pressures measured in a cadaveric knee in vitro. Several models of the implant, some including embedded reinforcement fibers of different nature, were tested. An optimal implant configuration was then selected based on the ability to restore pressure distribution in the knee, manufacturability, and long-term safety.

The compression of an initial meniscal implant design, composed solely of PCU, resulted in relatively large distortions in the implant structure and peripheral extrusion under load with respect to reinforced implant configurations. Circumferential reinforcement of the PCU implant with fibers improved its performance. First, it considerably reduced circumferential expansion under load by 95% to 2 mm. Second, it resulted in an improved ability to distribute the tibial plataue pressure. The pressure distribution maps attained for reinforced PCU had a closer form to that attained for the natural meniscus (Fig. 3). Importantly, the contact area was predominantly in the outer third of the tibial plateau surface and was not concentrated in the central region

The optimal implant design entailed a PCU meniscus embedded with circumferential reinforcement made of polyethylene fibers. This selected design can be manufactured in various sizes, without risking its integrity under joint loads. Importantly, it produces an optimal pressure distribution, similar in shape and values to that of natural meniscus.

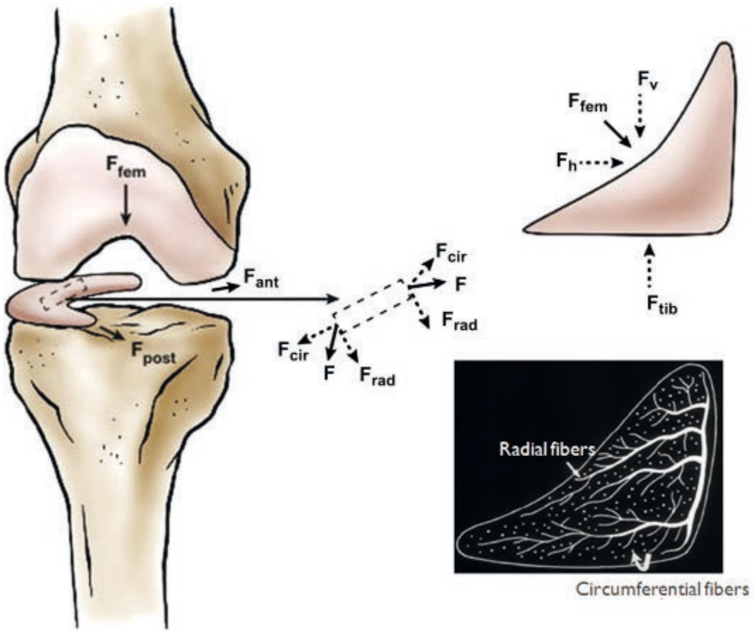

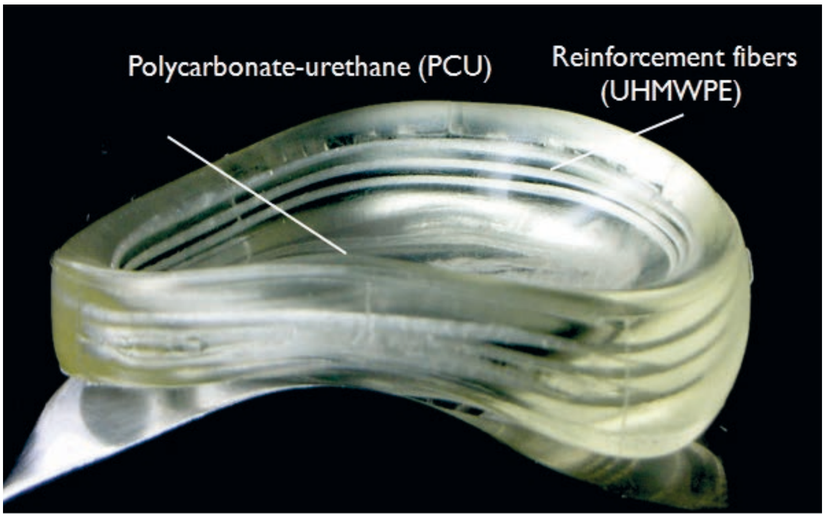

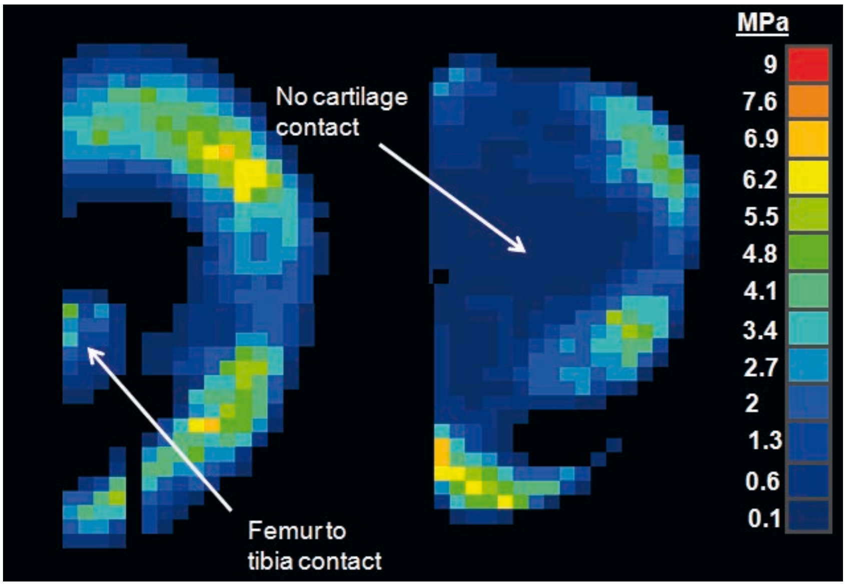

-Microstructure and biomechanical function of the natural meniscus. Translation of femoral compression into hoop stresses (Markis et al., 2011).
-A composite aritficial meniscus, based on a polycarbonate-urethane matrix reinforced with UHMWPE
-Pressure distrbution under the natural meniscus (left), and artificial implant (right), during joint compression

THE FINANCIAL BURDEN OF PERFORMING JOINT ARTHROPLASTY IN OBESE PATIENTS

Benjamin Bradley
South Devon Hospitals NHS Trust, Devon, UK

Introduction:

The current financial climate is placing immense strain on state-funded health care organisations, presenting an increasing need to justify expenditure. It is perceived within the orthopaedic community that operating on obese patients is associated with increased financial costs. There are currently 78,000 primary hip and 86,000 primary knee arthroplasties performed per year in the UK. The prevalence of obesity is increasing and the cost of performing joint arthroplasty is set to increase in line with this.

Performing joint arthroplasty in obese patients is demanding and technically challenging. It is well documented that arthroplasty in these patients is associated with an increased complication rate. This study aims to investigate and quantify the financial cost of performing primary hip and knee arthroplasty in obese patients.

Method:

A single-centre retrospective review of all patients undergoing primary hip and knee arthroplasty in a one year period was performed. Patients were stratified according to their BMI using the WHO classification. Patient case notes and the Theatre Administration System was interrogated with surgeon-specific operative time and length of inpatient stay being recorded.

Results:

545 primary hip and knee arthroplasty procedures were reviewed. 41 patients were excluded due to the complex nature of their surgical procedure.

There was a significant increase in mean operative time for total hip arthroplasty between overweight patients (BMI 25-29) and obese patients (BMI 30-34) of 30 minutes (88mins Vs 118mins, p

There was also a significant increase in the length of inpatient stay between overweight and obese patients for both hip and knee arthoplasties. In obese patients undergoing total hip arthroplasty the mean inpatient stay increased by 1.5 days (4.1 Vs 5.6, $p < 0.0001$). Mean inpatient stay for obese patients undergoing total knee arthroplasty was increased by 1.6 days (3.9 Vs 5.5, $p < 0.0001$).

Conclusions:

Patients undergoing primary hip and knee arthroplasty with a BMI in excess of 30 require a significantly longer operative time and inpatient stay.

Each obese patient listed for total hip arthroplasty will potentially cost the NHS an extra £1095 in terms of increased theatre time and longer bed occupancy alone. The potential extra cost of an obese patient undergoing total knee arthoplasty is £1028 using the same measures. There are further financial implications of obesity in surgery that have not been explored in this study.

In our institution obese patients undergoing these procedures are now listed for extra theatre time. This has improved theatre efficiency, reducing list over-runs and limiting patient cancellations. We have not yet addressed the increased length of stay presented by obese patients.

With rising rates of obesity in an ageing population the need for joint arthroplasty is set to increase placing potentially unsustainable demands on the NHS within the UK.

The effect of shortening the walkway in clinical inertia-based gait analysis.

Rachel Senden
Ahorse, Atrium MC Heerlen, Heerlen, The Netherlands

A minimum walking distance is required to obtain reproducible results from a gait test. With an inertia-based gait test, the walkway can be shortened from 20m to 15m. Further shortening seems possible when the start/stop phases are excluded from analysis.

Introduction

Gait analysis is frequently used in orthopaedic practice as clinical outcome tool. Currently, gait is assessed by visual observation which lacks discriminative power to identify subtle gait deviations. Laboratory-based gait analysis is reliable and accurate, but complex and lacks the ability to measure clinically relevant parameters such as gait variability which rely on several successive steps. Inertia-based motion analysis (IMA) showed to be reliable and clinically suitable for analysing (pathological) gait (1). IMA allows to measure many steps outside the laboratory, allowing for a natural gait pattern to be measured. However studies showed that a 20-25m undisturbed walkway is recommended to produce reproducible data (1,2). This makes the gait test less suitable for clinical use as an undisturbed 20m walkway is not often available in clinical practice and because some patients are unable to walk a 20m distance.

This study investigates whether the walking distance for IMA can be shortened, ensuring that gait parameters are reproducibly measured.

Methods

Five healthy subjects (range 21-54yrs, 5F/1M) walked two times a 5m, 10m, 15m and 20m distance at preferred speed while wearing comfortable shoes and while wearing an inertia sensor (3D accelero-, 3D gyrometer) at the level of the sacrum. Self-designed, published peak detection algorithms (3) were used to derive gait parameters from the inertia signal. Spatiotemporal gait parameters (e.g. speed, step length, cadence) and other clinically relevant gait parameters (e.g. step time asymmetry and variability, expressed by step time irregularity and step time variance coefficient) were determined. To calculate the asymmetry and variability, the first and last steps were excluded due to respectively acceleration vs. deceleration. The average of two walks was used for analysis (2). Gait parameters measured over 5m, 10m, and 15m walkway were compared with the 20m walkway using repeated measurement ANOVA ($p<0.05$).

Results

Spatiotemporal gait parameters were significantly affected by a shorter walkway showing a longer step time, smaller step length and slower walking speed during the 5m and 10m distance with regard to the 20m walking test. The spatiotemporal gait parameters measured over the 15m and 20m distance were similar. No effect of walk distance on step time asymmetry and variability parameters was found.

Conclusion

Walk distance has an effect on spatiotemporal gait parameters, but not on step time asymmetry and variability parameters. This suggests that the acceleration and deceleration phase of gait, which is included in the calculation of spatiotemporal parameters, has a considerable effect on IMA parameters. No differences in gait parameters were found between 15 and 20m distance indicating that the walkway for IMA-based gait analysis can be shortened from 20m tot 15m. This however may not solve the limitation for clinical use. Further shortening the walkway seems possible if the start and stop phase is excluded, but this needs further investigation. A 5m walkway however is not recommended, as this covers too few steps to determine clinically relevant parameters like gait variability.

References

Senden et al. Gait Posture 2009, 2. Zijlstra et al Gait Posture 2003, 3. Senden et al. EORS 2010

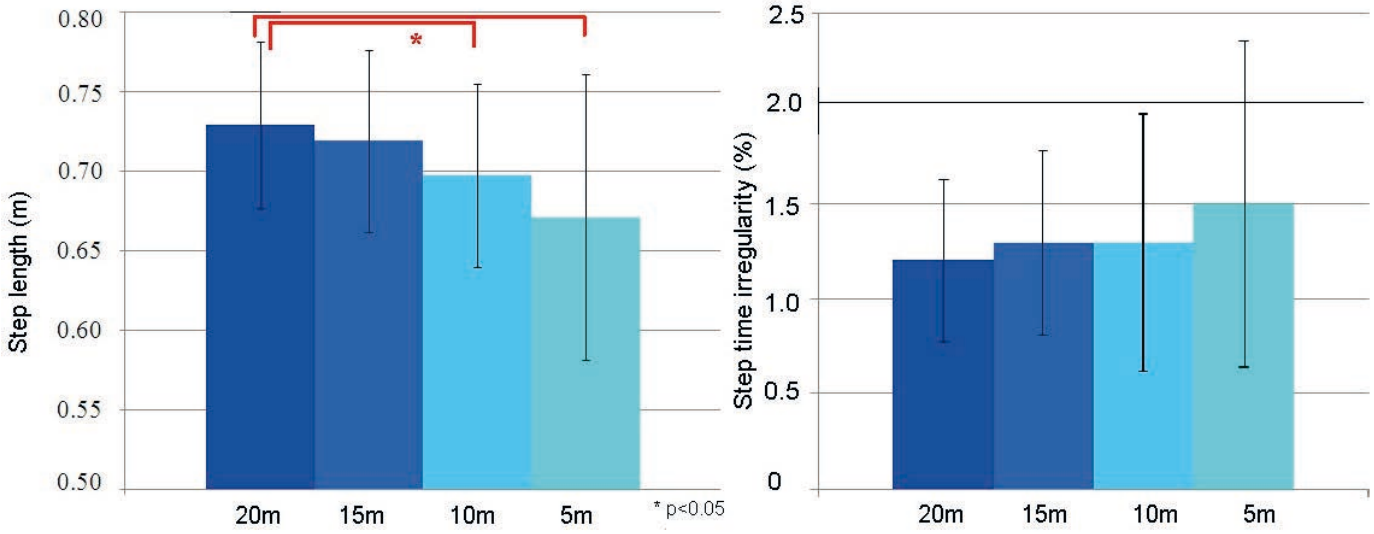

IMA-based step length and step time irregularity measured at different walking distances

Teres major tendon transfer surgery for massive irreparable posterosuperior rotator cuff tears

Jan Ferdinand Henseler
Leiden University Medical Center, Leiden, The Netherlands

The teres major transfer effectively restores function and relieves pain of irreparable posterosuperior (i.e. supraspinatus and infraspinatus) rotator cuff tear patients and can be considered as an alternative to the latissimus dorsi transfer

Introduction:

Degenerative massive rotator cuff tears have high failure rates when surgically repaired. Alternatively, a tendon transfer can compensate for lost rotator cuff function. The purpose of this prospective cohort study is to evaluate the clinical results of the teres major transfer for patients with an irreparable posterosuperior rotator cuff tear.

Patients and Methods:

Twenty-eight patients were treated consecutive with a teres major tendon transfer for an irreparable posterosuperior (i.e. supraspinatus and infraspinatus) rotator cuff tear in this prospective cohort study. Clinical outcomes included active range of motion, Constant score and VAS scores for pain.

Results:

All patients had a minimum follow-up of 12 months with an average follow-up of 25 months (12-80 months). Thirteen of the twenty-eight patients had a history of prior surgery on the affected shoulder. In these cases the teres major transfer was used as a salvage procedure.

Active forward elevation improved to an average of 113 compared to 89 preoperatively (paired t-test, $p = 0.01$), active abduction improved to 105 from 79 preoperative (paired t-test, $p = 0.01$), the average postoperative active external rotation in adduction was 33, from 23 preoperative (paired t-test, $p = 0.03$) and the average postoperative active external rotation in 90 abduction was 55, from 25 preoperative (paired t-test, $p < 0.001$). The average postoperative Constant Score was 65, increased from 43 preoperatively (paired t-test, $p < 0.001$). The average postoperative VAS score for pain decreased to 1.5 postoperatively from 5.2 preoperatively (Wilcoxon's signed-ranks test, $p < 0.001$).

In the salvage surgery group slightly better results were obtained group compared to the primary surgery group. However, the mean improvement of the active range of motion, Constant score and VAS scores for pain between salvage and primary group did not differ significantly.

Discussion and Conclusion:

The main goal of the teres major tendon transfer is to improve arm function by restoring external rotation in abduction. With its transferred orientation projecting over the infraspinatus into the supraspinatus footprint, the teres major cannot completely replace lost external rotation force of the infraspinatus. Improvement of forward flexion and abduction follows as the directional force of the transferred teres major becomes more optimal in elevated positions of the arm. The humeral head is centered onto the glenoid in the anteroposterior plane by reinforced external rotation, thereby reducing pain and allowing for an effective fulcrum for abduction by the deltoids.

In conclusion, the teres major transfer is a valid alternative to the latissimus dorsi transfer for the treatment of irreparable posterosuperior rotator cuff tears. The teres major transfer effectively restores function and relieves pain, leading to an overall clinical improvement in a relatively young, active and demanding patient group.

The stem cells therapy in longs bone non-unions

Viorel Nacu
SMPhU Nicolae Testemitanu, Chisinau, Rep. Of Moldova

The aim was to evaluate the capcity of cord blood cells or autogenous BMC to stimulate bone formation in 175 patients with non-unions by X-Ray, scintigraphy and CT. The bone healing were obtained in 82,1% cases.

Introduction. Repair of bone defects, and also non-unions remains a major concern in bone reconstructive surgery, because of: limited supply of autograft, donor site morbidity, risks and complications in allografting and synthetic bone substitutes.

After blood, the bone is the most frequently transplanted tissue in this century.

The sources of autogenous stem cells: Bone marrow, Fat tissue, Peripheral blood, Deciduous teethes, CBC.

Unfortunately number of stem cells in bone marrow for mature individual is quite small 0.1% from nucleated cells, and to have sufficient cells for cellular therapy it should be multiplied in vitro.

It was identified that cord blood, like bone marrow, is a rich source of stem cells including hematopoietic stem cells, mesenchymal stem cells and embryonic-like stem cells.

There are a hi number of potential donors and the UCBC could be transplanted when the HLA incompatibility is more envident by BMC.

The aim of presented study was to evaluate the grafts containing alogenous cord blood cells or autogenous bone marrow cells with alogenic demineralized bone to stimulate bone formation in nonunion and pseudartroses.

Patients and methods. This prospective study which was done on 175 patients with long bones non-unions. The Upper limb bones (61): clavicle - 3, the arm - 17; the radial bone - 9; the ulna - 7; the both bones of the forearm - 8, the scaphoide bone of the wrist - 14, the flanges - 3. The Lower limb bones (114): the femoral neck - 3; the femoral bone - 35; rotula -2, the tibial bone -74 cases. The ability of cells grafts to stimulate bone formation in nonunions and pseudarthroses were evaluated by X-Ray, scintigraphy and by Computed Tomography at every month until the bone healing.

Results

In 16 cases as a cellulare grafts were used alogenous cord blood cells and the rest (159) autogenous Bone marrow stem cells. The bone healing were obtained in 82,1% of cases, in the rest of the cases patients needed surgical methods of treatment with autogenous cancelous bone grafts.

Discussions The combination grafts from demineralized, morselized alogenic bone with autogenous bone marrow cells or cord blood cells were shown to promote good bone healing.

Conclusions

The used cells grafts were compatible with the recipients, provides active and uniform osteogenesis to the bone, which could be comparable with the use of the autogenous cancelous bone.

1A.1

Bone substitute reduces significantly the secondary loss of reduction: A biomechanical study of tibial depression fractures

Stephanie Doht
Department of Trauma, Hand, Plastic and Reconstructive Surgery, Wuerzburg, Germany

In the operative treatment of tibial depression fractures, only the combination of bone substitute (Norian drillable) and screws prevented secondary loss of reduction and, at the same time, provided enough stability under maximum load.

Introduction:

Tibial plateau depression fractures (Type AO-B2, Schatzker III) are frequently seen after low velocity injuries in the elderly. Depression of the articular surface requires fragment elevation and safe retention. Compression defects of cancellous bone after articular reconstruction may lead to secondary loss of the reduction. One therapeutic option is an arthroscopically controlled reduction and fixation with screws with or without filling up the metaphyseal defect. In patients with osteoporosis, iliac crest bone graft is unsatisfying and bone substitutes are used instead. A human cadaver model was used to investigate, whether filling the bone defect with new drillable calcium phosphate cement (Norian Drillable) with or without additional screws provides adequate fragment stability.

Methods:

A tibial depression plateau fracture was created in osteoporotic human tibiae. Soft tissue was removed from bone. The tibial shaft was fixed in bone cement in 5° valgus 20 cm below the joint line. A depression fracture of the lateral tibial plateau was induced resulting in a 1.2 cm^2 and a 1.5 cm deep depression fracture. The fracture was reduced indirectly using a guiding k-wire and cannulated ram until the articular plane was restored anatomically. Three different stabilization techniques were compared: In the 1st group, calcium phosphate cement (Norian Drillable) was inserted to support the elevated depression fragment (Figure 1A). Additional four crossing screws in the jail technique were used in the 2nd group, set after filling up the defect (Figure 1B). The 3rd group represented an unfilled defect, only fixed by four screws in the jail technique without bone substitute (Figure 1C). Seven specimens were investigated per group. After fixation load was applied with 250 N in 3000 cycles. Displacement was measured and in a load-to-failure tests, maximum load and stiffness were scaled (test machine Zwick/Roell 2020). All results underwent statistical analysis for normal distribution. Data was evaluated statistically by analysis of variance (ANOVA).

Results:

The 1st and 2nd group revealed a significantly lower displacement (Figure 2) and higher stiffness than group 3 without bone substitute (only fixed with screws). The maximum load was higher for the groups with screws (group 2 and 3) compared to the group with bone substitute (Norian Drillable) only (Figure 3).

Discussion:

A metaphyseal defect remains after reduction of the articular fragment in tibial plateau depression fractures, particularly in the presence of osteoporosis. Drillable calcium phosphate cement (Norian drillable) as bone substitute reduces the displacement of the depression fracture fragment under conditions simulating a clinical relevant partial weight bearing, and screws in the jail technique increase the maximum load. Thus, in the operative treatment of tibial depression fractures, for the primary stability, only a combination of bone substitute and screws appears favorable.

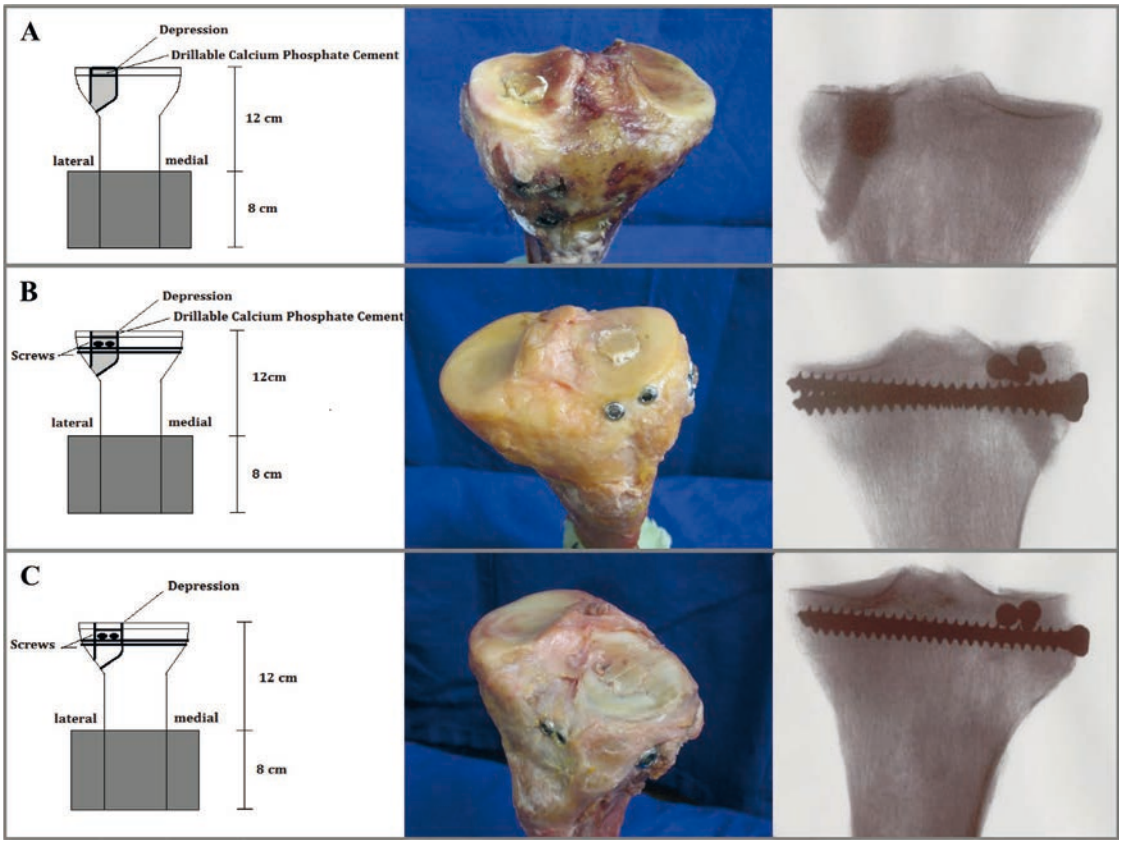

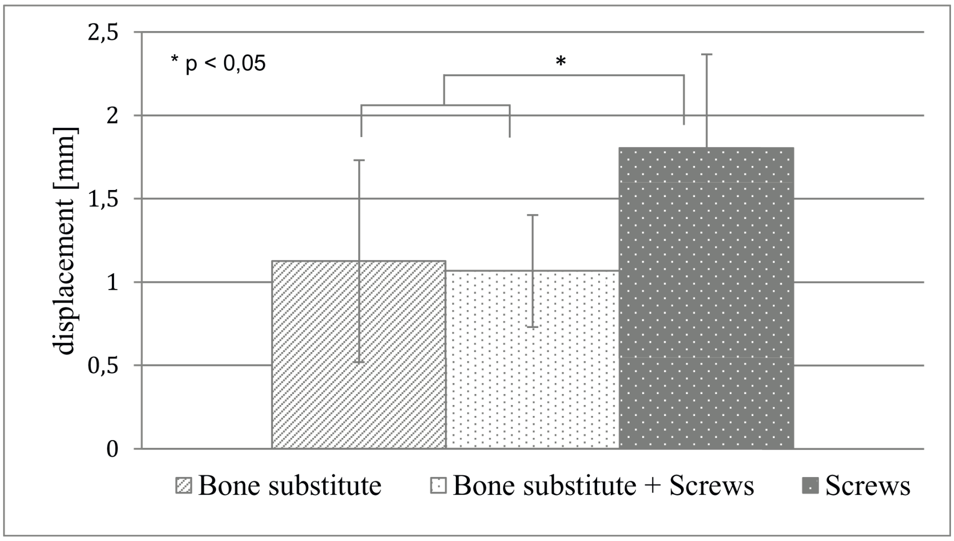

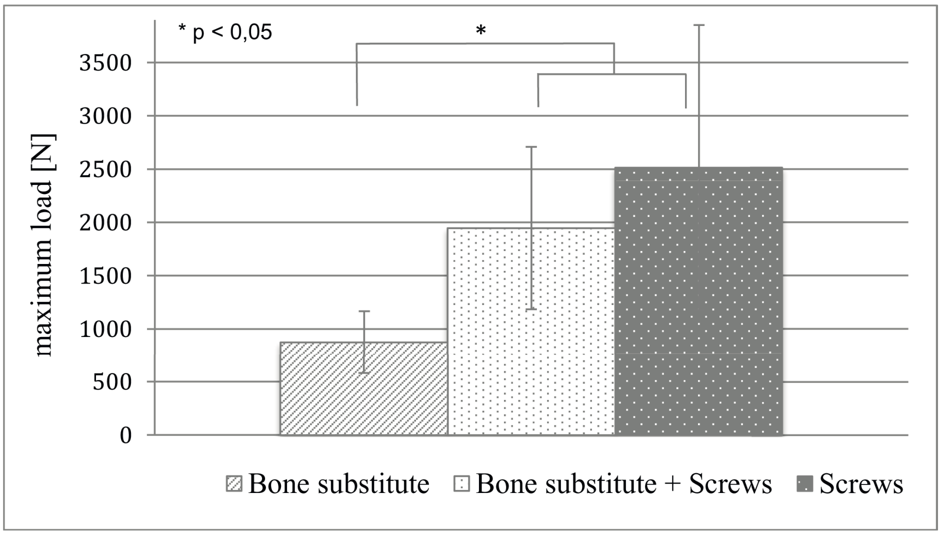

Figure1_groups
Figure2_displacement
Figure3_maximumload

1A.2

Stem cell response to mechanical stretch is dependent on surface microtopography

Laura Saldana
La Paz University Hospital, Madrid, Spain

This study examines the influence of tensile forces applied to plasma membrane of osteoblast precursor cells cultured on metallic surfaces with different roughnesses. The effect of mechanical stretch on cell behavior was strongly dependent on the surface microtopography.

The importance of physical factors in the development and maintenance of bone tissue has long been recognized. The biological response of bone-related cells to mechanical stimuli is the result of a complex mechanotransduction process to accommodate the new loading environment. The interactions between bone tissue and orthopedic implants are strongly affected by mechanical forces at the bone-implant interface. Numerous investigations have established the ability to direct cellular behavior by manipulating the topographical features of existing conventional metals. Optimizing cell-material interactions under mechanical stress is critical to enhance the therapeutic performance of biomaterials, but the interplay between surface topographies, mechanical stimuli and cell behavior is complex and not well understood. This study aimed to examine the influence of mechanical stretch applied to osteoblast precursor cells cultured on stainless steel surfaces with different roughnesses. The effect of physical stimuli on cell proliferation, matrix production, osteoblastic differentiation, secretion of signaling molecules and underlying mechanisms of load transduction on the tested surfaces were investigated. Controlled forces were applied to plasma membrane of substrate-attached cells using a magnetic particle-electromagnet model (1). A ceramic permanent magnet was used to generate tensile forces on ferric oxide magnetic beads, coated with collagen and attached to the dorsal surface of cells. Human mesenchymal stem cells (MSC) were seeded on austenitic stainless steel processed by polishing or by sand-blasting, treated with beads suspensions and subjected to a 30-min period of continuous force application. As controls, cells were treated with beads but not subjected to any force. Cell viability was assessed in cells cultured up to 9 days after physical stretching, using the alamarBlue assay. Cell maturation to the osteoblastic lineage was analyzed after incubating MSC in media supplemented with specific osteogenic inducers for 11 days, and determined using Alizarin Red staining. Human specific ELISA kits were used to measure PGE_2 and VEGF in culture media and FN, total FAK and p-FAK (Tyr-397) in cell layers. Cell viability and FN production decreased when surface roughness increased, while MSC maturated to the osteoblastic lineage to a similar extent in all surfaces. Increasing roughness of stainless steel increased PGE_2 secretion and the p-FAK/FAK ratio, but unaffected VEGF levels. The effect of mechanical stretch on these cellular parameters was surface-sensitive. Mechanical stress decreased cell viability, FN levels and MSC osteoblastic differentiation on polished surfaces but not on rough samples. PGE_2 production increased after physical stretching on all surfaces, although to a greater extent on polished substrates. Mechanical stimulation only induced VEGF secretion on polished surfaces. MSC exposed to mechanical stress underwent an increase in the p-FAK/FAK protein ratio on rough surfaces while no such effect was observed on polished samples. In summary, mechanical stimuli impaired several MSC functions and failed to promote FAK phosphorylation on polished surfaces. This study shows that collagen-magnetite bead model is well suited to characterize cellular responses to tensile forces on metallic surfaces and reveals that the effect of mechanical stretch on MSC behavior is strongly dependent on the surface microtopography. 1. Glogauer M et al. Am J Physiol. 1995;269:C1093-104.

1A.4

Assessment of the mechanical properties of plantar tissue by a combined CT imaging and modelling approach

Michiel Oosterwaal
Maastricht University Medical Centre, Maastricht, The Netherlands

To predict the effect of an insole on pressure distribution a detailed biomechanical model of the foot and ankle has been developed and validated. The model accounts for the integrated effect of bone kinematics and soft tissue properties.

Introduction

Foot orthotics are prescribed for a broad range of foot and ankle pathologies. Due to inter subject variations the prediction of the effect of such orthotics is difficult. In clinical practice it is impossible to evaluate many different designs to provide the patient with the best solution. Alternatively, biomechanical, in silico, models offer the potential to predict a-priori the functional outcome for a particular footshape and motion. Existing FE models of foot and ankle are of high detail, however there computational complexity renders them unsuitable for simulation of realistic dynamic loading conditions. Recently, a new foot and ankle model has been developed, which can be used efficiently in a dynamic situation to predict the effects of an insole on a highly detailed plantar surface [1]. The outcome of this model is highly influenced by the anatomical structures and mechanical properties of the foot and ankle. The aim of this study was to develop a method to characterise these properties for an individual patient. Therefore, the geometry of anatomical structures are directly derived from CT scans, while the mechanical properties are estimated from optimal correspondence between model and a series of weight bearing CT scans.

Patients & Methods

Ten healthy subjects, seven patients with a flexible flatfoot deformity and seven patients suffering on metatarsalgia have been measured. [2] Three loaded CT scans of the subjects right foot and 1 unloaded CT scan of the right lower leg have been made (figure 1). During scanning, plantar pressure has been measured with a pedar insole (Novel gmbh, Munich, Germany). These images were segmented with MIMICS (Materialise, Leuven, Belgium) and a finite element mesh has been generated with 3-matic (Materialise, Leuven, Belgium). Tissue parameters were adjusted to optimize the agreement between FE mesh and CT data. The final outcome of the finite element simulation is validated with the plantar pressure measurement obtained during CT-measurement.

Results

Complete CT datasets were obtained for all subjects and all CT data has been segmented. A 2.5D mesh has been defined that accurately captures the foot geometry (figure 2). Additional thresholding was required to define the boundary between bones and soft tissue. Preliminary results show that the mechanical properties of the plantar tissue can be estimated using this optimisation procedure.

Discussion/Conclusion

A method has been developed that determines the anatomy of the foot and ankle from the segmented CT images and allows direct implementation in a patient specific model. Mechanical properties of the plantar tissue can be derived via finite element simulation and implemented to estimate the effect of an insole.

References

1. Oosterwaal M, Telfer S, Carbes S, Torholm S, Meijer K, Woodburn J, Rhijn Lv: Generation of a dataset to develop a subject-specific, multibody, finite element, dynamic foot model. In EUROMECH Colloquium 511. Ponta Delgada, Azores, Portugal; 2011.
2. Oosterwaal M, Telfer S, Torholm S, Carbes S, van Rhijn LW, Macduff R, Meijer K, Woodburn J: Generation of subject-specific, dynamic, multisegment ankle and foot models to improve orthotic design: a feasibility study. BMC Musculoskelet Disord 2011, 12:256.

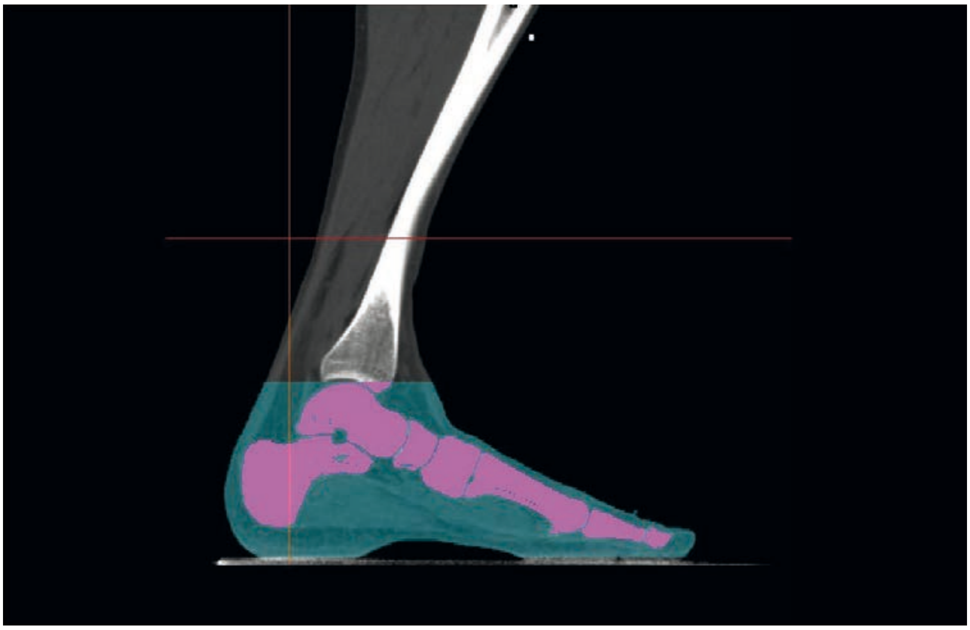

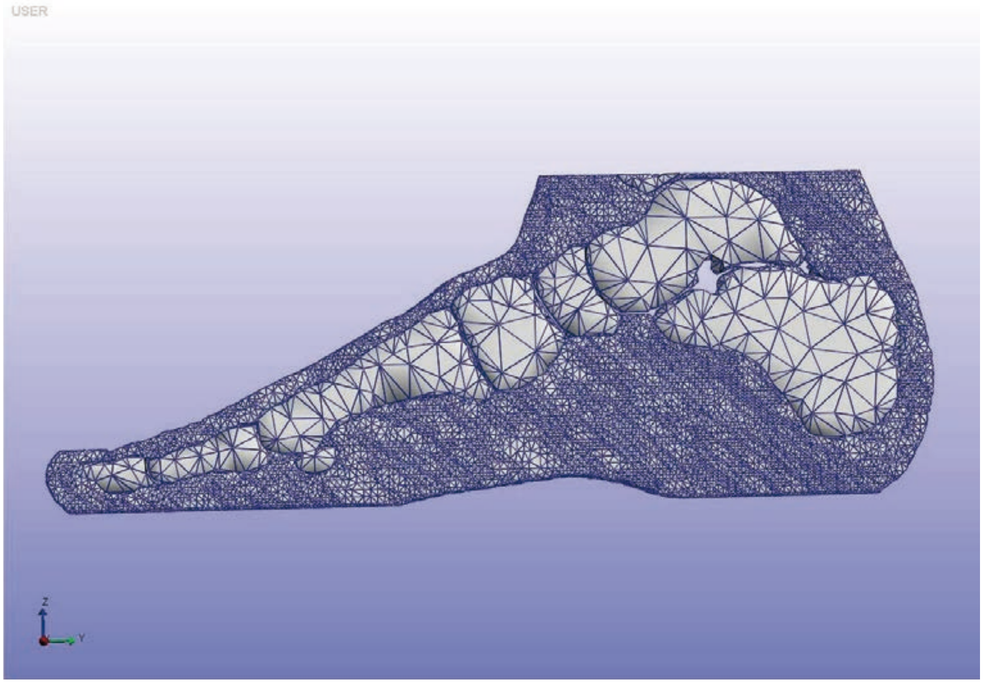

CT Image of the foot
FE mesh for assement of plantar tissue mechanical characteristics

1A.6
A patient-specific musculoskeletal mandible model using force-dependent kinematics

Michael Skipper Andersen
Department of Mechanical and Manifacturing Engineering, Aalborg University, Denmark

Force-dependent kinematics (FDK) was used to compute the joint reaction forces in the temporomandibular joint and the results compared to a planar constraint model. FDK model captured the change in reaction force direction due to the mandibular fossa shape.

Introduction Although only few joints in the human body can reasonably be considered idealized joints, most inverse dynamics-based musculoskeletal models available in the literature apply such models [1,2]. One example is the model of the temporomandibular joint (TMJ) reported by de Zee et al. [2,3], where it was modelled as a planar constraint and a unilateral reaction force. However, in reality, the detailed joint mechanics are governed by the contact between the condyle and the mandibular fossa, the ligaments, the muscle forces and the external load.

To enable modeling of complex joints in terms of force elements and still allow computation of muscle forces, joint reactions and ligament forces in an inverse dynamics-like manner, Andersen et al. [4] recently proposed the Force-dependent kinematics (FDK) analysis framework. FDK computes the detailed joint motions as well as the muscle and joint reaction forces under an assumption of static force equilibrium within the joint.

In this study, we extended the previously reported patient-specific mandible model of de Zee et al. [3] with a detailed TMJ joint model taking into acount the joint contact forces and the Temporomadibular ligaments using the FDK methodology.

Patients & Methods

A patient-specific mandible model was built in the AnyBody Modelling System v. 5.1 using the FDK solver. The model is illustrated in Fig. 1.

Detailed information about the patient, the Computed Tomography (CT) scan, muscle insertions and mechanical properties are described in de Zee et al. [3].

The TMJ was modelled with four FDK degrees-of-freedom (DOF); the three rotational DOF between the skull and the mandible as well as medial/lateral translation. Both temporomandibular ligaments were modelled as three nonlinear springs [5] and contact forces computed based on the bone surfaces using a rigid contact model.

Three clinching tasks with 0.0, 1.0 and 2.0 cm mouth opening and a 150 N bite force were simulated and the resulting joint reaction forces compared between the two models.

Results

The computed joint reaction forces using the detailed FDK-based model and the planar constraint model are depicted in Fig. 2. Both models show asymmetric loading due to the patient impairment with largest joint reactions on the unaffected side. Independent of mouth opening, the planar constraint model only has a compression force component. Contrary, the FDK model has joint reaction force components in all three directions, which changes direction and magnitude as a function of mouth opening.

Discussion/Conclusion

In this study, we demonstrated the use of FDK to construct a detailed TMJ model. It will be possible now with this model to analyse the effects of joint morphology during different tasks and predict the detailed effects of interventions on the loading of the joint like distraction and orthodontic treatments.

References

1. Crowninshild RD, J Biomed Engin.100: 88-92, 1978.
2. de Zee M, et al. J Biomech.40(6): 1192-1201, 2007.
3. de Zee M, et al. J Biomech.42(8): 1049-1053, 2009.
4. Andersen MS, et al. Proceedings of ISB XIII, Brussels, Belgium, Abstract 343, 2011.
5. Mommersteeg TJA, et al. J Biomech.29(12): 1659-1664, 1996.

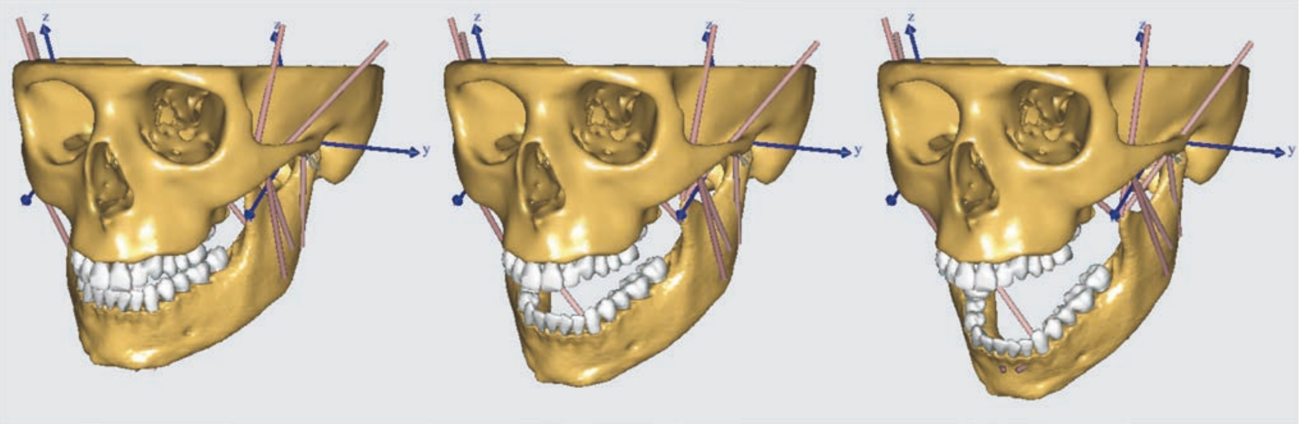

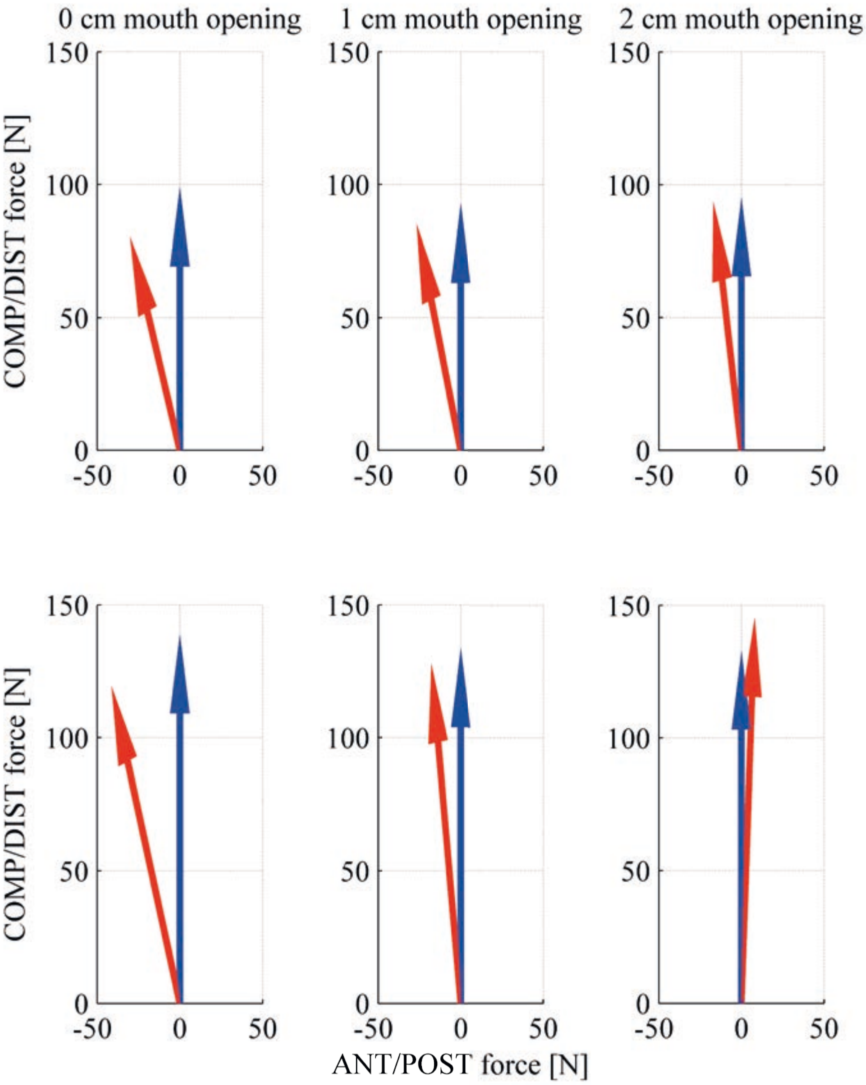

-The mandible model. The blue skull-fixed reference frames were used to represent the joint reaction forces. From left to right: 0.0, 1.0 and 2.0 cm mouth opening.

-Computed compressive forces plotted against anterior/posterior reaction forces for 0.0, 1.0 and 2.0 cm mouth opening and a bite force of 150 N. Top row: the right TMJ. Bottom row: the left TMJ. The red arrows show the TMJ reaction forces obtained using the FDK-modelled TMJ and the blue the results using the planar constraint model.

1A.9

Measurement of fluid pressures behind an acetabular cup in vitro.

Sarah Sydney
University of Bath, Bath, UK

A novel test rig was developed for the purpose of measuring periprosthetic fluid pressures in vitro.

Introduction

Osteolysis is a significant postoperative complication in hip replacements [1]. Current theories on osteolysis centre on particulate debris, but fluid pressures have also been implicated. It is believed that high fluid pressures may damage the bone-implant interface and allow access of fluid and wear debris into periprosthetic spaces [2].

The pressures generated in vitro by a loose femoral component have been investigated [3], as have pressures in osteolytic lesions [4]; however, fluid pressures behind a loose cup have not been extensively explored. The aim of this project was to design and test a rig capable of measuring pressures generated by the loading of an acetabular cup with different levels of fixation including the presence of interfacial fibrous tissue.

Methods

A test rig was developed that could measure pressure at three locations behind an acetabular cup (see Figure 1). A Stryker Trident hemispherical cup with PE liner was seated in a polyurethane hemisphere (M650 PU model board, John Burn, UK) with similar properties to Sawbones 30pcf foam. The cup was cyclically loaded to 1kN at 1Hz for 50 cycles, through a 28mm femoral head. Load was applied axially and at an angle of 30°. Synovial fluid was represented by vegetable oil, which was constrained by a rigid chamber. Pressures were measured using four miniature pressure transducers (XT-190, Kulite, UK). A static pressure was applied to the joint space by an elevated oil reservoir and measured by the top transducer. A synthetic material to simulate the presence of fibrous tissue was also used in some tests. Tests were carried out under different implant and loading conditions. Data were analysed using Matlab and Excel, and statistics packages R and SPSS.

Results

Pressure differences were measured at the rim and pole transducers, implying the presence of a pressure gradient, which would induce fluid flow behind the cup. The average pole pressure amplitude under axial loading was 62 kPa. The presence of a fibrous membrane decreased the pressure amplitudes measured behind the cup. The presence of screw holes in the acetabular shell produced a significant reduction in localised pressure on the angled transducer but not at the pole of the cup.

Discussion and Conclusions

This rig can be used to explore the fluid pressure generation potential of different implants and fixation conditions within the hip. Pressure results are comparable with similar studies [3, 4], although further development is required to improve the rig's loading capability. Improved understanding of periprosthetic fluid pressure can help investigate the causes of osteolysis and improve prosthetic component design.

References [1] Harris, W. H. (1995). Clin Orthop Relat Res(311): 46-53.
[2] Schmalzried, T. P., et al. (1992). J Bone Joint Surg Am 74(6): 849-863.
[3] Bartlett, G. E., et al. (2008). Med Eng Phys 30: 1042-1048.
[4] Walter, W. L., et al. (2005). J Arth 20(8): 1042-1048.

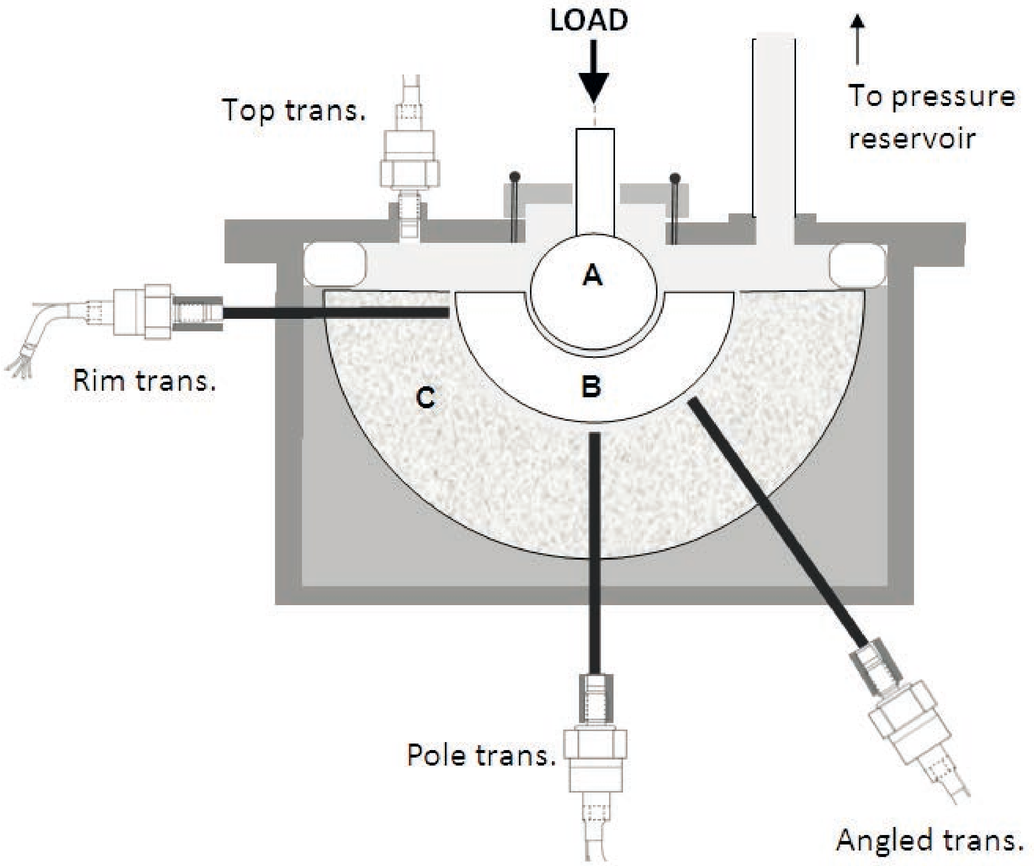

Figure 1: Simplified image of rig showing A) femoral head, B) Prosthetic cup, C) bone analogue hemisphere

1B.1

Preosteoblasts response to Ti6Al7Nb surfaces modified by plasma electrolytic oxidation

Nicole de Groot
Delft Technical University, Delft, The Netherlands.

The morphology of preosteoblasts, their metabolic activity and matrix mineralization potential are affected by the change in surface characteristics following plasma electrolytic oxidation of Ti6Al7Nb alloy under different conditions.

One possibility to extend the lifetime of metallic endosseous implants is to provide surface stimuli that favor cellular interactions involved in osseointegration. The porous TiO_2 layers produced by plasma electrolytic oxidation (PEO) on titanium and its biomedical alloys offer attractive features that include chemical biocompatibility, very good adhesion to the metallic substrate, micro-porous topographies and specific surface chemistries. The effects of oxide characteristics on cellular functionsare however not yet clearly established.

The aim of this study was to assesspreosteoblasts responseto two different surfaces produced by PEO on Ti6Al7Nb alloy. Therefore, the metallic substrates have been oxidized galvanostatically to153 V and 242 V using calcium-acetate/calcium glycerophosphate electrolyte. The oxidized samples were sterilized by thermal treatment at 110°C for 1h. The response of preosteoblasts (Simian-Virus Human Fetal Osteoblasts) included cells morphology and metabolic activity up to 7 incubation days and extracellular matrix mineralization after 7, 14 and 21 days. The in vitro cell response was assessed by Scanning Electron Microscopy, Fluorescence Microscopy, Alamar Blue test and Xylenol Orange staining. All the experiments have been performed at least in triplicates with polystyrene cultures as positive controls. Prior to cell culturing, the oxidized surfaces have been characterized for average roughness, pore size and porosity, chemistry and wettability using Mechanical Stylus Profilometry, Scanning Electron Microscopy with Energy Dispersive X-ray analysis and Drop Shape Analysis.

With increasing the final oxidation voltage, morphology and chemistry of surfaces changed significantly. The surfaces produced at 153 V (PEO153) revealed a fine porous morphology with most of the pores in the submicron range, an average roughness of 0.19 ± 0.03 µm and a Ca/P atomic ratio of about 1.0. In comparison, the surfaces produced at the highest voltage (PEO242) were relatively rough (1.43 ± 0.08 µm) and less porous, showing some larger pores protruding from the surface and an increased Ca/P ratio. The PEO treatment enhanced the hydrophilicity of titanium surfaces.

The in vitro cell results indicated that both surfaces assisted cells growthover the investigated period of 21 days (see Fig.1 forPEO153 surface). However, after one day of culture, cells on the PEO153 surfaces revealed a well spread morphology, with numerous, thin pseudopodia extending on the porous surface, and a more uniform surface coverage. On the PEO242 surface, cells were mostly confined between the protruding pores and showed a relatively less spread morphology. Further, the metabolic activity of cells after 7 days was higher on the PEO153. Matrix mineralization was evidenced on both surfaces after 14 incubation days. However, a larger mineralized area was visible on the PEO153 surface and the trend was maintained after 21 days.

Under the conditions used in this study, the smoother surface with higher porosity and lower Ca/P ratio favored spreading of SV-HFO cells and enhanced their metabolic activity and mineralization potential.

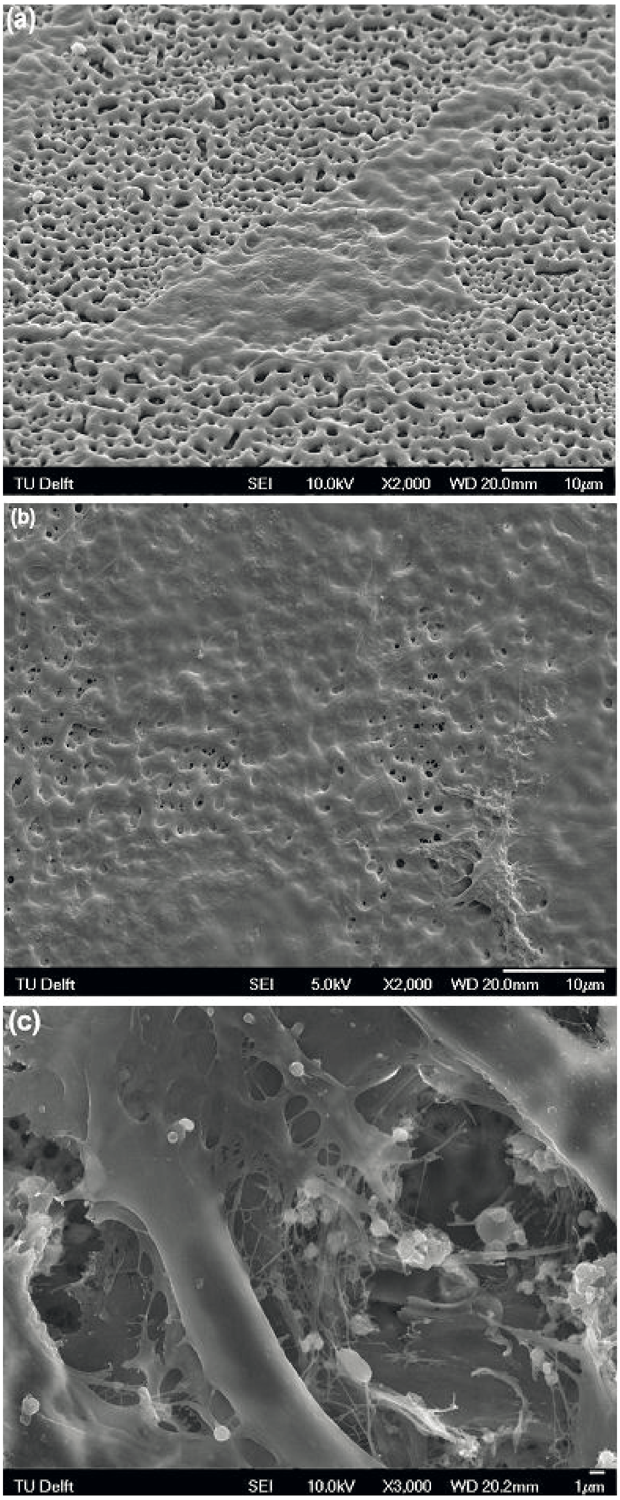

Fig.1 Evolution of surface-cells interface with incubation time: (a) 1 day; (b) 12 days; (c) 21 days. The SEM images show the potential of PEO153 surface to support SV-HFO cells adhesion, extracellular matrix synthesis and mineralization.

1B.2

Bacterial adherence to MWCNT/UHMWPE composites: searching new clinical applications for multi wall carbon nanotubes structures.

Gema del Prado
Instituto de Ciencia y Materiales (ICMA) CSIC-Universidad de Zaragoza, Zaragoza, Spain

The adherence of seven bacterial species to UHMWPE reinforced with carbon nanotubes was evaluated in this study. Adherence of five strains was significantly reduced ($p \leq 0.001$) when compared to that found on raw UHMWPE.

Introduction/ Objectives

Bacterial adherence has high clinical importance (1), being of particular concern in implant- related infections (2). Molecular functionalization using carbon nanotubes has recently shown some potential applications in biomedicine (3). Searching new biomaterials for prostheses engineering, this study has evaluated the adherence of seven bacterial species to a MWCNT reinforced polyethylene versus the raw material.

Material and Methods

The collection strain Staphylococcus aureus 15981 (4), and the reference strains Staphylococcus epidermidis ATCC 35984, Escherichia coli ATCC 29225, Pseudomonas aeruginosa ATCC 27853, Corynebacterium urealyticum ATCC 43044, Enterococcus faecalis ATCC 29212 and Mycobacterium fortuitum ATCC 6841, were included in the study. UHMWPE (GUR 1050®, Orthoplastic Ltd., Lancashire UK) discs with a diameter of 8 mm and 2 mm thick, containing or not 3 % wt multi wall carbon nanotubes, (MWCNT/ UHMWPE; NANOCYL® Nanocyl, Sambreville, Belgium) were tested as accretion surfaces.

For adherence studies, methodology of Pérez-Tanoira et al. (5) was applied, with minor modifications. Bacterial inoculum was prepared from an overnight culture in TSB-T at 37º C excepting for C. urealyticum and M. fortuitum, which were incubated in TSB-T plus Tween 80 for 72 hours. The sterilized surfaces were exposed to ≈10⁸ colony forming units (CFU)/mL during 90 minutes at 35º, washed with PBS (X 3) and incubated 24 hours at4ºC. Finally, surfaces were stained with Acridine Orange for 2 min. Adhered bacteria were visualized by fluorescence microscopy. Images of 10-20 fields/ surface were photographed at 40x magnification. Assays were always made in triplicates.

The percentage of bacterial coverage was determined by ImageJ software. Differences in bacterial adherence among surfaces as well as strains were individually analysed by unpaired t tests. Statistical significance was considered for $p \leq 0.001$.

Results

Figure shows the percentage of bacterial coverage per surface type (mean ± S.D). Significant reduction was observed in five bacterial species (S. aureus, P. aeruginosa, E. coli, C. urealyticum, and E. faecalis) when compared UHMWPE to the composite material.

E. coli registered the lowest adherence to UHMWPE compared to all the strains ($p \leq 0.001$) and equaled that S. aureus to MWCNT/ UHMWPE. S. epidermidis and E. faecalis were the most adherent strains, finding significant differences respect all the other strains in MWCNT/ UHMWPE composites and raw UHMWPE, respectively.

Discusion / Conclusions

Regarding to the experimental data, the capability of MWCNT/UHMWPE in diminishing bacterial adherence seems to be species-dependent. Although neither the adherence of S. epidermidis or M. fortuitum was significantly reduced, the use of composite reinforced with MWCNT could be interesting against S. aureus (a leading cause of biomaterial-related infection) and other pathogens, with several applications. Since differences between laboratory and clinical strains could be found, further studies must be performed using clinical isolates.

References

1 Donlan et al.Clin Microbiol Rev (2002)15:167-193
2. Kurtz et al. J Arthroplasty (2008) 23: 984-91
3. Wenrong-Yang et al. Nanotechnology (2007) 41: 412011 (12pp)
4. Valle et al. Mol Microbiol (2003) 48: 1075-87
5. Pérez-Tanoira et al. J Biomed Mat Research A (2012).100:1521-1528

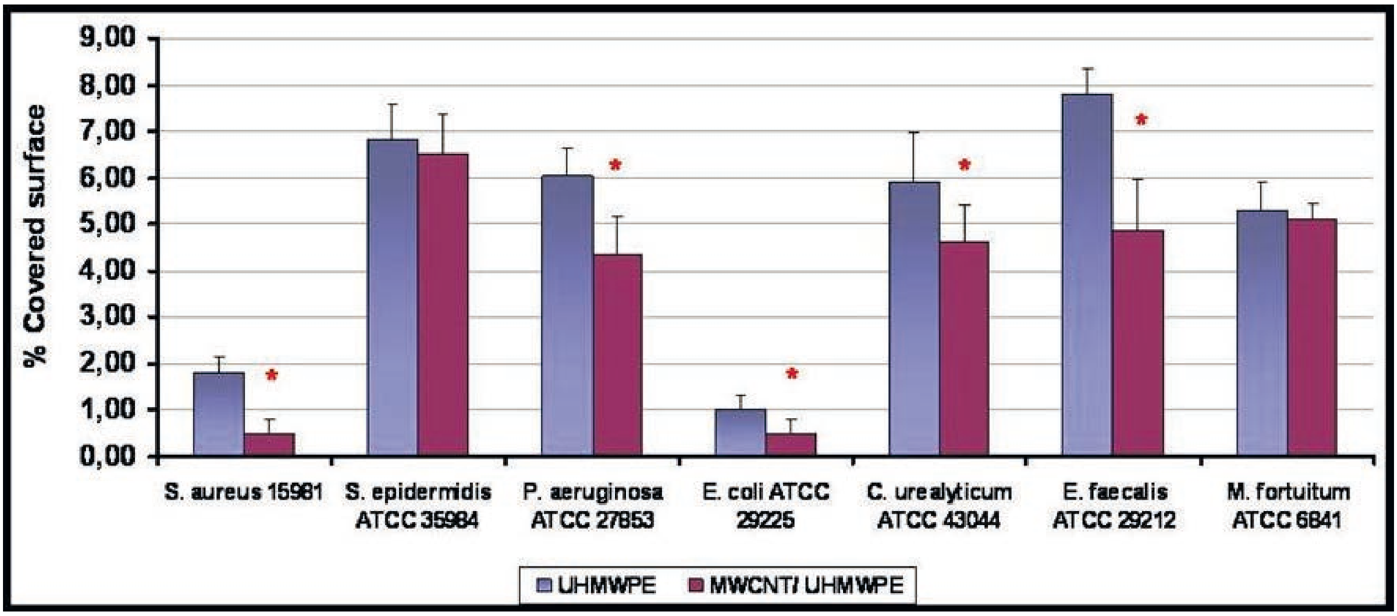

Percentage of bacterial coverage found in UHMWPE and MWCNT/UHMWPE (mean ± S.D).

1B.3

Human Polyethylene Granuloma Tissues Inhibit Bone Healing In A Novel Xenograft Animal Model

Christina Esposito
Surgical and Orthopaedic Research Labs, Sydney, Australia

Surgeons should remove polyethylene granuloma tissues during revision surgery, since these tissues may slow bone healing around a newly implanted prosthesis. This model provides a method for delivering clinically relevant sized particles into an in vivo model for investigation.

Introduction

Progressive periprosthetic bone loss, or osteolysis, is a biological response to wear debris that threatens the survival of joint replacements. To understand the pathogenesis of periprosthetic osteolysis, it is important to consider both phagocytic cells producing cytokines in the pseudocapsule and the cells they effect, that is the osteoclasts and osteoblasts in bone adjacent to the prosthesis.

In patients with conventional polyethylene joint replacements, surgeons can usually remove the source of osteolysis (polyethylene) during revision surgery but cannot always remove all of the inflammatory granulomatous tissues in the joint. We used a human/rat xenograft model to evaluate the effects of polyethylene granuloma tissues on bone healing.

Patients and Methods

Human osteoarthritic (OA) and periprosthetic tissues collected during primary and revision hip arthroplasty surgeries were transplanted into the distal femora of athymic (nude) rats (Figure 1 shows xrays of revision patients). The morphology of the tissues was assessed before and after implantation and the bone response to the tissues was evaluated after 1 week and 3 weeks using micro-computed tomography (CT), histology, and immunohistochemistry.

Results

The bone volume fraction (% bone in defects) measured with micro-CT was higher in defects filled with OA tissues compared to those with polyethylene granuloma tissues after 3 weeks in vivo (Figure 2). The majority (7 out of 10) of defects filled with osteoarthritic tissues healed, while only 3 out of 14 (21%) of defects with polyethylene granuloma tissues healed ($p=0.01$). No difference was not found after 1 week in vivo ($p=0.15$). The morphology of Figure 3 shows viable human tissues prior to implantation (A and D), and various degrees of necrosis after 1 week (B and E) and 3 weeks in vivo (C and F). New bone was confirmed histologically in 61% of defects after 1 week and 81% of defects after 3 weeks. Defects with granuloma tissues contained viable macrophages with polyethylene debris. Multinucleated cells in polyethylene granuloma tissues expressed Cathepsin-K after 1 week in vivo.

Conclusions

Polyethylene granuloma tissues in trabecular bone defects inhibited bone healing.

Surgeons should remove polyethylene granuloma tissues during revision surgery when possible, since these tissues may slow bone healing around a newly implanted prosthesis. This model provides a method for delivering clinically relevant sized particles into an in vivo model for investigation.

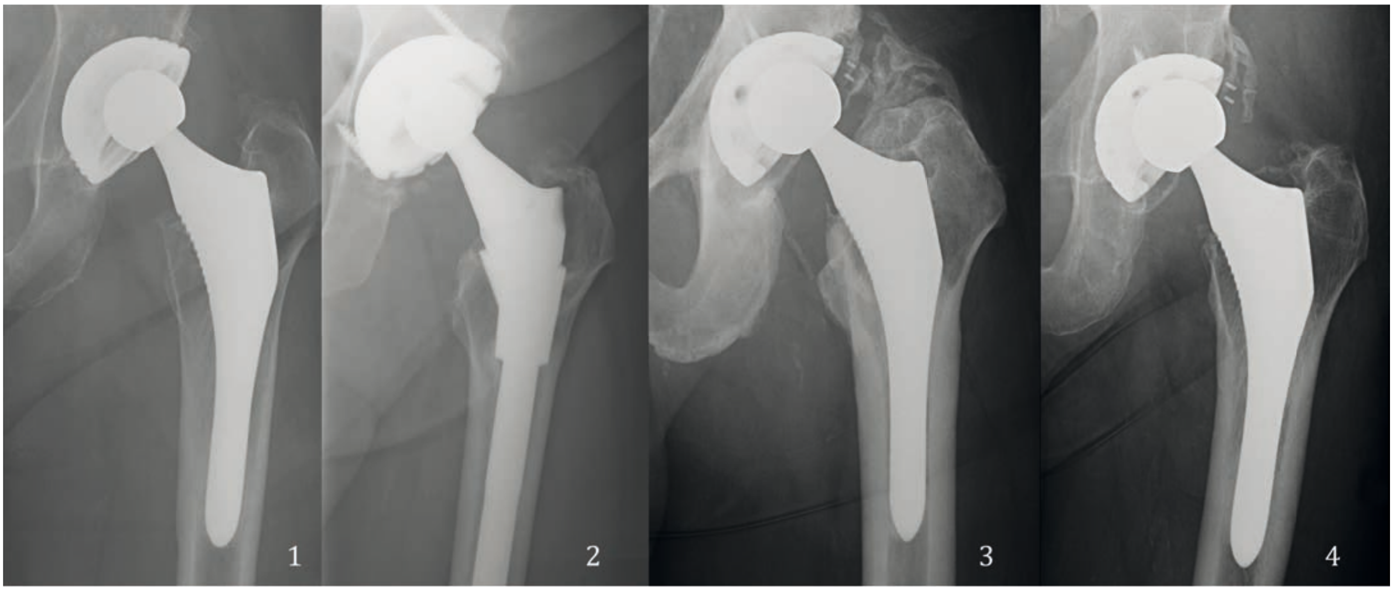

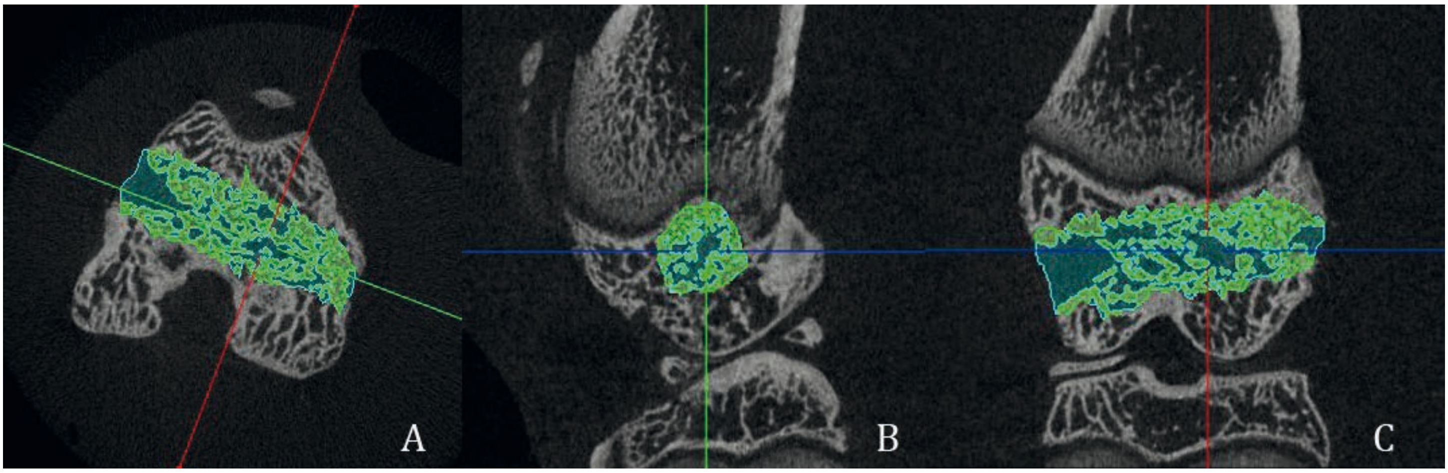

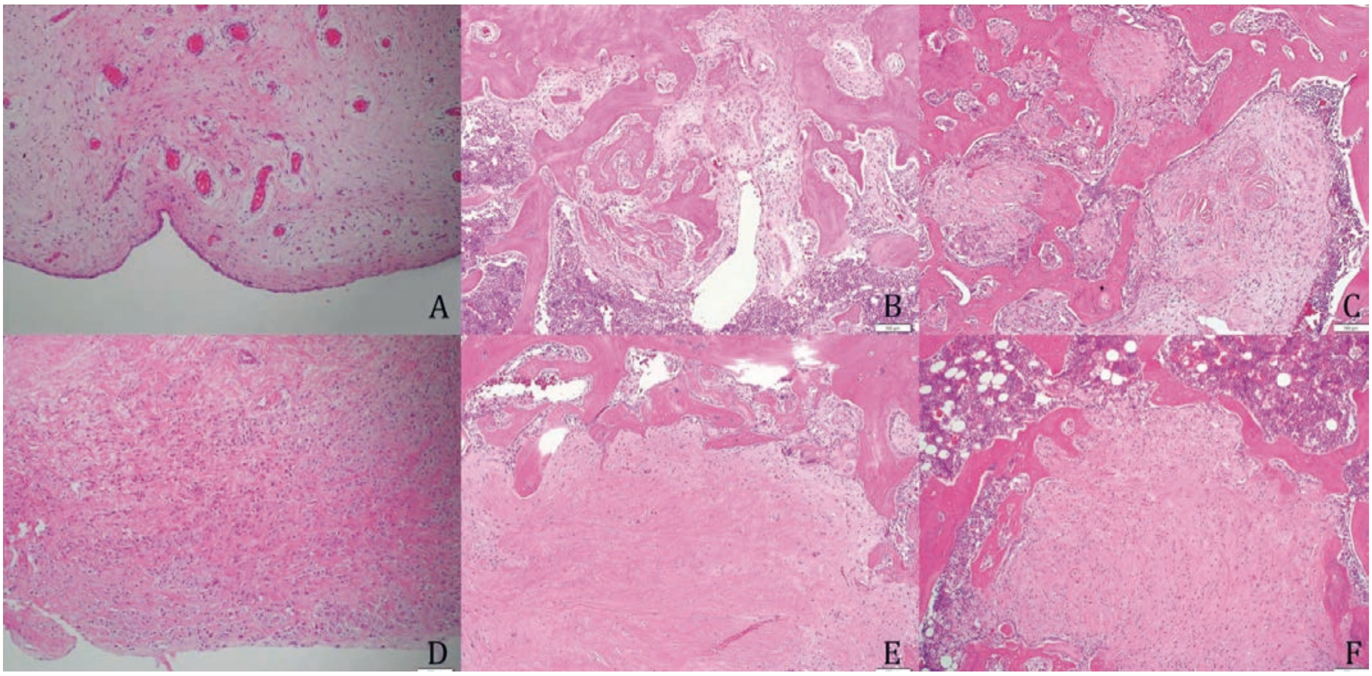

Radiographs of patients with conventional polyethylene hip replacements in vivo for a minimum of 15 years. Femoral and acetabular radiolucencies with irregular borders show osteolysis around the implants.

-Axial (A), sagittal (B) and coronal (C) micro-CT images of a distal femur of a 12 weeks old nude rat with a drill-hole defect. This defect was filled with osteoarthritic tissues and healed after 3 weeks.

-Representative photomicrographs (10x objective magnification) of human hematoxylin and eosin stained osteoarthritic tissues (A) prior to implantation, (B) 1 week after implantation and (C) 3 weeks after implantation, and micrographs of human polyethylene granuloma tissues (D) prior to implantation, (E) 1 week after implantation and (F) 3 weeks after implantation (F) in bone defects in nude rats.

1B.5

A method to preserve tensile properties of radiation crosslinked polyethylene

Andrew George
Department of Orthopedic Surgery, Brigham and Women's Hospital, Harvard Medical School, Boston MA02115, USA

Radiation crosslinking has been shown to decrease wear rate in polyethylene used in joint replacements but it also decreases tensile properties. This study shows that decrease in tensile strength and ductility can be minimized by melt-compression prior to irradiation.

Introduction:

Radiation crosslinking has been shown to decrease the rate of wear of polyethylene (PE) in total joint replacement prostheses substantially, however, also decreases several mechanical properties such as tensile strength and ductility [1, 2]. In this study, we hypothesized that disentangling PE via melt compression followed by strain recovery and recrystallization would, after irradiation, minimize the reduction in tensile strength and ductility (or maximum strain). Such a PE containing Vitamin E would be resistant to oxidation [3], resistant to wear due to crosslinking and maintain high tensile properties with a potential for use in joint replacements where they are subjected to high stresses.

Methods:

Compression molded sheets of GUR 1020 grade PE containing 0.1% Vitamin E served as control PE. Cylinders of 25.4mm diameter and 25.4mm height were compressed to a strain of 4.75t at 160°C in a hydraulic press and maintained for 16 hours. Thereafter, the load was released and the resulting discs were allowed to relax prior to recrystallization. These samples (C-XPE) and a set of sheets of 1mm thickness, which were heated to 160°C and cooled without any deformation (XPE) were irradiated to a dose of 100kGy using electron beam radiation at room temperature. Equilibrium swelling experiments were conducted to provide crosslink density; differential scanning calorimeter measurements provided degree of crystallinity and tensile tests provided modulus, yield stress, ultimate tensile stress and maximum strain.

Results:

Equilibrium swelling experiments showed that XPE had 18% higher crosslink density compared to C-XPE (ANOVA, p

Discussion/Conclusions:

This study shows that XPE, which was not deformed in the melt state and relaxed, had a higher crosslink density than C-XPE despite having a slightly higher crystallinity and thereby less amorphous region available for crosslinking. This indicates that the melt-deformation led to disentangling of the macromolecules of PE since the 'effective' crosslink density observed via equilibrium swelling is the sum of both crosslinks due to the irradiation and the trapped entanglements, which act as physical crosslinks. The lower overall entanglement density of C-XPE is the most plausible reason for its enhanced ductility and tensile strength compared to XPE which was not disentangled prior to irradiation. In summary, disentangling PE by melt-deformation and relaxation prior to irradiation at room temperature can enhance the tensile strength and ductility of XPE by decreasing its 'effective' crosslink density.

References:

[1] McKellop H, et al. J Orthop Res 1999; 17(2):157-67 [2] Muratoglu O, et al. Biomat 1999; 29:1463-70 [3] Kurtz SM, et al. J Biomed Mater Res A, 2009;90(2):549-63

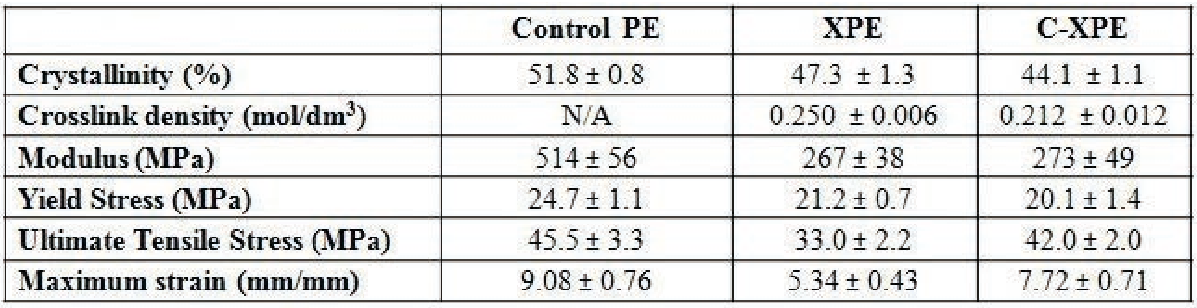

	Control PE	XPE	C-XPE
Crystallinity (%)	51.8 ± 0.8	47.3 ± 1.3	44.1 ± 1.1
Crosslink density (mol/dm^3)	N/A	0.250 ± 0.006	0.212 ± 0.012
Modulus (MPa)	514 ± 56	267 ± 38	273 ± 49
Yield Stress (MPa)	24.7 ± 1.1	21.2 ± 0.7	20.1 ± 1.4
Ultimate Tensile Stress (MPa)	45.5 ± 3.3	33.0 ± 2.2	42.0 ± 2.0
Maximum strain (mm/mm)	9.08 ± 0.76	5.34 ± 0.43	7.72 ± 0.71

Table 1. Crystallinity, Crosslink density and Tensile properties of Control PE, XPE and C-XPE

1B.7

Synthetic material to replicate fibrous tissue occurring in joint replacement.

Samantha Wright
University of Bath, Bath, UK

The study of the implant-bone interface membrane that forms following joint replacement is crucial for the understanding of long-term fixation stability. A synthetic material analogous to the natural membrane was assessed for use in future in-vitro studies.

Introduction

The formation of a fibrous membrane at the implant-bone interface following total hip replacement is thought to be a contributing factor to the occurrence of periprosthetic osteolysis. Some form of fibrous membrane will develop at the interface between the bone and implant or cement post-surgery (1). Although the shape and effect of this membrane can vary, in the acetabulum it usually takes the form of focal defects with uncemented cups and grows linearly around the hemisphere from the equator when the cup is cemented (2). There is currently no standard analogous synthetic material to the fibrous membrane, and its presence is rarely accounted for during in vitro implant testing, despite its compromising effect on joint stability. This study aimed to select a suitable material that was analogous to the natural membrane in terms of its key mechanical properties which include; an ability to release and reimbibe synovial fluid and an elastic modulus similar to that of the natural membrane (1.98MPa) (3).

A preliminary test was then carried out to establish the effect that the synthetic membrane has on implant stability. By proving that the presence of a fibrous membrane substitute significantly affects the results of implant stability testing, the material can be incorporated into future in vitro testing.

Methods

After identifying and sourcing various potential candidate materials, permeability, resorption and compression tests were performed on each sample to assess their suitability. Bespoke permeability and reabsorption test rigs were designed to assess which candidates fulfilled the criteria, followed by compression testing to establish the elastic modulus.

A micromotion investigation was then conducted using the selected material to analyse the effect of the synthetic membrane on implant stability. A rig was designed to replicate the hip joint which could allow the relative motion between a press-fit cup and a model of the acetabulum to be measured using an LVDT, whilst the cup was subjected a cyclic load simulating walking (Fig 1). Tests were carried out with and without membrane present and with axial and 30° loading.

Results

From the materials selection testing, an all-purpose cloth (comprised viscose, cotton, polypropylene and polyester) was selected to be used as substitute for the natural fibrous membrane, which had an elastic modulus of 2.81MPa.

A comparison of the micromotion results between tests with and without the presence of the membrane concluded that there was a significant increase in micromotion between bone and implant when a membrane was present (Fig 2).

Discussion and Conclusion

The study demonstrated that a synthetic material exhibiting mechanical properties analogous to that of the natural fibrous membrane currently exists. A micromotion test confirmed that the presence of such material reduced the stability of the implant. The material has the potential to be used to replicate the commonly occurring focal defects at the interface for more physiological in vitro testing.

References

Goldring, S.R., et al., JBJS (1983); 65: 575-584.
Agarwal, S., Current Orthopaedics (2004); 18(3): 220-231.
Hori, R.Y. et al., J Biomed Mater Res (1982); 16(6): 911-27.

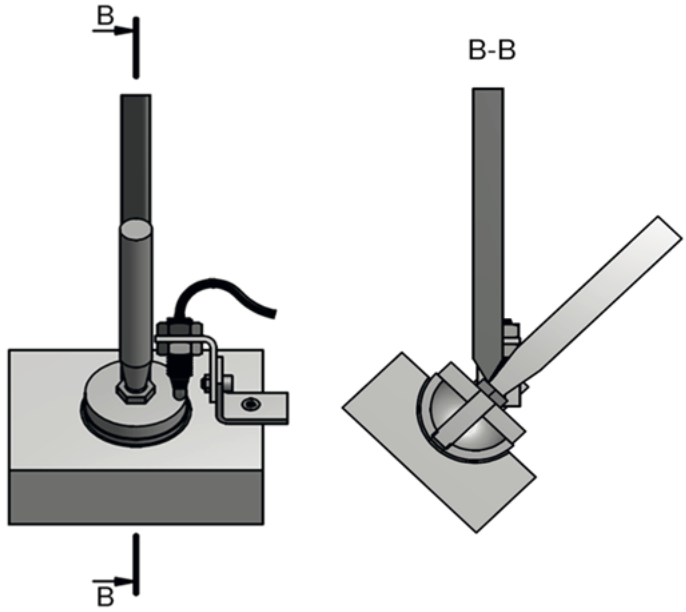

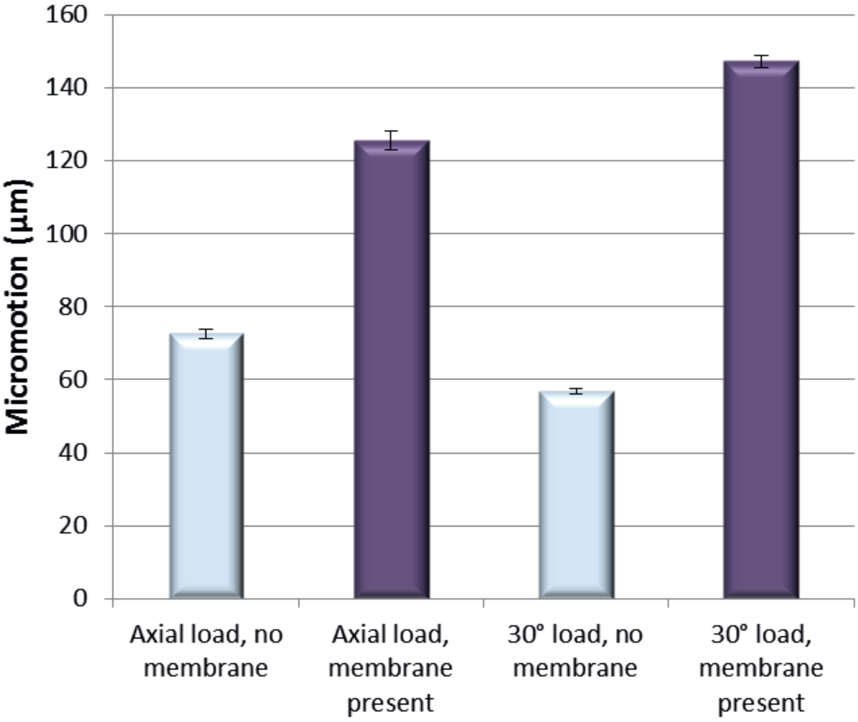

-A representation of the Micromotion Rig in its testing position

-A chart comparing the average micromotion levels and standard deviations with and without the membrane present

1B.9

Biodegradation of magnesium implants ZX50 and WZ21 in a transepiphyseal rat model

Tanja Kraus
Medical University Graz, Graz, Austria

Slow degrading magnesium alloy WZ21 does not induce adverse effects on the epiphyseal growth plate, which is a prerequisite for biodegradable implants that are considered as osteosynthetic devices in paediatric surgery.

Introduction

Biodegradable implants might present a promising approach for osteosynthesis in trauma surgery, as their self-degrading properties would render surgical interventions for implant removal unnecessary (1). For the purpose of Elastic Stable Intramedullary Nailing (ESIN) in paediatrics, magnesium seems to be an ideal material due to its excellent properties (2). As a follow-up study to a transcortical model (3), this study aims to investigate the epiphyseal reaction to two different magnesium alloys in a transepiphyseal rat model.

Methods

Twelve male Sprague-Dawley rats underwent a ‘patella slide bearing’ surgery. Drill holes with a diameter of 1.6mm were performed transepiphyseal through the distal femoral growth plate. Each rat received either a fast degrading ZX50 or a slow degrading WZ21 biodegradable magnesium pin (diameter 1.6mm, length 8mm; n=6 per group). The contralateral leg was also drilled and served as a control. Online µCT monitoring was performed to observe pin degradation rate, reactions of the growth plate and bone growth discrepancies for 3 months.

Results

Compared to the transcortical model, the pin degradation rate of both alloys (ZX50 and WZ21) were increased approximately by a factor 2 due to the transepiphyseal/intramedullary implantation ($p<0,05$). The ZX50 pins degraded fast and high amounts of gas were formed insidethe medullary cavity leading to a local destruction of the epiphyseal growth plate. The bone growth was consecutively reduced by 6,3% (+/-2,1) in the ZX50 group. Leg length discrepancies to the contralateral leg were significant ($p<0,05$). WZ21 implants did not induce an adverse reaction of the epiphyseal growth plate and did not show significant leg length discrepancy compared to the contralateral leg (7% (+/-3,3); $p=0,63$). Only few release of gas was exhibited, which was resorbed easily by the surrounding tissue.

Conclusion

The fast release of magnesium ions during ZX50 degradation leaded to massive gas formation according to the chemical reaction $Mg + 2H_2O$ → $Mg(OH)_2 + H_2$ which induced a degeneration of the epiphyseal growth plate. A consecutive diminished bone growth limits its use for clinical applications. WZ21, however, achieved good results and the effect on the growth plate did not differ to a solely drill hole lesion. Therefore WZ21 fulfils a prerequisite for a use as osteosynthetic device in paediatric trauma surgery.

References:

(1) Staiger MP, Pietak AM, Huadmai J, Dias G. Magnesium and its alloys as orthopedic biomaterials: a review. Biomaterials. 2006;27:1728-34.

(2) Claes L. Mechanical Characterization of Biodegradable Implants. Clinical Materials 1992;10:41-6.

(3) Kraus T, Fischerauer SF, Hänzi AC, Uggowitzer PJ, Löffler JF, Weinberg AM. Magnesium alloys for temporary implants in osteosynthesis: in vivo studies of their degradation and interaction with bone.Acta Biomater. 2012 Mar;8(3):1230-8. Epub 2011 Nov 11.

2A.1

The immune response to bacterial contamination of orthopaedic implant materials

Edward Rochford
AO Research Institute, Davos, Switzerland

A study into the role of material choice in infection risk, focusing on the immune system. Key aspects of the immune reaction were found to differ in vitro in response to different orthopaedic materials with and without additional bacterial stimulation.

Introduction:

The presence of any implant compromises local host immune responses and increases infection risk[1]. Previously it has been shown that implant material can alter the immune response, which subsequently may influence infection risk[2]. In this study, a range of orthopaedic biomaterials have been examined to identify the role of material choice in the immune response to infection in vitro.

Methods:

Materials: The following materials were used in this study to compare different surface chemistries and topographies: micro-rough titanium (TS), electropolished titanium (TE), Titanium-Aluminium-Niobium (NS), electropolished Titanium-Aluminium-Niobium (NE), stainless steel (SS)[a], injection moulded polyetheretherketone(PEEK) (PO), machined PEEK (PA) and oxygen plasma treated PO (PO30) and PA (PA30)^b as previously described[3]. For experiments requiring adherent bacteria, approximately 2x10^5 Staphylococcus aureus JAR cm^{-2}were adhered to the materials using a bacterial adhesion chamber[3]. All experiments were performed in triplicate.

Complement Activation: The activation of complement by the materials with and without pre-adhered S. aureus JAR was assessed by exposing the samples to human serum for one hour and measured using a C3a-desArg ELISA.

Leukocyte Stimulation: THP-1 monocyte cells were used to screen for NF-κB activation by the materials using the Quanti-blue assay with and without additional lipopolysaccharide (LPS) stimulation. Additionally, peripheral blood mononuclear cells (PBMC) were isolated from healthy donors and exposed to the materials, the materials and LPS or the materials pre-contaminated with S. aureus JAR for 48 hours. The PBMC were harvested for real-time PCR and samples of the cell media taken for multiplex analyte detection by Bioplex. The Bioplex screened for IL-8, IL-10, IL-12(p70), TNF-α, MIP-1α and G-CSF.

Results:

In general, TS produced the lowest level of immune-activation as illustrated by the complement (Fig.1), NF-κB and cytokine assays in the absence and presence of bacteria. However, in the presence of additional bacterial stimulation TS gave similar results as the other metals for complement activation and NF-κB stimulation. In contrast, PEEK was generally the most stimulatory of the materials; increasing complement activation, NF-κB, IL-12 and TNF-α secretion. Interestingly oxygen plasma treatment led to increased complement activation (Fig.1), TNF-α and IL-12 production but decreased NF-κB stimulation in the presence of bacteria or LPS. MIP-1α secretion was dependent on the material, though no clear trend for material classes could be identified (Fig.2).

Discussion / Conclusion

There appears to be differences in the immune response due to surface chemistry, particularly between TS and PEEK. TS was often the least immune-stimulatory of the materials which may be a reflection of biocompatibility of this material. In the presence of additional bacterial stimulation TS gave a similar response as the other metals which may benefit removal of contaminating bacteria. In contrast to surface chemistry, roughness did not have a consistent effect on the immune response. To understand how these differences affect the immune response to bacterial contamination of an implant in a trauma wound deserves further in vivo investigation.

References:

[1] Elek,S. and Conen, P. (1957) Br.J.Exp.Pathol. 38:573-586. [2] Boelens,J.J., et al. (2000) J Infect.Dis 181:1337-1349. [3] Rochford,E.T.J., et al. (2011) ESB2011.

ACKNOWLEDGEMENTS:[a]Metal samples from Synthes, ^bPEEK samples from Invibio Biomaterial Solutions.

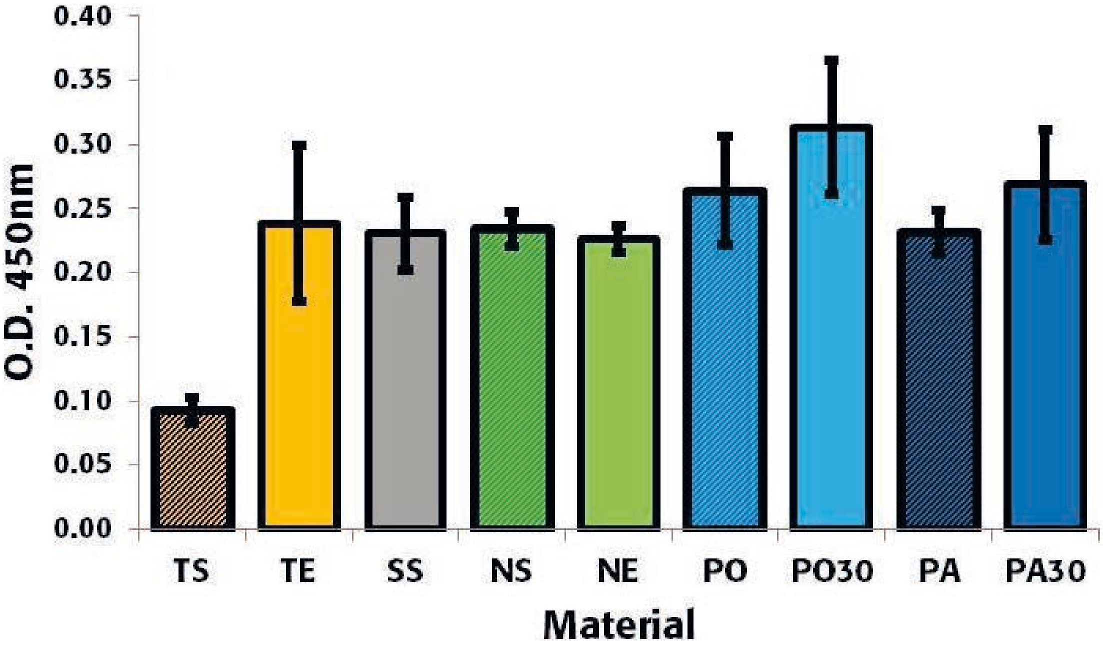

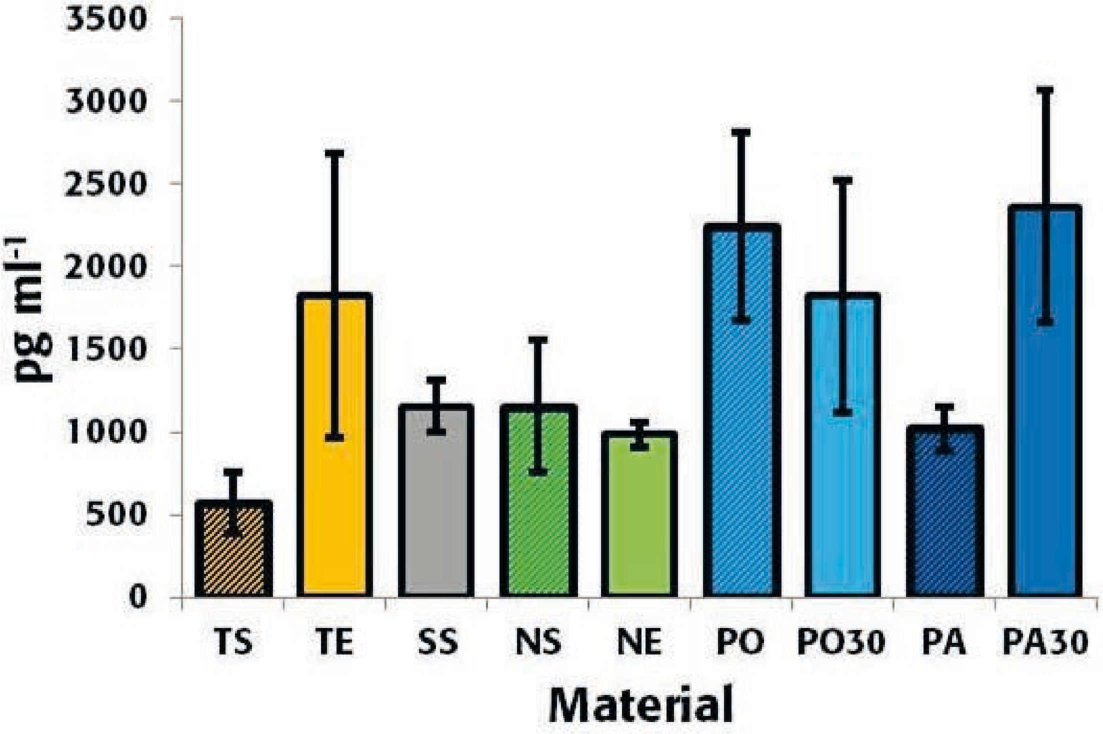

-Fig.1: Complement activation by the different materials without additional stimulation (n=3, ±s.e)
-Fig.2: MIP-1α secretion by PBMCs exposed to the materials coated with S. aureus JAR (n=3, ±s.e.)

2A.2

Augmented bone-implant constructs fail by shearing of the cement-screw interface: experimental and computational micromechanics

Samuel Basler
Institute for Biomechanics, ETH Zurich, Switzerland

Augmented bone-implant constructs showed non-linear deformation patterns in image-guided push-in tests and failed through shearing at the cement-screw interface. The ultimate force was highly correlated with the cement volume and trabecular bone morphometric parameters (R2 = 0.86).

Introduction

Augmentation using bone cement is a common treatment option to improve screw anchorage during fracture fixation in osteoporotic bone [1, 2]. However, little is known about the optimal parameters such as cement volume and distribution, as well as about the failure modes of augmented bone-implant constructs. It was the aim of this study to subject augmented trabecular bone screws to push-in tests combined with time-lapsed CT imaging. We hypothesized that the deformations and failure of augmented bone-screw specimens depend on the cement volume and on the peri-implant bone quality.

Methods

Trabecular bone screws (diameter: 2.7 mm) were inserted into bovine trabecular bone cylinders (diameter: 16 mm, height: 16mm) with a relatively narrow range of bone volume fractions (BV/TV between 23 % and 36 %). Augmentation was carried out using contrast-enhanced (ZrO_2) PMMA, resulting in a variety of cement volumes and distributions. Two non-augmented control specimens received the screw only. The specimens were subjected to stepwise quasi-static push-in tests in combination with high-resolution CT imaging according to the principle of image-guided failure assessment (IGFA). Deformable image registration was used to compute the peri-implant displacement fields. In order to study the interplay between trabecular bone, cement and screw, micro-finite element (µFE) models were additionally created based on the baseline CT image. Linear-elastic material properties were assigned to the components (E_{bone} = 6.8GPa, E_{cement}= 1.8 GPa, E_{screw} = 120 GPa) and fully bonded interfaces were assumed.

Results

Complex failure mechanisms were observed in the time-lapsed CT images (Fig 1). All specimens showed failure of the cement-screw interface and fragmentation of the cement. The ultimate force was highly correlated with the cement volume ($R^2 = 0.75$). In multiple linear regression additionally accounting for BV/TV and trabecular spacing (Tb. Sp), the coefficient of determination was $R^2 = 0.86$. Compared to non-augmented controls, up to a ten-fold increase in ultimate force was achieved. Highly non-linear displacement fields were found in the experiments, whereas in the computational models they were much more linear (Figs 2 and 3). In the experiments, only the cement and bone immediately adjacent to the screw were displaced, while the computational models predicted a displacement of the entire augmented construct.

Discussion / Conclusion

Our hypothesis was confirmed, since the ultimate force depended strongly on the cement volume as well as morphometric parameters in the peri-implant bone. The cement-screw interface seems to be a weak spot which underwent failure in all specimens. Our experimental and computational data provide evidence that the deformation patterns of augmented bone-implant constructs are governed by non-linear effects. The difference in elastic moduli alone did not produce non-linear displacement profiles in the computational models. Therefore, interfacial sliding and non-linear material behavior are believed to explain the non-linearities found in the experimental displacement fields. Bone debris at the bone-screw interface potentially weakens the connection between the two components. Clinically, a stronger interface may result from cement injection prior to implant insertion.

References

[1] Chen et al, Clin Biomech, 24:613-618, 2009.
[2] Stadelmann et al, J Biomech, 43:2869-2874, 2010.

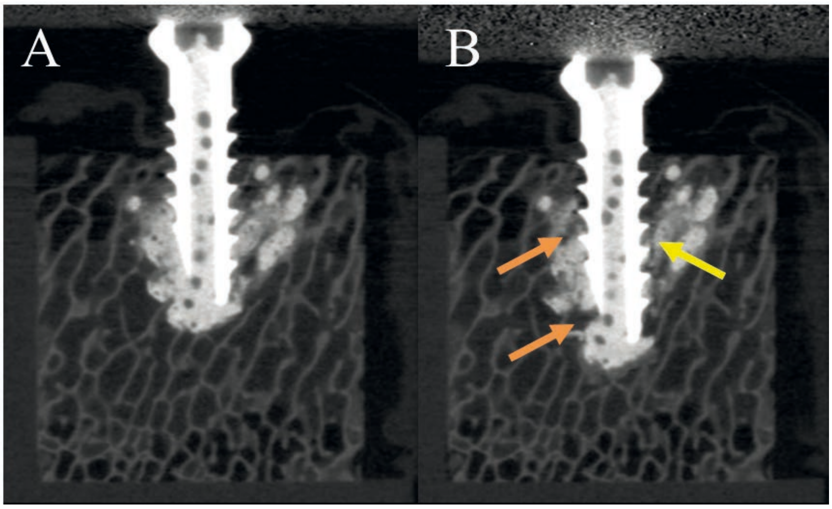

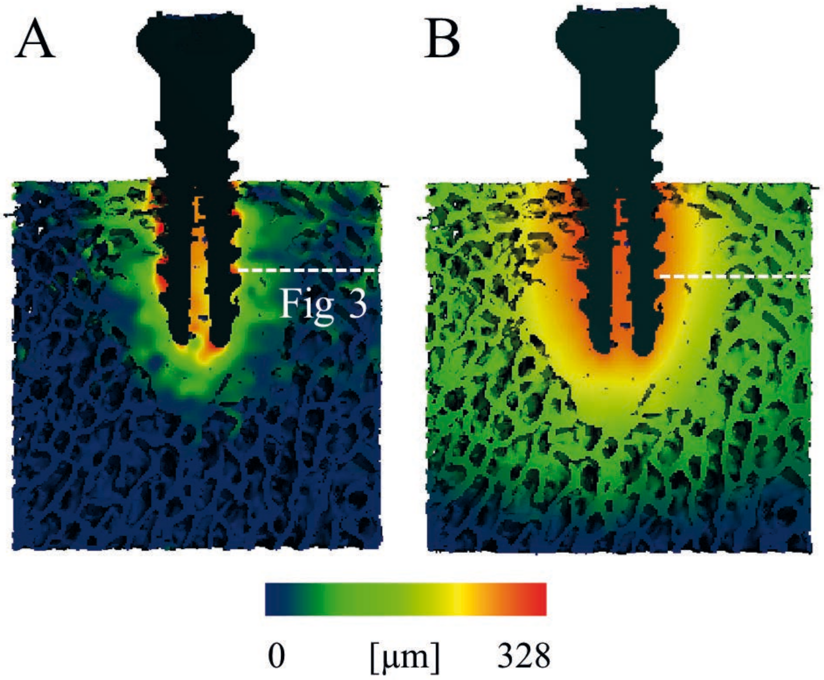

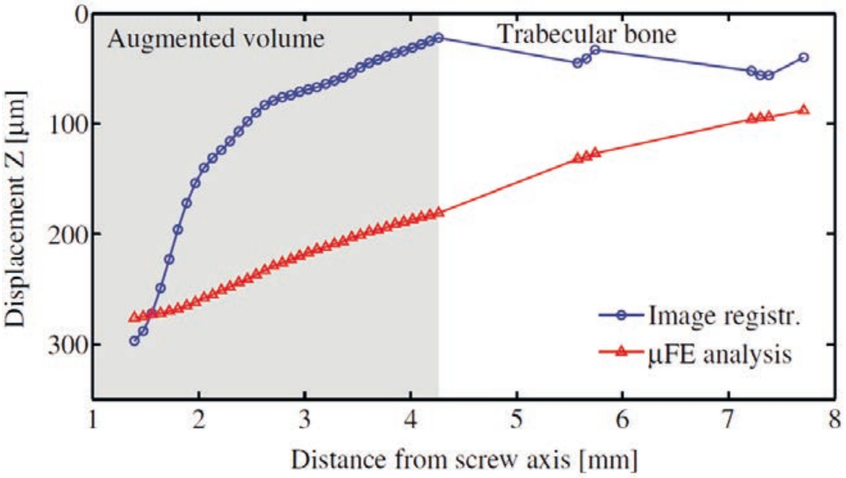

-Grayscale images of initial (A) and final (B) state of IGFA push-in test. Note: failure of cement-screw interface (yellow) and cement fragmentation (orange).
-Visualizations of the Z displacement fields obtained by experimental deformable image registration (A) and µFE analysis (B) for an augmented specimen at 328 µm nominal displacement. Note: dotted line represents location of displacement profile in Fig 3.
-One-dimensional profiles of Z displacements for location as indicated in Figure 3. The nominal displacement was 328 µm. Note: gaps in the profiles represent void spaces in the trabecular structure.

2A.3

IN VITRO SUSCEPTIBILITY TO ANTIBIOTICS IN BIOFILMS OF STAPHYLOCOCCI ISOLATED FROM ORTHOPAEDIC INFECTIONS

Diana Molina-Manso
IIS-Fundación Jiménez Díaz, Madrid, Spain

Biofilm susceptibility of two collection strains and 34 staphylococci isolated from prosthetic joint infection against nine antibiotics was studied. All the antibiotics tested lost their efficacy among sessile bacteria, being rifampin and tigecycline the less affected ones.

OBJECTIVES:
Prosthetic joint infections (PJI) are related to the formation of biofilms mainly by Staphylococcus aureus and Staphylococcus epidermidis (1). The antibiotic susceptibility is normally measured by MIC/MBC, but these data may be insufficient to detect the true antibiotic susceptibility in the biofilm. The aim of this study was to evaluate the sensitivity of biofilm-forming clinical strains of S. aureus and S. epidermidis isolated from PJI.

METHODS:
32 clinical strains (17 S. aureus and 15 S. epidermidis) isolated from patients with PJI, as well as 2 collection strains (S. aureus 15981 and S. epidermidis ATCC 35984) were tested against 9 antibiotics (rifampin, vancomycin, tigecycline, clindamycin, cotrimoxazole, ciprofloxacin, cloxacillin, daptomycin and fosfomycin). MIC was determined by microdilution method or agar dilution according to EUCAST recommendations (2). MBC was also determined by plating the contents of the wells without visible growth after exposure to antibiotics. The Minimal Biofilm Eradication Concentration (MBEC) was determined using the Calgary Biofilm Device (CBD) (3). MIC and MBEC determinations were performed by triplicate. S. aureus ATCC 29213 was used as quality control strain.

RESULTS:
The antibiotics which showed the best antimicrobial activity against planktonic bacteria were tigecycline and daptomycin, with low MIC_{90} values (0.5 and 1 mg/L for S. aureus and 0.25 and 1 mg/L for S. epidermidis, respectively) and no resistant strains were detected. Fosfomycin, rifampin and vancomycin also showed good activity. Ciprofloxacin and cloxacillin exhibited a high percentage of resistant strains among both bacterial species (66.7% for both antibiotics in S. aureus; 37.5 and 62.5% for S. epidermidis respectively). Bactericidal activity was detected for most strains of both species with vancomycin, ciprofloxacin, cloxacillin and daptomycin.

Regarding the MBEC data, none of the antibiotics proved to be totally effective against biofilms in both species, with concentrations highly above MIC results. The best results were obtained with rifampin and tigecycline (Table). It is especially remarkable that only two S. epidermidis strains showed MBEC values similar to MIC with some of the antibiotics tested (≤8 mg/L).

CONCLUSION:
All the antibiotics tested in this study lost its efficacy when the bacteria grown in a biofilm. The concentration of antibiotic required to eradicate staphylococcal biofilms in PJI are much higher than that required to eradicate planktonic bacteria in almost all cases, being rifampin and tigecycline the most active antibiotics against sessile bacteria.

REFERENCES

1. Del Pozo JL, Patel R. Clinical practice. Infection associated with prosthetic joints. N Engl J Med.2009; 361(8):787-94.
2. EUCAST. Breakpoint tables for interpretation of MICs and zone diameters. In Version 2.0.2012.
3. Ceri H, Olson ME, Stremick C, Read RR, Morck D, Buret A. The Calgary Biofilm Device: new technology for rapid determination of antibiotic susceptibilities of bacterial biofilms. J Clin Microbiol.1999; 37 (6):1771-76.

Table 1. Susceptibility results in both species (*S. aureus* and *S. epidermidis*).

ANTIBIOTIC	***S. aureus***						***S. epidermidis***					
	MIC		MBC		MBEC		MIC		MBC		MBEC	
	MIC_{50}	MIC_{90}	MBC_{50}	MBC_{90}	$MBEC_{50}$	$MBEC_{90}$	MIC_{50}	MIC_{90}	MBC_{50}	MBC_{90}	$MBEC_{50}$	$MBEC_{90}$
RIFAMPIN	0.015	4	2	>8	64	>64	0.015	0.015	0.06	0.5	32	64
VANCOMYCIN	1	2	4	16	>1024	>1024	2	4	2	4	>1024	>1024
TIGECYCLINE	0.25	0.5	4	>8	512	512	0.12	0.25	8	>8	256	512
CLINDAMYCIN	0.12	>8	4	>8	>1024	>1024	0.12	>8	4	>8	>1024	>1024
COTRIMOXAZOLE	1	4	4	32	>1024	>1024	2	>32	16	>32	>1024	>1024
CIPROFLOXACIN	>8	>8	>8	>8	>1024	>1024	0.5	>8	1	>8	512	>1024
CLOXACILLIN	>32	>32	>32	>32	>1024	>1024	0.5	>32	1	>32	>1024	>1024
DAPTOMYCIN	0.5	1	1	2	>1024	>1024	0.5	1	1	1	>1024	>1024
FOSFOMYCIN	1	16	64	128	>1024	>1024	1	4	6	64	>1024	>1024

2A.4

THE MASQUELET TECHNIQUE FOR SEGMENTAL TIBIAL DEFECTS A PRECLINICAL OVINE MODEL

Chris Christou
Surgical and Orthopaedic Research Labs, Sydney, Australia

The Masquelet technique is an effective and promising technique for the surgical management of large segmental defects. The optimal bone healing adjuncts to be used with this technique are yet to be discovered.

Introduction

The treatment of large segmental bone defects remains a clinical problem. This study examined the Masquelet technique and allograft alone and combined with autograft in an ovine critical sized defect model.

Methods

The Masquelet technique is a two stage procedure. A pseudo-synovial membrane is created by implanting a polymethylmethacrylate (PMMA) cement spacer for 4 weeks. The PMMA spacer is removed at 4 weeks and the site grafted. The Masquelet technique was performed in 14 adult sheep. The sites were grafted with either 100% gamma sterilised (25kGray) corticocancellous allograft (n=7) or 66% allograft/33% cancellous autograft (n=7). A sample of the induced membrane was collected at 4 weeks for histology and immunohistochemistry for VEGF. Tibias were harvested at 6 and 12 weeks after stage 2 for radiology, micro CT, histology and immunohistochemistry. The results were compared to a previously established control group (n=12) using the same experimental techniques.

Results

Histology of the induced membrane at 4 weeks revealed smooth fibrous pseudo-synovial membrane. The membrane consisted of a 2-3 cell layer of densely packed fibroblastic type cells adjacent and aligned parallel to the cement spacer, with deeper layers of randomly orientated collagen fibres and fibroblasts. The absence of macrophages indicated no immuno-reactivity to the presence of the cement spacer. VEGF expression in the membrane was found in the deeper layers of the capsular tissue and not in the 2-3 cell layer adjacent the spacer.

Radiographs confirmed callus formation at the osteotomy ends and the presence of graft material at 6 weeks. By 12 weeks the forming callus had progressed but did not manage to bridge the defect site, there was no indication of the presence of any graft material. MicroCT further confirmed the radiographic findings.

Conclusion

The Masquelet technique appears to be an effective method for providing a well enclosed cavity for the graft containment to assist the healing of critical sized segmental defects. The lack of full tissue bridging at the 12 week time point demonstrates the extreme healing environment encountered in the 5cm ovine tibial defect model. The presence of an increased radio dense tissue in both groups when compared to the empty (negative) control animals indicates a greater healing response, despite the incomplete union. No significant difference was found between 100% allograft or the mix. The graft materials were not visible radiographically at 12 weeks. The biologically active nature of the induced membrane may have increased the rate of graft resorption. Thus the ideal graft material to be used with this technique needs further investigation.

2A.6

Reduction of bacterial adhesion on Ti6Al4V surfaces functionalized with siloxanes

Miguel Angel Pacha Olivenza
Networking Research Center on Bioengineering, Biomaterials and Nanomedicine CIBER-BBN, Badajoz and Department of Applied Physics, Faculty of Sciences, Badajoz, Spain

This research will present the benefits, in relation to bacterial adhesion, of modifying the surface of the alloy Ti6Al4V with a bioactive surface coating composed of siloxanes molecules.

Introduction:
The development of biocompatible implants, employed in surgery and prosthetic devices, constitutes an active and challenging research domain in biomedicine. The titanium alloy Ti6Al4V combine robustness, high corrosion resistance and an acceptable biocompatibility that leads to researches on the material endeavoring better host responses. Nevertheless, after the implantation, microbial adhesion to its surface can provoke severe health problems associated to the development of biofilms and subsequent infectious processes.

This alloy has an outer layer dominated by Ti-OH groups after chemical oxidation, that can be functionalized. Focusing on these aspects, several routes are at present open to modify the surface. Coating with bioactive molecules, that stimulate osteoblast maturation and minimize bacterial adhesion and biofilm formation [1], is expected to improve biological response to the implant. This is usually accomplished by means of phosphate-and/or siloxane-based coupling reagents which displace a proton from surface hydroxyl groups and give rise to layers of organic molecules covalently bonded onto the metal surface. Siloxane-reactive head groups, typically amino or halogen substituents, enable the subsequent attach of such bioactive molecules whose antifouling properties protect the surface against non-specific microbial adhesion [2].

Materials and Methods:
Ti6Al4V discs were first subjected to a chemical oxidation process by immersing in a piranha solution. Samples used as controls were not subjected to any further treatment. A second set of samples were immersed into a crystallizer containing 1 M solution of APTMS (3-aminopropyltrimethoxysilane) in wet toluene and were cured by heating in a oven at 120 ºC for 24 h (samples 100 % silanized). A third set of samples silanized 100 % with APTMS was immersed in a phosphate buffer solution (PBS) at room temperature under stirring for 48 h (samples 37 % silanized).

Two gram-positive strains with different EPS-production were used: Staphylococcus epidermidis ATCC35984 and Staphylococcus epidermidis ATCC35983.

Bacterial adhesion experiments were carried out with the help of a sterile reusable silicone chamber fixed to the sample surface. Then the bacterial suspension was added to the chamber well and the contact with the alloy surface was allowed for 30, 60 and 90 min. After the adhesion time, the silicone chamber was removed and adhered bacteria were counted using a kit Live/Dead Baclight L-7012.

Results and Discussion:
In general, bacterial adhesion is increased when the contact time is higher, except in the case of S. epidermidis3 adhered to the 100 % silanized surface for which adhesion remains constant no matter the contact time. The coating with siloxane molecules (37% and 100 % silanization) of the alloy provokes a statistically significant reduction in bacterial adhesion for any time tested (see Fig.1 and Fig.2).

References:
[1] Lowery C.A. et al., J Med Chem 53(2010) 7467-7489.
[2] Bosker W.T.E. et al., J Colloid Interf Sci 286(2005) 496-503.

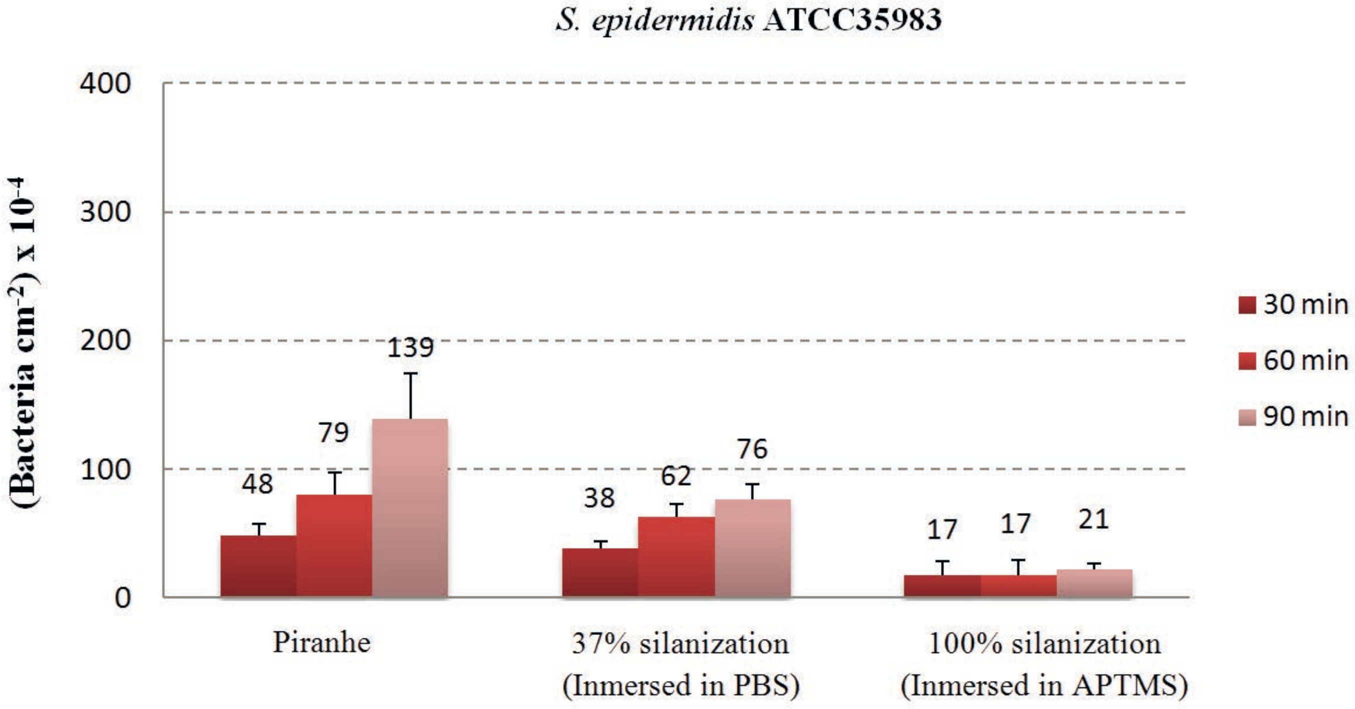

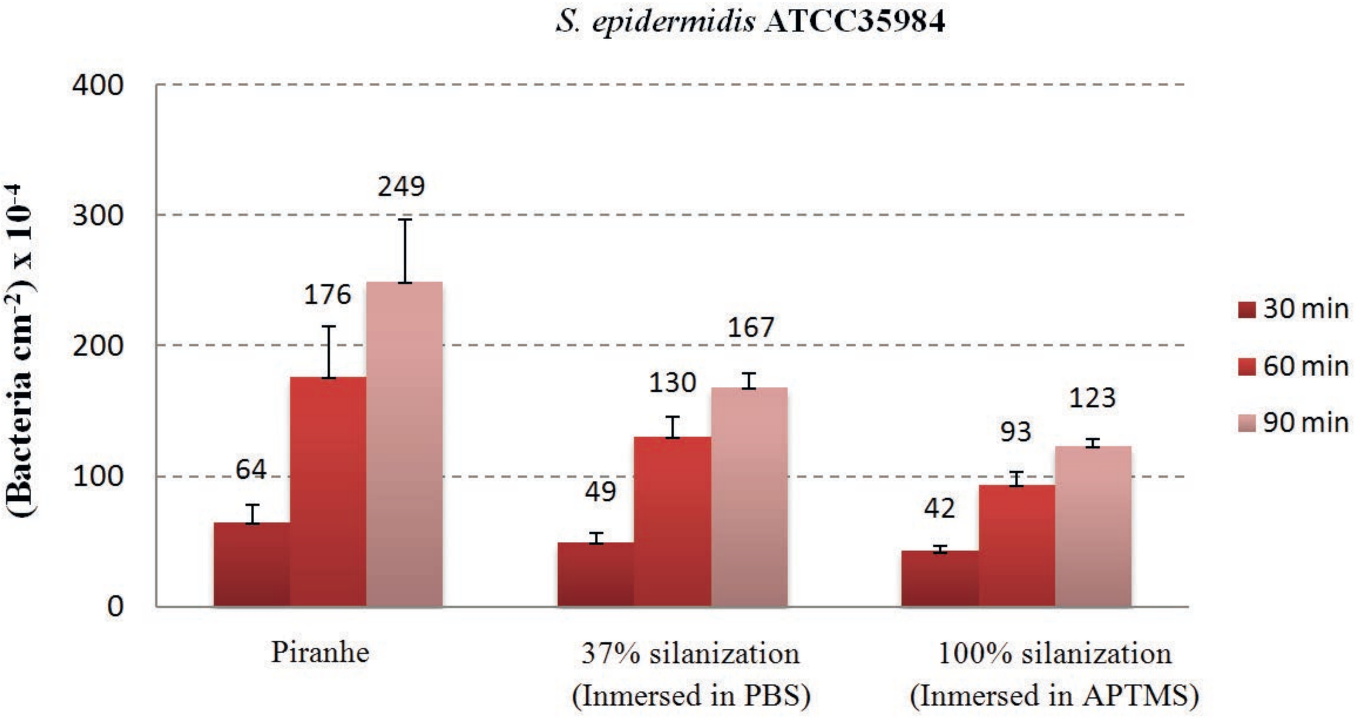

-Number of adhered bacteria on the Ti6Al4V surface treated with piranha, 37% silanization and 100% silanization for contact times of 30, 60 and 90 min for S. epidermidis ATCC35983

-Number of adhered bacteria on the Ti6Al4V surface treated with piranha, 37% silanization and 100% silanization for contact times of 30, 60 and 90 min for S. epidermidis ATCC35984

2A.7

Pre-vascularized 3D constructs for bone critical size defects.

Sophie Verrier
AO Research Institute, Davos, Switzerland

Our aim is to establish a pre-vascularized bone graft using scaffolds co-seeded with Endothelial Progenitor Cells and bone marrow Mesenchymal Stem Cells. We showed the cooperation of those cell types on implant's neovascularization and MSC osteogenic differentiation.

Introduction:

Angiogenesis is a key factor in early stages of wound healing and is also crucial for tissue regeneration. In cases of large bone defect, to date most of the efforts have been focused on the filling of the gap with autologous bone grafts, or various bio-active materials associated or not with bone forming cells. However, vessels' ingrowth from nearby tissues and therefore implant neo-vascularization is insufficient in most large defect healing. In the present study we developed a in vitro pre-vascularized 3D polyurethane (PU) implant based on the association of Endothelial Progenitor Cells (CD34+ and CD133+) with Mesenchymal Stem Cells (MSC) both autologous.

Methods:

MSCs were isolated by Ficoll-Paque density-gradient centrifugation from human bone marrow (KEK_Bern126/03). EPCs (CD133+/CD34+) were isolated from MSC fractions using magnetic-activated cell sorting (MACS®). For 2D Matrigel® assays, MSC and EPCs were pre-stained using PKH26-red® and PKH67-green® respectively before seeded either alone or in combination. In 3D set-up, cells in different proportions were embedded in autologous growth factor rich gel (Platelet Rich Plasma) and seeded in PU scaffolds. Constructs were cultured in different media (osteogenic, angiogenic, or mixed), and after 7 days, some samples were analysed in histology (toluidine blue, endothelial-cell- , pericyte-specific antibodies), while other were implanted subcutaneously in nude mice and sacrificed at 8 weeks.

Results:

On growth factor reduced Matrigel® we could observe rapid formation of cellular networks in which EPC and some of the MSC population participated. The MSC enrolled in these cells re-organizations showed positive staining with CD146 specific antibody.

In 3D scaffolds, the formation of luminal tubular structures in the co-seeded scaffolds as early as day 7 in culture could be observed. These tubular structures were proven positive for endothelial markers vWF and PECAM-1. Of special significance in our constructs is the presence of CD146 positive cells, as a part of neo-vasculature scaffolding. These cells coming from the mesenchymal stem cells population (MSC or EPC-depleted-MSC) also expressed further markers of pericytes cells (NG2 and αSMA), known to have a pivotal function in the stabilization of new formed pre-vascular network. In parallel, in co-cultures, osteogenic differentiation of MSC occurred earlier as in MSC monoculture, suggesting the close cooperation between the two cell populations in each other's differentiation and function.

Discussion & conclusions:

In conclusion, we were able to demonstrate the beneficial effect of MSC and EPC (CD34+ and CD133+) 3D co-culture on each other differentiation toward a functional osteoblastic- and endothelial phenotype respectively. The cell culture medium has proven to be as important as the cells co-seeding. The presence of angiogenic factors (from autologous platelet lysates) in association with osteogenic factors seems to be crucial for this synergy.

2A.8

Periprosthetic Fractures Around the Hip in a UK North West Trauma Unit

Zuned Hakim
Royal Preston Hospital, Preston, UK

Periprosthetic fractures around the hip are increasing in the UK with an expected increase of 4 fold within our unit compared to last year. Fractures are higher in women with the Vancouver type being influenced by the stem design.

Introduction

The Mayo and Scandanavian registries have reported consecutive annual increases in periperiprosthetic fractures around the hip over recent years. Little data exists from theUK with regards to epidemiology of these fractures. Our aim was to identify the epidemiology of these fractures in a busy North West Trauma unit.

Patients and methods

A restrospective review identified 54 patients over 5 years with periprosthetic fractures. Data were gathered on patient demographics, time of original surgery, time since surgery to fracture, implanted stem, and any revision surgery following fixation. All fractures were classified according to Vancouver by the senior author. The data was analysed to ascertain the epidemiology.

Results

61% of cases were female with an average age of 76. Mean time to fracture was 5.9 years from initial surgery. There has been an increase incidence from 2 cases in 2006 to 15 in the first 4 months of 2012. 46% of fractures were in polished tapered stems. 39% were Vancouver B1, 37% B2, 4% B3 and 20% C. Type C fractures were higher in composite beam and uncemented stems compared to polished tapered stems. 11% of all fractures fixed required further revision for complications within a mean of 14 weeks (range 3-30). There was no association between age and fracture pattern, nor time period from initial surgery and fracture pattern.

Discussion

Periprosthetic fracture rates are increasing considerably. This is likely to be associated with an increased rate of arthroplasty, increased life expectancy and greater levels of physical activity. At the current 2012 rate, if unchanged, will result in a 4 fold increase compared to 2011 and a 15 fold increase compared to 2006. A difference in fracture type was noted dependent on the stem implanted at time of first operation. Most cases of complication occurred within the first 4 weeks of fixation suggesting failure, if going to occur, does so at an early stage. Age and time period from THR do not influence fracture pattern seen.

References

H. Lindahl, H. Malchau, P. Herberts, G. Garellick Periprosthetic femoral fractures: classification and demographics of 1049 periprosthetic femoral fractures from the Swedish National Hip Arthroplasty Register J Arthroplasty, 20 (2005), pp. 857-865

Lindahl H. Epidemiology of periprosthetic femur fracture around a total hip arthroplasty. Injury. 2007;38:651-4.

2B.1

BMP-2 and BMP-7: Differential Regulation of Chondrogenic Differentiation

Marjolein Caron
Maastricht University Medical Centre, dept. Orthopaedic Surgery, Maastricht, The Netherlands

BMP-2 and BMP-7 show differential effects on chondrogenic differentiation of chondroprogenitors: BMP-2 induces chondrocyte hypertrophy, while BMP-7 increases or maintains the chondrogenic potential and prevents chondrocyte hypertrophy. Studies into the possible underlying mechanism revealed Bapx1 signalling as a potential candidate.

Introduction:

Bone morphogenic protein (BMP)-2 and BMP-7 are known to induce (ectopic) bone formation. The recombinant human versions of these proteins are clinically approved and used to promote osteogenesis at sites of poor fracture healing (non-unions) and as additional factors to enhance integration of bone grafts. Recently, molecular studies have shown that BMPs are also able to regulate the chondrogenic regenerative potential. However, the differential influence of different BMPs on the chondrogenesis of progenitor cells is unknown.

Methods:

Equimolar concentrations of BMP-2 and BMP-7 were added from the initiation of chondrogenic differentiation of ATDC5 and hBMSCs onward. Chondrogenic markers (Col2a1, Sox9), chondrocyte hypertrophic markers (Col10a1, Runx2) and chondrogenic regulatory mediator Bapx1 were analysed by gene- and protein expression analysis. In addition the requirement of Bapx1 for during chondrogenic differentiation under BMP treatment was investigated by genetically targeting Bapx1 by specific siRNAs.

Results:

Supplementing BMP-7 to chondrogenically differentiating ATDC5 cells resulted in an overall increased Col2a1 expression and decreased chondrocyte hypertrophy. In contrast, BMP-2 dose-dependently increased chondrocyte hypertrophic markers Col10a1 and Runx2, whereas Col2a1 levels did not differ from control conditions. This profound differential action of BMP-2 and BMP-7 on ATDC5 endochondral differentiation could also be confirmed in hBMSC chondrogenic differentiation. Bapx1/Nkx3.2 expression was decreased in the BMP-2 conditions and increased in BMP-7 conditions, which could possibly explain the differential effects of BMPs on chondrogenic outcome. Indeed, knockdown of Bapx1 under BMP-7 conditions treatment abolished the anti-hypertrophic effect of BMP-7 to control levels or even higher.

Conclusion:

BMP-2 and BMP-7 differentially direct the chondrogenic outcome of differentiating chondroprogenitor cells: BMP-2 acts a specific inducer of chondrocyte hypertrophy, while BMP-7 increases or maintains the chondrogenic potential and prevents chondrocyte hypertrophy. Studies into the possible underlying mechanism revealed Bapx1 signalling as a potential candidate. Our results may provide novel leads to optimize cartilage and bone regenerative techniques on a differential BMP basis and might prevent unwanted ossification of cartilage grafts by usage of different BMPs.

2B.2

Macrophages response to wear particles is determined by macrophage polarization

Jukka Pajarinen
Department of Medicine, Institute of Clinical Medicine, University of Helsinki, Helsinki, Finland

M1 macrophages respond to wear particles by producing osteolytic cytokines while M2 macrophages restrict particles into intracellular compartment without inflammatory reaction. Controlling macrophage polarization in the interface tissue might be a way to limit the osteolysis caused by wear particles.

Introduction

The main long-term complication of total joint replacements is aseptic loosening caused by a foreign body reaction to wear particles. Wear particles in the interface tissue are phagocytosed by macrophages which respond to this foreign material by secreting proinflammatory cytokines and chemokines leading into increased osteoclastogenesis and finally osteolysis. Wear particle recognition, phagocytosis and subsequent macrophage activation to proinflammatory phenotype are thus considered as fundamental events in the pathogenesis of aseptic osteolysis.

In the field of immunology it has become clear that macrophages represent heterogeneous population of cells, which are readily capable of adopting different phenotypes and activation states as a response to multitude of signals derived from the local microenvironment. Classically and alternatively activated or M1 and M2 macrophages, respectively, represent the extremes of this macrophage activation continuum.

This concept of macrophage polarization has received little attention in the context of wear particle recognition and subsequent foreign body reaction. This is somewhat surprising considering e.g. that M1 and M2 macrophages express different levels of pattern regognition receptors and have different abilities to produce pro-inflammatory and chemotactic mediators. It is thus well possible that the nature of macrophages response to wear particle is depended on the polarization state of the peri-implant macrophages.

Patients & Methods

To test this hypothesis, we generated non-activated M0 macrophages as well as M1 and M2 polarized macrophages in vitro from human peripheral blood monocytes and compared their responses to titanium particles using genome wide microarray analysis and multiplex cytokine assay. Particle phagocytosis was observed using real-time phase contrast microscopy.

Results

M0, M1 and M2 polarized macrophages responded to standardized titanium particle stimulus with a unique profile of transcriptome and proteome changes. In M1 macrophages the wear particle responses were enhanced and especially the production of inflammatory cytokines (e.g TNF-α) as well as chemokines (e.g. CCL3) were typical for M1 wear particle response. In addition genome wide approach revealed several novel, potentially osteolytic, wear particle induced genes (e.g. oncostatin M). In M2 macrophages all these wear particle responses were systematically suppressed, despite the fact that they effectively moved around the culture dish and engulfed the wear particles.

Discussion/Conclusion

Our results show that macrophage polarization is an important factor in determining the macrophages response to wear particles: M1 macrophages responded to wear particle stimulus by producing proinflammatory and osteolytic cytokines while M2 macrophages restricted wear particles into intracellular compartment without inflammatory reaction. Our results thus provide clear a proof of principle that it is possible to biologically suppress the host response against wear particles. By limiting the action of M1 polarizing factors (e.g. bacterial biofilm formation) in the interface tissue and perhaps promoting M2 macrophage polarization by biomaterial solutions or pharmacologically, it might be possible to restrict the osteolysis caused by the inevitably forming wear particles. Exiting is also the arising hypothesis that the low-grade inflammation in systemic level, associated e.g. to obesity, might be a determinant in the general M1-M2 balance of macrophages and thus in the susceptibility of an individual to develop aseptic osteolysis.

2B.2

Macrophages response to wear particles is determined by macrophage polarization

Jukka Pajarinen
Department of Medicine, Institute of Clinical Medicine, University of Helsinki, Helsinki, Finland

M1 macrophages respond to wear particles by producing osteolytic cytokines while M2 macrophages restrict particles into intracellular compartment without inflammatory reaction. Controlling macrophage polarization in the interface tissue might be a way to limit the osteolysis caused by wear particles.

Introduction

The main long-term complication of total joint replacements is aseptic loosening caused by a foreign body reaction to wear particles. Wear particles in the interface tissue are phagocytosed by macrophages which respond to this foreign material by secreting proinflammatory cytokines and chemokines leading into increased osteoclastogenesis and finally osteolysis. Wear particle recognition, phagocytosis and subsequent macrophage activation to proinflammatory phenotype are thus considered as fundamental events in the pathogenesis of aseptic osteolysis.

In the field of immunology it has become clear that macrophages represent heterogeneous population of cells, which are readily capable of adopting different phenotypes and activation states as a response to multitude of signals derived from the local microenvironment. Classically and alternatively activated or M1 and M2 macrophages, respectively, represent the extremes of this macrophage activation continuum.

This concept of macrophage polarization has received little attention in the context of wear particle recognition and subsequent foreign body reaction. This is somewhat surprising considering e.g. that M1 and M2 macrophages express different levels of pattern regognition receptors and have different abilities to produce pro-inflammatory and chemotactic mediators. It is thus well possible that the nature of macrophages response to wear particle is depended on the polarization state of the peri-implant macrophages.

Patients & Methods

To test this hypothesis, we generated non-activated M0 macrophages as well as M1 and M2 polarized macrophages in vitro from human peripheral blood monocytes and compared their responses to titanium particles using genome wide microarray analysis and multiplex cytokine assay. Particle phagocytosis was observed using real-time phase contrast microscopy.

Results

M0, M1 and M2 polarized macrophages responded to standardized titanium particle stimulus with a unique profile of transcriptome and proteome changes. In M1 macrophages the wear particle responses were enhanced and especially the production of inflammatory cytokines (e.g TNF-α) as well as chemokines (e.g. CCL3) were typical for M1 wear particle response. In addition genome wide approach revealed several novel, potentially osteolytic, wear particle induced genes (e.g. oncostatin M). In M2 macrophages all these wear particle responses were systematically suppressed, despite the fact that they effectively moved around the culture dish and engulfed the wear particles.

Discussion/Conclusion

Our results show that macrophage polarization is an important factor in determining the macrophages response to wear particles: M1 macrophages responded to wear particle stimulus by producing proinflammatory and osteolytic cytokines while M2 macrophages restricted wear particles into intracellular compartment without inflammatory reaction. Our results thus provide clear a proof of principle that it is possible to biologically suppress the host response against wear particles. By limiting the action of M1 polarizing factors (e.g. bacterial biofilm formation) in the interface tissue and perhaps promoting M2 macrophage polarization by biomaterial solutions or pharmacologically, it might be possible to restrict the osteolysis caused by the inevitably forming wear particles. Exiting is also the arising hypothesis that the low-grade inflammation in systemic level, associated e.g. to obesity, might be a determinant in the general M1-M2 balance of macrophages and thus in the susceptibility of an individual to develop aseptic osteolysis.

2B.3

Inhibition of NF-kB activation delays the onset of age-dependent spinal degeneration in a murine model of human progeria

Luigi Aurelio Nasto
Department of Orthopaedic Surgery, Catholic University of Rome, Rome, Italy

Our findings demonstrates that the IKK/NF-kB signaling pathway is a key mediator of age-dependent disc degeneration and represents a therapeutic target for mitigating disc degenerative diseases associated with aging.

Introduction: Activity of NF-κB, a family of transcription factors activated in response to cellular stress, increases with age and is implicated in the pathogenesis of numerous age-related degenerative diseases. (1,2,3) Micedeficient in the DNA repair (Errc1$^{\Delta}$mice) exhibit accelerated aging spine phenotype, including kyphosis, vertebral osteoporosis, loss of disc matrix proteoglycans and disc height. (4) Because NF-κB transcriptional activity is upregulated in aged discs, (5) wehypothesized that blocking NF-κB activation slows the onset of age-dependent degenerative changes in the spines of Errc1$^{\Delta}$mice.

Methods: Systemic inhibition of NF-kB activation was achieved either genetically by deletion of one allele of the NF-kB subunit p65 (Ercc1$^{\Delta}$p65$^{+/-}$ mice) or pharmacologically by chronic intra-peritoneal administration of the NEMO Binding Domain (8K-NBD) peptide to block the formation of the upstream activator of NF-κB, IkB Inducible Kinase (IKK), in Ercc1$^{\Delta}$ mice. Sibling pairs of Errc1$^{\Delta}$mice were treated with 8K-NBD or 8K-mNBD (10 mg/Kg three times per week intraperitoneally) starting at 5 weeks of age before they were symptomatic and continued until 18-20 weeks of age. 8K-NBD, a synthetic octalysine peptide transduction domain fused to the NEMO binding domain (NBD) of IκB kinase (IKK) ß, blocks NF-kB activation by IKK without inhibiting basal NF-kB activity. 8K-mNBD is a mutant peptide control that does not block IKK mediated activation of NF-kB.

Results:

Onset of kyphosis was delayed (13 wks in 8K-NBD vs. 12 wks in 8K-mNBD treated mice). mCT analysis revealed higher vertebral bone density in 8K-NBD treated mice (757+25 mg HA/ccm) than 8K-mNBD treated mice (710+48 mg HA/ccm). Discs of 8K-NBD treated mice showed greater safranin O histological staining for proteoglycan than those in 8K-mNBD treated animals. Disc organ culture derived from 8K-NBD treated Errc1$^{\Delta}$mice showed a two fold increase in proteoglycan synthesis (^{35}S-sulfate incorporation) compared to untreated control. Similar results were confirmed genetically by using Ercc1$^{\Delta}$p65$^{+/-}$ mice.

Conclusion: The 8K-NBD peptide has been shown to be efficacious in animal models of inflammatory bowel disease, muscular dystrophy, and arthritis. Here we showed that treatment of an accelerated aging animal model with the same therapeutic peptide delayed the onset of kyphosis, reduced vertebral osteoporosis, and decreased loss of disc matrix proteoglycans. These findings suggest that NF-κB plays a vital role in the development of age-dependent spinal degeneration and represents a potentially important therapeutic target.

Bibliografy:

Hayden, M.S. & Ghosh, S. Shared principles in NF-kappaB signaling. Cell132, 344-62 (2008).
Helenius, M., Hanninen, M., Lehtinen, S.K. & Salminen, A. Aging-induced up-regulation of nuclear binding activities of oxidative stress responsive NF-kB transcription factor in mouse cardiac muscle. J Mol Cell Cardiol28, 487-98 (1996).
Korhonen, P., Helenius, M. & Salminen, A. Age-related changes in the regulation of transcription factor NF-kappa B in rat brain. Neurosci Lett225, 61-4 (1997).
Vo, N. et al. Accelerated aging of intervertebral discs in a mouse model of progeria. J Orthop Res28, 1600-7.
Nerlich, A.G. et al. Immunomorphological analysis of RAGE receptor expression and NF-kappaB activation in tissue samples from normal and degenerated intervertebral discs of various ages. Ann N Y Acad Sci1096, 239-48 (2007).

2B.5

Modulation of osteoclast formation by cyclically-strained myotubes is mediated by IL-6

Petra Juffer
Department of Oral Cell Biology, Academic Centre for Dentistry Amsterdam (ACTA), University of Amsterdam and VU University Amsterdam, MOVE Research Institute, Amsterdam, The Netherlands

Skeletal muscle is an endocrine organ that produces numerous myokines affecting other tissues. We found that cyclically-strained myotubes secrete soluble factors that modulate osteoclast formation via IL-6. Our data suggest that biochemical communication between muscle and bone is possible.

Skeletal muscle is an endocrine organ that produces numerous growth factors and cytokines, such as IL-6, in response to mechanical loading. In bone, these factors can affect osteoblastic bone formation, but it is unknown whether osteoclasts are also affected. Therefore we aimed to investigate whether mechanically-loaded myotubes produce soluble factors that affect osteoclast formation, and whether IL-6 is one of these factors.

C2C12 myoblasts were seeded on laminin-coated Bioflex® 6-wells plates, and differentiated into C2C12 myotubes. C2C12 myotubes were mechanically stimulated for 1 h by applying an uni-axial cyclic strain (0-15% deformation, 1 Hz), or kept under static control conditions, and post-incubated without cyclic strain up to 24 h. Conditioned medium (CM) was collected directly after 1 h cyclic strain/static culture, and after 24 h post-cyclic strain/static culture. RNA was isolated directly after 1 h cyclic strain. IL-6 mRNA levels were measured by RT-PCR. Mouse bone marrow cells were cultured in the presence of M-CSF and RANKL, with/without myotube-CM, and with/without mouse IL-6 antibody (10 ng/mL). After 6 days of culture, osteoclast formation was quantified by counting tartrate-resistant acid phosphatase (TRACP) positive multinucleated (≥3 nuclei) cells.

CM harvested from C2C12 myotubes after 1 h static culture and 24 h post-static culture decreased the formation of TRACP+-multinucleated cells by 3.5-fold (1 h static) and 7.0-fold (24 h post-static) compared to non-CM. CM harvested from C2C12 myotubes after 1 h cyclic strain increased the formation of TRACP+-multinucleated cells by 1.7-fold compared to CM harvested after 1 h static culture. CM harvested from C2C12 myotubes after 24 h post-cyclic strain did not affect the formation of TRACP+-multinucleated cells. Cyclic strain increased IL-6 mRNA levels in C2C12 myotubes by 3.0-fold. Addition of IL-6 antibody to the myotube-CM nullified the effect of soluble factors produced by cyclically-strained myotubes on osteoclast formation.

Our data indicate that C2C12 myotubes secrete soluble factors that inhibit osteoclast formation, and that mechanical loading of C2C12 myotubes by cyclic strain stimulates osteoclast formation via IL-6. Since it is known that IL-6 plasma concentations increase substantially during muscular activity, our data suggest that muscle cells in vivo might affect osteoclasts via IL-6.

2B.6

Eicosapentanoic acid prolongs survival and attenuates inflammatory response in an experimental model of lethal trauma.

Stephanos Koutsostathis
Fourth Orthopaedic Department, KAT Hospital, Kifissia, Greece

An animal model of lethal trauma was studied, in order to define the efficacy of eicosapentanoic acid (EPA) in preventing fatal outcome. Results suggest that EPA may improve the survival rate, probably through the restoration of oxidative burst of neutrophils.

Introduction

In an attempt to define the efficacy of intravenously administered n-3 polyunsaturated fatty acids (PUFAs) in the prevention of fatal outcome of severe trauma, an animal model of lethal trauma following an open femur fracture was studied.

Animals and methods

For the purpose of the study, 25 rabbits were used. After causing a femur fracture- which was left open for 4 hours- to all of them, an intravenous solution of eicosapentanoic acid (EPA)- one n-3 PUFA- was administered; 13 were controls and 12 were treated with EPA 30 min after fracture. Vital signs were recorded and serum concentration of tumor necrosis factor- alpha (TNF-α) and respiratory burst of neutrophils were assessed.

Results

Survival of controls was 7.7% and of animals treated with EPA 50% (log-rank: 5.162; p: 0.023). Vital signs of both groups did not differ. Oxidative burst of neutrophils was greater among EPA- treated animals compared to controls at 48 h (p:0.010). Serum levels of TNF-α of the former group were decreased compared to the latter at 48 h (p: 0.019). Bacterial growth of enterobacteriacae from liver and spleen after death or euthanasia was lower among EPA- treated rabbits than controls.

Discussion

These results suggest that EPA possesses considerable immunomodulatory activities improving survival in a model of lethal trauma. Restoration of oxidative burst conferring efficient phagocytosis of evading bacteria seems the most probable mechanism of action.

2B.8

Deleterious interaction between BMP2 and TGF-beta signaling in articular chondrocytes: Harmful role for BMP2 in OA?

Esmeralda Blaney Davidson
Radboud University Nijmegen Medical Centre, Nijmegen, The Netherlands

BMP2 induces osteoarthritis-like effects in articular cartilage, which can be overcome by enhanced TGF-beta signaling.

Introduction:
TGF-beta signaling via Smad2/3 is crucial for cartilage maintenance. Smad2/3 maintains a healthy chondrocyte phenotype by inhibiting chondrocyte hypertrophy. We have previously shown that loss of Smad2/3 signaling is a hallmark of both ageing and Osteoarthritis (OA). BMP2, a TGF beta family member, signals via Smad1/5/8 instead of Smad2/3. During OA we found that BMP2 is elevated near lesions. We have investigated whether BMP2, and as a consequence Smad1/5/8 signaling, affects Smad2/3 signaling and what are the biological consequences of this.
Methods:
Primary bovine chondrocytes were exposed to BMP2, TGFb1 or a combination of both. Smad phosphorylation was analyzed by Western blotting and gene expression by qPCR. Adenoviral constructs for BMP2 and the control Luc were injected i.a. into murine knee joints. Knee joints were isolated after 3 days for immunohistochemistry. Human OA cartilage explants were obtained, after informed consent, from patients undergoing joint replacement surgery and exposed to TGFb1 or the Smad2/3P inhibitor SB-505124 for 48 hours. Subsequently RNA was isolated and gene expression was analyzed with qPCR.
Results: Exposing primary bovine chondrocytes to 15 or 50 ng BMP2 led to a decrease in Smad2/3 phosphorylation on Western Blot already after 60 minutes and that was sustained until at least 420 minutes compared to non-stimulated controls. We confirmed this effect in vivo as over expression of BMP2 in murine knee joints led to decreased Smad2/3P positive cells in both patella and tibia by 55% and 43% respectively. To investigate the functional consequence of decreased Smad2/3 signaling we cultured human OA cartilage explants in the presence of SB-505124. This significantly increased MMP13 expression 13.6 fold. A similar increase in MMP13 expression was also observed in cultures of primary bovine chondrocytes 48 hours after stimulation with BMP2. Interestingly, the effect of either 15 or 50 ng BMP2 could be prevented by addition of TGF-beta, which prevented the decrease in Smad2/3P levels, but only when a dose of 10 ng/ml TGF-beta was used. A lower dose of 0.5 ng/ml TGF-beta was insufficient to overcome the BMP2-induced Smad2/3P decrease. This indicates that TGF-beta can overcome the BMP2 effect in a dose-dependent manner. Even in human OA cartilage that had spontaneously reduced Smad2/3P levels addition of 10ng/ml TGF-beta could still decrease MMP13 expression by 6.6 fold ($p<0.005$).
Discussion/Conclusion:
Our data confirm that BMP2 down regulates Smad2/3 signaling in articular chondrocytes both in vitro and in vivo. A decreased Smad2/3 signaling results in up regulated levels of MMP13 expression suggesting that BMP2 up regulation, as found adjacent to OA lesions, is deleterious for articular cartilage. Moreover, we show that this negative effect of BMP2 can be overcome by addition of TGF-beta, thereby raising levels of Smad2/3P. Even in human OA cartilage that has naturally high levels of MMP13 and low levels of Smad2/3P, TGF-beta addition can still reduce MMP13 expression levels. Overall our data suggest that BMP2 induces OA-like effects in articular cartilage, down regulating Smad2/3P and up regulating MMP13, which can be overcome by enhanced TGF-beta signaling.

3A.1

Lumbar Posterolateral Spinal Fusion with a Collagen/TCP Scaffold in an Ovine Model

Ali Ismailoglu
NuVasive, San Diego, CA, USA

A novel microstructured tricalcium phosphate material which has previously demonstrated increased and accelerated bone formation was prepared with fibrillar collagen as a bone graft substitute investigated in a sheep posterolateral fusion model, and compared to iliac crest bone.

Introduction:

Autologous bone harvested from iliac crest has been the gold standard for spinal fusion grafting. Due to its limited availability and donor site morbidity, alternative materials like collagen/calcium phosphate composites have been studied[1]. These materials have similar chemical properties to mammalian bone and have been used successfully as bone graft substitutes due to their excellent biocompatibility, unlimited supply and safety. In the current study, a novel microstructured tricalcium phosphate (mTCP) material, which has previously demonstrated increased and accelerated bone formation[2], was prepared with fibrillar-collagen and investigated in a sheep posterolateral fusion (PLF) model versus iliac crest bone graft (ICBG).

Patients & Methods:

mTCP with a fibrillar-collagen composite was compared to ICBG in an instrumented 2 level (L2-L3 and L4-L5) ovine PLF model. A total of 12 operative levels were included in this study. Collagen/TCP scaffold is a composite bone graft material comprising Type-I fibrillar bovine collagen and mTCP ceramic in the form of ß-TCP(> 90%)/HA(< 10%) with particle size between 0.5-1mm and surface average pore size of 500nm. The total graft porosity was 72%, determined by Hg-intrusion porosimetry, allows for absorption of bone marrow aspirate. At 12 weeks, the fusion sites were assessed biomechanically (Figure 1) and by computed tomography (Figure 2). Each level was instrumented with transpedicular fixation with 10cc of graft per side placed laterally between the decorticated transverse processes. Prior to implantation, each collagen/TCP scaffold was hydrated with 10cc of bone marrow. At 12 weeks, animals were euthanized and biomechanical stiffness by manual palpation was correlated to quantitative multidirectional range of motion (ROM). Each segment was loaded in flexion/extension (f/e) with a pure moment of ±4Nm using a six degree of freedom spine simulator and measured by OptoTrak.

Results:

Fusion rates by manual palpation for collagen/TCP scaffold were 5/6 while autograft was 4/6 fused and 1/6 partially fused. Manual palpation results were confirmed by biomechanical testing where less than 2° ROM was indicative of fusion and greater than 2° ROM was suggestive of non-union. Segments treated with Collagen/TCP scaffold and ICBG demonstrated similar average ROM; 1.99°±1.66 and 1.65°±1.16 respectively ($p > 0.05$). Fusion rates with ICBG at 12 weeks are in agreement with published literature in this model[3]. The manual palpation, ROM results and radiograph scores demonstrate that ICBG and collagen/TCP treatment groups had similar fusion rates and suggest that this newly developed scaffold may be an ideal candidate for replacement of autograft for spinal fusion.

Conclusions:

This study has shown that collagen/TCP scaffold bone graft material resulted in similar biomechanical performance and fusion rates when compared to ICBG after 12 weeks in the sheep instrumented posterolateral fusion model. Additionally based on flexion/extension ROM results a threshold of >2° motion correlated with non-union from manual palpation. Based on the fusion results such material may be a good candidate in spinal fusion as a substitute for autograft.

References:

1. Damien CJ, P, J Appl Biomater, 1991 2(3):187-208
2. Habibovic P, J Orth Res, 2006; 24(5): 867-876
3. Kanayama, M., et al., Spine, 1999, 24(11): 1058-65

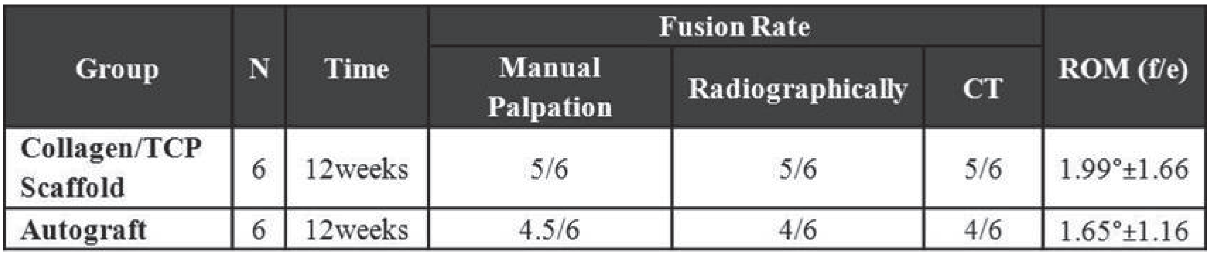

Group	N	Time	Fusion Rate			ROM (f/e)
			Manual Palpation	Radiographically	CT	
Collagen/TCP Scaffold	6	12weeks	5/6	5/6	5/6	1.99°±1.66
Autograft	6	12weeks	4.5/6	4/6	4/6	1.65°±1.16

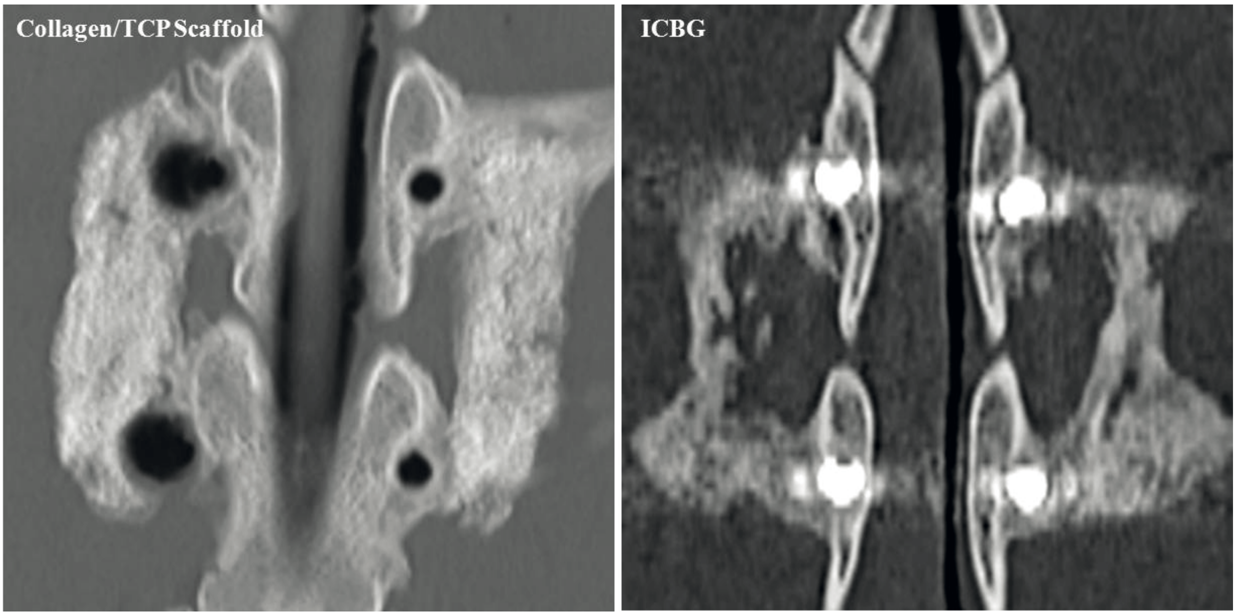

-The image on the left shows a CT scan of Collagen/TCP scaffold and the image on the right show a CT scan for ICBG treatment group. Solid bridging bone is evident on both sides for both groups.

3A.10

T1rho magnetic resonance imaging quantification of early lumbar intervertebral disc degeneration in healthy young adults

Gianluca Vadalà
University Campus Bio-Medico, Rome, Italy

The early intervertebral disc degeneration (IDD) in the lumbar spine was quantified by T1rho weighted MRI in a population of asymptomatic young adults. The data showed a significant difference in IDD onset among gender.

Introduction:
Intervertebral disc (IVD) starts early to degenerate losing glycosaminoglycan content in the nucleus pulposus (NP). A potential tool for the study of early stage of intervertebral disc degeneration (IDD) is T1ρ magnetic resonance imaging (MRI). T1ρ relaxation time of human discs has been correlated to glycosaminoglycan content in previous studies.[1]
The porpuse of the study was to evaluate early intervertebral disc degeneration (IDD) in the lumbar spine quantified by T1ρ and T2-weighted MRI in a population of asymptomatic young adults and to by correlating T1ρ value with Pfirrmann degenerative grade, gender and body mass index (BMI).
Materials and Methods.
T1ρ- and T2-weighted images of the lumbar spine were obtained with a 1.5T MRI scanner of 63 asymptomatic young subjects (male 34, female 29; mean age 22.95±1.8). T1ρ mapping and values in the NP and anulus fibrosus (AF) (n=315) were obtained. Degenerative grade was assessed using T2-weighted images according to the Pfirrmann scale. Differences in T1ρ value among gender, BMI, and linear regression analyses with degenerative grade were determined.
Results:
T1ρ values of NPs were significantly higher then AF at all levels. T1ρ values were significantly lower in female at L3-L4 and L4-L5 discs ($p<0.05$). T1ρ values decreased linearly with degenerative grade ($R^2=0.97$). However, bivariate scattergram analysis of non-degenerated disc (grade 1-2) showed a wide heterogeneity distribution of T1ρ values. No significant correlation was observed between T1ρ value and BMI.
Conclusion:
The data of this study showed a significant difference in IDD onset among gender. T1ρ values correlate with Pfirrmann degenerative grade in young adults. However, the wide distribution of T1ρ values in healthy IVD highlights the low sensitivity of Pfirrmann grade to detect the early IDD changes. T1ρ can be potentially used as a clinical tool to identify early IDD and to create a reliable quantitative scale.

References:

1. Johannessen, Spine (Phila Pa 1976) 2006.

3A.11

Proteomic Analysis of Ligamentum Flavum from Lumbar Spinal Canal Stenosis

Yuchiro Goda

This is the first study which could reveal the difference of protein components between ligamentum flavum from LCS patients and that from LDH patients.

Introduction

The lumbar spinal canal stenosis (LCS) is the common lumbar disorder in the aged population. Hypertrophy of ligamentum flavum is one of the main factors of the LCS but the patho-mechanism of hypertrophy has not been clarified yet. In many other diseases, proteomic analysis can contribute to understanding of pathogenesis. Although proteomic analysis of ligamentum flavum was difficult due to insolubility, Sato et al. succeeded in solubilization of ligamentum flavum using cyanogens bromide (CNBr) and some proteolytic enzymes, and proteomic analysis using liquid chromatography (LC)-mass spectrometry (MS)/MS. The purpose of this study is to compare protein components of ligamentum flavum from LCS patients with that from lumbar disc herniation (LDH) patients.

Patients & Methods

The ligamentum flavum samples were obtained from patients at the time of operation for LCS or LDH. This study was approved by institutional review board of Tokushima University, and the patients gave their informed consent. The samples were divided two groups. One group was ligamentum flavum with hypertrophy from LCS patients. The LCS patients were 80 (A), 74 (B), and 59 (C) years old. All of them were male. The other group was that without hypertrophy from LDH patients. The LDH patients were 17 (D) year-old male and 22 (E), 30 (F) year-old female. Samples were washed extensively for removal of blood cells and axially cut into 1-μm slices with cryotome. They were treated with CNBr under N_2 gas and digested with various enzymes (elastase, lysyl endopeptidase, and trypsin). The digestion mixtures were centrifuged and the supernatants were used for LC-MS/MS, although there was not any pellet. Searches were performed using the Mascot software to identify proteins.

Result

In the LCS group, the ratio of elastin was (A)14%, (B)38%, (C)50%, and the ratio of collagen were (A)78%, (B)55%, (C)39% (see Fig. 1). In the LDH group, the ratio of elastin were (D)57%, (E)66%, (F)57%, and the ratio of collagen were (D)36%, (E)15%, (F)33% (see Fig. 2). The ratio of elastin in LCS group were lower than that in LDH group and the ratio of collagen in LCS group was higher than that in LDH group. In addition, we mentioned about representative collagens that the ratio of COL1A1 were (A)29%, (B)15%, (C)11%, (D)12%, (E)4%, (F)9% and that of COL1A2 were (A)18%, (B)15%, (C)3%, (D)6%, (E)1%, (F)6% and that of COL3A1 were (A)25%, (B)14%, (C)11%, (D)9%, (E)7%, (F)10% (see Fig 3). LCS group tended to be higher than LDH group.

[Discussion/Conclusion] In this study, we could analyze and compare elastin and various kinds of collagens. The ligamentum flavum with hypertrophy had lower elastin contents and higher collagen contents than that without hypertrophy. It will be helpful to reveal the pathophysiology of hypertrophied ligamentum flavum.

Figure 1: Samples from LCS patients

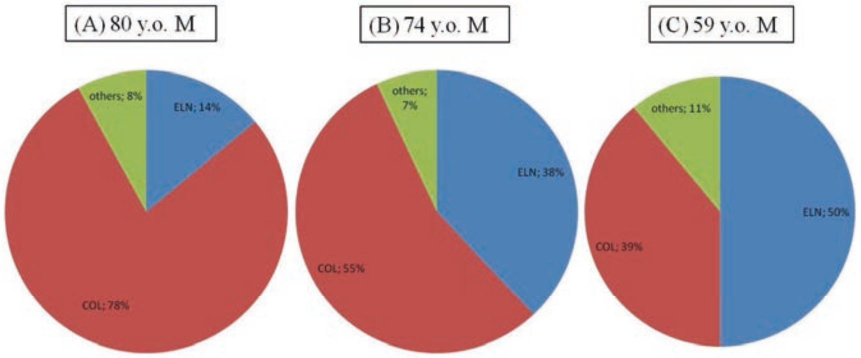
(A) 80 y.o. M
(B) 74 y.o. M
(C) 59 y.o. M

Figure 2: Samples from LDH patients

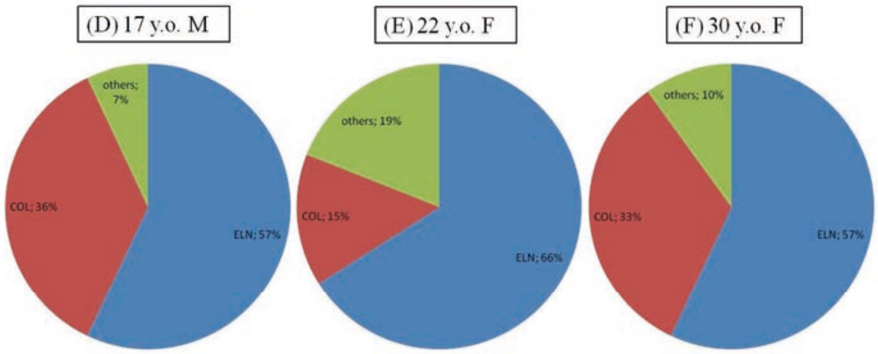
(D) 17 y.o. M
(E) 22 y.o. F
(F) 30 y.o. F

Figure 3: Representative Collagens from LCS and LDH patients

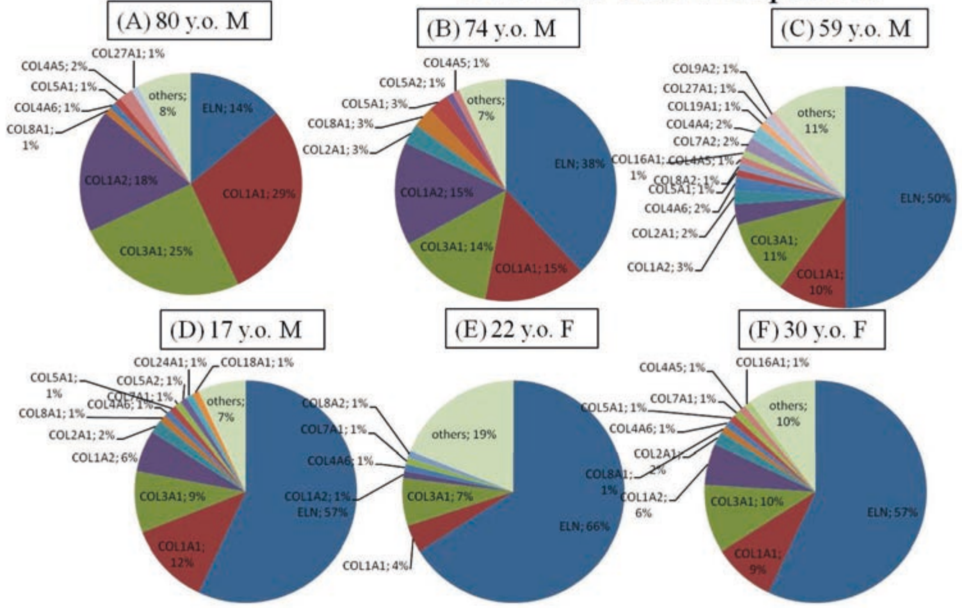
(A) 80 y.o. M
(B) 74 y.o. M
(C) 59 y.o. M
(D) 17 y.o. M
(E) 22 y.o. F
(F) 30 y.o. F

- Samples from LCS patients
- Samples from LDH patients
- Representative Collagens from LCS and LDH patients

3A.3

How do Tamoxifene and Raloxifene effect bipedal scoliotic mice?

Nadir Yalcin
Ataturk Training and Research Hospital, Ankara, Turkey

Our findings are important as they suggest the possibility of a medical treatment for the prevention of progression in AIS, otherwise treated with cumbersome orthoses and/or surgery with relatively high morbidity.

Introduction:
Our previous studies demonstrate that a Selective Estrogen Receptor Modulator (SERM) Tamoxifene (TMX) may decrease the incidence and progression of the scoliotic curve in both chicken and bipedal mouse models (1,2). Raloxifene (RLX) is another SERM, which is more specifically targeted to bone and has fewer side effects than TMX.
Materials and Methods:
All procedures were approved by the institutional committee of animal use for research at Hacettepe University, Ankara, Turkey. Ninety, 3-week-old, female C57BL6 mice were made bipedal according to the technique defined by Machida et al (3) and divided into three groups: 1. TMX, 2. RLX 3. Control. TMX and RLX groups received 10mg/lt in drinking water beginning from the 3rd week. Anteroposterior X-rays were obtained at the 20th and 40th weeks. On these, curves in different locations in the spinal column were identified according to the SRS guidelines and the Cobb angle was measured.
For histomorphological analysis, spinal columns were collected at 20th and 40th weeks (n=4/group). The lumbar 2nd vertebrae, L2-L3 discs and growth plates on both sides of all specimens were analysed after histologic staining. Total corpus volume (TCV), total trabecular volume (TTV), percentage of TTV to TCV (%TTV/TCV), total disc volume (TDV), total nucleus pulposus volume (TNPV) and total growth plate volume (TGPV) were calculated using the equation for a conical frustum.
Results:
Radiology:40th week analysis revealed similar curve rates among groups. RLX group had significantly lower upper and lower thoracic curve magnitudes compared to control group (p
Histology: TCV of both groups were similar at 20 weeks whereas there was a significant difference between RLX treated and control animals at 40 weeks. The vertebral body of RLX treated mice were smaller than the control group. TTV had the same distribution as TCV at 20 weeks. However, at 40 weeks, TMX-treated animals had higher TTV than controls but this was not significant. The TTV of RLX animals was almost the same as controls at the 40th week, but the ratio of TTV to TCV in both TMX and RLX groups were greater compared to controls. Both TDV and TNPV were decreased in treated groups at 20 weeks but this was not significant statistically. At 40 weeks, TDV in animals treated with RLX was significantly lower than controls. The growth plates of treated groups were smaller and thinner compared to controls at 20 weeks (Fig. 2,3).
Conclusions: RLX is as effective as TMX in preventing progression of scoliotic curves. Both drugs did not reduce the incidence of scoliosis, but the curve magnitudes between groups were reduced. Our findings suggest that the mechanism associated with this is the early maturation of growth plates thereby possible deceleration of the growth rate of the vertebral column. The mechanisms of action of these drugs on the growth plate and the intervetebral disc needs to be explored in further studies.

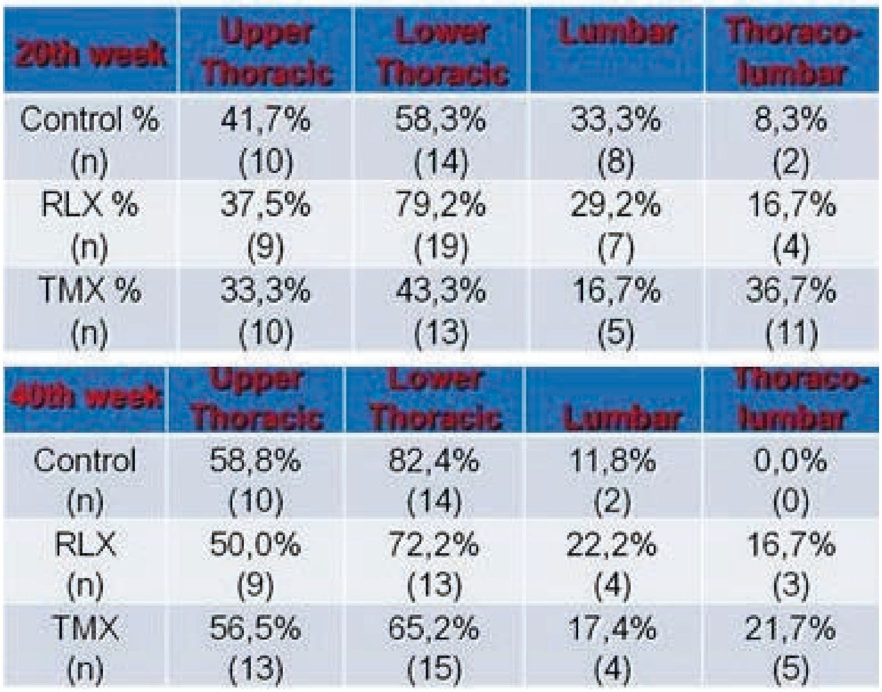

20th week	Upper Thoracic	Lower Thoracic	Lumbar	Thoraco-lumbar
Control % (n)	41,7% (10)	58,3% (14)	33,3% (8)	8,3% (2)
RLX % (n)	37,5% (9)	79,2% (19)	29,2% (7)	16,7% (4)
TMX % (n)	33,3% (10)	43,3% (13)	16,7% (5)	36,7% (11)

40th week	Upper Thoracic	Lower Thoracic	Lumbar	Thoraco-lumbar
Control (n)	58,8% (10)	82,4% (14)	11,8% (2)	0,0% (0)
RLX (n)	50,0% (9)	72,2% (13)	22,2% (4)	16,7% (3)
TMX (n)	56,5% (13)	65,2% (15)	17,4% (4)	21,7% (5)

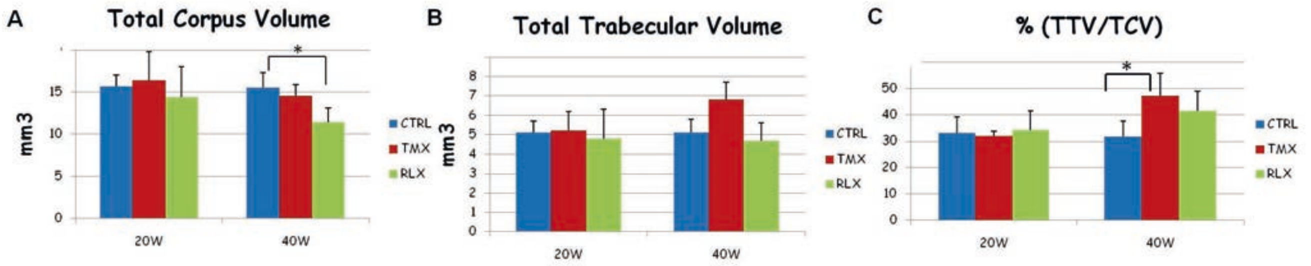

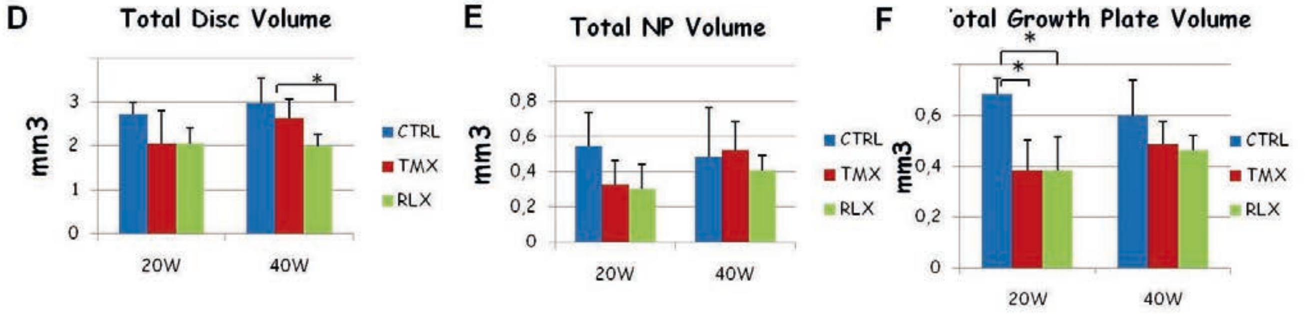

-Rates and average magnitudes of scoliotic curves by location and type of treatment at 20th and 40thweek

-Results of histomorphometric analysis. Total corpus volume, Total trabecular volume and Trabecular density by treatment and time pf analysis * $p<0.05$.

-Results of histomorphometric analysis. Total disc volume, Total NP volume and Total growth plate volume by treatment and time pf analysis * $p<0.05$.

3A.5

Near Infrared Spectroscopy for the Intra-operative Assessment of Human Spinal Cord Blood Perfusion.

Amir Amiri
Royal National Orthopaedic Hospital, London, UK

We describe the successful use of near infrared spectroscopy (NIRS) for intraoperative detection of changes to human spinal cord perfusion. With the advancement of technology it might be possible to use NIRS as a spinal monitoring tool.

Introduction:
Despite the significant interest in the assessment of human cerebral perfusion, investigations into human spinal cord blood perfusion (SCP) are scarce. Current intra-operative monitoring of the spinal cord relies on the assessment of neural conduction as a surrogate for SCP. However, there are various inherent limitations associated with the use of these techniques. A method of direct assessment of SCP may result in earlier warning of impending spinal cord damage. Near infrared spectroscopy (NIRS) has been successfully used for monitoring and assessing human cerebral perfusion and has shown promising results in intra-operative assessment of SCP in animal models.
The aim of this study was to investigate whether it is possible to monitor physiological changes in human SCP intra-operatively using NIRS with indocyanine green (ICG) tracer technique. We used this technique to calculate the human spinal cord carbon dioxide (CO_2) reactivity index. In addition, we investigated whether the lamina causes significant attenuation of NIRS signals.
Patients and Methods:
18 patients undergoing elective posterior cervical spine surgery provided informed consent to take part in this Intra-operative human experimental study. Nine patients underwent trans-dural assessment of SCP, while the other nine patients had trans-laminar measurements. Patients' SCP was continuously monitored using a NIRO-500 NIRS monitor via a set of purpose built optodes. Their arterial ICG concentration was simultaneously assessed using a pulse dye densitometer. Patients' end tidal CO_2 was gradually increased by 7.5 mmHg and then returned back to baseline. Three sets of measurements were taken by rapid intravenous administration of 0.1 mg/Kg of ICG; baseline, hypercapnic, and return to baseline.
Results:
Following hypercapnia, an increase in SCP by a mean of 57.2 ± 23.3 % in the trans-dural group and 46.6 ± 36.3 % in the trans-laminar group was detected. CO_2 reactivity index was 7.6 ± 3.2 %ΔSCP/mmHg in the trans-dural group and 6.4 ± 5.3 %ΔSCP/mmHg in the trans-laminar group. There was no significant difference in the increase in SCP ($p=0.475$) or the CO_2 reactivity index ($p=0.581$) observed between the trans-dural and the trans-laminar groups.
Conclusion: This is the first study to investigate the use of NIRS during spinal surgery in human subjects. To the best of our knowledge there are no other reports of CO2 reactivity index for human spinal cord in the literature. Intra-operative NIRS with ICG tracer technique can clearly identify increase in the SCP in response to hypercapnia. It is possible to use this technique for monitoring SCP over the dura as well as the lamina. With the advancement of technology it might be possible to insert a fine NIRS optical fibre through a spinal needle in to the extradural space for continuous monitoring of the SCP. Such minimally invasive monitoring will be useful during spinal surgery, thoraco-abdominal aneurysm repair surgery, as well as monitoring of patients in the high dependency unit. This technique could also potentially be used to provide insight into the pathophysiology and autoregulation of commonly acquired spinal cord conditions.

3A.6
With or without the long head of the biceps tendon?

Marco Hoozemans
Orthopaedic outpatient department, Medical Centre Alkmaar, Alkmaar, The Netherlands

Simulations using a musculoskeletal model of the upper extremity show that absence of the long head of the biceps tendon minimally affects other muscle forces, while keeping the glenohumeral joint reaction force directed inside the glenoid.

Introduction

The function of the long head of the biceps tendon (LHBT) is poorly understood. LHBT related pathology is often treated with tenotomy or tenodesis, which might lead to a decrease in glenohumeral joint stability. In this study the effect of an absence of the LHBT on upper extremity muscle forces and moments, and the trajectory of the glenohumeral joint reaction force inside the glenoid was studied.

Patients & Methods

The Delft Shoulder and Elbow Model (DSEM) is a musculoskeletal model for the upper extremity, based on three-dimensional anatomical information. This model was developed to increase the functional insight in the mechanical behaviour of the upper extremity and comprises all shoulder and arm muscles, divided into 139 muscle elements. Kinematic data of a person lifting a 2.5 kg box from waist height to a level above shoulder height and subsequently lowering the box was used as input for the model. Model simulations were run with and without LHBT to estimate the effect of tenotomy on upper extremity muscle forces and moments, and the trajectory of the glenohumeral joint reaction force inside the glenoid.

Results

In case of the LHBT being present, muscle forces generated by the long head of the biceps were estimated to be maximally 50 N when performing the lifting and lowering task. When leaving out the LHBT in the model, changes in muscle forces and moments were small and were relatively most pronounced in the deltoid, supraspinatus, short head of the biceps (SHB) and in the brachioradialis (see figure 1), especially when an elbow flexion moment was needed. In the elbow, the flexion moment of the SHB increased from maximally 8 to 10 Nm. This led to an increased (and unwanted) adduction moment around the glenohumeral joint, which required additional compensating abduction moments of the deltoid (pars spinalis) and supraspinatus. Finally, the trajectory of the glenohumeral joint reaction force inside the glenoid proved to be somewhat wider in case of the LHBT being absent in mainly superior direction (see figure 2), but still well within the borders of the glenoid surface.

Discussion/Conclusion

Absence of the LHBT affects muscle moments at both the elbow and glenohumeral joint. For the lifting activity studied, the decrease in required (internal) flexion moment around the elbow because of leaving out the LHBT is compensated by an increase in activity of the SHB at the elbow. This results in an unfavourable adduction moment around the glenohumeral joint that has to be compensated by an increase in deltoid and supraspinatus activity. This might also explain the shift of the trajectory of the glenohumeral joint reaction force inside the glenoid in superior direction, although we believe this is unlikely to be of clinical significance as it stays well within the borders of the glenoid surface. Our findings indicate biceps tenodesis more favourable over tenotomy as a tenodesis would preserve its flexion generating effect at the elbow, rendering the increase in SHB activity unnecessary and therefore not requiring an increase in deltoid and supraspinatus activity.

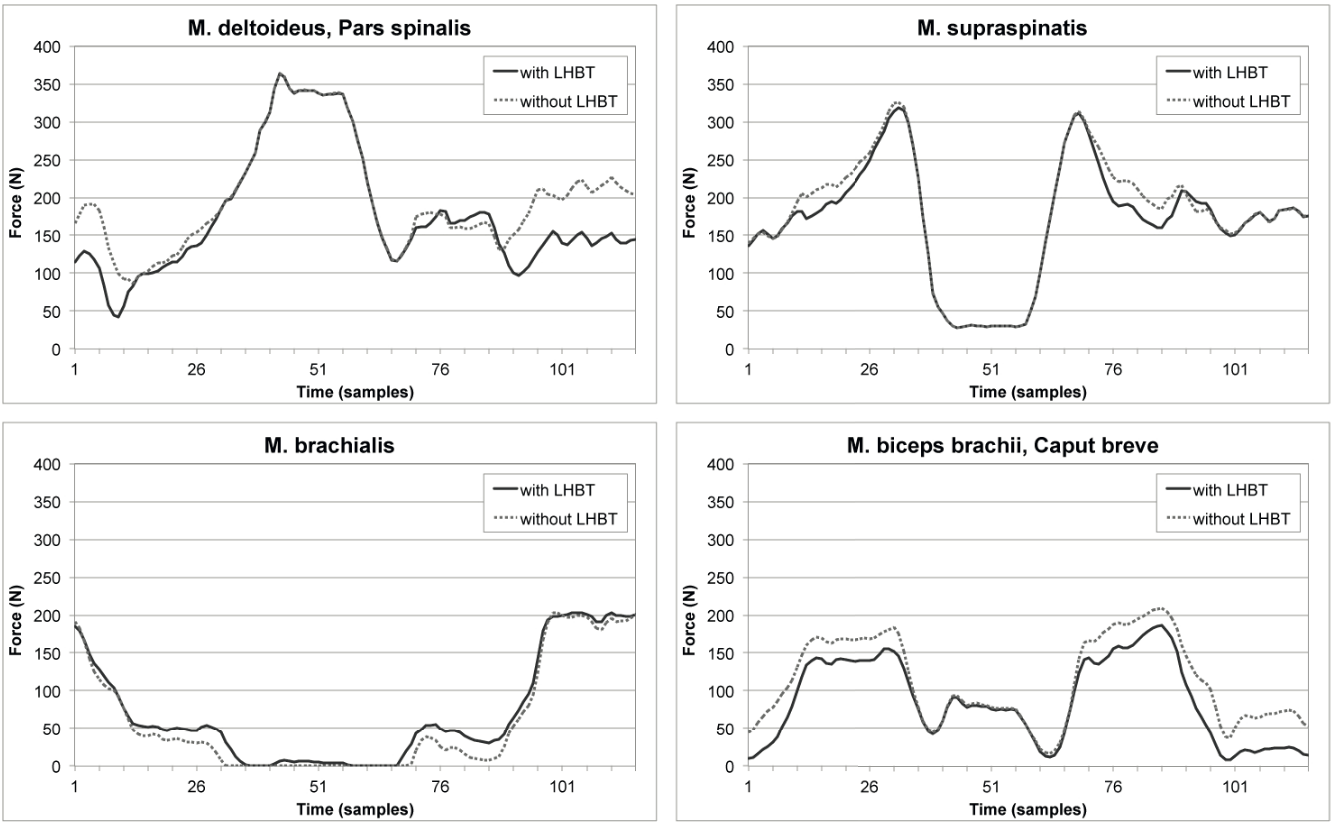

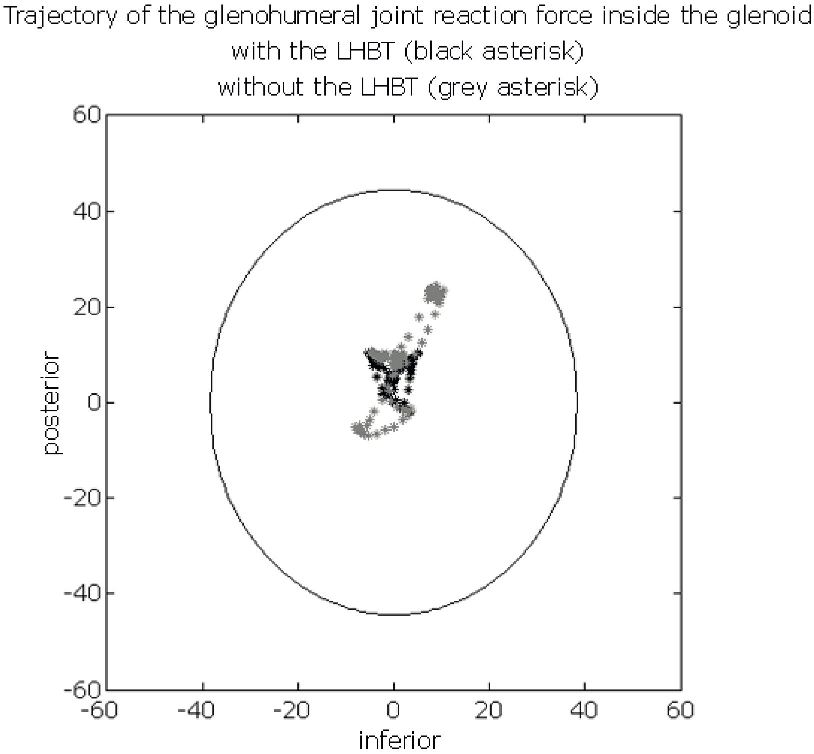

-Forces (N) of relevant muscles estimated using the Delft Shoulder and Elbow Model, for lifting a 2.5 kg box above shoulder height and subsequently lowering the box. Forces are presented for the situation in which the LHBT is present (solid line) and in which the LHBT is not present (dashed line).
-The trajectory of the glenohumeral joint reaction force inside the glenoid, estimated using the Delft Shoulder and Elbow Model, for lifting a 2.5 kg box above shoulder height and subsequently lowering the box. The trajectory is presented for the situation in which the LHBT is present (black asterisk) and in which the LHBT is not present (grey asterisk).

3A.7

Botulinum toxin injections to reduce internal rotation contractures in obstetric brachial plexus injuries

Bouke Duijnisveld
Leiden University Medical Center, Department of Orthopaedics, The Netherlands.

This prospective comparative study shows that internal rotation contractures of the shoulder associated with obstetric brachial plexus injuries can be reduced by botulinum toxin injections. The need for tendon transfer surgery is decreased while subscapularis degeneration negatively influences clinical outcome.

Introduction:
Obstetric brachial plexus injuries (OBPI) are frequently associated with internal rotation contractures of the shoulder as a result of muscle imbalance. The purpose of this study was to assess the effect of botulinum toxin A (BTX-A) injection in the subscapularis muscle on the passive external rotation (PER) and relation to the indication for tendon transfer surgery in children with OBPI.
Patients and Methods:
Prospective cohort study on 15 consecutive patients with an internal rotation contracture of the shoulder with BTX injection in the subscapularis and a minimum follow-up of 2 years. BTX-A (2 U/kg body weight) was injected under general anesthesia after MRI. A control group of 67 patients with an internal rotation contracture of a historic prospective cohort was used. The PER was assessed pre-MRI and at clinical follow-up at 3, 12 and 24 months. Subscapularis quality was evaluated at MRI as normal, atrophic, or atrophic with fatty degeneration. Logarithmic regression analysis was used to determine the effect of BTX-A injection and subcapularis degeneration on the need for tendon transfer surgery.
Results:
At 3 months, the BTX-A group showed a mean increase in PER in adduction of 43° compared to the control group (95% CI 27 to 58, PP=0.001) and is increased in patients with subscapularis fatty degeneration (OR=21, P=0.04).
Discussion/Conclusion:
BTX-A injections in the subscapularis of OBPI patients could reduce internal rotation contractures and the number of patients that are candidates for tendon transfer while subscapularis degeneration negatively influences clinical outcome. MRI evaluation of muscles and glenohumeral conformity prior to internal rotation contracture treatment of the shoulder is mandatory.

3A.9

Fusion less 3-D correction of idiopathic scoliosis. Feasibility of concept and pilot study results.

Jacobus Arts
Maastricht University Medical Centre, Maastricht, The Netherlands

A surgical technique for idiopathic scoliosis treatment providing 3-D deformity correction over time while allowing spinal growth and preservation of spine mobility is currently beyond our capabilities. When proven feasible it will greatly improve patients quality of life.

Introduction

Idiopathic scoliosis is a complex 3-D spinal deformity. Surgical correction is usually performed with a fusion technique using metal rods and metal sublaminar wires. Lack of spinal column growth, loss of correction over time, neurological complications and wire breakage are the main clinical problems during the introduction and removal of the metal wires.

A surgical option maintaining spinal mobility and spinal growth while also providing correction of lateral and rotational deformity would be advantageous over current treatment options.

Conceptually an ‘internal brace’, metal rod linked to a construction of UHMWPE fibre (Dyneema Purity®, DSM) per spinal level would allow growth (UHMWPE fibre can slide along metal rod) while also providing better rotational correction and preservation of spine mobility. (Figure 1). In vitro mechanical tests and in vivo animal models are used to assess the feasibility of this proposed technique.

Methods

1. Mechanical test:

Five different sublaminar wires were tested in four fresh frozen human thoraco-lumbar spines: one titanium cable (Atlas, Medtronic), two UHMWPE braids made of Dyneema Purity® (round 1mm; flat 5mm) and two UHMWPE woven constructions made of Dyneema Purity® (flat 3 and 5mm). The sublaminar wires were pulled upwards at a constant speed of 10 mm/min until failure of either the lamina or wire.

2. Animal study

In 6 immature Tesselaar sheep, two pedicle screws were placed at L4 and four consecutive laminae were attached to two titanium rods using UHMWPE sublaminar wires of different (3 and 5mm) diameter. The sublaminar wires were tightened with a tensioning device. Titanium sublaminar wires were applied in one animal as a control. The animals were sacrificed after 16 weeks. Radiographs and CT-scans were evaluated and histological analysis was performed.

Results

1. Mechanical test: The cut-through forces for constructions made with Dyneema Purity® measured up to those for titanium cable. The woven 3mm wide construction showed the highest mean cut-through force, however not statistical significantly different. 4 out of 7 titanium wires broke before cutting through the lamina (mean force 895 Newton). Only one UHMWPE constructions made with Dyneema Purity® broke (mean force 1325 Newton).

2. Animal study: Growth of the operated segment was observed (average growth 8.7 mm (sd ± 1.2). The reconstructions remained stable during follow-up as confirmed by CT-scans and radiographs. Macroscopic analysis showed that none of the 3 or 5 mm knots loosened and cryogenic sections showed no inflammation at lamina and dura levels.

Discussion

These preliminary study results indicate that Dyneema Purity® constructs are as strong as Ti laminar wires and able to provide sufficient stability, while allowing growth of a fixed segment in an animal model.

Furthermore they showed that UHMWPE laminar wires made with Dyneema Purity® fiber can provide sufficient stability in fusionless spinal surgery techniques.

Future animal studies will entail more clinical realistic models in which we first induce a scoliosis deformity which is subsequently reconstructed. After 6 months again stability of the reconstruction, biocompatibility of the reconstruction and growth of the spinal column will be assessed.

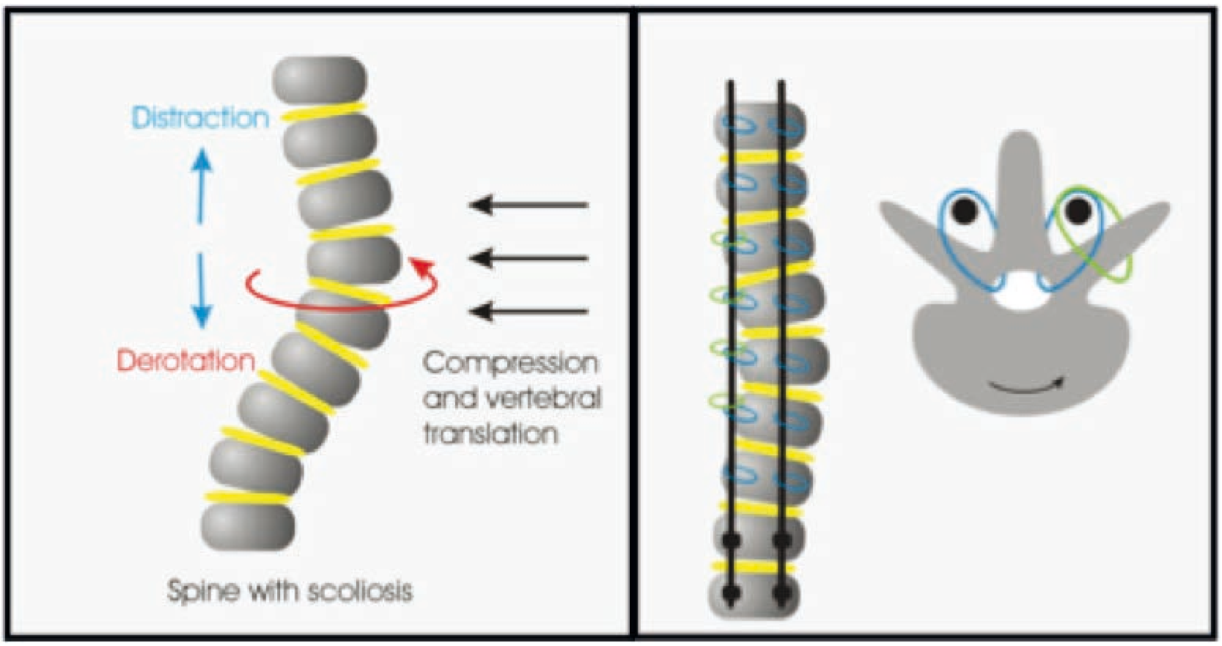

Left: types of correction needed for idiopathic scoliosis treatment. Right: our method of correction with metal rods along the spinal processus and sublaminar wiring with UHMWPE constructions made with Dyneema Purity allowing spinal column growth and a better 3-D deformity correction as compared to metal laminar wires.

3B.1

Mechanical stimulation of tendon-derived cells and investigation of its influence on gene expression

Cvetan Popov
Ludwig-Maximilians-University (LMU), Munich, Germany

This study represents a systematic approach to identify genes which are responsive to mechanical stress in tendon-derived cells. Hence, we identified that the expression of genes involved in cell-matrix interactions and matrix remodelling are altered in the mechanically stimulated cells.

Introduction:

Tendons are dense connective tissues subjected periodically to mechanical stress upon which complex responsive mechanisms are activated. These mechanisms affect not only the development of these tissues but also their healing process. Despite of the acknowledged importance of mechanical stress for tendon function and repair, the mechanotransduction mechanisms in tendon are still unclear and their elucidation remains one of the key goals in tendon research. Thus, the aims of this study were first, to stimulate mechanically tendon-derived cells and second, to analyse gene expression changes in the mechanically loaded cells. In this pilot study, we focused on the expression of tendon-related genes such as collagens and proteoglycans (major components of the tendon extracellular matrix), integrins (major cell mechanoreceptors) and MMPs (matrix metalloproteases which are involved in matrix degradation and thereby turnover).

Methods & Results:

Primary Achilles tendon-derived cells were isolated from two human donors and after an initial expansion in vitro, were subjected to cyclical stretching at a frequency of 1Hz and amplitude of 1, 5 and 8% for 1 and 3 days. After the mechanical stimulation, mRNA was collected from the cells and converted into cDNA. In the first phase of the study, we performed semi-quantitative PCR for the tendon-related matrix molecules, namely, collagen 1 and 3, COMP, tenascin C, decorin, byglican, fibromodulin and lumican. This analysis showed no apparent alteration in their gene expression upon mechanical stimulation. Next, since the collagen I is the major matrix protein in tendons, we continued with more precise analysis of the collagen I-binding integrins which are α1, α2 and α11 subunits. We applied LightCycler PCR technology allowing for estimation of quantitative differences in the receptor expression prior and after stimulation. We detected a clear upregulation of the three integrin subunits in tendon cells stimulated with 8% amplitude for 3 days. Stimulation with lower amplitudes and for just 1 day did not result in integrin expression changes. Using this technology, in the final phase of the study, we investigated the gene expression of 5 different MMPs and interestingly, we observed a definitive mechanoresponce of MMP13 and 14. Their gene expression was upregulated only after 3 days of stimulation but a positive effect was observed at each of the tested amplitudes.

Conclusions:

Taken together, here, we can convincingly report that expression of collagen I-binding integrins, namely α1, α2 and α11 as well as MMP13 and 14 is enhanced in the tendon-derived cells after 3 days mechanical stimulation with higher amplitudes such as 8%. Interestingly, a link between mechanical stress, integrins and MMPs has been reported in mesenchymal fibroblasts and it has been suggested to play an important role in matrix remodelling. Thus, our study contributes to a better understanding of the mechanotransduction mechanisms in tendon-derived cells which in long term, after further translational research between tendon cell biology and orthopaedic medicine, can be beneficial to the management of tendon repair.

3B.10
The BMP2-eNOS Axis Regulates Bone Development and Anabolic Effects of Statins

Megan Weivoda
University of Oxford, Oxford, UK

BMP-2 is essential for normal skeletal development and bone growth. Our studies identify a signaling pathway through which BMP-2 may mediate development and statin-induced bone growth, via the endothelial Nitric Oxide Synthase pathway.

Bone morphogenetic protein (BMP)-2 is essential for normal skeletal development and bone formation. It has been demonstrated that BMP2 mediates the bone anabolic properties of statins although the mechanism by which this occurs is unclear. As statins induce beneficial vascular effects via endothelial nitric oxide synthase (eNOS), and eNOS KO mice have a skeletal phenotype strongly resembling that of BMP2 KO mice, we hypothesize that eNOS plays a central role in mediating the anabolic effect of statins by controlling BMP2 expression.

We employed in vitro studies, ex vivo calvariae assays, and genetically modified mouse models to assess the effect of statins and/or NO donors or NOS inhibitors on gene expression and bone formation in tissues from normal, BMP2KO, and eNOS KO animals. In addition, we characterized the skeletal phenotype of DN-BMPRII:eNOS KO mice by μCT scanning and histomorphometry.

Simvastatin (10μM) increased eNOS and BMP2 mRNA and led to a 50% increase in NO in osteoblastic cells (p-3). Inhibition of NOS with L-NAME (10uM) returned bone growth to levels comparable with vehicle treatment alone (2.8±0.5 sq mm x10^{-3}). In addition, simvastatin treatment of eNOS KO murine calvariae demonstrated no significant increase in bone growth.

Osteoblastic cells treated with NO donors increased BMP2 protein by 2-fold, while BMP2 treatment did not result in any change in eNOS. Also, osteoblasts isolated from eNOS KO mice exhibited decreased BMP2 expression. These data support a linear pathway in which statin treatment increases BMP2 via eNOS. To assess the skeletal effects of this pathway in vivo, we examined DN-BMPRII and eNOS KO mouse models. DN-BMPRII mice displayed a decrease in BV/TV by μCT analysis compared to wildtype (17.83±.16% vs 5.6±1.12%, p

Together these data support a signaling system in which statins trigger eNOS activity to stimulate BMP2 expression. These findings demonstrate a clear physiological mechanism controlling skeletal development through which the bone anabolic effects of statins may be mediated.

3B.11

Nfat5 is involved in in vitro chondrogenic differentiation under normal and increased tonicity

Marjolein Caron
Maastricht University Medical Centre, dept. Orthopaedic Surgery, Maastricht, The Netherlands

Chondrogenic differentiation of progenitor cells is enhanced by increasing the tonicity of the culture medium to 380 mOsm. Nfat5 is important for chondrogenic differentiation of these cells under both tonicities and mediates related effects through influencing Sox9 expression.

Introduction:
New techniques promoting chondrogenic differentiation of progenitor and stem cells to chondrocytes are of interest to improve hyaline cartilage regenerative medicine approaches. Several studies have shown that human articular chondrocytes in vitro are tonicity-responsive and increase matrix synthesis under physiological tonicity and that Nuclear factor of activated T-cells 5 (Nfat5) plays an essential role in this response. The effects of increased tonicity (380 mOsm) on chondrogenic differentiation of progenitor cells in vitro are largely unknown. In addition, the expression and a (tonicity-independent) function of Nfat5 during this process and potential cross-talk to chondrogenic regulators remain elusive.
Methods:
ATDC5 cells and human bone marrow stem cells (hBMSCs) were differentiated in the chondrogenic lineage in control (280mOsm) and increased tonicity (380mOsm) cultures. Chondrogenic outcome was measured by gene- and protein expression analysis. RNAi was used to determine the role of Nfat5 in chondrogenic differentiation under normal and increased tonicity.
Results:
Overall, increasing tonicity from 280 mOsm to 380 mOsm resulted in an improved chondrogenic marker expression (Col2a1, Col10a1, Acan, Sox9, Runx2 and GAGs) during the differentiation of the chondroprogenitors ATDC5 and hBMSCs. Furthermore, Nfat5 knockdown shows that this transcription factor is involved in chondrogenic differentiation under both tonicity conditions and responsible for the improved chondrogenic marker expression under increased tonicity. Knockdown of Nfat5 decreased early Sox9 expression and may explain the decreased Col2a1 and Acan expression observed in these cultures. In contrast, Sox9 knockdown resulted in decreased levels of its targets Col2a1 and Acan, but did not affect mRNA levels of Nfat5 or its target genes.
Conclusions:
Increasing the tonicity from plasma levels (i.e. 280 mOsm) to 380 mOsm significantly increased chondrogenic marker expression during the course of chondrogenic differentiation of progenitor cells (ATDC5 and hBMSCs). Nfat5 is important for chondrogenic differentiation of these cells under both tonicities and mediates related effects through influencing Sox9 expression.

3B.3

Heat Shock proteins 70 and 90 in osteoarthritis progression

Michiel Siebelt

Hsp proteins (Hsp) regulate cellular stress responses and play an important role in chondrocytes and osteoarthritis development. Inhibition of Hsp90 proved to be beneficial for articular cartilage during strenuous running induced osteoarthritis.

Introduction

Heat shock proteins (Hsp) can be upregulated in chondrocytes in order to cope with increased stress levels. Hsp70 upregulation has shown to protect chondrocytes from apoptosis and prevents extra-cellular matrix (ECM) degradation by inhibition of NFkß. However, persistent mechanical stress abolishes the protective effect of Hsp70. Hsp90 upregulation stimulates NFkß. Possibly, Hsp90 might be responsible for the loss of beneficial effect from Hsp70. This study investigated the specific role of Hsp70 and Hsp90 during OA progression in an in-vivo rat model and tried to intervene with disease progression via specific Hsp90 inhibition (Hsp90i).

Methods

Thirthy-eight male Wistar rats were divided over three groups: baseline (n=6), OA control (n=12), Hsp90i (n=20). All baseline rats were immediately processed with an analysis sequence that consisted of in-vivo ^{111}In-DTPA-folate SPECT/CT for macrophage imaging, ex-vivo EPIC-µCT for bone and cartilage analysis and western blot analysis for measurement of Hsp70/Hsp90 protein levels in cartilage. Rats in the Hsp90i received 7mg of BIIB021 (Hsp90 inhibitor; SelleckChem) via an oral probe thrice weekly. All rats were forced to run (1km in 1hr, 5´/wk) six weeks on a rodent treadmill to induce OA, then six OA controls and ten Hsp90i rats were subjected to the analysis sequence. All other rats remained for another six weeks of rest in the experiment and then processed with the analysis sequence. Differences between means of both groups were compared with unpaired-t-tests.

Results

Our preliminary results from western blot analysis, showed that chondrocytes raised Hsp90 levels ~100 fold in the Hsp90i group. This is a compensatory response due to the loss of Hsp90 function through the inhibitor. Effective Hsp90i induces cells to switch to Hsp70 production, which explained the four times increase of Hsp70 Animals in the Hsp90i groups were able to increase the sGAG content of the cartilage and did not show signs of OA progression. Medial subchondral bone thickness increased more swift in Hsp90i animals. Lateral subchondral bone decreased slightly in OA control animals, but Hsp90i animals sustained a thicker subchondral plate. Macrophages did not become evidentially activated in OA controls, but surprisingly, after six weeks the activation level was significant lower in Hsp90i rats.

Conclusions

The results of this study demonstrate that stress related Hsp70 and Hsp90 production plays an important role in the onset of biomechanically induced OA. Hsp90 inhibition led to sustained levels of Hsp70, which protected against cartilage degradation and improved the quality of the ECM. Besides the effect of Hsp90i on cartilage, bone and macrophages also showed a beneficial response. These findings are interesting for therapeutic OA management.

3B.5

UTILIZATION OF PLATELET RICH PLASMA (PRP) IN ORTHOPEADIC PRACTICE: CLINICAL AND BIOLOGICAL ANALYSIS OF TERAPEUTIC EFFECTIVENES

Rocco Papalia
Campus Biomedico University Hospital, Department of Orthopaedic and Trauma Surgery, Rome, Italy

The literature provides little information about the variability of the clinical efficacy of PRP in relation to the biological characteristics of the product. Several more (P=0.01) or less (P=0.05) significant correlations were identified, both with clinical scores and haematological index.

Introduction

PRP is obtained by centrifugation of whole blood with the aim of producing plasma with high concentration of platelets. The literature provides little information about the variability of the clinical efficacy of PRP in relation to the biological characteristics of the product. Objectives of the study in question are: clinical evaluation of effectiveness of PRP "home made" a group of 89 patients, analysis of cytokine profile and concentrations of growth factors in a 10 patients homogeneous group, during treatment with intra-articular and peritendinous injections of PRP; description of possible correlation between changes in cytokine pattern and concentration of growth factors with clinical response to treatment in the same group of patients.

Patients & methods

89 patients were selected and declared fit to receive treatment with PRP "home made". In view of the underlying disease, (Tendinopathy, Epicondylitis, Chondral Lesions, Degenerative lesions of grade I-II-III-IV, Rotator Cuff Lesions) patients underwent to 3-5 cycles of intra-articular or peritendinous injections of PRP, at intervals of 7 or 15 days apart.

Scores of clinical evaluation were administered to each patient before treatment, before any infiltration, and six months after the last injection. The concentration of growth factors, and inflammatory cytokines present in the PRP, were evaluated in a homogeneous group of 10 patients with degenerative lesions of the knee cartilage of grade III-IV sec. Kellgren-Lawrence century. Finally correlation between growth factors, cytochine and haematological parameters of the patient and PRP with clinical parameters was analyzed.

Results

Overall Response Rate (ORR) was noted in 69 of 83 patients (84%).In addition, all the scores used have shown a significant rate in the period immediately after the second injection.Analysis of the growth factors showed a progressive increase in concentration than baseline, after the first application, with a peak level at the second (beginning of the period of clinical improvement statistically significant), and subsequent decrease at the third infiltration. Several more (P=0.01) or less (P=0.05) significant correlations were identified, both with clinical scores and haematological index. The pattern of inflammatory cytokines, after a stable trend from time 0, showed a decrease after the second clinical application, at the peak of growth factors and beginning of the patient's clinical improvement.

Discussion/conclusion

The results reported clinical efficacy in 84% of patients treated. In addition, the biological analysis showed at the beginning of the clinical improvement the increase in growth factors and decrease in inflammatory cytokines. More level I studies are necessary to identify the best production methodology and application of the product.

References

1. Marx, R.E. Platelet-rich plasma (PRP): what is PRP and what is not PRP? Implant Dent 10, 225-228 (2001).
2. Castillo, T.N., Pouliot, M.A., Kim, H.J. & Dragoo, J.L. Comparison of growth factor and platelet concentration from commercial platelet-rich plasma separation systems. Am J Sports Med 39, 266-271 (2011).
3. Ehrenfest, M. Classification of platelet concentrates:from pure platelet-rich plasma (P-PRP) to leucocyte- and platelet-rich fibrin (L-PRF). Trends in Biotechnology 27, 158-167 (2009).

3B.7

Synovial Wnt and WISP1 expression leads to OA-like cartilage damage by skewing of TGF-beta signaling

Martijn van den Bosch
Radboud University Nijmegen Medical Centre, Nijmegen, The Netherlands

Synovial upregulation of canonical Wnts and WISP1, as is found in experimental OA, leads to cartilage damage, probably by skewing TGF-ß signaling from the preserving Smad 2/3 towards the chondrocyte-hypertrophy-inducing Smad 1/5/8 pathway.

Introduction:

Although many osteoarthritis (OA) patients show synovial involvement, consequences are largely unknown. We found strong upregulation of canonical Wnts 2b and 16 and Wnt-1-induced secreted protein 1 (WISP1), in knee joints in two experimental OA models. Wnt signaling has been implicated in OA incidence and modulation of the ß-catenin pathway leads to OA-like changes in cartilage. In addition, TGF-ß signaling is critical in cartilage maintenance. TGF-ß signals via both ALK5 and ALK1 and downstream via phosphorylation of Smad 2/3 and Smad 1/5/8 respectively.

In this study we investigated the potency of canonical Wnts, produced by synovial cells, to induce OA pathology and whether canonical Wnts skew TGF-ß signaling from the protective Smad 2/3 pathway to the chondrocyte-hypertrophy-inducing Smad 1/5/8 pathway.

Methods:

Pathway analysis of microarray data from the synovium of a collagenase-induced OA mouse model was done using DAVID software. Detection of Smad 2/3 and Smad 1/5/8 phosphorylation was done by Western blot analysis. In vivo synovial overexpression of genes from the canonical Wnt signaling pathway was achieved by intra-articular injection of adenoviral vectors. Joint pathology was assessed by histology at several time points after injection. Gene expression was analyzed by qPCR after overexpression of Wnt genes in isolated human chondrocytes.

Results:

Pathway analysis using DAVID showed that both the Wnt and TGF-ß signaling pathway were enriched in the synovium of mice with collagenase-induced OA. To determine if synovial overexpression of canonical Wnts leads to cartilage damage, adenoviral vectors for Wnts 8a and 16, specifically targeting synovial cells, were injected in murine knee joints. At day 7 a highly significant induction of OA pathology was found at the medial margin of the medial tibial plateau. The incidence was 92% (n=12) for Wnt8a overexpression compared to 17% (N=12) for the control virus and 80% (N=5) for Wnt16 overexpression, but only 20% (N=5) for the control virus. Because of their relatively small size, Wnts and WISP1 proteins can migrate to the cartilage and possibly alter chondrocyte phenotype. Synovial Wnt8a and Wnt16 overexpression led to ß-catenin accumulation in chondrocytes, a tell-tale sign of canonical Wnt signaling, indicating diffusion of Wnts to the cartilage. Moreover, overexpression of canonical Wnts and WISP1 in human chondrocytes led to a significant increase of collagen type I and a significant decrease in type II collagen expression, suggesting a loss of chondrocyte phenotype. Pre-incubation with Wnt3a or WISP alone or Wnt3a + WISP1 together resulted in decreased TGF-ß-induced phosphorylation of Smad 2/3, whereas phosphorylation of Smad 1/5/8 was increased. This implies a shift towards dominant TGF-ß signaling via the hypertrophy-inducing ALK1 pathway.

Discussion:

Canonical Wnts produced in the synovium may play an important role in OA pathology by inducing ß-catenin signaling in the cartilage followed by cartilage damage. Synovial overexpression of canonical Wnts, as is found in experimental OA, may lead to chondrocyte phenotype changes, probably via modulation of the important TGF-ß signaling pathway. This underlines that synovial Wnt/WISP1 expression may be a potential target for OA therapy.

3B.9

Continued cell exposure to parathyroid hormone-related peptide (1-36) decreases osteogenic and angiogenic gene expression

Timothy Hardwick
Department of Biomaterials, Biomimetics and Biophotonics, The dental institute, Kings College London, London, UK

Summary: Continued cell exposure to the N-terminal domain of PTHrP (1-36) results in downregulation of osteogenic and angiogenic gene expression. Cell exposures up to 48 hours were shown to have an upregulatory effect on osteogenic and angiogenic gene expression.

Introduction:

Parathyroid hormone-related peptide (PTHrP) has been shown to be an important regulator of bone remodelling, via the promotion of osteoblast differentiation[1]. To date, in vivo tests have mainly focused on the C-terminal domain of the peptide (107-139). The aim of this study was to investigate the effect of the N-terminal domain of PTHrP (1-36) on osteogenic gene expression in human osteoblasts (HOB) and bone marrow stromal cells (BMSCs), as a potential therapeutic for bone repair. The effect of PTHrP (1-36)'s on pro-angiogenic factors was also assessed, as the formation of an integrated vascular network is vital for bone regeneration. Our hypothesis was that PTHrP (1-36) would increase both osteogenic and angiogenic markers.

Materials and Methods:

Primary human BMSC's and primary HOB cells were cultured in standard or osteogenic media with 0 nM, 1 nM or 10 nM PTHrP (1-36). At 8, 24 and 48 hours, gene expression was analysed via RT-qPCR. In order to assess early and middle stages of osteogenic and angiogenic differentiation, relative levels of runt-related transcription factor 2 (RUNX-2), alkaline phosphatase (ALP) and Collagen 1, as well as the angiogenic marker; vascular endothelial growth factor (VEGF) were quantified.

Results:

Exposure to PTHrP (1-36) resulted in an upregulation of VEGF expression in both BMSC's and HOB cells peaking at 1 nM concentration at 24 and 48 hrs respectively. At 10nM PTHrP, there was a reduction in VEGF expression compared to the control group. BMSCs cultured in osteogenic media showed a dose-dependent increase in the transcription of VEGF with the 1nM and 10nM group, with a 166% and 314% increase respectively in expression, compared to control cells (0 mM PTHrP). Continuous exposure of HOBs to PTHrP (1-36) for 48 hours also resulted in an upregulation in the gene expression of the osteogenic markers, RUNX-2, ALP and Collagen 1. BMSCs also showed a minimal upregulation in RUNX-2. Continuous exposure to PTHrP (1-36) for a total of 9 days resulted in a downregulation of all osteogenic and angiogenic gene expression markers. This effect was dose-dependent, with a relatively biphasic distribution. Interestingly, BMSC's were more sensitive to the peptide, showing 50-75% less expression compared to HOB cells.

Discussion and Conclusion: Exposure of both HOB cells and BMSC's to PTHrP (1-36) was shown to have a positive effect on osteogenic and angiogenic gene expression at 24 and 48 hours. Continuous exposure to 9 days however had the opposite effect with a downregulation in ostoegenic and angiogenic transcription. In this study, PTHrP (1-36) had a more pronounced effect on BMSCs compared to HOBs, which may be related to the BMSCs' lower passage number or increased sensitivity.

Ongoing work is examining the effect of intermittent doses of PTHrP (1-36) and whether the peptide can be effectively incorporated into a mesoporous bioceramic scaffold for direct delivery to sites of bone injury. The findings will help support or dispute our hypothesis that PTHrP (1-36)-loaded bioceramic scaffolds are suitable for the direct stimulation of bone repair.

4A.1

A potential mechanism of cobalt-induced inflammation found in MOM hip implants.

Agata Nyga
Imperial College London, London, UK

Cobalt is one of the metal components of MOM hip implants and its wear debris. Its role in MOM failure is not fully understood, however, it has a potential impact on the inflammation due to activation of the HIF pathway.

Introduction

Implant derived cobalt has been implicated in the mechanism of failure of metal-on-metal (MOM) hip implants. The wear debris from MOM is different from usual particulate wear debris as it is at nano-size (lower than 100μm in dimension). Also the nanoparticles (NP) consisting of cobalt have the potential to release cobalt in ionic form. Cobalt has been shown to act as a hypoxia-inducible factor (HIF) stabilizer. This stabilization mimics the processes associated with hypoxic condition (oxygen levels below normal). Hypoxic-related genes are activated, with many of them influencing inflammation and pain pathway (Fig. 1). This study presents the potential role of cobalt in ionic and nanoparticulate form in activation of hypoxia-related pathways of inflammation and pain.

Patients & Method

In order to isolate ions released from cobalt NP a conditioned media was prepared by incubating cobalt NP (20 nm, American elements, concentrations between 0-100 μg/mL)in tissue culture media at 37°C for 3,6 and 24 hours. After each time point NP solutions were ultracentrifuged to sediment NP and the supernatant was filtered through 0.2μm filter. Supernatant was analysed with ICP-MS to measure released cobalt. U937, a monocytic cell line, was used as a model for inflammatory response to cobalt nanoparticles and ions. U937 were stimulated with PMA in order to acquire a macrophage-like phenotype and were exposed to NP conditioned media, NP and cobalt chloride (0-100 μM)for up to 24 hours. After each exposure media was collected for cytokines analysis using ELISA. Cytotoxicity effects of each condition were assessed with MTT assay and cells were lysed for protein studies.

Results

NPs have shown highest toxicity potential depending on the concentration with toxic levels of ions released after 24 hours (Fig.2). After exposure to either nanoparticles or ions cells released TNF-α and showed decrease release of IL-10. No changes were observed with IL-1ß release. HIF-1α stabilization was confirmed in all conditions using Western Blot. Protein studies also confirmed increased expression of hypoxia-mediated proteins HO-1 and COX-2.

Discussion/Conclusion

This study has shown the potential role of cobalt as the important stimulant of the inflammation at the site of MOM due to the activation of the HIF pathway. Cytokine release studies showed increase in a pro-inflammatory cytokine, TNF-α, with a decrease in an anti-inflammatory mediator IL-10. No changes in IL-1ß indicate that the inflammasome has not been activated in U937 cell line upon exposure to either nanoparticles or ions. Inflammasome activation results in release of IL-1ß which acts upon activation of cyclooxygenase-2 (COX-2) which is responsible for the inflammation and pain pathway via prostaglandin release. However, COX-2 was induced both at the protein and gene level, which can be explained by the activation of HIF pathway, as COX-2 contains functional elements for HIF. Therefore, it is possible that the inflammation caused by wear debris in MOM implants is stimulated greatly by cobalt via activation of HIF pathway.

4A.2

How important is the femoral cup thickness in hip resurfacing?

António Ramos
TEMA, Biomechanics Research Group, Department of Mechanical Engineer, University of Aveiro, Portugal

Within this study we assessed how the thickness of the femoral cup of the hip resurfacing implant can change the relative mobility at the bone-implant interface. Numerical models with different femoral head thicknesses were constructed and analyzed.

Introduction:

The use of hip resurfacing technique in hip arthroplasty has increased in these last year's. This solution presents some biomechanical advantages comparatively to traditional total hip arthoplasty since bone support is higher and it is much easier to extract the implant if revision is necessary. The major problems in the load transfer process are associated to neck fracture and stress shielding. The excess of head deformation can provoke an abnormal tribology contact and induce higher rate of wear and mobility at the bone-implant interface.

Methods:

Five numerical models were constructed based on an in vitro resurfaced hip performed with synthetic Sawbones® (large left femur model). The femoral cup used is a Wright conserve model (Wright Medical Technology, Arlington, TN, USA) with 48 mm head size (figure 1). The thickness of head CAD model was increased and decreased in (20-40%) relatively to the model used in the femoral replacement.

The bone properties (manufacturer's data) were considered as linear elastic. A glued contact (no cemented) with a coefficient of friction of 0.3 was considered at the bone-implant interface. The load was applied in the distal region of femur and the acetabular cup was fixed to simulate the contact of the joint.

Results:

The bone-stem contact region is biomechanically the most critical one, namely in the frontal plane (figure 1). The small stem in the center of head improves the fixation and centralization of hip resurfacing, but induces high strains and deformation near its tip.

Figure 2 depicts the bone-implant interface strain distribution for the commercial model and those with higher and lower thickness. The strain distribution in the anterior-superior region is the most critical, but the thickness of head not changes significantly the strain intensity and distribution.

Relatively to the micro motion between the implant and bone head, we observed that the increase of thickness decreases the interface micro motion. The inferior regions evidence higher levels of micro motion.

Discussion:

The increase/decrease of the femoral cup thickness does not present any relevant changes concerning the interface strain distribution, which has also been pointed out by other authors.

The thickness of the femoral head cup changes the interface micro motions and induces changes on the load transfer mechanism. The increase of thickness decreases the head deformation and improves implant stability.

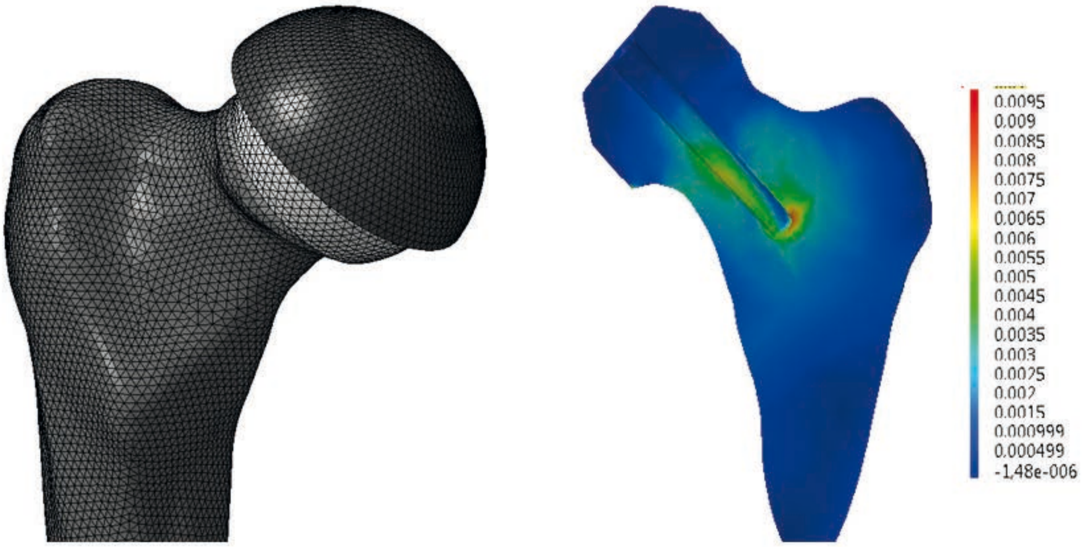

Figure 1: Finite element model of hip resurfacing and maximum strain distribution

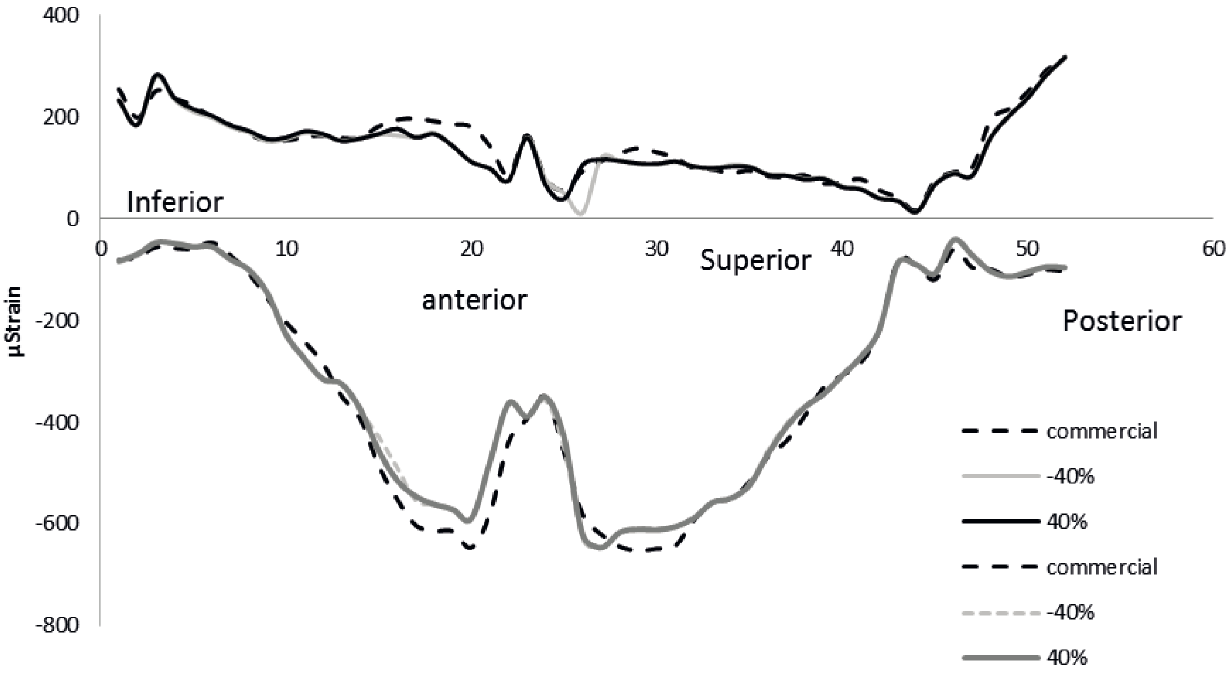

Figure 2: Maximum principal strain distribution versus femoral head cup thickness

4A.3

Mal-positioning Alone Does Not Necessarily Lead to Increased Wear in Metal-on-Metal Hip Resurfacing

Stephen Mellon
University of Oxford, Oxford, UK

Hip reaction force and the intersection of this force with the acetabular component was determined for subjects with well-positioned or mal-positioned acetabular components. Results suggest that edge-loading is induced by a combination of mal-positioning and intrinsic subject activity patterns.

Introduction:

Metal-on-metal hip resurfacing arthroplasty (MoMHRA) is a popular alternative to total hip replacement for younger patients. Despite low wear rates, metal-on-metal bearings release cobalt (Co) and chromium (Cr) ions into the body. There is evidence to suggest that these ions lead to adverse biological reactions1. Edge-loading caused by mal-positioned acetabular components has been suggested as a cause of increased metal wear2. The risk of biological reaction is lower for an acetabular orientation of 45° (±10) inclination and 20° (±10) anteversion3. However, mal-positioned acetabular components do not always lead to adverse reactions and studies have suggested that patient activity patterns may influence metal wear4. The aim of this study was to compute the hip reaction forces of subjects with well-positioned or mal-positioned acetabular components during functional activity, determine the point of intersection of this force with the acetabular component, and relate this to their serum metal ion levels.

Patients & methods:

Fourteen subjects, with either a Birmingham Hip Resurfacing (Smith and Nephew, Birmingham, UK) or a Conserve Plus (Wright Medical Technology, Arlington, TN, USA), were selected for this IRB approved study. The subjects were divided into three groups: Well positioned with low serum metal ion levels (n=6), mal positioned with high serum metal ion levels (n=4) and mal positioned with low serum metal ion levels (n=4) (Table 1).

Motion analysis data of each subject performing gait was captured with a 12 camera VICON MX (Vicon, Oxford, UK) using a Plug-in-Gait marker protocol with additional markers on the fifth and first metatarsals. Ground reaction forces were recorded using 3 force plates (AMTI, MA, USA). Immediately following motion capture, 10 retro-reflective markers on the pelvis and thighs were replaced with multi-modality markers and the subjects underwent a CT scan. This data was used to build musculoskeletal models for each subject in the AnyBody Modeling System v. 5.0 (AnyBody Technology A/S, Den) based on the Twente Lower Extremity Model (TLEM). Each subjects' hip joint centre (HJC) for the implanted and unimplanted side was incorporated into the model. For the implanted side the HJC was calculated by choosing points around the edge of the acetabular component and fitting a plane to the face of the cup. The HJC for the unimplanted side was determined by segmenting the CT scan of the femur (Mimics, Materialise, Netherlands) and fitting a sphere to the femoral head.

Subject specific hip reaction forces (HRF) were computed. These were transformed into the local coordinate system of the acetabular component and the angle the HRF vector made with the edge of the acetabular component was determined for the stance phase of gait (0 - 60%).

Results & Discussion:

The HRF of subjects with mal-positioned acetabular components and high metal ion levels were closest to the edge of the acetabular component (Figure 1). The mean angle for this group remained within 10° of the edge for the duration of the stance phase of gait.The HRF of the subjects with mal-positioned components and low ions were on average 5° further from the edge than subjects with mal-positioned components and high ions. The subjects with well-positioned components and low serum ion levels had HRF which were the furthest from the edge throughout the stance phase of gait. The subjects with well-positioned components showed the greatest variation in angle to acetabular component edge (Figure 2).

REFERENCES:

[1] Mabilleau, G. et al., Acta Orthop., 2008; 79(6):734-47.
[2] De Haan, R. et al., JBJR(Br), 2008;90-B:1158-63.
[3] Grammatopoulos, G. et al., JBJR(Br) 2010; 92-B:1072-8.
[4] Mellon, S. J. et al. Med. Eng. Phys. 2011;33(10)1212-20

4B.1
JIP1-inhibition sensitises osteosarcoma to doxorubicin

Jantine Posthuma de Boer
VU University Medical Center, Amsterdam, The Netherlands

Chemoresistance contributes to treatment failure in osteosarcoma. Inhibition of JIP1-kinase increases doxorubicin-induced cytotoxicity in osteosarcoma cells. JIP1 is expressed in a majority of OS specimens and is thus a clinically relevant target to enhance the treatment efficacy of doxorubicin.

Background

Osteosarcoma (OS) is the most common primary malignant bone tumour in children and adolescents. The gold standard for therapy consists of multi-agent chemotherapy and radical surgery when feasible. Despite this aggressive treatment regimen, survival outcomes remain unsatisfactory, especially in patients with metastatic and/or recurrent disease and patients with a poor response to induction chemotherapy [1, 2]. Chemoresistance contributes heavily to treatment failure and therefore to inferior survival outcomes. Targeting essential survival pathways concurrently with conventional chemotherapy treatment could possibly increase the efficacy of existing therapy. The aim of this study was to identify new drug targets that can be used as sensitisers to doxorubicin treatment in OS.

Methods Using an siRNA kinome library (Dharmacon), we systematically screened 788 kinase- and kinase-associated genes for their influence on survival after doxorubicin treatment in the OS cell line SaOS-2. Screens were executed three times, in a pair-wise fashion, i.e. either with or without doxorubicin treatment at approximately IC20. After data normalization, the treatment effects were studied by an empirical- Bayes linear model, using the limma software package [3]. Relative cytotoxicity was defined as the ratio of mean cytotoxicity after combination treatment (siRNA+doxorubicin) mean cytotoxicity after doxorubicin.

One candidate, JNK-interacting protein 1 (JIP1) was further explored as potential chemosensitiser in OS. The effect of JIP1 inhibition on doxorubicin response was verified using a small molecule JIP1-inhibitor (BI-78D3, Sigma) on a panel of OS cell lines and healthy bone cells. Western blot analysis was used to assess JIP1 protein expression and regulation of JIP1 activity was assessed by analysis of phosphorylated JNK (p-JNK) by immunoprecipitation with a JIP1-antibody followed by Western blot. JIP1 expression in human OS was investigated by immunohistochemistry on tissue micro arrays (TMAs) and correlated to survival outcome.

Results

RNAi-mediated silencing of JIP1 gave the most potent and significant sensitization to doxorubicin-induced cell death in SaOS-2 cells (relative cytotoxicity = 8.6; p = 0,0001, FDR = 2%) and was therefore selected for further investigations. BI-78D3 sensitised three out of four OS cell lines to doxorubicin treatment, but not healthy osteoblasts (Fig 1). We examined JIP1-JNK interaction and JNK phosphorylation in SaOS-LM7 and U2OS cells, which respectively showed a strong and poor sensitisation to doxorubicin using BI-78D3. Doxorubicin treatment increased p-JNK/JIP1 complex formation in LM7 cells, but not in U2OS cells. Concurrent treatment with BI-78D3 diminished p-JNK in both cell lines to undetectable levels, indicating successful inhibition of JIP1-JNK interaction and thus inhibition of JNK phosphorylation (Fig 2). Finally, JIP1 was expressed in two-thirds of human OS tissue samples and patients with JIP1 positive tumours showed a trend toward inferior overall survival (log rank; p = 0.056) (Fig 3).

Conclusion

Downregulation of JIP1 either by RNAi targeting or by pharmacological inhibition sensitises OS cells to doxorubicin treatment, but not healthy bone cells. JIP1 is expressed in a majority of OS specimens and is thus a clinically relevant target. JIP1 may have potential as a novel drug target in OS to enhance the treatment efficacy of doxorubicin.

References

1. Bielack SS et al., J Clin Oncol 2002; 20(3): 776-790
2. Hughes DP et al., Expert Opin Drug Deliv 2009; 6(12): 1311-1321
3. Smyth GK., Stat Appl Genet Mol Biol 2004;3:Article3.

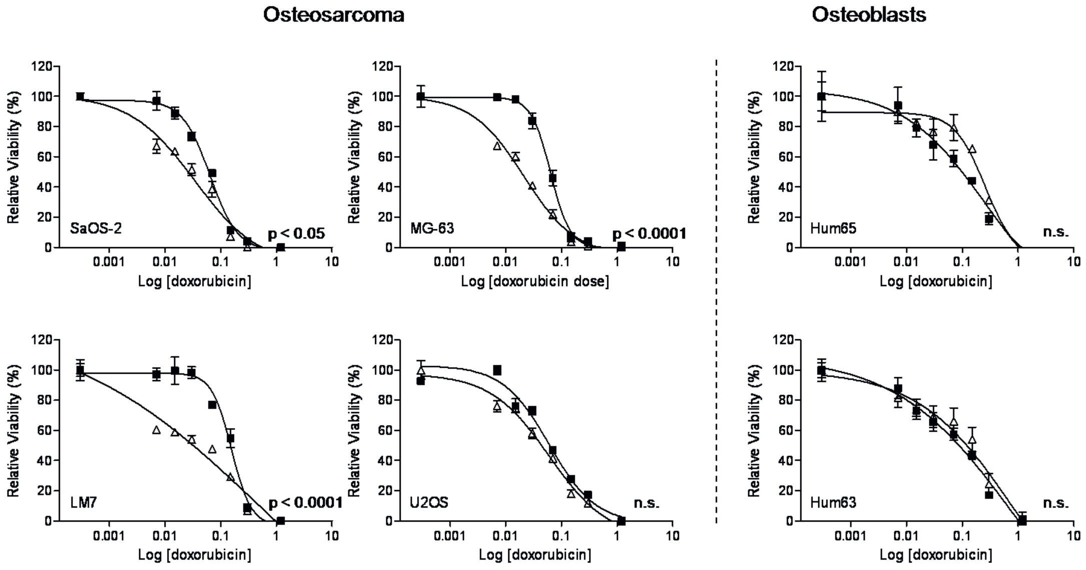

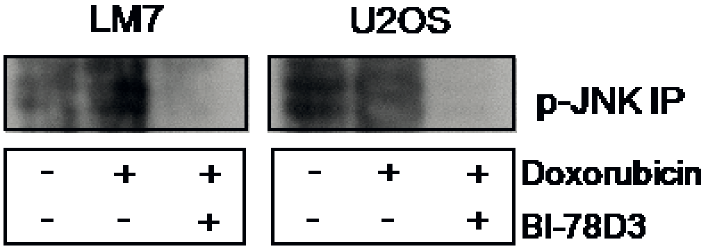

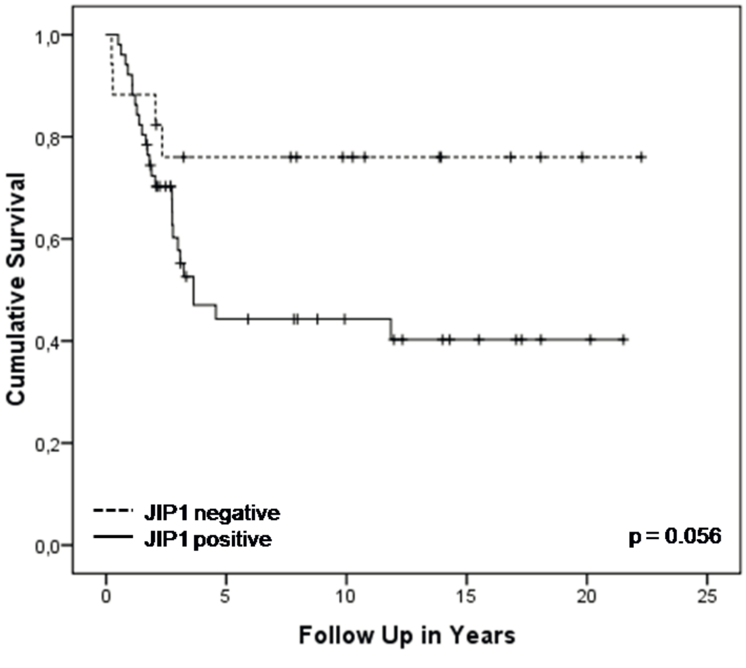

-Figure 1: JIP1 inhibition sensitizes OS cells but not normal osteoblasts to doxorubicin treatment. Cells were treated in triplicate with doxorubicin (closed squares) or with doxorubicin and JIP1-inhibitor BI-78D3 (open triangles). Sigmoidal dose-response curves were created and IC50 values were calculated. The sensitizing effect of JIP1 inhibition to doxorubicin treatment is significant in three out of four OS cell lines. Human primary osteoblasts Hum63 and Hum65 do not show sensitisation to doxorubicin treatment in the presence of the JIP1-inhibitor.

-Figure 2: JIP1-inhibitor BI-78D3 inhibits JIP1-JNK interaction leading to decreased phosphorylated JNK levels in doxorubicin treated cells. Doxorubicin treatment increased p-JNK in complex with JIP1 in LM7 cells, but not in U2OS cells. Concurrent treatment with BI-78D3 diminished p-JNK in both cell lines to undetectable levels, indicating successful inhibition of the JIP1-JNK interaction and JNK phosphorylation.

-Figure 3: Kaplan-Meier overall survival analysis of OS patients with JIP1 positive or negative tumours. Kaplan-Meier plots showing the cumulative survival of patients suffering from localised OS.

4B.2

Tumours Outside of the Local Skeletal Environment Contribute to Generalized Bone Loss

Seint Lwin
University of Oxford, Oxford, UK

With increasing detection and treatment options, cancer suffers are surviving longer. However, systemic, long-term effects are poorly understood. Our findings demonstrate that even without skeletal metastases, bone mass is markedly reduced by the presence of tumours outside of the skeleton.

The production and sustained release of ectopic hormones by cancer cells, induce striking systemic effects in tissues distant to the tumor site. For example, untreated breast cancer patients develop decreased Bone Mineral Density (BMD) leading to increased vertebral fractures, compared to healthy individuals. Based on these clinical observations, we hypothesized that tumors at locations distant to bone may result in a generalized bone loss.

To investigate this we employed well-established murine tumor models of melanoma, breast cancer and multiple myeloma, to induce tumors at sites distant to the assessed region of bone. All in vivo models conformed to national and institutional IACUC approved guidelines. Bone volume was analysed by uCT scanning and histomorphometric analysis. Subcutaneous (s.c.) tumor growth was measured daily and tumor growth in bone quantified by GFP fluorescence. The 5TGM1 myeloma tumor burden was determined by serum IgG2κ paraprotein levels. Urinary markers of bone resorption were also examined and dual-label fluorescent imaging used to assess bone formation rates (BFR). Statistical significance was determined using a students t-test with p values less than 0.05 considered significant.

Intravenous inoculation of 5TGM1 cells resulted in myeloma bone disease, with homing of myeloma cells to bone, osteolytic bone lesions, increased osteoclast number and decreased trabecular bone and BFR. In contrast, s.c. inoculation resulted in a time-dependent growth of a plasmacytoma, accompanied by a significant increase in serum IgG2κ levels. Flow cytometric analysis detected no significant increase in GFP+ cells within the marrow, demonstrating that myeloma cells inoculated s.c. do not home to the bone marrow.

Despite the absence of myeloma cells within the bone, uCT analysis demonstrated a 23% reduction in trabecular bone volume/total volume (BV/TV), and decreased vBMD and mBMD in mice bearing plasmacytomas compared with non-tumor controls (p

In addition, melanoma s.c. tumors resulted in a 20% decrease in BV/TV, along with decreased vBMD, mBMD and trabecular number, thickness and increased separation, while untreated bones in the intra-tibial MDA-MB-231 model showed a 47% decrease in BV/TV accompanied by decreased trabecular number, thickness and increased separation, along with decreased vBMD and mBMD compared to non-tumor bearing animals ($p<0.01$).

Our data demonstrate that myeloma, melanoma and breast cancer cells induce generalized bone loss, providing evidence for the development of cancer-induced osteoporosis from tumors at sites distant to bone.

4B.3

Surface proteomic analysis of osteosarcoma identifies EPHA2 as receptor for targeted drug delivery

Jantine Posthuma de Boer
VU University Medical Center, Amsterdam, The Netherlands

Targeted delivery of drugs to tumours can increase chemotherapeutic doses at the site of the tumour while sparing healthy tissues. EPHA2 is a suited receptor for the targeted delivery of treatment to osteosarcoma, thereby improving the efficacy of current therapy-regimens.

Background
Osteosarcoma (OS) is the most common primary malignant bone tumour in children and adolescents. The gold standard for therapy consists of multi-agent chemotherapy and radical surgery when feasible. Despite this aggressive treatment regimen, survival outcomes remain unsatisfactory, especially in patients with metastatic and/or recurrent disease and in patients with a poor response to induction chemotherapy [1, 2]. By employing the targeted delivery of drugs, higher chemotherapy doses can be achieved at the site of the tumour while sparing healthy tissues. The aim of this study was to identify a cell surface protein that can serve as a receptor for targeted drug delivery in OS.
Methods
Mass spectrometry was performed for the identification and relative quantification of proteins. The surface proteomes of five osteosarcoma cell-lines and three human primary osteoblast cultures we isolated using the Pierce cell surface isolation kit (ThermoScientific). Proteins were prepared for mass spectrometry by 1D-gel-electrophoresis followed by processing into peptides by in-gel tryptic digestion. The peptides were separated by nano-LC and identified by mass spectrometry (MS/MS) on a LTQ-TF. The measured spectra were searched against the IPI database using Sequest software to identify the corresponding peptides. The peptides were then validated and organised using Scaffold software to generate the final protein dataset. [3]. Protein abundance was assessed by spectral counting. Differential protein expression was analysed using the ß-binominal test [4].
One candidate, the Ephrin-A2-receptor (EPHA2) was further investigated for its suitability as a receptor for targeted drug delivery. Surface expression of EPHA2 on cell-lines was validated using FACS analysis. EPHA2 expression on human tumour samples was analysed by immunohistochemistry. Receptor-mediated uptake via EPHA2 was investigated using a GFP-expressing adenovirus specifically targeted to EPHA2 (AdYSA). The specificity of viral uptake was tested by competition experiments using the synthetic YSA peptide to compete with AdYSA for receptor binding [5].
Results
In total, 2841 proteins were identified using MS/MS, of which 156 were surface proteins that were significantly overexpressed on OS cells compared to osteoblasts. The EPHA2 receptor was the most abundant surface protein on OS cells, with an average of 100 spectral counts per OS cell line. EPHA2 was 12-fold upregulated on OS cells compared to osteoblasts (ß-binominal test; $p = 0.0005$). FACS analysis confirmed EPHA2 surface overexpression on OS cells compared to osteoblasts (Fig 1). Immunohistochemistry verified a significant overexpression of EPHA2 on osteosarcoma tissue compared to healthy bone tissue, both in primary and in metastatic lesions (Table 1). The EPHA2 expressing OS cells are efficiently infected with the targeted adenovirus AdYSA, whereas osteoblasts, poorly expressing EPHA2, are not. Receptor blocking by pre-incubation with a the synthetic YSA peptide resulted in EPHA2 receptor blockage and consequently a significant reduction of infection in the EPHA2-expressing (OS) cells. This indicates that AdYSA uptake is mediated by EPHA2 specifically (Fig 3).
Conclusion
The EPHA2 receptor is abundantly expressed on OS cell lines and expressed on a majority of OS tissue samples. EPHA2 specifically mediated internalisation of targeted adenoviral vectors into OS cells. EPHA2 seems a promising candidate receptor for targeted drug delivery to osteosarcoma.

References
1. Bielack SS et al., J Clin Oncol 2002; 20(3): 776-790
2. Hughes DP et al., Expert Opin Drug Deliv 2009; 6(12): 1311-1321
3. Pham TV et al., Bioinformatics 2010; 26(3): 363-369

4. Piersma SR et al., J Proteome Res 2010; 9: 1913-1922
5. Van Geer et al., Int J Oncol 2010; 36(1): 233-244

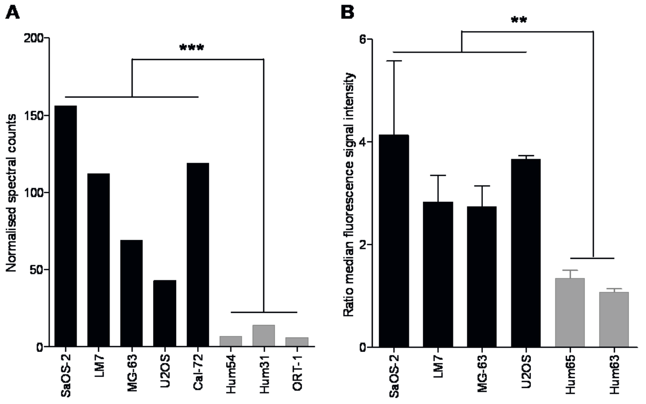

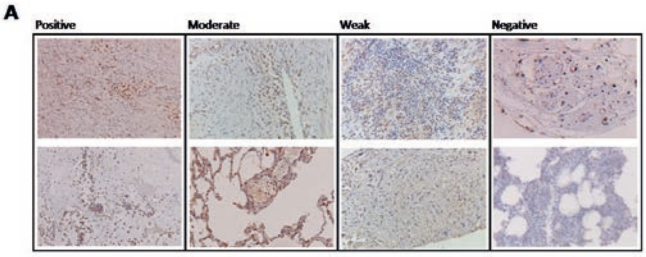

B

Summary:	bone (n = 11)	OS (n = 18)	*primary* (*n = 10*)	*metastatic* (*n = 8*)
Positive	–	12	*5*	*7*
Moderate	1	4	*4*	--
Weak	2	--	–	--
Negative	7	2	*1*	*1*
N/A	1			
χ-square test		*p = 0.0046*	*p = 0.0027*	*p = 0.0023*

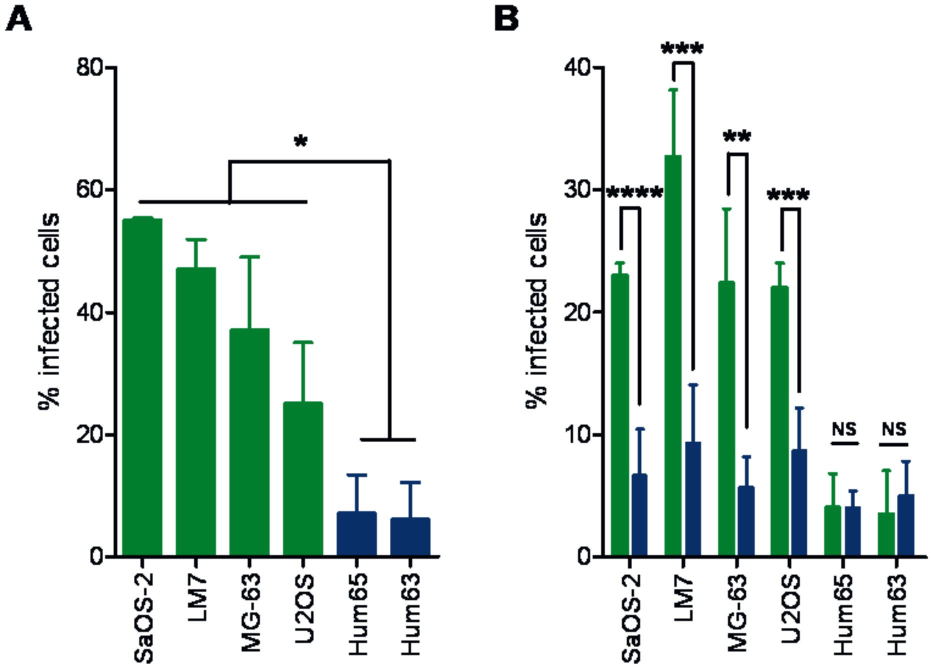

-Figure 1: EPHA2 is significantly overexpressed on osteosarcoma cells compared to osteoblasts. (A) The EPHA2 receptor was the most abundant surface protein on OS cells, with an average of 100 spectral counts per OS cell line and is 12-fold upregulated on OS cell lines (black bars) compared to osteoblasts (grey bars) (beta-binominal test, ***, p = 0.0005). (B) FACS analysis confirms the differential expression between the OS cell lines (black bars) and the osteoblasts (grey bars) (student's t-test, **, p < 0.01).

-Table 1: EPHA2 is significantly overexpressed in osteosarcoma tissue compared to healthy bone tissue. (A) Immunohistochemical staining results for EPHA2 on human OS and normal bone tissue sections. Per category, two examples are shown. (B) Tissue staining per group. Staining was scored based on the percentage of positive cells and the intensity of the staining of the cells and allotted to the categories: negative, weak, moderate, or positive. One bone sample could not be scored because of limited sample quality (N/A). The Chisquare test was applied to analyse the difference in staining results between the groups. The staining intensity was significantly higher in the OS samples compared to healthy bone tissue, both in the primary and metastatic lesions (p < 0.005).

-Figure 3: EPHA2 receptor specifically mediates targeted adenoviral vector internalisation into OS cells. (A) Transduction of OS cell lines (green bars) and hp-OBs (blue bars) with EPHA2-targeted

4B.4

Effects of Low Intensity Pulsed Ultrasound (LIPUS) on Cancer Cells

Yasushi Sawai
Department of Orthopaedics, Kyoto Prefectural University of Medicine, Kyoto, Japan

Although the effects of LIPUS were different according to the kind of cancers, LIPUS used for bone metastases might induce osteoblast differentiation without cancer proliferation and vascularization. LIPUS might be a new method of treatment for metastatic bone tumors.

Introduction:

Metastatic bone tumors cause pain and pathological fractures due to bone destruction. If we could enhance new osteogenic activities and prevent to progress osteolytic change by cancer cells, patients with these disease would achieved their satisfactory activity of daily living (ADL). While, low intensity pulsed ultrasound (LIPUS) stimulation was known as one of the methods for bone formation in orthopedics. We considered that LIPUS stimulated bone formation similar to normal fracture healing and prevented progression of pathological fractures. LIPUS stimulation has been reported to affect osteoblast differentiation and vascularization and unaffect osteoblast proliferation. However, changes of LIPUS to cancer cells have not been discussed. In this study, we investigated the in vitro effects of LIPUS treatment on cancer cell lines.

Materials and Methods:

We used a mouse osteoblast cell line (MC3T3-E1), a human renal cancer cell line (786-O), a human prostate cancer cell line (PC-3) and a human lung cancer cell line (A549). The temporal average intensity of LIPUS was 30mW/cm^2 and the frequency was 1.5 MHz with a 200-μs tone burst repeated at 1.0 KHz. LIPUS was administered for 20 minutes every day in a span of this experiment. For the cell growth study, after the cells were cultured for 24 hours, the number of cells was counted with time for two groups, with or without LIPUS. Extracellular signal-regulated kinase (ERK1/2), phosphorylated ERK1/2 (pERK1/2), Akt, phosphorylated Akt (pAkt) and ß-catenin were analyzed by western blotting with time. ELISA assays for vascular endothelial growth factor (VEGF) were performed.

Results:

LIPUS stimulation for up to 3 days did not affect the rate of all cell growth (Fig.1). The expressions of pERK1/2 and pAkt significantly increased by LIPUS stimulation on MC3T3-E1 and A549 cells. However, they showed no difference between two groups on PC-3 and 786-O cells. LIPUS stimulation on all cells did not significantly increased ß-catenin (Fig.2). VEGF protein levels on MC3T3-E1 at 12, 24 and 48 hs after LIPUS stimulation were significantly increased compared with the control and not significantly increased on PC-3, 786-O and A549 (Fig.3).

Discussions:

It was reported that the integrin/MAPK pathway, integrin/phosphatidylinositol 3-OH kinase/Akt pathway and Wnt/ß-catenin pathway were activated on osteoblast cell by LIPUS stimulation. Additionally, VEGF expression has been reported to be increased by LIPUS stimulation on osteoblast cell. In the current study, the results of cell number, phosphorylation of ERK1/2 and Akt, and expression of VEGF on MC3T3-E1 correspond to previous study. 786-O and PC-3 were not affected by LIPUS stimulation in all experiments. As a result, LIPUS used for bone metastases from renal and prostate cancer might induce osteoblast differentiation without cancer proliferation and vascularization. The effects of LIPUS stimulation on A549 indicated that LIPUS stimulation affected phosphorylation of ERK1/2 and Akt but did not affect cell growth and VEGF expression. Our findings demonstrate that the effects of LIPUS on cancer cells were different according to the kind of cancers. The results of our study suggested that LIPUS might be a new method of treatment for metastatic bone tumors.

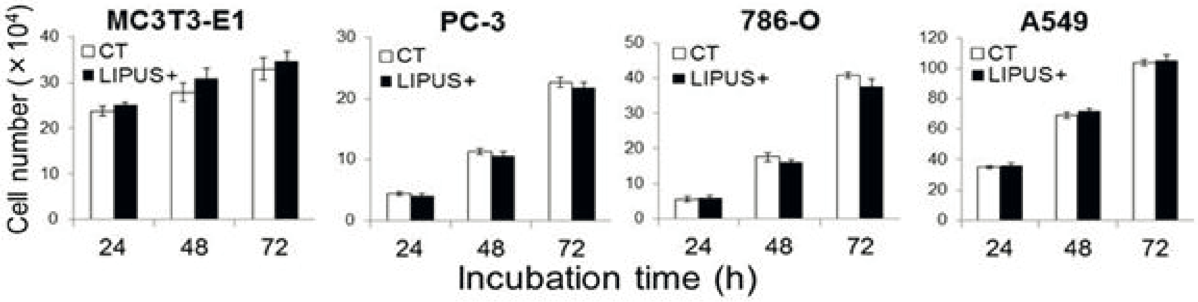
MC3T3-E1
PC-3
786-O
A549
Cell number (×10⁴)
□CT
■LIPUS+
40
30
20
10
0
50
120
100
80
60
24
48
72
Incubation time (h)

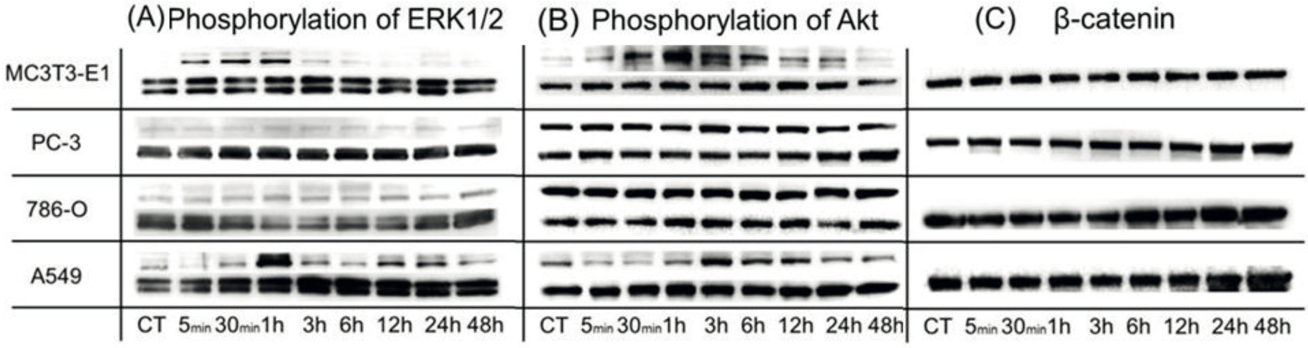
(A) Phosphorylation of ERK1/2
(B) Phosphorylation of Akt
(C) β-catenin
MC3T3-E1
PC-3
786-O
A549
CT
5min
30min
1h
3h
6h
12h
24h
48h

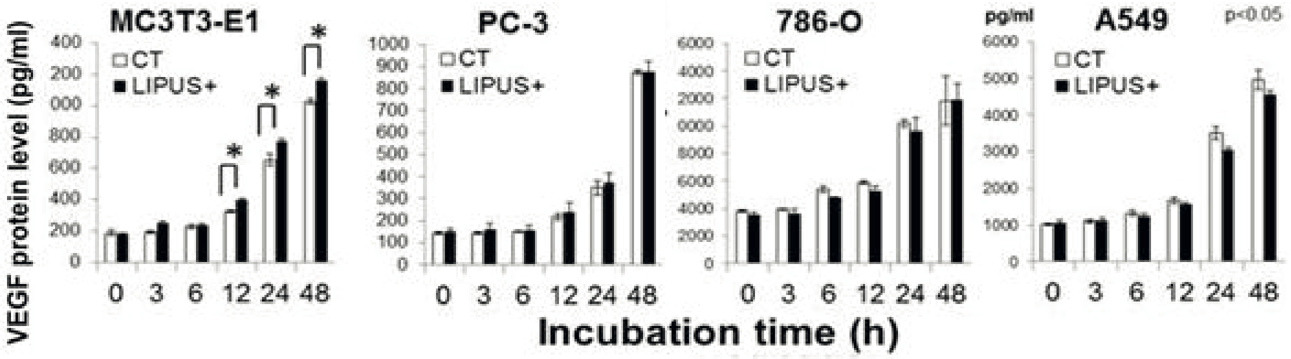
MC3T3-E1
PC-3
786-O
A549
pg/ml
p<0.05
VEGF protein level (pg/ml)
□CT
■LIPUS+
*
400
200
000
800
600
1000
900
700
500
300
100
0
6000
4000
2000
0000
8000
5000
3000
1000
3
6
12
24
48
Incubation time (h)

4B.5

Autologous vaccine for dog osteosarcomas

Patrick Frayssinet
Urodelia, St. Lys, France

Autologous specific proteins were purified from biopsies of dog sarcomas and used to vaccine a series of 7 dogs suffereing from osteosarcoma. The OS and PFS were measured and were much higher than those reported in the litterature.

Dog osteosarcomas have a very poor prognosis. The median overall survival is about two months. Amputation does not greatly improve survival rates. Amputation and chemotherapy show better results, but amputation is not always possible as osteosarcomas occur in heavy, middle-aged dogs generally unable to walk after amputation.

Cancer cells are genetically unstable and synthesize dozens of abnormal proteins which change as the tumour develops and differ from patient to patient. This variation is the rationale for an autologous vaccine in order to integrate in the vaccine the most numerous abnormal proteins being synthesized by the tumour at the time it is discovered.

Cancer cells also synthesize heat shock proteins (HSPs) due to stress triggered by various metabolic and mechanical anomalies in cancer tissue. These molecules are chaperone proteins and thus associated with almost all the normal and numerous abnormal peptides synthesized by the cancer cells. They also participate in the crosspriming of CD8 cells against the cancer cells processing their associated normal and abnormal peptides at the surface of class I HLA so they can be presented to CD8 lymphocytes.

The aim of this study was to check whether a method of vaccination based on the injection of autologous heat shock proteins could have a clinical effect on naturally-occurring osteosarcomas in veterinary medicine, which could constitute a good model for human osteosarcomas.

We purified heat shock proteins from dog osteosarcoma biopsies then combined them with calcium phosphate powders to make an autologous vaccine which was administered as eight injections at different time intervals. Seven dogs consulting in veterinary medicine for a tumour of the appendicular skeleton were enrolled in the study once their owners signed an informed consent form. Three dogs were amputated at the request of their owners. The dogs were staged and monitored up to their death. Both overall survival (OS) and progression free survival (PFS) were noted and compared to results in the literature. A test of antigen presenting cells (APCs) stimulation was developed to check that the loaded powders could stimulate these cells. A tumour extract was injected intradermally before the first injection and after the fourth. The induration was measured 48 hours later in order to check the change in immunological status with respect to the tumour.

No local or systemic secondary effects were evidenced. It was shown that the overall survival rate of all the treated dogs, whether amputated or not, was much higher than the median OS of dogs reported in the literature. It was also demonstrated that the PFS was very close to the OS and that the inflammation of the tumour zone for non-amputated dogs regressed after every injection. X-rays showed a remodelling of the tumour region after vaccination. All the non-amputated dogs were able to walk during the follow up period and none of them broke what remained of the cortical bone around the tumour during the same period.

Conclusions. Autologous osteosarcoma vaccines could be a good adjuvant therapy to eliminate disseminated cells and/or slow down micrometastasis development.

4B.7
Recurrence rate and progression of Chondrosarcoma correlates with Heat shock protein expression

Klemens Trieb
Department of Orthopedics, Wels, Austria

The expression of heat shock proteins in chondrosarcoma is correlated with outcome.

Heat shock proteins are involved in tumour immunity and correlation with survival and drug resistance in many cancers. Our study investigated the expression of heat shock proteins and multiple drug resistance in human chondrosarcoma.

The evaluation of heat shock protein and p-glycoprotein (multiple drug resistance gene 1 product) expression was done by immunhistochemistry on paraffin-embedded sections of 37 patients with chondrosarcoma (19 male, 18 female, aged 33 to 85 years ; mean 48.5 years).

Hsp 73 and hsp 90 were significantly overexpressed in patients with local recurrence, for hsp 73 7 of 7 cases were positive (100%) in patients with local recurrence and 9 of 18 positive (50%) without recurrence $p < .02$). For hsp 90, all cases were positive in patients with recurrence and only 8 of 18 (44%) in patients without recurrence ($p < .02$).

There was also found a strong relationship between hsp expression and survival.

Hsp 72 and hsp 73 were significantly overexpressed in tumours from patients, who died from disease (all positive for hsp 72 and 73, $p < 0.05$).

No differences were observed recording to age or gender between hsp 72, hsp 73 or hsp 90 positive or negative tumours. In addition hsp 72 expression showed a correlation with respect to differentiation of the tumours ($p < .02$).

Due to these results hsp 72, hsp 73 and hsp 90 could function as new prognostic markers in chondrosarcoma and initiate further studies to introduce markers for identification patients with a poor prognosis.

Figure 1: Heat shock proteins and Chondrosarcoma

A: Immunostaining for hsp 73; note exclusive cytoplasmic expression of this protein (Immunoperoxidase stain, original magnification x40)

B: Immunostaining for hsp 90 (Immunoperoxidase stain, original magnification x60)

(A)

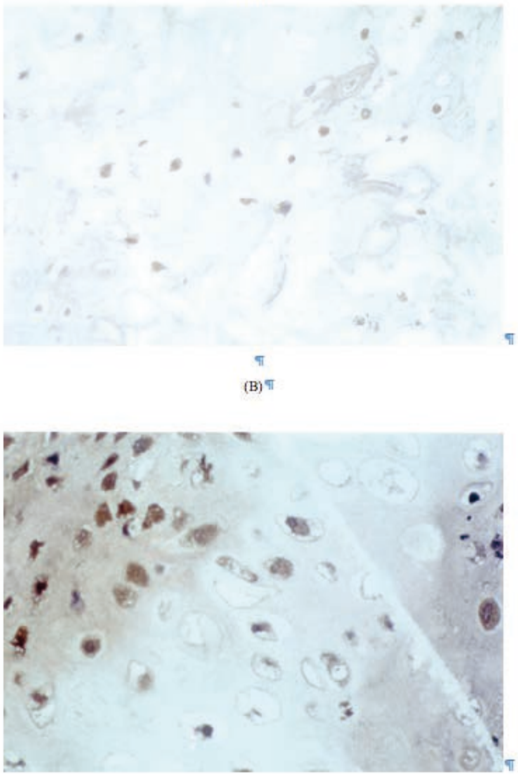

5A.2

Knee angle measurements on 3D-CT are influenced by femur orientation, slice thickness and reslicing.

Rachel Senden
Ahorse, Atrium MC Heerlen, Heerlen, The Netherlands

Femur rotation, slice thickness and reslicing affect the measurement of knee angles used in preoperative TKA planning. These effects can be bigger than the accuracy claimed by navigation or shape matching technology. Patient positioning in the scanner must be controlled.

Introduction

Preoperative planning receives growing attention regarding shape matching technology (SMT) which mainly relies on MRI or low resolution CT's. SMT claims high accuracy for component placement with errors ≤1º and ≤1mm. This study investigates the effect of slice thickness, successively reslicing and femur rotation on various knee axes measured using high-resolution CT's. Moreover the influence of age and ethnicity is investigated.

Methods

Knee axes were identified in 93 CT's of femora of 50 elderly (27M/22F, avg. 83±3yrs,1.72±0.10m) and 16 young subjects (11M/5F avg. 52±19yrs,1.74±0.10m) from the Netherlands and 27 subjects from India (24M/3F, avg. 58±12yrs,1.68±0.11m). Subsequently various knee angles were calculated: posterior condylar angle (PCA), condylar twist angle (CTA), femoral neck anteversion angle (FNA), angle between Whitesideline and surgical epicondylar axis (WS-EP) and angle between Whitesideline and posterior condylar line (WS-PC). All measurements were taken after reslicing the CT's along the mechanical axis (MA) of the femur with a slice thickness of 1mm using CAD-software Mimics. In a subgroup of 21 elderly intra- and interreliability was investigated by repeating the measurements by the same and a second observer. Intraclass Correlations (ICC) were calculated. In a subgroup of 50 CTs (elderly), measurements were repeated with the femur rotated 2°, 5°, 10° in the coronal plane relative to MA, the PCA was repeatedly calculated with the femur rotating from 0° to 10° with intervals of 2° and angles were repeatedly measured using a slice thickness of 3mm, 5mm and in a subgroup of 20 subjects of 10mm. Pearson correlations and repeated measurements ANOVA was used to investigate the effect of rotation, slice thickness and reslicing. The influence of age and ethnicity was study using ANOVA.

Results:

All angles were measured with high inter- (ICC-range 0.75-0.97) and intra-reliability (ICC-range 0.82-0.98). The WS-EP and WS-PC angle were affected by age (r=0.25 and 0.27 respectively) showing significantly higher WS-EP and WS-PC in the young Dutch group (90.5±3.1, 92.4±2.7) and young Indian group (90.6±3.8, 93.0±4.0) compared to the old Dutch group (93.5±3.4°, 95.7±2.9°). Femur rotation had an effect on WSEP, WSPC and FNA showing increased angles with increased femur rotation (3° to 4° increase when femur is rotated 10°, fig.1,2). Also an effect of reslicing was found. The PCA differed significantly by ca. 1º whether resliced directly or in successive steps (fig.3). No significant effect of slice thickness was found, although at trend was shown towards increased knee angles with increasing slice thickness.

Discussion

Femur rotation, reslicing and slice thickness can have a bigger effect on knee angles than the accuracy claimed by SMT. Femur rotation has a bigger influence than slice thickness. With changing slice thickness, the voxel volume changes but no change in resolution occurs (x and y direction) explaining the lack of a significant effect of slice thickness. A larger effect is however expected with increased slice thickness (>10mm). Age differences in knee angles can be due to osteoarthritis as 11 of 50 elderly had severe characteristics of OA. In clinical practice, patient positioning in the scanner must be well controlled to achieve the benefits of image based navigation or SMT.

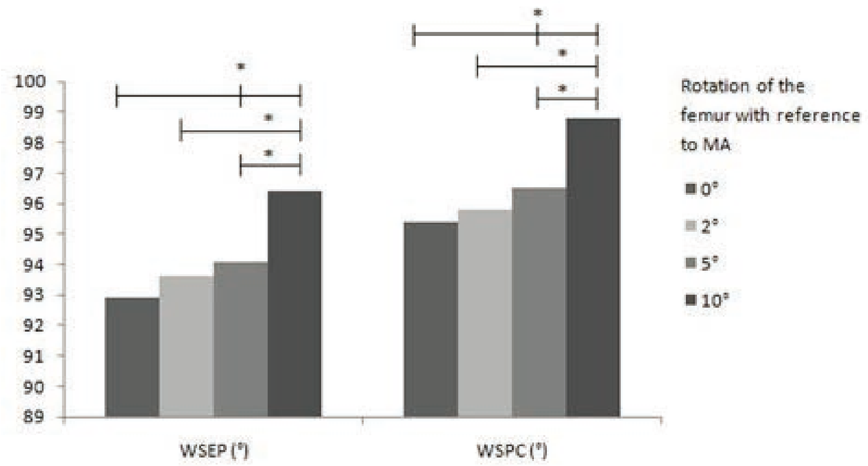

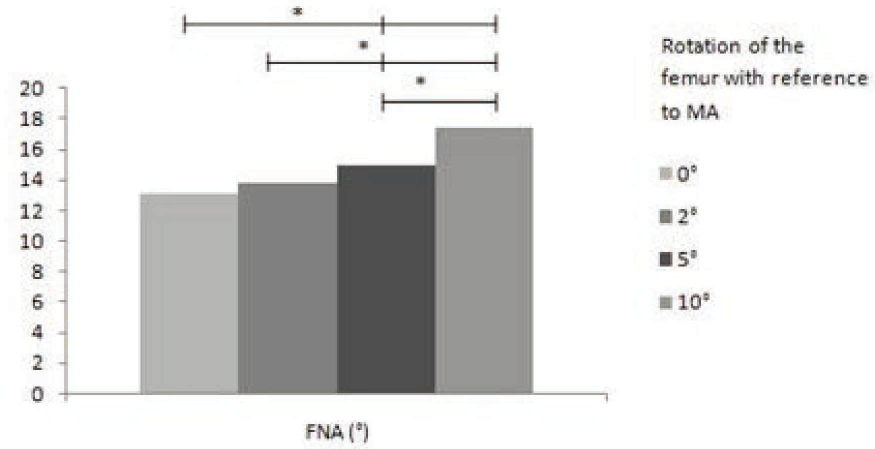

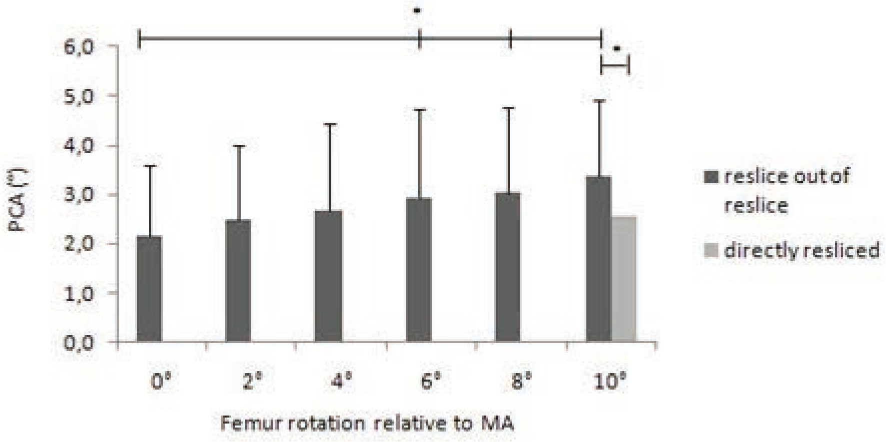

-Influence of femur rotation on WSEP and WSPC, *p<0.05
-Influence of femur rotation on NAA, * p<0.05
-Influence of successively reslicing on PCA, *p<0.05

5A.3
Quantifying periprosthetic osteolysis of the hip using CT images

Francois Malan
Leiden University Medical Center, Leiden, The Netherlands

We developed image analysis techniques that allow three dimensional detection and measurement of peri-prosthetic osteolysis of the hip. These techniques deal with metal artefacts and low image contrast, while avoiding labour intensive manual intervention.

Introduction:

The most significant complication in long-term survival of total hip prostheses is peri-prosthetic osteolysis, which involves resorption of bone and its replacement by soft fibrotic tissue. For such patients, open revision surgery may be substituted with minimally invasive cement injection to fixate the loosened prosthesis. Pre-operative planning using finite element (FEM) analysis may aid a surgeon to choose an optimal cement injection strategy. This requires three-dimensional (3D) tissue segmentation for creating patient-specific models. Metal artefacts and ambiguous computed tomography (CT) image intensities in the peri-prosthetic region are frequent imaging problems.

Methods:

We developed a tissue segmentation pipeline (Figures 1, 3) that can correctly identify the majority of peri-prosthetic tissues, including pathological fibrous lesions, using a combination of statistical classification of per-voxel image features, and segmentation by graph cuts. The output of our software is a patient-specific 3D tissue map that may aid a surgeon in modelling and planning a minimally invasive procedure.

We tested our methods using clinical CT images of twelve different patients. Tissues surrounding the metal hip prostheses were automatically identified and compared to manually segmented ground truth.

Once a segmentation has been obtained, care should be taken in deriving mechanical properties from CT image values. Using standard orthopaedic imaging settings, we investigated deviations in CT image intensities in regions enclosed by varying thicknesses of a cortical bone phantom (Figure 2).

Result:

Our automated segmentation method determined healthy tissue distributions in clinical scans with sensitivities greater than 82% and pathological fibrous interface tissue with a sensitivity exceeding 73%. Specificity exceeded 96% for all tissues. This provides us with a good starting point for constructing automatically generated patient-specific FEM models.

We show that CT metal artefact reduction is detrimental when used in isolation, but beneficial in our integrated multiple-feature approach.

Taking note of CT beam hardening effects, we investigated what the error in derived mechanical properties in bony structures may be. We estimate that inaccuracies in derived mechanical strength of enclosed trabecular bone, caused by beam hardening, may exceed 33%. Recent skeletal FEM studies seem to insufficiently guard against this issue.

Discussion:

Three dimensional image-based planning may improve the planning of minimally invasive refixation procedures. Such planning will typically consist of 3D tissue segmentation followed by patient-specific FEM modelling.

We showed that patient specific FEM modelling requires careful model validation, since derived mechanical properties are strongly dependent on image intensities, which may unduly be influenced by the proximity of bony structures, even after proper CT calibration. Multi-feature image-based techniques including metal artefact reduction, similar to that of our tissue segmentation algorithm, may protect against these phenomena.

Our image-based segmentation pipeline for modelling aseptic osteolysis around a femoral prosthesis can easily be modified to apply to other anatomical regions. Strengths of our method include the ability to combine different imaging filters or modalities and its ability to enforce geometrical constraints without specifying an explicit shape model. The pipeline described in this paper therefore represents a practical approach to segmenting multiple tissues and pathological lesions in CT.

5A.4

Effect of Sagittal Cutting Angel for Morphology of Anterior Cruciate Ligament in MRI

Ho-Joong Jung
Chung-Ang University, Seoul, Korea

Because the incidence of ACL bowing was higher in perpendicular cutting compared with oblique sagittal in MRI, sagittal orientation of ACL as a sign of partial tear of ACL should be carefully reviewed considering sagittal cutting angle.

Introduction:
Redundant ACL relative to the Blumensaat line has been regarded as a important sign of complete ACL tear in sagittal section of MRI. However, in some cases, ACL showed redundancy without injury. The aim of this study was to elucidate the effect of sagittal cutting angel for morphology of ACL in MRI.
Patients & Methods:
Three dimensional (3D) MRI was performed to the 30 knees which have no ACL injuries. 3D-MRI data was reformatted in multi-planar reformatting mode in OsiriX program and checked the ACL angle and Blumensaat angle according to two different sagittal cutting angle, 0° & ER 15°(Fig 1).
Results:
ACL orientation showed significantly different features according to the sagittal cutting angle of MRI (Fig2).
Eleven cases of 30 knees(37%) showed redundant ACL in 0° sagittal cutting, However in 15° oblique sagittal cutting, no cases showed redundancy of ACL
Conclusion :
Redundancy of ACL relative to the Blumensaat line should be carefully interpreted as a sign of partial tear of ACL, when the MRI was checked in perpendicular the coronal plane.

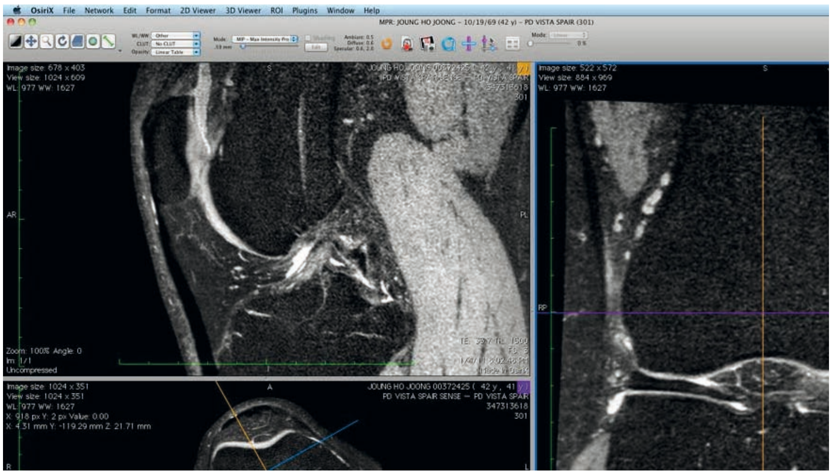

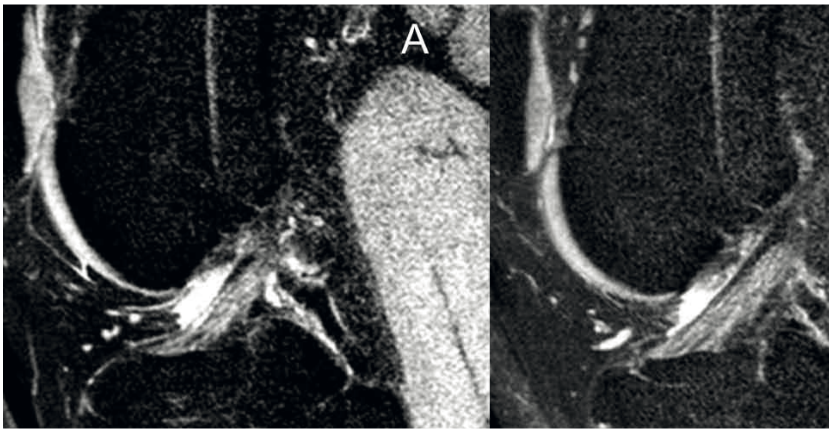

-3D multi-planar reformatting mode (3D MPR) in OsiriX
-MRI finding in different sagittal cutting. (A) perpendicular to the knee, ACL fiber shows redundancy, (B) 15° external rotation cutting view, ACL shows tight

5A.6

Sensitivity and specificity of ultrasound for detecting small (osteo-)chondral defects in the talus in a cadaveric study

Aimee-Claire Kok
Dept. of Orthopaedic Surgery, Academical Medical Center Amsterdam, Amsterdam, The Netherlands

Ultrasound is a reliable and promising method for detecting and classifying small talar chondral and osteochondral defects in the talus, though protocol improvement is needed to increase the accuracy of locating these defects.

Introduction:
The purpose of this study is to determine the potential of ultrasound in diagnosing the presence or absence of chondral and osteochondral defects in the talus with intact overlying tissue at locations that can be visualized with ultrasound and to develop a reproducible registration method to minimize the inter-observer variability in defect measurements and defect localisation.

Methods:
In ten cadaveric human ankles, chondral and osteochondral defects (ø 1,5 mm and ø 3 mm) were created arthroscopically by an orthopaedic surgeon in order to leave the ankles intact as much as possible. The ankles were examined with ultrasound by two blinded observers. In each ankle, a randomized combination of four conditions were created: no defect, a pure chondral defect with ø 3 mm drill, an osteochondral defect with ø 3 mm drill, a pure chondral defect with ø 1,5 mm drill, osteochondral defect with ø 1,5 mm drill. One condition always was no defect. A scan-and-detect protocol was set up that specified patient position, scan direction, localization of a defect based on division of the talar surface in three zones using overlying tendons, classification and sizing of the defect as either chondral or osteochondral. Observations were validated using CT scans of the ankles and pictures of the dissected tali. Additionally, video material that was recorded during the measurement of the defects was used to compare to the shape, size and location of defects between the CT-scans and pictures and determine exactly what defects were and were not detected and measured by both observers.

Results:
For the detection of all defects irrespective of defect type, we found a sensitivity of 85% and 74% for Observers 1 and 2 with a specificity of 100% and 89%. The detection of osteochondral defects had a higher sensitivity and specificity (Se 88% and 92%, Sp 100% and 94% for Observers 1 and 2). The correctly located defects out of the total number of defects located by Observer 1 and 2 was 67% and 63%. Observer 1 classified 95% of all the defects correct as either chondral or osteochondral, Observer 2 classified 81% of the defects correct. Of the total measurements taken by Observer 1 and 2, 89% were accurate according to the limits of agreement found for measurements taken by Observer 1 (-0,1±2,6) and 2 (0,2±2,8). An ICC of 0,62 was calculated with no significant difference between measurements taken by Observer 1 and Observer 2 (mean, 0.1 mm., 95% CI, -.5 to 0.6 mm).

Conclusion:
Ultrasound has the potential to make accurate measurements of small (ø 1,5 mm. and ø 3 mm.) cadaveric talar defects. The scan protocol developed for this study can be used for detecting defects in the talus and classifying them as chondral or osteochondral, though it could be improved to increase the accuracy of locating defect locations. Based on these results further research is justified to determine the exact place of ultrasound in relation to CT and MRI for OCD detection in surfaces that can be accessed by ultrasound.

5A.7

Registration and Quantification of T1Rho MRI on Patients with Knee Osteoarthritis

Pieter Oomen
Maastricht University Medical Centre, Maastricht, The Netherlands

This study shows that quantification of T1Rho is applicable to patients with knee osteoarthritis. Slightly elevated relaxation times were found in the outer layer of the cartilage in patients with knee osteoarthritis compared to healthy controls.

Introduction

Magnetic Resonance Imaging (MRI) of the articular cartilage of the knee gives information about the degenerative processes of the soft tissue (Gold, 1998). T1Rho is a non-invasive MRI method to detect early cartilage degeneration, by use of a cluster of spin lock pulses. A method to quantify T1Rho images on healthy volunteers has been developed by Pedersen et al (2011). This study aimed to reproduce the method of Pedersen et al in patients with knee osteoarthritis (KNOA). Additionally, this study evaluated the influence of several registration methods.

Patients & Methods

In this study patients with KNOA (N=4) and healthy controls (N=2) were included. The studie is part of a larger study on determinants of KNOA in women between 50-65 years. Patients with Kellgren Lawrence grade 3-4 were excluded. A MRI protocol was used including the T1Rho scan with 1, 10, 20, 30, 40 ms spin lock times (Phillips, 3 Tesla), in order to detect relaxation times. Correlation, translation, similarity, rigid and non-rigid registration methods were used to find an optimal match between the different spin lock images. Furthermore the method proposed by Pedersen et al was applied to define reproducibly sections of cartilage layer at 3 levels: 0.5, 1.0 and 1.5 mm from the bone-cartilage-interface (Fig.1).

Results

Registration of the T1Rho spin lock images increased accuracy of the relaxation time (Fig.2). However, excluding non-rigid registration, the type of registration used in this study did not influenced matching outcomes. The preliminary results showed an increased T1Rho relaxation time on the outer layer of the cartilage between 10 and 45 degrees from the sulcus region (Fig.3)

Discussion/Conclusion

This study showed that the method of Pedersen et al is applicable to both healthy subjects and KNOA patients. Moreover, relaxation times of healthy controls are comparable to Pedersen et al. Registration of T1Rho images should be included for better quantification of relaxation time. The slightly elevated relaxation time near the sulcus region in KNOA patients compared to healthy controls is in line with literature (Regatte et al 2004). The method does require the presence of a discernable cartilage layer, hence patients with severe loss of articular cartilage cannot be included.

References

Gold et al., MR imaging of articular cartilage of the knee: new methods using ultrashort TEs. Eckstein, F., 1998.170(5)
Pedersen et al., A comparative method for finding and folding RNA secondary structures within protein-coding regions. Nucleic Acids Res, 2004. 32(16)
Regatte et al., 3D-T1rho-relaxation mapping of articular cartilage: in vivo assessment of early degenerative changes in symptomatic osteoarthritic subjects. Bottger, T., 2004. 11(7)

5B.1

Decreased range of motion differentiates the incidental radiographic finding from clinical femoroacetabular impingement

Jan Van Houcke
Ghent University Hospital, Ghent, Belgium

The present study confirms that clinical femoroacetabular impingement presents with decreased range of motion. The incidental finding of a cam lesion does not necessarily present with limited or painful hip motion.

Introduction

Femoroacetabular impingement (FAI) is a mechanical hip disorder defined as early and/or repetitive contact between the acetabular rim and the proximal femur, potentially resulting in damage to the hip joint cartilage and labrum in young adults. Despite the growing awareness of the condition and the exponential growth of the literature on FAI, many discrepancies and controversies still remain. One of these controversies is the question whether radiographic findings such as loss of femoral head sphericity or reduced anterior offset, which appear to be highly prevalent in the general population, are pathognomonic of the condition or merely represent common anatomical variations. As a decreased range of motion (ROM) has been suggested by several authors to be an important sign of FAI, we hypothesized that evaluation of hip ROM could be a means for differentiating true patients from healthy cases with incidental radiographic findings. The purpose of the present study was to describe and analyze differences in ROM between FAI patients, asymptomatic cases with incidental radiographic findings and healthy controls. Furthermore, it was evaluated which motions were clinically relevant and could be used to differentiate between these groups.

Patients and Methods

The study population (see figure 1) was composed of three subgroups: cam patients (18 subjects, 24 symptomatic hips), asymptomatic cases with radiographic features specific for FAI (12 subjects, 24 asymptomatic hips) and healthy controls (12 subjects, 24 asymptomatic hips). All subjects were men, aged 18-35 years. Patients were recruited from cam type FAI patients scheduled for hip arthroscopy. Simultaneously, healthy controls and asymptomatic cases were recruited from a cohort of healthy volunteers with a negative history of groin pain and negative impingement test. Different radiographic parameters describing FAI or parameters that might have an influence on the condition were measured in each subject in a standardized fashion: alpha angle, caput-collum-diaphyseal angle and lateral center-edge angle. An alpha angle $> 55°$ distinguished the asymptomatic cases from the healthy controls (alpha angle $< 50°$). Kinematic measurements were performed using the Fastrak electromagnetic tracking system (Polhemus, Colchester, Vt.). The system and applied protocol have previously been validated for use in the applied setting, i.e. the evaluation of end ROM positions in FAI (Audenaert et al., 2011).

Results

Patients and asymptomatic cases with radiographic features specific of FAI did not significantly differ in terms of radiographic measures, height, weight and BMI. No significant differences in ROM between asymptomatic cases and controls could be demonstrated. However, compared to the control group, patients showed significantly decreased flexion ($p < 0.001$) and internal rotation during impingement testing ($p < 0.001$) as well as decreased neutral internal and external femoral rotation ($p < 0.05$).

Conclusion

The results of the present study confirm that a limited range of internal rotation during impingement testing is an important feature in the clinical presentation of hip impingement. The incidental finding of a cam lesion does not necessarily present with limited hip ROM. Neutral femoral rotation seems to be limited in FAI cases, a finding that needs further confirmation.

Patients	Asymptomatic cases	Controls
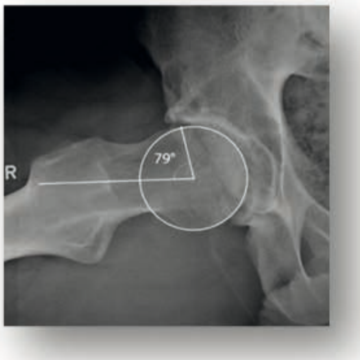		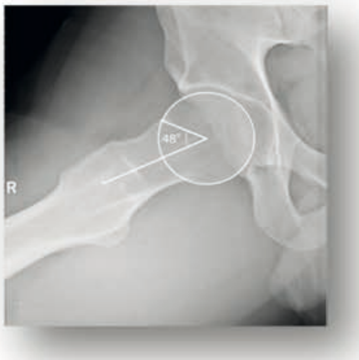
Male	Male	Male
Age 18-35 years	Age 18-35 years	Age 18-35 years
History of groin pain	No history of groin pain	No history of groin pain
Painful impingement test	Negative impingement test	Negative impingement test
Alpha angle > 55°	Alpha angle > 55°	Alpha angle < 50°
CE angle between 28-40°	CE angle between 28-40°	CE angle between 28-40°
Cam type FAI confirmed	Healthy volunteer	Healthy volunteer

Recruitment criteria for patients, asymptomatic cases and controls. (CE angle: Center-edge angle)

5B.2
Fluoroscopic assessment of femoral kinematics using a statistical shape model

Nora Baka
Leiden University Medical Center, Leiden, The Netherlands

We present a method for kinematic analysis of the femur from biplane X-ray fluoroscopy sequences with minimal user interaction. The method uses a statistical shape model, eliminating the need of prior CT or MR acquisition.

Purpose Kinematic analyses are performed to assess pre-operative, post-operative, and normal knee function. Kinematic joint analysis using fluoroscopy is an emerging field of research since its accuracy is much improved compared to traditional motion capture systems. State of the art workflow involves CT or MR acquisition of the subject's joint, with subsequent bone segmentation and shape reconstruction. The bone shape is then aligned to match the fluoroscopic sequences frame by frame. This alignment requires manual interaction in every fluoroscopy frame in the form of manual alignment or in the form of edge selection [1]. We aimed to eliminate the need for 3D imaging to create the bone model, and to minimize manual interaction.

Method and experiments

Our method reconstructs the subject specific bone from the biplane fluoroscopic sequence, rather than from CT or MR imaging, with the use of a statistical shape model. This model is optimized to match the bone edges in the fluoroscopic images. Bone edges are automatically selected from all image edges based on their location, orientation and appearance [2]. Manual interaction is thereby minimized to one starting pose per sequence. Model pose is optimized per frame, and model shape on the entire sequence.

Biplane fluoroscopy sequences of the drop-landing of 10 individuals from a previous study were used for evaluation [3]. The fluoroscopic data of the knee was collected in about one second at an effective frame rate of 125 frames/sec. The statistical model of the distal femur was created on 43 femora. The reconstruction and tracking accuracy of our novel method was compared with a manual interaction and CT segmentation based reference method (model-based roentgen stereophotogrammetric analysis) [1].

Results

Our method converged in 91% of all reconstructed frames. When converged, translation and two rotation directions had low bias (between 0.02 and 0.41 [mm and degree]), and a precision between 0.93 and 1.53 [mm and degree], defined as the standard deviation from several reconstructing attempts. The rotation around the proximal-distal axis of the femur was the most difficult to optimize, and resulted in -1.03 degree bias with 2.51 degree precision. An example frame with projected contours of our method (red) and the reference standard (green) are shown in Figure 1.

Discussion

A promising new method for fluoroscopic kinematic analysis was presented for the femur. Our framework is expected to be generally applicable to other joints such as the elbow and to other bones such as the tibia. Future work focuses on tracking femur and tibia simultaneously for deriving clinically relevant motion measurements.

[1] Kaptein, B. L., et al. (2003). A new model-based RSA method validated using CAD models and models from reversed engineering. J Biomech

[2] Baka, N., et al. (2012). Statistical Shape Model Based Femur Kinematics from Biplane Fluoroscopy. IEEE TMI

[3] Torry, M. R., et al. (2010). Knee Kinematic Profiles During Drop Landings: A Biplane Fluoroscopy Study. Med Sci Sports Exerc.

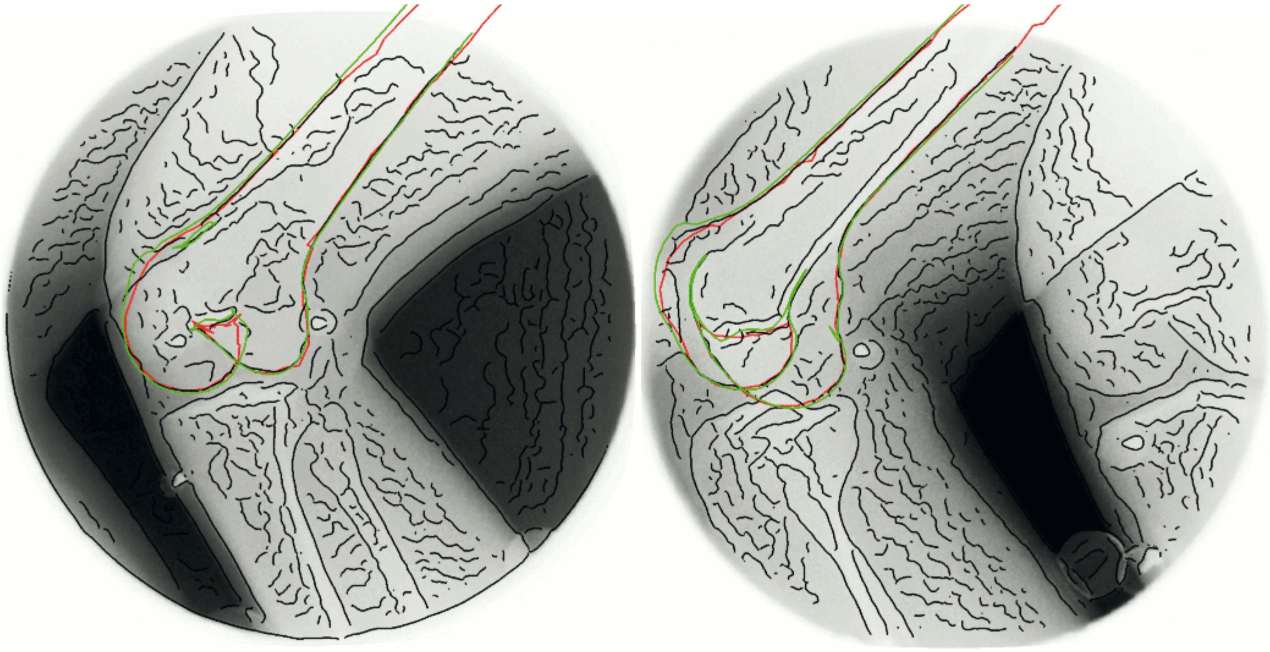

An example frame with edges (black), projected result (red) and projected reference standard (green).

5B.3

Subject-specific kinematic modelling of clavicular and scapular movements

Bart Bolsterlee
Delft University of Technology, Delft, The Netherlands

Subject-specific modelling leads to a closer match between measured and simulated shoulder kinematics, but better validation of model individualisation assumptions is required before it can be concluded that a dynamic subject-specific shoulder model is an improvement to a generic model.

Introduction

Movements of the human clavicle and scapula are constrained by the thorax at the sternoclavicular joint and the scapulothoracic gliding plane, and by the coracoclavicular ligaments. These motion constraints limit the combinations of clavicular and scapular depending on an individual's anthropometry. For a generic musculoskeletal shoulder model that uses morphological cadaver data this implies that experimentally recorded motions are not exactly reproducible by the model. For instance, the scapula moves inside the ribcage. For realistic kinematic simulation of shoulder movements either the measurements should be adjusted to fit the model, or the model should be scaled to the subject. In this study, both approaches are compared by calculating to what extent measurements should be adjusted for realistic simulation of measured shoulder movements when using a generic or a subject-specific (= scaled) morphology and for two methods of modelling motion constraints (hard vs. soft constraints).

Methods

Orientations of thorax, scapula and humerus of five healthy subjects were measured with a marker-based motion-capture system during a humeral abduction (ABD) and anteflexion (FLEX) movement. From measured orientation angles of clavicle and scapula, realistic simulated angles were calculated by mathematical minimisation of the difference between measurements and simulations, while satisfying three motion constraints: two bony landmarks on the medial border of the scapula (trigonum spinae and angulus inferior) are on a fixed distance to the thorax and the conoid ligament length is constant. Per subject and motion, simulation angles were calculated for two morphologies - generic and subject-specific - and two methods of modelling motion constraints - hard (exactly fulfil motion constraints) and soft (allow some variation). Root mean square differences (RMSD) between measured and simulated angles were calculated for all four conditions. A small RMSD means good resemblance between experimental recordings and simulation and is therefore desirable.

Results

Figures 1 and 2 illustrate the results of kinematic optimisation with respectively hard vs. soft constraints and generic vs. subject-specific. Figure 3 shows RMSD averaged over all 5 subjects.

Discussion

Both adaptations are an improvement to the existing method (Figure 3, generic, hard constraints): by individualizing the model geometry 23% and 43% improvement in RMSD results for respectively ABD and FLEX (subj.spec, hard constraints) and by applying soft constraints with the generic morphology the RMSD also increases significantly (45% for ABD and 40% for FLEX).

This study only considered kinematics. However, for more clinically relevant model results (joint contact forces), soft tissues need to be included. Individualizing the bone geometry means that soft tissue parameters (e.g. muscle attachment sites, force-length-velocity characteristics) need to be scaled as well. The current challenge in subject-specific modelling is to evaluate whether assumptions to scale soft tissue parameters are more valid than the assumptions of a generic model. This study shows that small model adaptations (soft constraints) can sometimes achieve a similar improvement in modelling results as individualization.

References De Groot, J.H., "The shoulder: a kinematic and dynamic analysis of motion and loading," Delft University of Technology, 1998.

5B.4

Unicondylar Knee Arthroplasty kinematics in vitro

Thomas Heyse
Department of Orthopedics and Rheumatology, University Hospital Marburg, Germany

Following UKA, loaded kinematic patterns resemble those found in knees with significant loss of function of the medial meniscus.

Introduction:
It is assumed that unicondylar knee arthroplasty (UKA) features kinematics close to the natural knee. Clinical studies have also shown functional benefits for UKA. There is to date only little biomechanical data to support or explain these findings.Material and Methods:
Six fresh frozen full leg cadaver specimens were prepared to be mounted in a kinematic rig with six degrees of freedom for the knee joint. Three motion patterns were applied before and after medial UKA: passive flexion-extension, open chain extension, and squatting. During the loaded motions, quadriceps and hamstrings muscle forces were applied. Infrared cameras continuously recorded the trajectories of marker frames rigidly attached to femur, tibia and patella. Prior computer tomography allowed identification of coordinate frames of the bones and calculations of anatomical rotations and translations.Results: Native kinematics was reproduced after UKA in all the specimens. In the unloaded knee and during open chain extension, femoral rollback patterns after UKA were very close to those in the native knee. During squatting, the medial femoral condyle after UKA tended to be more posteriorly and superiorly with flexion and there was less tibial internal rotation. The tibia was found to be in more valgus after UKA during all motion patterns.Discussion: This in vitro setup shows that UKA allows for reproducible restoration of kinematics that are close to the native knee, particularly in the unloaded situation. Following UKA, loaded kinematic patterns resemble those found in knees with significant loss of function of the medial meniscus.

5B.6

Intraoperative kinematic analysis of mobile bearing TKA using imageless navigation

Danilo Bruni
Rizzoli Orthopaedic Institute, Bologna, Italy

MB TKA reduces screw-home and increases mid-flexion instability.

Introduction:

The purpose of our work was to evaluate changes in clinical scores, passive knee kinematics and stability after mobile bearing TKA surgery.

Material & methods:

60 patients were treated with a mobile bearing prosthesis (Gemini, Waldemar Link, Hamburg, Germany). PCL was always resected. Inclusion criteria were BMI >30, age range 60-80yrs. Preoperative KSS, KOOS and SF36 scores were recorded. Surgeries were performed with a navigation system (BLU-IGS, Orthokey Italia, Firenze, Italy) to verify bone cuts, ligament balancing and implant positioning. Kinematic tests were executed to determine: tibial rotation and femoral translation through flexion range. Stability tests were performed using varus-valgus stress in extension and at 30° of flexion and drawer test. Acquisition were perfomed with menisci and cruciate ligaments intact , and repeated after final implant fixation. Clinical scores were rrecorded at 6 months follow-up.

Results:

All clinical scores showed increased value at 6 months follow up. KSS changed from 35±16.6 to 89.6±17.2; KOOS changed from 45.1 ±15.7 to 89.4 ±20.6; SF 36 changed from 22.5±21.4 to 85.1±24.6.

Average preoperative kinematics showed a rotation pattern of 10° during flexion, mostly occurring at first 30° of flexion. All tibiae resulted externally rotated preoperatively. After TKA the similar rotational pattern was maintained; screw-home was slighlty reduced, but tibial external rotation was corrected. Traslation patterns showed no differences.

VV stability was reduced in extension but not at 30° of flexion. AP stability at 90° of flexion increased after TKA (from 8.2mm±4.9 to 13.2mm±5.4).

Discussion

Mobile bearing PCS TKA was effective in increasing funtionality of the patients. Clinical scores improved after implant. Kinematics didn't change significantly. The correction of preoperative external rotation was noted, and similar AP translation pattern was obtained. Screw-home mechanism was reduced, and IE rotation pattern is more distributed throughout the flexion range. Stability in extension was restored, while it was not at 30° of flexion, as also drawer test resulted increased after TKA. This may be due to the absence of both cruciate ligaments.

6A.1

Laser-modified CoCrMo- and Al2O3- surfaces for use in the total joint Arthroplasty - A tribological in vitro investigation

Robert Wendlandt
University Lübeck, Biomechanics, Lübeck, Germany

Wear particles inducing osteolysis are among the top reasons for aseptic implant loosening. We describe a novel method to reduce wear by advanced laser pattering.

Introduction:

Surface wear of corresponding tribological pairings is still a major problem in artificial joint surgery. Wear particles are mainly produced by friction of artificial joint pairings, the so-called sliding bearings. Optimizing the wear behaviour of the articulating surfaces is crucial for the extension of the prostheses useful life. The study presented here aims at developing wear reduced surfaces to utilize them in total joint arthroplasty.

Method:

Using a pico-second laser, samples of medical CoCrMo metal alloy and Al2O3 ceramic were permanently patterned by material removal (Figure 1). Using a picosecond laser, longitudinal, transverse, and spiral-shaped channels as well as Dimples were created on the surfaces. The channels embed the scattered wear particles. Thus, the grooving of wear particles on the surface is minimized, consequently reducing the 3-body-wear between the contact surfaces.

The subsequent tribological investigation employed a ring-on-disc method, the structured surfaces have been tribologically tested according to ISO 6474. The samples were manufactured with a disc diameter of 25 mm and a ring of 20 mm outer and 14 mm inner diameter, loaded with an axial force of 1500 N. The ring has a countersunk of 2 mm, thus creating a contact surface between disc and ring. The ring oscillates with a rotation angle of ± 25 ° on the fixed disk. The test ran for 100h at a frequency of 1 Hz

Results:

The results showed that those samples with modified surfaces were more wear resistant than those with a regular surface. Using calf serum as lubricating medium, the wear volume of the structured CoCrMo samples was 8 times lower than that of regular samples. The wear volume of structured Al2O3 samples decreased by 4.5 times. Compared to distilled water, using calf serum as lubricating medium reduced the wear volume of CoCrMo samples by about 3.5 times. Investigations with the scanning electron microscope (SEM) showed that the slots generated by laser were filled with wear particles. In a 1000-fold magnification, large particles, which have been pressed at the intersection of the channels, become visible. The sharp-edged geometry is a characteristic feature of these particles resulting from the brittleness of these particles (see Figure 2). The energy dispersive X-ray spectroscopy system (EDX) of the SEM illustrates that the deposited Agglomerates are composed of high amounts of chromium and cobalt. Other substances such as Na, Mg, Mn and P are found in small quantities. These findings indicate that the agglomerates are derived from abrasion materials of the structured surface.

Discussion:

The results of the ring-on disc method indicate, that structuring CoCrMo- and Al2O3- surfaces by laser decreases abrasion. The contact surfaces get worn out only at the edges of the generated patterns. Therefore, the contact area between the two contact partners stays relatively small. In summary, using different materials and lubrications, structured surfaces store abrasive particles. Especially the spread of hard carbides of CoCrMo alloys, which are mainly responsible for the abrasive wear of the metal-metal bearings, is diminished. The results from this study are very promising. Further research is warranted. The use of simulators meeting the natural conditions in the joint and in vivo studies with living organism are the logical consequence to the positive results.

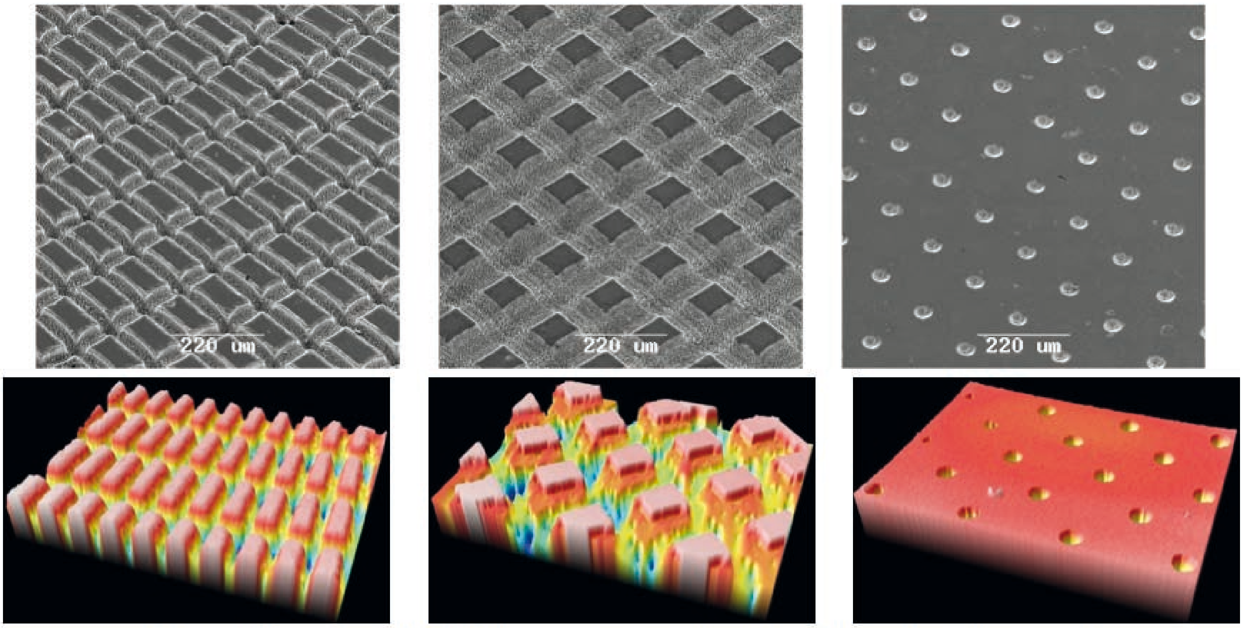

Figure 1 Exemplary SEM pictures (upper row) and isometric views (lower row) of CoCrMo-samples I.1 to I.3 (left to right) with modified surfaces

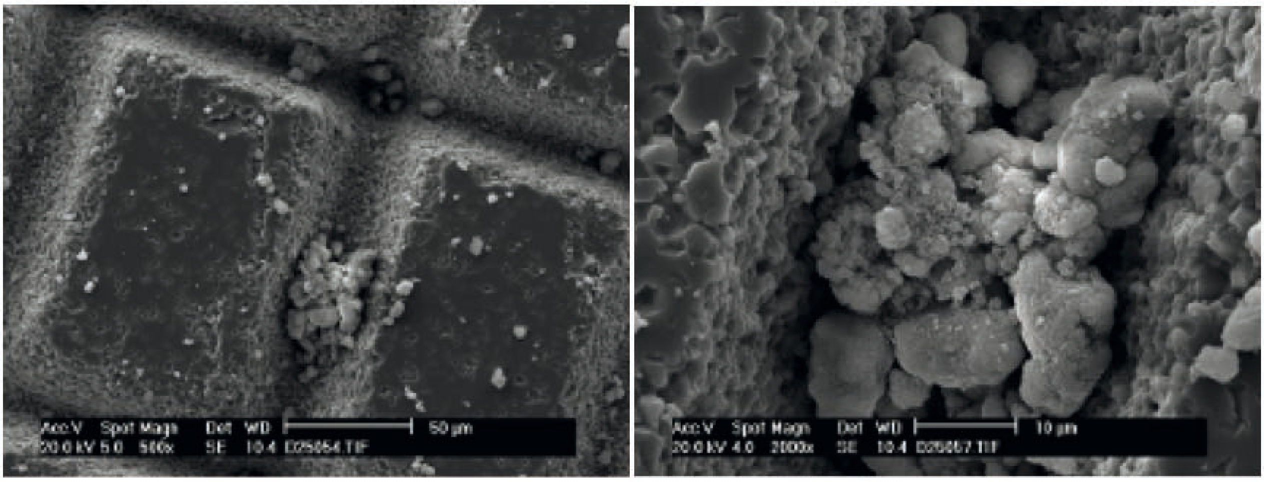

Figure 2: BIOLOX-Forte ceramic structured surfaces with wear articles

6A.3

Evaluation of Interleukins and TNF alfa in Serum and Synovial Fluid as Markers for Aseptic Loosening of Hip Arthroplasty

Maria Angeles Cuadrado-Cenzual
Hospital Universitario, Salamanca, Spain

Aseptic loosening is one of the major complications of total hip arthroplasty,The aim was to analyze the role of Interleukins in aseptic loosening and to evaluate the ratio IL-10/alfa-TNF in synovial fluid and serum as a marker of aseptic loosening

Introduction

Most of hip revisions after hip replacement are performed to aseptic loosening and one of the most important factors that seems to be involved is periprosthetic osteolysis. A reliable biological marker would be useful to diagnosis osteolysis early.

The aim of the present work was: to analyze the role of Interleukins (ILs) in aseptic loosening and , to evaluate if one of them can also predict hip implant loosening and to analize the value of the Interleukin 10 (IL-10)-alfaTNF ratio in serum and synovial fluid as a marker of aseptic loosening fluid and to determine whether these cytokines could be used as markers of enhanced periprosthetic osteolysis, leading to aseptic loosening of total/partial hip arthroplasty

Patients & methods

Blood synovial fluid samples were collected in 27 patients with a cemented Hip Arthroplasty (Group A) , 32 healthy subjects comparable for age and gender who were programmed for total hip arthroplasty because of primary osteoarthritis (group B) and 21 patients undergoing hip revision due to aseptic loosening (group C) in this last group; ,five cases had suffered a prosthesis fracture

The levels of IL-1α, 1ß, 6, 8, and 10 and alfa-TNF in synovial fluid and IL10 y alfa TNF in serum were examined, using a high sensitivity enzyme-linked immunosorbent assay (ELISA) test

Results

ILs 6 and 8 were significantly higher in the revisions compared with the primary arthroplasties ($p<0.001$) including cases with prosthesis fracture .

There was no significant difference in levels of IL10 by the two groups. However, the IL10/alphaTNF ratio was significantly higher in group A. . ILs 6 and 8 were significantly higher in group C ($p<0.001$) compared with Group A . IL-1ß levels were significantly higher ($p<0.01$) in Group C. No statistically significant differences in IL levels were found between osteoarthritis samples and those of other diseases

Discussion

IL6 and IL8 might be considered as markers to predict prosthesis loosening. The IL10/alphaTNF ratio alone was significantly correlated with aseptic loosening both in synovial and serum. IL10 or alphaTNF did not alone correlate in all conditions. These results show that the validity of this ratio is supported by its local and general correlation. A comparative prospective study in healthy subjects should be conducted to confirm the clinical pertinence of this marker

References

1- Trisha N. Peel, Kirsty L. Buising† and Peter F. M. Choong. Prosthetic joint infection: challenges of diagnosis and treatment ANZ J Surg 81 (2011) 32-39

2. Janja Zupan, Radko Komadina, and Janja Marc: The relationship between osteoclastogenic and anti-osteoclastogenic pro-inflammatory cytokines differs in human osteoporotic and osteoarthritic bone tissues Journal of Biomedical Science 2012, 19:28

6A.4

Antibiotic loaded plaster of Paris: Wear of artificial hip joints in the presence of gypsum particles

Roman Heuberger
RMS Foundation, Bettlach, Switzerland

In the presence of gypsum particles the wear of artificial hip joints increased by a small amount only. Thus antibiotic loaded plaster of Paris can be added to infected joints without making a two-stage-procedure necessary.

Introduction

Bacterial infections at artificial joints require a removal of the joint and a treatment with antibiotics. After recovering, a new joint is implanted. This two-stage-procedure is an enormous stress, especially for elderly patients. An alternative could be that plaster of Paris loaded with antibiotics is given into the centre of inflammation without removing the joint. The plaster of Paris is slowly dissolved and thus antibiotics are locally released to fight the bacteria. In this study the influence of gypsum particles from the hydrolysis of plaster of Paris on the wear of artificial hip joints is investigated.

Materials and methods

Inlays made of ultra-high-molecular-weight polyethylene (UHMWPE) and cross linked polyethylene (XLPE: vitamys®) against 28mm CoCrMo heads and alumina pairings (36mm, Bionit®2) were investigated (all seleXys®, provided by Mathys Ltd. Bettlach, Switzerland). The tests with n=3 each were conducted on a hydraulic six station hip simulator from Endolab (Germany) according to ISO 14242 for 5 million cycles (MC).

10g/L calcium sulphate hemihydrate (VWR, 1-100µm particle sizes, solubility in H_2O 2g/L) was added to the test liquid composed of 30 g/L newborn calf serum (NZ, GIBCO®), 2g/L sodium azide and 3g/L EDTA immediately prior to the tests. The calcium sulphate hemihydrate called plaster of Paris forms in the presence of water the more stable dihydrate called gypsum. The polymer inlays tested for 5MC in the presence of gypsum particles were subsequently tested for 1MC without particles.

Results

Both with and without gypsum particles in the test liquid, the wear of the polymer inlays increased continuously (Fig. 1). In presence of the gypsum particles, the wear rates of the polymer inlays were with 35±4mg/MC for the UHMWPE and 9±2mg/MC for the XLPE slightly higher than without gypsum with 29±2mg/MC and 5±1mg/MC respectively (Fig. 2). The wear rates of the alumina inlays were 0.3±0.1 mg/MC both with and without gypsum. When no more gypsum was added to the polymer articulations, the wear decreased to 18±4mg/MC and 7±2mg/MC for the UHMWPE and XLPE inlays respectively.

All heads and inlays showed few scratches, but there was no significant difference between the articulations with and without gypsum particles. On the polymer inlays, additionally some pitting was observed.

Discussion

Neither the alumina articulations nor the CoCrMo heads were affected by the gypsum particles since gypsum is a relatively soft material. Only the much softer polymers were worn 20-70 % more, but they recovered when no more particles were added. For the ceramic-on-polymer articulations and the further developed ceramics even less effects by the gypsum is expected, since these heads/materials are more scratch resistant.

The results show, that if bacteria are fought successfully with the antibiotic plaster of Paris, this leads to higher wear of polymer inlays during probably one year or MC respectively, but the two-stage-procedure can be omitted.

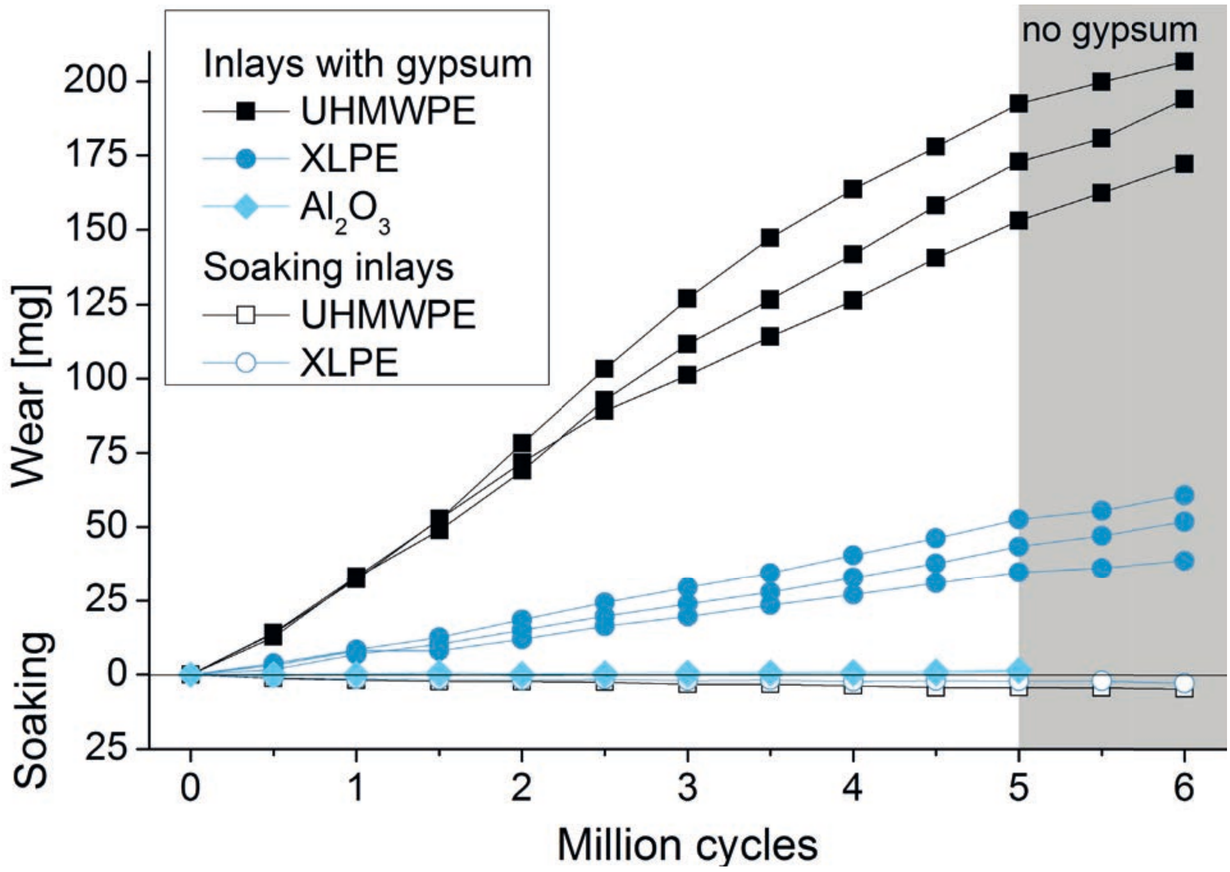

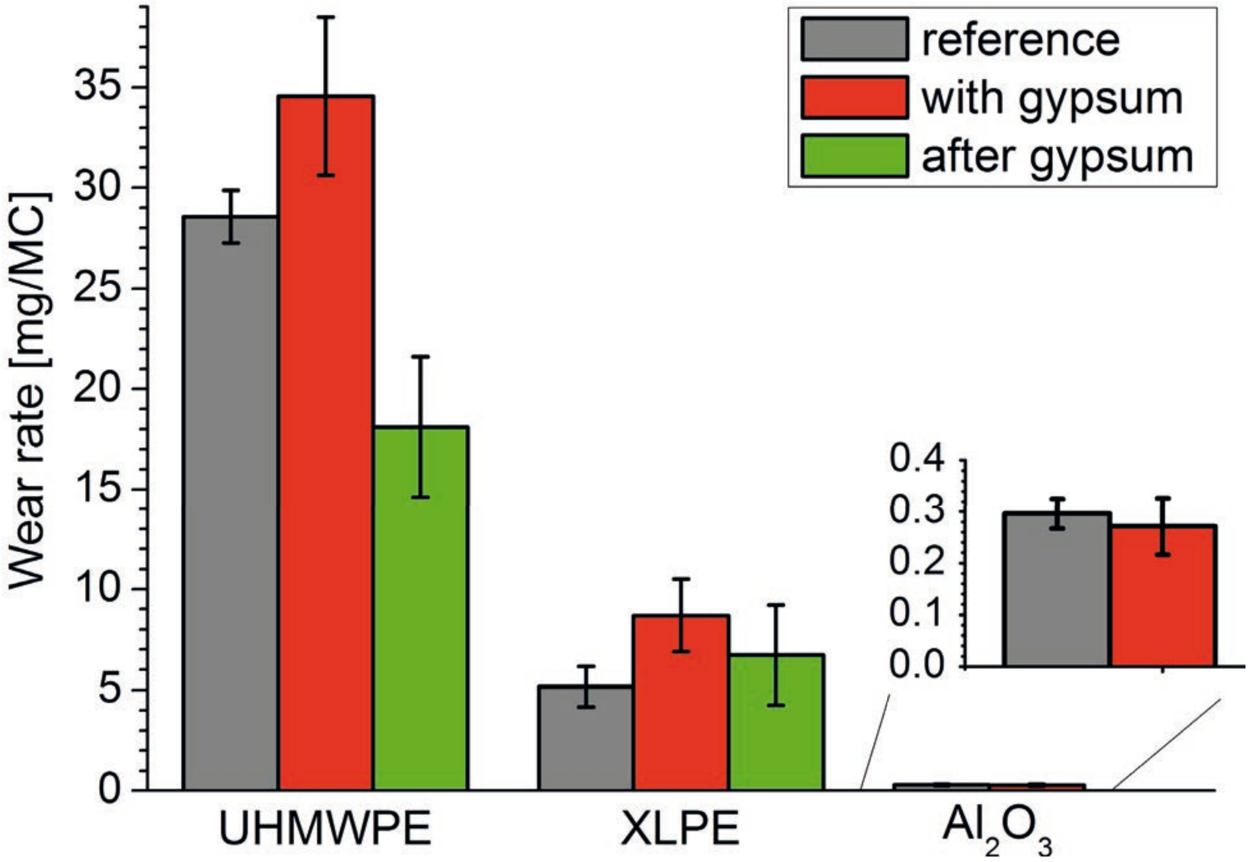

-Figure 1: Wear rate of the hip inlays in presence of gypsum particles in the test liquid. After 5 million cycles the polymer inlays were tested without gypsum particles.

-Figure 2: Wear rate of the inlays of artificial hip joints made of UHMWPE, cross linked PE (XLPE) and alumina. 3 inlays each were tested in the presence of gypsum particles and 3 or more without. After 5 mill. cycles in presence of the gypsum particles, the polymer inlays were tested for 1 mill. cycles without particles.

6A.6

Surgical reconstruction of failed hip Abductors - A new technique using Graft Jacket allograft human dermal matrix

Biyyam Madhusudhan Rao
St.Richards Hospital, Western Sussex Hospitals NHS Trust, Chichester, West Sussex, UK

Avulsion of abductors from hip can be debilitating complication after total hip arthroplasty performed through a trans-gluteal approach.We describe a new surgical technique of trans-osseous repair of hip abductors augmented by a Graft Jacket allograft acellular human dermal matrix.

Introduction

Avulsion of abductors from hip is a debilitating complication after total hip arthroplasty performed through a trans-gluteal approach. It results in intractable pain, Trendelenberg limp and instability of the hip.

Techniques described for repairing these abductor tears including direct trans osseous repairs[1], endoscopic repair techniques[2], Achilles tendon allograft[3], Gluteus Maximus⁴ and Vastus Lateralis⁵ muscle transfers. The aim of our study was to assess improvement in pain, limp and abductor strength in patients operated upon surgically for confirmed abductor avulsion using a modified trans osseous repair and augmentation of repair with a Graft Jacket allograft acellular human dermal matrix (Graft jacket; Wright Medical Technology, Arlington, TN).

Patients and Methods

In this prospective study we include 16 consecutive patients with hip abductor avulsions following a primary total hip arthroplasty through Hardinge approach for osteoarthritis.All the patients presented with pain around lateral aspect of hip, walking with a significant Trendelenberg limp and used a crutch or a stick in the opposite hand. Diagnosis was made by clinical examination and confirmed by ultrasound or MRI scans.

Surgical Technique

Surgical procedure was through lateral approach using the old scar to mobilise combined aponeurosis of the Gluteal Medius and Gluteus Minimus from the bony bed on the ilium to permit advancement onto the trochanter. The conjoint Gluteus Medius and Minimus insertion was affixed to the greater trochanter with No.5 non absorbable trans osseous suture using a Krackow suture through a series of transverse tunnels made in anterior aspect of greater trochanter. An onlay augmentation (Fig.1) of the osseo-tendinous junction was performed using a Graft Jacket matrix of 4 X 7 cms in size after rehydration according to the manufacturer's instructions.

Results

At mean follow up of 22 months (15-34 months), pain improved in all patients with mean VAS score improving from 8.25 to 2.33 (p value-0.05). All the patients had improvement in their abductor strength with MRC grade 4 out of 5 in 14 patients and 3 out of 5 in 2 patients. Trendelenberg sign disappeared in all but two. Mean Harris hip score improved from 34.05 to 81.26 (p value-0.001). All patients had improvement in gait except mild noticeable limp in two patients.11 patients did not use any walking aids and five felt more secure using a walking stick in the contralateral hand. The mean SF 36 PCS was 53.47 and MCS was 56.07

Conclusions

The procedure is safe and associated with high patient satisfaction, without the morbidity of tendon or muscle transfers. The Graft Jacket Matrix provides biological bridging between the hip abductors and its insertion into greater trochanter. It provides a biological scaffold for cellular and vascular in-growth and constructive tissue remodelling. The described procedure appears to enhance the mechanical strength of repaired tendon immediately following surgery. This Graft Jacketmatrix has already been used successfully in rotator cuff repairs of shoulder⁶ and has showed encouraging results.The early success of this new procedure warrants further study with more patients, longer follow-up and possibly histological study of retrieved specimens.

References

Hermes H.Miozzari, et al. Late repair of abductor avulsion after the transgluteal approach for hip arthroplasty. J Arthroplasty. 2010 Apr; 25(3):450-457.
Voos JE et al. Endoscopic repair of gluteus medius tendon tears of the hip. Am J Sports Med 2009; 37(4):743-747.
Fehm MN et al. Repair of a deficient abductor mechanism with Achilles tendon allograft after total hip replacement. J Bone Joint Surg Am 2010; 92(13):2305-2311.

Whiteside LA et al. Gluteus maximus flap transfer for greater trochanter reconstruction in revision THA. Clin Orthop Relat Res2006; 453:203-210.
Beck M, Leunig M, Ellis T, Granz R. Advancement of the vastus lateralis muscle for the treatment of hip abductor discontinuity. J Arthroplasty 2004; 19:476.
Bond JL, Dopirak RM, Higgins J, Burns J, Snyder SJ. Arthroscopic replacement of massive, irreparable rotator cuff tears using a graft jacket allograft: technique and preliminary results. Arthroscopy 2008; 24:403-9.

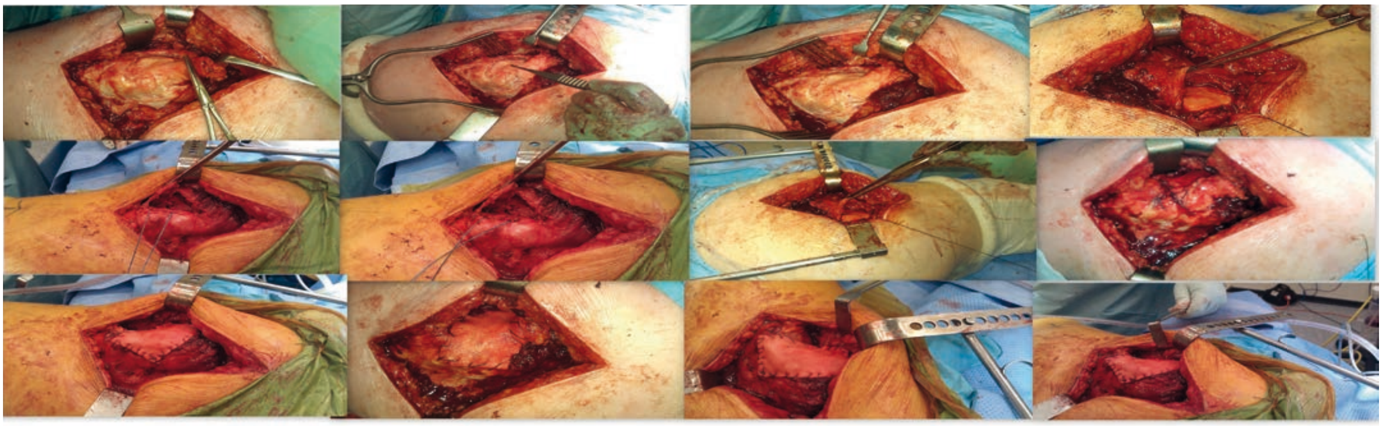

-Abductor avulsion and technique of trans-osseous repair augmented by Graft jacket matrix.

6A.7
Statins may reduce femoral osteolysis in patients with total hip arthroplasty

Anne Lübbeke
Geneva University Hospitals, Geneva, Switzerland

Statin use was associated with a reduced risk of developing femoral osteolysis in the first five years after primary THA. However, the number of events in this study is relativley small and further larger studies are necessary for confirmation.

Introduction:
Periprothetic osteolysis is still the main long-term complication after total hip arthroplasty (THA). Statins are frequently taken by elderly patients. Their use has been associated in experimental studies[1] [2] [3] with reduction of osteoclastic activity and subsequent periprosthetic osteolysis as well as promotion of bone formation. Recently, a large clinical study reported on a reduced risk of revision for aseptic loosening among statin users with THA[4].
Our objective was to evaluate the influence of statin use on the development of femoral osteolysis within the first five years after primary THA.
Patients & methods:
Since March 1996 all patients undergoing THA in our UniversityHospitalare routinely enrolled in a prospective hospital-based cohort and followed longitudinally. Eligible for this study were all primary THAs with the same un-cemented press-fit cup and a 28mm head operated upon between 1/2001 and 10/2005. Five years after surgery all patients still alive were contacted for a clinical and radiographic evaluation. Information on statin use was obtained(1) at the time of operation and(2)at the 5-year follow-up visit during the interview. Patients were classified as statin ever-users when they had a recorded statin use(1)both at the time of operation and follow-up,(2)at the time of operation but not at follow-up anymore and(3)at the time of follow-up. All others were classified as statin never-users. Main outcome was the incidence of focal or linear osteolysis around the femoral stem. Radiographs were analysed by an experienced orthopaedic surgeon who was blinded to the patient characteristics.
We used the case-cohort design, a type of nested case-control study. We employed both stratification and multiple logistic regression analysis to control for confounding.
Results sectin:
735 primary THAs (mean age 68 years, 54% women) were included. Five years postoperative focal or linear osteolysis was found around 40 (5.4%) femoral components; the cases in our analysis. The remaining 695 THAs that did not show osteolytic lesions were the controls. Among all patients, the prevalence of ever use of statins was 27.8% (204/735 THAs). Compared with never-users of statins, ever-users were more likely to be men, were less often engaged in high activity, had a higher BMI, more often an ASA score of 3 or 4, and more co-morbidities. The two groups differed only slightly with respect to age, diagnosis, and bearing surface, and were similar for the other baseline characteristics. Ever use of statins was much less frequent among cases (5 of 40, 12.5%) than among controls (199 of 695, 28.6%). The crude RR of statin use was 0.36 (95% CI 0.14; 0.92). After adjustment for age, sex, patient activity, BMI, diagnosis, type of bearing surface, and type of stem the adjusted RR was 0.38 (95% CI 0.15; 0.99).
Discussion & conclusion:
Statin use was associated with a reduced risk of developing femoral osteolysis in the first five years after primary THA. However, the number of events in this study is relativley small and further larger studies are necessary for confirmation.

References:
[1] Von Knoch F et al. Effect of simvastatin on polyethylene particle-induced osteolysis. Biomaterials, 2005
[2] Laing A et al. Statins attenuate PMMA-mediated monocyte activation. Acta Orthopaedica, 2008
[3] Yin H et al. Effects of simvastatin on osseointegration in a canine THA model. J Arthroplasty, 2011
[4] Thillemann T et al. Risk of revision after primary THA among statin users. JBJS Am, 2010

6A.8

Long term results of Müller reinforcement rings in acetabular revision surgery for large bone defects.

Stephanos Koutsostathis
Fourth Orthopaedic Department, KAT Hospital, Kifissia, Greece

Reinforcement rings are considered to be a valuable solution in acetabular revision surgery, when large bone defects are present. In our series, MŸller rings, combined with morsellized allografts, proved to perform successfully, clinically and radiologically in the long term.

Introduction:

Acetabular revision surgery in the presence of large bone defects is a challenging procedure. Reinforcement rings are considered to be a valuable solution. However function in the long term is a major concern. We present our long term results after reconstruction of the acetabulum with bone grafting and a Müller reinforcement device.

Patients and methods:

From 1992 to 1999, we performed 28 acetabular revisions in 25 patients (21 females, 4 males) using the Müller reinforcement ring, with an average follow-up period of 13.5 years. Mean age at surgery was 58 (40 - 78) years. Using the Paprosky classification, 5 cases were IIC, 13 were IIIA, and 10 were IIIB. Acetabular defects were filled with morsellized allografts from frozen femoral heads. Rings were secured with 2-5 screws. The polyethylene was cemented inside the ring. In all cases the Müller ring was optimally placed and the center of hip rotation was restored.

Results:

4 patients (5 hips) were lost to follow-up for several reasons. The average Harris hip score improved from 34.6 to 84.2 points at the final follow-up. Incorporation of the bone grafts took place in all cases at a mean time of 5 months. Overall survival was 91.3% using acetabular re-revision for all reasons as endpoint. One hip was reoperated for recurrent dislocation at 2 years postoperatively. One case was re-revised at 15 years for aseptic loosening. Radiolucent lines according to DeLee and Charnley were observed once in zone I, once in zone II and twice in zone III.

Discussion: Allograft collapse - resorption, aseptic loosening and failure in the long term are major concerns in acetabular revision arthroplasty. In our series, in cases with large acetabular defects, Müller rings, combined with morsellized allografts, proved to perform successfully, clinically and radiologically in the long term.

6B.1

Hyaluronic Acid-Based Hydrogel Enhances Neuronal Survival in Mouse Organotypic Spinal Cord Slice Cultures

Nikos Schizas
KTH, Stockholm, Sweden

Organotypic slice cultures have limitations such as early motorneuron loss. These limitations are counteracted when cultures are maintained on a substrate of hyaluronic acid based hydrogel.

Spinal cord slice cultures represent an in vitro model that is used for studies on spinal cord injury. However, limitations such as early motorneuron loss and severe tissue degeneration have been observed in these cultures.

It was the aim of this study to investigate whether spinal cord cultures maintained on hyaluronic acid (HA)-based hydrogel show improved neuronal survival and tissue preservation.

Spinal cord slices were obtained from p6-p9 mice and cultured for 4 days in vitro, either on a substrate of HA-based hydrogel (HA-gel group), or directly on polyethylene terephthalate (PET) membrane inserts (control group), or in the presence of soluble HA. Hematoxyline-eosine staining and histochemistry for neuronal nuclei (NeuN), choline acetyltransferance (ChAT), glial fibrillary acidic protein (GFAP), and Griffonia simplicifolia isolectin B_4 (IB_4) followed by quantitative analysis were performed in order to evaluate and characterise neuronal and glial populations.

Spinal cord slices maintained on HA-based hydrogel showed significantly improved tissue preservation and neuronal survival when compared to the PET group (figure 1).Survival of ChAT-positive motorneurons was 5.9-fold (p=0.008), resting microglial cells were 2-fold more numerous in the white matter (p=0.031), and the number of activated microglial cells within the grey matter was reduced by 61.4% (p=0.05) in these cultures. In contrast, cultures maintained in the presence of soluble HA showed no improvement when compared to the PET group.

In conclusion, HA-based hydrogel vastly improved neuronal and - most notably - motorneuron survival in spinal cord slice cultures derived from postnatal mice. Previously observed limitations in organotypic cultures such as early motorneuron death were thus counteracted. Moreover, microglial activation is limited both within the white and grey matter. We also conclude that the chemical properties of HA-based hydrogel are not as decisive as its mechanical properties since cultures maintained in the presence of soluble HA showed no improvement over controls. Our findings open up for experiments on hydrogels loaded with neuroprotective substances.

6B.2

Bone Cell Proliferation, Differentiation, and Cytokine Production on Titanium-Nitride versus Cobalt-Chromium-Molybdenum Surface

Ruud van Hove
Dept of Orthopaedics, Spaarne Hospital, Hoofddorp, The Netherlands

Titanium-nitride (TiN) coating is used to improve cobalt-chromium-molybdenum (CoCrMo) implant survival in total knee arthroplasty, but its effect on osteoconduction is unknown. Our findings show increased osteoblast proliferation and decreased differentiation suggesting improved osteoconduction on TiN compared to CoCrMo-surface.

Introduction

Uncemented total knee arthroplasty for painful, disabling osteoarthritis of the knee sometimes fail due to aseptic loosening. The tibial and femoral component of total knee prostheses are manufactured of cobalt, chromium, and molybdenum (CoCrMo) alloy because of its high wear resistance 1, 2. TiN provides the CoCrMo surface with increased hardness, a low coefficient of friction, and higher resistance to adhesive wear compared with CoCrMo, which are favorable characteristics for long-term survival of the implant, since it prevents the potentially harmful effects of accumulation of chromium and cobalt ions in the body 2, 3. Chromium and cobalt ions negatively affect the growth and metabolism of cultured osteoblasts while enhancing osteoclastogenic cytokine production 4-6. Therefore it was hypothesized that a TiN-surface would enhance osteoblast proliferation and/or differentiation and reduce osteoclastogenic cytokine production compared with a CoCrMo-surface.

Material & Methods

Hundred and ninety-two discs composed of CoCrMo alloy (diameter 25.5 mm, height 3.3 mm) were tested. Ninety-six discs were composed of CoCrMo alloy, of which 48 discs were uncoated (smooth discs) and 48 discs were coated with spherical CoCrMo beads (porous discs) as used at the bone-implant interface of total knee arthroplasty for bone ingrowth (Fig. 1). Ninety-six other discs composed of CoCrMo alloy (48 smooth discs and 48 porous discs) were coated with a thin TiN layer (~4 μm thickness) (Fig. 1). MC3T3-E1 osteoblasts were cultured on porous or smooth CoCrMo and TiN implant surfaces for 1-7 days in culture medium in a CO_2 incubator at 37°C in a 99% humidity atmosphere and 5% CO_2 in air. At day 1, 2, 4 and 7, culture medium was collected and adhered MC3T3-E1 osteoblasts were lysed. DNA concentration and alkaline phosphatase activity was measured in the cell lysate as measure for proliferation and differentiation respectively. Cytokines IL-1ß, IL-6, and TNF-α were quantitatively determined in culture medium using ELISA.

Results

MC3T3-E1 osteoblasts on porous TiN showed increased proliferation on day 2 ($p < 0.01$) and 7 ($p < 0.01$) compared with porous CoCrMo. MC3T3-E1 osteoblasts on porous TiN showed lower ALP activity on day 2 ($p < 0.01$) and 7 ($p = 0.04$) compared with porous CoCrMo. IL-6 production by MC3T3-E1 osteoblasts was higher on porous CoCrMo compared with porous TiN ($p < 0.05$) (Table 1).

MC3T3-E1 osteoblasts on smooth TiN showed increased proliferation compared with porous CoCrMo ($p < 0.05$). MC3T3-E1 osteoblasts on smooth TiN showed higher ALP activity on day 4 ($p = 0.03$) and 7 ($p = 0.03$) compared with smooth CoCrMo (Table 2). IL-6 production by osteoblasts expressed per amount of DNA did not show a difference between smooth TiN and CoCrMo. IL-1ß was only detected in a few cultures on either surface. TNF-α was not detected in any culture.

Discussion In conclusion

MC3T3-E1 osteoblasts cultured on porous or smooth TiN surfaces showed similar differentiation but increased proliferation compared with CoCrMo surfaces. IL-6 production by osteoblasts on TiN surfaces was decreased on porous surfaces and similar on smooth surfaces. The clinical implications of these findings might be decreased bone resorption and enhanced osteoconduction leading to improved osseointegration.

References

1. Marti, A. Cobalt-base alloys used in bone surgery, Injury, 2000: 31 Suppl 4: 18-21.
2. Wisbey, A., Gregson, P.J. and Tuke, M. Application of PVD TiN coating to Co-Cr-Mo based surgical implants, Biomaterials, 1987: 8: 477-480.
3. Mezger, P.R. and Creugers, N.H.J. Titanium nitride coatings in clinical dentistry, J Dent., 1992: 20: 342-3

4. Allen, M.J., Myer, B.J., Millett, P.J. and Rushton, N. The effects of particulate cobalt, chromium and cobalt-chromium alloy on human osteoblast-like cells in vitro, J. Bone Joint Surg. (Br), 1997: 79: 475-482.
5. Fleury, C., Petit, A., Mwale, F., Antoniou, J., Zukor, D.J., Tabrizian, M. and Huk, O.L. Effect of cobalt and chromium ions on human MG-63 osteoblasts in vitro: morphology, cytotoxicity, and oxidative stress, Biomaterials, 2006: 27: 3351-3360.
6. Wang, J.Y., Wicklund, B.H., Gustilo, R.B. and Tsukayama, D.T. Prosthetic metals interfere with the functions of human osteoblast cells in vitro, Clin. Orthop. Relat. Res., 1997: 339: 216-226.

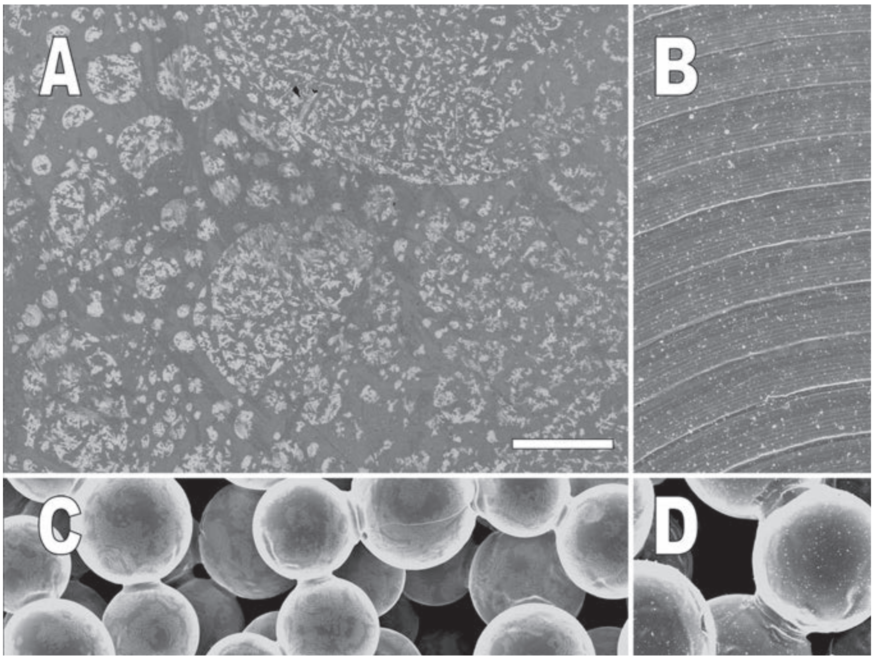

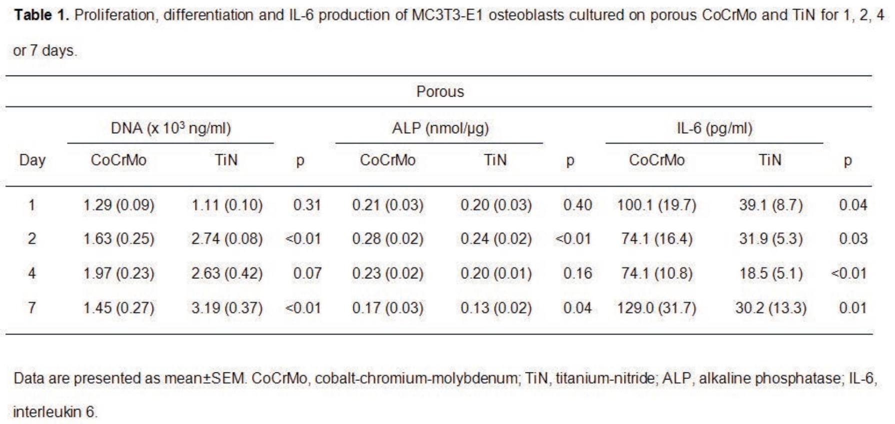
Table 1. Proliferation, differentiation and IL-6 production of MC3T3-E1 osteoblasts cultured on porous CoCrMo and TiN for 1, 2, 4 or 7 days.

	Porous								
	DNA (x 10^3 ng/ml)			ALP (nmol/µg)			IL-6 (pg/ml)		
Day	CoCrMo	TiN	p	CoCrMo	TiN	p	CoCrMo	TiN	p
1	1.29 (0.09)	1.11 (0.10)	0.31	0.21 (0.03)	0.20 (0.03)	0.40	100.1 (19.7)	39.1 (8.7)	0.04
2	1.63 (0.25)	2.74 (0.08)	<0.01	0.28 (0.02)	0.24 (0.02)	<0.01	74.1 (16.4)	31.9 (5.3)	0.03
4	1.97 (0.23)	2.63 (0.42)	0.07	0.23 (0.02)	0.20 (0.01)	0.16	74.1 (10.8)	18.5 (5.1)	<0.01
7	1.45 (0.27)	3.19 (0.37)	<0.01	0.17 (0.03)	0.13 (0.02)	0.04	129.0 (31.7)	30.2 (13.3)	0.01

Data are presented as mean±SEM. CoCrMo, cobalt-chromium-molybdenum; TiN, titanium-nitride; ALP, alkaline phosphatase; IL-6, interleukin 6.

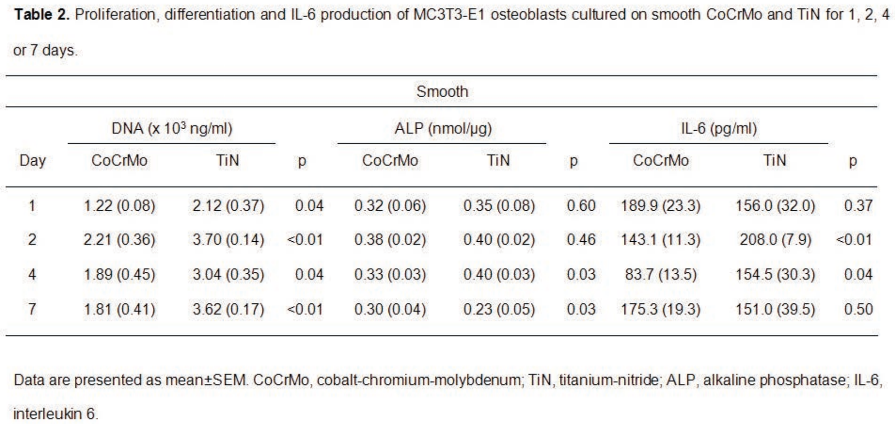
Table 2. Proliferation, differentiation and IL-6 production of MC3T3-E1 osteoblasts cultured on smooth CoCrMo and TiN for 1, 2, 4 or 7 days.

	Smooth								
	DNA (x 10^3 ng/ml)			ALP (nmol/µg)			IL-6 (pg/ml)		
Day	CoCrMo	TiN	p	CoCrMo	TiN	p	CoCrMo	TiN	p
1	1.22 (0.08)	2.12 (0.37)	0.04	0.32 (0.06)	0.35 (0.08)	0.60	189.9 (23.3)	156.0 (32.0)	0.37
2	2.21 (0.36)	3.70 (0.14)	<0.01	0.38 (0.02)	0.40 (0.02)	0.46	143.1 (11.3)	208.0 (7.9)	<0.01
4	1.89 (0.45)	3.04 (0.35)	0.04	0.33 (0.03)	0.40 (0.03)	0.03	83.7 (13.5)	154.5 (30.3)	0.04
7	1.81 (0.41)	3.62 (0.17)	<0.01	0.30 (0.04)	0.23 (0.05)	0.03	175.3 (19.3)	151.0 (39.5)	0.50

Data are presented as mean±SEM. CoCrMo, cobalt-chromium-molybdenum; TiN, titanium-nitride; ALP, alkaline phosphatase; IL-6, interleukin 6.

-Figure 1. Scanning electron microscopy images of discs with A) CoCrMo surface, B) TiN surface, C) Porous coated CoCrMo surface, and D) Porous coated TiN surface. Scale bar, 200 µm. Magnification, x100.

6B.3
Developing Robocast Ceramic/Polymer Scaffolds for Bone Implants

Pedro Miranda
Universidad de Extremadura, Badajoz, Spain

Hybrid ceramic/polymer structures are developed by infiltration of biodegradable polymers into bioceramic scaffolds with controlled pore architecture fabricated by robocasting. Mechanical properties of the composites closely match those of human cortical or cancellous bone depending on composition and fabrication process.

Introduction:

Optimal materials for bone tissue replacement should exhibit bone-like properties (low density and stiffness and high strength) and be able to interact with the tissues, so that they can actively induce bone regeneration. A strategy to achieve interaction with surrounding tissue is to use porous matrices of osteophilic materials.

Among the materials most commonly used to fabricate these porous substrates several calcium phosphates stand out. The main drawback of these bioceramic materials is their low fracture strength, which limits their use to low-load bearing applications (e.g. cranial implants). One of the reasons for this low mechanical resistance of bioceramic scaffolds is that their porosity must be interconnected and with a certain interconnection size, to allow vascularization, cell penetration and nutrient diffusion into the scaffold. In conventional scaffold fabrication methods it is difficult to precisely control pore size, geometry, and spatial distribution, and therefore high porosities are required to achieve the necessary interconnectivity, which translate into very low strengths.

To overcome these obstacles, this work uses a dual strategy: on the one hand, robocasting is used to fabricate scaffolds with controlled, pre-designed pore architecture exhibiting a large degree of interconnectivity with a reduced total porosity; and on the other, novel inorganic/organic composite biomaterials are fabricated by impregnating the robocast scaffolds with biodegradable polymers.

Materials & Methods

Bioceramic scaffolds with controlled pore architecture were fabricated from tricalcium phosphate powders by robocasting, a novel extrusion-based additive fabrication technique. These ceramic skeletons are then either fully impregnated or simply coated with different biodegradable polymers (polylactic acid and poly (e-caprolactone)) by in situ polymerization of the corresponding monomers within the ceramic structures. The microstructure and mechanical performance of the developed materials are thoroughly characterized and compared to results from the literature and to bone properties.

Results

The infiltration method developed allows the full impregnation of both the pre-designed robocast scaffolds' macroporosity and the intrinsic scaffold microporosity (Fig. 1). Alternatively, homogeneous polymeric coatings (Fig. 2) can be deposited onto the scaffolds surfaces, producing infiltration of the scaffold microporosity but preserving the pre-designed macroporosity. Porous ceramic scaffolds fabricated by robocasting exhibit mechanical strengths superior to conventional scaffolds thanks to their optimized architecture, and their mechanical performance is further boosted, both in terms of strength and toughness, after they are impregnated/coated. The results show that these hybrid materials have a mechanical response not attainable with conventional porous ceramic scaffolds and closely matching human bone performance (Fig.3).

Discussion/Conclusion

Scaffolds fully impregnated with PLA can exhibit performances similar to cortical bone in terms of modulus and strength, and a superior toughness (Fig. 3). This comes at the price of sacrificing pre-existing porosity, but such dense biodegradable composites can find application as temporary fixation devices. Bioceramics scaffolds simply coated with PCL, and thus preserving macroporosity, come close to cancellous bone mechanical performance and are deemed more appropriate for its replacement. Combinations of both types of structures could become optimal materials for bone regeneration.

Acknowledgements:
This work was supported by Junta de Extremadura (IB10006) and FEDER funds.

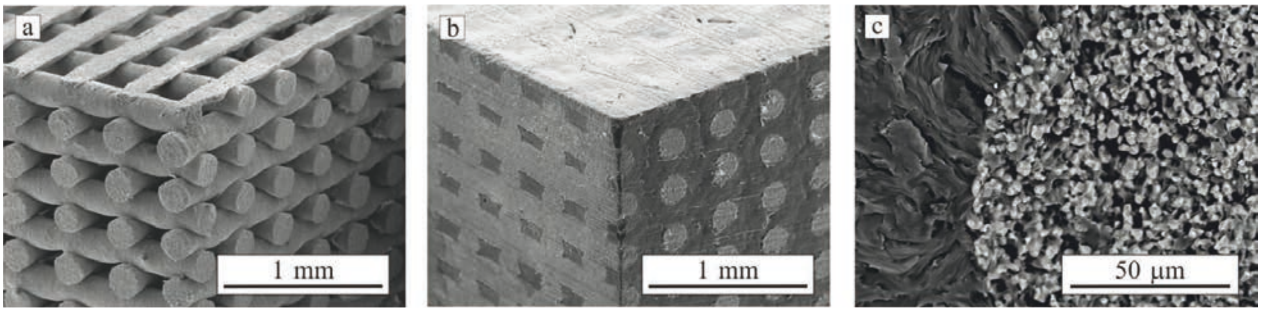

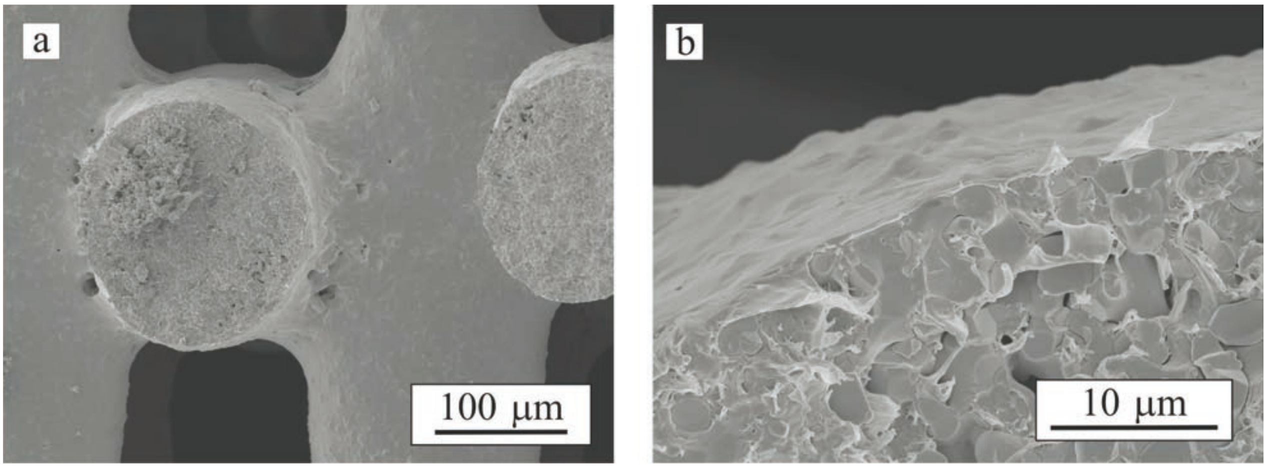

-<a

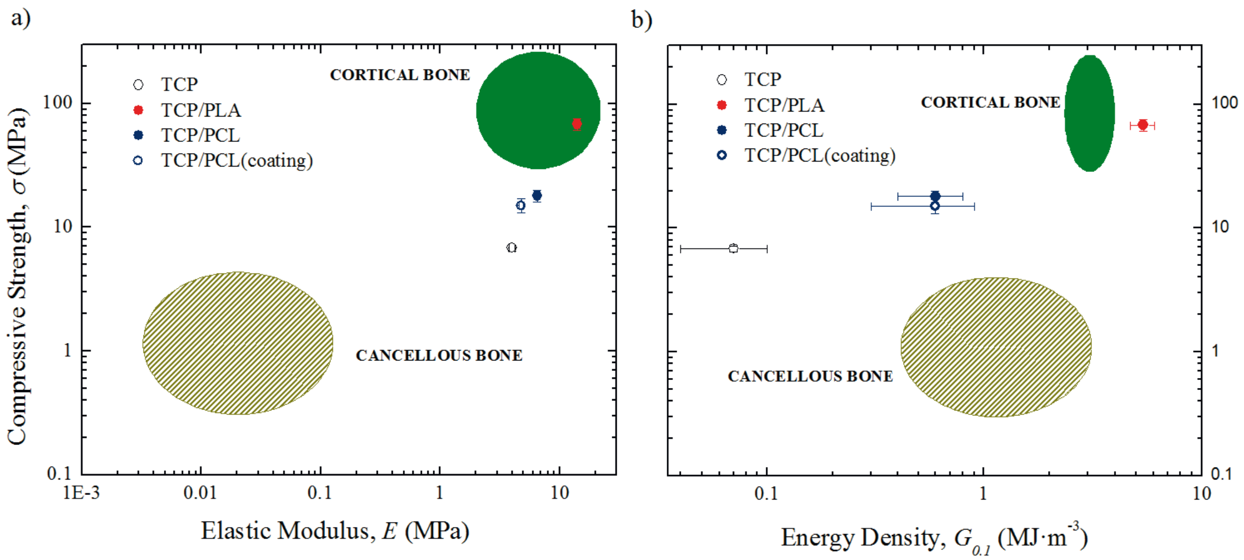

-Figure 1. SEM micrographs showing: (a) the bare robocast scaffold, (b) a similar scaffold after impregnation with PLA, and (c) a fracture surface on the impregnated structure evidencing the presence of PLA on the scaffold micro-porosity.

-Figure 2. SEM micrographs showing details of a robocast scaffold coated with PCL.

-Figure 3. Ashby diagrams comparing the mechanical properties of the fabricated scaffolds with natural bone properties: (a) compressive strength vs. elastic modulus and (b) compressive strength vs. toughness (estimated as strain energy density at 10 % strain).

6B.4

Comparison of cellular behavior with different bone grafting materials

Massimiliano Leigheb
Orthopaedics and Traumatology, “Maggiore d.c.” Hospital, University of Eastern Piedmont, Novara, Italy

Introduction:

Even if the autogenous bone still remains the gold standard to augment or bridge osseous defects, bone substitute materials of natural or synthetic origin are becoming more and more used to avoid the risks associated with autogenous bone grafting such as perioperative morbidity and complications. The literature reports only few comparative studies on these materials, and most of them are histologic and morphometric evaluations, or microradiograph measurements obtained from in vivo explants. Moreover, we do not find in vitro studies on bone cells that compare their behavior when cultured in contact with these bone substitutes.

Purpose of this work is to study and compare the behavior of macrophages and human osteoclasts cultured in contact with different bone substitutes used in orthopaedic surgery for non-unions, traumatic loss of substance, after oncological resections and whenever a graft is needed to fill bone defects.

Materials & Methods:

Bone substitutes of natural and synthetic origin were used: human, bovine, hydroxyapatite and hydroxyapatite + b-tricalcium phosphate. Macrophage activation and cytokine release were evaluated using SEM analysis and a sandwich ELISA kit while the activity of human osteoclast-like cells was studied quantifying Calcium released from the studied substrata together with SEM analysis of cell morphology and of pit formation on the bone substitutes.

Results:

Hydroxyapatite resulted to be the greatest macrophage activator, while the bovine derived material resulted to be the only bone substitute that doesn’t induce macrophages to release IFNg. No material had direct induction of osteoclast precursor differentiation even if mature osteoclasts showed the greater activity on the human derived material, while the bovine one was the substrate with the minor osteoclast’s activity.

Discussion: The strategies involved in the repair of bone defects include the use of autogenous bone, bone cement, metals, polymers and ceramics. Local and systemic factors are involved in favoring or inhibiting bone repair, and a fundamental role is played by the cells of macrophage lineage, which, producing cytokines, mediate inflammation, bone cells differentiation, and bone cells activity. A growing body of evidence suggests that inflammatory signals are critical for the initiation of the fracture healing response, and the effect of inflammatory cytokines on bone depends on the timing and context of their expression.

Conclusions:

The four tested materials reacted differently with the tested cells and between them, the bovine derived bone, being the lower macrophages and osteoclasts activator may be considered a good bone substitute for clinical situations requiring greater time of permanence of the material in the site of implantation while the human derived bone will be better suitable for clinical applications that require lower time of permanence. Compared to bone autograft, all these osteo-conductive biomaterials combined with proper osteo-inductive agents can provide better regenerative effects with less undesired effects.

6B.6
In vivo biological fixation of selective laser melted bone scaffolds

Jan Demol
Mobelife, Leuven, Belgium

The in vivo osseointegration potential of selective laser melted Ti6Al4V scaffolds was evaluated. New bone formation inside the scaffoldÕs interconnected porous network resulted in an increasingly strong fixation, making them a valuable option for the treatment of extensive bone defects.

Introduction:
Custom-made implants are applied clinically nowadays to reconstruct massive bone defects encountered during revision surgery of total hip arthroplasties. CT-based preoperative planning combined with additive manufacturing provides the flexibility to produce orthopaedic implants with a personalized external shape and a controllable internal network of pores. Rapid and extensive bone infiltration into the scaffold's pores is essential to obtain strong and durable biological fixation. In this study, the in vivo bone ingrowth and biological fixation of clinically used titanium scaffolds were quantified in an in vivo goat model.
Methods:
Ti6Al4V constructs were manufactured by additive manufacturing (selective laser melting (SLM)). The cylindrical constructs (Ø8mm x 14mm) had an interconnected, regular porous network (75% porosity). Constructs with or without hydroxyapatite coating were implanted in six goats. Three unicortical defects were created in the distal femur and medial tibia of both hind legs and constructs were inserted in a press-fit manner. After insertion and prior to explantation, implant stability was evaluated through resonance frequency analysis. Fluorochrome labeling was performed at 3, 6 and 9 weeks after surgery to monitor new bone formation. After 6 and 12 weeks, samples were explanted, fixated, imaged with micro-CT and processed for histological analysis. In addition, pull-out tests were performed to measure the fixation strength at the bone-scaffold interface.
Results:
Histological analysis indicated good bone apposition and active bone ingrowth for all implants at 6 and 12 weeks. Quantification of the microCT data showed that on average 10.5% of the void volume inside the scaffold was filled with newly formed bone. The presence of a hydroxyapatite coating tended to increase the bone volume inside the scaffolds. Analysis of the frequency response functions indicated a reduction in modal damping of more than 30% in 89% of the samples. The stiffness of the bone-implant interface increased and changed (as measured by the increase in resonance frequency and change in mode shape) due to the osseointegration of the scaffolds. Pull-out forces increased over time. At 12 weeks, maximal forces above 1kN were measured.
Conclusion:
SLM manufactured titanium scaffold allow bone ingrowth and obtain strong biological fixation in a 3 months goat model. As custom-made bone augments, they provide a promising approach to the reconstruction of severe bone defects.

6B.7
Bone marrow aspirate and biomaterials for osteoregeneration

Claudia Eder
Orthopedic Hospital Speising, Vienna, Austria

A combination of native bone marrow aspirate with Demineralised Bone Matrix, Calcium Phosphate or Hydroxyl Apatite Biomaterials can only deliver low amounts of stem cells and results in tissue formation resembling bone marrow rather than trabecular bone.

Introduction:
The limited supply of autografts for spinal fusion has prompted extensive research on bone graft substitutes. Various biomaterials have been applied either stand alone or impregnated with blood or bone marrow aspirate to promote spinal fusion. Bone marrow aspirate harvested from the iliac crest is known to contain osteoprogenitor cells, which are supposed to differentiate into osteoblasts and form new bone at the desired fusion site. According to literature, only 0,001% - 0,01% of bone marrow aspirate cells are in fact osteoprogenitor cells (Science 1999;248:143). Aim of the presented study is to analyze the potential of native bone marrow aspirate in combination with 3 different biomaterials and try to improve results by cell concentration and pre-cultivation.
Materials & Methods:
Surplus material remaining after cage and intervertebral space preparation for routine spinal fusion surgery was assessed from 5 patients. Bone marrow aspirate was analyzed native as well as after concentration of stem cells by density gradient centrifugation and the potential of the stem cells to differentiate into the osteogenic, chondrogenic and adipogenic lineage was investigated. Three different biomaterials - Demineralised Bone Matrix (DBX), ß-Tricalciumphosphate (ChronOS®)and Hydroxylapatite (HealOS®) were impregnated with bone marrow aspirate according to specifications of the supplier and analyzed immediately after seeding and after a 2 weeks pre-culture period.
Results:
Most of the cells in native bone marrow aspirate were identified as erythrocytes while only a small fraction was identified as nucleated stem cells. Density gradient centrifugation resulted in a homogenous fraction of stem cells with an average cell yield of $6{,}5\times10^6$ mononuclear cells per ml. Concentrated cells from all patients could be differentiated into the osteoblastic, chondrogenic and adipogenic lineage according to the mesenchymal stem cell definiton.
After biomaterial impregnation with native bone marrow aspirate, average stem cell density was 1,13 cells/mm^2 (ChronOS®), 0,92 cells/mm^2 (HealOS®) and 0,008 cells/mm^2 (DBX). Pre-cultivation of the constructs in vitro did not significantly alter stem cell densities in ChronOS® and HealOS® , but significantly increased cell density to 8,7 cells/mm^2 if combined with DBX (p
After 2 weeks, some tissue islands formed by the mesenchymal stem cells were visible in all biomaterials tested. The tissue consisted of a heterogenous cell population resembling bone marrow rather than bone and did not exhibit typical osteogenic markers.
Conclusion:
Impregnation of biomaterials with native bone marrow aspirate can only deliver very small amounts of osteoprogenitor cells to the implantation site. Density gradient centrifugation represents a rapid and effective method to purify stem cells from bone marrow aspirate and allow the transplantation of higher cell densities. If applied in combination with demineralized bone matrix, a pre-culture period of stem cells together with the biomaterial significantly improves cell seeding density and tissue formation. Irregular tissue formation was visible in all biomaterials tested, but the further addition of ostegenic differentiation factors might be required to enforce the differentiation into trabelcular bone tissue.

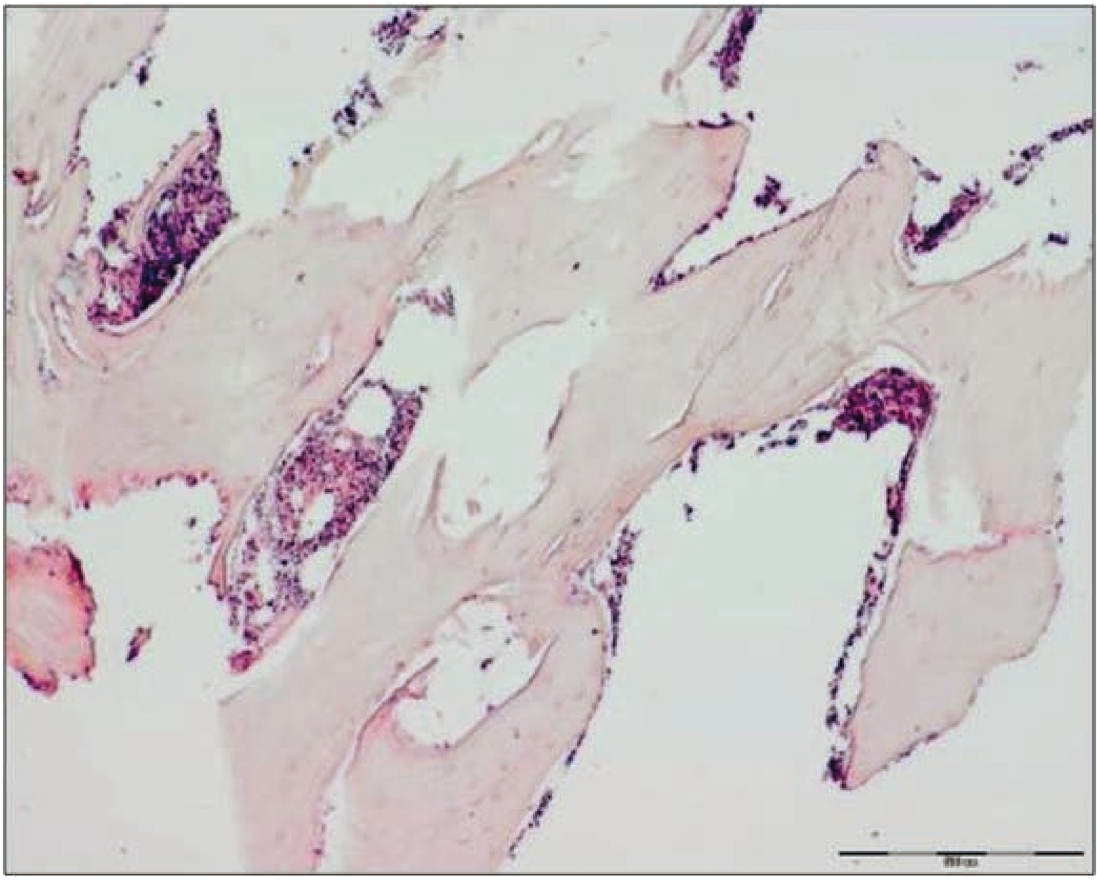

Formation of tissue bridges between the bone fragments

6B.9

EFFECT OF INTRARTICULAR PLATELET-RICH PLASMA (PRP) INJECTION IN OSTEOCHONDRITIS. AN EXPERIMENTAL HISTOLOGICAL STUDY IN RABBITS.

Javier Cervero
Hospital San Agustín, Avilés. Spain.

Intraarticular injection of PRP after osteochondritic lesions made to rabbits' knees enhances cartilage regeneration and improves surface regularity, structural integrity and the bonding of newly formed cartilage to the adjacent cartilage after 4 weeks as compared with control animals.

Introduction:
Trauma and age-related degeneration of articular cartilage often results in severe and chronic lesions, partly due to the low regeneration potential of cartilage. These osteochondrotic lesions are of important clinical and social relevance. Strategies to treat cartilage defects include the use of biomaterials, growth factors, stem cells, and platelet-derived products.
Material and method:
In our work, we employed New Zealand rabbits (12).Six animals were used as controls: an intrarticular osteochondrotic lesion was made to the femoral condyles on their knees and the animals were sacrificed at 2 week (3 animals) and 4 weeks (3 animals). Another six animals were subjected to the same lesion and the same operative procedure and the lesions were filled with platelet-rich plasma (PRP). These animals were also sacrificed at 2 (3 animals) and 4 (3 animals) weeks. After sacrifice, blocks including the lesion and the neighbouring articular tissue were taken, fixed in formaldehyde, decalcified, and embedded in paraffin. Sections (10 microns) were obtained from the blocks and stained with H/E. The sections were assessed following the criteria of O'Driscoll (1).
Results:
The main difference between the experimental and control groups was the nature of the predominant tissue in the lesion: cartilage in the groups treated with PRP, mesenchimal tissue in the control groups.
O´Driscoll, S.W., et al: J.Bone and Joint Surg., Vol. 68-A (7): 1017-1035, 1986

7A.10

Assessing Results After Distal Radius Fracture Treatment: A Comparison of Objective and Subjective Tools

Iris Kwok
Queen Mary Hospital, Hong Kong

Functional outcomes following distal radius fractures are directly influenced by the choice of outcome assessment instruments used. In this study we compare four commonest scoring systems, each comprising of objective and/or subjective assessment components.

Introduction:
Functional outcomes following distal radius fractures are directly influenced by the choice of outcome assessment instruments used. Our objective was to compare scoring systems in measuring patient functional outcomes, and determine which scoring system compared most favourably with the widely-used Disabilities of the Arm, Shoulder and Hand (DASH) questionnaire.

Methods:
108 patients between May 2004 and November 2006 were treated operatively following distal radius fractures. Follow-up was at three months, six months, one year and two years post-surgery, during which anatomical and functional assessments were performed. Patient outcomes were recorded using DASH, the Green and O'Brien system, Gartland and Werley system and Sarmiento radiological scoring system.

Results:
There was a stronger correlation between the Green and O'Brien scoring system and DASH (r = -0.54) than Gartland and Werley and DASH (r = 0.44). The Green and O'Brien scoring system was more demanding so patients rated 'excellent' or 'good' had better functional outcome than those bearing the same grade in the Gartland and Werley system. Nonetheless the Green and O'Brien score and Gartland and Werley score showed good correlation with each other (r = 0.66). The Sarmiento radiological score had no significant correlation with any of the other scoring systems. Significant predictors of the DASH score were function (r = 0.42), power grip (r = 0.41), pain (r = 0.37) and range of motion (r = 0.28).

Conclusion:
The Green and O'Brien scoring system correlated most strongly with the DASH score. Radiological scoring (reflecting anatomical deformity) was not significantly correlated with functional outcome. Whilst subjective parameters 'pain' and 'function' are influenced by psychosocial factors and thus highly variable, it is paramount to include subjective tools in outcome assessment in future studies on wrist fractures.

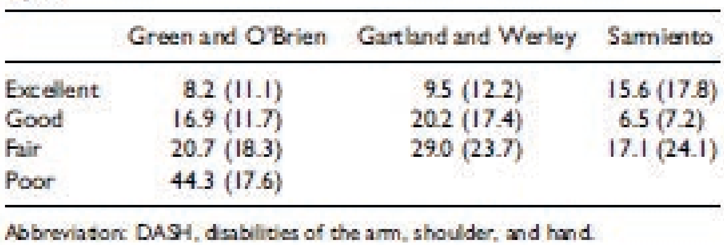

Table 2. Mean DASH Scores (Standard Deviation) for Each Final Grade When Using Different Scoring Systems—Includes Patients of all Ages

	Green and O'Brien	Gartland and Werley	Sarmiento
Excellent	8.2 (11.1)	9.5 (12.2)	15.6 (17.8)
Good	16.9 (11.7)	20.2 (17.4)	6.5 (7.2)
Fair	20.7 (18.3)	29.0 (23.7)	17.1 (24.1)
Poor	44.3 (17.6)		

Abbreviation: DASH, disabilities of the arm, shoulder, and hand.

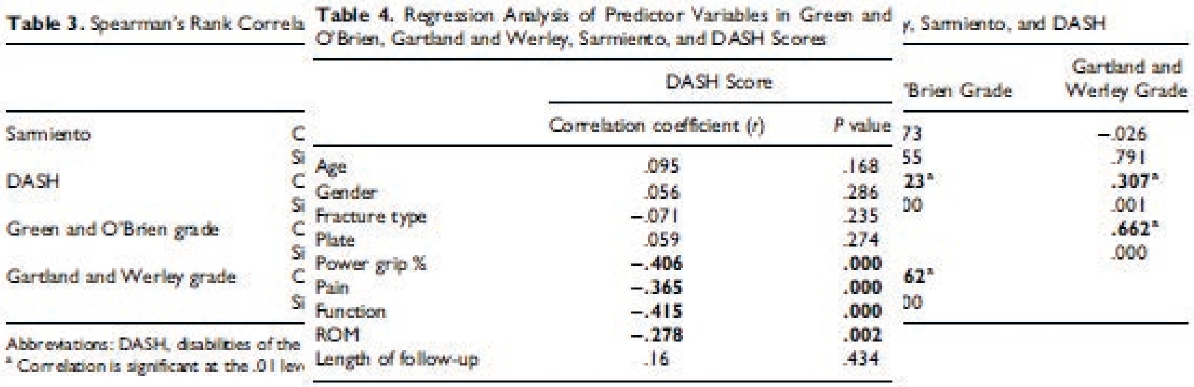

Table 3. Spearman's Rank Correla y, Sarmiento, and DASH

		'Brien Grade	Gartland and Werley Grade
Sarmiento	C	73	−.026
	Si	55	.791
DASH	C	23ᵃ	.307ᵃ
	Si	00	.001
Green and O'Brien grade	C		.662ᵃ
	Si		.000
Gartland and Werley grade	C	62ᵃ	
	Si	00	

Abbreviations: DASH, disabilities of the

ᵃ Correlation is significant at the .01 lev

Table 4. Regression Analysis of Predictor Variables in Green and O'Brien, Gartland and Werley, Sarmiento, and DASH Scores

	DASH Score	
	Correlation coefficient (*r*)	*P* value
Age	.095	.168
Gender	.056	.286
Fracture type	−.071	.235
Plate	.059	.274
Power grip %	**−.406**	**.000**
Pain	**−.365**	**.000**
Function	**−.415**	**.000**
ROM	**−.278**	**.002**
Length of follow-up	.16	.434

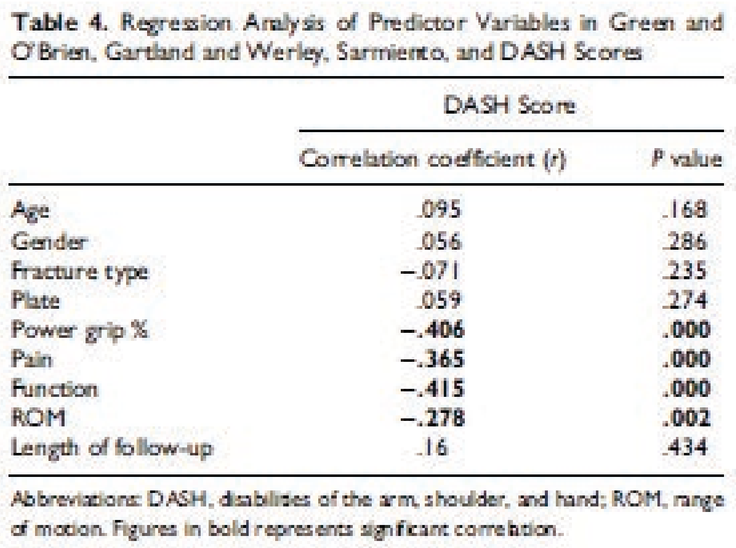

Table 4. Regression Analysis of Predictor Variables in Green and O'Brien, Gartland and Werley, Sarmiento, and DASH Scores

	DASH Score	
	Correlation coefficient (*r*)	*P* value
Age	.095	.168
Gender	.056	.286
Fracture type	−.071	.235
Plate	.059	.274
Power grip %	**−.406**	**.000**
Pain	**−.365**	**.000**
Function	**−.415**	**.000**
ROM	**−.278**	**.002**
Length of follow-up	.16	.434

Abbreviations: DASH, disabilities of the arm, shoulder, and hand; ROM, range of motion. Figures in bold represents significant correlation.

-Mean DASH scores (standard deviation) for each final grade when using different scoring systems - includes patients of all ages.

-Spearman's rank correlation between final grading in Green and O'Brien, Gartland and Werley, Sarmiento and DASH.

-Regression analysis of predictor variables in Green and O'Brien, Gartland and Werley, Sarmiento and DASH scores.

7A.11

Analysis of how knee flexion characteristics can be used as an outcome assessment for knee osteoarthritis

Diana Hodgins
European Technology for Business Ltd, Codicote, UK

The purpose of this study was to examine the differences in gait profile between patients with knee osteoarthritis (OA) and healthy controls using inertial measurement units (IMUs). Results identified knee flexion on stance as the motion characteristics that will differentiate between them.

Introduction:

Around 2.5% of the adult population suffer from Osteoarthritis (OA) of the hip or knee, most of whom are over 45 and this increases to 10% for women over 75. Current diagnosis in an orthopaedic clinic is done using a standard X-ray machine, and the level of degeneration is assessed. Previous studies have reported that changes to the knee joint occur even before radiographic changes are detected. Furthermore, poor correlation between radiographic changes and symptoms of pain and function has been reported. There is evidence that the maximum knee flexion angle in stance is reduced with the severity of the OA when compared to normal subjects, and some suggest that this is in order to care for and prevent knee OA progress [1, 2].

The current study had four aims. First, to provide further evidence to support the claim that patients with knee OA demonstrate altered gait pattern compared to healthy subjects, and specifically to examine the differences between groups in knee flexion angle during the stance and the swing phases. Second, to demonstrate that knee flexion in swing and stance is not age dependent in healthy subjects. Third, to demonstrate that knee motion can be measured using a sensor based system that can be used in a clinic. Finally, to define a parameter that would differentiate between patients with knee OA and matched controls.

Methods:

Twenty three patients (mean±sd age was 65.1 ± 7.7 years) diagnosed with knee OA, 21 healthy age-matched controls (mean±sd age was 71.3 ± 6.1 years), and 31 young healthy controls (mean±sd age was 33.0 ± 7.5 years) underwent a gait test using an IMU system (gaitWALK). Gait parameters evaluated were: stride duration, knee flexion range of motion (ROM) in swing and stance. One-way ANOVA was used to evaluate significant differences between groups ($P<0.05$).

Results:

Patients with knee OA had significant lower knee flexion ROM (10.3°±4.0°) during stance than age-matched controls (18.0°±4.0°) ($P<0.001$).

For the younger healthy subjects the values were marginally higher (18.8°±4.4°). Patients with knee OA had significant lower knee flexion ROM (54.8°±5.5°) during swing than age matched controls (61.2°±6.1) ($P=0.003$). For the younger healthy subjects the values were marginally higher (65.4°±7.4°). Patients with knee OA also had longer stride duration (1.12s±0.09s) than age matched controls (1.06 s±0.11 s), but this was not statistically significant ($P=0.073$). There were no statistically significant differences between the age-matched controls and the younger subjects.

Discussions and Conclusions:

The characteristic that differentiates between a patient with knee OA and a healthy one is knee flexion ROM in stance, with a sensitivity of 0.952 and a specificity of 0.783. Knee flexion ROM in swing and stride duration are not good discriminators as there is significant overlap between the two groups. This parameter might help clinicians identify and evaluate a knee problem from a simple gait test.

References:

Astephen JL, et al: Journal of Orthopaedic Research 2008, 26:332-341.
Zeni JA, et al: Clinical Biomechanics 2009, 24:372-378.

7A.3
Total Knee Arthroplasty: do custom cutting blocks improve mechanical axis reconstruction?

Nemanja Polic
CHUV, Lausanne, Switzerland

Mechanical axis reconstruction in Total Knee Arthroplasty plays a central role in longevity of the implants, particularly in young active patients. TKA with custom cutting blocks seems to be a promising technique to improve the precision of reconstruction.

Introduction

The efficiency of Total Knee Arthroplasty (TKA) on pain removal and function improvement in primary osteoarthritis is well accepted. Anatomical reconstruction of limb mechanical axis is known to play a central role in longevity of the implants, particularly in young active patients. This is why TKA using custom made cutting blocks have been developed recently by several manufacturers.

The purpose of this study was to evaluate the mechanical axis reconstruction together with the functional outcome after a TKA implantation with custom instrumentation.

Patients and Methods

We prospectively followed a consecutive series of 64 patients who have undergone a posterior-stabilized (mobile bearing plate in rotation) TKA implantation with custom made instrumentation for primary knee osteoarthritis.

Method

Custom cutting blocks were manufactured on the basis of a preoperative knee CT-scan with a three-dimensional planification of femoral and tibial bone cuts(see Fig. 2).

Both operative technique and postoperative care were the same as those used for standard cuts with the same TKA implant in our department. The outcomes were measured using both clinical (subjective-WOMAC/objective-KSS) and radiological (KSS) pre- and post-operative scores (6 weeks, 3-6 and 12 months).

'Results

Sixty-four patients with a mean age of 68.6 +/- 9.7 years were included in the study after informed and signed consent. Themean6 months WOMAC scoreimproved to25.3 +/-17.0 points(thepre-operative onewas 58.1 +/- 16.2 points). The KSS-function has improved from 62.6 +/-20.84 points to 88.8 +/- 15.5 points, and the KSS total score from 48.9 +/-14.8 points to 84.0 +/- 16.3 points.

As forthe mechanical axis reconstruction, total femoro-tibial valgus angle on KSS scorewas 185.0° +/- 2.8 at 6 months. Femoral flexionwas measured at -3.9° +/- 3.1. Tibial slopewasabout five degrees (as recommended by the manufacturer) with a prosthesis-tibia angle of 85.2° +/- 4.2 on lateral plain film...

Discussion Conclusion

At 6 months of follow-up, both clinical and radiological results after TKA using custom instrumentation aregood. The mechanical axis reconstruction appeared to be improved by this instrumentation (in comparison with our data in our knee implant register).

TKA with custom cutting blocks seem to be a promising technique to improve the quality of reconstruction and thus the longevity of the implants.

References

1. Nunley RM, Ellison BS, Zhu J, Ruh EL, Howell SM, Barrack RL.Do patient-specific guides improve coronal alignment in total knee arthroplasty? Clin Orthop Relat Res. 2012 Mar;470(3):895-902. Epub 2011 Dec 20.
2. Ng VY, DeClaire JH, Berend KR, Gulick BC, Lombardi AV Jr. Improved accuracy of alignment with patient-specific positioning guides compared with manual instrumentation in TKA. Clin Orthop Relat Res. 2012 Jan;470(1):99-107.
3. Jeffery RS, Morris RW, Denham RA. Coronal alignment after total knee replacement. J Bone Joint Surg Br. 1991 Sep;73(5):709-14.
4. Lotke PA, Ecker ML. Influence of positioning of prosthesis in total knee replacement. J Bone Joint Surg Am. 1977 Jan;59(1):77-9.

7A.4

Survivorship, Patient Reported Outcome and Satisfaction Following Resurfacing and Total Hip Replacement

Alexander Aquilina
Orthopaedic research, Avon Orthopaedic Centre, Southmead Hospital, Bristol, UK

The ASR resurfacing shows poorer survival than MoM, CoC THRs and the BHR. Highest functional scores were achieved with the BHR and the CoC THR which were equivalent. Metal wear debris related phenomenon remain a cause for concern.

Background

Resurfacing (RA) and total hip replacement (THR) are arthroplasty options in the treatment of patients with debilitating hip pathology. There remains doubt as to the best option in terms of postoperative function and survivorship 1.

Patients and Methods

381 patients that had undergone hip arthroplasty with a BHR RA, ASR RA, metal-on-metal (MoM) THR or ceramic-on-ceramic (CoC) THR were reviewed at a median follow up of 51 months (IQR 36-64). Validated outcome questionnaires for satisfaction (SAPS), function (OHS) and health (SF-12) were administered and survivorship assessed with revision of any part of the construct and reoperation for any reason assessed.

Outcome data was checked for normality using Kolmogorov-Smirnov test. The outcome scores (OHS, SF12 MCS, SF12 PCS and SAPS) were not normally distributed and therefore were compared by means of a Kruskal-Wallis one-way analysis of variance by ranks with a Dunn's multiple comparison post-test. In order to ensure sufficient power a priori power calculation was performed on the basis of pilot data using an alpha value of 0.05 and a power of 0.8. This indicated 196 patients would be required for a calculated effect size of 0.239.

Results

Significantly lower survivorship for revision and reoperation was observed in the ASR group compared to all other groups (see figure 1). There was a non-significant trend towards increased survivorship in the CoC group compared to the BHR and MoM group. The BHR demonstrated better outcome scores than the ASR (OHS and SAPS) (see figures 2 and 3) and the MoM (OHS and SF12 PCS). The CoC demonstrated better outcome scores than the ASR (OHS and SAPS). The MoM demonstrated a better SAPS than the ASR.

Log-rank comparison of the survival curves revealed a significantly lower survival with revision as the end point in the ASR compared to the MoM (p=0.021), CoC (p=0.047) and BHR (p=0.015). When reoperation for any reason was considered the same pattern was observed (MoM, p=0.005; CoC, p=0.0006, BHR, p=0.0007) (MoM 88.2% at 74 months [+6.5%/-13.3%], CoC 97.1% at 98 months [+1.9%/-5.8%], ASR 71.0% at 91 months [+9.1%/-12.1%], BHR 85.2% at 95 months [+9.1%/-20.8%]).

Conclusions

In the short to medium term, survivorship for the best performing RA (BHR) and THR (CoC) were comparable as were the outcome scores. There was a non-significant trend towards poorer outcome scores in the MoM THR group which may be due to confounding factors such as age and preoperative function or may represent the beginning of a decline in function due to wear debris related phenomenon.

References

1. Smith AJ, Dieppe P, Vernon K, Porter M, Blom AW, on behalf of the National Joint Registry of England and Wales. Failure rates of stemmed metal-on-metal hip replacements: analysis of data from the National Joint Registry of England and Wales. Lancet. 2012 Mar. 12.i

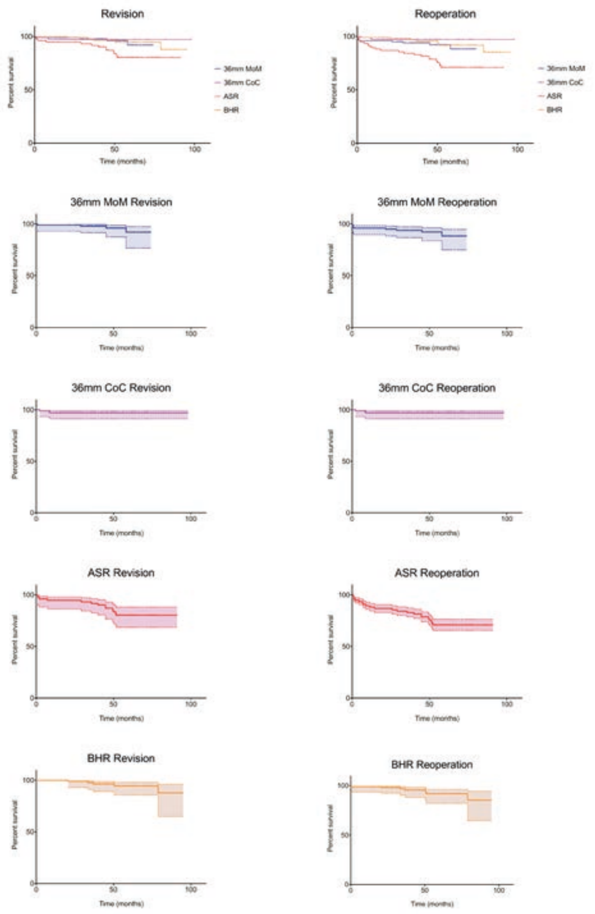

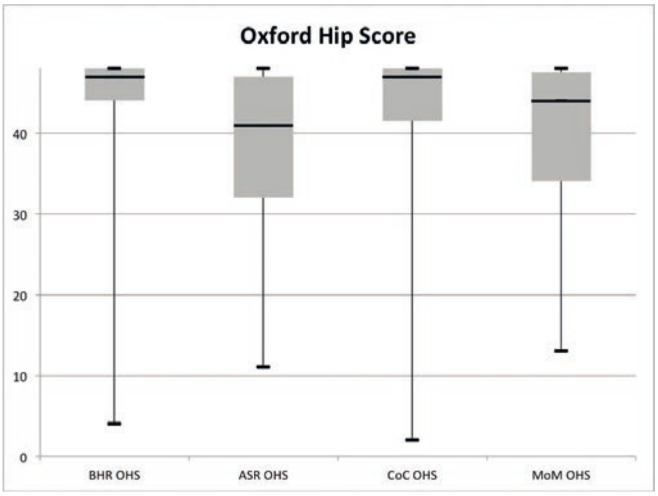

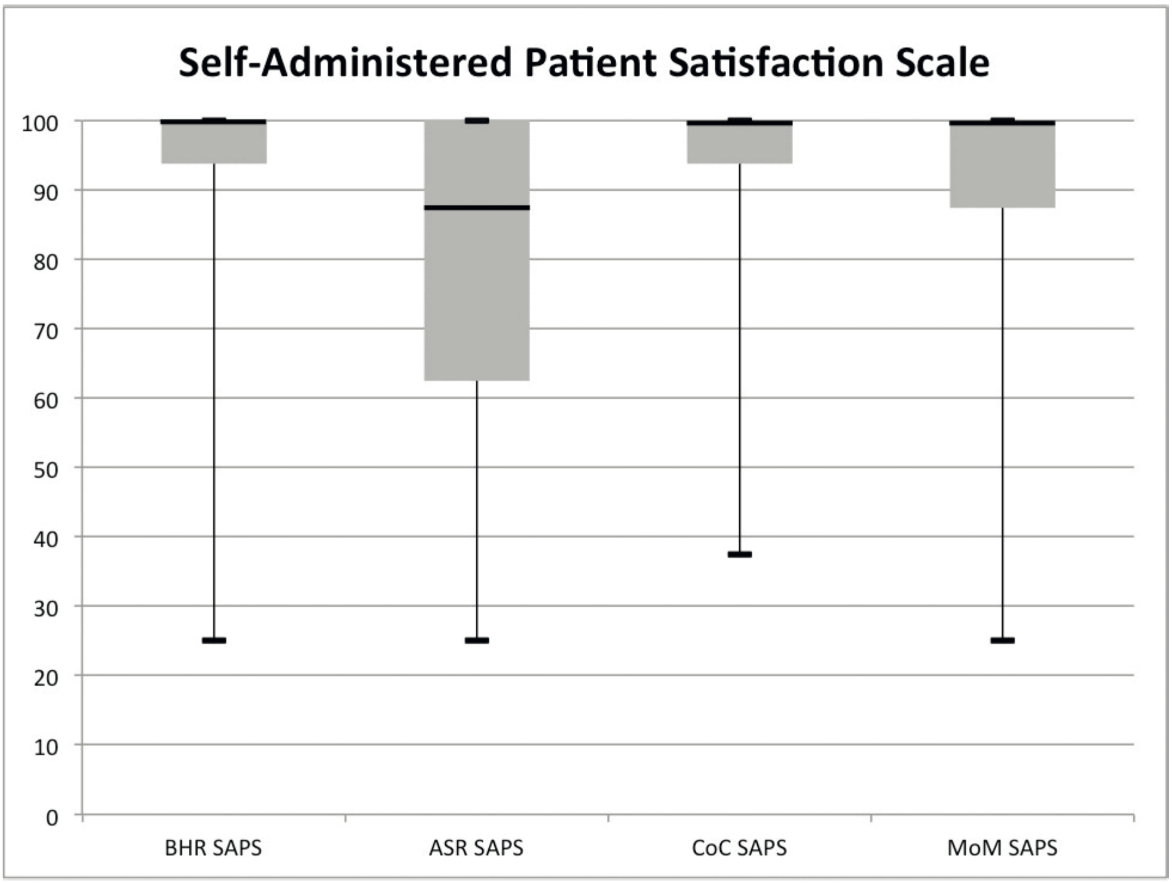

-Figure 1. Kaplan Meier survivorship curves
-Figure 2. Oxford hip score
-Figure 3. Self-administered pataient satisfaction scale

7A.5
Effect of PCL Over-tightness in Cruciate Retaining Total Knee Arthroplasty

Bo Gao
Exactech, Gainesville, USA

Over-tightness of posterior cruciate ligament (PCL) in cruciate retaining total knee arthroplasty produces significantly increased contact stress in polyethylene tibial insert. This supported that PCL over-tightening could be the cause of excessive wear and early failure seen in some cases.

Introduction

Properly balanced posterior cruciate ligament (PCL) is critical for satisfactory clinical outcome in cruciate retaining (CR) total knee arthroplasty (TKA). However, this is often considered challenging. PCL is a rather stiff anatomical structure and any subtle misbalance of the flexion gap could cause the PCL to be either loose or too tight. A loose PCL won't accomplish the designed function of the CR TKA due to lack of femoral rollback, while an over-tightened PCL may generate excessive load on the tibial insert. It has been clinically observed that some CR patients develop excessive wear and early failure on the polyethylene tibial insert [1, 2]. Over-tightening of the PCL is often suspected to be the cause, but there has been little quantitative research on this subject. The objective of this study was to evaluate the effect of PCL over-tightness on contact stress of polyethylene tibial insert in CR TKA.

Methods

Finite element analysis (FEA) was performed to evaluate contact stresses on a CR tibial insert under various PCL tightening conditions. CAD models of a CR prosthesis (Optetrak Logic CR, size 3, Exactech) including a femoral component, a 9 mm tibial insert and a tibial baseplate were used in the study. Polyethylene wear is usually generated by repeated loading during daily activities, and the PCL is tensioned when the knee is in flexion. The knee could flex over 60° during walking. Being relevant, 60° flexion was used in the analysis. Surface-surface contact was established in the FEA model between the femoral component and the tibial insert, and between the tibial insert and the baseplate. The compressive load at maximum flexion during walking is about 40% of a patient's body weight (BW) and shearing loads are minimal [3]. Considering the patient's BW is 90 kg, a 353 N compressive force was applied when no PCL over-tensioning was assumed. To model the additional compressive force caused by an over-tightened PCL, a 204 N/mm stiffness and a 50° elevation angle of the ligament were used [4,5]. Von Mises stress on the tibial insert under PCL over-tightness from 0 to 5 mm was analyzed.

Results

Without PCL over-tightening, the peak stress on the polyethylene tibial insert was about 14.1 MPa. When the PCL was over-tightened by 1, 2, 3, 4, and 5 mm, the peak stress in the insert increased to 16.8 MPa, 19.1 MPa, 21.0 MPa, 22.8 MPa, and 24.5 MPa, respectively. The stress value exceeded yield strength of polyethylene (about 21 MPa) when the over-tightness was above 3 mm. (Figure 1).

Discussion/Conclusion

This study demonstrated that moderate PCL unbalance (tightness) could increase the polyethylene stress significantly in CR TKA. When higher stress is coupled with repeated loading during daily activities, excessive wear and even catastrophic failure could occur on the tibial insert. The finding supported the clinical observations [1, 2]. To avoid excessive wear and early failure, over-tightening PCL should be prevented in CR TKA. In addition to proper surgical techniques, improved prosthesis and instrumentation designs could be beneficial to address this challenge.

References

[1] Swany et al., J Arthroplasty, 1993.
[2] Kim et al., JBJS Br. 2010.
[3] Kutzner et al., J Biomech, 2010.
[4] Prietto et al., Trans Orthop Res Soc. 1988.
[5] DeFrate et al., Am J Sports Med, 2004

7A.6

A short-form of the new KSS is a valid and practical clinical outcome tool for the younger and more demanding patient

R. Dinjens
Ahorse, Atrium MC Heerlen, Heerlen, The Netherlands

Effectively shortening and simplifying the New-KSS outcome score dramatically improves completion rate while retaining clinimetric quality.

Introduction:
The New-KSS, which is based on the popular KSS and recently promoted by the Knee Society, has been developed to better capture the outcome of the younger and more demanding TKA patients [1]. The New-KSS consists of 34 questions, categorized into a satisfaction, expectation, function (patient-reported outcome measures= PROMs) and objective (clinician-administered) subscale. A recent study showed the internal consistency, construct validity and responsiveness of the New-KSS. However further optimisations were recommended to improve the unsatisfactory completion rate (33%) [2]. Based on these findings, a shortened version (New-KSS-SF) was developed and evaluated in a group of 494 Dutch patients.
Methods:
Redundant questions (Crohnbachs alpha ≥0.95) and questions that frequently remained unanswered (e.g. advanced activities) in the New-KSS were removed and several discretional activities (e.g. aerobics) were grouped together as ‘hobbies’. A ‘not applicable option’, was added and associated with the worst score (based on unpublished pilot study). A subscale ‘symptoms’ was separated from the objective-subscale as this contains patient information about pain, complaints. Moreover a simplified design was chosen. Thus, the New-KSS-SF, consists of 5 clinician-administered questions (objective subscale, not further evaluated) and 20 patient-reported questions (5min to complete) which are categorized into symptoms, satisfaction, expectations and functions (sub-divided into standing & walking, standard & advanced activities).
A total of 494 post-operative (6 weeks to >5 years) TKA patients received the New-KSS by mail including an explanatory letter and stamped returning envelop. Scores were collected 6 weeks after they were send. A subgroup of 266 post-operative patients also completed the KOOS-PS. In 33 patients (6-12 weeks follow-up), PROMs were also collected preoperatively. The response rate, completion rate, internal consistency (Cronbach’s alpha), construct validity (Pearson’s correlation with KOOS-PS) and floor/ceiling effects (>15% score the lowest or highest possible score) were evaluated. Pre- and postoperative scores were compared using paired-sample t-test.
Results:
Seventy percent of the patients returned the questionnaire by mail, of which 90% was completely filled in. This resulted in 288 complete scores available for analysis (patient age 70±10yrs, 162F/126M). Cronbach’s Alpha ranged from 0.79-0.92 showing sufficient homogeneity but no redundancy (Alpha ≥0.95) between the items of a subscale. Strong correlations (r-range 0.61-0.87) were found between the KOOS-PS and the new-KSS-SF function-subscales (Table 1). Postoperatively, all subscales were significantly improved with regards to preoperative (range 14-33%, Fig 1.). Ceiling effects were found in subscales symptoms (16%) and walking & standing (26%) in the postoperative group. No floor/ ceiling effects were found in the preoperative group.
Discussion/Conclusion:
Completion rate of the New-KSS-SF was excellent at 90% compared to unacceptably low 33% with the original full-length New-KSS [2]. The short-form had comparable internal consistency, construct validity and responsiveness to the full-length New-KSS. This shows that the New-KSS was effectively shortened and simplified to near perfect completion rate while maintaining clinimetric value. The New-KSS-SF is a valid and practical outcome tool for the younger and more demanding TKA patient.

Reference:
Noble et al. Clin Orthop Relat Res 2012
Senden et al. NOF 2012.

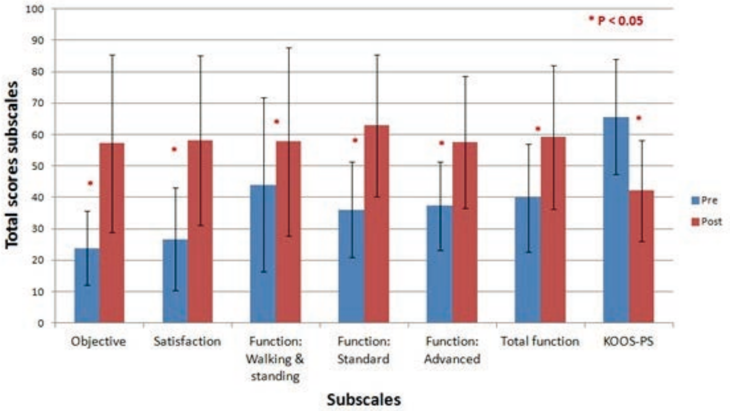

Fig. 1. Responsiveness of the new-KSS-SF and KOOS-PS.

-Responsiveness of the New-KSS-SF

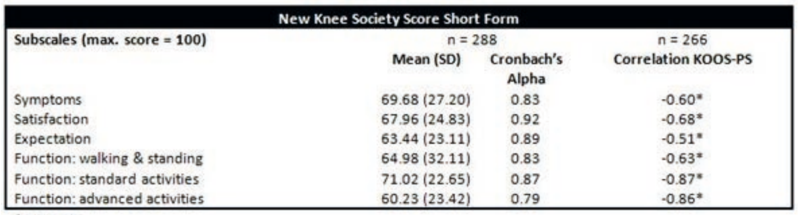

New Knee Society Score Short Form			
Subscales (max. score = 100)	n = 288		n = 266
	Mean (SD)	**Cronbach's Alpha**	**Correlation KOOS-PS**
Symptoms	69.68 (27.20)	0.83	-0.60*
Satisfaction	67.96 (24.83)	0.92	-0.68*
Expectation	63.44 (23.11)	0.89	-0.51*
Function: walking & standing	64.98 (32.11)	0.83	-0.63*
Function: standard activities	71.02 (22.65)	0.87	-0.87*
Function: advanced activities	60.23 (23.42)	0.79	-0.86*

* p < 0.05

-Averages, crohnbachs alfa (intern consistency) and pearson

7A.7

Total hip replacement can be predicted by shape variations of the hip: A nationwide prospective cohort study

Rintje Agricola
Erasmus Medical Centre, Rotterdam, The Netherlands

The shape of the hip as quantified by statistical shape modeling has a good predictive value for the development of end-stage osteoarthritis. Minor shape variations may be used as a biomarker to predict the future risk for total hip replacement.

Introduction:
Osteoarthritis (OA) of the hip can be defined by both radiographic and clinical criteria. Previously, it has been shown that radiographic criteria associate to the shape of the hip. However, it is unknown whether shape variations of the hip also associate with hip OA defined by clinical criteria. We aimed to determine the contribution of hip shape in the prediction of both total hip replacement (THR) and general clinical OA (ACR criteria) in a prospective cohort.
Methods:
Individuals were extracted from the CHECK (cohort hip and cohort knee) study. CHECK is aprospective cohort study of individuals with assumed early symptomatic OA of knee or hip. Anteroposterior pelvic radiographs of sufficient quality were obtained in 723 subjects at baseline and in 770 subjects at 5 years follow-up. The shape of the proximal femur and acetabulum on the AP radiographs was assessed using statistical shape modelling (SSM). The shape was defined by a set of landmark points that are positioned along the contour of the bone in the image (Figure 1). An SSM describes all variation in shape of the complete cohort by several independent shape aspects. Outcome measures were hips that had received THR within 5 years and hips fulfilling the ACR criteria after 5 years based on history, physical examination, and laboratory findings. The association between each mode and both outcome measures was calculated by Generalized Estimating Equations (GEE), corrected for sex and age. The predictive value of the GEE model including all univariate significant modes was then tested by the area under the ROC curve (AUC).
Results:
For this study, 575 females and 148 males (mean age 55.9) were included. At baseline, 76% of the hips had no signs of OA (K&L=0) whereas 24% had doubtful OA (K&L=1). When corrected for age and sex, nine modes at baseline associated significantly with THR within 5 years (table 1). For example, mode 4 and 12, which resulted in the largest odds ratio, illustrates superior joint space narrowing and a nonspehrical femoral head, respectively. When combining these modes, only the four modes which associated most with THR (mode 4, 7, 12, 15) were selected for calculating the AUC, to prevent overfitting of the model. The predictive value of those four modes in the GEE model resulted in an AUC of 0.81. At baseline, no modes associated significantly with the presence of clinical OA at 5 years.
Discussion:
These results show that the shape of the hip as quantified by an SSM is able to predict the risk of THR, whereas variation in shape can not predict the development of clinical OA. The latter might be a result of the poor reliability of the ACR criteria. We observed that 87% of the individuals who had clinical OA at baseline, did not have clinical OA anymore after 5 years. In conclusion, minor shape variations at baseline have a good predictive value for the development of end-stage OA and may be used as a biomarker to predict the future risk for THR.

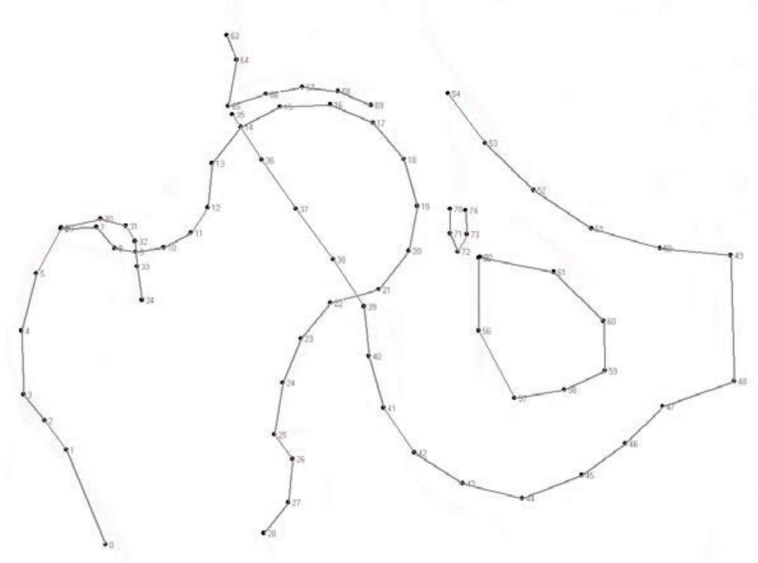

-Figure 1. The statistical shape model which consisted of 74 points.

Shape variation	OR	95% CI	p-value
2	1.74	1.21 - 2.51	0.003
4	1.97	1.27 - 3.07	0.003
7	0.53	0.38 – 0.76	<0.001
11	1.76	1.28 - 2.42	0.001
12	1.97	1.38 - 2.82	<0.001
13	0.56	0.39 - 0.81	0.002
15	1.86	1.38 - 2.51	<0.001
16	0.61	0.42 - 0.88	0.008
22	0.55	0.40 - 0.76	<0.001

-Table 1. Modes which significantly associated with THR are shown.

7A.8

TOWARDS AN INSTRUMENT FOR THE INTRAOPERATIVE ASSESSMENT OF THE INITIAL STABILITY OF ACETABULAR IMPLANTS

Steven Leuridan
Department of Mechanical Engineering, Division of Biomechanics, Katholieke Universiteit Leuven, Leuven, Belgium

This papers reports on the numerical and experimental development of an intraoperative instrument to monitor the acetabular component insertion and to assess the initial stability of the implant based on vibration techniques.

Introduction

Total hip arthroplasty (THA) typically comprises both a femoral and an acetabular implant. Acetabular implant failure is an important cause for the failure of a THA and is deemed more critical to a good long-term surgical outcome than the failure of the femoral component [Havelin, 2000]. One of the main reasons for premature failure of cementless acetabular implants is a lack of initial stability of the implant achieved during surgery [Ramamurti, 1997]. Monitoring the insertion and obtaining the optimal initial stability is a challenging task for the surgeon, hereby relying solely on his tactile and auditory senses. Inspired by the success of vibration techniques in dentistry to determine initial stability (e.g. Ostell), [Pastrav,2009] demonstrated unique aptness of vibrational techniques to provide the surgeon with additional information during the insertion process of the femoral stem. These techniques are explored numerically and experimentally to asses there validity and potential as an intraoperative method to monitor the acetabular component inertion and asses the initial stability of the implant.

Methods

A numerical and experimental test setup was developed (figure 1) to simulate the acetabular insertion process. Both setups consist of an inserter attached to the acetabular implant, a Sawbones block (40 pcf) prepared with a spherical cavity mimicking the acetabular cavity and a mass. The implant is inserted both numerically as well as experimentally in 4 equal length steps, where step 4 is the insertion endpoint (optimal fixation). A vibration analysis was performed using accelerometers mounted on the inserter at every insertion step from which modal parameters were extracted (resonance frequencies, mode shapes,...).

Results

Features such as mode shape displacement and curvature differences, resonance frequency differences and modal damping changes are found to be sensitive to the changing conditions around the implant during implant insertion. Good correlation was found between numerical simula-tion and the experiments. Table 1 lists two features (frequency and standard deviation) that prove sensitive to detect the insertion endpoint (step 4).

Discussion

Several sensitive vibration features are defined that allow to track the insertion and stability of the implant. As measurements are taken only on the inserter, which is removed after surgery, an intraoperative implementation of these techniques is very feasible.

References

Havelin et al, 67th Annual Meeting AAOS, 2000.
Pastrav et al., JOSR, 4:10, 2009.
Ramamurti et al., J Biomed Mater Res, 36(2): 274-280, 1997

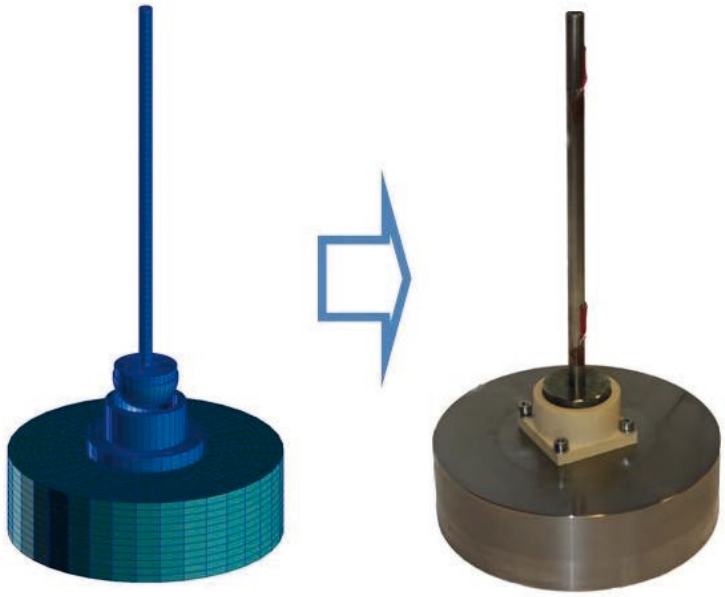

-Figure 1: Numerical and experimental test setup

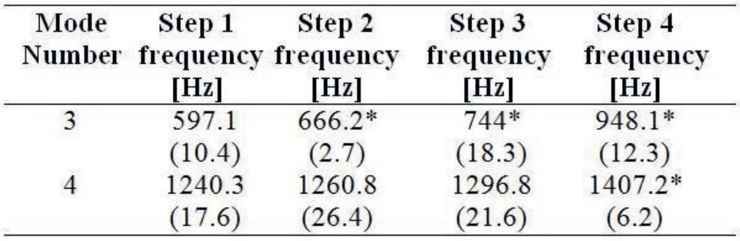

Mode Number	Step 1 frequency [Hz]	Step 2 frequency [Hz]	Step 3 frequency [Hz]	Step 4 frequency [Hz]
3	597.1	666.2*	744*	948.1*
	(10.4)	(2.7)	(18.3)	(12.3)
4	1240.3	1260.8	1296.8	1407.2*
	(17.6)	(26.4)	(21.6)	(6.2)

-Table 1: Two possible frequency based features that allow for monitoring and differentiating between the different insertion stages in the experimental model. * indicates a significant difference from the previous step at the 5% level.

7A.9

Age Related Changes in Lower Limb Segment Movement during Gait in a Healthy Population Measured by Inertial Measurement Units

Ian McCarthy
UCL Institute of Orthopaedics and Musculoskeletal Science, London; UK

In a healthy active population, little change was observed in movement of lower limb segments during walking until after the age of 80. A normal range has been defined that can be used to assess age-related changes in mobility.

Introduction:
Walking ability is a key aspect of maintaining independence during ageing; impairment of gait has also been shown to be associated with falls in the elderly. The use of inertial measurement units (IMUs) allows measurement of some parameters of gait outside a laboratory setting, which can be advantageous for population-based studies. In this study, we have investigated how the kinematics of limb segment movement changes in healthy ageing using inertial measurement units, which allows measurements to be performed in a variety of environments.
Patients and Methods:
Subjects were recruited who were in general good health and active for their age. Participants were excluded if they had had previous surgery on their lower limbs, had a neuromuscular condition that might affect gait (e.g. stroke, Parkinson's disease), had current back pain, were not able to walk 10 metres without a walking aid, or if they could not give informed consent. The study used four IMUs, with one sensor strapped to each shank and thigh. Participants were then asked to walk for 10 metres at their normal pace. The ranges of motion (ROM) were calculated for thigh and shank; knee ROM was calculated for both swing and stance phase; stride duration was also calculated. Ethical approval for the study was given by UCL Research Ethics Committee, and all participants gave informed consent.
Results:
128 participants were recruited with an age range from 18 to 97. Results for knee, thigh and shank ROM showed little change until after the age of 80. Knee ROM during swing was 67.8° + 3.9° in the < 30 years age group and 53.3° + 6.5° in the > 80 years group, and knee ROM during stance was 20.8° + 3.1° and 12.3° + 6.0° respectively in the two groups. Overall, the relationship between angle and age was best fitted with a cubic relationship (see Figure 1). Stride duration showed a slight linear increase with age, increasing by about 0.1% a year. Although walking ability declined on average after the age of 80, several subjects in this age group were still within the normal range for younger subjects.
Discussion:
The IMUs were able to provide data on limb segment kinematics in a community setting. In this study of an active population, there was little change in limb segment range of motion until about the age of 80. It is known that peak muscle power declines with age. We propose that after the age of 80, peak muscle power has decreased below a threshold, at which point it has an effect on normal gait and mobility. The decrease in peak muscle power may impact at a lower age in other activities of daily living, such as stair climbing or sitting-to-standing, which require greater muscle power, but a similar approach could be used to investigate age-related performance in these activities.

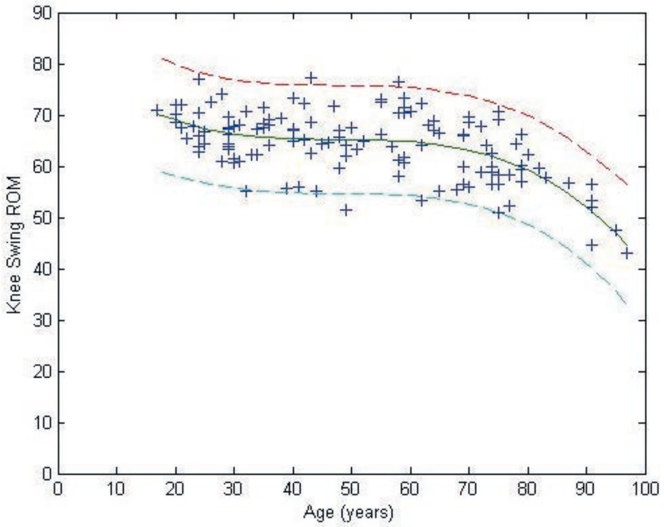

-Figure 1. Age-related changes in knee swing ROM showing the calculated cubic regression with 95% confidence limits.

7B.2

Intra articular infusion of autologous expanded bone marrow mesenchymal cells (MSCs) in knee osteoarthritis (OA)

Francesc Soler
ITRT, Barcelona, Spain

The articular infusion of autologous expanded bone marrow MSC in knee OA showed an optimal improvement in pain and function after 1 year follow up as well as significant changes in MRI (Cartigram¨ software)

Introduction:

The treatment of knee OA is well known: From NAIDs to arthroplasty. At the moment, there is no other option to improve pain and function significantly. Many treatments have been proposed in focal cartilage injuries, but not to restore normal cartilage in advanced OA. Several studies have reported excellent results with intra-articular infusion of bone marrow expanded MSC in animal models, but very few in human applications. Our research group leads different studies in this direction.

Patients And Methods:

We conducted a study under clinical trial format, approved by the Ethics Committee of Centro Medico Teknon (Barcelona) and the Spanish Medicines Agency (AEMPS), registered in ClinicalTrials.gov. We treated 12 patients affected of knee OA grade II -IV (Kellgren-Lawrence Classification) by means of a single infusion of 40 x 10^6autologous bone marrow expanded MSC.

The MSC are harvested by aspiration from the posterior iliac crest under local anesthesia + sedation. The sample is sent to the cell therapy laboratory were, following GLPs, MSC are isolated by direct plating subjecting the whole marrow sample to fractionation on a density gradient solution. MSC cultures are maintained and expanded for three weeks, during which time the nonadherent haematopoietic cell fraction is depleted and the MSC population is adherent to the plastic substrata. The dose obtained, 40 x 10^6 MSC, is infused into the knee joint in a single application.

Results:

We found significant improvement in pain and function scores (VAS, Lequesne, WOMAC and SF-36) comparing pre-infusion and 3 - 6 - 12 months post-infusion. We performed a quantitative MRI (Cartigram® software) before the application and 1 year post-infusion, showing important differences. There were no adverse effects or complications.

Discussion/Conclusion:

We present an innovative treatment based in cellular therapy (expanded autologous MSC) in order to achieve important improvement in pain and function in patients with advanced knee OA, implying minimal aggression and risk.

7B.3
Regulation of players involved in the osteogenic differentiation of mesenchymal stem cells

Serena Rubina Baglio
Instituto Ortopedico Rizzoli, Bologna, Italy

The mRNA and microRNA expression profiling of bone marrow mesenchymal stem cells during osteogenic differentiation represents a useful tool to understand the molecular events underlying osteogenesis and to monitor the osteogenic process in physiological and pathological conditions.

Introduction:
Bone marrow is the most common source of adult mesenchymal stem cells (MSCs), defined for their ability to differentiate into multiple cell types including osteoblasts, chondrocytes and adipocytes. MSCs are currently a focus of great interest because of their ability to function in tissue repair and regeneration, and have been evaluated for the restoration of function in damaged skeletal tissue both in cell therapy and tissue engineering approaches. The aim of this study was to define gene expression patterns underlying the differentiation of MSCs into mature osteoblasts during in vitro expansion.
Patients & Methods:
We performed a microarray analysis on the whole transcriptome of bone marrow-derived MSCs obtained from the femoral canal of patients undergoing hip replacement. By defining different time-points within the differentiation and mineralization processes of MSCs, temporal gene expression changes were visualised. Bone marrow adherent mononuclear cells were used as reference and, in addition, only the cultures able to form mineral nodules at the final time-point were considered for the gene expression analysis. To obtain the genes of our interest, we only focused on genes i) whose expression was significantly upregulated; ii) which are involved in pathways or biological processes relevant to bone cell biology; iii) which changed considerably during the different steps of differentiation and mineralization. Subsequently we set out to investigate the involvement of microRNAs (miRNAs) in the differentiation of MSC into osteoblasts and, in particular, in the regulation of the bone-specific transcription factor Osterix. We analysed the miRNA expression profile of MSCs during osteogenic differentiation by miRNA microarray analysis. Then, we verified that one of the modulated miRNAs, miR-31, is able to control Osterix expression and we evaluated the effect of this regulation on Osterix downstream targets.
Results:
We obtained 213 differentially upregulated genes, some belonging to well-known pathways and some having Gene Ontology annotations related to bone cell biology, including angiogenesis, bone-related genes, cell communication, development and morphogenesis, transforming growth factor-beta signaling, and Wnt signaling. Interestingly, twenty-nine genes, whose role in bone cell pathophysiology has not been described yet, have been highlighted. In addition, we found 28 miRNAs significantly modulated during osteogenic differentiation and we demonstrated that miR-31 controls Osterix expression through association of the microRNA to the 3'untranslated region of this transcription factor. By analyzing miR-31 and target gene expression levels we found an inverse trend during osteogenic differentiation both in mesenchymal stem cells and in osteoblast-like cell lines. Finally, the inhibition of microRNA activity led to an increase in the endogenous expression of Osterix and downstream targets, including Collagen type 1 and Osteocalcin.
Discussion/Conclusion:
We defined mRNA and miRNA expression patterns characterizing the osteogenic differentiation of bone marrow-derived MSCs. These signatures represent a useful tool to monitor the osteogenic process, and to analyze a broad spectrum of functions of MSCs in pathological conditions or when cultured on scaffolds to promote bone regeneration. Moreover, we provide evidence for the involvement of miR-31 in the regulation of the bone-specific transcription factor Osterix and suggest a role for this microRNA in osteogenic differentiation.
(Poster presentation)

7B.4

To die or not to die: glucose as a determinant of the survival of human mesenchymal stem cells upon implantation

Mickael Deschepper
B2OA, Paris, France

In this study, we challenged the current paradigm of human Mesenchymal Stem Cells survival, which assigned a pivotal role to oxygen, by testing the hypothesis that exogenous glucose may be key to their survival.

Introduction

The survival of human mesenchymal stem cells (hMSCs) has elicited a great deal of interest, because it is relevant to the efficacy of engineered tissues. However, to date, hMSCs have not met this promise, in part due to the high death rate of cells upon transplantation. In this study, we challenged the current paradigm of hMSC survival, which assigned a pivotal role to oxygen, by testing the hypothesis that exogenous glucose may be key to hMSC survival.

Materials and methods

In vitro model of ischemia

‘2.10^4 hMSCs from five donors, were seeded into individual wells of a 24-well plate, cultured overnight, washed twice with PBS and then maintained in hypoxia (0.1% oxygen) under serum (FBS) free αMEM medium in either the absence or in the presence (1 or 5 g/L) of glucose for 21 days. (fig 1)

In vitroCell viability:

To assess the role of glucose on hMSCs viability, cells were cultured under hypoxia in the absence or in the presence of glucose (1 and 5g/L), At days 0, 3,7,14 and 21, cell viability was evaluated by flow cytometry and ATP content per cell quantified.

In vivo effect of glucose supply on hMSCs viability

‘3.10^5 eGFG-luc hMSCs were seeded on a cylindrical AN-69 scaffolds. At the time of implantation, 100 µl of hyaluronic acide (HA) (2%) containing either 0g/L (negative control) or 10g/L of glucose was gently injected inside the construct. Cell- constructs were implanted subcutaneously in eight week-old mice (2 per animal) and were imaged by bioluminescence imaging (BLI) at day 1, 4, 7 and 14 until sacrifice.

Results

hMSCs were able to survive and to maintain their ATP content 21 days under sustained hypoxia providing that they were cultured in the presence of a sufficient glucose supply (i.e. 5g/L). In contrast, hMSCs cultured without or with 1g/L of glucose failed to survive (figure 2). These results established that glucose depletion but not sustained hypoxia affected cell survival (fig 2).

In vivo results showed a striking increase of cell viability in cell constructs loaded with glucose. At day 14, a five-fold increase in cell number was observed in cell constructs loaded with glucose when compared to the control cell constructs without glucose. (fig 3)

Discussion

The present study challenge the current paradigm that gives a pivotal role to oxygen on hMSCs massive cell death. By using an in vitro model of hypoxia/ischemia, we demonstrated that in the presence of sufficient glucose, hMSCs were able to survive 21 days under sustained hypoxia.

Most importantly, an appropriate glucose supply strongly increases cell viability of hMSCs implanted subcutaneously in a mice model. This study provides evidences that glucose depletion but not hypoxia affects hMSCs viability. Further investigations need to be performed to develop hydrogels that ensure continuous glucose delivery to the implanted cells. Theses findings are particularly relevant because they pave the way to the development of new delivery systems to ensure hMSCs viability in order to increase their therapeutical potential after implantation.

7B.5
Regenerative potential of human muscle stem cells in chronic inflammation

Bouke Duijnisveld
Leiden University Medical Center, Department of Orthopaedics, The Netherlands.

Chronic inflammation could affect cellular microenvironment and change survival, repair and maintenance of muscle stem cells. Proliferation, differentiation, protein expression and telomere length showed that chronic inflammation does not affect the in vitro regenerative potential of human muscle stem cells.

Introduction: Chronic inflammation is a profound systemic modification of the cellular microenvironment which could affect survival, repair and maintenance of muscle stem cells. The aim of this study is to define the role of chronic inflammation on the regenerative potential of satellite cells in human muscle.
Patients and Methods:
As a model for chronic inflammation, 11 patients suffering from rheumatoid arthritis (RA) were included together with 16 patients with osteoarthritis (OA) as controls. The mean age of both groups was 64 years, with more females in the RA group compared to the OA group. During elective knee replacement surgery, a muscle biopsy was taken from the distal musculus vastus medialis.
Cell populations from 4 RA and 8 OA patients were used for extensive phenotyping because these cell populations showed no spontaneous differentiation and myogenic purity greater than 75% after explantation.
Results:
After mononuclear cell explantation,
myogenic purity, viability, proliferation index, number of colonies, myogenic colonies, growth speed and fusion index were not different between RA and OA patients.
The growth curve showed no differences in the maximum number of population doublings (figure 1). The expression of proteins involved in replicative and stress induced premature senescence and apoptosis was measured by western blot and showed no difference between RA and OA patients including p16, p21, p53, hTERT and cleaved caspase-3 (figure 2). Mean telomere length was measured by flow cytometry comparing sample cells to control cells in G0/1 phase which showed shorter telomeres in the RA group compared to the OA group (figure 3).
Discussion/Conclusion. In the present study we found evidence that chronic inflammation in RA does not affect the in vitro regenerative potential of human satellite cells. Identification of mechanisms influencing muscle regeneration by modulation of its microenvironment may therefore be more appropriate.

Figure 1: Growth curve of human satellite cells

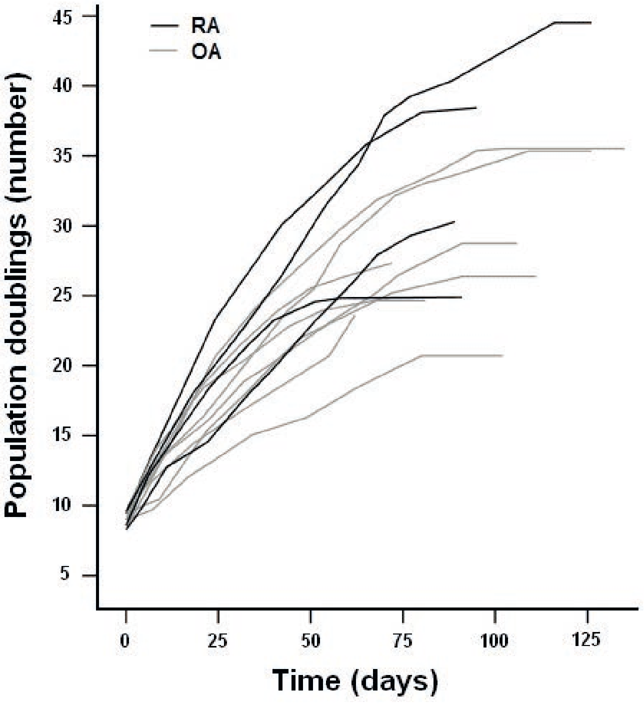

-Figure 1: Growth curve of human satellite cells

Figure 2: Western blot image (A) and normalized protein expression (B) of human satellite cells

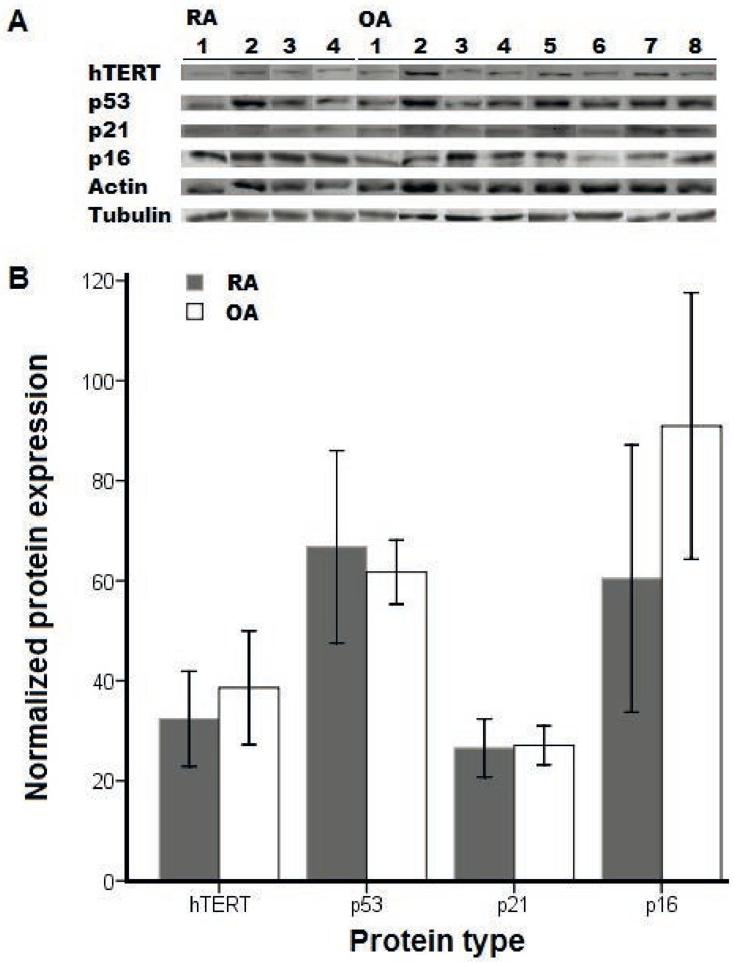

-Figure 2: Western blot image (A) and normalized protein expression (B) of human satellite cells

Figure 3: Telomere length of human satellite cells measured by flow cytometry using fluorescence in situ hybridization without (A) or with the fluorescein-conjugated telomere probe (B)

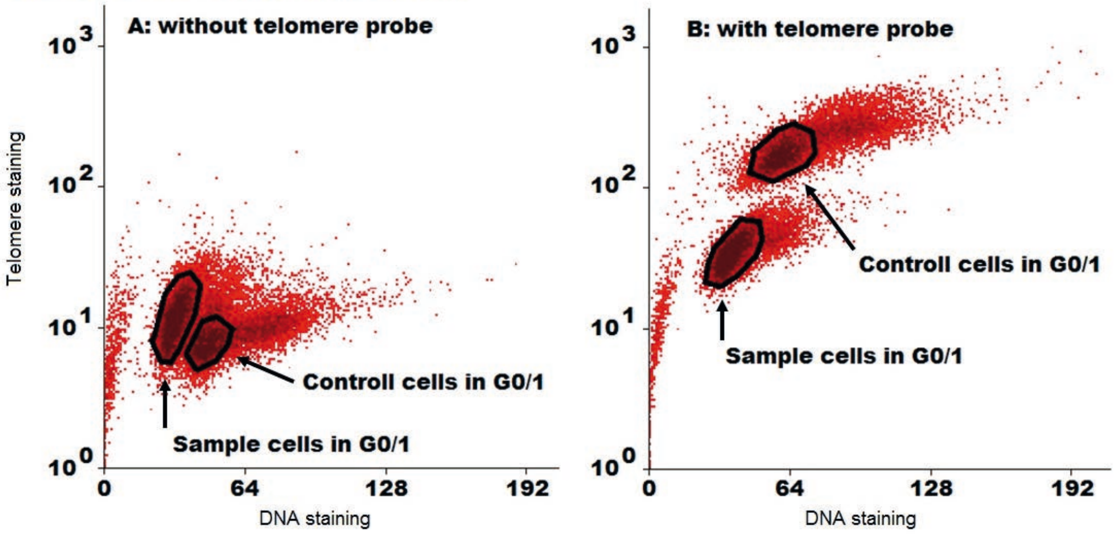

-Figure 3: Telomere length of human satellite cells measured by flow cytometry using fluorescence in situ hybridization without (A) or with the fluorescein-conjugated telomere probe (B)

7B.8

Adipose stem cells for the treatment of bone lesions in an animal model

Alonso Moreno
Hospital Universitario La Paz, Madrid, Spain

The histological results of our animal model suggest that the use of adipose stem cells improves the repairing process of bone lesions.

Introduction:
Recent progress in adult stem cell research opens new possibilities in bone and joint surgery. Stem cells have therapeutic potential in the realm of orthopaedic surgery because of their capacity to self-renew and differentiate into various types of mature cells and tissues, including bone. We have developed an animal model to essay the possible effect of adipose stem cells (ASC) in the healing of a bone defect.
Methods:
Human ASC (Inbiobank) were cultured in DMEM, 1g/l glucose, 10% fetal bovine serum and antibiotics, with subcultures once a week taking care not to reach more than 30 cumulative population doublings since initial thawing. Granules of TCP/HA (tricalcic phosphate / hydorxiapatite: triosite®, Zimmer) were incubated 3h at37°C under light shaking with hASC, 5x10^4/mg, before administering to rabbits. One cortical of the proximal diaphysis of both humeri was perforated with a 3mm drillbit, filling the lesion with 50mg of TCP/HA granules containing or not hASC. Four weeks later, animals were sacrificed, humeri were removed and fixed in 4% paraformaldehyde, decalcified, embedded in paraffin, and 5µm sections stained with H&E and Masson trichrome. Pictures of 3-6 different fields were analyzed with ImageJ software, calculating the ratio of the surface (in pixels) of osteoid vs. remaining TCP/HA matrix. For the in vitro experiments, ultra low attachment plates (Corning) were used to differentiate hASC adhered to TCP/HA granules to an osteogenic phenotype by incubation with osteogenic differentiating medium (StemPro, Invitrogen) for 4 weeks. At different time points, 0.1% triton X-100 extracts were obtained to determine total protein content (Bradford Assay), alkaline phosphatase activity (p-N-phenyl-phosphate hydrolysis in 1M DEA buffer, pH 9.8), and osteocalcin (ELISA, Invitrogen).
Statistical analysis was performed with appropriate tests, considering $p<0.05$ as significant value.
Results:
hASC adhered stably to TCP/HA granules within 3h at37°C. During the 4 week treatment with osteogenic differentiating medium, hASC presented a maximal AP activity at 2 weeks, declining afterwards, and BGP production rising progressively until maximal levels at 4 weeks, similarly to cells cultured directly on plastic.
In vivo, bones treated with TCP/HA containing hASC showed a statistical significant higher ratio of osteoid vs. TCP/HA matrix than bones treated with TCP/HA alone (1.06±0.21 vs. 0.76±0.22, mean±SEM, $p=0.0139$).
Conclusions:
TCP/HA is an adequate vehicle for the implantation of hASC.
In our animal model of bone lesion repair, the use of TCP/HA + hASC may improve the bone repair process due to a greater production of osteoid tissue.

7B.9

Stem cells transplantation and core decompression therapies for osteonecrosis of the femoral head (ONFH)

Sun Mengyao
CJUH, Changchun, China

The article summarized our retrospective study of early stage avascular necrosis of the femoral head (stage I and II) treated with stem cells transplantation and core decompression.

Introduction

Osteonecrosis of the femoral head (ONFH) is a debilitating disease that ultimately leads to hip joint destruction. Various efforts have been made in an attempt to enhance the healing of osseous defects in the femoral head before collapse occurs. Total hip arthroplasty or hip resurfacing is indicated for patients with late-stage disease. However, alternative treatment options, including core decompression, osteotomy, and bone grafting, may improve long-term outcomes in those with less advanced disease. Stem cell transplantation is another alternative therapy for early stage ONFH. In current study, we treated early stage ONFH with stem cell transplantation and core decompression.

Subjects and methods

From March 2006 to February 2010, 23 patients (18 male, 5 female, 36 symptomatic hips) were diagnosed as osteonecrosis of the femoral head (ONFH) with MRI. The number of hips affected by osteonecrosis in current series of 36 hips was 5 in patients taking corticosteroids, 5 in patients with excessive alcohol intake, 5 in patients with hip trauma, and 21 in patients with idiopathic osteonecrosis. The mean age of the patients was 38 (range: 15-59). Hips were graded for severity according to ARCO's system. 12 hips in 8 patients were stage I, and 24 hips in 15 patients were stage II. The patients were undergone with stem cells transplantation and core decompression in our hospital. All patients were permitted to move without any help one month post-operation, and the follow-up period was from 15 to 36 months, average 18.5 months. Follow-up visits were scheduled at the 1st, 3rd, 6th month, 1 year, and annually thereafter. The outcome was demonstrated according to the changes in the Harris hip score.

Results

The average Harris hip score was 78.5 ± 11.2 at 6th month post-operation, significantly higher than that pre-operation, 53 ± 10.7 ($P<0.05$). But 7 of 10 patients (6 in stage II) complained of an improving aggravation of pain since 6th month post-operation, proving by a reduction of the pain part of Harris hip score which showed an average of 15 at pre-operation, 40.2 at 3rd month, and 21.8 at 6th month post-operation, respectively. The Harris hip score at 12th month post-operation was 64.5 ± 8.8. Three patients in stage II were treated with total hip arthroplasty at 10th and 20th month post-operation due to unbearable pain and movement disability.

Conclusion

The ONFH patients felt great improvement post-operation, proving by a statistical comparison between the Harris hip scores of pre-operation and post-operation. An aggravation of pain was found at 6th month post-operation in patients most from stage of ARCO II. It might be somehow the sign of increased pressure in femoral head.

PC.16

Stem cells transplantation and core decompression therapies for osteonecrosis of the femoral head (ONFH)

Fei Chang
China-Japan Union Hospital, Jilin University, Changchun, China

The article summarized our retrospective study of early stage avascular necrosis of the femoral head (stage I and II) treated with stem cells transplantation and core decompression.

Introduction

The article summarized our retrospective study of early stage avascular necrosis of the femoral head (stage I and II) treated with stem cells transplantation and core decompression.

Subjects and methods

From July 2008 to February 2010, eleven patients (10 male, 1 female, 13 symptomatic hips) were diagnosed as avascular necrosis of the femoral head with MRI. The number of hips affected by avascular necrosis in current series of 13 hips was 3 in patients taking corticosteroids, 5 in patients with excessive alcohol intake, and 5 in patients with idiopathic osteonecrosis. The mean age of the patients was 44 (range: 23-52). Hips were graded for severity according to ARCO's system. Five hips in 4 patients were stage I, and 8 hips in 7 patients were stage II. The patient were underwent with stem cells transplantation and core decompression in our hospital. All patients were permitted to move without any help one month post-operation, and the follow-up period was from 15 to 36 months, average 18.5 months.

Results

Follow-up visits were scheduled at the 1st, 3rd, 6thmonth, 1 year, and annually thereafter. The outcome was demonstrated according to the changes in the Harris' hip score. The average Harris' hip score was 78.5 ± 11.2 at 6thmonth post-operation, significantly higher than the score pre-operation (53 ± 10.7, $P<0.05$). But 7 of 10 patients (6 in stage II) complained of an improving aggravation of pain from 6 months post-operation, proving by a reduction of the pain part of Harris' hip score which showed an average of 15 at pre-operation, 40.2 at 3rdmonth post-operation and 21.8 at 6thmonth. The Harris' hip score at 12thmonth post-operation was 64.5 ± 8.8. Three patients in stage II were treated with total hip arthroplasty at 10thand 20thmonth post-operation due to unbearable pain and movement disability

Conclusion

The patients felt great improvement post-operation, proving by a statistical comparison between the Harris' hip scores of pre-operation and post-operation. An aggravation of pain was found at the 6thmonth post-operation in patients most from stage of ARCO II. It might be somehow the sign of increased pressure in femoral head.

8A.1
A computational platform for design-phase evaluation of knee replacement

Clare Fitzpatrick
UNIVERSITY OF DENVER, DENVER COLORADO, USA

Computational models are the primary tools for efficient design-phase exploration of knee replacement concepts before in vitro testing. To improve design-phase efficiency, a computational platform was developed that allows designers to assess devices under a series of important loading conditions.

Introduction:

Early in the design-phase of new implant design, numerous in vitro tests would be desirable to assess the influence of design parameters or component alignment on the performance of the device. However, cadaveric testing of knee replacement devices is a costly and time-consuming procedure, requiring manufacture of parts, preparation of cadaveric specimens, and personnel to carry of the experiments. Validated computational models are ideally suited for pre-clinical, high-volume design evaluation. Initial development of these models requires substantial time and expertise; once developed, however, computational simulations may be applied for comparative evaluation of devices in an extremely efficient manner. The objective of the current study was to develop a suite of semi-automated tools which perform a series of knee simulations of varying complexity, from basic contact to simulation of activities of daily living. The system integrates with commercially available finite element software to allow for direct, efficient comparison of designs and surgical alignment under a host of different boundary conditions.

Patients & Methods:

A suite of five simulation tools were developed in Abaqus/Explicit (SIMULIA, Providence, RI) which modeled (1) basic tibiofemoral (TF) component contact (Figure 1), (2) TF mechanical constraint, or joint laxity assessment [Haider and Walker, 2005], (3) TF joint laxity including ligamentous constraint, (4) TF wear during gait [Knight et al., 2007], (5) whole joint (TF and patellofemoral (PF)) mechanics during dynamic activities of daily living (e.g. gait, squat, chair-rise) (Figure 2). These models were developed in a software environment which integrates with Abaqus' interactive Complete Abaqus Environment (CAE), with a custom interface developed to allow easy conversion from rigid to deformable structures, adjustment of mechanical properties and component alignment, editing of material properties and boundary conditions, and presentation of simulation results (Figure 3).

Results:

The suite of tools provides a platform for baseline evaluation of design factors, comparison of new implant designs with predicate devices, and assessment of robustness to surgical alignment during five different loading conditions. Implant material properties, ligament properties and initial conditions can be varied, and results compared, to evaluate the influence of a host of design, surgical and subject-specific factors on implant performance. The interface allows users without complex finite element expertise to setup, analyze and compare devices and interpret results.

Discussion/Conclusion:

A platform which allows implant designers to evaluate their design ideas and compare with predicate devices has the potential to substantially decrease the development time for new devices. Designers can perform iterative modification to their devices to focus on an optimal design solution prior to in vitro testing, reducing the number of pre-clinical cadaveric experiments that may be required, and ultimately improving TKR mechanics in the patient population.

References:

Haider H, Walker PS, 2005. Measurements of constraint of total knee replacement. J Biomech 38:341-8.
Knight LA, Pal S, Coleman JC, Bronson F, Haider H, Levine DL, Taylor M, Rullkoetter PJ, 2007. Comparison of long-term numerical and experimental total knee replacement wear during simulated gait loading.J Biomech 40:1550-8.

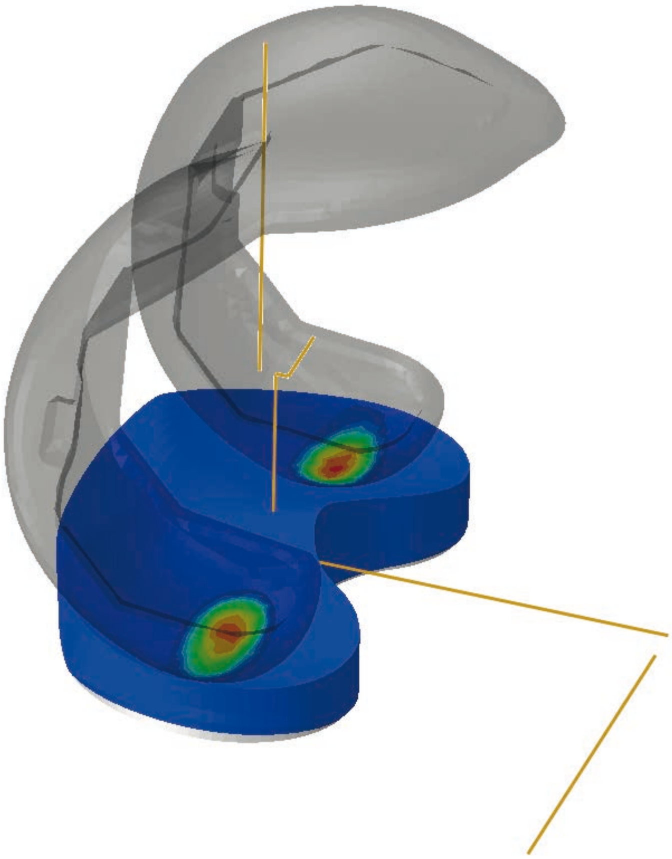

Basic contact analysis of the tibiofemoral joint, showing actuators through which loads (compressive force, internal-external and varus-valgus torque, anterior-posterior force) and kinematics may be applied.

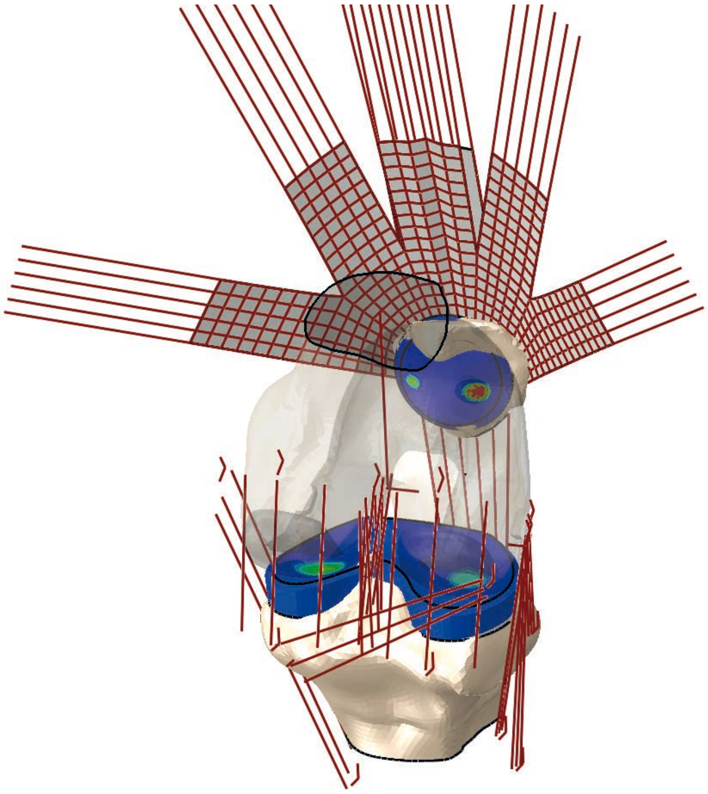

-Whole joint (including extensor mechanism and 1-D tibiofemoral ligaments) during a squat simulation (shown with transparent femoral bone and implant).

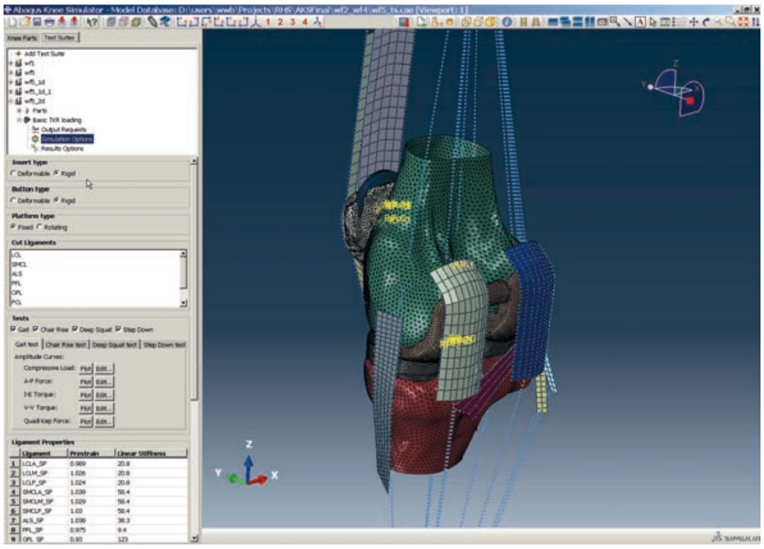

Insert type
○ Deformable ● Rigid

Button type
○ Deformable ● Rigid

Platform type
● Fixed ○ Rotating

Cut Ligaments
LCL
SMCL
ALS
PFL
OPL
PCL

Tests
☑ Gait ☑ Chair Rise ☑ Deep Squat ☑ Step Down

Ligament Properties

	Ligament	Prestrain	Linear Stiffness
1	LCLA_SP	0.989	20.8
2	LCLM_SP	1.026	20.8
3	LCLP_SP	1.024	20.8
4	SMCLA_SP	1.039	58.4
5	SMCLM_SP	1.029	58.4
6	SMCLP_SP	1.03	58.4
7	ALS_SP	1.038	38.3
8	PFL_SP	0.975	9.4
9	OPL_SP	0.93	123

-Custom interface developed in Abaqus CAE which allows efficient implementation and alteration of component alignment, muscle representation, soft-tissue mechanical properties, material properties and loading conditions.

8A.10
Sensitivity of total knee volumetric wear measurement using RSA

Emiel van IJsseldijk
Centre Hospitalier Universitaire de Caen, Caen, France

In this study the sensitivity of an in vivo volumetric wear measurement for knee prostheses is assessed. Large tolerances should be taken into account due to pose uncertainty in RSA and variation in the liner thickness.

Introduction

Model-matching techniques in Roentgen Stereogrammetric Analysis (RSA) allow accurate pose estimation of femur and tibia components in Total Knee Arthroplasty (TKA). From these measured poses, volumetric wear of the tibial insert can be calculated. This would be a valuable tool to estimate the amount of polyethylene debris, which is considered an important risk factor for TKA revision. However, little is known about the precision of this measurement. In this study, we investigated the response of the measurement to effects of pose uncertainty in Model-based RSA and variations in insert thickness due to manufacturing tolerance.

Methods

Clinical data from two patients with a Stryker (Raheen, Ireland) Triathlon PS total knee replacement were used. For both patients, RSA images were acquired at 7 weeks, 6 month, 1 year and 2 years follow-up. All data were analyzed in Model-Based RSA and the wear volume was detected using the overlap between the femoral model and insert model.

A Monte Carlo simulation was used to mimic the effect of pose uncertainty in Model-based RSA, using a standard deviation of (0.06mm, 0.06mm, 0.16mm, 0.24°, 0.29°, 0.16°) for the three translational and rotational parameters of the Model-based RSA pose. The wear volumes were detected for 500 generated poses. The 95% central range of these volumes was used as an estimate for thetolerance due to pose uncertainty. The tolerance due to insert thickness variation was investigated by repeating the measurement with a liner thickness offset of ±0.12mm. These experiments were conducted for all eight patient / follow-up data.

Results

The detected wear volumes in the patient data ranged between 51 and 304mm^3. For these two data, the measurement tolerance due to pose uncertainty were [12-120]and [185-456]mm^3 respectively, which is [0.24 - 2.4] and [0.6 - 1.5] times the original detection. The tolerances due to liner thickness variation were [21-95] and [222 - 396]mm^3 respectively. In relative terms these were [0.4 - 1.9] and [0.73 - 1.3] respectively. The widths of the measurement tolerances scaled with the value of the original volume detected. The tolerance of pose uncertainty was slightly larger than for the liner thickness variation.

Discussion

The results show that volumetric wear measurements in Model-Based RSA are viable, but a large tolerance interval should be taken into account. The liner thickness variation is a fixed patient effect and its tolerance could be reduced by careful measurements in the early follow-up stage.

8A.4

Collateral ligament strain after implantation of a total knee arthroplasty with measured resection technique

Hendrik Delport
Department of Orthopedics, K.U. Leuven, Leuven, Belgium

Testing strains in collateral ligaments before and after TKA shows different behavior in MCL and LCL.

Introduction

The last years have deepened the knowledge of biomechanics before and after implantation of total knee arthroplasty (TKA). It has been shown that TKA should respect the soft tissue envelope to be successful. More specifically since the collateral ligaments have a neurosensory function in knee joint behavior.

The aim of this project is to determine how collateral ligament strains compare before and after TKA using a measured resection technique with specimen specific cutting blocks.

Materials and methods

An MRI scan and full leg radiograph were made of the knee joint in six fresh frozen full leg cadaver specimens and specimen-specific cutting blocks (Visionnaire, S&N) for a primary PS TKA were designed based on the images. Frames with reflective markers were rigidly fixed to tibia, femur and patella of six and a computed tomography (CT) scan was made.

Femur and tibia were embedded, properly aligned in frontal and sagittal planes. The medial and lateral hamstrings tendons were prepared for attachment to constant load springs (50 N each). The quadriceps tendon was prepared to be clamped to a motor. Two extensometers were firmly sutured to the lateral and medial superficial collateral ligaments. The knees were mounted in a kinematic rig that provides six degrees of freedom to the knee joint.

The specimens were subjected to three motion patterns: a passive motion cycle, an open chain extension with 3 kg of load hung to the distal tibia, and a squat between 30° and 120° of flexion with a constant vertical ankle force of 130 N. Infrared cameras continuously recorded the trajectories of the markers. The strains in the collateral ligaments during the different motion patterns were recorded using the extensometers.

After testing the native knee, a PS TKA was performed using a measured resection technique with the cutting blocks and the tests were redone.

Ligament strains before and after TKA were then calculated as a function of knee flexion.

Results

Figure 1 shows the strains after TKA in medial and lateral collateral ligaments during the three investigated motor tasks compared to their native values.

It is clear that insertion of a total knee leads to minimal differences compared to the native knee on the medial side, at least during passive and open chain motions with differences in strain of less than ±3% over the flexion range. However, during squatting, the MCL strains are increased threefold.

The lateral ligament shows quite different behavior. This ligament is stretched by 6% more compared to the native situation during open chain and passive motion. It relaxes more during squatting after TKA reaching almost 6% less strain at 120° compared to the native situation.

Discussion and conclusion

The loaded activities of the patient after a TKA will interfere with the neuro-sensor properties of the ligaments if the isometric nature of these ligaments is not reproduced. This is by no means trivial as the surgeon can peroperatively only check unloaded situations.

This in vitro biomechanical study showed indeed a considerable difference, both medially and laterally, in strain after TKA during loaded squatting.

8A.6

Intra-Articular injections for degenerative cartilage lesions of the knee: Platelet Rich Plasma VS Hyaluronic Acid

Rocco Papalia
Campus Biomedico University Hospital, Department of Orthopaedic and Trauma Surgery, Rome, Italy

PRP represents a promising method to manage cartilage lesion, despite its mechanism of action is still troublesome, its positive effects is encouraging. Overall cohort improved significantly from the pre- to post-treatment time, but PRP is markedly more effective than HA.

Introduction:

In recent years the conservative management of degenerative cartilage lesions has received particular attention. Hyaluronic Acid is a widely used product, but newer solutions have been introduced in this field. Platelet Rich Plasma represents a promising method to manage degenerative cartilage lesion, despite its mechanism of action is still troublesome, its positive effects is encouraging. To better understand the PRP effectiveness we decided to compare this latter to hyaluronic acid. Purpose of this study is to compare clinical outcomes in patients undergoing injections of Hyaluronic Acid and Platelet Rich Plasma to the knee for treatment of degenerative chondral lesion.

Patients & Methods:

One hundred and fifty (73 men and 77 women, mean age 55.6) patients with clinical and radiographic evidence of degenerative changes to the knee were enrolled. The lesions were classified according to the Kellgren-Lawrence radiographic system. Patients were randomized into 3 groups: 50 patients (Group A) received 3 intra-articular injections of 5.5 mL PRP ‘Regen’, 50 patients (Group B) received 3 injections of 5.5 mL ‘Home made’ PRP, and 50 patients (Group C) underwent 4 injections of Hyaluronic Acid. IKDC, KOOS and VAS score were administered to all patients before starting the treatment, at 1, 6 and 12 months from the end of the management.

Results:

At 1 month and 6 months, PRP Regen Lab provided the best outcomes. Patients underwent home made PRP administration reported significant higher score than those undergoing hyaluronan injections , but lesser than PRP Regen Lab since the 6th post-injection month.

Discussion/Conclusion:

The overall cohort improved significantly from the pre- to the post-treatment time, but PRP is markedly more effective than hyaluronic acid. In particular, Regen Lab PRP injections provided significantly better outcomes than home made PRP.

(References)

1. Castillo, T.N., Pouliot, M.A., Kim, H.J. & Dragoo, J.L. Comparison of growth factor and platelet concentration from commercial platelet-rich plasma separation systems. Am J Sports Med 39, 266-271 (2011).
2. Ehrenfest, M. Classification of platelet concentrates:from pure platelet-rich plasma (P-PRP) to leucocyte- and platelet-rich fibrin (L-PRF). Trends in Biotechnology 27, 158-167 (2009).
3. Mishra, A., et al. Buffered platelet-rich plasma enhances mesenchymal stem cell proliferation and chondrogenic differentiation. Tissue Eng Part C Methods 15, 431-435 (2009).
4. Randelli, P., Arrigoni, P., Ragone, V., Aliprandi, A. & Cabitza, P. Platelet rich plasma in arthroscopic rotator cuff repair: a prospective RCT study, 2-year follow-up. J Shoulder Elbow Surg 20, 518-528 (2011).
5. Castricini, R., et al. Platelet-rich plasma augmentation for arthroscopic rotator cuff repair: a randomized controlled trial. Am J Sports Med 39, 258-265 (2011).
7. Sun, Y., Feng, Y., Zhang, C.Q., Chen, S.B. & Cheng, X.G. The regenerative effect of platelet-rich plasma on healing in large osteochondral defects. Int Orthop 34, 589-597 (2010).

8A.7

Effect of extramedullary tibial jig pin placement on the tibial alingment in Total Knee Replacement

Priyanka Jani
Diana Princess of Wales Hospital, Grimsby, UK

The success of the TKR is dictated by biomechanical stability therefore alignment of femoral and tibial component is vital. We aim to assess whether number and placement of the pins for the extramedullary tibial jig affects the tibial alignment.

Introduction

During a TKR the tibial plateau can be cut and prepared by using either an intramedullary or extramedullary cutting jigs. The use of extramedullary cutting jigs is less invasive and therefore minimizes blood loss and risk of embolization of fat and marrow elements. However, periarticular soft tissue / lateral knee ligaments can impair the surgeon's ability to translate the guide laterally at the knee resulting in a varus cut. The cutting jig is held in situ by use of medial and lateral pins. This study aimed to assess whether the number of pins used and the placement of the pins influence the alignment of the tibial component.

Patients & Methods

Methodology - Prospective clinical trial. The study involves 102 knees in patients undergoing Primary total knee replacement for osteoarthritis.

Participants & Intervention

N=102. These participants are divided into two groups. Group I - included 65 patients where the extramedullary tibial jig was secured with two lateral and one medial pin. Group II included 37 patients where the extramedullary tibial jig was secured with 1 medial and 1 lateral pin.

Outcomes

The patients all underwent a post operative CT scanogram. The mechanical axes, coronal, tibial and femoral angles at the CT scanograms were compared.

Results

There was a significant difference in the tibial component alignment between the patients in the two groups. In Group A - 49 of 65 (75%) attained a postoperative mechanical axis of $< 2^\circ$ varus / valgus whereas in Group B - only 25 of 37(67%) has similar post operative knee alignment in knees.

Discussion / Conclusion

We noted a definite improvement in the tibial component alignment confirmed by CT scanograms by using 2 lateral pins rather than just 1 lateral pin. The added lateral pins helped restrict the medialisation of the tibial jig and thereby improve the tibial cut and the alignment of the knee prosthesis.

8B.4

Bioplasty for vertebral fractures: a pre-clinical study on goats using autologous modified skin fibroblasts

Enrico Pola
Department of Orthopaedic Surgery, Catholic University of Rome, Rome, Italy

In vivo percutaneous gene therapy approach using Ad-hBMP-2 modified dermal fibroblasts in a goat model of anterior column vertebral bone defect was developed and showed to be effective in inducing new bone formation and bone defect repair.

Introduction:
Approximately, 160.000 patients/year sustain an injury of the spinal column in United States. (1) Themost common mechanism of injury of the thoracolumbar spine involves flexion/distraction forces causing eccentric compression of the vertebral bodies and discs resulting in anterior wedge compression fractures. (2)Even if non-operative treatment is still a viable and effective treatment for a good number of patients, many patients still need to be treated surgically in order to restore a correct spinal sagittal alignment.
The reduction of vertebral compression fractures leaves residual bone defects that pose a significant challenge to the practicing spinal surgeon. (3) Bone-grafting procedures often allow filling of bone defects, but the materials commonly used in everyday practice have many limitations. (4,5) Theselimitations include morbidity of donor sites, limited availability of graft materials for autografts, risks of disease transmission, and complications such as infection, fracture, and nonunion of allografts. We previously developed a clinically relevant gene therapy approach using modified dermal fibroblasts for inducing bone healing and bone formation in vivo. (6) Theaim of our study was to test the feasibility of a minimally invasive percutaneous intrasomatic ex vivo gene therapy approach to treat thoracolumbar vertebral fractures and anterior column bone defects.
Methods: Ten wild-type female goats, 8 months old, were used for this study. Primary dermal fibroblast cultures were established using a 0.5-cm-diameter punch biopsy of shaved skin obtained from the lumbar region of each animal under general anesthesia and in aseptic conditions. Subconfluent dermal fibroblasts were transduced with Ad-hBMP-2 or Ad-ψ5 (control vector) using a MOI of 100 pfus per cell. Cells were harvested 24 hours after viral infection and absorbed on a gel biomaterial composed of porous HA and collagen. The mixture of biomaterial + autologous dermal fibroblasts transduced with Ad-hBMP-2 was used as case and injected in the fourth lumbar vertebra of each goat after the creation of an intrasomatic bone defect by means of a percutaneous instrumentation. In the same manner the mixture of biomaterial and non-trasduced cells was injected in the fifth lumbar vertebra and the biomaterial + dermal fibroblasts transduced with Ad-ψ5 was injected in the sixth lumbar vertebra of each goat and both were considered as negative controls.
Results:
One animal has been sacrificed 5 days after surgery due to a post-operative infection. After 1 month vertebrae treated with Ad-hBMP-2 transduced skin fibroblasts without the biomaterial scaffold showed an advanced healing of the bone defect with a 60% filling of the bone defect. At 3 months the bone defect filling was about 85-90% in all Ad-hBMP-2 + biomaterial vertebrae.
Conclusions:
Our findings suggest the feasibility of using a minimally invasive percutaneous approach to deliver gene therapy engineered cells in the intrasomatic bone. The main advantage of this kind of approach is to promote and enhance bone healing of complex fractures and anterior column bone defects. Moreover, the use of autologous dermal fibroblast prevent the risk of an autoimmune reaction. However, more studies need to be done on the fate and the systemic diffusion of the transduced skin fibroblasts after the in vivo implant.
Bibliografy:

1. Hauser CJ, Visvikis G, Hinrichs C, Eber CD, Cho K, Lavery RF, Livingston DH. Prospective validation of computed tomographic screening of the thoracolumbar spine in trauma. J Trauma, 2003, 55:228-34.
2. Gertzbein SD. Scoliosis Research Society. Multicenter spine fracture study. Spine, 1992, 17:528-40.
3. Lindner T, Kanakaris NK, Marx B, Cockbain A, Kontakis G, Giannoudis PV. Fractures of the hip and osteoporosis: the role of bone substitutes. J Bone Joint Surg Br, 2009, 91:294-303.
4. Younger EM, Chapman MW. Morbidity at bone graft donor sites. J Orthop Trauma, 1989, 3:192-195.

5. Nemzek JA, Arnoczky SP, Swenson CL. Retroviral transmission in bone allotransplantation: the effects of tissue processing. Clin Orthop Relat Res, 1996, 324:275-282.
6. Lattanzi W, Parrilla C, Fetoni A, Logroscino G, Straface G, Pecorini G, Stigliano E, Tampieri A, Bedini R, Pecci R, Michetti F, Gamboto A, Robbins PD, Pola E. Ex vivo-transduced autologous skin fibroblasts expressing human Lim mineralization protein-3 efficiently form new bone in animal models. Gene Ther, 2008, 15:1330-1343

8B.6

Coral particle size influences human mesenchymal stem cell osteogenesis but not cell survival in an ectopic mouse model

Martina Sladkova
University Paris 7, Paris, France

Rapid decline of viable human mesenchymal stem cells (associated with coral scaffolds) after implantation in the ectopic mouse model, did not prevent their osteogenic potential. It was the size of scaffolds that affected the morphology and quantity of formed bone.

Mathieu M MSc. mathieumanassero@wanadoo.fr University Paris 7 Paris France
Myrtil Valentin V valentin.myrtil@paris7.jussieu.fr University Paris 7 Paris France
Savari Hema H savarihema@hotmail.com University Paris 7 Paris France
Fall Madelaine M madoma@hotmail.fr University Paris 7 Paris France
Thomas Daila D MSc. dialat82@hotmail.fr University Paris 7 Paris France
Logeart-Avramoglou Delphine D PhD. delphine.logeart@univ-paris-diderot.fr University Paris 7 Paris France Petite

Introduction:
Mesenchymal stem cells (MSCs) loaded onto osteoconductive scaffolds showed great promise for treating large bone defects. In the present study, we hypothesized that in vivo osteogenic potential of MSCs could be enhanced by optimizing the size of scaffolds. The objective of the present study was to assess the effect of the scaffold size on the osteogenic potential of human MSCs (hMSCs) that were seeded on coral scaffolds of various sizes and implanted in the ectopic mouse model. Furthermore, to fill the gap in the knowledge about the fate of hMSCs after their subcutaneous implantation, hMSCs were tracked in the present study early after implantation via bioluminescence imaging (BLI) system.
Materials and Methods:
10^6 hMSCs (transduced by a gene to express luciferase) were loaded on either coral particles (size: 45-80 µm, 80-200 µm, 300-450 µm, 600-1000 µm) or coral cube 3x3x3 mm^3, wrapped in fibrin gel, and transplanted subcutaneously into nude mice (n=8/group). As control, scaffolds with no hMSCs were used. Cell survival was monitored using the BLI system during first 15 days after implantation. Osteogenesis was quantified 2 months after implantation on non-decalcified samples.
Results:
After implantation, the number of viable hMSCs decreased progressively in time regardless of the coral scaffold size. At day 15 post-implantation, less than 4% of initially seeded hMSCs were observed to be viable in all groups tested. The frequency of bone formation was similar in all tested conditions (more than 75% of all samples), except for the particles 45-80 µm (only 2/8 samples have formed bone). Control scaffolds, with no hMSCs, did not form bone. The morphology of new formed bone was affected by the scaffold size. Both bone and bone marrow (a rim of bone filled with bone marrow) was formed in groups containing particles of small (up to 300-450 µm) size. While all samples positive for bone were also positive for bone marrow formation in groups containing particles 45-80 µm and 80-200 µm, only 3/8 samples were positive for bone marrow in the case of particles 300-450 µm. Quantification of bone formation shown that group containing particles 80-200 µm promoted the highest bone formation which was 10-time higher compared to particles 45-80 µm and cube ($p<0.05$). The group containing particles 80-200 µm promoted also the highest bone marrow formation which was more than 6-time higher ($p<0.05$) compared to that observed in the rest of groups. Coral resorption increased with increasing scaffold size. Significantly ($p<0.05$) more coral remained in the group containing cube compared to groups containing the particles.
Conclusion:
In the present study, hMSCs were required for new bone formation in the ectopic mouse model. The osteogenic potential of hMSCs was highly enhanced by associating them with particles 80-200 µm. Importantly; rapid decline of viable hMSCs did not prevent new bone formation in the implanted hMSC-containing scaffolds.Further investigations are needed to elucidate the fate of implanted hMSCs and how the extent of the trophic action of hMSCs (i.e., their capability to secrete growth factors and cytokines) affects the process of osteogenesis.

Submitted by:Sladkova, Martina MSc

8B.7
THE ROLE OF PERICELLULAR MATRIX HYALURONAN IN CELL ADHESION TO POLYELECTROLYTES

Caterina Fotia
Pathophysiology Lab, Instituto Orthopedico Rizzoli, Bologna, Italy

Pericellular matrix mediates the first interaction cell/surface showing a fundamental role when cells interact with substrates that do not favour adhesion.

Introduction

The build-up of polyelectrolyte multilayer (PEM) films is now a well-established concept that enables surface modification for the coating of biomaterials in clinical applications, such as implant materials and artificial organs. The formation of focal adhesion complexes, together with the resulting cytoskeletal reorganisation, has a short- and long-term effects on cell adhesion and differentiation. However, prior to this integrin-mediated step, the initial cell-ECM/surface interaction is mediated by a hyaluronan-dependent pericellular matrix (PCM). PCM is a thick coat lying between the cell membrane and the extracellular matrix, which recognizes the substrate and holds the cells close to the surface until stable contacts are established.

In this study, we investigated the role of PCM in the interaction of cells with positive (PEI) and negative (PSS) charged polyelectrolytes.

Methods

PEM were built up using the layer-by-layer method on chamber slides. A PEI-PSS-PEI film with a cationic surface (PEI), and a PEI-PSS film with an anionic surface (PSS) were obtained. The resulting films were 6 ±1.2 nanometer thick as characterized by XPS and AFM analyses.

GFP-expressing MG63 cells were seeded on the substrates and the presence of PCM was assessed by using specific hyaluronan binding proteins (HABP). To evaluate the role of the PCM, the matrix was removed by hyaluronidase treatment. The organization of cytoskeleton and focal contacts was then analysed via immunostaining of integrin b1, paxillin, vinculin, and actin. The expression and the activation of Fak were evaluated by Western blotting. Adhesion and spreading of MG63 cells were evaluated after 1, 3, and 6 hours of culture by image analysis.

Results

MG63 cells secreted and organized an extensive PCM, which was removed after hyaluronidase treatment. The PCM appeared as a thick border around the cells on PEI and Permanox®, which keep a round shape after 3 hours. Instead, MG63 seeded on PSS and fibronectin were spread and the PCM was visible only around a few cells and mainly distributed along the border of the cells (fig 1).

Many cells adhered to PSS and no differences were evident after hyaluronidase treatment. On PSS cells were elongated, actin stress fibers thethered into focal adhesion contacts and cell area increased over time. Cells pre-treated with hyaluronidase showed a fewer number of focal contacts. On PEI the number of adherent cells was significantly reduced over time, and cells treated with hyaluronidase revealed a significant lower ability to adhere. Cells maintained a round shape over time and actin was present only at the cell edge as a cortical layer, while the adhesion molecules did not organize into focal contacts. On both substrates the PCM removal induced a reduction of Fak levels, in particular on PEI where a two-fold decrease was observed.

Conclusion

PCM is fundamental for cell adhesion to substrates with different charges, in particular for surfaces that do not favour cell adhesion, such as PEI. Further studies will be necessary to increase our knowledge on the nature and function of this matrix and to evaluate its contribution to cell-matrix and cell-to-cell interactions.

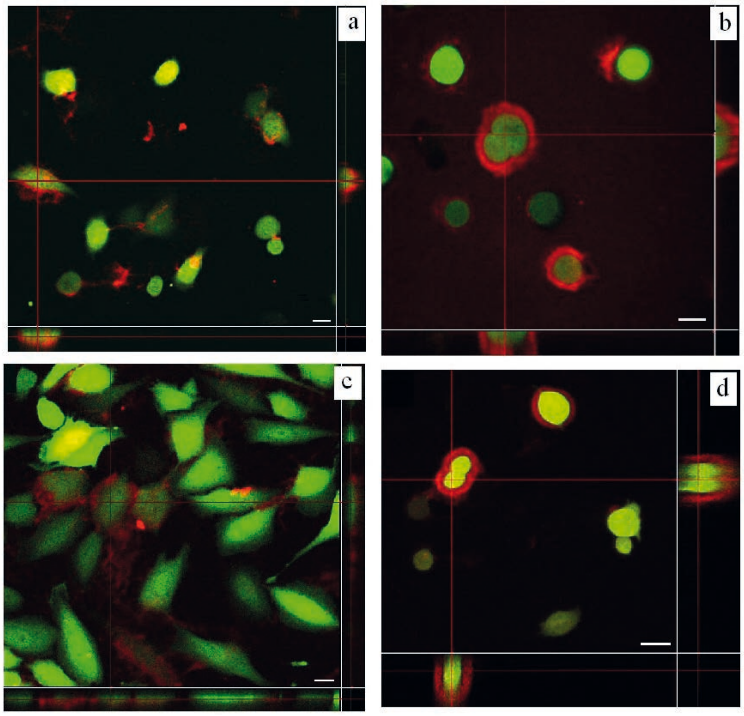

Distribution of the pericellular matrix (red) of GFP cells (green), seeded on the substrates. a) PEI; b) PSS; c) fibronectin; d) Permanox®.

8B.8

Factors affecting stability of osteochondral grafts: effect of graft length, depth of defect and congruency.

Kathryn Lowery
Institute of Medical and Biological Engineering, Leeds University, UK

This study investigated factors influencing the pressfit stability of osteochondral grafts. Short grafts in bottomed defects had significantly greater stability after displacement of 1 mm below congruency.

Introduction

The aim of this study was to investigate factors influencing the stability of surgical fixation for osteochondral grafts. The press-fit stability of the grafts was evaluated through investigation of the effect of graft length, defect depth, graft congruency and alignment.

Materials and Methods

Cylindrical osteochondral grafts (8.5 mm diameter) were harvested from bovine medial condyles using a Mosaicplasty system. Grafts were implanted into bovine medial femoral condyles and push-in tests were performed using an Instron compression rig to assess the press-fit stability of the grafts. Grafts were inserted to congruency using the Mosaicplasty system, then pushed 4 mm below congruency. Ten millimetre length grafts were inserted into defects with depths of 10, 12 and 15 mm (n=4 per medial femoral condyle; n=12 in total) which, represented 'bottomed' or 'unbottomed' grafts. Grafts 15 mm in length were also inserted into defects (n=12) but with depths of 20 mm. Ten millimetre length grafts were inserted into 10, 12 and 15 mm length defects (n=12 per group) and, a silicone rubber was applied in order to replicate the surface profile. The profiles were measured using a Form Talysurf profilometer and congruency of the grafts was determined. Graft alignment was visualised using micro-computed tomography (Micro-CT).

Results

All 'bottomed' grafts needed a significantly greater amount of force to push-in than 'unbottomed' grafts beyond 1 mm below congruency (0 mm, 2 mm and 5 mm (difference between graft length and defect depth)). However, at 0.5 mm and 1 mm below congruency there were no significant differences between 'unbottomed' and 'bottomed' grafts. The force required to 'push-in' the 10 mm and 15 mm length grafts below congruency showed no significant differences. The 10 mm length grafts required a significantly higher force to push-in beyond 1 mm below congruency compared to the 15 mm length grafts. Talysurf measurements demonstrated that fewer 'unbottomed' grafts were proud in respect to the surrounding articular cartilage than the 'bottomed' grafts; a finding visually confirmed by Micro-CT images.

Discussion

This study demonstrated that at greater than 1 mm displacement below congruency shorter 'bottomed' grafts exhibited significantly greater stability, however talysurf data demonstrated that 'bottomed' grafts result in a higher proportion of proud grafts. This study suggested that in order to optimise surgical outcomes, a shorter graft in a bottomed defect provided a more stable construct, however surface congruency may be compromised.

Acknowledgments:
University of Leeds, Institute of Medical and Biological Engineering. Funding; University of Leeds

8B.9

Osteoinductive properties of platelet gels prepared by different techniques

Francesca Perut
Laboratory for Orthopaedic Pathophysiology and Regenerative Medicine, Istituto Ortopedico Rizzoli, Bologna, Italy

Different preparation techniques of platelet rich plasma influence platelet content and growth factor release from platelet gels. The osteoinductive properties of the platelet gels are comparable, but L-PRP is a more effective method for stimulating the proliferation of osteogenic precursors.

Introduction.

An extensive debate about clinical benefits of platelet concentrates used as treatment option for patients with orthopaedic injuries is still ongoing, as well as there is no accepted standard for its preparation [1,2]. The aim of this study was to investigate the osteoinductive properties of platelet gels (PGS) prepared from platelet rich plasma (PRP) obtained with two different techniques.

Methods.

After signing written consent, 10 healthy male volunteers underwent blood harvesting (age 28-37). The Pure Platelet Rich Plasma (P-PRP) was obtained by a one-step separation technique, by using a commercial device [3] , while the Leukocyte-PRP (L-PRP) was obtained by a two-step separation technique by using a literature-based method [4]. PRPs were characterized for platelets and leukocytes content. PGs were prepared starting from P-PRP, fresh L-PRP, L-PRP after thawing, and Platelet Poor Plasma (PPP). The release of bFGF from PGs was measured at 1, 18, 48, 72 hours and 7 days. The ability of different PGs to induce proliferation and differentiation of human bone marrow stromal cells (BMSC) was evaluated by using a metabolic assay (AlamarBlue test) and Alizarin red staining, respectively.

Results.

The platelet recovery was significantly higher in L-PRP, either fresh or frozen compared to P-PRP. bFGF release was faster in both fresh or frozen L-PRP preparations, but a negative correlation was found between bFGF and number of polymorphonuclear cells. L-PRP induced a significantly higher proliferation of BMSC compared to P-PRP or PPP samples. The mineralization activity of BMSC was not influenced by different PGs preparations, while it showed a positive correlation with bFGF release.

Conclusion.

Platelet content and growth factor release by PGs are strongly influenced by the different preparation techniques. Leukocyte content plays a crucial role in growth factors spreading. Both proliferative and osteoinductive properties of BMSC strictly depend on the growth factor availability. L-PRP and PRP show similar osteoinductive properties, but L-PRP seems to be more effective in stimulating the proliferation of osteogenic precursors.

References

1. Sheth U et al M. J Bone Joint Surg Am. 2012;94:298-307.
2. Mazzocca AD et al. J Bone Joint Surg Am. 2012;94:308-16.
3. Anitua E. Int J Oral Maxillofac Implants.1999;14:529-35.
4. Kon E et al. Arthroscopy. 2011;27:1490-50.

9A.1

AN INDEXATION ALGORITHM FOR FEMORAL SHAPE AND BMD CAN PERFORM BONE SIMILARITY SEARCHES AND GENERATE SYNTHETIC BONES

Ilaria Palmadori
Istituto Ortopedico Rizzoli, Bologna, Italy

This work presents and successfully evaluates an indexation method that can be used to (i) characterise the variability of femoral shape and bone mineral density in a population, (ii) make “best match” searches, and (iii) generate synthetic anatomies.

Introduction

A statistical description of the high existing variability of bone shape and mineral density (BMD) could help in computational biomechanics for (i) defining risk factors (e.g. fracture susceptibility in osteoporosis, shape degeneration in osteoarthritis), (ii) pre-clinically evaluating prosthetic designs[1], and (iii) computer assisted surgery [2].

One main limitation of current studies (usually relying on CT-based subject-specific finite element (FE) models) is the low sample numerosity, because CT scans cannot be taken on volunteers, privacy policies limit sharing, cadaver specimens are scarcely available.

A general method to obtain bone shape and BMD indexation based on principal component analysis (PCA) has been recently proposed and evaluated on the femur in terms of convergence and in-vitro accuracy [3]. The aim of this study is to verify if this method can be used to define similarity criteria and to generate synthetic bones.

Methods

CT datasets of 150 normal femurs were used. Each femur was mesh-morphed with a validated algorithm [4] and materials were mapped to CT [5] obtaining isotopological FE meshes.

Shape-bmd indexation

The algorithm consists of: (i) pre-processing of morphed meshes (normalising rigid transformation and scaling); (ii) PCA computation of eigenvalues and eigenvectors (modes), i.e. the space of shape and BMD variability.

Projection and similarity criterion

A generic given bone can be projected to the indexation space, i.e. approximated by a linear combination of modes, by using the bone coordinates after removing rigid body transformation and optionally scaling. The most similar bone to a given bone can be identified by calculating the range of modes (ROM) distance.

Synthetic bones generation

Linear combination of indexation modes generates synthetic bones. To avoid generation of uncertain instances, the combination of modes is limited within the range of eigenvalues of the indexed bones.

Evaluation procedure

The ROM distance was tested for accuracy and speed against standard methods (normal distance for shape, element-by-element norm for BMD).

The quality of synthetic bones was evaluated by visual inspection, morphological descriptors, and leave-one-out tests (each femur is in turn excluded from the indexation database, re-generated through projection in the database, compared to the re-generated instance).

Results and discussion

similarity criterion

The nearest bone to a given one was univocally defined among 150 femurs by ROM distance (few seconds) and standard methods (~20 minutes). The difference is expected to grow for larger databases.

Synthetic bones generation.

Visual inspection could not reveal unrealistic features. Morphological descriptors were within the range of normal bones. The mean error in leave-one-out tests was around 0.5 mm (shape) and 0.05 g/cm^3 (BMD).

In summary, the proposed tools are reliable for use in simulation studies, and prospectively in clinical contexts. To approach wider clinical contexts, future studies will attempt the reconstruction of 3D anatomies from 2D images.

References
1. Bryan et al., Medical Engineering & Physics, 2010. 32(1):57-65
2. Cootes et al., Image and Vision Computing, 1994. 12(6):355-365
3. Grassi et al., ISB 2011 Congress, www.isbweb.org
4. Grassi et al., Medical Engineering & Physics, 2010. 33(1):112-120
5. Taddei et al., Medical Engineering & Physics, 2007. 29(9):973-9

9A.2

Biomechanical considerations in the development of a Novel Polycarbonate-Urethane Meniscal Implant

Jonathan Elsner
Active Implants Corp., Netanya, Israel

A prosthetic medial meniscal implant is proposed as a bridge treatment for middle-aged patients suffering from joint pain. A meniscal implant with a reliable biomechanical performance which doesn't rely on regeneration hasn't thus far been offered in the clinical practice.

Meniscal tears often lead to degenerative arthritis, attributed primarily to the changes in the magnitude and pattern of stress distribution in the knee. While meniscal replacement traditionally involves implantation of allografts; problems related to availability, size matching, and cost limit their use. Artificial prostheses offered thus far are based principally on tissue engineering concepts. The variability in the body response to them and the quality of the tissue formed still pose a problem in this respect, thus making it difficult to attain satisfying results from scaffold-type meniscal implants under intense knee loading conditions, especially in older patients (Fig. 1). The goal of this study was to develop a bio-stable synthetic meniscal implant which combines durability with a dependable biomechanical performance resembling that of the natural meniscus.

A composite, non-fixed self-centering discoid-shaped polycarbonate-urethane meniscus implant, reinforced circumferentially with UHMWPE fibers is proposed. The implant's form was based on extensive MRI study that included the geometrical analysis of more than 100 knee scans. Biomechanical evaluation of the implant was focused on several in-vitro measurements of contact pressure under the implant in cadaver knees and computational finite element (FE) analyses. Pressure distribution under the meniscus was measured by using pressure sensitive films and quantified with respect to the natural meniscus. The effects of changes in the geometry and material properties of the composite structure were investigated. Finite element analyses were used to evaluate internal stresses and strains, and to support the selection of optimal implant configuration. The last pre-clinical step was a sheep study in which both implant and surrounding tissue (specifically cartilage) were evaluated, quantitatively, over six months.

Contact pressure distributions were in good agreement with those measured under the intact natural meniscus prior to meniscectomy. Specifically, peak and average pressures developed under the implant were found to be similar to those of the natural meniscus (Fig. 2). The contact area measured under the implant was also restored when compared to the natural meniscus. Outputs of the FE model confirmed that internal strains/stresses within the device components remained within the materials' allowed limits. The evaluation of an implant adapted to sheep showed no signs of wear or degradation of the materials. Histology showed no significant difference between the control and the 3 and 6 month groups. First clinical results with 3 years follow-up, demonstrate encouraging prospects for this concept in terms of pain relief and quality of life measures.

A new implant which is able to reduce the overall cartilage load associated with meniscectomy was presented. First implantations have shown that arthroscopic implantation of the device is short and uncomplicated. Clinical follow-up of the device is underway.

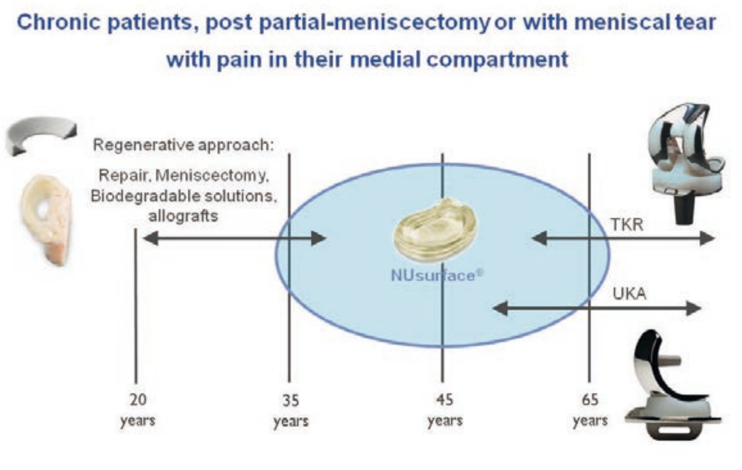

-Treatment options for chronic patients post meniscectomy or meniscal tear with medial pain

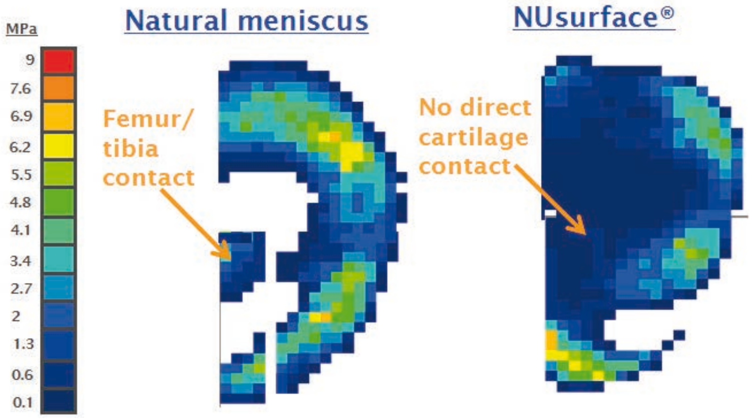

-Pressure distrbution under the natural meniscus (left), and artificial implant (right), during joint compression

9A.3

Is double-looped double pegged? A biomechanical study on different cerclage configurations

Mark Lenz
AO Research Institute, Davos, Switzerland

Double looping cerclages can significantly enhance lasting pretension, stability and strength.

Introduction:
Periprosthetic fracture surgery evoked a new interest in cerclage technology. Different wiring techniques can be applied on cable cerclages to enhance fixation capacity. Their stability and strength was biomechanically compared in a cyclic loading test.
Methods:
Different configurations of cerclage cables (Ø1.7mm, crimp closure) and solid cerclage wires (Ø1.5mm, twist closure), forming 7 groups (n=6), fixed two cortical half shells of human femoral shaft mounted on a testing jig (one single cerclage looped once around the shells, one single cerclage looped twice, two cerclages each looped once, two braided wires, twisted around each other looped once). Cerclage pretension, load leading to onset of plastic construct deformation (LPD) and load at total failure were identified during sinusoidal cyclic loading with constantly increasing force (0.1N/cycle), starting at 50N peak load. Statistical differences between the groups were detected by univariate ANOVA with Tukey B post hoc correction.
Results:
The LPD was 1334N ±319 for double looped cables, significantly better than single looped cable 646N ±108, but comparable to two single looped cables 1191N ±334. Double loop wires 752N ±119 performed superior to two single wires LPD 520N ±58 and comparable to single looped cables. Braided wires exhibited early plastic deformation (119N ±55).
Conclusion:
Double looped cerclages provide higher stability under cyclic loading leading to a more reliable fracture fixation being applicable via the same approach. The use of braided wires could mechanically not be recommended.

9A.4

FE-BASED STRENGTH ESTIMATION FOR THE PREDICTION OF FEMORAL NECK FRACTURE

Cristina Falcinelli
Instituto Ortopedico Rizzoli, Bologna, Italy

A preliminary retrospective study on 48 patients shows that FE-based bone strength from CT data (using validated FE models) is a suitable candidate to discriminate fractured versus controls within a clinical cohort.

Introduction

Finite element (FE) models from CT data are a promising tool to non-invasively assess the bone strength and the risk of fracture of bones in vivo in individual patients. They are often used to predict bone strength in a pre-defined and usually simplified loading case. When used to this purpose, they have demonstrated a high accuracy in predicting bone strains and bone strength in vitro and have also been applied in clinical studies, but routine clinical applications have not started since their superiority in clinical predictivity has not been proved yet. The aim of this work is to use validated FE modelling procedure [Schileo, 2008] to identify fracture cases within a clinical cohort.

Patients and Methods

Each patient (48 patients, 10 fractured, 38 non-fractured) underwent a clinical hip CT and a DXA, from which femoral neck and total hip aBMD were measured.

The FE models (right femur for non-fractured and contralateral femur for fractured) were generated starting from CT using an in-vitro validated procedure [Schileo, 2008].

Bone strength was evaluated in quasi-axial loading conditions, for a set of 12 different configurations sampling the cone of recorded in vivo hip joint reactions [Bergmann, 2001], and was defined as the minimum load inducing on the femoral neck surface an elastic principal strain value greater than a limit value [Bayraktar, 2004].

Results and Discussion

FE predicted femoral strength had a weak correlation with femoral neck and total hip aBMD. Spearman r was respectively 0.66 and 0.57 significantly lower than those reported by [Orwoll, 2009] and [Keyak, 2011]. This indicates that the proposed FE prediction is not equivalent to BMD derived indices, while the existing studies concluded for a sustantial equivalence of FE-derived and BMD-derived indices in classifying fracture cases.

The mean FE predicted strength of fractured cases was 28% less than that of non-fractured cases. This value is greater than those reported by [Keyak, 2011] for women (13% in quasi-axial loading, 18% in side-fall), indicating a good potential of the proposed method to classify fracture cases.

In order to derive an optimal threshold to classify cases at risk, a logistic regression was performed and a ROC curve for the discrimination of fractured versus non fractured cases was derived based on the value of the predicted FE strength. An optimal threshold value of 3000N was identified, concordantly to [Amin, 2011]. The AUC (Area under curve) was 0.81, similar to that reported in [Amin, 2011]. This performance was obtained despite two main limitations of this study: the low number of fractured cases, that will increase in the prosecution of the study, and the absence of side-fall modelling that has already recived in-vitro validation [Grassi, 2011] and will soon be included.

References

Amin et al, JBMR, 26:1593-1600, 2011
Bayraktar et al, J Biomech, 37:27-35, 2004
Bergmann et al, J Biomech, 34:859-871, 2001
Keyak et al, Bone, 48:1239-1245, 2011
Orwoll et al, JBMR, 24:475-483, 2009
Schileo et al, J Biomech, 41:356-367, 2008
Tremollieres et al, JBMR, 25:1002-1009, 2010
Grassi et al, J Biomech, 45:394-9, 2012

9A.5

The influence of porosity on fracture toughness of human cortical bone: An xFEM study

Silke Besdo
Institute of Continuum Mechanics, Leibniz Universität Hannover, Hannover, Germany

The significance of this study lies in demonstrating the feasibility and application of xFEM to predict fracture behaviour of compact bone from high resolution CT images without apriori defining the crack initiation and propagation.

Introduction:

Fracture risk increases with ageing. The reasons are not well understood. One reason seems to be changes in the bone structure and the loss of bone mass. The extended Finite Element Method (xFEM) offers the possibility to determine the different aspects, by changing single parameters like geometry or the material properties, without predefining the crack path. Consequently the influence of microstructural features on initiation and propagation of fracture can be determined. Thus, the aim of this study was to develop an xFEM model for compact bone and demonstrate its feasibility in determining the effects of intracortical porosity, captured through a microCT, on fracture properties of bone.

Methods:

FE-meshes were generated using the microCT data of compact bone fracture toughness samples of 19 and 81 years old donors showing distinct differences in intracortical porosity. The meshes for this study were generated using Mimics. To reduce the number of elements the bottom and the top areas were meshed with huge elements and the cavities in these areas were neglected. The crack area was meshed with a higher amount of elements. In both cases linear tetrahedrons of the type C3D4 were used. In order to determine the effect of porosity on fracture properties, same material were chosen for both donors. The quadratic nominal stress criterion was used. Crack propagation was only allowed in the middle part of the samples to reduce the calculation time. The crack initiation was defined by a small plate in the middle of the sample.

Results:

A comparison of the slopes of the R-curves obtained by assuming one set of material properties for the whole model and the calculations with homogenized material properties in the areas with simplified geometry shows, that they are nearly similar in more porous 81-year sample. In the case of the 19 year old donor sample with the homogenized material properties, the FE-estimated slope is 86.9 % of the slope obtained by assuming only a single set of material properties. If the changes in the material properties obtained by neglecting the cavities are not taken into account, the slope of the R-curve of the 81 year old donor is 69,7 % of the slope of the 19 year old donor. In the case of the effective material properties the slope of the 81 year old donor versus the 19 year old donor is 79.9 %.

Discussion / conclusion:

The results show that xFEM successfully captured the fracture behaviour of compact bone, demonstrated here by a rising crack, without the use of a predefined crack path. xFEM can be used to determine the influence of microstructural features including the porosity on. Because the present study used the same material properties but different geometries the observed difference in fracture properties are due to the differences in the intracortical porosity.

Acknowledgement

This work is supported by the DFG Project BE-3990/2-1 and by National Institutes of Health Grant AR49635. Thanks to the Imaging Core at the CBIS, RPI for the use of Micocomputed tomography facility.

9B.1

A curious effect in the jaw joint following bisphosphonate treatment.

Greetje Renders
Academic Center for Dentistry Amsterdam, Amsterdam, The Netherlands

The application of BP resulted in bone-site specific changes in mineralization; an effect that to our knowledge has never been reported before.

Bisphosphonates (BPs) are commonly used for the treatment of osteoporosis and bone metastases. BPs have a positive treatment effect on the long bones (e.g., increase in bone density), however a negative effect (e.g., osteonecrosis) on the mandible is reported. It is not known whether the jaw joint is also affected by BP treatment. We hypothesized that application of bisphosphonates affects the jaw joint. To test our hypothesis, female C57BL/6J mice (n=18/group; n=6/time point) were injected intraperitoneally with zoledronic acid (0.5 mg/kg; BP group) or saline (control group) once a week. At baseline or after 1, 3 and 6 months, the animals were killed to collect the jaw joints. The joints were scanned with a µCT system (8 µm resolution). The mineral density was analyzed and the samples were examined for bone pathologies. To test for differences within and between both groups 1-way ANOVAs and independent t-tests were applied, respectively. Our results showed remarkable bone pathologies, some of them characteristic for osteoarthritis. For instance, pits (likely cysts) were seen after 1, 3, and 6 months in both groups. Also osteophytosis was seen after 1, 3, and 6 months in both groups and increased over time. The mineral density increased significantly with age in the control group. This effect was in the BP group only seen after 1 month. BP-treated mice showed an intriguing regional phenomenon; the subchondral bone had a signficantly lower mineral density, whereas the condylar core had a higher mineral density (Fig.1). This phenomenon did not exist in the control group. To conclude, our findings show a time-dependent occurence of an osteoarthritis-like bone phenotype in both control and BP groups. The application of BP resulted in bone-site specific changes in mineralization, that to our knowledge have never been reported before.

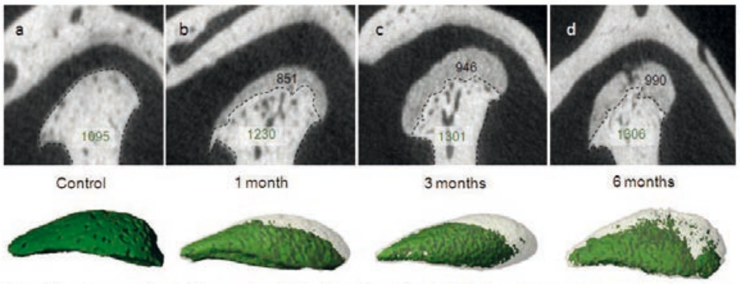

Figure 1: Upper images are frontal µCT cross-sections of the jaw joint: a) Control 1 month, b-d) bisphosphonate-treated group over time. Lower images represent the 3-D-reconstructions of the same condylar samples (lateral view). The dark green area represents the traced core region with a higher mineral density compared to the transparent subchondral region. The values represent the average degree of mineralization of bone (mg hydroxyapatite/cm^3)

Bone-site specific mineral density in jaw joint.

9B.2

Biological membranes for bone repair

Florelle Gindraux
University of Franche-Comté, CIC-BT, Besançon, France

Induced membrane, Amniotic membrane, Mesenchymal stem cell, Bone repair

1 Induced membrane concept

The reconstruction of wide long bone diaphyseal defects is often the major challenge in limb salvage whatever the etiology of bone loss. Bone defects can occur in case of open diaphyseal fracture or in case of bone non union (10% to 30% of diaphyseal fractures
do not consolidate after 6 months and are known as 'bone non union').

The most common and widely accepted procedures are the vascularized bone free transfer and the Ilizarov bone transport method. Bone autograft is not advocated when the defect is over 4 to 5 cm. When diaphyseal defects larger than 6 cm are reconstructed with autologous bone graft, healing is incomplete because of graft resorption even in a good vascularized muscular envelope.

Previous clinical and experimental studies have shown the efficacy for bone regeneration of a foreign body 'induced membrane' (Fig 1) combined with bone autograft. This membrane has the properties to avoid the resorption of the bone autograft and to promote the consolidation by revascularisation of the bone and secretion of growth factors. The technique needs to have two different surgical stages: the first is the insertion of a cement spacer in the defect, the second is the removing of the spacer and the filling of the cavity by bone autograft harvested from the iliac crest.

We observed in in vitro studies that this induced membrane is rich in mesenchymal stem cells (MSC).

2 Amniotic membrane

The human placenta consists of the amniotic and chorionic foetal membranes (each containing MSC). Many beneficial properties of amniotic membrane (Fig 2) tissue, including bacteriostatic (anti-microbial properties), anti-inflammatory, analgesic, wound healing, anti-fibrotic, reepithelialization, reduced scarring, anatomical vapor barrier and capacity to synthesize and release biologically active substances (including cytokines and signalling molecules) have been reported. In addition to its almost unlimited availability, easy procurement from the placenta, low processing costs for therapeutic application, and low immunogenicity, the amniotic membrane is widely described as a good candidate in regenerative medicine.

At Besançon, the bank of cells and tissues of the French Blood Agency has been organizing the collection and the qualification of the amniotic membranes since 2003 and retroceded them for clinical ophthalmologic indications (corneal ulcerations and severe destruction of the surface of the cornea).

3 Status report

From a clinical point of view, we believe that it would be better to use minimally manipulated amniotic membrane rather than placenta-derived cells or subpopulations of these cells. To our knowledge, the use of amniotic membrane for bone repair in clinical situations is not described in the literature to date.

So, we plan to use amniotic membrane instead of the induced membrane in the event of large bone defects (in case of open diaphyseal fracture and bone non union) to avoid the need of two different surgical stages.

We are studying:

- The histology and immunohistochemistry of these tissues to observe the similarities.
- The in vivo and in vitro osteogenic potential of MSC derived from these tissues.

The results are currently being analyzed.

9B.3

THE LACUNAR - CANALICULAR STRUCTURE OF IRRADIATED MANDIBLE STUDIED BY SCANNING ELECTRON MICROSCOPY

Timo Ruotsalainen
Inst. Of Dentistry, Oulu, Finland

The lacunar-canalicular network of alveolar bone of irradiated mandible were analyzed with scanning electron microscopy, which helps in distinguishing changes in this network due to irradiation and also new bone formation process especially at the bone-implant interface.

Osteocytes are a key component of bone physiology. They are contained within its own lacuna, which is connected to adjacent osteocytes via fillipodial processes forming a lacunar-canalicular network. Further, it is important to study the osseointegration of dental implants in the mandible, because the alveolar bone differs from those of the appendicular skeleton. The alveolar process of the mandible normally is subject to a high rate of bone turnover, and it has been shown that the bone turnover in the alveolar region of the mandible is 15-20x higher than in bones from the appendicular skeleton (Huja et al.2006). The aim of this study was to analyze the lacunar-canalicular system in irradiated mandible by scanning electron microscopy, because there are no reports about the canalicular changes of irradiated mandible.

In ten skeletally mature beagle dogs (1-2 years), one side of each mandible was irradiated in 2 sessions, lasting one week. The total dosages were 40 Gy (Group A, 5 dogs) and 50 Gy (Group B, 5 dogs). The irradiation source used was a linear accelerator (Saturne III, CGR, France) with 6 MeV electrons. The size of the treatment area was 4.5 cm x 3 cm. After the animals were sacrificed, the mandible bone blocks containing implants were dissected and fixed in 10 % formalin. Tissue segments were processed by bulk staining en bloc in basic fuchsin, which identifies the microdamage in bone and distinguishes it from the artefact caused by histological processing and sectioning. Basic fuchsin stains cells and empty spaces in the bone matrix - blood cells, lacunae, canaliculi, microcracks. The specimens were embedded routinely in polymethyl methacrylate resin without preliminary decalcification. Thin sections for analysis by light microscopy were prepared using cutting and grinding systems (Exakt, Nordenstedt, Germany).

Secondly, about 3 mm thick slice were cut and polished. The polished sections were acid-etched with 9% phosphoric acid for 60 s. Following etching, sections were immersed in sodium hypochlorite for 5 min and rinsed by hand in dH_2O. (Kubek et al. 2010) Thereafter the slices were coated by a thin gold layer for SEM imaging.

In light microscopy, areas that do not stain with fuchsin lack a canalicular network. The three-dimensional visualization of the lacunar-canalicular network is different in alveolar bone than in mandibular cortex. Scanning electron microscopy helps in distinguishing changes in lacunar-canalicular network due to irradiation and also new bone formation process especially at the bone-implant interface.

References:

1) Huja SS, Fernandez SA, Hill KJ, Li Y. Remodeling dynamics in the alveolar process in skeletally mature dogs. Anat Rec 2006;288A: 1243-1249.
2) Kubek DJ, Gattone II VH, Allen MR. Methodological assessment of acid-etching for visualizaing the osteocyte lacunar-canalicular networks using scanning electron microscopy. Microsc Res Tech 2010; 73: 182-186.

9B.4

Evolution simulations predict variable mechanoregulated endochondral ossification process in animal populations

Hanifeh Khayyeri
Trinity Centre for Bioengineering, Trinity College Dublin, Dublin, Ireland

A new computational framework, combining a mechanoregulated tissue differentiation model and an evolutionary model predict that the mechanoregulated endochondral ossification process is variable within a population of same-species.

Introduction

Mechanical forces regulate the differentiation of mesenchymal stem cell (MSC) into skeletal cells and tissues. However, little is known about the emergence of these differentiation pathways in evolution and the fundamental role of mechanobiology in this process.

It is believed that the ability of cells to adapt to changing mechanical environments, utilising their capacity of modulating their synthetic activities and differentiation pathways, has led to the emergence of novel tissue differentiation processes in evolution, such as the endochondral ossification process. We hypothesise that the emergence of mechanosensitive genes that enable the mechanoregulated endochondral ossification process is sufficient to stabilise the process in a population, since it gives a greater fitness for survival. In particular, we propose that the endochondral ossification process is not optimised in evolution but exists with variability in animal populations.

Methods

The hypothesis of this study was investigated through a computation approach, combining a mechanoregulated tissue differentiation simulation and an evolutionary simulation.

Tissue differentiation simulations: A 3D finite element model of a fracture callus was created and a lattice modelling approach was adopted to model stochastic cell activities. Depending on the magnitudes of biophysical stimulus (fluid flow and shear strain), MSCs could differentiate into osteoblasts, fibroblasts and chondrocytes. Fracture healing simulations were performed with variable biophysical stimulus boundaries (m-value) for the endochondral ossification process, giving different fracture healing times. A fitness function was generated based on the fracture healing times, where animals with fast healing were assigned higher fitness as they had higher chance to survive, compared to individuals with slow healing.

Evolution simulations: A population with 1000 individuals, each equipped with genes (10 alleles) that determined the endochondral ossification response due to loading, was created (initially all allelic values were zero, i.e. the endochondral ossification process did not exist). Random mutations, during recombination, enabled the ability of endochondral ossification (allelic values became non-zero). In each generation, some individuals fractured their bones and those that could heal in shortest time (i.e. had higher fitness) had higher chances to survive and reunite with the non-fractured individuals for mating through random selection. This evolution process was simulated for 1000 generations.

Results and discussion

The simulations predicted that the emergence of mechanosensitive genes that trigger endochondral ossification were favoured by natural selection since they provided greater fitness (through faster healing). The simulations show that after 1000 generations the new gene values have generated a distribution of m-values in the population (Fig. 1), representing a variable mechanoregulated endochondral ossification process in the animal population, which can be associated with the variability reported of in current animal populations. Furthermore, the evolutionary simulation suggest that different distributions of m-values exist for different species, depending on their body weight, where heavier animals require to higher magnitudes of mechanical stimulus and lighter animals respond to lower magnitudes of mechanical stimulus for an endochondral differentiation pathway.

The results have corroborated the hypothesis and emphasised that this kind of model can be used to better understand the fundamental interactions between mechanical forces and biological processes.

Acknowledgements

This work has been funded by Science Foundation Ireland under Grant No. [SFI/06/IN.1/B86].

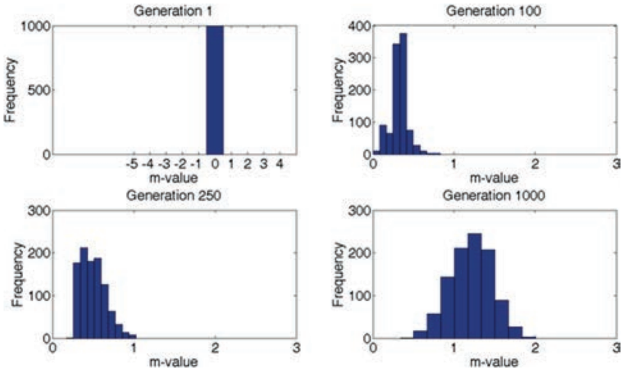

Fig. 1: The emergence of the mechanoregualted endochondral ossification process (m-value) in evolution, after 1, 100, 250 and 1000 generations.

9B.5

A Novel Method for Generating Crack Extension Resistance Curves in Small Bone Samples using High-Speed Videography

Orestis Katsamenis
Bioengineering Sciences Research Group, Faculty of Engineering and the Environment, University of Southampton, Southampton, UK

The research proposes a novel method to overcome the size limitations of measuring strain energy release rate in miniature samples. The method, high speed videography, differentiates between young and old donors and is validated against reference point indentation.

Introduction

Measurement of fracture toughness behaviour of bone tissue, in terms of critical stress intensity factor (K_c) and/or critical strain energy release rate (J-Integral), is becoming increasingly popular as a quantitative way to evaluate bone quality. In many cases, because of bone tissue size limitations, fracture toughness experiments have to be conducted in miniature specimens. The experimental procedure for determining the crack extension resistance curve of a material (R-curve or J-R curve) requires the measurement of the crack extension (Δa; Δa = a_(i) - a₀) that occurs during the loading of a pre-cracked specimen. In the case of small samples, crack propagation may be difficult to assess directly by optical methods. However, damage propagation may be evaluated instead by exploiting the whitening effect which develops in front of the crack tip and extends in a self-similar manner with it. Consequently, whitening front propagation serves as a metric of crack extension. Here we present a new method for generating 'crack' extension resistance curves in miniature bone samples (< 1mm x 1mm x Length) in three-point bending using high-speed videography. Our approach is based on tracking the whitening front propagation and this way indirectly assessing the actual crack propagation (Figure 1). Reference point indentation (RPI) is then utilised as a cross-validation method to measure the indentation distance increase (IDI), known to be inversely proportional to crack growth resistance.

Materials and Methods

Four human femora (females; aged 43, 47, 80 and 83) stored at -80^{ο}C were obtained from IIAM tissue bank. Single-edge notched SE(B) specimens (n = 20) of 0.8 - 0.9 mm width - height and 10 mm long oriented in the antiplane longitudinal orientation where machined from the femora (5 per femur). Toughness experiments were conducted in three-point bending (6 mm span) to failure by means of Bose ElectroForce3200 and recorded using a high speed camera. A custom made Matlab algorithm was developed to track the damage propagation (whitening effect) from the notched edge. Non-elastic fracture mechanics was used for calculating 'crack'-extension resistance curves. RPI measurements were conducted by means of BioDent reference point indenter (Active Life Scientific) onto the same SE(B) samples after the fracture toughness experiments.

Results

Determination of crack (or more accurately 'damage') extension resistance curves were achieved by means of 'Whitening front tracking' method. Our fracture toughness results as expressed by K_{eff} were consistent with the IDI measurements showing that the group of older donors (n=10) exhibits lower fracture toughness (2.13±0.3 MPa.m^{1/2}) and higher IDI (8.2±0.4 μm), while the opposite was true for the group of younger donors (4.7±0.7 MPa.m^{1/2} and 6.9±0.5 μm); $p < 0.05$ in all cases.

Conclusions

Here we present a novel method for generating crack extension resistance curves in miniature bone samples by means of high-speed videography. We show that, for the geometry tested, the whitening effect can be used to generate 'crack' extension resistance curves in small bone samples in a simple and fast manner, with corresponding toughness estimates being seen to be consistent with IDI measurement.

PA.02
HISTOLOGICAL EVALUATION OF A NEW CALCIUM PHOSPATE BIOMATERIAL IN SHEEP

Lorena Benito
University of Salamanca-Faculty of Medicine, Salamanca, Spain

Biocompatible and bioreabsorbible monetite granulates tested in sheep«s bone critical defects showed better defect regeneration and osteointegration than controls with Bio-Oss¨.

Introduction:
Bone autografts are the gold standard of bone defect regeneration and fractures, but owing to their limited availability and their possible side effects it is necessary to search for alternative synthetic materials. Some of the most widely applied synthetic materials are calcium phosphates such as hydroxyapatite (HA) or tricalcium phosphates (TCP) due to their biocompatibility, bioactivity and osteoconductivity.
Based on these materials, in this work a new biomaterial (Sil-Oss®) developed by Azurebio S.L. (Madrid) was evaluated for application in bone regeneration. This biomaterial is composed by monetite partly substituted by zinc and deficient calcium hydroxyapatite (DCHA) granulates embedded in a silica gel matrix. These granulates are biocompatible, reabsorbable and release ionic species such as calcium, phosphorus and silica, which are potentially able to stimulate bone regeneration. The aim of this work was to make a histological evaluation of the tissue response of this biomaterial in osseous defects in a sheep model. Its capacity to stimulate bone regeneration was compared with BioOss®, used as controls.
Material and methods:
The Sil-Oss® and Bio-Oss® granulates, with a particle size between 250 and 1000 µm, were placed in bilateral cylindrical bone defects (8mm x 13mm) in sheep. Some empty defects were kept as controls. After 16 weeks, the animals were sacrificed and bone blocks with osseous defects were radiographed and cut with a saw for their subsequent histologic study. The non-decalcified osseous fragments were fixed, dehydrated and embedded in PMMA. Once polymerized, bone fragments were microtome-sectioned and stained for histological evaluation.
Results:
The empty defects with spontaneous healing used as controls, showed no signs of bone regeneration. These were observed as empty cavities in which adipose tissue had developed.
Regarding the bone defects with BioOss®, these were regenerated but showed many remains of material. These BioOss® remains were integrated into the regenerated trabecular bone (see Fig.1).
Moreover, histological evaluation of the Sil-Oss® granules showed an almost complete reabsorption at 16 weeks. The few remaining granulates were perfectly osteointegrated in the neoformed trabecular bone. Sil-Oss® showed almost complete bone regeneration in bone defects. The neoformed bone was disorganized, with wide and anastomosed trabecular bone (see Fig.2).
A considerable difference was observed between the bone regeneration capacity of the BioOss® and Sil-Oss® granules. The Sil-Oss® granules led to more bone regeneration than remaining material. However, the BioOss® granulates showed the opposite behavior, where remains of osteointegrated material predominated over bone formation.
Discussion/ conclusion:
From the histological evaluation, Sil-Oss® can be said to be biocompatible, bioactive and reabsorbable. In comparison with to BioOss®, the Sil-Oss® granulates showed a greater bone regeneration rate, because its trabecular bone was wider and bone regeneration was enhanced.
Also, the Sil-Oss® granulates showed a greater degree of reabsorption as compared with BioOss®. This was confirmed in the histological evaluation, where more BioOss® particles were integrated into bone trabeculae. The reabsorption rate of Sil-Oss® granulates was variable, due to its chemical composition.
The results show that the Sil-Oss® granulates evaluated could be considered a promising bone regeneration biomaterial.

Granted by MAT2010-18155

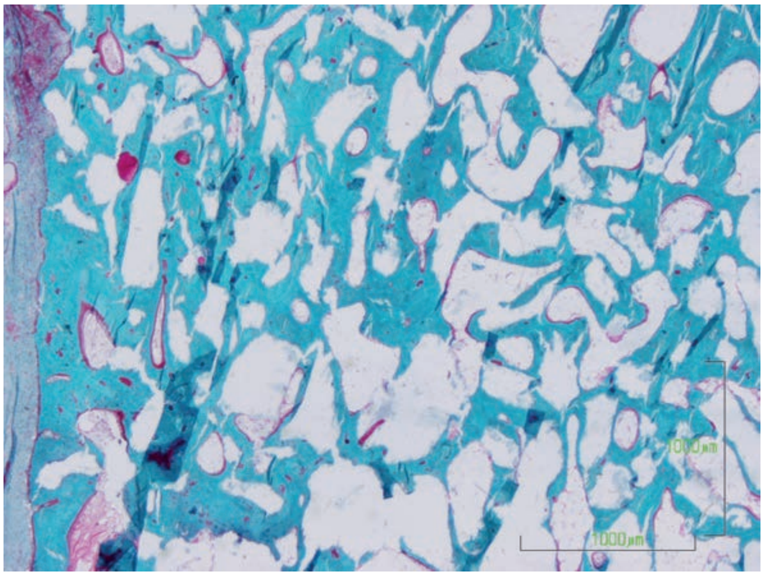

-Fig. 1 (2x) Panoramic view of a defect regenerated with Bio-Oss® granulates. A remarkable degree of Bio-Oss® integration is evident. The neoformed trabecular bone is thin and acicular due to the angular shape of the BioOss® granulates.

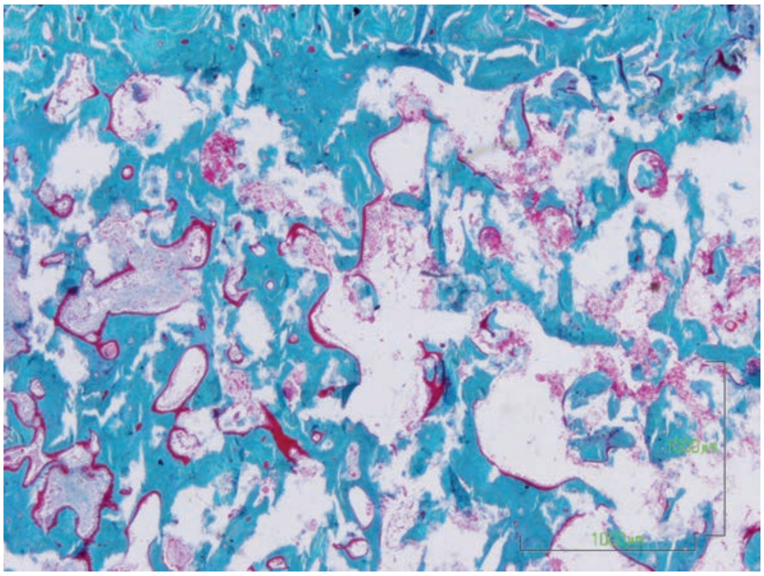

-Fig. 2 (2x) Histological image of the defect regenerated with Sil-Oss® granulates. Wide and anastomosed neoformed trabecular bone is noticeable. Sil-Oss® osteointegration can be observed.

PA.03
Development of Gene Activated Matrices for osteochondral regeneration in osteoarthritis

Matteo D'Este
AO Research Institute, Davos Platz, Switzerland

Thermoresponsive hydrogels were proven to be suitable matrices for biphasic calcium phosphate and magnetic nanoparticles used for hyperthermia induction and transfection. The composites are injectable osteoconductive bone void fillers and gene activated matrices featured by on demand" gene activation."

Introduction

Thermoresponsive hydrogels are promising matrices in musculoskeletal tissue engineering [1]. In this work, we assessed the suitability of a thermoresponsive hyaluronan hydrogel as carrier for smart bioceramics [2] and magnetic nanoparticles (MNPs). Layering of the different composites and the activation of gene expression "on demand" via a heat-inducible plasmid by an alternating magnetic field are tools for the spatiotemporal control of gene expression essential for the regeneration of different musculoskeletal tissues.

Materials and Methods

Amino-terminated poly(N-isopropylacrylamide)(pNIPAM-NH_2) was conjugated to hyaluronic acid (Hyal) via amidation chemistry to give Hyal-pNIPAM thermoresponsive hydrogels. Degree of substitution determined via ^1H NMR spectroscopy was 6.5±1% mol. Hyal-pNIPAM was dissolved at 10 % w/w in PBS solution. Biphasic Calcium Phosphate (BCP) unsintered powder with a granule size ranging from 2 to 200 µm (Biomatlante SA, France) were added at 1:1 to 1:8 polymer:granules weight ratio and mixed manually into the Hyal-pNIPAM solution. MNPs composites were prepared similarly [3]. Sterilization was performed on freeze-dried samples by treatment with gamma (25 kGy) and beta (15, 25, 40 kGy) radiation followed by rehydration for rheological characterization. Sol-gel transition capability was assessed as ratio between elastic moduli at 25°C and 35°C. Rheology: composites were subjected to 1 °C/min heating from 20 to 40°C at 1 Hz using a TA Instruments AR2000ex Rheometer equipped with a Peltier controller and plate-plate geometry. Differential Scanning Calorimetry (DSC) was performed on a Pyris DSC-1 Perkin-Elmer instrument calibrated with indium.

Results

The rheological analysis demonstrated that composites exhibit the temperature induced gelation up to 1:8 polymer:granules weight ratio. Even at the highest particle content viscoelastic shear moduli of the composites resulted < 100 Pa, making them injectable through a cannula. DSC confirmed the trend of the rheology data, showing decrease in transition temperature at increasing particles concentration. Radiation sterilization resulted in a minor loss of viscoelasticity, without compromising the temperature-induced sol-gel transition.

Conclusion

We have demonstrated that Hyal-pNIPAM hydrogels are suitable carriers for osteoconductive granules and selected MNPs. Composites maintain thermoresponsiveness and gamma- or beta-irradiation is a suitable method for their sterilization. Injectability makes them suitable for minimally invasive surgery. The non-covalent gelation of the composites improves cohesion potentially avoiding the delayed implant colonization observed for chemically crosslinked carriers [4]. Bioceramic composites are osteoconductive, while MNP composites can activate osteoinductive growth factors expression "on demand" under an alternative magnetic field. These features are meant to provide different gene activated matrices for the regeneration of the different tissues involved in osteoarthritis.

Acknowledgments

The research leading to these results has received funding from the European Union's 7th Framework Program under grant agreement n° NMP3-SL-2010-245993.

References

[1] M. Peroglio, et al, Eur Spine J. 2011.
[2] G.Daculsi, F.Jegoux and P. Layrolle (2009). in Advanced Biomaterials: Fundamentals, Processing, and Applications book, Advanced Biomaterials: Fundamentals, Processing, and Applications, B.Basu et al ed, John Wiley and sons Inc., pp 101-141
[3] V. Ortner, et al, J Control Release, 2012,158,424-432.
[4] G. Daculsi, et al J Mater Sci: Mater Med, 2010, 21, 855-861.

PA.04
ANTIBACTERIAL PROPERTIES OF TI-O DOPED WITH DIFFERENT CONCENTRATIONS OF SILVER

Jaime Esteban Moreno
IIS-Foundation Jimenez Diaz, Madrid, Spain

This study evaluates the adherence of Staphylococcus spp to a Titanium-Aluminium-Vanadium (Ti-Al-V) surface modified by cathodic arc deposition of a Ti-O layer with several concentrations of silver oxide.

Introduction

Implant infection still represents a major clinical problem in orthopedic surgery and adherence is the first step in the pathogenic process. Interactions between bacteria and a substratum surface depend largely on the surface and near-surface atomic structure and composition of implanted biomaterials. It is known that TiO2 possesses potential antimicrobial activity due to its strong photo-oxidation ability. It is desirable to combine the advantages of Ag with TiO2 to produce a kind of low-cost Ag-doped TiO2 coating with allweather antimicrobial property. Ag can act as both an antimicrobial auxiliary agent and a sink for electrons and redox catalyst that may enhance the overall photo-oxidation ability of TiO2.

Material & Methods

On the surface of a sample of Ti-6Al-4V films doped with Ag and Ti-O by pulsed cathodic arc technique, yielding 3 different samples: a) Ti-O, b) Ti-O with low concentration of silver (6,4%) c) Ti-O with high concentration of silver (17,3%).

Microbial adhesion tests, using collection strains of Staphylococcus aureus 15981 (Valle et al.) and Staphylococcus epidermidis ATCC 35984 and two clinical strains of each species, were performed in triplicates using Kinnari et al. protocol (J Biomed Mat Res Part A. 2008. 86:760-8).

For the statistical study non parametric tests were used. Mann-Whitney or Wilcoxon were used for two samples and the Kruskal-Wallis test was used for more than two samples. EPI-Info software version 3.5.1 (CDC, Atlanta, GA. USA) was used to perform these studies.

Results

Both collection strains showed a statistically significant decrease in adherence to the modified materials compared to unmodified material ($p < 0.0001$, Kruskal-Wallis)(Fig.1). The adhesion decreases as concentration of silver increases. S. epidermidis showed greater adherence than S. aureus for all materials ($p < 0.0001$, Kruskal-Wallis test). The only difference that was not statistically significant was the adhesion between Ti-O and Ti-O with low concentration of silver (2%) for S. epidermidis.

With respect to the clinical strains(Fig1), P53 is the only one that showed statistically significant differences in adhesion between material modified with Ti-O and the unmodified one and also statistically significant decrease of adhesion between the materials modified with silver in favor of a lower concentration. All others have no statistically significant differences between the materials modified with silver. All other strains showed significant differences only with to the materials modified with silver.

Discussion/Conclusion

Our results showed that both S. aureus and S. epidermidis decreases significatively the bacterial adherence on materials modified with silver. Ti-O in the absence of silver does not diminish such adhesion. A lower concentration of silver is enough to exert its catalytic effect with Ti-O achieving a decrease in bacterial adherence. These results demonstrate also the antibacterial properties for titanium oxide in the absence of UV light and enable the use of cheaper silver coatings.

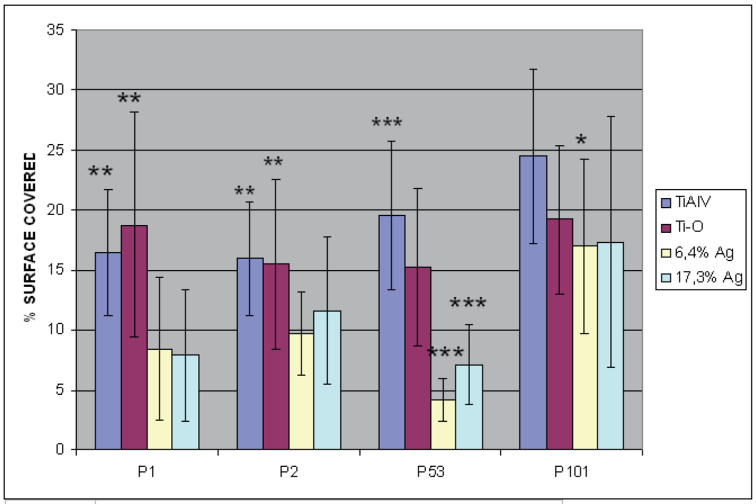

*	Difference statistically significant with Ti-Al-V
**	Difference statistically significant with the materials modified with silver
***	Difference statistically significant with all the other materials

Percentage of area covered by each type of material for clinical strain

PA.05

COMBINED DIFFUSIVE/PVD COATNG SOLUTIONS IN MODULAR COUPLINGS TO IMPROVE IN VIVO LIFE-TIME OF ORTHOPAEDIC IMPLANTS

Elia Marin
University of Udine, Udine, Italy

In this work, innovative combined PVD/diffusive treatments were used on biomedical titanium alloys in order to improve the durability of modular titanium prosthetic implants. The combination of nitriding and PVD enhanced the durability of Grade 5 titanium under corrosion-fretting conditions.

Introduction and Aim:
Titanium alloys are nowadays used for a wide range of biomedical applications, thanks to their combination of high mechanical resistance, high corrosion resistance and biocompatibility. Nevertheless, the applicability of titanium alloys is sometimes limited due to their low microhardness and tribological resistance and thus may fail or break if applied on prosthetic joint couplings (Rodrigues 2009). A wide range of surface treatments have been used in order to improve the tribological behaviour of titanium alloys and in particular PVD coatings such as CrN and TiN (Fu 2000), but the low microhardness of the titanium substrate often resulted in coating failure due to cracks and delamination (Goldberg 2004). The aim of this study has been the development of hybrid technologies based on microhardness enhancing-diffusive treatments and subsequent PVD coatings to improve the overall coating resistance and prevent delamination, particularly in-vivo.
Materials and Methods:
In this work, two series of samples of different coatings in CrN (A) and TiCN (B) on a Ti Grade 5 alloy substrate have been characterized. Serie 1 consisted of conventional PVD coatings; while Serie 2 was obtained from a combination of a diffusive thermal treatment and PVD. The different treatments have been studied by means of Scanning Electron Microscopy both on the sample surface and in cross-section. In-depth composition profiles have been obtained using Glow Discharge Optical Emission Spectrometry (GDOES) and localized Energy Dispersive X-Ray Diffraction (EDXS) on linear scan-lines. The micro-hardness and adhesion properties of the different treatments have been evaluated using Vickers micro-hardness tests at different load conditions. The corrosion resistance of the different treatments has been studied using Linear Voltammetry in a 9 g/l NaCl solution and in an aggressive solution containing 9 g/l of NaCl, 5 ml/l of HCl and 2 g/l of Tri-Calcium-Phosphate, to obtain an accelerated simulation of the most challenging conditions that may be found in-vivo after the implantation of a titanium joint prosthesis. The tribological behaviour of the different treatments has been tested both in dry conditions and in the two different lubricant fluids.
Discussion and Conclusion:
The standalone PVD coatings showed a limited tribological resistance due to the low hardness of the substrate, which resulted in fractures and delamination. The combination of a diffusive process and a subsequent PVD coating showed a stronger effect in improving the tribo-corrosion resistance of the substrate, particularly in aggressive media, resulting in a sensibly longer component life even in extreme conditions.

-A fractured modular Titanium/Titanium junction

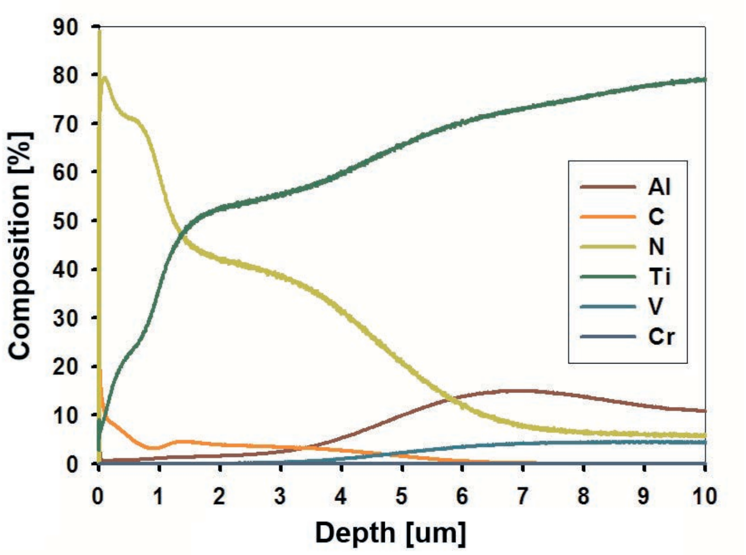

-Example of composition in-depth profile for nitrided + PVD (TiCN) coated samples, as obtained by GDOES technique.

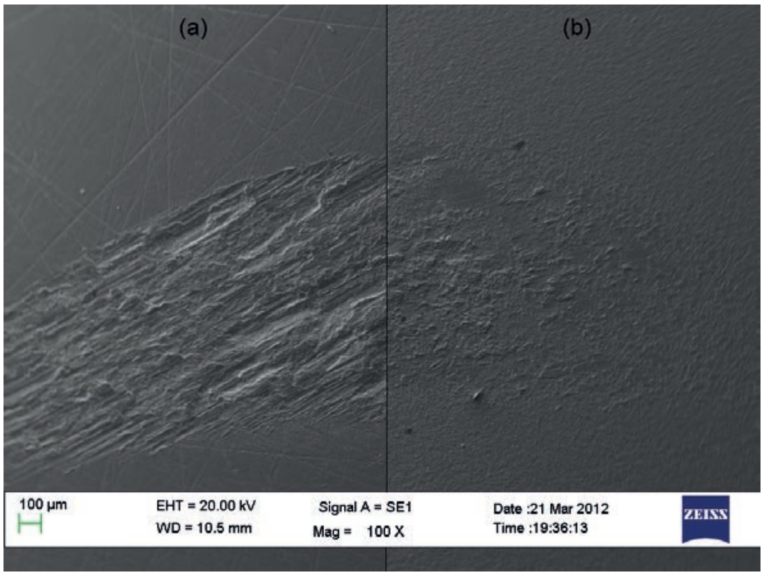

-SEM images of (a) the intense wear of Grade 5 titanium and (b) the low wear of nitrided + PVD coated titanium after tribological testing.

PA.06
EVALUATION OF A NEW CALCIUM PHOSPATE BIOMATERIAL BY MULTIPLE FLUORESCENCE BONE-LABELLING

Lorena Benito
University of Salamanca-Faculty of Medicine, Salamanca, Spain

The use of fluorochromes allows the study of bone formation dynamics in order to test the bone regeneration capacity of new biomaterials.

Introduction:
Labelling of the skeleton with intravital marker substances allows qualitative and quantitative estimations of bone formation and remodeling to be made. Fluorochromes used for bone labelling are calcium-seeking substances that are incorporated into the mineralization front of mineralizing surfaces. In this work, the bone regeneration dynamics of a new biomaterial (Sil-Oss®) developed by Azurebio S.L. (Madrid) is evaluated. This biomaterial is made up of monetite and deficient calcium hydroxyapatite granulates embedded in a silica gel matrix. The aim of this work is to assess its bone regeneration potential in osseous defects in a sheep model. Its capacity to stimulate bone regeneration is compared with BioOss®.
Material and methods:
The Sil-Oss ®granulates, with a particle size between 250 y 1000 µm, were placed in bilateral cylindrical bone defects (8mm x 13mm) in sheep. Some defects were filled with BioOss® granulates, as regenerative bone controls. A multiple bone-labelling with four fluorochromes was performed. Each was administered intravenously every four weeks in the following correlative order: tetracycline (25mg/mL), calcein (20mg/mL), xylenol orange (90mg/mL) and alizarin complexone (30mg/mL). After 16 weeks, the animals were sacrificed and bone blocks with the osseous defects were cut with a saw. The non-decalcified osseous fragments were fixed, dehydrated, and embedded in PMMA. Once polymerized, the bone fragments were microtome-sectioned. The histological specimens were observed with fluorescence light microscopy using different filters to show each fluorochrome colour: yellow-tetracycline, green-calcein, orange-xylenol and red-alizarin.
Results:
The bone defects filled with BioOss® were almost completely regenerated. They showed a predominant signal of the two first fluorochromes administered. Tetracycline marks in the inner part of the new formed bone were observed, whereas signals of calcein, administered 8 weeks after BioOss® implantation, were mostly localized in the regenerated trabecular bone surface (see Fig.1). The osteointegration of many BioOss® particles was also clearly evident.
Additionally, fluorescence microscopy of Sil-Oss® granulates samples indicated three bone marking labels (see Fig.2). Calcein, xylenol and alizarin were consistently observed to lie in parallel and with a certain distance between one another. In some cases, calcein was seen to be in direct contact with the surface of the osteointegrated monetite granulates. No tetracycline marks were evident. The biomaterial studied showed almost total bone regeneration in the bone defects. The few remaining granulates were perfectly osteointegrated into the trabecular neoformed bone.
Discussion/ conclusion:
From the fluorescence evaluation, it may be inferred that bone regeneration follows different dynamics in BioOss® and Sil-Oss® granulates. In BioOss®, mainly the first two fluorochromes were detected, showing that bone formation was almost complete at 8 weeks. In contrast, in the monetite granulates the three latest markers appeared, revealing continuous bone formation during the 16 weeks of study. Also, the absence of tetracycline marks indicated remodelling or reabsorbing processes. In fact, the differences in bone-labelling highlighted the better and more sustained capacity of bone regeneration in the case of Sil-Oss® granulates in comparison with BioOss®.
The results show that the Sil-Oss® granulates evaluated could be considered as a promising bone regeneration biomaterial.
Granted by MAT2010-18155.

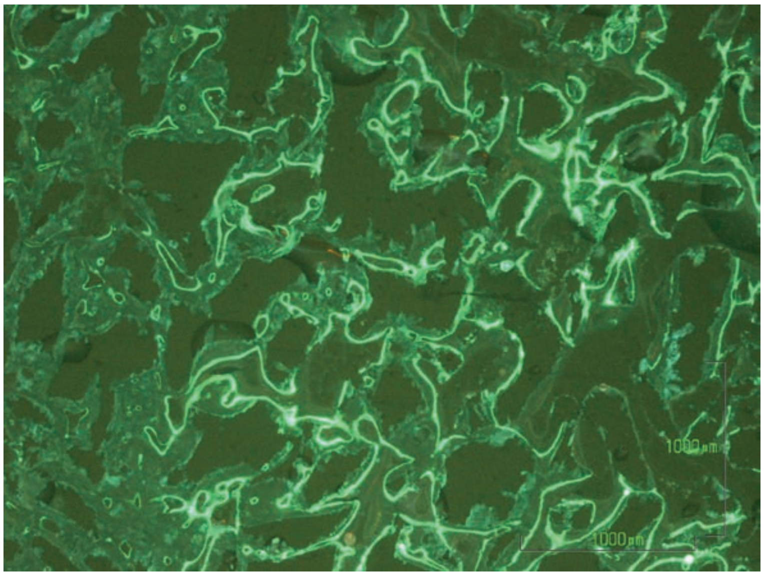

Fig. 1 (2x). Panoramic view of a defect regeneration with BioOss®. Calcein marks were the most abundant. Yellow-tetracycline lines were less evident.

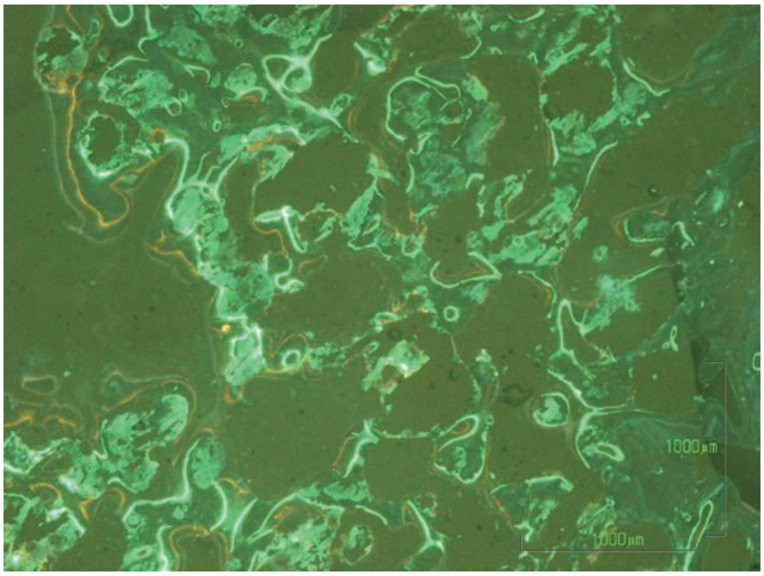

Fig. 2 (2x). Fluorochrome-labelled bone within Sil-Oss® granulates. Different marks can be distinguished (green- calcein, orange-xylenol and red-alizarin).

PA.07
Seeding of mesenchymal stromal cells on high and low porosity tricalcium phosphate scaffolds

Arina Buizer
University Medical Center, Department of Orthopedic Surgery, Groningen, The Netherlands

The porosity of tricalcium phosphate scaffolds is of influence on the efficacy and homogeneity of hMSC cell seeding. In low porosity scaffolds a vacuum cell seeding method is suitable, while in high porosity scaffolds a static seeding method is preferred.

Introduction

Constructs of porous tricalcium phosphates seeded with human mesenchymal stem cells (hMSCs) are a promising replacement for autologous bone grafts in the repair of bone defects. An adequate cell seeding technique is essential for effective bone regeneration. Static seeding, in which cells are passively mixed with a scaffold, is the most frequently used cell seeding technique. Several dynamic cell seeding techniques, in which an external force is applied, have attracted attention lately. A suitable seeding technique has several requirements: efficient cell seeding, homogenous distribution of seeded cells, minimized cell damage due to seeding, reproducibility and ease of use. In case of point-of-care seeding, the technique should be rapid. Tricalcium phosphate products are available in different porosities. We hypothesize that the porosity of the scaffold influences cell seeding efficiency and homogeneity. In previous studies, vacuum seeding seemed more effective than static seeding on low porosity TCP scaffolds. The aim of this study was to determine which cell seeding technique is most suitable for high porosity scaffolds in a point-of-care setting: static or vacuum seeding.

Patients and Methods

Human mesenchymal stem cells (hMSCs) were isolated by Ficoll density gradient centrifugation from reaming debris that was collected during total hip replacement. The cells were seeded on low porosity (45%) and high porosity (90%) tricalcium phosphate scaffolds by a static and a vacuum seeding technique. At 1, 3, and 7 days after seeding, cell proliferation was measured by a cell proliferation assay. Cell distribution was imaged by confocal microscopy after LIVE/ DEAD® staining of the cell-scaffold constructs. Cell seeding efficiency was assessed for each technique. Cell viability was assessed by creating growth curves of vacuum treated and cells not treated with vacuum .

Results

Neither static nor vacuum seeding methods did result in homogenous cell seeding in both scaffold materials. In low porosity tricalcium phosphate scaffolds hMSCs seeded with a static seeding method did not penetrate into the core of the scaffold, while with a vacuum seeding method inhomogeneous cell distribution was accomplished. In high porosity tricalcium phosphate scaffolds, a vacuum hMSC seeding method resulted in higher cell death after seeding than static seeding. After 7 days the difference in cell death was negligible. The number of life cells after seeding on a high porosity scaffold was higher in static cell seeding than in vacuum seeding at all time points.

Discussion / Conclusion

Vacuum cell seeding appears the preferred cell seeding method for low porosity tricalcium phosphate scaffolds, as cells penetrate into the scaffold deeper than in a static cell seeding method. Static seeding is the preferred cell seeding method on high porosity scaffolds in a point-of-care setting, as there is higher cell survival after seeding and it is easier to use than a vacuum seeding technique.

PA.08

Effect of thermal treatment on the nanostructure and mechanical properties of crosslinked Vitamin-E-blended UHMWPE

Andrew George
Department of Orthopedic Surgery, Brigham and Women's Hospital, Harvard Medical School, Boston MA02115, USA

It is widely accepted that radiation crosslinking for polyethylene used in prostheses results in improved wear resistance but a reduction in ultimate tensile properties. This study shows how various thermal treatments prior to crosslinking are able to enhance these properties.

To be reviewed
Introduction:
Incorporation of Vitamin E into polyethylene (PE) used in total joint replacements can decrease the rate of oxidative degradation while radiation crosslinking is known to substantially increase the wear resistance of PE. However, crosslinking also results in a decrease in mechanical properties, especially ultimate tensile strength and ductility (maximum strain), which has been a concern especially for joints where such components are subjected to high stresses. The goal of this study was to determine the effect of thermal treatments on the morphology and mechanical properties of Vitamin-E-containing PE. We hypothesised that ultimate tensile properties could be enhanced using thermal treatments prior to radiation crosslinking.
Methods:
Compression moulded sheets (MediTech Medical Polymers Inc) of 0.1% vitamin-E-blended GUR 1020 PE (Ticona,Oberhausen,Germany) were machined into 2mm slices. Samples were melted at 180°C before quenching in ice water. A second group was quenched followed by annealing at 126°C for 24 hours. One-half of each material was then irradiated at a dose of 100kGy at room temperature using electron beam radiation. All samples were compared to untreated control PE. Tensile tests were carried out on ASTM 638-Type V specimens punched from each sheet by stretching at a nominal strain rate of 10mm/min to determine: ultimate tensile strength (UTS), maximum strain and work of Fracture (WOF). Differential scanning calorimetry (DSC) was performed to determine the degree of crystallinity and lamellar thickness of samples and equilibrium swelling experiments provided the crosslink density of irradiated samples.
Results:
Average crosslink density for irradiated samples was 0.200mol/dm3 ± 0.009. Quenched PE had 27% reduced crystallinity and 26% lower lamellar thickness as compared to the control whereas quench 126 PE only had 7% reduced crystallinity and 11% lower thickness than control PE (p0.05). WOF was also significantly lower in the crosslinked samples (p0.05) but the maximum strain was 18% higher ($p<0.05$).
Discussion/Conclusion:
This study shows how significant differences in tensile properties can be achieved by varying thermal treatments. Quenching increases the ductility (maximum strain) of PE substantially while decreasing UTS. Further annealing at 126°C for 24 hours increases the UTS substantially so that both UTS and ductility are high. After radiation, UTS becomes comparable to control irradiated PE but the ductility remains higher. Thus, it may be possible to offset the reduction afforded by radiation crosslinking by optimisation of processing conditions to provide enhancement in tensile properties prior to crosslinking; especially ductility, which is a measure of brittleness of the polymer.

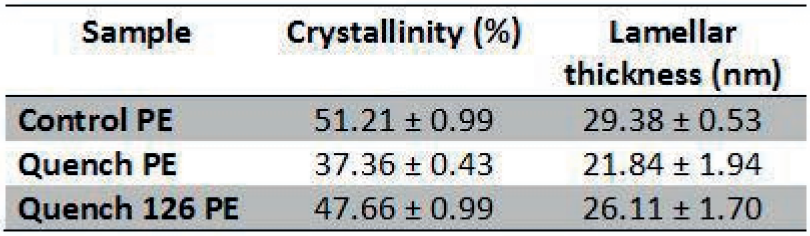

Sample	Crystallinity (%)	Lamellar thickness (nm)
Control PE	51.21 ± 0.99	29.38 ± 0.53
Quench PE	37.36 ± 0.43	21.84 ± 1.94
Quench 126 PE	47.66 ± 0.99	26.11 ± 1.70

-Table 1. Crystallinity and lamellar thickness for sample groups (mean ± standard deviation)

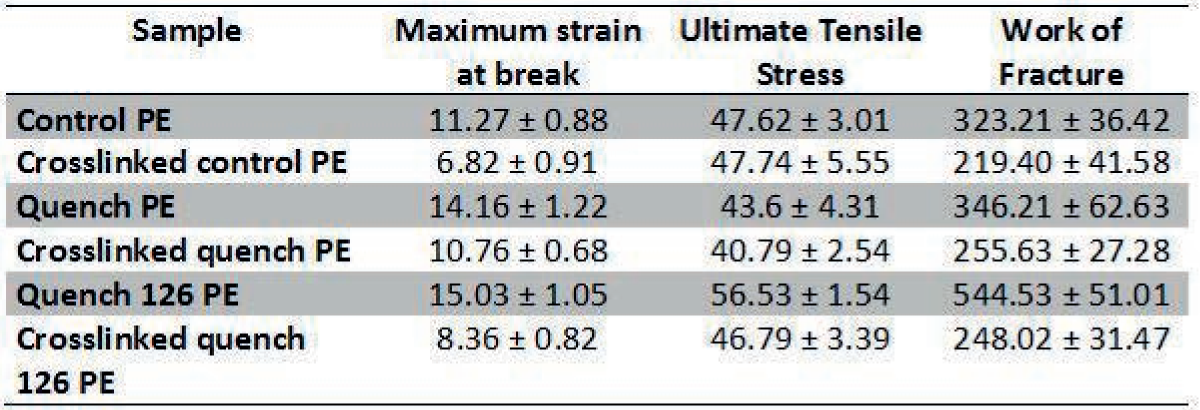

Sample	Maximum strain at break	Ultimate Tensile Stress	Work of Fracture
Control PE	11.27 ± 0.88	47.62 ± 3.01	323.21 ± 36.42
Crosslinked control PE	6.82 ± 0.91	47.74 ± 5.55	219.40 ± 41.58
Quench PE	14.16 ± 1.22	43.6 ± 4.31	346.21 ± 62.63
Crosslinked quench PE	10.76 ± 0.68	40.79 ± 2.54	255.63 ± 27.28
Quench 126 PE	15.03 ± 1.05	56.53 ± 1.54	544.53 ± 51.01
Crosslinked quench 126 PE	8.36 ± 0.82	46.79 ± 3.39	248.02 ± 31.47

-Table 2. Tensile properties for sample groups (mean ± standard deviation)

PA.09
Osteoinductive Potential of Different Collagen/TCP Scaffolds in Canine Intramuscular Defect

Ali Ismailoglu
NuVasive, San Diego, CA, USA

Osteoinductive potential of two different types of in-house developed collagen/TCP scaffolds with varying collagen sources and different structures were compared to commercially available Vitoss BA (Orthovita/Stryker Inc., Malvern, PA) in an intramuscular defect model in canines.

Introduction:
Calcium phosphate-based bioceramics have been used as synthetic bone graft substitutes for several decades due to their close resemblance to the mineral component of bone. To enhance bone regeneration, researchers have focused on the effect of chemical composition of these materials as well as on the micro and macro surface topographies and porosity. Recently, several research groups have reported intramuscular bone formation of calcium phosphate based materials in different animal models[1]. We have developed a novel scaffold composite material that is composed of a microstructured tricalcium phosphate (TCP) known to induce bone formation when implanted intramuscularly, combined with fibrillar collagen. The goal of this study is to evaluate the tissue responses after intramuscular implantation of various collagen/TCP scaffolds.
Patients & Methods:
in vivo performance of commercially available Vitoss BA (Orthovita/Stryker Inc., Malvern, PA) was compared to two different types of collagen/TCP scaffolds with varying collagen sources and different structures (Figure 1). The in-house developed collagen/TCP scaffolds were prepared with the same weight percentage either with fibrillar Type I tendon collagen (Proto1) or non-fibrillar Type I dermal collagen (Proto2). For both prototypes, a microstructured TCP (ßTCP/HA) ceramic material with consistent surface micro features with particle size range between 0.5-1mm and surface average pore size of 500nm was used. A canine intramuscular model was performed to measure bone induction with these materials. Following IACUC approval, intramuscular implantation was performed on 10 dogs. 1cc of implant was inserted in each muscle pocket without addition of bone marrow or growth factors. End of 12 weeks animals were euthanized and implants were prepared for histology and histomorphometry evaluation.
Results:
Bone induction occurred only with the prototypes containing microstructured TCP but the amount of bone varied by the collagen type (Figure 2). After 12 weeks the bone incidence was 7/7 for Proto1, 1/9 for Proto2 and 0/7 for Vitoss BA. Bone apposition was significantly higher ($p< 0.05$) in Proto1 (2.7±1.8%) and followed by Proto2 (0.01±0.03%) and Vitoss BA (0%). According to the histological and histomorphometrical results intramuscular bone formation is affected by TCP microstructure and collagen microstructure (Figure 3). The results confirm that intramuscular bone formation is achievable with specific microstructured TCP granules and a collagen matrix. However, the structure of the collagen may also play a significant role in this bone forming response, since dermal collagen almost totally inhibited bone formation, while the fibrillar collagen supported bone formation. Additionally, in Vitoss BA, intramuscular bone formation was not observed.
Conclusions:
In this study we have demonstrated a novel collagen/TCP scaffold that is able to induce intramuscular bone formation without the addition of bone marrow or growth factors. To our knowledge, this is the first reported instance of a collagen/TCP composite with this property. While it is known that the submicron morphology properties of the TCP granules need to be within a critical range[2], this study demonstrated that the structure of the collagen was also important.

References:
1. Yuan H., Proc Natl Acad Sci., 2010, 107:13614-9
2. Fellah B., Key Eng Mat., 2007, 330-332:1063-1066

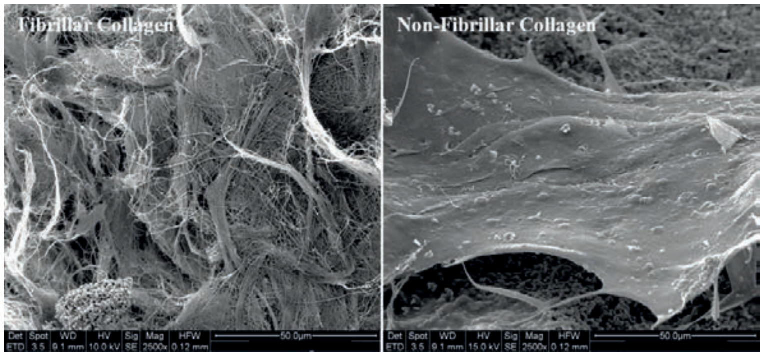

-SEM images comparison of two different types of collagens (fibrillar vs. non-fibrillar)

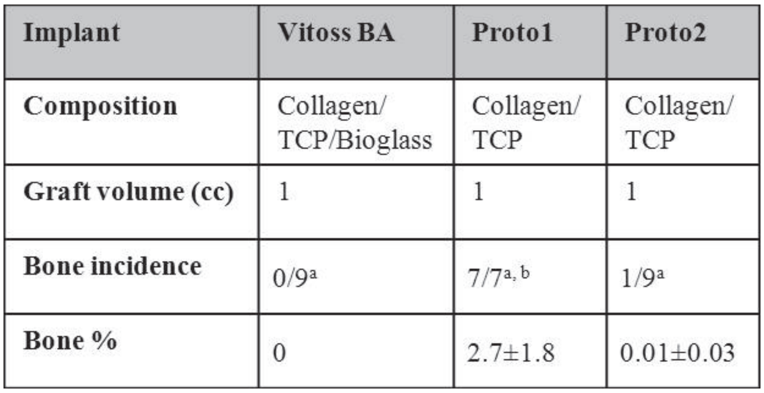

Implant	**Vitoss BA**	**Proto1**	**Proto2**
Composition	Collagen/ TCP/Bioglass	Collagen/ TCP	Collagen/ TCP
Graft volume (cc)	1	1	1
Bone incidence	0/9[a]	7/7[a, b]	1/9[a]
Bone %	0	2.7±1.8	0.01±0.03

-Histology results (a; 1 animal was lost due to infection, b; 2 samples were lost)

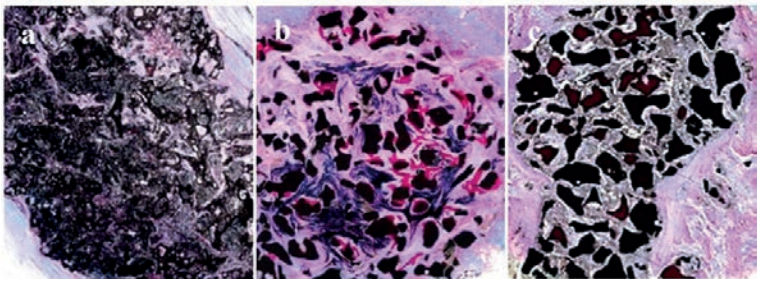

-Histological comparison of implants. (a) Vitoss BA, (b) Proto1, (c) Proto2. Black: granules Red: new bone. No bone formation was observed with Vitoss BA

PA.11
Ti6Al4V after UV-C irradiation: Bactericidal and electrical surface behavior

Miguel Angel Pacha Olivenza
Networking Research Center on Bioengineering, Biomaterials and Nanomedicine CIBER-BBN, Badajoz and Department of Applied Physics, Faculty of Sciences, Badajoz, Spain

Ti6Al4V surface exhibits bactericidal properties and modifications in its electrical characteristics after UV-C exposure. In this research, as part of a larger study to understand that simultaneous bactericidal behavior, we analyze electrochemically how its conductivity is affected after UV-C exposure.

Introduction:

Microbial infection is one of the most destructive complications related to orthopedic implants because antimicrobial therapy usually lacks efficacy when the infection process is detected. In addition, the standarised biomaterial antibiotic-coating has sometimes been criticized because it can increase the microbial resistance to such drugs. By this reason, recent research has been focused on proposing alternative surface modifications able to minimize or even avoid the proliferation of microbial cells on the implant surface.

In this context, the Ti6Al4V alloy is one of the most widely used biomaterials in orthopedic and dental applications due to their excellent mechanical properties and resistance to corrosion, which, in turn, is also due to a thin and chemically stable oxide film predominantly composed of TiO_2 that spontaneously develops on the material surface under ambient conditions. TiO_2 is a n type photoactive oxide semiconductor, able to change its physico-chemical properties after exposure to UV irradiation [1]. The photoactivation of TiO_2 under UV-light has been associated to bactericidal properties in different environmental areas. However its translation to the biomedical field has been limited to the necessity to irradiate the implant in situ.

This research presents the beneficial bactericidal post-UV-radiation and the electrochemistry behind the simultaneous surface conductivity change of the Ti6Al4V.

Materials and Methods:

The Ti6Al4V samples were used without being irradiated (control) and after 15 h irradiation (UV) with a UV lamp (257 nm). Three gram-positive bacteria with different EPS-production were used: Staphylococcus aureus ATCC29213, Staphylococcus epidermidis ATCC35984 and Staphylococcus epidermidis HAM 892.

Bacterial adhesion experiments were carried out with the help of a sterile reusable silicone chamber fixed to the sample surface. Then the bacterial suspension was added to the chamber well and the contact with the alloy surface was allowed for 60 min. After the adhesion time, the silicone chamber was removed and the viability test Live/Dead Baclight L-7012 were carried out to show the viability of adhered bacteria to the Ti6Al4V surface.

The electrochemical characterization (electrochemical impedance spectroscopy (EIS), potentiodynamic polarization studies and Mott-Schottky analysis) was carried out in a conventional electrochemical cell.

Results and Discussion:

All bacteria deposited directly on the control surface are 100 % viable (green), while bacteria attached to the irradiated surface show a progressively loss in viability. After 60 min of contact all bacteria are completely damaged-dead (red). We hypothesized that there is some correlation between the degradation of the bacterial cells and the changes in conductivity in the surface. To test this hypothesis a thin opaque conducting film was placed over the irradiated surface immediately after turning off the lamp so, bacteria were not in direct contact with the irradiated surface but “connected” to it through a conductor. The viability test confirmed the degradation of bacteria in such condition (see Fig.1). EIS and Mott-Schottky curves further confirmed this electrical change in the surface and the anionic polarization curves detected higher corrosion currents after irradiation.

References:

[1] Pacha-Olivenza et al. J Colloid Interf Sci 320(2008) 117-124.

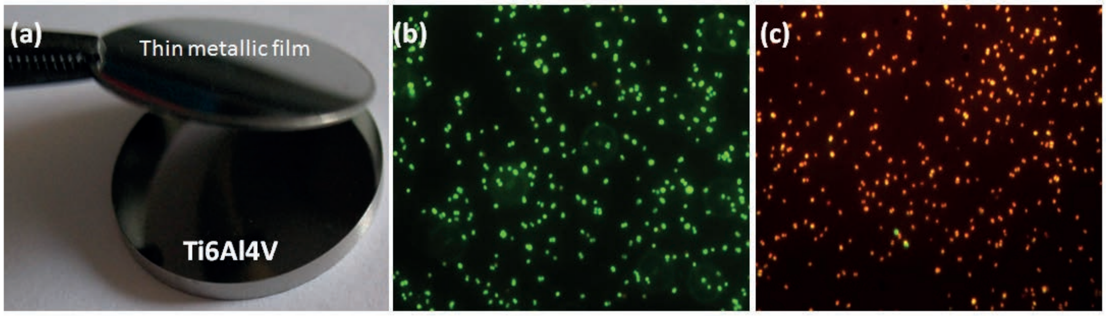

Adhesion experiment in which bacteria were not deposited directly in contact with the Ti6Al4V surface but on a thin metallic film dropped previously on the Ti6Al4V surface (a). Images of green (live) or red-like (dead or damaged) stained adhered bacteria on the control (b) or UV (c) Ti6Al4V surface.

PA.12
ANTIBACTERIAL EFFECTS OF SILVER ION IMPLANTATION

Jaime Esteban Moreno
IIS-Foundation Jimenez Diaz, Madrid, Spain

Implant infection still represents a major clinical problem in orthopedic surgery. We therefore tested the in vitro antibacterial effects of silver (Ag)-ion implantation.

Introduction
'Infections associated with surgical implants generally starts with bacterial adhesion to the biomaterial. The number of adhered bacteria depends on several properties of the surface. To avoid bacterial adhesion without drugs may be one of the best ways to reduce orthopedic implant infection. It would be desirable to develop implant coatings that are repellent to bacteria in order to minimize the implant colonization.
'Patients & Methods
'Discs of a commonly used titanium alloy (Ti_6Al_4V) surface were treated by Ag-ion implantation with different silver dosage ($2x10^{17}$ $5x10^{16}$ and $1x10^{16}$(ion/cm^2) at energie of 100keV). Ti_6Al_4V coupons modified were compared with controls Ti_6Al_4V coupons.
'Microbial adhesion tests using collection strains of Staphylococcus aureus 15981 (Valle et al.) and Staphylococcus epidermidis ATCC 35984 were performed in triplicates using Kinnari et al. protocol (J Biomed Mat Res Part A. 2008. 86:760-8). The number of microphotographs studied was 24 per each material and bacterium.
'For the statistical study non parametric tests were used. Mann-Whitney or Wilcoxon were used for two samples and the Kruskal-Wallis test was used for more than two samples. EPI-Info software version 3.5.1 (CDC, Atlanta, GA. USA) was used to perform the statistical studies.
'Results
'Both strains showed decreased adherence to modified materials. The differences between Ti_6Al_4V surface and Ti_6Al_4V with Ag were statiscally significant for S. aureus and S. epidermidis (pS. epidermidis showed higher adherence to these materials than S. aureus.). The only difference that was not statistically significant differences was the adhesion between surface treated by Ag-ion implantation with dosages of $2x10^{17}$ and $5x10^{16}$.
'Discussion/Conclusion
'No statistically significant differences were observed with a dosage of $5x10^{16}$ in bacterial adherence. These results indicate that Ag-ion implantation may have a potential role in the prevention of implant-related infections though avoiding bacterial adherence.

PA.13

A Novel Mixing Method For The Incorporation Of Gentamicin Into Orthopaedic Bone Cement

Davinder Bhachu
Department of Biomaterials, King's College London, London, UK

We present a novel method of incorporating Gentamicin into orthopaedic bone cement. Results have shown a reduced peak polymerisation termperature and significantly improved compressive strength compared with bone cement formulations with and without antibiotic incorporation.

Background :
Antibiotic loaded bone cement (ALBC) was introduced in 1970 as a means to reduce prosthesis related infections[1]. Antibiotic inclusion into bone cement has been poorly studied and currently factory mixing and intraoperative manual incorporation are the two most common methods used. It has been documented that manual mixing of antibiotics can lead to a significant decline it it's mechanical properties[2]. It is postulated that these methods lead to heterogenous distribution of antibiotic which in turn could lead to poor reproducibility of clinical outcomes.
Methods :
A novel concept of antibiotic incorporation was devised to solve the problem of heterogenous distribution. Gentamicin, a commonly used antibiotic in orthopaedic surgery was combined with ethanol and then combined with the powder component of bone cement (Smartset MV, DePuy) and allowed to dry. The concept is to coat the individual beads of the bone cement power component with antibiotic in order to achieve a more homogenous distribution. Analysis of the tensile and compressive strengths under dry conditions as well as the thermokinetic properties (dough time, working time and setting time) were performed. Comparisons were made to that of factory produced gentamicin loaded bone cement (Smartset GMV, DePuy) & (Smartset CMW 2000 Gentamicin, DePuy), manually mixed powdered gentamicin with Smartset MV(DePuy) and bone cement without any antibiotic incorporated (Smartset MV, DePuy)
Results :
Analysis of the ultimate tensile strength (UTS) revealed no statistical difference between the novel cement and it's comparators. There was however a statistical increase in the compressive strength between the novel cement and Smartset GMV and manually combined Smartset MV with Gentamicin. Peak polymerisation temperature of the novel cement was between 16% and 36% lower than the other cements compared.
Discussion :
The development of a novel mixing method is yet in its early stages. However initial results reveal promising results which could prove useful in an operative and clinical setting.

References

1) Bucholz HW, Engelbrecht H. Uber die Depotwirkung einiger antibiotic bei Vermischung mit dem Kunstharz Palacos. Chirurg. 1970 Nov;41(11):511-515
2) DeLuise M, Scott CP. Addition of hand blended generic tobramycin in bone cement : effect on mechanical strength. Orthopaedics. 2004 Dec;27(12):1289-91

PA.14
In vivo evaluation of novel injectable hydrogel for viscosupplementation treatment

William Walsh
University of New South Wales, Sydney, Australia

In this work, an innovative resorbable composite material was applied on induced articular defects in the sheep-knee joint. The new injectable hydrogel can be considered as a valid and safe alternative to traditional viscosupplementation.

Introduction
Viscosupplementation is a symptomatic treatment of moderate osteoarthritis in articular joints where the lubricating and cushioning properties of the synovial fluid may be reduced. Various motivations lead to develop new materials apt to compete with HA-based products. The biological response to a single injection of a new viscosupplement based on an amidic derivative of carboxymethylcellulose (CMCA)[1] seven days after the induced defect was examined using adult sheep.
Material and Methods
Bilateral chondral defects (6 mm diameter) with a central osteochondral component (2 mm diameter, 6 mm deep) were created in the weight bearing region of the medial femoral condyle in a bilateral fashion in 15 adult sheep (2-3 years old). Blood was taken prior to surgery and at euthanasia for routine parameters. Animals were allowed unrestricted activity following surgery and given a saline or hydrogel treatment injection on day 7. A total volume of 5 mls was injected into each knee. Animals were allowed unrestricted activity following injection.
The hydrogel is a non-Newtonian viscoelastic system[1] composed by chemically crosslinked CMCA gel dispersed in CMCA polymer and hydrated in saline solution up to obtain a concentration of 3.6% (W/W)
Animals were euthanizedat 3months (n=5), 6 months (n=5) and 12 months (n=5) following surgery. AP and lateral radiographs, MRI, macroscopic dissection and paraffin histology of the fat pad, capsular tissues and menisci were performed. The medial (defect side) and lateral femoral condyle, medial and lateral tibial plateau were fixed in formalin and decalcified in formic acid for paraffin histology. H&E and Safranin O stains were used to assess changes in multiple tissues and any arthritic changes using a modified O'Driscoll grading scale.
Results and Discussion
All animals recovered uneventfully following surgery and after injections at 7 days. Macroscopic examination of the knees at 3, 6 and 12 months did not reveal any arthritic changes or damage to the menisci. Blood work and necropsy results were normal for all animals at any time point. The hydrogel was found in the capsular tissues at 3 and 6 months. Hydrogel resorption was complete by 12 months with no evidence of CMCA found. White tissue partially covered the defects at 3 and 6 months although no differences were noted between groups macroscopically. The bony aspects of the defect were filled with fibrocartilage in both groups although the hydrogel treated sites had a noted vascular response at 3 months. Histology revealed some repair tissue in both groups at 3 and 6 months. No discernable differences in the quality of the repair tissue filling the chondral defects were identified between the two groups using both radiographic and histologic endpoints at 52 weeks.
Conclusions The hydrogel used in the current study is biocompatible and biodegradable, the single injection does not induce any local, or systemic adverse reaction at any time point. On the basis of these preliminary data, the CMCA polysaccharide can be considered to be a valid alternative to traditional hyaluronic acid. There were no macro evidences in the extent of healing between the saline vs. the hydrogel. Additional studies should be performed to determine efficacy

References
1)R. Lapasin, M. Suerz, M. Grassi,F. Segatti, S. Fusi, D. Mercuri, G. De Conti. In Proceedings of XVIth International Congress on Rheology, 2012 (In press).

PA.15
A Collagen Augmented Acrylic Bone Cement

Mohamed Hachem
Department of Biomaterials, King's College London Institute, London, UK

Addition of collagen in a cement matrix has shown no marked effect on working and setting time and produces cement with good injectability. The compressive strength is not affected but the modulus shows the material is less brittle than PMMA

Introduction:
Polymethylmethacrylate (PMMA) bone cement has been widely used in joint reconstruction surgery and recently has been introduced into spine reconstructive surgery as part of the treatment of osteoporotic vertebral compression fracture. However, the use of PMMA bone cement in vertebroplasty leads to extensive bone stiffening and high rate of adjacent vertebrae fracture.
Aim:
The purpose of this study was to investigate the properties of PMMA bone cement augmented with collagen and assess its characteristics and its relevance for the reduction of complication rate associated with vertebroplasty.
Methods:
Bone cement was produced using 2 types of PMMA based bone cement. Augmented groups were prepared using 40 gm of PMMA base bone cement with 1% of rat tail liquid collagen. The mixing was conducted in controlled laboratory environment and at room temperature. The working and setting time and the mechanical properties were determined in accordance to ASTM standards for acrylic cements. The effect of ageing in simulated body fluid (SBF) on the mechanical properties of these cements and the microstructure were studied.
Results:
The effect of addition of collagen in a cement matrix has shown that there is no marked effect on the working and setting time and produces bone cement with good injectability. The compressive strength is not affected but the modulus shows the material is less brittle than PMMA.
Conclusion:
The addition of liquid collagen to PMMA based bone cement does not necessarily compromise the properties of the cements and produce cement with good injectability and less brittle than PMMA based bone cement alone. However, bone cement augmented with different concentration of collagen need to be studied further in order to assess its clinical relevance especially in vertebroplasty.

PA.16

Functionalization of silk-fibroin meshes with polypyrrole for medical purposes. Pilot study.

Luis Meseguer-Olmo
Arrixaca University Hospital, Murcia, Spain

Silk fibroin nanofibers coated with polypyrrol present high electroactivity and have the ability to support hMSCs and hFb growth.

Introduction

Scaffolds for cellular growth made of silk fibroin (SF) have demonstrated excellent biocompatibility in experimental studies[1]. However, potential applications could be expanded by fabricating electrospun mats with conductive properties for applications in biosensing, controlled drug delivery and tissue engineering[2].

Methods

Mats: Cocoons were boiled in Na_2CO_3 aqueous solution. The extracted SF was dissolved in LiBr to generate a 20% w/v dissolution and that was dialyzed. Then, a 17% w/v SF solution in Hexafluoroisopropanol was generated. The electrospinning setup used was Yflow™ 2.2.S-300.

Polypyrrole coating: Pyrrole (Fluka 97 % content) was distilled under vacuum using a vacuum pump MZ 2C SCHOOT. A SF mats (16 x 7 x 0.085 mm) was put pyrrole and NaCl aqueous solution in a 250 mL beaker. Electrochemical experiments were performed in a Metrohm system.

Cells: hMSCs (CD73+, CD90+, CD105+, $CD34_-$ and $CD45_-$) from bone marrow and dermal fibroblast (hFb) were obtained from 3 healthy donors. hMSCs were isolated from buffy coat by SEPAX™ System and maintained in basal DMEM supplemented with FBS and routin antibiotics, and incubated (37_0C, 7.5% CO_2, 95% humidity). Fibroblasts where obtained from a skin biopsy by enzymatic digestion (0.1 % w/v collagenase/DMEM). Cells from passage 3 (P3) were used for all experiments. Pieces of mats were seeded (2.0×10^4 cells/cm^2) into 24 wells plates and proliferation was measured by MTT staining at 1, 7, 14 and 21 days. SEM and phase contrast microscopy were used to examine hMSCs and hFb cultured on the mats.

Statistical: Data are presented as mean ± SD (standard deviation). The statistical significance was determined using Student´s t-test ($p<0.05$) or ANOVA ($p<0.05$) for two or more groups comparisons, respectively.

Results

No significant differences were found between SF and SF-pPy fiber sizes ($p>0.05$). So, pPy coating does not diminish the free space between fibers in the mats available for cell adherence and proliferation (see Fig. 1). A slight growing tendency was observed in hMSCs cultures being always slower in the coated mats. Significant absorbance differences ($p<0.05$) were found from hFb between coated and un-coated SF mats at the beginning (1 day) and at the end of the study (21 days). At 7 and 14 days no differences were detected between both materials ($p>0.05$) (see Fig. 2). Proliferation was followed by cell's visualization of images obtained by SEM. Excellent adhesions on the tested materials (SF and pPy-SF mats) were observed for both, hFb and hMSCs cells, 3 days after the seeding (see Fig. 3)

Conclusions

Our results show the ability of conductive silk matrices to support hMSCs and hFb attachment and growth. Using conducting polymers (pPy) adsorbed to SF fibers, could improve the applications of the mats in the fields of bone and neural tissue engineering.

References

1. Wang YZ, et al. Biomaterials, 2006; 27:6064-82.
2. Guimard NK, et al. Prog. Polym. Sci. 2007; 32:876-921.

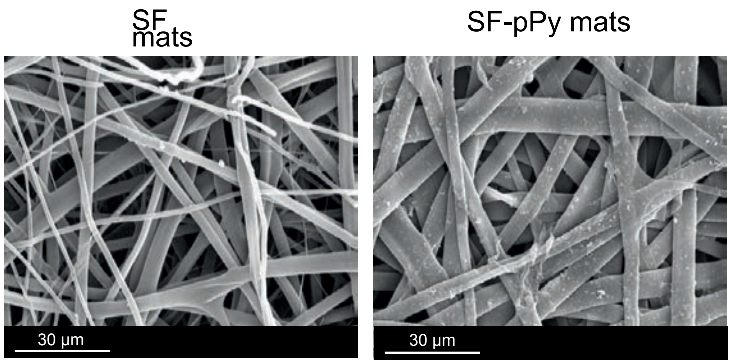

Fig. 1: SEM micrographs of SF and SF-pPy mesh (bar 30 µm).

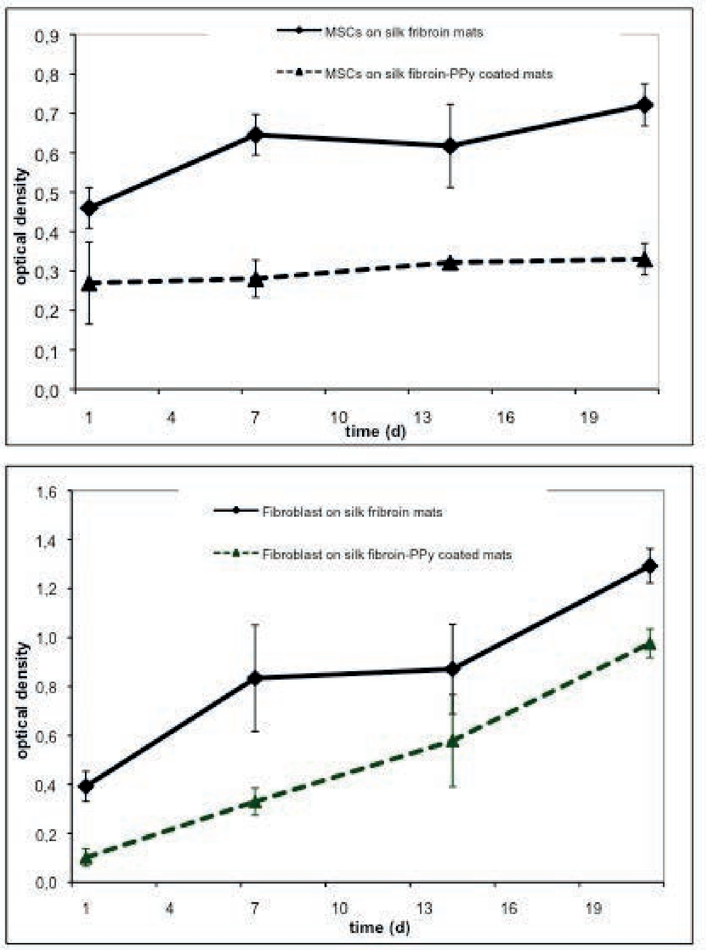

Fig. 2: MTT assay results.

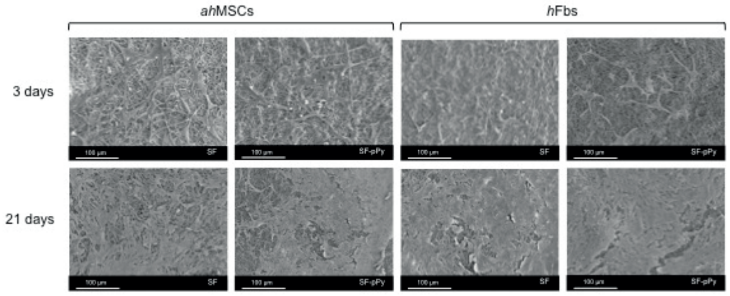

Fig. 3: Representative SEM micrographs of *h*MSCs and *h*Fb growing on both maths during 21 days.

PA.17

Incorporation of Raloxifene-impregnated Allograft around Orthopaedic Titanium Implants

Lars Lykke Hermansen
Orthopaedic Research Laboratory, Aarhuns University Hospital, Nørrebrogade 44, Building 1A, 8000 Aarhus C, Denmark

Local application of Raloxifene in conjunction with morselized bone graft around orthopaedic titanium implants revealed an anabolic side of Raloxifene in our settings. Instead of being solely anti-catabolic as generally held, Raloxifene may impact both aspects of bone turnover dose-dependently.

Introduction

Due to peri-implant osteolysis, hip revisions are a more complex procedure compared to primary hip arthroplasties. Early fixation of the revision prosthesis is crucial to its long-term survival [1]. The anti-osteoporotic drug Raloxifene decreases the risk of vertebral fractures by maintaining bone mass density. Raloxifene acts as an estrogen agonist on bone, and the mechanism of action by Raloxifene is purportedly by inhibition of the recruitment and activation of osteoclasts. We investigated whether Raloxifene offers any benefits in augmenting early fixation of orthopaedic implants in the setting of impaction bone grafting. Our hypothesis was that Raloxifene-impregnated morselized cancellous allograft bone would increase early implant fixation compared to normal, untreated morselized cancellous allograft. This was to obtained by an alteration of the balance between bone formation and resorption in favour of less resorption, thereby preserving bone graft as a mechanical stabilizer for the implant and keeping it available as a scaffold for new bone.

Methods

We used a non-weight-bearing, grafted gap model in 12 dogs. The cylindrical titanium alloy implants coated with a porous surface (Fig. 1) were inserted in the proximal metaphyseal ends of each tibia. Each animal received a control and intervention implant. The 2.5-mm peri-implant gap was filled with either Raloxifene-impregnated or untreated bone allograft. A dose of 10.0 mg Raloxifene was chosen. The implants were harvested after an observation period of 28 days, and implant fixation was assessed by mechanical push out testing and histomorphometrical evaluation.

Results

Using Raloxifene-treated allograft significantly decreased early implant fixation compared to untreated allograft illustrated by inferior maximum shear strength ($p < 0.01$) and apparent shear stiffness ($p < 0.01$) (Fig. 2). This result was explained by a significantly higher amount of new bone formation ($p < 0.02$) accompanied with accelerated allograft resorption ($p < 0.03$) in the Raloxifene-treated group (Table 1).

Discussion/Conclusions

Within our study design of grafted implants, and with a 4-week observation period, we demonstrated a striking similarity between the actions of BMP's and Raloxifene [2]. Our results are not consistent with current theory regarding the mechanism of how Raloxifene counteracts the decrease in BMD in postmenopausal women. Instead of being solely anti-catabolic as generally held, we report an anabolic side of Raloxifene. Studies using high dose estradiol implant therapy have provided direct histological evidence that high dose estrogen produces anabolic skeletal effects by stimulating osteoblast activity [3]. It is possible that we may have arrived at a therapeutic window of Raloxifene, where it acts similar to high doses of estrogen, hereby explaining the anabolic effects of the local Raloxifene treatment.

References

[1] Ryd L et al. Roentgen stereophotogrammetric analysis as a predictor of mechanical loosening of knee prostheses. J Bone Joint Surg Br 1995;77(3):377-83.
[2] Baas J et al. The effect of pretreating morselized allograft bone with rhBMP-2 and/or pamidronate on the fixation of porous Ti and HA-coated implants. Biomaterials 2008;29(19):2915-22.
[3] Khastgir G et al. Anabolic effect of estrogen replacement on bone in postmenopausal women with osteoporosis: histomorphometric evidence in a longitudinal study. J Clin Endocrinol Metab 2001;86(1):289-95.

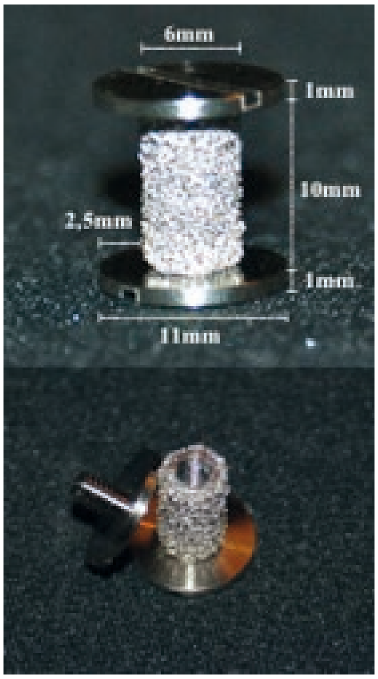

Figure 1: The implant is 6 mm in diameter and it is placed in a drill hole of 11mm in diameter. Central positioning is secured by 2 endplates, and a 2.5 mm gap is generated. This gap is impacted with either Raloxifene-impregnated or untreated allograft bone chips. After the observation period of 28 days, the outermost 3.5 mm of the implant is prepared for mechanical push out test, while the rest is embedded and stained for histomorphometrical evaluation.

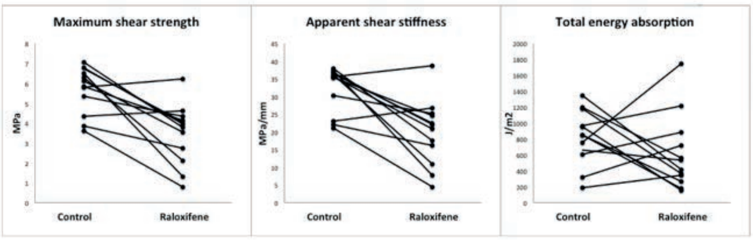

Figure 2: Mechanical push out test. The control and intervention implant within the same animal is connected with a line to illustrate the differences seen in each dog. Mean values (95%CI) for maximum shear strength was 5.7 MPa (4.9-6.4) for the control group and 3.5 MPa (2.5-4.4) for the Raloxifene-treated group (p < 0.01). Apparent shear stiffness was 32.3 MPa/mm (28.2-36.4) for the control group and 19.8 MPa/mm (13.9-25.7) in the Raloxifene-treated group (p < 0.01). Total energy absorption was 823 J/m2 (602-1043) for the control group and 616 J/m2 (317-915) for the Raloxifene-treated group (p < 0.269).

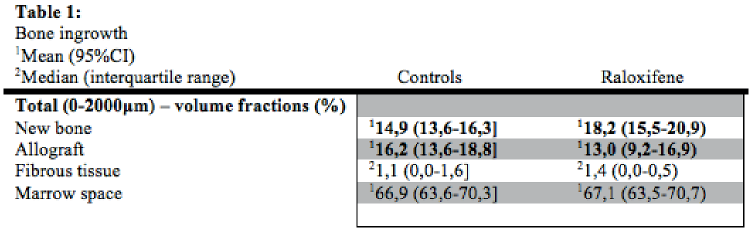

Table 1:
Bone ingrowth
^{1}Mean (95%CI)

^{2}Median (interquartile range)	Controls	Raloxifene
Total (0-2000µm) – volume fractions (%)		
New bone	**^{1}14,9 (13,6-16,3]**	**^{1}18,2 (15,5-20,9)**
Allograft	**^{1}16,2 (13,6-18,8]**	**^{1}13,0 (9,2-16,9)**
Fibrous tissue	^{2}1,1 (0,0-1,6]	^{2}1,4 (0,0-0,5)
Marrow space	^{1}66,9 (63,6-70,3]	^{1}67,1 (63,5-70,7)

Table 1: Paired comparisons of bone ingrowth with p-values below 0,05 are marked bold.

PB.01
Prediction of the elastic strain limit of the tendon using a shape-based comparative method

Alejandra Magaly Reyes Lúa
University Medical Center Rotterdam, Rotterdam, The Netherlands

The current study presents a new method for predicting the elastic strain limit of tendons with an acceptable level of accuracy. This will allow the choice of appropriate load magnitude when studying the response of tendons to fatigue loading.

Introduction:
The lack of parameters that are indicative of the fatigue resistance of tendons makes it difficult to understand the differences between energy-storing and positional tendons in the human and equine athletic population with respect of susceptibility to overuse injuries. Repetitive mechanical loading of tendon explants is an effective method for studying the fatigue resistance of tendons. One needs to apply a repetitive load that does not exceed the elastic strain limit, E_{max}, (where elastic deformation turns into plastic deformation) of the tendon but is substantial enough to induce fatigue damage. The variability of the elastic strain limit between different individuals makes it difficult to choose the correct load magnitude. The objective of the current study is to obtain a reliable method by which the elastic strain limit may be predicted using only a small fraction of the stress-strain curve.
Methods:
A series of failure stress-strain curves of porcine superficial and deep digital flexor tendon explants (n=34) were measured and their respective elastic strain limit was determined. In order to estimate the elastic strain limit of any given sample, a fraction of its measured stress-strain curve was used. That fraction of the stress-strain curve was then compared to the rest of the stress-strain curves available in the database. The most similar stress-strain curve from the database (Fig 1.), determined by the minimum L2 norm error between the fraction of the stress-strain curve of the sample and the corresponding fraction of the curves in the database, was used to estimate the elastic strain limit, E_{max}, of the sample. The accuracy of the prediction method was examined using the 'leave-one-out' test. The same procedure was used three times varying the fraction of the stress-strain curve that was available for comparison with the stress-strain curves of the database (5%, 6%, and 7%) (Fig. 2.)
Results:
The measured ultimate tensile strengths (UTS) varied between 6.5 and 29.7 MPa, while the Young's modulus varied between 0.1 and 0.29 GPa. Despite these relatively large differences between the minimum and maximum values of the UTS and Young's modulus, the database approach proved useful for predicting the elastic strain limit with a mean absolute percentage error of 8.46 % (SD ± 8.15%).
Discussion and conclusion:
The elastic strain limit may be predicted with this shape-based comparative method with an acceptable level of accuracy. The accuracy will improve when the number of samples in the database increases. Using the proposed technique, future research on overuse injuries may be able to predict the tendon-specific elastic strain limit and study the structural, mechanical and biological changes in response to fatigue loading.

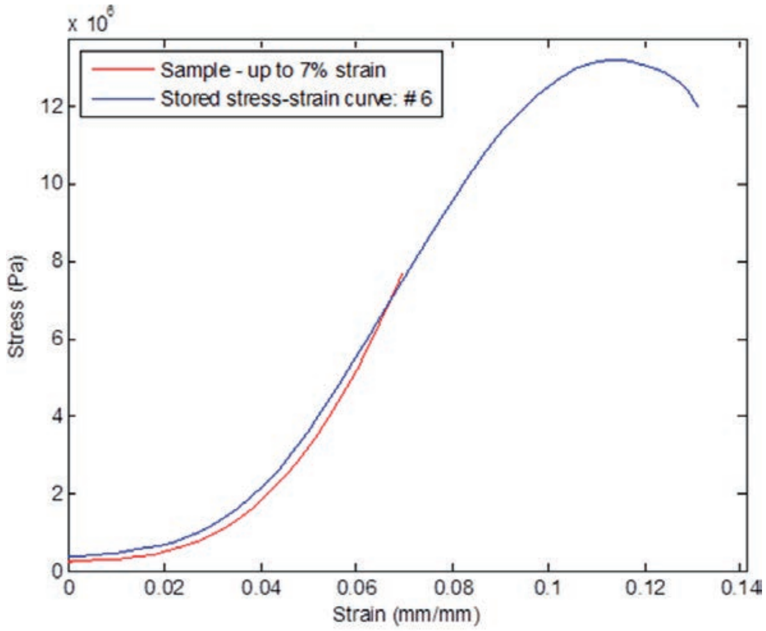

Figure 1 : Prediction of the strain at E_{max} by comparing a fraction of the stress-strain curve (red line) with the stress-strain curves stored in the database and finding the most similar stress-strain curve (blue line).

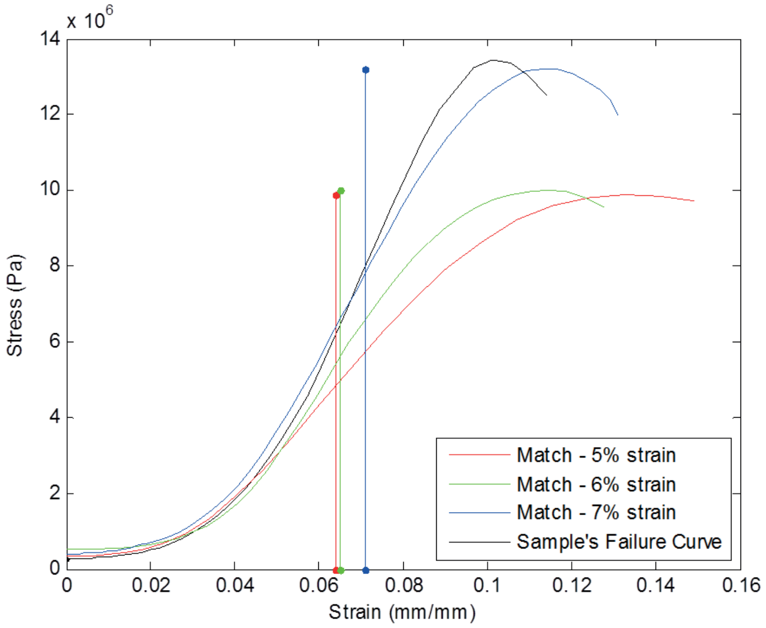

Figure 2 : Prediction of the strain at E_{max} of one sample (black) using stress-strain information of its failure curve up to 5%, 6% and 7%. The best match in each analysis is shown in red, green and blue, respectively.

PB.02

Waterjet drilling in bone: the effects of nozzle diameter and joint type on hole depth and diameter

Steven den Dunnen
Delft University of Technology, Delft, The Netherlands

For waterjet technology to be safely used for orthopedic drilling, depth control is a crucial requirement. This study shows a positive correlation between nozzle diameter and hole dimensions, which is an important step in the design of clinically safe nozzles.

Introduction:

In orthopedic surgery, waterjet technology (WJT) can be used as a clean, precise and always sharp tool for machining bone tissue. For the safe application of waterjet drilling in a clinical setting, control over the depth of a hole is required and the amount of added water should be minimized. One way of controlling the depth and water flow rate is by adjusting the nozzle diameter. The goals of this study were: 1. Finding a correlation between the nozzle diameter and hole depth; 2. Finding the minimum nozzle diameter that, regardless the articular bone type, is required to machine 3 mm deep holes.

Materials and Methods:

210 holes were drilled in the articular surfaces of 10 pig tali and 10 femora (4-6 months) by waterjet diameters of 0.3 (femora only), 0.4, 0.5 and 0.6mm. Pressure, standoff distance and jet time were kept constant at 700 bar, 8 mm and 5 seconds, respectively. All tests were performed submerged in water to mimic regular arthroscopic treatment. Post-experimental microCT scans were used to measure hole depths, diameters, and thicknesses of cartilage and subchondral plate layers. A Pearson test was used to correlate the nozzle diameters and thicknesses of articular layers to the hole depths and diameters for both tali and femora joints (P=0.05).

Results:

Increasing the waterjet diameter increases the hole depth (tali: p2= 0.57; femora: p2=0,84) and hole diameter (tali: p2= 0.52; femora: p2=0,57). The depths and diameters of the holes are significantly smaller in tali than in femora (Figure 1). The thicknesses of the subchondral bone plate and the cartilage do not correlate with the hole depth and diameter for either bone type.

Discussion/Conclusion:

An increase in waterjet nozzle diameter significantly increases the hole depth and diameter. The larger variations in depth in the tali are likely to be caused by the larger heterogeneity of the bone material which was seen on the microCT scans. For waterjet drilling of articular bone to a depth of at least 3 mm, 0.4 mm and 0.3 mm nozzles are to be used for pig tali (minimum hole depth 3.4 mm) and femora (minimum hole depth 3.3) respectively. Choosing the right nozzle diameter for specific bones can increase the control over the hole depth and thus improve the safe application of waterjet technology in orthopedic surgery.

The nozzle diameter plotted against the hole depth for pig tali (left) and pig femora (right).

PB.04
Influence of tool geometry on drilling performance of cortical and trabecular bone

Gabrielle Tuijthof
Dept. of BioMechanical Engineering, Delft University of Technology, Delft, The Netherlands

To design innovative drilling tools, forces in cortical and trabecular bone were measured for different conditions. Thrust forces ranged up to 110 N for cortical to 65 N for trabecular bone. Drill geometry has dominant influence on thrust force magnitude.

Introduction

Minimally invasive surgery poses high demands on tool design. Only a small set of steerable instruments is actually used in the clinic. One of the reasons might be the fact that typical human tissue properties (e.g. machining force, or hardness) are insufficiently available to set proper design criteria for innovative instrument development. The goal was to measure the influence of drill bit geometry relative to the known influence of feed rate on maximum thrust forces, and to compare these forces between cortical to trabecular bone.

Methods

Cadaveric pelvic bones of 20 pigs (adolescent) and 11 goats (full grown) were drilled perpendicular to the iliac crest up to 10 mm depth with eight different drill bits of Ø 3-3.2 mm. Subsequently, holes were drilled through all perpendicular to the ilium with the same drill bits at three different feed rates (0.58 mm/s, 0.83 mm/s, 1.08 mm/s) (Saha et al., 1982). The rotational speed was 200 rpm (Ohashi et al., 2003) and thrust force and drill depth were simultaneously measured at 54 Hz. A multivariable linear regression analysis was performed to determine the factors that significantly influenced the values of maximum thrust force for drilling in the iliac crest and ilium, separately. As reference condition drilling in porcine bone was chosen with a kirschner wire at a feed rate of 0.58 mm/s. The factors, animal (goat and pig), feed rate, and each of the drill bits were entered in the multivariable linear regression model. The significance level was adjusted for multiple comparisons (alpha = 0.01). To determine the difference between the maximum thrust force of cortical and trabecular bone, paired T-tests (2-tailed) were performed separately (alpha = 0.005).

Results

The mean maximum thrust force ranges from 10 to 110 N for cortical bone, and from 3 to 65 N for trabecular bone. The results show that both drill bit geometry and feed rate have a significant influence on the maximum thrust forces with a dominant influence of drill bit geometry. A higher feed rate requires higher forces, whereas larger flutes allowing removal of a steady stream of material, sharp cutting edges and a positive point angle contribute to minimization of the forces. All paired T-tests (2-tailed) show a significant mean difference between the maximum thrust forces of cortical bone and trabecular bone, with the cortical bone thrust forces always being higher.

Discussion

The substantial differences in thrust forces between cortical and trabecular bone can be used for drill design, and drill geometry is important to reduce the maximum thrust forces.

References

1. Saha S, Pal S, Albright JA. Surgical drilling: design and performance of an improved drill. J Biomech Eng. 1982;104:245-252.
2. Ohashi K, Hata N, Matsumura T et al. Stem Cell Harvesting Device with Passive Flexible Drilling Unit for Bone Marrow Transplantation. IEEE Transactions on Robotics and Automation 19(5), 810-817. 2003.

PB.05

Biomechanical evaluation of a new fixation concept for intramedullary nailing of proximal humerus fractures

Boyko Gueorguiev
AO Research Institute Davos, Davos Switzerland

Biomechanical evaluation of new concept for intramedullary nailing of proximal humerus fractures revealed that introduction of additional screw-in-screws and a calcar screw could increase osteosynthesis stability in poor bone quality and reduce the risk of secondary redislocation in clinical use.

Background

The osteosynthesis treatment of unstable proximal humerus fractures still remains challenging. The aim of this study was to investigate a new fixation concept for intramedullary nailing with different locking options in a three-part fracture proximal humerus model and prove whether its design adaptations, introducing additional two locking screw-in-screw, inserted through the head of the primary proximal screws, and one calcar screw, provide better stability, considering the peri-implant bone quality in the humeral head regions engaged by the locking screws.

Methods

A biomechanical testing model for three-part proximal humerus fractures, including cyclic axial loading with increasing peak load and simultaneous pulling forces at the rotator cuff, whose test set-up shown in Figure 1, was used to test twelve pairs of fresh human cadaver humeri, assigned to four study groups and intramedullary nailed with either Targon PH (Aesculap Othopeadics; T1) or MultiLoc PHN (Synthes, Inc.; standard M1; additional two screw-in-screw M2; additional one calcar screw and two screw-in-screw M3) (Figure 2). Bone mineral density (BMD) was evaluated in the humeral head at the exact locations along the locking screw paths via high resolution peripheral quantitative computed tomography using XtremeCT (Scanco Medical).

Results

Initial range of motion in internal-external rotation and mediolateral translation was smallest in M3 (1.82±0.38°; 0.11±0.11 mm), biggest in T1 (3.63±0.49°; 0.51±0.17 mm) and significantly different between these two groups ($p=0.02$ and $p=0.04$, respectively). M3 showed minimum head migration along the nail and varus deformation after 5000 cycles (0.31±0.14 mm; 0.20±0.05°) and 10000 cycles (1.59±0.68 mm; 0.34±0.19°) (Figure 2). The head migration increased significantly between 5000 and 10000 cycles in all study groups ($p=0.02$). The additional two locking screw-in-screw in M2 and M3 were aimed at bone volumes in the posteromedial part of the humeral head with significantly higher BMD, compared to the respective primary proximal screws, through whose heads they were inserted ($p\leq0.03$). M2 and M3 performed better than M1 and T1 with regard to varus collapse. The highest number of cycles to failure was observed for M3 (20733±1669) and the lowest for T1 (10083±3939) with significant difference between these two groups ($p=0.04$).

Conclusion

Both nail constructs performed very well biomechanically and would be a good choice for treatment of proximal humerus fractures. The locking configuration with two screw-in-screw and one calcar screw was superior in most aspects, while both options with two screw-in-screw showed better behavior with regard to varus collapse. This confirms that the introduction of additional two screw-in-screw and one calcar screw could increase osteosynthesis stability in poor bone quality and reduce the risk of secondary redislocation in clinical use.

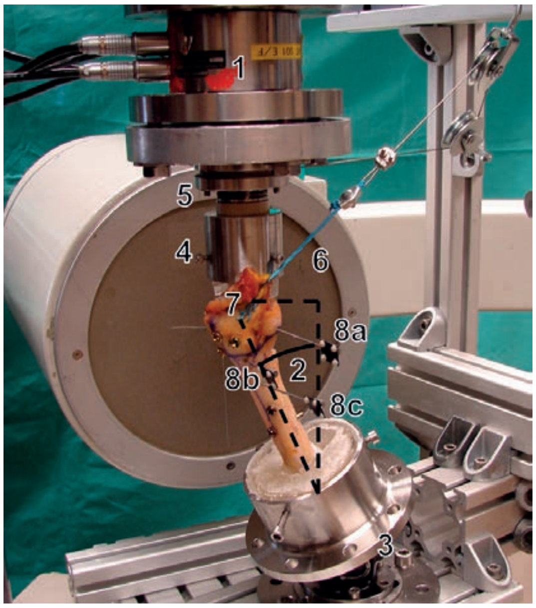

Figure 1. Test set-up: (1) Load cell; (2) 25° lateral angulation of the humeral shaft axis; (3) Cardan joint; (4) PMMA cup simulating glenoid fossa; (5) Notched flange decoupling axial and torsional loading; (6) Direction of the pulling force 110° to the shaft axis; (7) Attachment of the sutures to the muscle tendons; (8a-c) Marker sets for motion tracking.

Figure 2. Left: MultiLoc PHN with additional one calcar screw and two screw-in-screw (M3); right: Targon PH (T1).

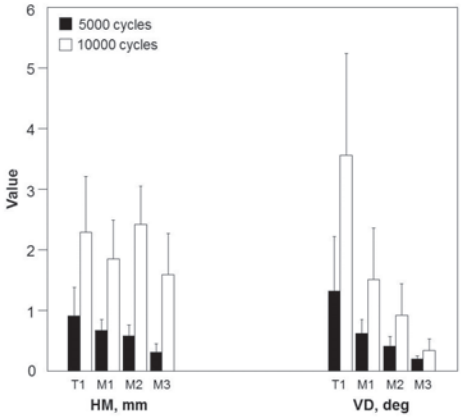

Figure 3. Mean value with standard error of mean of the head migration (HM) and varus deformation (VD) in the study groups T1, M1, M2 and M3 after 5000 cycles (black) and 10000 cycles (white) during the cyclic test.

PB.09
Fixation of the Fitmore® stem - A biomechanical Analysis.

Jan Nadorf
University of Heidelberg, Heidelberg, Germany

This study presents an overview on the correlation of implant design, mechanical stiffness and biomechanical force transmission at the implant-bone-interface, which might clinically influence bone remodelling processes.

Introduction:

Implantation of total hip arthroplasty (THA) may induce remodelling of the periprosthetic bone structure. Many implant-related parameters, like material and elasticity influence the remodelling processes. During the past years, there is a tendency to shorter hip stems to preserve femoral bone stock and to reduce the risk of proximal stress shielding.

After clinical introduction of the Fitmore® stem (Zimmer) we noticed the formation of cortical hyperthrophies in some cases.

The aim of this biomechanical study was to analyse possible biomechanical reasons for the formation of these distal hyperthrophies. Therefore we determined the primary stability, which has notable influence on long-term stability of the implant. We compared the Fitmore® stem to the well established CLS® stem (Zimmer).

Methods:

A standardized neck resection was preformed using eight synthetic femurs. Four Fitmore® and four CLS® stems were implanted. Micromotions of the stems and femurs were measured with a high precision measuring device at defined sites under two different cyclic load applications. An axial torque of +/-7Nm around the stem axis was applied to classify the rotational implant stability. In a second step a varus-valgus-torque of +/-3.5Nm was applied to analyse the bending-behaviour of the stem. Comparing the motions of the stem and femur at different sites allowed the calculation of relative micromotions at the bone-implant-interface.

Results:

The lowest relative micromotions were detected within the proximal part of the stems near the Trochanter minor (Fitmore® = 7.18 (SD ±0.79) mgrad/Nm und CLS® = 6.49 (SD ±0.87) mgrad/Nm). Maximum relative micromotions were found at the distal tip of the stem for both designs, in which the shorter Fitmore® stem showed lower relative micromotions (11.91 (SD ±2.58) mgrad/Nm) compared to the CLS® (12.32 (SD ±3.68) mdeg/Nm), indicating a proximal fixation of both stems.

Regarding the medio-lateral bending behaviour, the CLS® stem followed the bending of the bone. Contrary to this, the Fitmore® stem acted rigidly, indicating less flexibility.

Discussion:

Both stems showed low micromotions within the proximal part of the stem. Under medio-lateral torque application, the CLS® stem followed the physiological bending of the bone, whereas the shorter Fitmore® stem seemed to act like a rigid body and tilted instead of bending. This may be due to an enlarged axial cross-section of the stem and therefore an enlarged implant stiffness of the Fitmore® compared to the CLS®. Such a tilting of the stem may induce high intra-femoral stresses which may possibly lead to cortical hypertrophies.

PB.10
Accuracy of robot spine drilling

Rumen Kastelov
Institute of Mechanics – Bulgarian Academy of Sciences, Sofia, Bulgaria

The purpose of the work is to present a robot application for vertebra drilling in surgery and to underline its advantages concerning accuracy and safety.

Introduction

Various cases of adopting of robots as direct participants in surgery intervention are known. The surgery requires instruments with drives, which the surgeon holds in his hands. By reports the drilling devices are used approximately in 95% in orthopaedic trauma surgery. Hand-drilling leads to problems as getting the big outlets, breaking the tendons or blood vessels, overheating etc. and surgeons have to use X-ray machines. The average error in drilling accuracy beyond far cortex is 6.31 mm! As it is made by hand the subjective behaviour is decisive for the final result quality. The drilling automation can neutralize the subjective factor and avoid the existing problems.

The purpose

of the work is to present a robot application for vertebra drilling in surgery and to underline its advantages concerning accuracy and safety.

Methods

The research method concerning robot application for spine column drilling is experimental one. Beef vertebras is used. Laboratory experiments are executing under various conditions - drilling speed, rotation, force, different size and diameter of drilling bits. The contact with the bone is realised by the surgeon holding the machine in hands. Surgeon can stop any time just by releasing the button as well as can prolong it by pressing again. When the pressing is continuously, the robot executes the desired settings, stops automatically and returns back to its initial position. The robot works in two modes: hand and automatic. The last has three sub modes: desired depth, one wall (cortex I) and the whole bone (cortex II) drilling. The experiments concern the desired depth drilling. The surgeon sets the mode and the desired depth.

Results

The robot executes the drilling with high precision (0.2 mm) and minimal time (average 6 sec). Three types of drilling bit are used: diameter 2mm, 4mm and 6 mm. The temperature increases relatively 4 $_{o}$C, 7 $_{o}$C and 10 $_{o}$C. The information in real time is seen online on the display. The error is 0 % - all the experiments show exactly execution of the set task.

Discussion / conclusion

The experimental setup is designed to identify main parameters of drilling as the resistant force due to variable density, temperature, and angular and linear speed. In comparison with the existing similar systems, which are complex, expensive and require special maintenance and training of the working team, ours is very compact and not expensive, performing high accuracy and safety. The surgeon can operate easy and the required task is set simply. The information is received in real time. The surgeon does not exert influence on the process; he has only to take care of keeping the contact with the bone. The identification reveals the size of the both corteces and the bone marrow length. That helps to choose optimal screw implant length. The automatic drilling eliminates one manipulation - measuring the depth handily after any hole. It shortens the operation time.

The advantages of the automatic drilling are underlined: prevention of overheating and soft tissue near the drilled bone, high accuracy and patient safety.

Fig.1. The executive module of the robot.

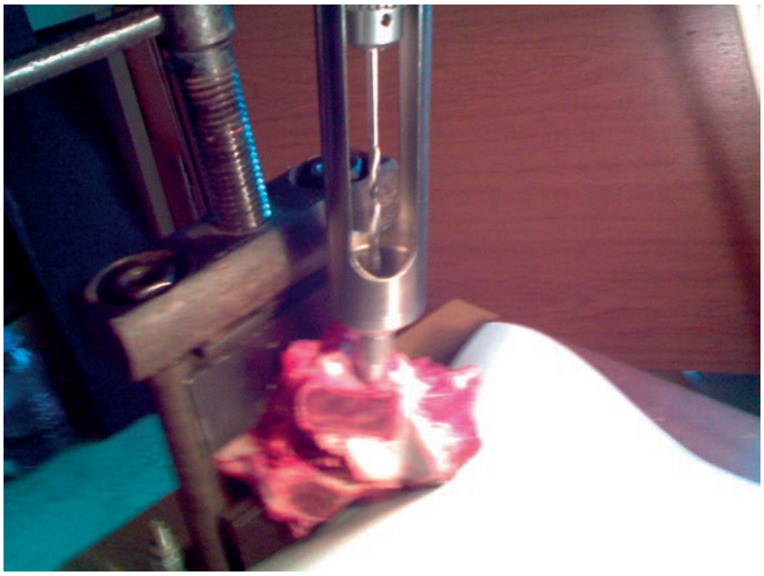

Fig.2. The experimental setup.

Fig.3. Real time information on the display. The right number (20 mm) is preliminary set

PB.11

The interprosthetic gap as a risk factor for peri-prosthetic fractures of the femur. A biomechanical evaluation.

Thomas Quirynen
BMe - Biomechanics Section, Faculty of Engineering, KU Leuven, Belgium and Orthopaedic Surgery Department, University Hospital Pellenberg, Pellenberg, Belgium

In contrary to what is intuitively expected, interprosthetic femoral gap distances

Introduction
An interprosthetic gap between the tip of a total hip (THA) or total knee (TKA) replacement stem can be a stress riser that might jeopardize the biomechanical properties of the femur. However, little is known about the optimal gap distance to minimize the fracture risk. It also remains unclear whether the interprosthetic gap distance would influence the biomechanical properties of a lateral plate construct used to treat these fractures.
Objectives
It was our aim (1) to evaluate the effect of the interprosthetic gap distance on the biomechanical properties of the femur, (2) to describe the inter-prosthetic fracture morphology and (3) to evaluate the effect of the interprosthetic gap distance on the stability of 3 different lateral plate constructs.
Methods
The maximal load to failure (Fmax), the compression at failure (Cmax) and the absorbed energy at failure of 7 inter-prosthetic gaps between a cemented THA and TKA stem in 33 validated sawbone specimens were evaluated. Similarly, the same parameters of 3 different constructs used to fix these fractures were evaluated.
Results
The mean Fmax decreased 800N when an interprosthetic gap was present. A mean Fmax of 7500N was noted for gaps between 5 to 20 cm. The Fmax increased to >9220N with gap distances shorter than 5 cm. There was a higher Cmax with a gap distance15 cm and the absorption of energy prior to failure was lowest with gap distances between 5 and 15 cm. Gaps shorter than 5 cm required more energy to fail. The femur fractured with a butterfly fragment at the site of the gap. Lateral plate and screw constructs reached the initial Fmax only with gap distances
Conclusions
In contrary to what is intuitively expected, gap distances
Clinical relevance
Avoiding an interprosthetic gap between 5 and 15 cm can minimize the risk for a peri-prosthetic fracture. With small sized gaps it is advisable to decrease the distance to between 0 and 3 cm. An anterior strut augment with a lateral plate and screw construct should be considered in case a gap >5 cm is present.

PB.12
Progressive failure in the femoral neck during a sideways fall

Mohamed Ridzwan
Biomechanics Group, Department of Mechanical Engineering, Imperial College, South Kensington, SW7 2AZ, London, UK

Damage development in femoral neck during a sideways fall was modelled using finite element method until a complete failure. The failure was simulated using the maximum principal strain criterion. The evolution of damage was consistent with previous studies.

Introduction:
Finite element (FE) models of bone predict femoral strength better than other non-invasive tools [1]. Previous FE studies estimated femoral fracture load and fracture patterns when at least one shell element or few solid elements exceeded yield stress or strain in the model [2,3]. Recently, several authors investigated on complete failure and compared to ex-vivo and clinical observations [4,5]. Even though these studies appear promising, however they did not consider strain direction in failure criterion or was modelled only for one-legged stance loading condition. This study incorporated differences in yield strain for bone in compression and under tension to simulate progressive failure in the femur during a sideways fall.

Patients & Methods:
The left femur of 69-year-old subject was segmented using Avizo Standard software. The 3D model was then imported into Marc/Mentat 2010 for volume mesh generation. Each element was assigned to isotropic heterogeneous material using relationship of E = 6.850 ρ_{app}^{1.49}, where E is elastic modulus (GPa) and ρ_{app} is apparent bone density [6]. A constant Poisson's ratio was 0.3.

The femur was orientated to simulate a sideways fall [4]. Initially, 500N was applied to the proximal head surface. The load was then increased by 500N in each load cases until it reaches a first yield (in compression/tensile) and by 100N increments when the yield limit was reached. Subsequently, once a second yield (in compression/tensile) was reached, the applied load was reduced until a complete failure was observed. The distal end of the femur was restrained from axial movement and the lower part of the greater trochanter was prohibited from vertical displacement [7].

The femoral failure was simulated using the maximum principal strain criterion. The maximum and minimum principal strains were 0.62% and -1.04% respectively [5]. After yielding occurs, element that failed in compression was assigned low elastic modulus of 0.1GPa whereas in tension was removed from the model to simulate the broken zone. The model was then updated and solved again until a complete fracture was observed. The load displacement curve was determined for further comparison.

Results:
The damage was initiated at the junction of the superior aspect of the femoral neck and greater trochanter when elements exceeded the yield compression strain at 4100N. The compressive damages were accumulated to anterior-superior medial femoral neck as the applied load increased to the ultimate load (4650N). Then the applied load was reduced as some elements at the inferior aspect of the femoral neck exceeded the yield strain in tension were removed. Finally, at the maximum displacement of 3.85 mm (corresponding to 3600N), a complete transcervical fracture was observed and failure line was less than 50° from the horizontal plane (Pauwels type II).

Discussion/Conclusion: This study investigated progressive femoral failure of subject-specific FE during a sideways fall. The predicted fracture load was within the range of failure load found in elderly cadaveric test [8]. The number of yielded elements increased with increased load that lead to the complete failure. The evolution of damage was consistent with previous studies [4,5].

References:
[1] Cody et al 1999, Femoral strength is better predicted by finite element models than QCT and DXA, Journal of Biomechanics 32, pp. 1013-1020
[2] Keyak et al., (1998), Prediction of femoral fracture load using automated finite element modelling, Journal of Biomechanics, 31, pp. 125-133.
[3] Bessho et al., (2009) Prediction of proximal femur strength using a CT-based nonlinear finite element method: Differences in predicted fracture load and site with changing load and boundary conditions, Bone, 45, pp. 226-231.

[4] Dragomir-Daescu et al., 2011, Robust QCT/FEA models of proximal femur stiffness and fracture load during a sideways fall on the hip, Annals of Biomedical Engineering, 39(2), pp. 742-755.
[5] Hambli et al., 2012, Finite element prediction of proximal femur fracture pattern based on orthotropic behaviour law coupled to quasi-brittle damage, Medical Engineering & Physics, 34, pp. 202- 210,
[6] Morgan et al., 2003, Trabecular bone modulus-density relationships depend on anatomic site, Journal of Biomechanics, 36, pp. 897-904.
[7] Verhulp et al., 2008, Load distribution in the healthy and osteoporotic human proximal femur during a fall to the side, Bone, 42, pp. 30-35.
[8] Courtney et al 1994, Effects of loading rate on strength of the proximal femur, Calcif Tissue Int, 55, pp. 53-58.

PB.13

Changes in Core Suture Geometry within Repaired Flexor Tendons: Investigations with a novel radiographic method.

Tim Sebastian Peltz
University of New South Wales, Surgical & Orthopaedic Research Laboratories, Prince of Wales Hospital, Sydey, Australia

Several factors influence gap formation in tendon repairs and these are intimately related to 3-dimensional changes in the repair geometry when put under tension. We present a novel method to analyze these changes and investigate 4 prevalent tendon repair constructs.

Introduction

Early mobilization of a repaired deep flexor tendon promotes better outcomes than immobilization.Tension on the reconstruction, however, produces gap formation at the repair site, which is detrimental. The changes in the 3-dimensional suture geometry when a tendon repair is strained, and the relationship this has to gap formation have not clearly been characterized yet. Therefore, we present a novel X-ray technique to qualitatively and quantitatively examine the three-dimensional changes in the core suture repair configurations under tension.

Methods

40 adult sheep forelimb deep flexor tendons were randomized into 4 repair groups. The repair techniques used reflected prevalent 2-strand and 4-strand methods, using different grasping and locking variants: Kessler Repair (Fig 1), Cruciate Repair (Fig 2), Cross Locked Cruciate Repair (Adelaide Repair) (Fig 3) and a novel repair variation, we called the Modified Adelaide repair (Fig 4). 3-0 surgical steel wire was used for all repairs. Sutures were marked at the point of exit from the tendon with a Ligaclip. AP and lateral X-rays were taken. Thereafter the suture strands were loaded to 35N. X-rays were repeated and digitally ananalysed. Gap formation was measured and data pre and post tensioning were compared.

Results

The relative length of suture elongation at the repair site was most in the 2strand Kessler repairs. Significant narrowing of the tendon at the transverse suture component and a complete loss of the 3-dimensional Kessler configuration was noticed. In the 4strand cruciate repair significant cheese-wiring of the loop-locks was noted with a large resultant propensity for gapping. In contrast, the cross-locking variants (Adelaide Repair) locked in itself under tension and showed minimal tendency to cheese-wire. Least propensity for gapping was noticed in the interlocked modification of the Adelaide repair.

Discussion

Several factors influence gap formation and these are intimately related to 3-dimensional changes in the repair geometry. 2-strand grasping configurations like the Kessler technique not only allow great tendon constriction but also lose their three-dimensional configuration when tensioned. This results in elongation and therefore gapping. These effects are less observable in 4 strand configurations. Cross locks, like used in an Adelaide repair stabilize the construct and prevent cheese wiring. Our interlocked modification of the Adelaide technique showed least changes when put under tension. This study looked at the core suture in isolation to exaggerate the geometric effects. The sample size of n=10 per group, while small, was representative considering the in-vitro nature of the study and high reproducibility of findings.

Conclusion

X-ray is a useful method of investigating suture configuration changes. This evaluation provides a valuable new insight into the behavior of prevalent flexor tendon repair constructs.

-The modified Kessler Repair pre and post tensioning
-The Cruciate Repair pre and post tensioning
-The Adelaide and Modified Adelaide Repair pre and post tensioning

PB.14
Multi-scale Modelling of the Cement-Bone Interface

Dennis Janssen
Radboud University Nijmegen Medical Centre, Nijmegen, The Netherlands

Using cohesive modelling, the micro-mechanical behaviour of the cement-bone interface was incorporated in FEA models of sectioned cemented hip reconstructions, and compared against experiments. Information on interface morphology is essential for the application of cohesive modelling in full THA models.

Introduction

The cement-bone interface provides stability to the cement mantle in cemented total hip arthroplasty (THA). Finite Element Analysis (FEA) models of cemented hip reconstructions, have shown that it is crucial to include the proper mechanics of the cement-bone interface. Recently, a cohesive model was developed to incorporate the mixed-mode micromechanics of the cement-bone interface in macroscopic models. The goal of the current study was to validate this cohesive model on a macroscopic level, by simulating torque experiments performed on transverse sections of post-mortem retrieved cemented hip reconstructions.

Methods

Two post-mortem retrieved transverse sections of cemented hip reconstructions (Figure 1) were harvested from two different donors. The implants were subjected to a torque load, during which the micro-motions at the cement-bone interface were measured using Digital Image Correlation.

Two plane-strain FEA models of the transverse sections were generated. The cement-bone interface was modelled with cohesive elements, which mechanical response was based on a constitutive cohesive model. The mechanical behaviour of this model was dependent on the local gap thickness of the cement-bone interface, which was measured on the outer surface of the transverse sections.

The global stiffness and the total motions at the cement-bone interface were determined for both specimens.

Results

At maximum torque load, the magnitude of the interface motions of the two specimens differed considerably (Figure 2). The average motions of Donor 1 (0.68 and 0.73 mm for the experiment and FEA, resp.) were considerably larger than those of Donor 2 (0.0024 and 0.0040 mm for experiment and FEA, resp.). Donor 2 gave a better match of the circumferential distribution of micromotions than Donor 1 (Fig 2). While Donor 2 showed a positive match of the distribution of the motions around the circumference of the interface, Donor 1 did not.

The global stiffness of Donor 1 was underestimated (1374 and 265 Nm/deg for the experiment and FEA, resp.), while Donor 2 showed a better match of the experimental and FEA global stiffness (17,916 and 21,380 Nm/deg, resp.).

Discussion

The results of this study show that the surface of the experimental specimens provides insufficient Information on the morphology of the cement-bone interface to capture the mechanics of the structure, when implemented in a cohesive zone model. While this could be interpreted as a lack of validity of the cohesive model, it is more likely that the limitation lies in the inability to fully describe the complex morphology of the cement-bone interface. In clinical use, the actual detailed (micro-level) morphology would never be available. Therefore, modelling approaches that account for uncertainties in the interface morphology may be more appropriate to address this issue.

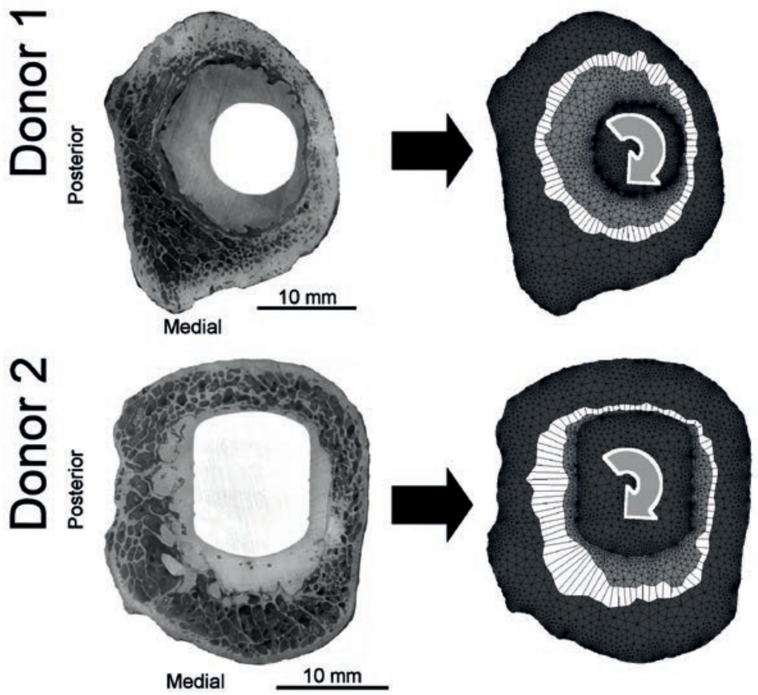

-Two transverse sections of the experiment (left) and the generated FEA models (right).

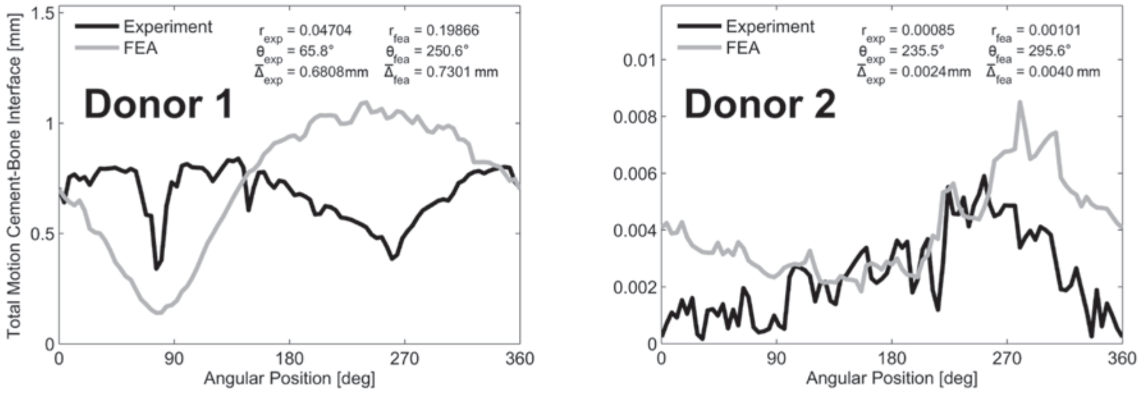

-The total motions of the cement-bone interface as measured at its circumference.

PB.15
A biomechanical knee model with deformable structural components to dynamically simulate TKR.

Dario Bovio
Politecnico di Milano, Milan, Italy

The potential of advanced simulation tools can be profitably exploited in designing prosthetic components while considering the effects of altered biomechanical properties of the anatomical structures.

Integration of multibody dynamics and finite element analysis offers very interesting opportunities to simulate the effects of total knee replacement (TKR). This approach can be helpful during both the prosthesis design phase and the functional assessment of patients, as it can lead to a better understanding of the influence of different anthropometric and pathological characteristics. In particular soft tissues modelling is fundamental for a good simulation of TKR, although the definition of the anatomical arrangement and constitutive properties of the altered material is particularly critical.

Aim of the present work was to implement a model of the knee joint that included the main anatomical structures and allowed us to change all the mechanical properties of soft tissues and see how they affect the knee function and how they interact with the prosthetic design in TKR.

A software tool specifically geared toward biological applications, FEBio [1], was used, which is a freely available open source. This package has embedded different modelling scenarios, relevant constitutive models and boundary conditions that can be used for both quasi-static and dynamic analyses. Different isotropic and anisotropic constitutive models are available to represent deformable bodies, up to the inclusion of hyperelasticity.

In our application, a lower limb model (consisting of pelvis, thigh, shank and ankle joint) has been developed, in which the natural knee joint could be replaced by prosthetic components.

Soft tissues considered were the medial and lateral collateral ligaments, posterior cruciate ligament (needed to simulate PCL retaining implants), as well as patellar tendon, quadriceps and hamstrings. These anatomical structures were modelled with three-dimensional finite elements, to which the appropriate mechanical properties were assigned. The stress-strain relationship of the materials were modelled with typically non-linear equations, that could represent hyperelasticity or viscoelasticity when appropriate, inhomogeneity and anisotropy related to muscle activation and fibres orientation [2]. As a preliminary application of this model, the deep knee bending movement of a generic male (weight 80 kg, height 1.80 m), was simulated and several trials were performed by changing prosthetic component geometries. Among the available output variables, antero-posterior displacements, internal-external rotation and the force distribution map at tibial-femur interface have been particularly analysed.

The results show the influence of the prosthetic design on ligaments balancing and on the patellofemoral kinematics. The force distribution map on the bone-implant interface gives an estimation of the strains within the underlying bone and permits to infer about the wear phenomena between the prosthetic components.

In conclusion, the investigation of implant performance through computational models that comprise kinematics, contact kinetics and non linear material properties represents a comprehensive method to test different prosthetic designs for achieving the most effective solutions with interesting perspectives for prosthesis customization.

1. Maas SA, Ellis BJ, Ateshian GA, Weiss JA. FEBio: Finite elements for biomechanics. J Biomech Eng, 134(1), 2012.
2. Gardiner JC, Weiss JA. Subject-specific finite element analysis of the human medial collateral ligament during valgus knee loading. J Orthop Res. 21(6):1098-106, 2003.

PB.16

Active isometric abduction causes cranial translation of the humeral head in rotator cuff tear patients

Jan Ferdinand Henseler
Leiden University Medical Center, Leiden, The Netherlands

Active abduction leads to dynamic cranial translation in rotator cuff tear patients. There is more cranial translation in posterosuperior tears (i.e. supraspinatus and infraspinatus) compared to full-thickness supraspinatus tears. Superior directed deltoid force causes excessive cranial translation during arm activity.

Background:
Cranial translation of the humeral head may be unapparent on routine shoulder radiographs in early stage massive rotator cuff tears. It is currently unclear if isometric abduction leads to active cranial humeral translation in rotator cuff tear patients. Alternatively, caudal directed adductor co-activation forces counteract to the superiorly directed forces of the deltoid, potentially modulating the effect of cranial translation of the humeral head.
Patients and Methods:
20 consecutive patients with 9 full thickness supraspinatus cuff tears and 11 posterosuperior tears (i.e. supraspinatus and infraspinatus) were assessed. Radiographs with active isometric abduction force tasks with the arm in 0_o abduction were used. Cranial translation was measured using the relative upper migration index (UMI, [1.00 > UMI < 1.50]) during rest and isometric abduction and adduction with simultaneous muscle activation measurements of the arm ab- and adductors, respectively.
Results:
There is significant cranial translation during active isometric abduction (1.18 SD 0.08), p>0.001 and adduction (1.23 SD 0.08), p > 0.001 compared to rest (1.27 SD 0.05). Cranial translation was more severe in the posterosuperior cuff tears (0.11 SD 0.05) compared to the supraspinatus tear group (0.04 SD 0.05), p = 0.021. There is a weak correlation between cranial translation and VAS for pain in rest and during abduction (r = 0.428), p = 0.006.
There is a significant increase of latissimus dorsi and teres major activation during adduction, but this was not present during abduction. Contrary, there was a significant mean increase of deltoid activation during both abduction and adduction tasks compared to rest. However, the correlation between cranial translation and deltoid activity was medium low (r = 0.301), p = 0.01. The correlations between cranial translation and the adductor for the latissimus dorsi (r = 0.110) and for the teres major (r = 0.115), were not clinically significant.
Conclusions:
Active isometric abduction leads to dynamic cranial translation in massive cuff tear patients. More cranial translation is present in posterosuperior cuff tears, compared to the less extensive supraspinatus tear group. The superior directed force of the deltoids causes excessive superior translation during arm activity. Although there is more cranial translation during abduction compared to adduction, the adductor (co-)activation is insufficient to prevent nett cranial translation of the humeral head.

PB.18

Development of a micro FE model of a titanium porous implantable material.

Fernando José Quevedo González
École de technologie supérieure, Montréal, Canada

FE analyses and mechanical testing were performed on a new porous titanium structure. The results showed that there is a relation between the microarchitecture of the structure and its mechanical properties.

Introduction

The mismatch in stiffness of human bone and implant leads to an unusual stress distribution in the bone that causes its resorption, which is believed to cause implant loosening [1]. Thanks to the advancements in additive manufacturing processes, complex structural materials, such as porous microstructures, can now be designed. These materials promote bone cells ingrowth into the structure, leading to a better osseointegration, and consequently a better fixation to the surrounding bone.

However, little is known about the relationship between the microarchitecture and the overall properties of porous microstructures. In particular, few finite element (FE) studies have investigated this relationship. In this study, a new porous titanium structure is developed by means of additive manufacturing. Mechanical testing is performed and a micro FE model is developed to study the influence of the geometric parameters on the overall mechanical behaviour.

Materials and methods

The porous structure, obtained by Electron Beam Melting, consists of a cube of 10.95 mm long, with straight struts along the Cartesian axes (Fig.1). Using an INSTRON 8874/287 Universal Test Machine, static compression tests of three different structures (total of 15 samples) were performed until failure was clearly observed (around 2mm of displacement).

Static non-linear simulations, using a 3D CAD model with ¼ of symmetry (Fig.2), and an isotropic homogeneous elastic-plastic material model were performed in ANSYS V13 software. Strut diameter was varied between 450 and 650 µm, and pore diameter between 500 and 700µm. FE analyses predicted the onset of plastic behaviour and studied the effect of the geometric parameters on the mechanical response.

Results

Mechanical tests showed that structures exhibit an irregular behaviour at the beginning of the compression test before an apparent elastic zone. Then, a non-linear behaviour is observed and failure process starts. The apparent elastic modulus obtained ($2,6<E$

In computational simulations, plastic behaviour is observed for small displacement values: displacements over 0,05 mm lead to widespread plastic behaviour (Fig.3). In addition, while keeping the same displacement, the greater the strut diameter is, the greater the reaction force is, showing a linear relation; whereas for the pore diameter, the relation is the opposite and non-linear

discusion/conclusion

A new cellular solid has been tested, showing a stiffness similar to human bone. Structure's mechanical behaviour can be varied by changes in the strut and pore diameters. This would allow tailoring its mechanical properties, achieving more suitable properties. An elastic-plastic material model is necessary to simulate the mechanical behaviour of such micro-structure in FE models.

References

[1] Heinl, Peter; Rottmair, Andreas; Körner, Carolin; Singer, Robert F. 'Cellular Titanium by Selective Electron Beam Melting'. Advanced Engineering Materials 2007, 9, n°5, 360-364.

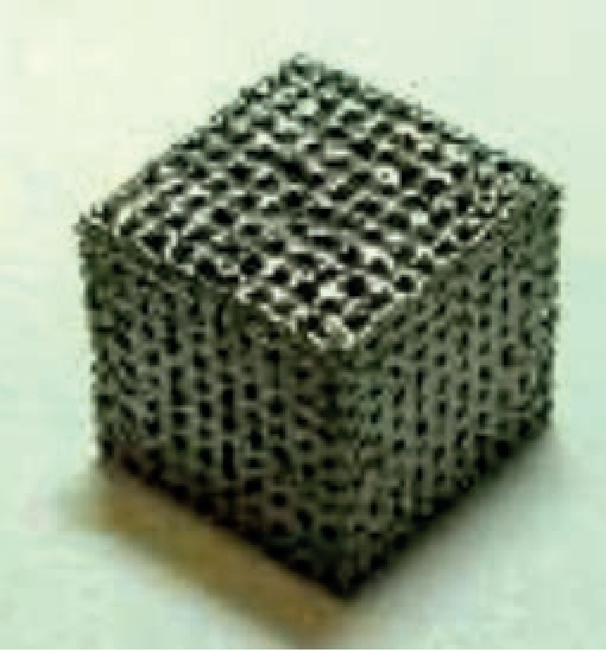

Porous microstructure.

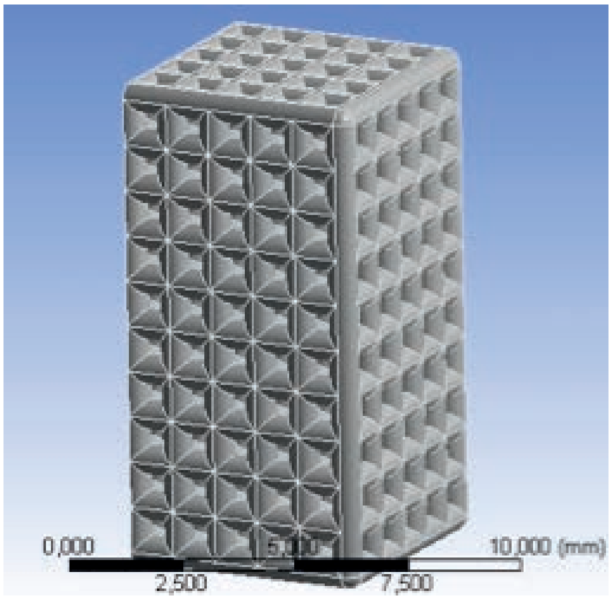

3D CAD of the porous microstructure.

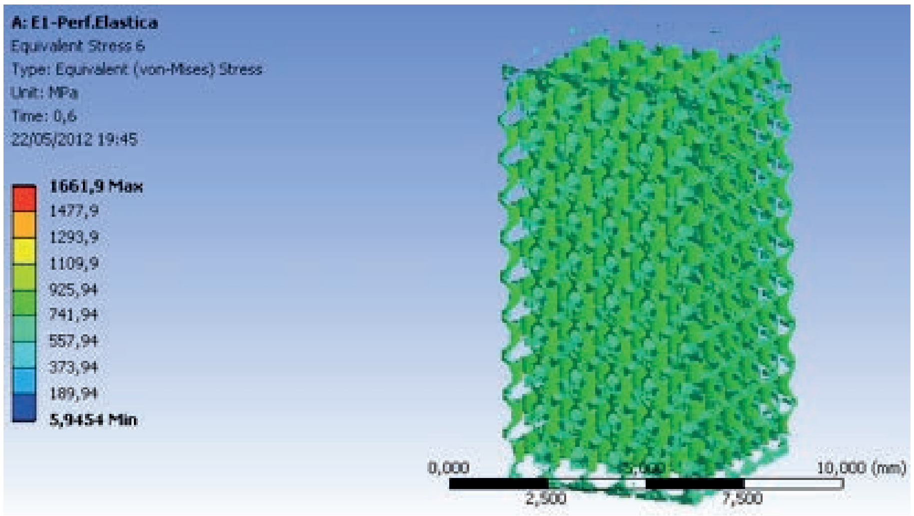

Widespread plastic behaviour at 0,06 mm of displacement.

PB.19

A NEW OSSEOINTEGRATABLE AND DAMAGEABLE INTERFACE ELEMENT FOR MODELING OF BONE-IMPLANT AND BONE-CEMENT INTERFACES

Christiane Caouette
École de technologie supérieure, Boucherville, Canada

We propose a new robust modeling method for the finite element modeling of load-transmitting bone-cement and bone-implant interfaces. This new modeling method allows simulation of osseointegration and progressive debonding.

Introduction

Finite element (FE) models are frequently used for preclinical evaluation of orthopaedic implants, but an aspect of these models remains neglected: the modeling method of load-transmitting bone-implant and bone-cement interfaces. Frictional or bonded contact elements are usually used, despite the fact that these elements cannot simulate behaviors such as osseointegration or progressive debonding. Furthermore, studies have demonstrated that the idealized Coulomb friction model of frictional contacts does not represent the non-linear behavior of bone-implant interfaces [1] and that bonded contacts overestimate bone-cement interface rigidity by a factor of 2 [2]. All of these aspects of load-transmitting interface modeling could affect the level of stress shielding predicted by FE models. The objective of the current study is to propose a new modeling method for bone-implant and bone-cement interfaces based on the work of Moreo et al. [3], a method allowing simulation of evolutive and progressive behaviors such as osseointegration and progressive debonding.

Methods

A FE model was constructed; the femur was obtained from CT-scan images and is modeled with heterogenous linear elastic isotropic properties. A commercially available model of hip resurfacing femoral component with a modified stem made of osseointegratable biomimetic composite and a 1-mm thick cement mantle is used. A static load case representing normal gait was applied to evaluate strain within the bone of the femoral head and neck. The bone-stem and bone-cement interfaces are modeled with an osseointegratable and damageable interface element that follows an exponential law based on experimental data from bone-cement interfaces [4]. This law uses an osseointegration parameter α that varies between 0 and 1, allowing the possibility of partially osseointegrated interfaces based on the mechanical conditions at the interface.

Results

Numerical results show that the biomimetic stem progressively osseointegrates (α averages 0,7 on the stem surface, with spot-welds) and that bone-stem micromotions decrease below 10 mm. Osseointegration also changes the load path within the femoral bone: a decrease of 300 me was observed in the femoral head, and the infero-medial part of the femoral neck showed a slight increase of 165 me. There was also increased stress in the implant stem (from 7 to 11 MPa after osseointegration), indicating that part of the load was supported through the stem.

Discussion

A new, robust modeling method for bone-implant and bone-cement interfaces has been presented. The use of this new osseointegratable interface element has shown the osseointegration potential of the biomimetic stem. Its ability to model partially osseointegrated interfaces based on the mechanical conditions at the interface means the new element could be used to study load transfer and osseointegration patterns on other models of uncemented hip resurfacing femoral components.

[1] Dammak et al. (1997) JBiomech30(2): 121-129. [2] Janssen et al. (2009) J Orthop Res27(10): 1312-8. [3] Moreo et al. (2007) Comp Meth Appl Mech Eng196(35-36): 3300-3314. [4] Mann et al. (2001) J Orthop Res19(6): 1153-1161.

PB.20

Local stresses around scapular implant in total shoulder arthroplasty: a finite element model

Ibrahim Kalouche
Bicetre University Hospital, Paris, France

Local stresses around pegs of a scapular implant were simulated using a finite element model. This model showed that effective primary fixation could not be assured by a press-fit technique.

Total shoulder prostheses have a limited survival due mainly to the loosening of the glenoid implant. The purpose of this study was to analyze the local stresses around the glenoid implant in the case of a press-fit technique of fixation. A finite element model of the glenoid cancellous bone based on anisotropy and heterogeneity of the mechanical properties of this bone was elaborated using the results of mechanical compression tests coupled with magnetic resonance imaging of the same specimens (scapulae).

Finite element simulation showed the inability of the glenoid cancellous bone to withstand minimal radial displacement of 32.5 μm (corresponding to a strain level lower than 10^{-4}) around implant's pegs, with local stresses exceeding the maximum strength of cancellous bone in the sagittal plane.

This model showed that effective primary fixation could not be assured by a press-fit technique of stabilization of the pegs of a glenoid implant.

New perspectives for the design of a cementless prosthesis should search other modes of fixation in the glenoid cancellous bone.

PB.21

Shaping Patient Specific Templates for Arthroplasty to obtain High Docking Robustness

Joost Mattheijer
Delft University of Technology, Delft, The Netherlands

Patient Specific Templates are designed to have a unique fit with the joint surface. The exact shape of the template determines the fit that may be perceived when the surgeon holds it in position and is topic of our research.

In arthroplasty, worn out and painful joints are replaced with a prosthesis. Alignment instruments are used to find where bone cuts need to be made, in order to place the prosthesis with the correct alignment. This process can often be problematic and prone for errors, because only a small part of the involved bones – the joint - is exposed. Computer Assisted Surgery (CAS) techniques are being used in arthroplasty, in order to obtain accurate alignment of prosthetic components.

Generally there are two CAS approaches used today: Camera-based CAS and Patient Specific Templates (PST's). Camera-based CAS relies on – time consuming – registration of the actual bone surfaces as exposed during surgery and the virtual bone models resulting from CT or MRI. Bone, instruments and prosthesis using markers are subsequently tracked by a camera. For the PST method, the virtual bone models are used to fabricate plastic templates, representing the negative imprint of the joint surface. During surgery, the templates are supposed to dock in the planned position only, taking away the need for a time-consuming registration process. Holes and slots that are incorporated in the templates are instantly aligned right and will be used to guide cutting instruments. Our research group is developing Configurable PST's: templates that can be customized for every surgery to have a patient specific fit.

As a first topic of research we are investigating the quality of the fit. The shape of the template – the location of bone-template contact and an application surface where the surgeon may push – determines the fit that may be perceived when the template is held in its planned position. The goal is to analyze the effect of the template's shape onto the range of forces that may be applied, i.e. the docking robustness. The bony geometry is hereto used as an input to find suitable locations for bone-template contact and the application surface. The wrench space theory widely used in the related research areas of robotic hands and workpart fixtures is employed to obtain an analytical method. With this method, templates can be fully shaped to obtain high docking robustness with minimal contact.

PC.02
POLYAMINE ROLE IN OSTEOGENESIS OF ADIPOSE DERIVED STEM CELLS

Giovanni Trisolino
Rizzoli Orthopaedic Institute, Bologna, Italy

Adipose derived stem cells (ASC) are an attractive cell source for regenerative purposes in orthopedics. Spermine can represent a potential tool to improve and speed the differentiation of ASC for bone tissue engineering .

Introduction:
‘Adipose derived stem cells (ASC) are an attractive cell source for regenerative purposes in orthopedics, because of their accessibility and high differentiation potential, upon delivery of appropriate stimuli which mimick the organogenetic natural microenvironment.
Polyamines are naturally occurring, positively charged polycations able to interact with negatively charged compounds and structures within the living cell thus controlling several cellular processes including cell differentiation and already implicated in bone growth and development. Hence, we investigated the effects of exogenously added spermine in osteogenesis of ASC, to tease out the effects on gene and protein expression of key regulatory transcription factors, markers and effectors.
Patients & Methods:
‘Adipose tissue was obtained from intra-operative biopsies of subcutaneous tissue from 24 OA patients (age 26-72) undergoing total hip replacement. ASC were obtained from the stromal vascular fraction with conventional procedures and used within p2-p3 passage. To monitor phenotypic homogeneity, flow cytometric analysis of the cells at p1 passage was carried out to evaluate the CD31, 34, 45, 271, 44, 73, 90 and 105 expression. Micromasses were seeded in control (D-MEM 10% FCS and 50 µg/ml ascorbic acid) or chondrogenic medium (Miltenyi), with or without the addition of 5 µM spermine to evaluate its osteogenic ability across 1, 2 and 3 weeks maturation. Osteogenic medium was used as positive control. We evaluated the effects of spermine addition on osteogenic differentiation molecular markers at gene level (real time PCR) and protein (western blot, immunohistochemistry and confocal microscopy) expression as well as the effects on extracellular matrix deposition and mineralization.
Results:
‘The number of ASC per unit (g) of adipose tissue was inversely correlated with the age of both male and female subjects and positively correlated with the body mass index. ASC samples were highly positive for CD44, CD73 and CD90, being the expression of the latter inversely correlated with the age of the subjects. In all micromass culture conditions, gene espression of osteogenesis markers far exceeded that of chondrogenesis markers. We observed an increase in osterix (the osteoblast commitment factor) and VEGF (a major contributor of neoangiogenesis associated to osteogenic differentiation). Indeed, early markers of the osteoblast lineage such as Runx-2 and alkaline phosphatase were highly expressed and further induced by 5 µM spermine addition. However, in most patients, Runx-2 protein expression did not increase upon spermine addition. Further evaluation by confocal microscopy are intended to investigate nuclear Runx-2 expression at the single cell level in control micromasses and following spermine addition. Mineralization evaluated in micromass lysates indicated an increased calcium content upon spermine addition.
Discussion/Conclusions:
‘Spermine can represent a potential tool to improve and speed the differentiation of ASC for bone tissue engineering favouring intramembraneous ossification rather than endochondral ossification.

References

‘Zuk PA, et al. Human adipose tissue is a source of multipotent stem cells. Mol Biol Cell. 2002 Dec;13(12):4279-95.

PC.03
Combination of Osteotomy with Autologous Chondrocyte Implantation

Atanu Bhattacharjee
Robert Jones and Agnes Hunt Orthopeadic Hospital, Oswestry, UK

Simultaneous correction of the axis of a joint and re-instating the biology of denuded cartilage by ACI can not only prolong requirement for primary joint replacements but can markedly reduce the revision joint replacement surgery.

Introduction

Knee arthroplasty is the end-stage procedure for biological joint failures. Surgically correcting underlying knee misalignments and promoting cartilage regeneration can delay such joint replacements in young patients. The aim of this study is to assess functional outcomes and survivorship of combining Osteotomy with Autologous Chondrocyte Implantation (ACI) for treatment of articular cartilage defects in early Osteoarthritis (OA) of knee.

Methods

Data was prospectively collected for functional outcomes and survivorship of combined osteotomy and ACI for chondral defects in early OA for 18 consecutive patients - 12 males, 6 females, aged 16 - 65 years (mean age 38.8 years) over a mean follow up period of 45.1 months. Of the total number of patients, 14 patients had associated meniscal pathology, with 4 requiring previous operative treatment. All patients had signed an informed consent prior to the planned treatment. Patients were followed up after they underwent both ACI and osteotomy - 14 patients had osteotomy and ACI done simultaneously, 4 patients had two procedures at an average interval of 9 months (time range 5-16 months). 7 patients had distal femoral varus osteotomy- 1 medial closing wedge and 6 lateral opening wedge osteotomies. 11 patients had proximal tibial osteotomies- 1 closing varus osteotomy, 1 closing valgus osteotomy and 9 had opening valgus osteotomies. Opening wedge osteotomies were done by Tensegrity technique. Lysholm scores, collected annually, were compared with pre-operative scores. Knee arthroplasty / pending knee replacements were considered failure of the existing treatment and defined as end of follow-up. A Kaplan-Meir curve was used to ascertain the survival probability at 5 and 10 years. Arthroscopy of the knee done 3 weeks prior to the ACI confirmed chondral defect size, site and allowed simultaneous cartilage biopsy from non-weight bearing areas to harvest chondrocytes. These chondrocytes were released by enzymatic digestion and expanded in vitro in Good Manufacturing Practice (GMP) standard laboratory of the hospital. On an average, 1.1 million cells per cm^2 of chondral defect were re-implanted at 21 days. Chondroguide (14 patients) and periosteal patch (4 patients) were used to contain these cells on the defects.

Results

The 5 and 10- year cumulative survival probability of combined procedures were 84.8 per cent and 72.8 per cent respectively, with 3 failed treatments. Mean pre-operative Lysholm score was 42.7 (SD 16.3), improving by 17.1 points (SD-23.3) to 59.8 (SD 27.1) at the last follow up. Oldham's method showed significant rise in post-operative Lysholm scores. The mean chondral defect size was 10.9 cm^2 (SD-9.3 cm^2) with 13 patients having interface chondral defects between tibia and femur. Student's T-test was used to ascertain the influence of meniscal pathology, interface chondral defects and location of osteotomy on the outcome following such procedures. Patients with co-existent meniscal pathology (n=14) or interface chondral defects (n=13) between femur and tibia had significantly less improvement of Lysholm scores at follow up (p-value < 0.05). Tibial osteotomies (n=14) had better outcomes than femoral osteotomies (n=4) (p-value <0.05).

Conclusion

Combining ACI and Osteotomy can delay joint replacements in young patients with large chondral defects for a period up to ten years. Improvement of post operative Lysholm scores through this method is comparable to outcomes of ACI for treatment of smaller chondral defects. Concurrent meniscal pathology or interface lesions between tibia and femur can impair the outcome following such procedures. Tibial osteotomies done to correct the alignment produce favourable outcome than femoral osteotomies. This study is restricted by a relatively small sample size, with a single surgeon recruiting patients in one tertiary care centre. Nevertheless, it ensures the uniformity of the surgical intervention and hence avoids discrepancies in outcome.

PC.04
Linking tendon stem/progenitor cells to tendon aging

Denitsa Docheva
Ludwig-Maximilians-University (LMU), Munich, Germany

There is substantial evidence that impaired stem cell functions can lead to tissue aging and cancer. Here, we could show that tendon-derived stem/progenitor cells accumulate functional deficits and hence we suggest that they contribute to the onset of tendon aging.

Introduction: With advancing age, tendons become more prone to tissue degeneration followed by injuries. Furthermore, in elderly patients tendon repair often requires lengthy periods of rehabilitation. It has been already recognized that altered stem cell properties are linked to aging and age-associated diseases. Therefore, the aim of this study was to determine if the functions of tendon stem/progenitor cells (TSPC) decline during tendon aging.
Methods & Results:
For this purpose, TSPC derived from human Achilles tendons of young (Y-TSPC) and elderly (A-TSPC) individuals were compared. FACS and PCR analyses showed that the isolated cells express mesenchymal stem cell markers (CD73, CD90 and CD105) and tendon-related genes (Scleraxis, Eya1, Six1) confirming their TSPC character. Long-term growth analysis and clonogenicity assay clearly demonstrated that A-TSPC enter earlier into growth arrest and have significantly lower colony forming potential compared to Y-TSPC. In addition, senescence analysis (ß-gal assay and p16INK4A expression) revealed that A-TSPC contain higher portion of senescent cells. Interestingly, both TSPC groups retained their multipotentiality as are able to differentiate into adipocytes, osteoblasts and chondrocytes. Next, in order to identify specific gene changes in tendon aging, genome-wide microarray and gene cluster analysis were performed. This data suggested a number of genes, mainly involved in cell cytoskeleton and migration, to be affected. Indeed, further examination by time lapse and actin staining revealed that A-TSPC are less migratory and have slower actin fibre turnover.
Conclusions:
Taken together, our data strongly suggest that during tendon aging TSPC become exhausted in number and functional performance. Thus, our study provides the first fundamental basis for understanding the mechanisms behind tendon aging.

PC.08

IN VITRO DIFFERENTIATION OF BONE MARROW DERIVED MESENCHYMAL STEM CELLS.

Annamalai Chandrasekaran
Department Of Orthopaedic Surgery, Sri Ramachandra University, Chennai, India

In vitro Bone marrow derived mesenchymal stem cells are isolated and expanded to osteoblast,chondrocyte, myofibrils, adiposites

Isolation and expansion of mesenchymal stem cells (MSC)
MSC characterization
Surface expression of CD44 & CD29 by flow cytometry
3. Induction of osteogenic differentiation
- Morphological follow up
- Alizarin red staining for calcium accumulation
- Gene expression analysis for osteocalcin and osteopontin by reverse transcriptase (RT) PCR
- Bone marrow from patient
- Stem cells identified and isolated
- Grown in special culture medium
- Temperature were regulated

Pittenger, Science 1999 et al
Mesenchymal stem cells were separated from the marrow aspirate
and expanded in lab to osteoblast, chondrocyte, lipocytes, myotubes
Mesenchymal stem cells were successfully isolated and characterised in vitro.
The cells could readily differentiate into Osteogenic lineages upon induction.
MSC’s is a very promising tool for regenerative medicine
Further engineering such osteogenic cells in scaffolds would allow us to transplant and repair bone defects.

PC.08

IN VITRO DIFFERENTIATION OF BONE MARROW DERIVED MESENCHYMAL STEM CELLS.

Annamalai Chandrasekaran
Department Of Orthopaedic Surgery, Sri Ramachandra University, Chennai, India

In vitro Bone marrow derived mesenchymal stem cells are isolated and expanded to osteoblast,chondrocyte, myofibrils, adiposites

Human mesenchymal stem cells are thought to be multipotent, which are present in adult marrow that can replicate as undifferentiated cells and that have the potential to differentiate to lineages of mesenchymal tissues, including bone, cartilage, fat, tendon, muscle and marrow stroma.
Our aim is to develop region specific stem cell in treating difficult orthopaedic problem where treatment is not available.
To do away animal experiment,
And we can establish STEM CELL BANK.
Our Objectives are
Isolation and expansion of mesenchymal stem cells (MSC)
MSC characterization by surface expression of CD44 & CD29 by flow cytometry
Induction of osteogenic differentiation - Morphological follow up
- Alizarin red staining for calcium accumulation
- Gene expression analysis for osteocalcin and osteopontin by reverse transcriptase (RT) PCR

Methodology
- Bone marrow from patient
- Stem cells identified and isolated
- Grown in special culture medium
- Temperature were regulated

Pittenger, Science 1999 et al
Mesenchymal stem cells were separated from the marrow aspirate
and expanded in lab to osteoblast, chondrocyte, lipocytes, myotubes.
The cells could readily differentiate into Osteogenic lineages upon induction.
MSC’s is a very promising tool for regenerative medicine.
Further engineering such osteogenic cells in scaffolds would allow us to transplant and repair bone defects.

PC.09
Differential Effects of Cyclooxygenase-1 and -2 specific NSAIDs on Chondrogenic Differentiation

Marjolein Caron
Maastricht University Medical Centre, dept. Orthopaedic Surgery, Maastricht, The Netherlands

COX-enzymes and PG-production have a differential role in chondrogenic differentiation.

Introduction:
NSAIDs are clinically used to relieve pain and decrease inflammation by inhibition of cyclooxygenase (COX)- catalyzed prostaglandin (PG) synthesis. As PGs are important fatty acid metabolites in bone and cartilage homeostasis, they thereby may provide a novel way to influence cartilage regeneration. In this study we aimed to define how different COX-1 or COX-2 specific NSAIDs influence extracellular matrix formation during chondrocyte differentiation.
Methods:
ATDC5 cells were differentiated in the presence of different COX-1 (SC-560, Mofezolac) or COX-2 (NS398, Celecoxib) specific inhibitors. COX-1 or COX-2 specificity of the NSAIDs and NSAID-specific inhibition of prostaglandin synthesis were determined by colorimetric enzymatic assays and PG-specific ELISAs. Specific prostaglandins were added during the differentiation process. Gene- and protein expression analyses were employed to determine the effects on chondrogenic extracellular matrix formation.
Results:
COX-specificity of the NSAIDs was confirmed and for subsequent experiments NSAID concentrations were selected that resulted in similar degrees of COX-1 or COX-2 inhibition. COX-1 specific NSAIDs inhibited both Col2a1 and Col10a1 expression. Inhibition of COX-2 resulted in substantial decrease of Col10a1 expression, while Col2a1 remained unaffected. To explain this difference we determined the expression patterns of both COX enzymes as well as specific prostaglandin synthesis during differentiation. COX-1 is upregulated during late chondrogenic differentiation only, whereas COX-2 is briefly expressed early in differentiation and increases again late in differentiation. PGD2 and PGE2 faithfully followed the COX-2 expression pattern, whereas PGF2a and TXA2 levels remained stably low. Furthermore, COX-2 inhibition resulted in decreased levels of all tested PGs, whereas COX-1 inhibition inhibited synthesis of all PGs, except for PGD2 and PGF2a, which were increased by COX-1 inhibition. Addition of PGE2 and PGF2a resulted in increased expression of chondrogenic markers.
Conclusions:
Our findings point towards a differential role for COX-enzymes and PG-production in chondrogenic differentiation. Ongoing research is focusing on further elucidating the functional partition of cyclooxygenases and specific prostaglandin production. Our data add to the pallet of possibilities for improving the collagen quality of cartilage constructs for better outcome of cartilage regenerative approaches.

PC.10

Early increase of serum angiopoietin-2 is associated with early progression to death in experimental injury.

Stephanos Koutsostathis
Fourth Orthopaedic Department, KAT Hospital, Kifissia, Greece

To define the role of Ang-2 in lethal injury, a model of lethal trauma in rabbits was studied. Results suggest that Ang-2 is markedly increased early in the course of SIRS where death is imminent within the first two days.

Introduction

Severe trauma induces systemic inflammatory response syndrome (SIRS) through the release of proinflammatory mediators. Angiopoietin-2 (Ang-2) is over-produced in sepsis and leads to dysfunction of endothelial cells and subsequent multiple organ dysfunction. In order to define the role of Ang-2 in lethal injury, a model of lethal trauma in rabbits was studied.

Animals and methods

For the purpose of this study, 45 rabbits were used; 8 were administered anesthesia, 26 were subject to femoral injury (a complete transverse fracture of the middle shaft of the right femur) and 11 were sham-operated (undergoing only the approach used to cause the fracture to the rabbits of the other group). Concentrations of Ang-2, malondialdehyde (MDA), tumor- necrosis factor- alpha (TNFα) and endotoxins (LPS) were determined in serum and of Ang-2 intissues. Vital signs and overall survival were recorded. Bacterial growth was quantitatively assessed in liver, spleen and lung of animal that died.

Results

Survival of injured animals was shorter than sham operated ones. Serum concentration of Ang-2 at 4 hours was greater among animals where death supervened early, i.e. within 48 hours after injury, than among rabbits that died later. That was also the case for systolic, diastolic and mean arterial pressures. All three arterial pressures at 4 hours were lower among rabbits that died early comparedto rabbits that died late after trauma. Serum MDA and TNFα and tissue bacterial growth did not differ between rabbits that died early and rabbits that died late. Serum LPS remained below the limit of detection (Figure 1).

Discussion

These results suggest that, in an animal model of lethal trauma, Ang-2 is markedly increased early in the course of SIRS in rabbits where death is imminent within the first two days from the onset of trauma. This is accompanied by rapid hemodynamic instability. The results highlight a significant role of Ang-2 inthe course of lethal trauma and that Ang-2 may be a potential target for therapeutic intervention for SIRS developed after multiple injuries.

PC.12
Immunologic factors underlying periprosthetic osteolysis in THA

Jiri Gallo
Department of Orthopaedic Surgery, Palacky University, University Hospital Olomouc, Czech Republic

We postulate that the local tissue homeostatic mechanisms more effectively regulate the adverse pro-inflammatory/ pro-osteolytic cells/ pathways in patients with none/ mild periprosthetic osteolysis (PPOL) than in patients with severe PPOL.

Total hip arthroplasty (THA) is an effective and safe method for treating severe osteoarthritis of the hip. With the extension of THAs to a younger and more active population, the expected time of service of THAs could be insufficient and the number of revision surgeries will therefore increase[1]. The main reasons for failure of THA is aseptic loosening accompanied by osteolysis[2]. Periprosthetic osteolysis is currently considered a multifactorial complication of THA in which prosthesis-related factors act in concert with genetically and environmentally determined host-responses[3]. The key concept in particle disease is that very small prosthetic particles (micrometers and less in size) stimulate periprosthetic cells to express proinflammatory/ pro-osteoclastic cytokines and other substances that orchestrate increased accumulation/activity/survival of osteoclasts, and inhibit the activity of osteoblasts and their progenitors^{4,5}. Additionally, mechanical stresses, tissue injury, hypoxia, and bacterial remnants can trigger innate immune responses and inflammation. However, when inflammatory sensors are activated, there is a concurrent activation of protective and regenerative mechanisms in order to restore the original tissue architecture and normal tissue metabolism once inducers are excluded. Oxygenated lipids, anti-inflammatory cytokines and other classes of molecules exert strong control of inflammation^{6,7}. Another such mechanism is erythropoietin-mediated tissue protective system that is up-regulated by inflammation and hypoxia.

The role of protective and homeostatic mechanisms in non-destructive local host tissue response to prosthesis-related stimuli in successful THAs has not been previously investigated despite the fact that such mechanisms should exist[8,9]. In the absence of a key negative feedback loop, the proinflammatory chemokines/ cytokines develop a severe inflammatory microenvironment associated with the predominance of activated macrophages, fibroblasts, synoviocytes, lymphocytes and osteoclasts over osteoblasts, resident-fibroblasts and other homeostatic repair cells. In this line, periprosthetic osteolysis can be considered as a failure of local tissue homeostatic mechanisms. This disturbance can be at the level of sensors, regulators and effectors of ‘particle disease’. Precise identification of the deregulated signaling pathways, mediators and cellular differentiation programs that contribute to periprosthetic osteolysis could facilitate the development of selective, targeted therapeutic strategies including new generation of mimetic, self-diagnosing and multifunctional prosthetic surfaces.

This study was supported by Internal Grant Agency Ministry of Health, Czech Republic (NT/11049-5).

References:

1. Kurtz SM, Lau E, Ong K, Zhao K, Kelly M, Bozic KJ. Future young patient demand for primary and revision joint replacement: national projections from 2010 to 2030. Clin Orthop Relat Res 2009;467-10:2606-12.
2. Bozic KJ, Ong K, Lau E, Kurtz SM, Vail TP, Rubash HE, Berry DJ. Risk of complication and revision total hip arthroplasty among Medicare patients with different bearing surfaces. Clin Orthop Relat Res 2010;468-9:2357-62.
3. Del Buono A, Denaro V, Maffulli N. Genetic susceptibility to aseptic loosening following total hip arthroplasty: a systematic review. Br Med Bull 2012;101:39-55.
4. Konttinen YT, Zhao D, Beklen A, Ma G, Takagi M, Kivela-Rajamaki M, Ashammakhi N, Santavirta S. The microenvironment around total hip replacement prostheses. Clin Orthop Relat Res 2005-430:28-38.
5. Ren PG, Irani A, Huang Z, Ma T, Biswal S, Goodman SB. Continuous infusion of UHMWPE particles induces increased bone macrophages and osteolysis. Clin Orthop Relat Res 2011;469-1:113-22.
6. Medzhitov R. Inflammation 2010: new adventures of an old flame. Cell 2010;140-6:771-6.
7. Nathan C, Ding A. Nonresolving inflammation. Cell 2010;140-6:871-82.
8. Gallo J, Konttinen, Y.T., Goodman, S.B., Thyssen, J.P. et al. Aseptic loosening of total hip arthroplasty as a result of local failure of tissue homeostasis. In: Fokter SK, ed. Recent advances in arthroplasty. Rijeka: InTech, 2012:319-62.
9. Zhang Y, Hou C, Yu S, Xiao J, Zhang Z, Zhai Q, Chen J, Li Z, Zhang X, Lehto M, Konttinen YT, Sheng P. IRAK-M in macrophages around septically and aseptically loosened hip implants. J Biomed Mater Res A 2012;100-1:261-8.

PC.13
The involvement of endoplasmic reticulum stress in FGFR3-related chondroplasias

Ryosuke Sato

This study is the first report that provide the new insight into molecular pathogenesis of chondrodysplasia due to mutant FGFR3 genes besides the hypothesis that activation of FGFR3 signaling contributes to chondrodysplasias.

Introduction

Point mutations of the Fibroblast Growth Factor Receptor3 Gene are known to cause short limb dwarfism which is called achondroplasia or hypochondroplasia. In achondroplasia, a majority of cases are caused by G380R mutation within transverse membrane domain, while various sites of mutations are reported in hypochondroplasia. Constitutive activationof the MAPK and JAK/STAT1 pathway byG380R mutant FGFR3 has been shown, but it is unclear whether various mutants in hypochondroplasia activate signaling pathways.

Newly synthesized secretory and membrane proteinsare folded and matured in the lumen of the endoplasmic reticulum (ER). Various physiological and pathological conditions perturb protein folding in the ER lumen and lead to accumulation of unfolded proteins, a cellular condition referred to as ER stress. To deal with ER stress, cells activate the unfolded protein response (UPR), involving the induction of molecularchaperones,translational attenuation, and ER-associated degradation. When theUPRis perturbed or not sufficient to restore normal ER function,apoptosis is induced (see Fig. 1), which is implicated in the pathophysiology of several diseases. Accumulating evidence indicates that the synthesis of mutant proteins such as collagen1, collagen2, collagen10, COMP and matrilin3 can trigger ER stress.

In this study, we examined whether mutant FGFR3 proteins of hypochondroplasia cause ER stress.

Method

The plasmids containing wild-type, R200C, I538V, N540K, N540S, N540T, K650N and K650Q mutant FGFR3 genes, cause hypochondroplasia, were constructed. HEK293 cells were transfected with wild-type or mutant FGFR3 expression vectors using polyethyleneimine by reverse transfection method. The activation of MAPK pathway were verified by western blotting analysis and quantified by densinometry. The activation of JAK/STAT1 were measured using Luminex xMAP technology. The ER stress reporter plasmid containing unfolded protein response element, which had the binding sites of XBP1 induced by ER stress, was constructed for detection of induction of ER stress. HEK293 cells were co-transfected with the ER stress reporter plasmid, plasmids expressing mutant FGFR3 and EGFP. Luciferase assay was performed 48hours after transfection. Luciferase signal was normalized by EGFP fluorescence to correctfor transfection efficiency.

Result

FGFR3^{R200C} and FGFR3^{N540T} mutants did not activate both MAPK and JAK/STAT1 pathway. FGFR3^{N540K} activated only MAPK pathway. FGFR3^{I538V}, FGFR3^{N540S}, FGFR3^{K650N} and FGFR3^{K650Q} mutants activated both pathways (see Fig. 2).

Luciferase signals in cells transfected with R200C, N540K and N540T mutant FGFR3 genes, increased compared to that of wild type FGFR3 (see Fig. 3).

Discussion

Membrane proteins, such as FGFR3, is necessary to be folded in their proper tertiary structure in the ER to work functionally, improperproteinfolding (misfolding)due to mutation can leads to the accumulation of unfolded proteins in the ER and might trigger apoptosis. It is generally accepted thatFGFR3is a negative regulator of chondrogenesis and thatconstitutive activationofFGFR3 signaling is the cause of chondrodysplasias. This study indicated that ER stress was induced by FGFR3 mutants, might lead to chondrodysplasia inducing anapoptosis of chondrocytes. Further molecular elucidation of role of ER stress in chondrodysplasia propose anewtreatment approach using ‘chemical chaperone’, that can stabilize various proteins against misfolding.

Unfolded protein response

-The activation of MAPK and JAK/STAT1 signaling by mutant FGFR3

-Induction of ER stress by mutant FGFR3

PC.14

Redifferentiation of Human Articular Chondrocytes in 2D versus 3D culture

Marjolein Caron
Maastricht University Medical Centre, dept. Orthopaedic Surgery, Maastricht, The Netherlands

For redifferentiation of dedifferentiated human articular chondrocytes, three-dimensional cultures like alginate beads and pellets exhibit the most potent chondrogenic potential, whereas a hypertrophic phenotype is best achieved in two-dimensional monolayer cultures.

Introduction:
For cartilage regenerative techniques human articular chondrocytes (HACs) are cultured in vitro. Unfortunately, long expansion time and multiple passaging lead to ‘dedifferentiation’. Many studies ‘redifferentiate’ chondrocytes in three-dimensional culturemodels (pellets, alginate cultures etc.). However, the rationale behind the choice for three-dimensional above two-dimensional cultures (monolayer) is poorly investigated, and is mainly based on mRNA expression and GAG content. The objective of this study was to determine the differential chondrogenic redifferentiation characteristics of human articular chondrocytes in monolayer, alginate beads and pellet culture.
Methods:
Dedifferentiated HACs (passage 5) from 6 individuals were redifferentiated in identical medium conditions for 7 days in monolayer, alginate beads or pellet culture. Read-out parameters were defined as expression of chondrogenic and hypertrophic mRNAs and proteins, GAG content and cell proliferation.
Results:
Three-dimensional cultures specifically induced chondrogenic mRNAs (COL2A1, SOX9, ACAN), whereas two-dimensional cultures did not. Hypertrophic mRNAs (COL10A1, RUNX2, MMP13, VEGFA, OPN, ALP) were highly increased in two-dimensional cultures and lower in three-dimensional cultures. Suggesting that redifferentiation in monolayer does not fully support a chondrogenic phenotype. Protein expression analysis supported most of the mRNA data, although an important discrepancy was found between mRNA and protein expression of COL2A1 and SOX9 in monolayer culture, stressing on the importance of protein expression analysis. GAG content was highest in three-dimensional cultures, whereas chondrocyte proliferation was almost specific for two-dimensional cultures.
Conclusion:
For redifferentiation of dedifferentiated HACs, three-dimensional cultures exhibit the most potent chondrogenic potential, whereas a hypertrophic phenotype is best achieved in two-dimensional cultures. This is the first human study that systematically evaluates the differences between proliferation, GAG content, protein expression and mRNA expression of commonly used two- and three-dimensional chondrocyte culture techniques.

PC.15
BMP 7 in the treatment of pseudoarthroses of the foot

Klemens Trieb
Department of Orthopedics, Wels, Austria

This paper presents the results of BMP 7 as a useful tool in treating pseudoarthroses of the foot.

Introduction:
Treatment of pseudarthroses is a highly demanding field with respect to bone healing. Treatment of tibial pseudoarthroses has been scuccessfully reported with the use of bone morphogenic proteine (bmp) 7. BMP 7 is a recombinant human protein produced in ovary cells of the chinese hamster. It is responsible for differentiation of mesenchymal stem cells from the periost, muscle and sponious bone and stimulates bone formation.
Methods:
It is the aim of our study to investgate the use of BMP 7 for other locations than the tibia, such as the foot. 10 pseudoarthroses of the foot (4 forefoot, 1 midfoot, 3 hindfoot, 2 tibia) were surgically treatet with stabilisation, resection and BMP 7 and followed after 19 months (5 - 40). 6 men and 4 women (mean age 58 years (range 33 - 80) were included, 14 previous surgeries are reported.
Results:
At follow-up all patients were satisfied with respect to pain and function, no operative complications occured and bone fusion was finished in 8 patients after 3 months, one ankle joint had a painfree fibrous fusion. One arthrodesis of the first metatarsophalangeal joint was turned to a resection arthroplasty, the pain is painfree and uses a normal shoe.
Discussion:
These results show that BMP 7 is a useful tool in treating pseudoarthroses of the foot.

PD.01

Fast Powder Sintering: an innovative process suitable for application of Ti foam onto challenging substrates

Luca Facchini
Eurocoating, pergine Valsugana-Trento, Italy

Fast Powder Sintering is a sintering process able to produce Functionally Graded Materials in one step.By FPS, tailored Ti foams can be applied to challenging substrates (e.g., Co-alloys, Ti-alloys or ceramics) thus enabling new designs in orthopedic devices.

Introduction.

In orthopedics, Co28Cr6Mo alloy is widely used due to its excellent wear performances required in joints reconstruction. Unfortunately poor osteointegration is achieved by the material itself even when a CoCrMo part is manufactured with a porous surface. At the moment long-term retention for prostheses using this type of material is mainly achieved using bone cement or adding additional HA or rough Ti coatings enabling limited bone ongrowth. On the other hand the golden standard in long term cementless fixation uses thick layers of osteoconductive materials with large size and interconnected pores (e.g. Trabecular Metal or similar solutions)

Fast Powder Sintering (FPS) is proposed as alternative technique to apply macro-porous Ti layers onto bioinert bulk substrates. FPS process starts from metal or ceramic powders as well as pre-sintered, ‘green’ or solid materials. This multiple working capability allows for new devices comprising Functionally Graded Materials (FGM) i.e. different biomaterials with different features in one single solid piece).

Methods.

In this work the sintering of pre-alloyed Co28Cr6Mo powders was carried out by FPS, together with c.p. Ti powder in a single manufacturing step, thus obtaining a near-net shape part presenting both fully dense CoCrMo and macro-porous interconnected Ti foam. FPS process involves DC pulsing currents that generate high temperature plasmas between the powder particles. Furthermore pressure, applied together with the current, promotes plastic flow during the sintering step. Described FPS process is hence characterized by high heating rates, relatively low sintering temperatures, small dwelling times. The obtained materials respect bio-composition and have improved performances.

FPS technology uses molds. The obtained products are near-net shape: depending on specific device requirements, further finishing operations can be required for total functionality (e.g., mirror like CoCrMo surface, burrs removal, etc.).

By animal testing bone ingrowth and fixation was showed using FGM specimens with Ti foam structures.

Results and discussion.

FPS process parameters were investigated by sintering CoCrMo in different conditions. Thanks to the relatively low sintering temperature and small soaking times, FPS avoids dramatic grain growth in the sintered material and allows the fine grained peculiar microstructures and well distributed carbides showed in (Fig. 1). Such microstructures are related to high mechanical performances, both in quasi-static (tensile) and dynamic (fatigue) conditions (Tab. 1).

At porous-bulk interface, titanium foams show adhesion in agreement with applicable norms as confirmed by pull-off and shear test results. C.p. Ti macro-porous surface (e.g. diameters 400-600 μm) have large and interconnected pores exhibiting high friction vs bone.

Biological evidences of bone ingrowth inside c.p.Ti pores (Fig. 2) have been collected as well as bone-implant fixation strength.

Conclusions.

FPS is a non-conventional technique suitable to quickly produce large numbers of near-net shape implants having a fully dense CoCrMo portion and a titanium macro-porous surface.

PD.03
Wear of vitamin-E blended polyethylene against large diameter CoCrMo metal and EBPVD chromium nitride coated femoral heads

Danielle de Villiers
Queen Mary, University of London, United Kingdom

Vitamin-E blended polyethylene is low wearing even at large diameters. Early stage wear rates of this polyethylene combined with CoCrMo and CrN coated metallic femoral heads are similar, although their head wear rates indicated higher wear of the uncoated components.

Introduction

Metal-on-polyethylene has been the ‘gold-standard’ in total hip replacement but is limited by wear of the polyethylene cup and the body’s resulting inflammatory response. Crosslinking ultra-high-molecular-weight polyethylene (UHMWPE) reduces wear but concern still remains over oxidation and material degradation. The introduction of an antioxidant (vitamin-E) has been shown to reduce oxidation [1].

Attempts to improve the wear resistance of UHMWPE have focussed on improvements to polyethylene, however wear reduction can also be achieved by optimisation of the femoral head component. Coating the femoral heads can decrease the wear of UHMWPE to levels comparable to ceramic-on-polyethylene [2]. Equally coating the metal head may reduce Co ion release into the surrounding tissues.

This study investigates the hypothesis that the wear performance of large diameter metal femoral heads articulating against vitamin-E blended UHMWPE can be enhanced by coating with chromium nitride (CrN).

Materials and Methods

Eight 52mm diameter GUR 1020 0.1wt% vitamin-E blended polyethylene liners, crosslinked at a dose of 120kGy and mechanically annealed (Corin, UK) were tested after pre-soaking for 9 weeks. Four were paired with CoCrMo heads and four with electron beam physical vapour deposition (EBPVD) CrN coated heads polished after coating (Tecvac, UK). Bearings were tested for three million cycles (mc) in an eight station hip simulator (MTS Systems, USA); gravimetric measurements were recorded and cobalt release measured from fluid samples taken over this period using graphite furnace atomic absorption spectroscopy (GFAAS).

Results

The volumetric wear of the vitamin-E polyethylene liners, Figure 1, showed there was no difference between their wear articulating against metal or CrN over 3mc with mean wear rates of 11.11 ± 2.57 and 9.70 ± 1.00 mm^3/mc, respectively.

Both types of femoral head showed measurable wear over the first million cycles with lower wear observed from the CrN heads, Figure 2. The cobalt release (ions and particles) increased over the test period, Figure 3, showing no difference from the CrN heads compared to soak controls.

Discussion

The results from this study show that vitamin-E blended polyethylene is a low wearing polyethylene at large (>50mm) diameters. The use of a coated metallic head compared to the CoCrMo metal had little effect on the wear rate of the liners but did influence the wear of the head itself and may lead to a cycle of increased wear clinically. The initial wear rates of 1.13 ± 0.07 and 0.80 ± 0.03 mm^3/mc for CoCrMo and CrN respectively were similar to standard metal-on-metal (MoM) testing, although mass gain prevented further measurement. Cobalt release from the CrN heads was approximately 20% that from CoCrMo heads and levels were much lower than those reported in MoM (6515 µg/L after 2mc [3]). The lower wear rates and a reduction in metal particle and ion release with CrN coated heads has clinical significance as the release of Co metal ions may be damaging to the surrounding cells.

References

1. Oral, E., et al Biomaterials, 2008.29
2. Galvin, A.L., et al., Wear, 2005.259
3. Royle, M., et al., ORS, 2011

PD.04

Pressures required for water jet dissection in minimally invasive hip refixation tested in interface tissue substitutes

Gert Kraaij
Delft University of Technology, Delft, The Netherlands

Minimally invasive refixation can be an alternative for the demanding revision surgery of loosened hip prostheses. Water jet dissection is a promising technique for removal of the interface tissue during the refixation procedure.

Introduction:
Worldwide about 1.5 million hip prostheses are implanted annually and this number is growing due to the longer life expectancy of people [1]. Within the first ten years approximately 10% of the hip prostheses fail because of aseptic loosening [2]. An alternative for the current invasive revision surgery, which requires complete removal of the loosened prosthesis and insertion of a new prosthesis, is a new Minimally Invasive Hip Refixation (MIHR) procedure. An important step in this procedure is the removal of the soft peri-prosthetic interface tissue. In a previous study laser and coblation were evaluated [3], however heat generation was an issue. This can be solved by using a coolant. But why not using the coolant itself, for water jet cutting, to cut the tissue? In medical field, the current applications of water jet are limited, but it is already used for liver resections. In experimental examinations Rau et al [4] found a pressure of 3-4 MPa (30-40 bar) and a nozzle diameter of 0.1 mm to be very effective to dissect normal liver tissue. The effect of a water jet on a material is influenced by the pressure and nozzle diameter combination. The aim of this pilot study is to evaluate the effect of the nozzle diameter on the required minimum water jet pressure to perforate soft elastic materials with different thicknesses.

Materials and Methods:
Water jets with nozzle diameters of 0.1, 0.2 and 0.6 mm were applied to specimens with thicknesses of 3, 6 and 9 mm and consisting of interface tissue substitutes: ballistic gel and silicone (Dragon Skin Pro). A specimen was placed under the water jet cutting head and by trial and error the minimum pressure was found to perforate the specimen. A low starting pressure was chosen and the water jet was activated for 2 seconds. At a new spot the water jet was activated again while the pressure was increased with 0.5 MPa. This procedure was repeated until the water jet pressure was high enough to perforate the specimen. To be sure the right minimum pressure was found, we performed three additional trials respectively with the minimum pressure and minimum pressure minus 0.5 MPa bar.

Results:
In Figure 1 the resulting minimum pressures for ballistic gel and silicone are shown. Minimum pressures for silicone were higher compared to those for ballistic gel. Pressure was (linear) increasing with increasing specimen thickness. A larger nozzle diameter resulted in a lower minimum water jet pressure. The largest drop in minimum pressure was found between a 0.1 and 0.2 mm nozzle.

Discussion/Conclusion: This pilot study shows that using larger nozzles results in reduced minimum water jet pressures to perforate soft elastic material. However, research with human interface tissue is necessary to find the optimal combination of nozzle diameter and associated minimum water jet pressure for interface dissection. Currently we are collecting human interface tissue to test water jet dissection.

References:
[1] R.J. Looney et al., Arthritis Research and Therapy, 4:59-63, 2002.
[2] H. Malchau et al., The wellcemented total hip arthroplasty: Theory and practice, chapter 11, pages 291-299. Springer Berlin Heidelberg, 2005.
[3] Kraaij et al., Medical Engineering & Physics, 34:370-377, 2012.
[4] Rau et al., HPB , 10: 275-280, 2008.

PD.06
Application And Survival Curve Of Total Hip Arthroplasties Using National Hip Arthroplasty Registers

Patrick Sadoghi
Ludwig-Maximilians University, Munich, Germany

This study revealed large differences in terms of the annual number of primary THAs per inhabitant and primary THA procedure type across Europe. Data can be used to rank local primary THA implantations within an international context.

Introduction:
The aim of the study was to compare primary total hip arthroplasty (THA) implantations between different countries in terms of THA number per inhabitant, age, and procedure type as well as to compare the survival curve including all THAs using hip arthroplasty registers.
Methods:
THA registers were compared between different countries with respect to the number of primary implantations per inhabitant and age, and procedure type and survival curve. We performed a literature search for all national hip arthroplasty registers providing annual reports for 2009 or, if not available, a more recent time period. The data of these reports were analyzed in terms of number, age distribution and procedure type of primary THAs and survival curves.
Results:
We identified nine hip arthroplasty registers, which comprised sufficient data to be included. A large variation was found in the annual number of primary THA implantations per inhabitant of more than the factor 2.5 for all age groups across regions. The procedure type varied strongly as well, e.g. in Sweden 67% are cemented THAs whereas in Emilia-Romagna (Italy) 89% are cementless THAs. Figure 1 illustrates the annual total number of primary total hip arthroplasty (THA) implantations per 100,000 inhabitants. Figure 2 for persons younger than 55 years, and figure 3 for persons between 55 and 64 years.
Discussion and Conclusion:
The present study revealed large differences in terms of the annual number of primary THAs per inhabitant and primary THA procedure type across regions. These data can be used to rank local primary THA implantations within an international context.

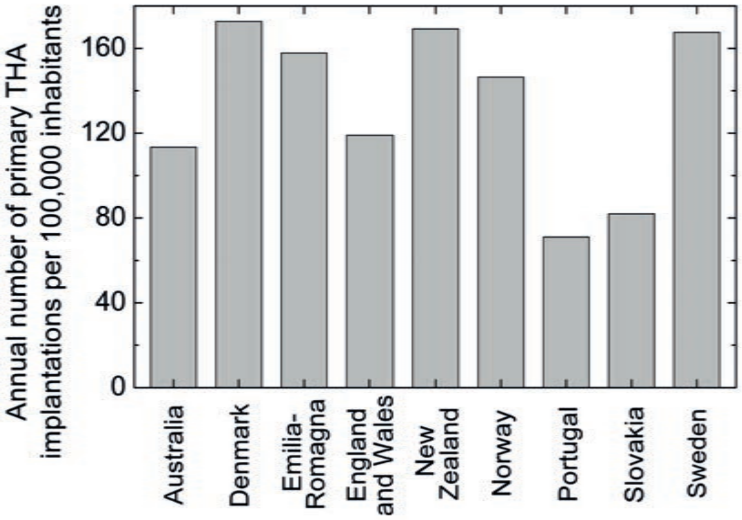

Figure 1 illustrates the annual total number of primary total hip arthroplasty (THA) implantations per 100,000 inhabitants.

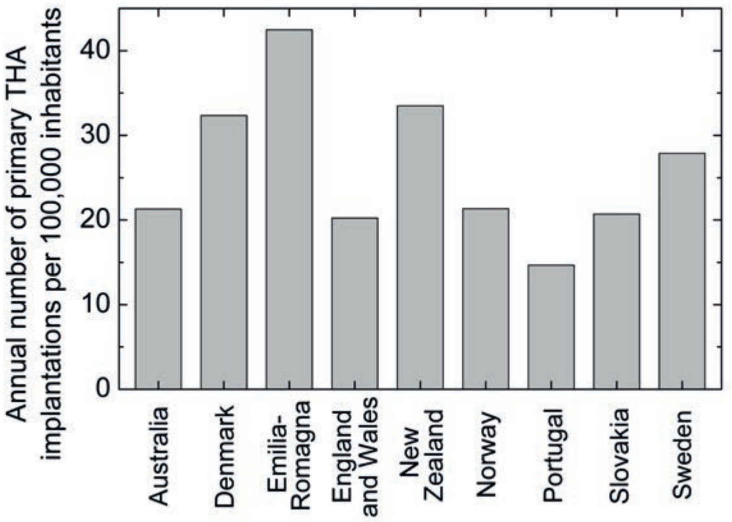

-Figure 2 illustrates the annual total number of primary total hip arthroplasty (THA) implantations per 100,000 inhabitants for persons younger than 55 years

PD.06

Application And Survival Curve Of Total Hip Arthroplasties Using National Hip Arthroplasty Registers

Patrick Sadoghi
Ludwig-Maximilians University, Munich, Germany

This study revealed large differences in terms of the annual number of primary THAs per inhabitant and primary THA procedure type across Europe. Data can be used to rank local primary THA implantations within an international context.

Introduction:
The aim of the study was to compare primary total hip arthroplasty (THA) implantations between different countries in terms of THA number per inhabitant, age, and procedure type as well as to compare the survival curve including all THAs using hip arthroplasty registers.
Methods:
THA registers were compared between different countries with respect to the number of primary implantations per inhabitant and age, and procedure type and survival curve. We performed a literature search for all national hip arthroplasty registers providing annual reports for 2009 or, if not available, a more recent time period. The data of these reports were analyzed in terms of number, age distribution and procedure type of primary THAs and survival curves.
Results:
We identified nine hip arthroplasty registers, which comprised sufficient data to be included. A large variation was found in the annual number of primary THA implantations per inhabitant of more than the factor 2.5 for all age groups across regions. The procedure type varied strongly as well, e.g. in Sweden 67% are cemented THAs whereas in Emilia-Romagna (Italy) 89% are cementless THAs. Figure 1 illustrates the annual total number of primary total hip arthroplasty (THA) implantations per 100,000 inhabitants. Figure 2 for persons younger than 55 years, and figure 3 for persons between 55 and 64 years.
Discussion and Conclusion:
The present study revealed large differences in terms of the annual number of primary THAs per inhabitant and primary THA procedure type across regions. These data can be used to rank local primary THA implantations within an international context.

PD.06

Application And Survival Curve Of Total Hip Arthroplasties Using National Hip Arthroplasty Registers

Patrick Sadoghi
Ludwig-Maximilians University, Munich, Germany

This study revealed large differences in terms of the annual number of primary THAs per inhabitant and primary THA procedure type across Europe. Data can be used to rank local primary THA implantations within an international context.

Introduction:
The aim of the study was to compare primary total hip arthroplasty (THA) implantations between different countries in terms of THA number per inhabitant, age, and procedure type as well as to compare the survival curve including all THAs using hip arthroplasty registers.
Methods:
THA registers were compared between different countries with respect to the number of primary implantations per inhabitant and age, and procedure type and survival curve. We performed a literature search for all national hip arthroplasty registers providing annual reports for 2009 or, if not available, a more recent time period. The data of these reports were analyzed in terms of number, age distribution and procedure type of primary THAs and survival curves.
Results:
We identified nine hip arthroplasty registers, which comprised sufficient data to be included. A large variation was found in the annual number of primary THA implantations per inhabitant of more than the factor 2.5 for all age groups across regions. The procedure type varied strongly as well, e.g. in Sweden 67% are cemented THAs whereas in Emilia-Romagna (Italy) 89% are cementless THAs.
Discussion and Conclusion:
The present study revealed large differences in terms of the annual number of primary THAs per inhabitant and primary THA procedure type across regions. These data can be used to rank local primary THA implantations within an international context.

PD.07
ANALYSIS OF THE DETECTION OF FEMORAL STEM LOOSENING

Evelyn García
Departamento de Mecánica Estructural E.T.S. de Ingenieros Industriales. Universidad Politécnica de Madrid, Madrid, Spain

Design, development, implementation and tuning of an experimental method of detection of femoral stems micromobility in total hip arthroplasty, based on free oscillations of samples instrumented with electric extensometry

Introduction

Aseptic loosening is recognized nowadays as the major reason of re-intervention in total joint arthroplasties. For those prostheses, aseptic loosening is mainly due to defective bone ingrowth, in most cases due to micro-mobility between bone and implant.

Since the first studies of Charnley in 1965 (Charnley et al., 1965), several techniques have been used for analysis of the stem stability. In the last 20 years a lot of experimental studies have been carried out which attempt to explore this problematic, with special emphasis on uncemented stems. Most studies are based on the use of Linear Variable Displacement Transducers (Monti et al., 1999; Götze et al., 2002; Østbyhaug et al., 2010) and vibration analysis (Puers et al., 2000; Georgiou et al., 2001; Rowlands et al., 2008) where the accelerometer has been the most used sensor Although there are a high number of papers dealing this problem and using different techniques, at present has not reached a enough simple procedure, reliable and affordable. This paperpresents a newapproach to the problemout to be moresimpleand affordable. The technique used is the analysis, in vitro, of free oscillation strain response of bone after a sudden release of an applied force, by using conventional strain gauges.

Material and methods

A dynamic test of free oscillation using real femurs was designed. Two types of uncemented stems (Salamanca, ABG) were implanted in femur by an expert surgeon, using surgical technique, and femurs were fixed by the condyles in a resin base upright.

Each femur was instrumented with 5 triaxial (rosettes) conventional strain gauges located in both medial and lateral sides. The gauges were aligned with the long dimension of femur.

A bending load previously placed at the top of the morse cone of the prosthetic stem was suddenly released. The subsequent free escalations were recorded by gages to 2 kHz sampling frequency. The signal was treated with Matlab program in order to study it in the time domain and in the frequency domain by means of the Fast Fourier Transformation. Three replicas of the experiment were carried out with different levels micromovility (the gap between bone and implant was filled in with a soft polymer).

Results

In the time domain, the gauges readings the repeatability was much better in the fixed situation, (see Fig. 1). In the frequency domain, clear changes were observed between the two situations in the second harmonic, both in amplitude and in frequency, (see Fig. 2).

Conclusion

This paper has developed and implemented a procedure for detection of femoralstem loosening in total hip replacement based on dynamic trial of free oscillationson actual samples of bone-joint prosthesis.

The results obtained, at this stage only qualitative ones, are very encouraging and seem to show that instrumental defects can be detected with a simple pre-clinical test.

References

-Buhler, D. W., Oxland, T. R., Nolte, L. P., 1997. Design and evaluation of a device for measuring three-dimensional micromotions of press-fit femoral stem prostheses. Medical Engineering & Physics 19, 187-199.
-Charnley, J., Kettlell, J., 1965. The elimination of slip between prosthesis and femur. The Journal of Bone and Joint Surgery.British Volume 47, 56-60.
-Georgiou, A. P., Cunningham, J. L., 2001. Accurate diagnosis of hip prosthesis loosening using a vibrational technique. Clinical Biomechanics 16, 315-323.
-Götze, C., Steens, W., Vieth, V., Poremba, C., Claes, L., Steinbeck, J., 2002. Primary stability in cementless femoral stems: custom-made versus conventional femoral prosthesis. Clinical Biomechanics 17, 267-273.
-Monti, L., Cristofolini, L., Viceconti, M., 1999. Methods for Quantitative Analysis of the Primary Stability in Uncemented Hip Prostheses. Artificial Organs 23, 851-859.
-Østbyhaug, P. O., Klaksvik, J., Romundstad, P., Aamodt, A., 2010. Primary stability of custom and anatomical uncemented femoral stems A method for three-dimensional in vitro measurement of implant stability. Clinical Biomechanics 25, 318-324.
-Puers, R., Catrysse, M., Vandevoorde, G., Collier, R. J., Louridas, E., Burny, F., Donkerwolcke, M., Moulart, F., 2000. A telemetry system for the detection of hip prosthesis loosening by vibration analysis. Sensors and Actuators A-Physical 85, 42-47.

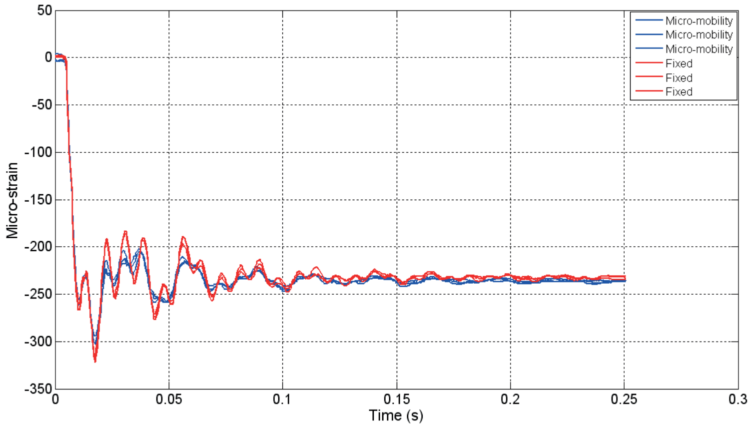

Time domain results. Gage on the stem tip.

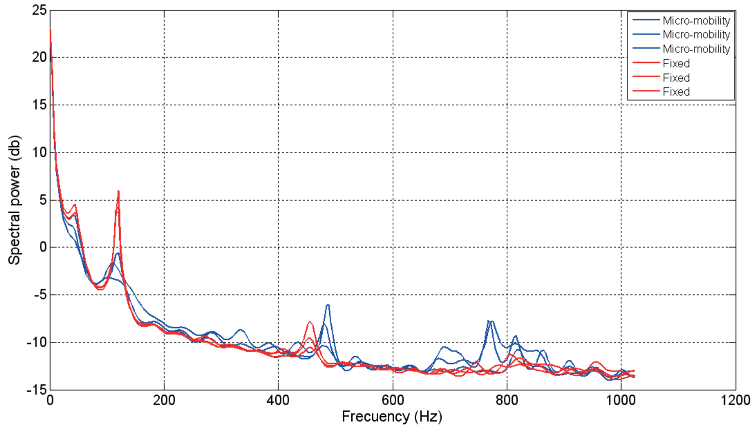

FFT results. Gage on the stem tip.

PD.08
Reconstruction of the Native Center of Rotation in Primary Total Hip Arthroplasty

Geert Meermans
Department of Orthopaedic Surgery, Lievensberg Hospital, Bergen op Zoom, The Netherlands

Reaming of the acetabulum is usually initiated directly medial to the floor which leads to displacement of the center of rotation. Peripheral reaming alone will lead to more accurate reconstruction of the native center of rotation.

Introduction:
The goal of total hip replacement is to restore normal hip anatomy. Traditionally, reaming of the acetabulum is initiated directly medial to the floor and followed by sequentially larger reamers in the anticipated cup position. The goal of this study was to compare this technique with a technique in which the cup is not deliberately medialized and the acetabulum is reamed immediately peripherally.
Methods:
we compared two cohorts of 40 patients with primary osteoarthritis that underwent total hip arthroplasty. In the first cohort (group F) the acetabulum was reamed to the floor followed by sequentially larger reamers. In the second cohort (group P) the acetabulum was only reamed peripherally with sequentially larger reamers with 2-mm increments in the preferred postion of the cup, starting with a reamer the same size as the native femoral head. Reaming was done until sufficient subchondral or cancellous bone has been exposed to ensure bone ingrowth. In all patients a hemispherical cementless porous coated acetabular component oversized 1 mm to ensure a tight press-fit was used. Postoperative anteroposterior pelvic radiographs were analyzed for vertical (interteardrop line to center of rotation) and horizontal acetabular offset (midline to center of rotation)
Results:
The mean preoperative vertical offset (13.18 mm in group P and 11.65 mm in group F) and horizontal offset (90.95 mm and 92.38 mm respectively) were similar in both groups. Compared to the preoperative values, postoperative vertical and horizontal offset were similar in group P (mean 14.08 mm and 90.58 mm respectively), but there was a significant difference in group F (mean 15.95 mm and 87.35 mm respectively; $p<0.001$).
Discussion:
Our results demonstrate that reaming the acetabulum to the floor can lead to significant displacement of the center of rotation medially and superiorly. Peripheral reaming will lead to more accurate reconstruction of the native center of rotation.

PD.09

MEASURING HIP WOUND AREA USING A TIME OF FLIGHT (TOF) CAMERA

David Putzer
Medical University Innsbruck, Experimantal Orthopaedics, Austria

An new algorithm is presented which is able to recognize the wound area of subjects which underwent minimally invasive hip surgery using a Time of flight camera.

Introduction For instrument design and for advanced navigation techniques in minimally invasive hip arthroplasty, it is important to identify precisely the available working space. Time of flight (ToF) cameras combine fast imaging, high lateral resolution with depth information of the captured scene. An algorithm was build for a ToF camera to recognize the wound area of 8 different cadavers which underwent minimally invasive hip surgery. Materials & Methods Distance, intensity, and amplitude images obtained with the ToF Camera were scaled to a gray image and the contrast was enhanced. Unnecessary information of the background was removed, and the amplitude values were corrected. To obtain the contours of the wound first a median filter was applied, then a canny edge detection filter was used on the distance, amplitude and intensity images and finally the contours were combined by a logic operation. Inspecting the neighbor pixels helps the contour extraction method overcome the problem of recognizing weak boarders. Enlarging the contours yields a closed contour line of the wound boarder. Using a fill function, the targeted region was filled in each frame and the bordering pixels were cleared away by an eroding function. The wound region had a shape of an ellipse and could be discriminated from other areas by this property. The recognized region was used as a mask to select values out of the point cloud provided by the ToF camera and by calculating its area by using a Delauney triangulation. The algorithm was tested on 8 different hip wounds of 5 cadavers, which underwent a minimally invasive hip surgery.

Results 10 different combinations of logic operations between intensity, amplitude and distance values in a 3x3 and a 5x5 pixel neighborhood were evaluated. Two of the combinations were excluded because they recognized the wound in 5 datasets only. Combinations using a 5x5 neighborhood were affected by outliers. To address this, lines were enlarged in order to enclose nearby borders. As a result, all remaining 8 combinations improved in recognizing the wound regions and in reducing outliers. After testing various filters, an median filter with a kernel of size 9x9 was chosen for the algorithm. The resulting algorithm, which combined amplitude and intensity values by a AND function in a 5x5 vicinity, was able to recognize 65 % of the wound areas. Discussion With the advent of new surgical techniques in hip arthroplasty, it is important to identify precisely the available working space for the movements of the surgical instruments. Time of flight (ToF) cameras may have the potential to do this. The ellipse shape of the wound may vary when instruments are inserted. Introducing a temporal filter will probably lead to a better outcome of the algorithm. Conclusion We believe the use of a ToF camera with the appropriate data filters and application of the relevant algorithms can intoduce a new tool for recognizing the wound area during minimally invasive hip surgery.

PD.10

Neck fractures in Modular Uncemented Femoral stem in Primary Total Hip Arthroplasty

Biyyam Madhusudhan Rao
St.Richards Hospital, Western Sussex Hospitals NHS Trust, Chichester, West Sussex, UK

Increasing modularity of femoral components has given rise to new complication of femoral neck fractures. We present a series of this complication and technique to extract broken cold welded neck from its Morse taper preventing revision of well-fixed femoral stem.

Introduction

Increasing modularity of femoral components to aid in recreating native femoral version, limb length, and offset in total hip arthroplasty (THA) has given rise to new complication of femoral neck fractures. The aim of this study is to present a case series of this complication and the technique to extract the broken cold welded distal part of neck from its Morse taper preventing unnecessary extraction of well-fixed femoral stem.

Methods and Materials

We include 4 patients with mean age of 63 years who underwent THA for osteoarthritis using uncemented hydroxyl apatite coated modular stem of Titanium alloy (Ti6Al4V) and long Titanium necks (Wright Medical Technology, Arlington, TN) with uncemented acetabular component. 3 of these patients had large metal heads Co-Cr (52-54 mm) with metal on metal articulation and 1 of them had ceramic on ceramic with 32 mm head. All four patients presented with modular neck fractures (Fig.1) without any preceding trauma or other hip symptoms at an average of 56 months after index procedure. Two of these had extended trochanteric osteotomies (ETO) to extract the well-fixed stems as the fractured neck had cold welded into the Morse taper of stem and it was not possible to extract it. In the next two patients with introduction of new instrumentation (Wright Medical Technology, Arlington, TN) it was possible to drill into broken neck using special carbide tip drills and tap threads. With the special extraction assembly tool it was possible to thread onto fractured cold welded titanium neck and extract it (Fig.2). The taper of neck apart from showing signs of somemildcorrosion looked pristine (Fig.3)and hence a new long neck Co-Cr was inserted avoiding any extraction of well-fixed stem. The fractured neck had corrosion and fretting with signs of fatigue due to stress at the fractured site. This was analysed microscopically and sent for further analysis to the manufacturers.

Results

At mean follow up of 26 months patients have mean Oxford scores of 39 and Harris Hip scores of 84 but are under long term surveillance. Following our case series and other sporadic reported cases in literature and few unreported casesfromUnited Kingdomthe manufacturers have realised the problem of Titanium long necks and have addressed this by changing them to Co-Cr in last three years.

Discussion

While offering several distinct advantages intra-operatively, the long-term success of adding a second modular junction has yet to be established. A fixed neck stem would be subject to the same increased bending moment, but in the modular neck, this stress is concentrated at the modular junction and is potentially subject to fretting and corrosion that could lead to a weakening and a fatigue fracture.

It has been suggested that once the neck has fractured in its Morse taper, it probably destroys the taper in spite of it careful extraction and a new neck to engage into it may not be advisable. In present time there is no published evidence for this and new described method avoids need for ETO and removal of well-fixed stem. Still one has to be aware of this and long term outcome results are awaited.

Fig 1 - Radiographs of Modular Neck fractures and subsequent revisions

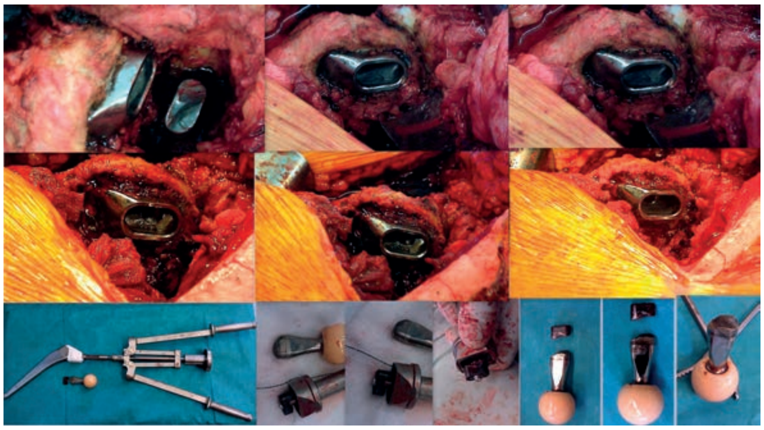

Fig.2 - Intraoperative pictures of fracture modular neck and its extraction using new instrumentation

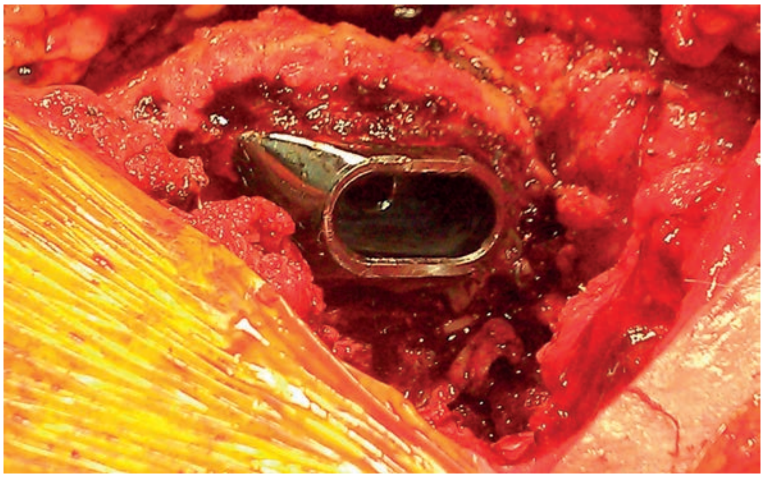

Taper of neck in the femoral stem after extraction of fractured neck

PD.13

The influence of cement modulus on fatigue performance of hip implants tested to ISO and ASTM standards

Amy Kinbrum
Corin, Cirencester, UK

ISO 7206-4 (1) stipulates a range of elastic moduli for the potting medium used to embed the femoral stem. Computational analysis and mechanical testing were completed to determine if elastic modulus significantly affects fatigue performance of femoral stems.

Introduction

To demonstrate that femoral stems have the required endurance properties to function without failure, fatigue testing can be carried out under the requirements of ISO 7206-4. The principal of ISO 7206-4 is to embed the lower portion of a femoral stem in a solid medium and apply a cyclic load to the attached femoral head until the femoral component exhibits failure or achieves the prescribed number of cycles. The resin modulus within which the head is held will affect the amount of flexion the stem undergoes and therefore the stresses incurred at the point of potential fracture. The purpose of this study was to determine the effect of changing the elastic modulus of the embedding medium within the range stipulated in ISO 7206-4 using finite element (FE) analysis validated with laboratory experimentation.

Method

For the FE analysis, an assembly was created in Solid Edge ST2 (Siemens PLM Software, Plano, US) , using a Metafix size 3 stem (Corin Ltd, Cirencester, UK) and an Optimom size 10 head (Corin Ltd, Cirencester, UK) in a suitable sized pot. The femoral component was oriented in accordance with ISO 7206-4. The distal stem was potted 80mm from the centre of the head. The geometry was imported into ANSYS 12.1 (Ansys Inc. Canonsburg, PA,USA). Three dimensional, 10-node, quadratic tetrahedrons were used to generate a solid mesh. A 2.3 kN load was applied vertically to the pole of the femoral head. The analysis was conducted with varying modulus of cement from 2.0 GPa to 6.0 GPa.

A laboratory experiment verified the outcome of the FE analysis. The same set-up and loading conditions as those described above were applied. Two tests were completed; ceramic grit was used to increase the modulus of the resin from 2.8 GPa to 5.0 GPa in order to mimic the most extreme range of the medium modulus.

Results

FE results show a first principle stress of 461 MPa, 532 MPa and 609 MPa for a cement modulus of 2.0 GPa, 4.0 GPa and 6.0 GPa respectively. Applying the Soderberg principal of fatigue to the FE results, the soderberg graph for Ti6Al4V shows that these three stresses could alter the number of cycles to failure such that the requirements of ISO 7206-4 may or may not be achieved. These results were validated by the laboratory test; the stem potted with the more compliant embedding medium performed better than the stem potted in the stiffer embedding medium.

Discussion / Conclusion

There is a higher risk of failure if a stem is potted in an embedding medium with a modulus close to the upper limit of the range given in the ISO standard. The associated clinical risk is clear; there is no clinical requirement for cement of the same modulus as that used in the standard.

It is recommended that femoral components are tested in embedding mediums with a modulus greater than 4 GPa to determine the fatigue resistance of femoral stems.

References:

ISO 7206-4:2010 Implants for surgery -- Partial and total hip joint prostheses -- Part 4: Determination of endurance properties and performance of stemmed femoral components

PD.15

An increasing trend of investigating occult hip fractures with CT scans

Robert Jordan
Birmingham Heartlands Hospital, Birmingham, UK

Our study has shown that clinicians are becoming increasingly reliant on CT for diagnosis of hip fractures despite evidence that this can delay time to theatre.

Introduction

Neck of femur fractures carry significant rates of mortality, morbidity and financial cost to the NHS. Early diagnosis allows prompt treatment which reduces mortality and increases compliance with the best practice tariff. The prevalence of occult fractures is estimated to be 3-4% and NICE recommend the use of MRI or, if not accessible within 24 hours, CT to establish the diagnosis in these cases. Little evidence exists to show whether the increasing use of CT scanning aids the overall treatment of these cohort of patients in terms of aiding clinician decision and shortening time to surgery. Our study aims to analyse the trends of its use over two separate one year periods.

Materials and method

Patients who underwent CT hip or pelvis to diagnose an occult hip fracture were identified from electronic records across two district general hospitals between 2006-2007 and 2010-2011. The times taken from initial radiograph to CT and initial radiograph to operation were recorded.

Results

In 2006-2007, of 547 hip fractures, 20 CT hips were performed and 6 fractured necks of femur were identified (30%). In 2010-2011, of 499 hip fractures, 239 CT hips were performed and 65 fractures were recognised (27%). The mean time from initial radiograph until CT scan was 2.0 days in the 2007 group (range 0-5 days) and 3.2 days in the 2011 group (range 0-93 days). For those with confirmed fracture on CT that underwent operative intervention, the mean and median times from the initial x-ray to surgery were 1.2 and 1.0 days in 2007 (range 0-4 days) and 3.6 and 3.0 days in 2011 (range 0-13 days). This difference in mean time until surgery was shown to be significant ($p=0.008$).

Conclusion

Clinicians are becoming increasingly reliant on CT for the diagnosis of hip fractures despite no demonstrable benefit in its use in the overall treatment of hip fracture patients.

PD.16
Non-Object Based Calibration of Digital Radiographs

Geert Meermans
Department of Orthopaedic Surgery, Lievensberg Hospital, Bergen op Zoom, The Netherlands

Calibration of digital radiographs is usually done by placing an object in the plane of the hip joint. Our data demonstrate that calibration can be reliably done without a reference object when adjusting for weigth and gender or BMI.

Introduction:
Pre-operative templating is paramount in planning total hip arthroplasty (THA) and can reduce complications. Different methods have been described to scale digital radiographs. These commonly involve placing a disc or a sphere of known size in the plane of the hip joint. This requires training and cooperation of the radiographers. The goal of this study was to compare different methods of non-object based calibration of digital radiographs when templating for primary THA
Methods:
In the first part of this study, we calculated the mean magnification factor of our radiology department on 100 (50 men and 50 women) standardized anteroposterior pelvic radiographs after THA. The relationship of magnification to gender, length, weight, and body mass index (BMI) was analyzed. In the second part of this study, we compared the accuracy of each calibration method on a different set of 100 anteroposterior pelvic radiographs.
Results:
The mean magnification was 121.78% (121.81% in women and 121.75% in men). The magnification was significantly correlated with the weight (r^2=0.17, p=0.001) and BMI (r^2=0.22, p2=0.15, p=0.003 in men and r^2=0.21, p=0.0002 in women) and gender and BMI (r^2=0.16, p=0.002 in men and r^2=0.28, p
Discussion:
These data demonstrate that calibration of digital radiographs can re reliably done without reference objects. This avoids problems of correct placement of the reference object. Exact-size templating can be achieved when weight and gender or BMI are taken into account.

PD.17

Taper Corrosion and Measurement of a Retrieved Metal-on-Poly Total Hip Joint Device

Chenxi Li Chenxi

Past studies have been using scoring systems to qualitatively evaluate the level of fretting and corrosion at a taper junction. This study demonstrates that it is feasible to quantify fretting and corrosion at a taper junction using straightness measurement.

Introduction:
This retrieval study examined the bearing surface and taper junction of a retrieved metal-on-poly total hip replacement (THR) device, and investigated the feasibility of using taper straightness measurement to quantify the depth of material loss at the taper junction.
Materials & method:
The retrieval examined was a 28 mm metal-on-poly (Corin) THR revised due to osteolysis and acetabular loosening after 11.6 years in vivo. The head had an off-set of +11 mm. The stem (Freeman) was left in situ.A Taylor-Hobson TR290 roundness machine was used to evaluate the depth of material loss at the head taper.This included nine roundness measurements at 2 mm intervals from distal to proximal end of the taper, and eight vertical straightness measurements at 45 degree intervals around the taper. An FEI Quanta 600 SEM was used to examine the taper surface.
Results:
Wear occurred over a large area on the bearing surface of the poly liner (Fig. 1a). A maximum linear wear depth of 2.53 mm was measured at the rim and 2.50 mm within the bearing surface.
No wear could be measured on the bearing surface of the Co-Cr head. However, severe discolouration and surface texture change were observed on the head taper in the region where it was in contact with the trunnion of the stem (Fig. 1b). In the non-contact region at the proximal end, the taper surface was intact with visible original machining marks. SEM examination confirmed that corrosion occurred in the contact region, and preferential etching revealed the crystallographic features of the Co-Cr alloy. A step was observed between the corroded and un-corroded regions at the distal end of the taper, which indicatesthe amount of material loss (Fig. 2).
The roundness measurement showed an average of less than 5 µm linear deviation from the best fit circle at the non-contact region of the taper. The deviation was increasing in the contact region toward the distal end. Close to the distal rim where a step was observed under SEM, a maximum linear deviation of 107µm was measured (Fig. 3a). The vertical straightness profiles showed distinct features between the contact and non-contact region along the taper (Fig. 3b). Using the non-contact region as reference, a maximum corrosion depth of 80µm was measured for the head taper. This is in good agreement with the corrosion depth estimated under SEM.
Discussion:
Taper junction in THR is a potential site for fretting and corrosion regardless of the bearing materials used. Studies have shown that even in some well-functioning metal-on-poly prosthesis, increase in chromium in serum and urine can be observed [1]. This study showed severe corrosion and material loss from the taper junction of the metal on poly device. Past studies have been using scoring systems to qualitatively evaluate the level of fretting and corrosion at a taper junction [2, 3]. This study demonstrates that it is feasible to quantify fretting and corrosion at a taper junction using straightness measurement.

Reference:

[1] JJ Jacobs et al, JBJS (Am), 80(10):1447-58, 1998. [2] Goldberg et al. CORR. No 401, pp. 149-161, 2002. [3] Kop et al, JOA, Vol. 24, pp. 1019-1023, 2009.

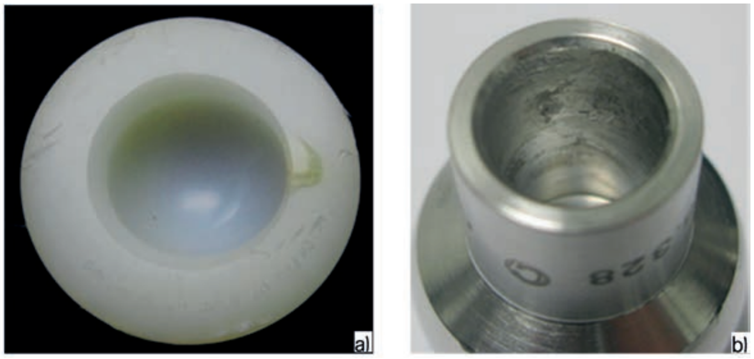

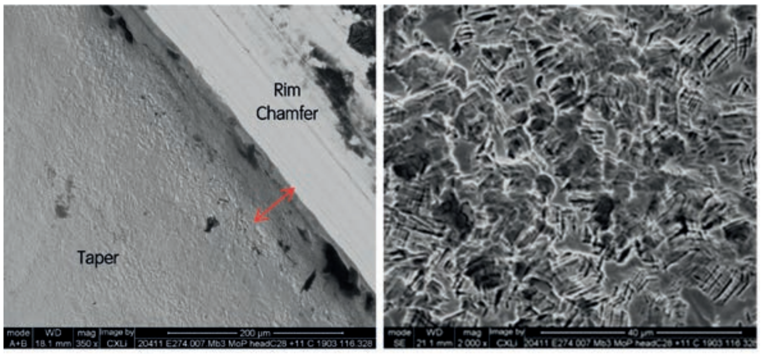

a) 350x

b) 1000 x

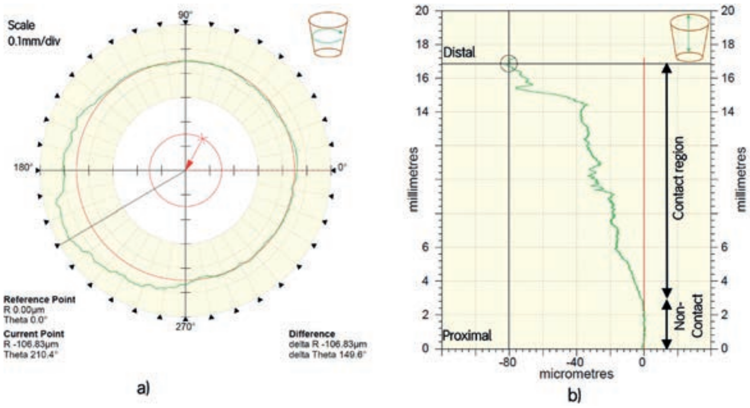

a)

b)

PD.18

Periprosthetic fracture after excessive stress shielding in a fully hydroxyapatite(HA)-coated femoral revision stem

Jacobus Arts
Maastricht University Medical Centre, Maastricht, The Netherlands

An alternative in revision THA to bypass proximal femoral stress shielding is the use of fully hydroxyapatite-coated stems. In this study we report and discuss the clinical consequences and implications for treatment of excessive stress shielding in fully HA-coated femoral revision stems.

Introduction

Adaptive bone remodeling due to stress shielding remains a concern in primary and revision total hip arthroplasty (THA). The redistribution of stress after prosthesis change, results in proximal femur bone mineral density decrease, which may influence prosthesis longevity. Potential adverse effects of stress shielding may be stem, bone, interface failure, or deficient bone stock when a (re)revision is required. Clinical and animal experimental studies have revealed factors governing stress shielding, which include stem stiffness, coating extent, stem shape, fit, bone quality and patient weight. An alternative in revison THA to bypass the proximal femoral stress shielding is the use of fully hydroxyapatite(HA)-coated stems. While the preliminary clinical results of these stems are promising, concerns over stress shielding still exist. In this study we report and discuss the clinical consequences and implications for treatment of excessive stress shielding in a fully HA-coated femoral revision stems.

Material and methods

Retrospectively, a cohort of revision THA patients operated at Maastricht University Medical Centre between 2002-2006 implanted with a fully HA-coated Restoration stem (Stryker, Mahwah, USA) were reviewed. Radiological assessment of bone remodelling of Gruen zones was performed at 1-2-3 and 5 years follow-up and clinical outcome scores (HHS) were matched to the follow-up dates. Cases with occurrence of excessive stress shielding were selected and analysed for risk of revision surgery.

Results

Restoration HA-coated revision THA cohort with minimum 5 year clinical follow-up included 85 patients. Four cases with excessive stress shielding were identified of which 1 patient (case 1) was already revised due to traumatic periprosthetic fracture.

Case 1: Male, 78 year with aseptic loosening of his left THA. Primary uncemented THA was implanted in 1981 and in 1983 a revision THA was performed using a cemented straight-stem Muller prosthesis. Due to polyethylene wear of the cup and osteolysis of the femoral component in 2005 a Restoration HA femoral stem was implanted combined with a cemented SHP cup. Two years later extensive bone remodeling around the femoral stem with cortical thickening around the distal stem was observed and at 5 year follow-up progressive loosening of Gruen zones 2,3,5,6,7,9,10,12,13 was observed. A Vancouver type-B3 periprosthetic fracture occurred after a low-impact fall. It was treated with a femoral strut graft, plate fixation and cerclage wires. Patient was followed with partial weight-bearing during the first three months postoperatively and full weight-bearing thereafter. The remaining postoperative course was uncomplicated with a consolidated fracture and HHS 90 points at lastest follow up.

Discussion

This is the only available study concerning the mid-term clinical consequences of excessive stress shielding in fully HA coated revison THA stems. While such problems have not been manifested as severe, the preservation of femoral bone stock is an important and desirable goal. There’s no literature about the implications of excessive stress shielding for follow-up and treatment. Should we follow these patients more strictly? When do we decide to do a re-intervention? We advocate surgeons using this type of implant to remain vigilant and be aware of possible stress shielding side effects.

PD.20

Comparative study of Caucasian and Chinese femur shapes for evidence-based implant design

Lara Vigneron
Materialise, Leuven, Belgium

With the increasing use of 3D medical imaging, it is possible to analyze 3D patient anatomy to extract features, trends and population specific shape information. This is applied to the development of 'standard implants' targeted to specific population groups.

Introduction

Human beings are diverse in their physical makeup while implants are often designed based on some key measurements taken from the literature or a limited sampling of patient data. The different implant sizes are often scaled versions of the 'average' implant, although in reality, the shape of anatomy changes as a function of the size of patient. The implant designs are often developed based on a certain demographic and ethnicity and then, simply applied to others, which can result in poor design fitment [1].Today, with the increasing use of 3D medical imaging (e.g. CT or MRI), it is possible to analyze 3D patient anatomy to extract features, trends and population specific shape information. This can be applied to the development of new 'standard implants' targeted to a specific population group [2].

Patients & Methods

Our population analysis was performed by creating a Statistical Shape Model (SSM) [3] of the dataset. In this study, 40 full Chinese femurs and 100 full Caucasian femurs were segmented from CT scans using Mimics®. Two different SSMs, specific to each population, were built using in-house software tools. These SSMs were validated using leave-one-out experiments, and then analyzed and compared in order to enhance the two population shape differences.

Results

An SSM is typically represented by an average model and a few independent modes of variation that capture most of the inherent variations in the data. Based on these main modes of variations (see Fig.1), the shape features, e.g. length, thickness, curvature neck angle and femoral version, presenting largest variations were determined, and correlations between these features were calculated. A special focus on features representing proximal and distal femoral parts separately was provided, which allows to evaluate the correlation between the shape of these two proximal and distal parts.

Conclusion

The advantage of using more advanced statistical analyses is that the 3D data are probed in an unbiased fashion, allowing the most important parameters of variation to be determined. These analyses are thus particularly effective to compare different populations, to evaluate how well existing implant designs fit specific populations, and to highlight the design parameters that need to be adapted for good fitment of specific populations.

References

-Kwak D., Han S., Han C.W., Han S. Resected femoral anthropometry for design of the femoral component of the total knee prosthesis in a Korean population, Anat Cell Biol. 43(3): 252-259, 2010.

-Plaster R.L., Starkman K.B., McGee J., The Gender Solutions Natural-Knee Flex System and Future Directions, Am J Orthop, 39(6 suppl):9-12, 2010.

-Cootes T.F., Taylor C.J., Cooper D.H., Graham J., Active shape models - their training and applications. Comput. Vis. Image Underst. 61 (1), 38-59, 1995.

PD.21

Optimization of Hip Resurfacing Arthroplasty Cement Penetration: The Role of Cement Mantle Space

Paulick Mark
University of California Davis Medical Center, Sacramento, CA, USA

The purpose of this study is to determine the role of the mantle space and whether it affects cement penetration. An increase in mantle space was found to have a significant predictable decrease of cement penetration from the dome, chamfer.

Introduction

Hip resurfacing arthroplasty has changed the treatment of end stage arthritis in young, active adults. Presently, there are various philosophies regarding optimal femoral component cement techniques and inner geometries. Cement penetration into the femoral head has been identified as one of the critical factors in the longevity of the resurfaced joint [1]. Adequate cement penetration is needed to secure the implant to the bone, while too much penetration may lead to thermal necrosis, possibly resulting in loss of normal bone remodeling and increased risk of failure. Current implant designs for hip resurfacing arthroplasties offer various offsets between the femoral component and reamer, representing differing theories as to the optimal offset and resulting cement mantle thickness for effective adherence of the implant to bone. The goal of this study was to explore the effect of a range of reamer-femoral component offsets on cement penetration into the femoral head.

Methods

Three sets of 6 plastic hip resurfacing femoral component models were designed using CAD and cast (Huntsman Pro-cast, Hong Kong) from silicone molds created by rapid prototyping. Models were designed with reamer-femoral component offsets of 0.0 mm (50 mm diameter, n=6), 0.5 mm (51 mm diameter, n=6), and 1.0 mm (52 mm diameter, n=6) relative to the outer diameter of the reamer.

Results

The femoral components were implanted onto models of reamed femoral heads made from high-density open-cell reticulated carbon foam (Pacific Research Laboratories, Vashon, WA) that simulated the density, porosity, and pore connectivity of trabecular bone [2]. For implantation, the femoral components were filled to 50% of their depth with PMMA bone cement. To ensure consistency in seating the implant on the foam, an Instron 8511 materials testing machine (Instron, Norwood, MA) and custom fixtures were utilized to insert the femoral component on the bone and maintain an approximately 20 N load on the construct while the cement cured. Following implantation, the components were cut longitudinally and cement penetration was assessed on four unique surfaces per foam-implant unit. Digital images were processed in ImageJ (NIH) to determine actual component offset and cement penetration depth, height, and area (Figures 1 and 2). An analysis of variance (ANOVA) was performed on the set of data to determine statistical significance between offsets for each of the measured values.

Discussion

Results from this study suggest that the reamer-femoral component offset significantly affects not only the cement mantle, but also the extent of cement penetration. Increasing the offset decreased the depth and area of cement penetration, while increasing the penetration height. Our study results indicate that, for the situation where cement is applied by filling the cup to 50% of its depth without applying cement directly to the head of the femur, the 1.0 mm offset provides the most cement coverage to the femoral head while reducing the amount penetrating into the bone, possibly reducing the risk of thermal necrosis and, ultimately, implant failure.

References

[1] Breusch et al., J Arthroplasty 16:648-657, 2001.
[2] Bitsch et al., JBJS-Am 90 (Suppl 3):102-110, 2008.

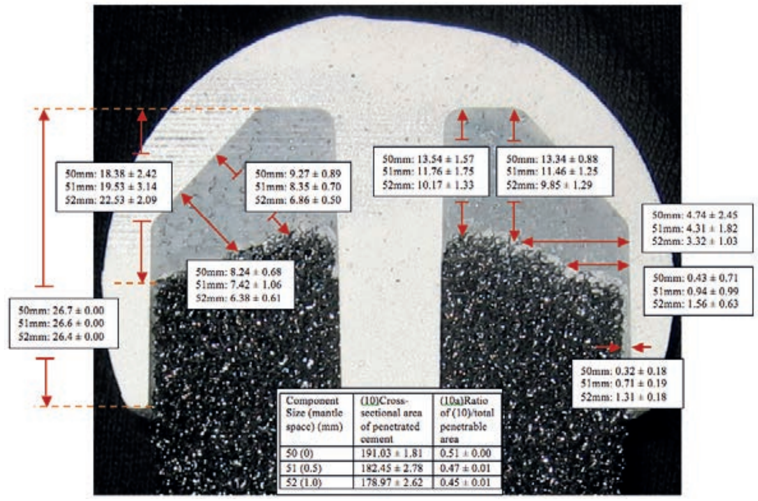

Component Size (mantle space) (mm)	(10)Cross-sectional area of penetrated cement	(10a)Ratio of (10)/total penetrable area
50 (0)	191.03 ± 1.81	0.51 ± 0.00
51 (0.5)	182.45 ± 2.78	0.47 ± 0.01
52 (1.0)	178.97 ± 2.62	0.45 ± 0.01

Mean cement penetration at each location (1-9) of each component size including cross-sectional area measurements and ratio calculations (mm ± SD)

PD.23

Hip Resurfacing Arthroplasty in Older Patients

Geert Meermans
Department of Orthopaedic Surgery, Lievensberg Hospital, Bergen op Zoom, The Netherlands

Hip resurfacing arthroplasty must be used with caution and good patient selection is mandatory. It can be safely done in well selected older patients with a complication rate similar to a young cohort.

Introduction:
Clinical results
of patients with hip resurfacing arthroplasty (HRA) are excellent. The advantages are femoral bone stock conservation and proposed suitability for younger and more active patients. Femoral neck fracture is the most common complication of HRA with its reported incidence of up to 2.8%. Older patients may be more susceptible to femoral neck fractures or aseptic loosening because of poor bone quality. The goal of this study was to compare the complication rate of HRA in young and old patients.
Method:
Between August 2006 and December 2008,
150 patients with primary osteoarthritis were managed with a HRA in our department. There were 26 women older and 36 younger than 55 years of age. Twenty-two men were older and 66 were younger than 60 years of age. Complications, radiographic alignement and radiographic lucencies were evaluated.
Results:
The mean age of the younger cohort was 49.81 SEM 0.74 (range 25-60) and of the older cohort 61.10 SEM 0.47 (range 56-67). There were 2 (1.96%) femoral neck fractures in the younger cohort and 1 (2.08%) in the older cohort (p=0.96). There were no differences regarding gender (p=0.39 for women and p=0.40 for men). Radiographic alignement was similar in both cohorts and there were no impending radiographic failures.
Discussion:
HRA may lead to large tensile strains and potential neck fracture. Our study demonstrates that HRA in older patients has a similar complication rate than in younger patients. Age as a single variable should not be used for selecting HRA. Older, active patients may benefit from HRA.

PD.24

Functional Outcome in Patients with High Body Mass Index Following Primary Total Hip Arthroplasty

Claire Louise Rutherford
Lancashire Teaching Hospitals NHS Trust, North West, UK

Patients with Body Mass Index (BMI) ≥30 have poorer pre-op and post-op functional scores but gain the same functional improvement compared to those with a BMI

Introduction

Obesity is becoming a crucial problem for developed nations. Within England the proportion of adults with a normal BMI decreased between 1993 and 2010, from 41.0% to 30.9% in men and from 49.5% to 40.4% in women. Those classed as obese have gradually increased over this period from 13.2% in 1993 to 26.2% in 2010 in men and from 16.4% in 1993 to 26.1% in 2010 in women.[1]

Based on existing trends the prevalence of obesity is predicted to will increase to 32.1% in men and 31.0% in women by the end of 2012. [2] Within England the North West Region has the second highest obesity prevalence rate, this being 11.5% and second only to the North East Region.[1]

The current trend to perform arthroplasty in younger, higher demand patients who may be overweight poses the question of whether any benefit is to be gained in patients with a BMI greater than 30.

We undertook a retrospective cohort study to determine if body mass index is an independent factor in determining patient outcome following total hip arthroplasty (THA).

Patients and methods

All THAs carried out on patients with a BMI of 30 or more over a 38 month period (220 operations), were identified and compared against 220 randomly selected THAs carried out on patients with a BMI of less than 30 within the same 38 month period.

For each case we recorded patient BMI, P score (analogous to the anaesthetic ASA score) and Oxford Hip Scores. We calculated the difference between pre-operative and one year post-operative Oxford Hip Scores (functional change). We used Kendall's rank correlation to assess any potential correlation between BMI and functional change. We used the Mann-Whitney U test to establish whether any difference in functional change between the groups was statistically significant.

Discussion

Our study indicated that BMI is not an independent factor in determining relative subjective functional change following THA. Although it showed that patients with a BMI of 30 or more have poorer function both before and after THA, there was no statistically significant difference between the two groups in terms of functional change ($p = 0.9902$).

Patients with a higher BMI should be considered for THA as they can expect the same degree of functional improvement, with the caveat that absolute function should not be expected to equal that of patients with a lower BMI. Given the trend for increasing numbers of obese people in the population these findings could have a significant impact on the future of THA operations.

PD.25

The Use of Preoperative DEXA Scans to Evaluate Bone Quality in Hip Resurfacing

Geert Meermans
Department of Orthopaedic Surgery, Lievensberg Hospital, Bergen op Zoom, The Netherlands

In this study the usefulness of a preoperative DEXA-scan to help in patient selection for hip resurfacing (HRA) is examined. DEXA scan is a reliable tool to assess femoral bone quality and can help in selecting appropriate candidates for HRA.

Introduction:
There is renewed interest in hip resurfacing arthroplasty (HRA). A fracture of the femoral neck is the most common complication and depends on patient and surgical factors. The goal of this study was to determine whether a preoperative DEXA scan is useful to assess poor proximal femoral bone stock and to help in patient selection for HRA.
Method:
We reviewed 35 patients with primary osteoarthritis who were good candidates for a HRA and had a preoperative DEXA scan of the hip region. The operating surgeon determined intraoperatively whether the patient had a HRA or a large head metal-on-metal total hip arthroplasty (MOM) according to the bone quality.
Results: Eventually, 8 patients (7 women and 1 man) had a MOM and 27 patients (19 women and 8 men) a HRA. The t-score and z-score were significantly lower in the MOM group compared to the HRA group ($p=0.021$ and $p=0.014$ respectively). The mean age of the MOM group (56.13 SEM 2.30) and the HRA group (57.04 SEM 1.24) was similar ($p=0.73$). There were no neck fractures in the HRA group at a minimum follow-up of 2 years.
Discussion:
Our study demonstrates that a preoperative DEXA scan can account for proximal femoral bone material quality. We believe that in relatively elderly candidates for a HRA, a preoperative DEXA scan should be performed. According to our data, HRA can be safely done in patients with a t-score > -1. In patients with a t-score < -1.5 a conventional total hip arthroplasty should be considered.

PD.27
Ceramic Large Diameter Ball Head in Total Hip Replacement

Bernard Masson

In the 60th, Sir John Charnley introduced small femoral head size. Today, big heads are in high demand. Joint stability and Range of Motion are decisive issues, then large head diameters are available. Which diameter offers the best stability?

In the sixties, Sir John Charnley introduced small femoral head size. This was to remain the trend for several decades based on the low friction theory. Today, big heads are in high demand. Wear is no longer an issue thanks to hard hard bearings and in particular the ceramic ceramic bearing

As mentioned on the latest Swedish registry report, aseptic loosening and dislocation are the main complications in Total Hip Arthroplasty (THA).

Joint stability and Range of Motion (ROM) are decisive issues, especially in younger patients with high expectations on their quality of life after a surgery. In consequence, a large variety of head diameters from 22mm to 60mm are available today.

Which ball head diameter offers the best stability without causing further complications?

Ball head diameter and stability

Larger heads increase the stability of a THA not only by reducing the risk for impingement but also by increasing the distance the head has to be lifted out of the cup

Head size directly influences the technical ROM. A benefit of 13° (from 123° to 136°) in technical ROM is achieved when the head size is increasing from 28mm to 36mm.

The ROM will obviously depend also on the design of the metal back and the neck of the stem. In this case the cup is hemispheric and the taper is a 12/14

The «real « ROM of the patient is influenced by the position of the component, the personal anatomy of the patient (soft tissue and muscles)

From a bio mechanism point of view, it is important to differentiate the «prosthetic impingement» that can lead to dislocation from the «bony impingement» that will have the same effect.

Increasing the ball head diameter is supposed to increase stability by increasing the technical ROM and therefore the «prosthetic impingement» however the «bony impingement» will occurs earlier.

The dislocation can also occur without any impingement if the «jumping distance» is small, this is called shear out dislocation. This mechanism can happen in case of special bearing and cup design.

The best compromise between several parameters such as ball head diameter, neck size, cup design should be investigate

Ball head diameter and wear

Excellent results can be achieved with ceramic-ceramic bearing total hip replacement (THR), particularly for younger patients thanks to the bearing couple's low wear performance and the material's biocompatibility.

Larger diameter hard on hard bearings may also change the wear characteristics due to larger wear areas or different lubrication behaviour. Many tribological tests demonstrate that a large ceramic bearing also has a very low wear rate. The influence of the clearance on the wear rate is negligible.

Using a ceramic ball head against a highly crosslinked polyethylene liner reduces the wear rate by 40% compared to metal ball heads.

Ball head diameter and design

Increasing the ball head diameter consequently increases the insert diameter then also the cup diameter. The cup diameter is limited by the physiological size of the acetabulum.

Current ceramic-on-ceramic THR bearings range from 28-36 mm to 40mm diameter but increasing the bearing diameter should not come at the expense of bone conservation,

There are several solutions to have the biggest ball head in the smallest cup. One solution is to reduce the thickness of the insert and/ or the metal back. Another solution is to change the design of the metal back from an hemispherical shape to a sub-hemispherical shape.

The limitation of the wall thickness of the ceramic insert depends on the deformability of the metal back. For a standard and direct fixation of the ceramic insert in a metal back, the minimum thickness of the ceramic insert is 3,5mm.

A new solution preassembled under standard, clean and controlled conditions can reduces both the thickness of the ceramic and the metal back. This system can offer a big ball head in an acceptable cup size with a high reliability.

Preassembled inserts and metal backs eliminate the risk of misalignment or third body at the interface.

The ceramic insert is secured by the metal back. This would not be possible in surgery, giving complete seating and superior strength both of the interface and the assembled cup

Conclusion

The effect of larger head sizes for THA on the type of impingement, ROM, and joint stability has been reported in the literature. Results have shown that femoral heads larger than 32 mm provide greater ROM and push the limits of prosthetic impingement.

Because the increase of the ball head diameter has also some surgical consequences, clinical trials will answer for the limit in size. Based on many biomechanical tests, it seems that the use of a 36mm ball head is a good compromise between strength, stability, safety and surgical technique.

PD.28
The Outcome of Extensively Porous Coated Stems for Revision Total Hip Arthroplasty

William Peace
Colorado Permanente Medical Group, Denver, CO, USA

Extensively porous-coated, cylindrical stems offer a straight-forward surgical technique that can be used to address the full spectrum of femoral bone defects that are typically encountered at revision.

Introduction:
As the number of total hip arthroplasty (THA) performed continues to increase, so do the numbers of revisions. Common diagnoses for femoral revision THA include aseptic loosening, osteolysis, and periprosthetic fractures. The tenants of revision femoral arthroplasty include obtaining rotational stability, inhibiting axial implant migration implant and restoration of hip biomechanics. The procedure of choice at our institution has been the use of extensively porous coated stems in revision THA; we have previously reported a 95% survivorship at 10 years with this type of implant. The purpose of this study was to review our institutional experience to date and evaluate the longterm survivorship of femoral revision THA using extensively porous coated cylindrical prostheses.
Methods:
In order to identify our study population, we queried our institutional database for all femoral revisions using extensively porous-coated stems with a cylindrical distal geometry. Patient demographics, including gender, age at the time of revision and the original THA diagnosis were queried from our database. At the time of revision surgery, any cement residue if present was removed with curettage or high speed drill. When necessary, a trochanteric osteotomy was employed in order to gain adequate access to the femoral canal. The femoral canal was prepared with sequentially larger cylindrical reamers prior to introduction of the revision stem. The surgical goal was to obtain scratch fit over at least a 5 to 7cm segment of healthy diaphyseal bone. Stem fixation was assessed radiographically and classified as bone ingrown, fibrous stable, or loose according to previously published criteria. Kaplan-Meier survivorship was evaluated using femoral rerevision for any reason as an endpoint.
Results:
The mean follow up among all 1000 cases was 6.9 ± 5.5 years (range, 0 to 26.8) years. Five-hundred forty of the stem revisions were followed less than 5 years, 218 were followed 5-10 years, 160 were followed 10-15 years, and 82 were followed 15 years or longer. Radiographically, 5% of the stems were graded as loose, 7% were fibrous stable, and the remaining stems were bone ingrown. Kaplan-Meier survivorship using stem rerevision for any reason as an endpoint was 98.6± 0.8% at two years, 97.0 ± 1.3% at five years, 95.6 ± 1.8% at ten years, and 94.5 ± 2.3% at fifteen years. There were no rerevisions after twelve years. We have had 27 stems undergo rerevision: 14 for aseptic loosening, 7 for implant fracture, 4 for infection and 2 in conjunction with periprosthetic femoral shaft fractures.
Discussion and Conclusion:
Mechanical loosening rates have been reported to be less than 5% at nominal 10-year follow-up when the level of femoral bone damage does not extend more than 10 cm below the lesser trochanter prior to revision. When the femoral bone damage extends more than 10 cm below the lesser trochanter, revision becomes more challenging. Prerevision bone stock is a factor affecting femoral fixation. We have documented lower survivorship when the femoral bone damage extends more than 10 cm below the lesser trochanter, but the overall survivorship for these types of cases is 89% at 10-year follow-up. Consistent with prior reports, failure to achieve bone ingrowth occurs in 10% to 20% of cases but the decision to rerevise a stem is typically driven by patient symptoms rather than radiographic appearance. Extensively porous-coated, cylindrical stems offer a straight-forward surgical technique that can be used to address the full spectrum of femoral bone defects that are typically encountered at revision. We regard the use cementless fixation with extensively porous-coated cylindrical stems as the gold standard in the femoral revision setting.

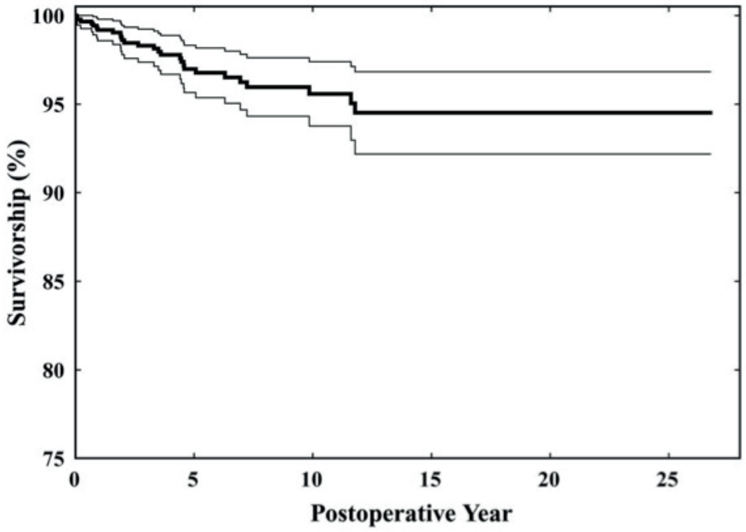

Kaplan-Meier survivorship using stem revision for any reason as an endpoint. The thinner lines represent the 95% confidence intervals.

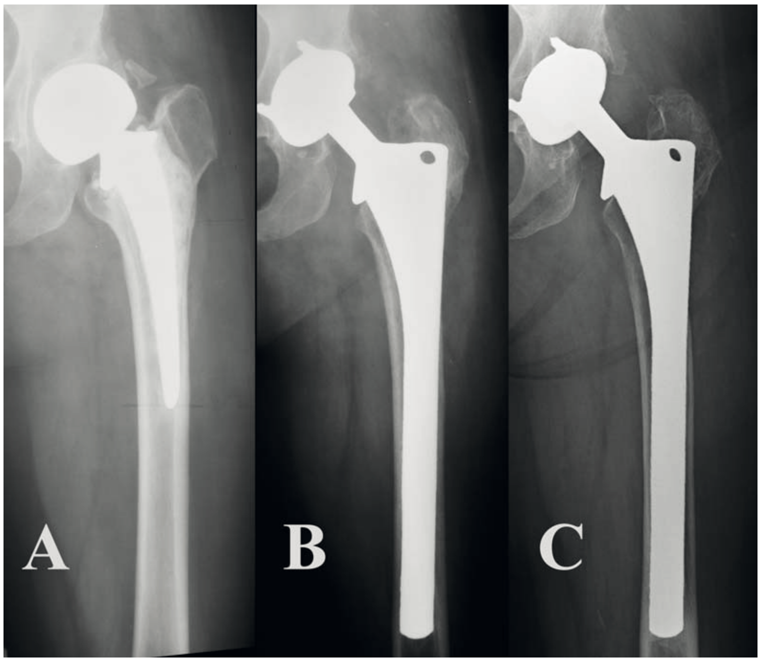

An x-ray taken 2 months prior to revision (A) demonstrates a loose bipolar with a cemented stem. The patient was 56 years old at the time of her revision. A 4 month postoperative radiograph (B) shows the fully porous-coated AML stem used at revision. At 26.1 year follow-up (C), the stem remains well-fixed with distal spot welds evidencing bone ingrowth.

PD.29

Marker wire position is an important factor in the risk of polyethlyene bearing fracture

Elise Pegg
University of Oxford, Oxford, UK

The marker wire position, if too central, was found to cause high tensile stresses within the bearings. Replacement of the wires with balls significantly reduced the stresses and risk of fracture.

Introduction

The Oxford Unicompartmental Knee Replacement (UKR) has a mobile bearing, which is known to reduce the wear rate and reproduce normal knee kinematics. The design of the bearing has a fully congruent spherical surface on the femoral side and a flat fully congruent surface on the tibial side. Unfortunately a small number of ultra-high molecular weight polyethylene (UHMWPE) bearings have fractured after several years (average 17 years) in vivo. The fractured bearings all showed signs of wear and impingement, indicating surgical technique may be to blame. In almost all cases the fracture was transverse across the centre of the bearing; these fractures were examined in a previous study [1]. In phase I and phase II Oxford UKR designs, the bearing had two embedded metal marker wires to help assess the position of the bearing on post-operative radiographs. This has been replaced by marker balls in the current, phase III, design. The purpose of the present study was to examine whether there may be a mechanical cause for the characteristic pattern of fracture observed.

Patients & Methods

A simplified parametric model of a phase I bearing was created, in which the marker wire position could be varied or replaced with marker balls. Finite element analyses (FEA) were performed explicitly (ABAQUS, Simulia), a symmetric quarter model was examined. The load applied was 2.4 kN and was applied in one loading-unloading step sinusoidally over 1 second. A J_2 plasticity model was used for the UHMWPE, the marker wires were modelled as linear elastic titanium and the femoral and tibial surfaces as rigid bodies.

Results

In models where the marker wire was near to the centre of the bearing, a line of tensile stresses were observed in the same pattern as the fractures. A reduction in the tensile stress was found when the marker wires were replaced by marker balls.

Discussion/Conclusion

These results indicate that the position and presence of the marker wire may be the cause of the typical fracture pattern observed in the fractured bearings. In the phase III component design, the posterior marker wires were replaced by two marker balls, after this a reduced incidence of bearing fracture was observed. Changing the marker wire to marker balls in the polyethylene bearing significantly reduces the tensile stresses within the bearing, thereby reducing the fracture risk.

References

[1] Pegg E, Pandit H, Gill HS, et al. 2011. Examination of ten fractured Oxford unicompartmental knee bearings. JBJS [Br] 93-B: 1610-1616.

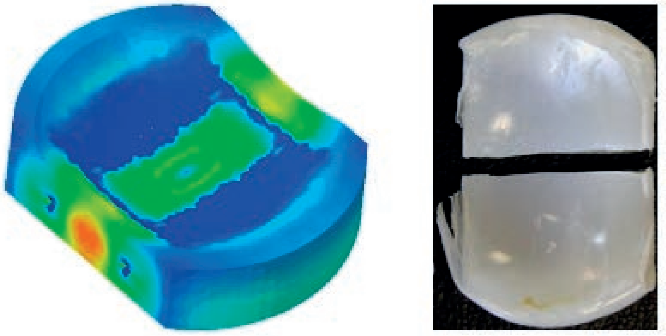

Tensile stresses measured within the bearing (none=blue, medium=green, high=red) correlated with the position of the characteristic transverse fracture line.

PE.01

Effect of Implant Alignment on Bone Resection Volume during Femoral Intercondylar Notch Preparation in PS TKA

Bo Gao
Exactech, Gainesville, USA

The effect of implant alignment on bone resection volume during intercondylar notch preparation in PS TKA was evaluated. The notch resection volume was more sensitive to translational deviations and internal/external rotation, while less sensitive to varus/valgus and flexion/extension deviations.

Introduction

Posterior stabilized (PS) knee implants account for more than 50% of total knee arthroplasty (TKA) surgeries these day. A PS knee prosthesis compensates for posterior cruciate ligament function through a tibial post-femoral cam mechanism that requires an intercondylar notch on the femur to accommodate the cam housing. Minimizing bone resection during notch preparation is a goal of modern PS prosthesis designs, especially for PS implants with high-flexion (HF) capability which usually requires even more bone resection. Studies have been performed to evaluate bone resection volumes during notch preparation for different PS prostheses at ideal implant alignment [1, 2]. However, in reality, prostheses may be implanted with deviations from its ideal position due to patient anatomy, surgeon preference, operational accuracy, etc. The effects of implant alignment deviation on notch resection volume have not been well understood. The objective of this study was to evaluate the effects of implant alignment on bone resection volume during intercondylar notch preparation.

Methods

A contemporary HF PS femoral prosthesis (Optetrak Logic PS, Exactech) was evaluated in this study. This implant features a cylindrical intercondylar box intended to simplify surgical technique and preserve bone. Five cadaveric femurs were scanned under computed tomography (CT) and 3D digital models were reconstructed from the CT images. Virtual TKA surgeries were performed on the femoral models in CAD software using digitally modeled implant and instrumentation. Standard bone cuts were performed on the distal femur, and the intercondylar notch was prepared using proper surgical procedures. In addition to the ideal implant position, deviations of -6° to +10° flexion, -8° to +8° varus, -6° to +6° internal rotation, -4 mm to +4 mm anterior translation, -10 mm to +10 mm medial translation, and -4 mm to +8 mm proximal translation were imposed to the prosthesis and resultant notch resection volumes were measured.

Results

The effect of prosthesis alignment deviation on notch resection volume varied by each degree of freedom, reflecting an interaction between resection location and intercondylar bone geometry. All five bone models revealed similar trends in terms of resection volume-alignment deviation dependency. The resection volume was most sensitive to translational deviations and internal/external rotation, less sensitive to varus/valgus, and insensitive to flexion/extension. The resection volume increased with implant anterior translation (about 387 mm^3/mm), proximal translation (about 141 mm^3/mm), external rotation (about 209 mm^3/deg), and extension (about 7 mm^3/deg). The resection volume curve was at a minimum with no medial/lateral and varus/valgus deviations, and increased with any medial (about 108 mm^3/mm), lateral (about 126 mm^3/mm), varus (about 91 mm^3/deg), or valgus (about 68 mm^3/deg) deviations. (Figure 1).

Discussion/Conclusion

This study systematically evaluated the effect of implant alignment on bone resection volume during femoral intercondylar notch preparation for a contemporary HF PS prosthesis. In general, the resection volume was more sensitive to translational deviations and internal/external rotation, while less sensitive to varus/valgus and flexion/extension deviations.

References
[1] Angibaud et al., The 56th ORS Annual Meeting, 2010.
[2] Gesell et al., The 21st AAHKS Annual Meeting, 2011.

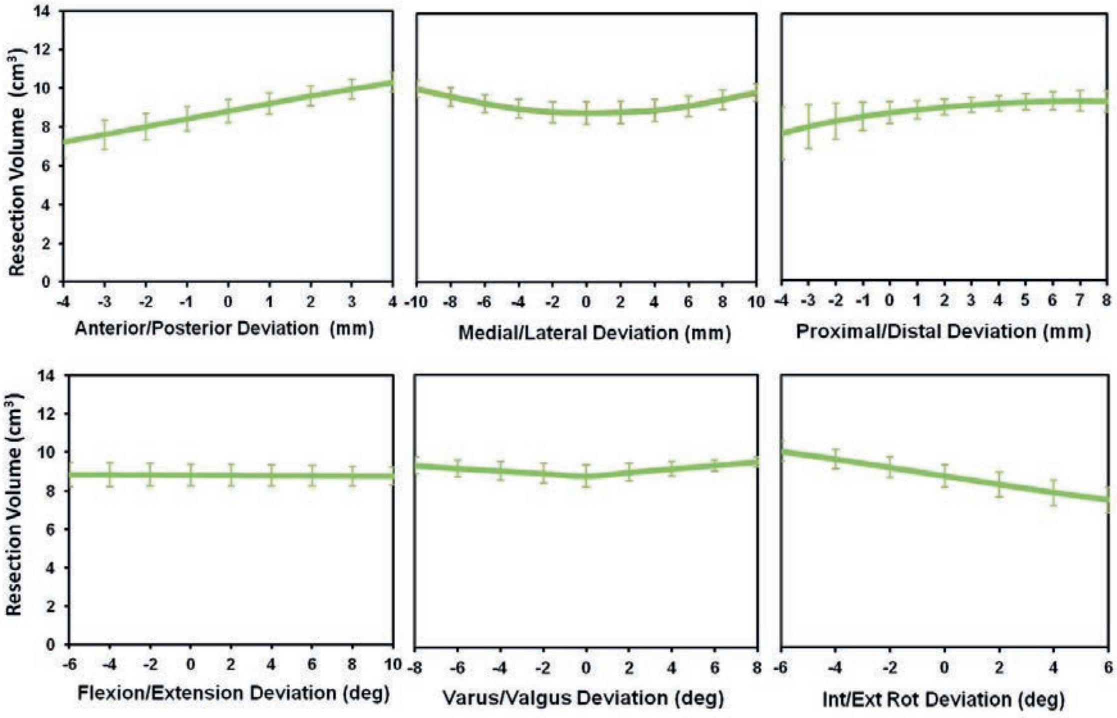

Intercondylar notch resection volume under alignment deviations of each degree of freedom.

PE.04

KNEE ARTHRODESIS WITH A PRESS-FIT MODULAR INTRAMEDULLARY NAIL WITHOUT BONE-ON-BONE FUSION AFTER AN INFECTED REVISION TKA

Danilo Bruni
Rizzoli Orthopaedic Institute, Bologna, Italy

Direct Bone-on-bone fusion is unnecessary to have good clinical outcome in knee arthrodesis after an infected revision arthroplasty

Introduction:
Knee arthrodesis can be an effective treatment after an infected revision Total Knee Arthroplasty (TKA). The main hypothesis of this study is that a two-stage arthrodesis of the knee using a press-fit, modular intramedullary nail and antibiotic loaded cement, to fill the residual gap between the bone surfaces, prevents an excessive limb shortening, providing satisfactory clinical and functional results even without direct bone-on-bone fusion.
Patients and methods:
The study included 22 patients who underwent knee arthrodesis between 2004 and 2009 because of recurrent infection following revision-TKA (R-TKA). Clinical and functional evaluations were =performed using the Visual Analogue Scale (VAS) and the Lequesne Algofunctional Score. A postoperative clinical and radiographical evaluation of the residual limb-length discrepancy was conducted by three independent observers.
Results:
VAS and LAS results showed a significant improvement =ith respect to the preoperative condition. The mean leg length discrepancy was less than 1 cm. There were three recurrent infections that needed further =urgical treatment.
Discussion:
This study demonstrated that reinfection after Revision of total knee Arthroplasty can be effectively treated with arthrodesis using a modular intramedullary nail, along with an antibiotic loaded cement spacer and that satisfactory results can be obtained without direct bone-on-bone fusion.

PE.06

Predicting Deformation and Recovery of UHMWPE in Total Knee Arthroplasty

Said Gomaa
DePuy Orthopaedics Inc, Indiana, USA

UHMWPE is the main bearing material used in total knee arthroplasty (TKA). Understanding the deformation and recovery response of the UHMWPE for in-vitro and in-vivo conditions is the first step in decoupling the deformation from wear during a volumetric, two dimensional, or linear wear quantification processes. The objective of this study was to use an advanced constitutive model to predict the time dependent deformation that occurs during a simplified in-vitro knee wear testing process.

Introduction:
UHMWPE is the main bearing material used in total knee arthroplasty (TKA). Understanding the deformation and recovery response of the UHMWPE for in-vitro and in-vivo conditions is the first step in decoupling the deformation from wear during a volumetric, two dimensional, or linear wear quantification processes. The objective of this study was to use an advanced constitutive model to predict the time dependent deformation that occurs during a simplified in-vitro knee wear testing process.
Methods:
To use the advanced constitutive model, a servo-hydraulic testing machine (MTS, Eden Prairie, MN), with direct measurement of load and displacement was used to test cylindrical specimens of moderately irradiated UHMWPE (GUR 1020). A series of monotonic tensile tests were used to reveal strain-rate sensitivity as well as creep and relaxation behaviors [3]. The data obtained from testing were fed into a material calibration program to obtain material parameters for the Three Network Model.
This new advanced constitutive model was then applied in ABAQUS to predict the deformation and recovery of a flat UHMWPE tibial insert in a simplified knee articulation. A three-dimensional finite element model was constructed for the Sigma® fixed-bearing cruciate-retaining femoral component (DePuy, Warsaw, IN) with 8 mm UHMWPE flat insert. The outer surface of the femoral component was meshed using 4 node rigid elements and the tibial insert was meshed using 8 node hex elements with a corresponding frictional coefficient of 0.04 between the two components. During loading a 1.8 kN compressive load was applied eccentrically while the femoral component was flexed for 10 cycles sinusoidally between 0[°] to 30[°] about a distal sagittal femoral radius. The femur was otherwise constrained in the anterior-posterior and medial-lateral motions as well as the varus-valgus and internal-external rotations. The nodes on the inferior surface of the tibial insert were constrained in all directions. Following the dynamic cycles, the compressive load was removed and the insert was left to recover.
Finally, the contact area and the depth of the vertical deformation of the insert were recorded in the computer model and then compared to a physical experiment.
Results and discussion:
The insert recovered about 65% of the deformation instantly after removing the load and recovered about 85% of the deformation one hour after removing the load (Figure 1). The results are in reasonable agreement with the results obtained experimentally. The compressive load was applied eccentrically to replicate imbalanced loading observed in the physical experiment.
The results strongly recommend that ample time be considered for deformation recovery when using volumetric, two dimensional or linear analyses in quantifying wear. This is especially important during wear creation as creep will increase the contact area, which has been shown to be influential in wear.
Using advanced constitutive models makes it easier to quantify the deformation and recovery of the UHMWPE under in-vivo or in-vitro conditions. That will open the door for more accurate methods to separate deformation from wear especially for in-vivo conditions. Future studies are required to better characterize this behavior and examine it in more complex loading conditions.

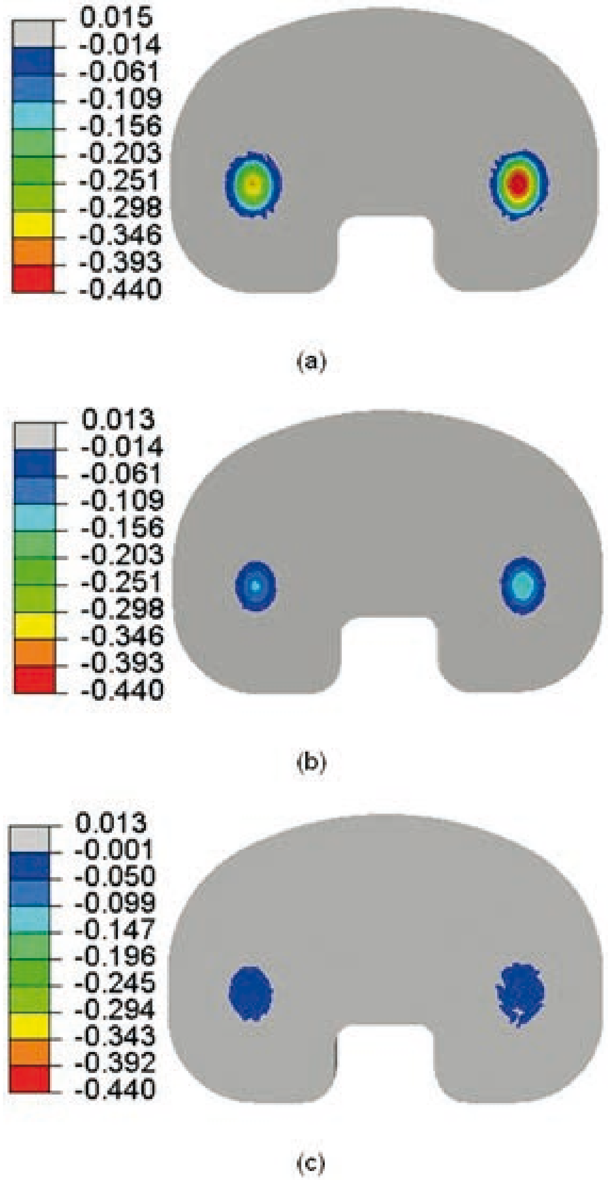

Vertical deformation in the tibial insert; (a) before removing the load, (b) just after removing the load and (c) one hour after removing the load, units in mm.

PE.09

Effect of Implant Design on Bone Resection Volume during Intercondylar Notch Preparation in Hi-Flexion PS TKA

Bo Gao
Exactech, Gainesville, USA

Benefiting from a cylindrical box design, the Optetrak Logic PS femoral prosthesis requires less bone resection during femoral notch preparation than its predecessor which has the conventional rectangular box design.

Introduction

In total knee arthroplasty (TKA), posterior stabilized (PS) knee prostheses provide functional compensation for the posterior cruciate ligament using a femoral cam-tibial post mechanism. Compared with the cruciate retaining approach, implanting a PS femoral component requires additional bone resection at intercondylar notch to accommodate the cam-post mechanism. Bone resection volume could be even greater for those prostheses with high-flexion (HF) capability to accommodate larger cam-post mechanism. Maintaining HF capability while minimizing bone resection is an effort seen in newer prosthesis designs. A study using a generic femur model has shown a new HF prosthesis reduces bone resection during notch preparation by 29% compared to a predicate prosthesis [1]. However, anatomical viabilities which could play a role in bone resection volumes were not considered in the previous study. The objective of this study was to compare the notch resection volume of two designs of HF PS prostheses, considering multiple anatomies from bone models reconstructed from cadaveric specimens.

Methods

Two HF PS prostheses from the same knee product family were selected in this study. The first one (OptetrakHi-Flex, Exactech) features a conventional rectangular intercondylar box, while the second one (Optetrak Logic PS, Exactech) features a cylindrical intercondylar box. Computed tomography (CT) scans were performed on five cadaveric femurs. CT images were segmented and reconstructed into 3D digital models. To exclude size variability, all five bone models were scaled to fit a size 3 implant. Digital TKA surgeries were performed on the femoral models in CAD software (NX 7.5, Siemens PLM, TX, USA). Standard five-step bone cuts were performed on the distal femur, and intercondylar notch was prepared for each femoral prosthesis using its appropriate surgical procedures. The resultant bone resection volume during notch preparation was measured and compared between the two designs using a paired t-test.

Results

The average bone resection volume during notch preparation was 11.66 ± 0.64 cm^3 for the Optetrak Hi-Flex femoral prosthesis, and was 8.82 ± 0.58 cm^3 for the Optetrak Logic PS femoral prosthesis. The difference (2.84 cm^{3}on average) was statistically significant ($P < 0.001$). The Optetrak Logic PS preserved about 24% bone on average at notch preparation compared to predecessor Optetrak Hi-Flex.

Discussion/Conclusion

Benefiting from a bone-preserving intercondylar box design, the Optetrak Logic PS femoral prosthesis requires less bone resection during femoral notch preparation than its predecessor Optetrak Hi-Flex which has the conventional rectangular box design. The findings from this study were also confirmed by a separate research group using larger specimen sample and multiple prosthesis sizes [2].

References

[1] Angibaud et al., The 56th ORS Annual Meeting, 2010.
[2] Gesell et al., The 21st AAHKS Annual Meeting, 2011.

PE.10

Navigated evaluation of the position of the patella and its relationship with early clinical results after a TKA

Danilo Bruni
Rizzoli Orthopaedic Institute, Bologna, Italy

Real time tracking of the patella is necessary to investigate with navigation how patellar position influences early clinical outcome.

Introduction:
The success of total knee arthroplasty depends on the correct positioning of the prosthetic components and restoring of the normal mechanical axis.Navigation is designed to help achieving these purposes but it does not give much importance to the patella which is usually prepared at the end of surgery with a free-hand bone cut. Many studies have highlighted the importance of restoring the normalpatellar trackingand that maltracking is a major cause of problems after a total knee replacement and accounting for a high percentage of failures.
Material and methods:
The present study was conductedto highlight the importance of tracking the patellar motionduring a TKR. With the knee at full extension and at 90° of flexion, the navigation system was used to determine some paramethers (anterior translation of the patella with respect to the anterior cortex of the femur, patellar tendon angle, distance from the lower pole of the patella and the tibial plateaux and the patellar shift with respect to the tibia and femur). With an offline analysis of these data,we determined the modification of the patellar position after TKA and investigated for a possible correlation with early clinical results.
Results:
We found a fair to good correlation between the position of the patella and clinical scores.
Conclusions:
We conclude that it is necessary to track the patella throughout the entire surgery by applying a third non invasive and light tracker to the anterior aspect of the patella.

PE.11

EVALUATION OF A PATIENT-SPECIFIC CUTTING BLOCK SYSTEM FOR TOTAL KNEE ARTHROPLASTY USING COMPUTER NAVIGATION.

Sébastien Lustig
Albert Trillat Center, Lyon, France

This study determined the efficacy of patient-specific cutting blocks by comparing them to navigation.

Introduction
This study determined the efficacy of patient-specific cutting blocks by comparing them to navigation.
Methods
60 total knee arthroplasty (TKA) patients were recruited to undergo their surgery guided by patient-matched cutting blocks. Continuous computer navigation was used during the surgery to evaluate the accuracy of the cutting blocks. The blocks were assessed for the fit to the articular surface, as well as alignment in the coronal, sagittal and rotational planes, sizing, and resection depth.
Results
All patient-matched cutting blocks were a good fit intra-operatively. They would have placed 79.3% of the sample within +3° of neutral in the coronal plane, while the rotational and sagittal alignment results within +3° were 77.2% and 54.5% respectively. The patient-matched cutting blocks system achieved unacceptable accuracy in the coronal plane and even less in the sagittal and rotational planes compared to computer navigation.
Conclusion
This study suggests the use of patient-matched cutting blocks is not accurate. Caution is recommended before PSCB are used routinely without objective verification of alignment.

PE.12

CORRELATION OF INTRAOPERATIVE NAVIGATION DATA AND POSTOPERATIVE OUTCOME MEASURES IN TOTAL KNEE ARTHROPLASTY

Sébastien Lustig
Albert Trillat Center, Lyon, France

Static knee alignment data obtained intraoperatively have limited capacity to explain the variance in functional outcome at one-year. While alignment and component position can be precisely measured intraoperatively, intrinsic patient factors remain dominant in determining outcome.

Introduction:
Computer assisted surgical navigation has played an increasingly central role in total knee arthroplasty (TKA). Given the recognized importance of component position changes in knee function, navigation has emerged as a promising tool for reducing the occurrence of significant malalignment. The ability of this technology to reliably measure multiple parameters intraoperatively allows analysis to possibly identify a correlation between intraoperative computer assisted surgical navigation data and functional outcomes of patients undergoing elective total knee arthroplasty.
Material and Methods:
Intraoperative navigation data was collected prospectively for 134 knees undergoing cemented, posterior stabilized TKA. Partial least squares regression analysis was used to test the association between patient demographics and intraoperative data collected with a computer assisted navigation system (coronal alignment, ligament balance, range of motion, external tibio-femoral rotation) with one year outcomes (SF36, Oxford Knee Score, range of motion).
Results:
Age at surgery displayed the largest coefficients of any other predictor. In contrast, navigation coefficients were variable in the strength and direction of their association with the outcomes variable.
Conclusion:
Static knee alignment data obtained intraoperatively have limited capacity to explain the variance in functional outcome at one-year. While alignment and component position can be precisely measured intraoperatively, intrinsic patient factors remain dominant in determining outcome.

PE.13

Medialised loading position may increase risk of pain after unicompartmental knee arthroplasty

Elise Pegg
University of Oxford, Oxford, UK

The position of loading through the medial compartment of the knee was shown to affect tibial strain. Strain significantly increased when loading was medialised >3mm and may be correlated with pain.

Introduction

Persistent pain is an important cause of patient dissatisfaction after unicompartmental knee arthroplasty (UKA) and some studies have correlated pain with localised tibial strain. The position of femoral loading through the medial side is dependent upon surgical factors (femoral and tibial component position) as well as patient factors (gait, varus deformity). The purpose of this study was to examine whether load position has an effect on tibial strain.

Patients & Methods

Using a previously validated finite element analysis (FEA) model [1], material properties of the bone were assigned using the Hounsfield units of the CT scan. Components were implanted according to the operative technique and the loads were calculated using measurements from an instrumented knee prosthesis. The tibia was cut 100 mm below the tibial plateau, this shortened model was validated. A mesh size of 2.4 mm was used after performing a mesh convergence study. Analyses were performed with the medial load positioned between 1 mm lateral to 7 mm medial from the centre, and 14 mm posterior to 14 mm anterior from the centre.

Results

Implanting the components increased the strain by 20%; this increase was significant. Movement of the loading position beyond 10 mm anteriorly and 8 mm posteriorly caused a significant increase in the mean von Mises strain in the proximal exterior cortex. Fluorscopy studies have shown anterior and posterior movement rarely exceed 7 mm so the movement is outside of this range and thought not to be of clinical impact. However, movement in excess of 3 mm medially also caused a significant increase in strain and is within the range of movement which could occur in vivo and potentially cause pain.

Discussion/Conclusion

Previous studies have found that patient with a tibial tray overhang of greater than 3 mm are more likely to have a poor outcome, the present study indicates the poor outcome may be due to medialisation of the load. These results suggest that a cause of early pain after UKR may be strain. Surgical factors which may move the load position medially, such as the use of a small tray in a large patient or medial placement of the tibial tray, should be avoided to minimise strain and possible consequent pain.

References

[1] Gray HA, Taddei F, Zavatsky AB, et al. 2008. Experimental Validation of a Finite Element Model of a Human Cadaveric Tibia. J Biomech Eng 130: 031016

Change in strain in the proximal tibial with the medial load position. Significant increase in strain ($p<0.05$) highlighted in grey.

PE.14
No clinical advantages of mobile-bearing total knee arthroplasty

Paul van der Voort
Leiden University Medical Center, Leiden, The Netherlands

Mobile-bearing total knee arthroplasty has no clinical advantages over the fixed-bearing regarding revision rates, postoperative range of motion and Knee Society Score. However, the type of mobile bearing appears to be of influence on postoperative range of motion.

Introduction

Mobile-bearings were introduced to reduce the risk of aseptic loosening and wear of polyethylene inserts in total knee arthroplasty. However, clinical advantages of the mobile-bearing (MB) over the fixed-bearing (FB) have not been consistently found in recent studies. However, few studies take different MB designs into account. There are various MB designs available each accommodating different types of mobility (e.g. rotating platform, meniscal bearing, anteroposterior gliding + rotating platform and floating platform). It may be a shortcoming to consider the MB as one entity. The different MB designs should therefore be evaluated for clinical functioning in a meta-analyses.

Methods

We conducted a systematic search of the literature to collect randomized clinical trials comparing MB with FB in primary total knee arthroplasty. The primary objective was to determine whether the MB is clinically superior to the FB, regarding revision rates, range of motion and Knee Society Score (KSS). The second objective was to search by meta-regression analysis for modifying variables (e.g. type op MB design) which affect the outcome. All data were combined for random-effect meta-analyses. Heterogeneity across studies was tested with the I^2 statistic and possible sources of heterogeneity were explored by meta-regression analysis.

Results

Our search yielded 1,827 unique references. We identified 48 studies which met our inclusion criteria, comprising almost 6,000 total knee arthroplasties. There were 66 revisions for any reason (2.3%) in the pooled MB group and 49 revisions for any reason (1.7%) in the pooled FB group. Meta-analyses showed no difference between the MB and FB TKA in revision rates for any reason (Figure 1), aseptic loosening and wear. There were also no differences in postoperative range of motion and KSS. We found considerable heterogeneity ($I^2 = 75\%$) across studies regarding postoperative range of motion. This heterogeneity could be explained by stratifying for MB design using meta-regression analysis. The rotating platform had a 1,44 degree (95% CI; 0.20 to 2.69) better range of motion in comparison to the FB TKA and the anteriorposterior gliding and rotating platform had a 3,14 degree (95% CI; -5.47 to -0,81) worse range of motion.

Conclusion

In this systematic review and meta-analysis we found no clinical advantages of the MB over the FB TKA regarding revision rates, postoperative range of motion and KSS. However, considerable heterogeneity exist among studies reporting postoperative range of motion. This heterogeneity could be explained by stratifying for different MB designs, with the best results for the rotating platform. Although there may be no difference between MB and FB TKA, the choose of mobile bearing appears to be of influence on postoperative range of motion.

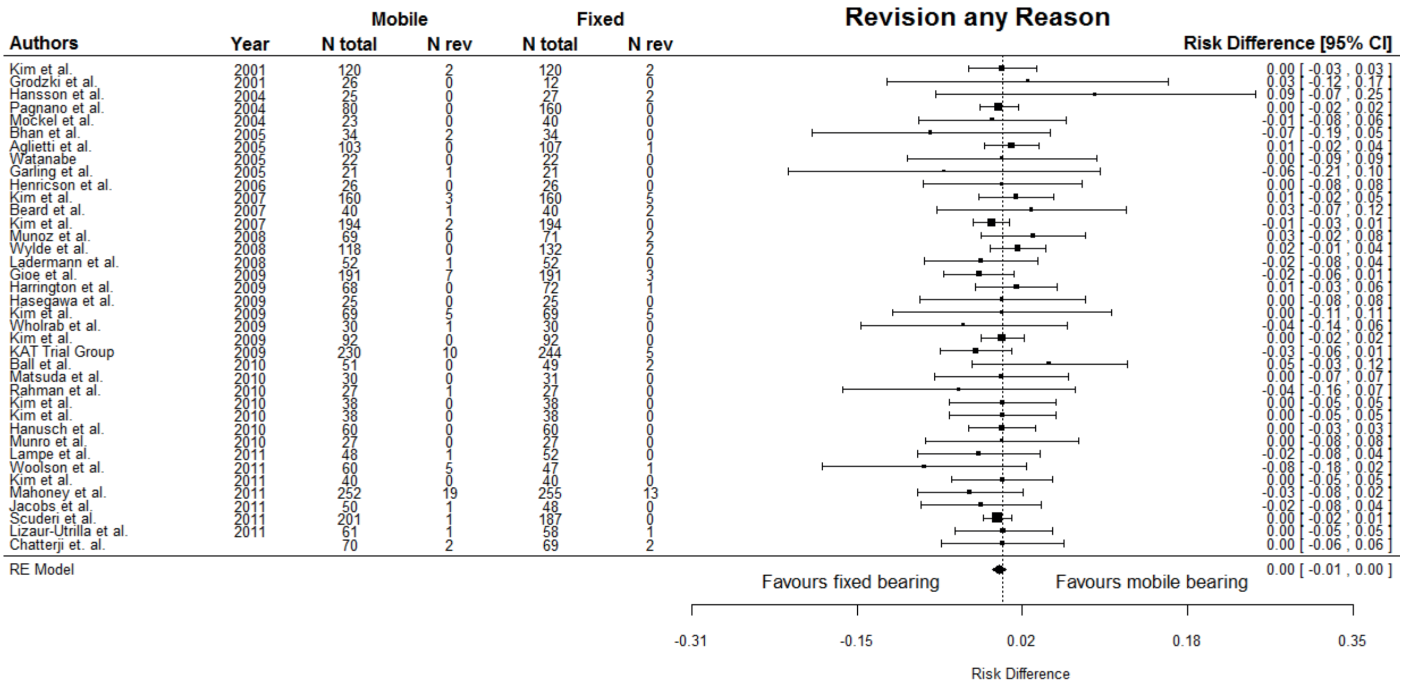

		Mobile		Fixed		
Authors	**Year**	**N total**	**N rev**	**N total**	**N rev**	**Risk Difference [95% CI]**
Kim et al.	2001	120	2	120	2	0.00 [-0.03 , 0.03]
Grodzki et al.	2001	26	0	12	0	0.03 [-0.12 , 0.17]
Hansson et al.	2004	25	0	27	2	0.09 [-0.07 , 0.25]
Pagnano et al.	2004	80	0	160	0	0.00 [-0.02 , 0.02]
Mockel et al.	2004	23	0	40	0	-0.01 [-0.08 , 0.06]
Bhan et al.	2005	34	2	34	0	-0.07 [-0.19 , 0.05]
Aglietti et al.	2005	103	0	107	1	0.01 [-0.02 , 0.04]
Watanabe	2005	22	0	22	0	0.00 [-0.09 , 0.09]
Garling et al.	2005	21	1	21	0	-0.06 [-0.21 , 0.10]
Henricson et al.	2006	26	0	26	0	0.00 [-0.08 , 0.08]
Kim et al.	2007	160	3	160	5	0.01 [-0.02 , 0.05]
Beard et al.	2007	40	1	40	2	0.03 [-0.07 , 0.12]
Kim et al.	2007	194	2	194	0	-0.01 [-0.03 , 0.01]
Munoz et al.	2008	69	0	71	2	0.03 [-0.02 , 0.08]
Wylde et al.	2008	118	0	132	2	0.02 [-0.01 , 0.04]
Ladermann et al.	2008	52	1	52	0	-0.02 [-0.08 , 0.04]
Gioe et al.	2009	191	7	191	3	-0.02 [-0.06 , 0.01]
Harrington et al.	2009	68	0	72	1	0.01 [-0.03 , 0.06]
Hasegawa et al.	2009	25	0	25	0	0.00 [-0.08 , 0.08]
Kim et al.	2009	69	5	69	5	0.00 [-0.11 , 0.11]
Wholrab et al.	2009	30	1	30	0	-0.04 [-0.14 , 0.06]
Kim et al.	2009	92	0	92	0	0.00 [-0.02 , 0.02]
KAT Trial Group	2009	230	10	244	5	-0.03 [-0.06 , 0.01]
Ball et al.	2010	51	0	49	2	0.05 [-0.03 , 0.12]
Matsuda et al.	2010	30	0	31	0	0.00 [-0.07 , 0.07]
Rahman et al.	2010	27	1	27	0	-0.04 [-0.16 , 0.07]
Kim et al.	2010	38	0	38	0	0.00 [-0.05 , 0.05]
Kim et al.	2010	38	0	38	0	0.00 [-0.05 , 0.05]
Hanusch et al.	2010	60	0	60	0	0.00 [-0.03 , 0.03]
Munro et al.	2010	27	0	27	0	0.00 [-0.08 , 0.08]
Lampe et al.	2011	48	1	52	0	-0.02 [-0.08 , 0.04]
Woolson et al.	2011	60	5	47	1	-0.08 [-0.18 , 0.02]
Kim et al.	2011	40	0	40	0	0.00 [-0.05 , 0.05]
Mahoney et al.	2011	252	19	255	13	-0.03 [-0.08 , 0.02]
Jacobs et al.	2011	50	1	48	0	-0.02 [-0.08 , 0.04]
Scuderi et al.	2011	201	1	187	0	0.00 [-0.02 , 0.01]
Lizaur-Utrilla et al.	2011	61	1	58	1	0.00 [-0.05 , 0.05]
Chatterji et. al.		70	2	69	2	0.00 [-0.06 , 0.06]
RE Model						0.00 [-0.01 , 0.00]

PE.15
MRI STUDY OF TIBIAL SLOPE CHANGES AFTER MEDIAL OPENING WEDGE HIGH TIBIAL OSTEOTOMY

Sébastien Lustig
Albert Trillat Center, Lyon, France

This study assessed the reliability of the measurement of bony and meniscal tibial slope and the changes of slope after a medial opening wedge high tibial osteotomy (MOWHTO) using MRI.

Introduction:
This study investigates changes of slope after a medial opening wedge high tibial osteotomy (MOWHTO) using MRI.
Methods:
MRI sagittal images from 101 patients were used to assess the reliability of the measurement of bony and meniscal slope. The measurements were carried out twice by two observers. The influence of gender and age on these parameters was analysed.
A prospective series of 21 patients (17 men and 4 women, mean age 52 +/- 9 years) undergoing a MOWHTO was then analysed using the same method. The difference between pre and post-operative tibial slope for both compartments was calculated as well as the correlation with the amount of frontal correction.
Results:
Repeated measures analysis of variance showed good inter and intra-observer reliability for both bony and meniscal slope (ICC (0.87 - 0.93) and (0.91-0.97) for inter and intra-observer reliability respectively). These differences were not influenced by age or gender.
There was a significant increase in bony tibial slope in both compartments following MOWHTO. When a change in bony tibial slope was detected in an individual patient, the change was larger in the medial compartment, with the average change also significantly greater (p
Conclusions:
This is the first study assessing the effect of MOWHTO on tibial slope using high-Tesla MRI measurement. The results suggest that tibial slope might increase after an OWHTO. The modification of the bony slope is larger in the medial compartment, probably related to the location of the hinge on the lateral cortex of the tibia.

PE.16
SOFTWARE ANALYSIS OF FEMORAL CARTILAGE VOLUME AFTER MENISCAL SURGERY

Sébastien Lustig
Albert Trillat Center, Lyon, France

Introduction

MRI offers a number of advantages over radiographs for the monitoring of knee cartilage changes. Software can be used to objectively quantify cartilage volume changes associated with osteoarthritis progression. Validity of such cartilage quantification software has been demonstrated [1, 2] however the reproducibility of cartilage volume analysis has not been well documented. This study aimed to assess the reproducibility of two different software packages across repeated measurements with respect to femoral cartilage volume.

Methods

9 patients with previous meniscal surgery (age 25.5 +/- 10.3 years; BMI 25.57 +/- 5.1) undertook a 3T volumetric MRI of their affected knee with a T1 weighted fat suppressed sequence using 2mm slice thickness. Scans were semi-automatically segmented and three dimensional femoral cartilage volumes were calculated using ScanIP and 3D Slicer software packages (Figure 1). This analysis was then repeated to determine intra-observerreliability. Cartilage volumes calculated for the femoral condyles were compared between medial and lateral compartments, tests and software packages.

Results and discussion

Results of the ANOVA showed no significant differences between test, compartment or software. Test-retest differences in cartilage volume for Scan-IP and 3D Slicer were 1.5% +0.6 and 1.8%+1.0 respectively. Inter-software reproducibility showed differences of 2.0% +1.6 for the medial femoral condyle, 3.2% +1.9 for the lateral condyle and 2.1 +1.2 overall.

Conclusions

Test-retest variation of femoral cartilage volume with the same software package was less than the differences between software packages. Nevertheless, the test-retest and inter-software variation were relatively high in this population when compared to the annual cartilage volume losses reported in the literature for healthy (3.1%/yr) and osteoarthritic (5-6%/yr) patients. Therefore, cartilage volume losses reported using these methods should be interpreted with caution. Further work is required to assess inter-observer reliability using the same software and explore ways of improving the reliability of quantifying cartilage volume. It is recommended that the test-retest variation be taken into account when planning the follow-up period between longitudinal measurements for monitoring cartilage volume changes.

References

1. Peterfy C.G., et al. Radiology. 192: 485-491. 1994
2. Cicuttini F., et al. Osteoarthritis and Cartilage, 7: 265-271. 1999

PE.17

In-vitro stability testing of a non-fixed meniscal implant: the effect of surgical technique and knee condition

Jonathan Elsner
Active Implants Corp., Netanya, Israel

This study aims to simulate the dynamic performance of a non-fixed interpositional device to replace the injured meniscus by subjecting it to various musculoskeletal loading conditions, to understand gross implant motion as a function of joint loading, and joint preparation.

The NUsurface® implant was developed as a non-fixed femur-conforming interpositional device to replace the injured meniscus, restore applicable functionality and relieve knee pain. The forthcoming study aims to simulate the dynamic performance of this implant, in-vitro, by subjecting it to various predicted musculoskeletal loading conditions, to understand gross implant motion as a function of joint loading, implant size, joint laxity, and the amount of posterior horn excised during the meniscectomy. Such characterization is necessary since the implant is free floating and is designed to be self-centering to prevent dislocation (fig. 1).

Joint loading conditions were determined following measurements of gait, ascending stairs, and pivoting kinematics for a representative subject. Six cadaveric knees were pre-assigned randomly to one of 3 levels of posterior horn removal (normal/excessive/total) and to display either normal laxity or increased laxity following a partial MCL release. Three implant sizes (nominal/undersized/oversized) were chosen for each of the joint loading conditions. The dislocation or subluxation of an implant was determined by either fluoroscopic visual observation or large unexpected changes in the kinematics /loads from the joint (Fig. 2).

Dislocation and subluxation of the implant did not occur under most conditions. Smaller implants experienced the most compromise in implant dislocation risk and joint integrity. Of the six specimens, there were two ACL tears that occurred during testing. The two selected surgical variables of MCL release and level of posterior horn removal had less of an effect than anticipated. Rather, undersized implants, ACL deficient joints, and major cartilage defects all significantly increased the risk for subluxation/dislocation of the implant. Interestingly, there were no subluxation or dislocation episodes when the implant was nominal or oversized in patients, even with complete removal of the posterior horn.

The dynamic performance of the NUsurface® indicated a relative sensitivity of the joint to smaller implant sizes. Complete dislocations only occurred in the absence of an ACL or with a major cartilage defect, supporting these as contraindications for use of this implant.

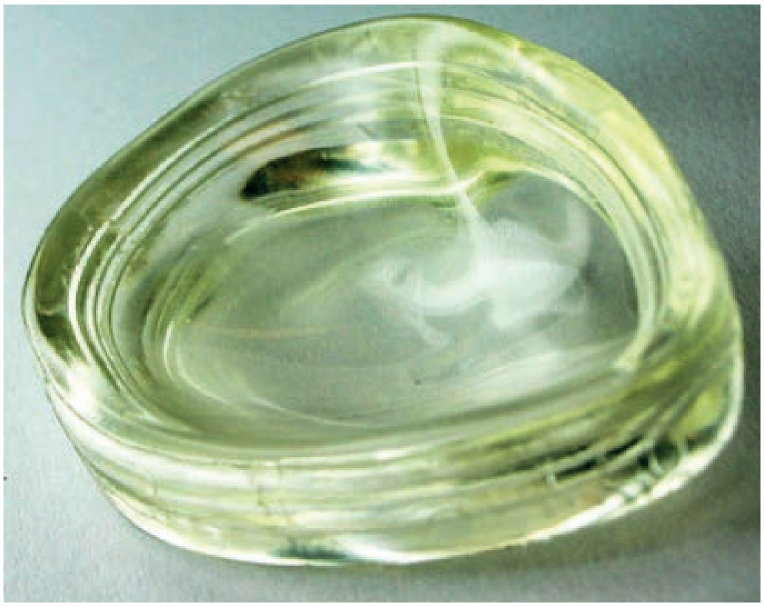

The NUsurface meniscal implant

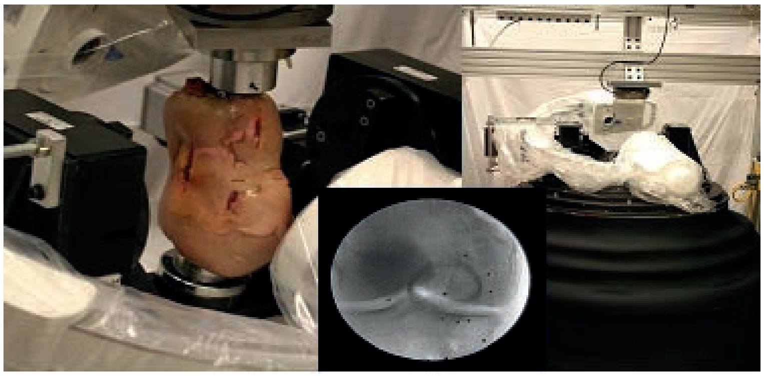

Robotic knee manipulator, and C-arm, used to track implant motion during simulated activities

PE.18
The New Knee Society Score: evaluation of the clinimetric quality in Dutch patients.

R. Dinjens
Ahorse, Atrium MC Heerlen, Heerlen, The Netherlands

The New Knee Society Score is an internal consistent, construct valid and responsive questionnaire to assess the outcome of the younger and more demanding patients. However, optimisations are recommended to increase the poor response and completion rate.

Introduction:
Most outcome assessments don't comply with the demands of the younger and more demanding TKA patients [1]. New questionnaires have therefore been developed (e.g. KOOS-PS) and current measures have been optimised by e.g. incorporating expectation, satisfaction and more demanding patient specific activities. In this way the New-KSS has been developed (based on popular KSS) and recently promoted by the Knee Society. This study evaluates the clinimetric quality of the New-KSS in Dutch TKA patients.
Methods:
Sixty-four preoperative and 114 postoperative primary TKA patients (avg. 68±9yrs, 112F/66M) were asked to complete the PROM part of the New-KSS, including a satisfaction, expectation and function (further divided into standing & walking, standard, advanced and discretional activities) subscale [2], which takes >10min. to complete. Clinicians completed the objective subscale of the New-KSS. A subgroup of 42 patients (avg. 66±9yrs,17F/25M) also completed the KOOS-PS and the current KSS was administered by clinicians in this subgroup. Moreover 14 patients completed the New-KSS and the KOOS-PS twice, pre-op and 6-12 weeks post-op TKA. The PROMs were send to patients by mail and were returned during their visit at the out-patient clinic or by mail.
Response rate, completeness rate and internal consistency (Cronbach's Alpha) was evaluated. Construct validity was assessed by measuring pearson's correlations with KOOS-PS and KSS (n=42). Responsiveness was tested by comparing pre- and postoperative new-KSS scores using paired-samples t-test (n=14). Floor and ceiling effects were examined (if >15% achieve lowest or highest possible score).
Results:
The New-KSS was returned by 97% of the patients of which 33% was completely filled in. The incomplete forms were mainly due to missing answers in the function advanced (39%) and discretional (38%) activity subscales. Further analysis relies on 57 patients. A Cronbach's α<span style="font-family: Gozl;"> >0.7 was found for all subscales, except the objective-subscale, with α = 0.95 for the satisfaction and standard activity subscale (table 1). Moderate to strong correlations were found between subscales which are intended to measure the same: New-KSS function-subscales correlated with KOOS-PS (r-range 0.59-0.85) and current KSS-function (r-range 0.60-0.79) and the new-KSS objective-subscale correlated with the current KSS-knee (r = 0.50). Moderate to strong correlations were also found between the New-KSS satisfaction-subscale and the KOOS-PS and the current KSS. No correlations were found with the expectation-subscale (table 1). All New-KSS subscales, except the objective-subscale, improved significantly after intervention (range 19%-39%, fig.1). Similar improvements were found in KOOS-PS. A floor and ceiling effect was found in respectively the preoperative (e.g. 15% in function advanced activities subscale) and postoperative group (e.g. 26% in function walking and standing subscale).
Discussion/Conclusion:
The new-KSS is internal consistent, construct valid and responsive for patients with TKA. However further improvements should be made. Shortening the scale e.g. by removing redundant items (Cronbach's Alpha ≥<span style="font-family: Gozl;">>0.95) or by removing questions causing ceiling/floor effects may improve the completion rate. Moreover an easier design and the addition of a 'not applicable' option may further optimise the New-KSS before it can be recommended for clinical use.

Reference:
[1] Alviar et al. J Rehabil Med 2011.
[2] Noble et al. Clin Orthop Relat Res 2012.

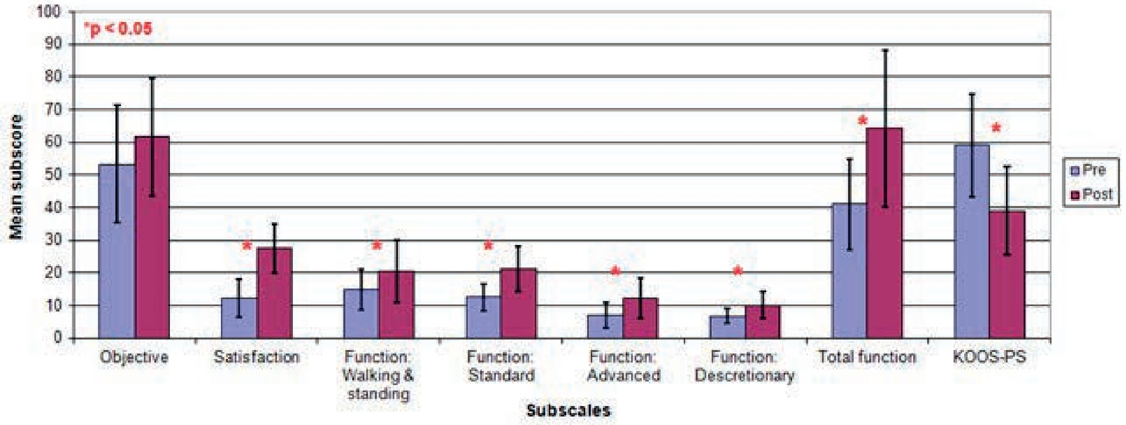

Fig.1. Changes in new-KSS subscales and KOOS-PS after surgery.

Changes in new-KSS subscales and KOOS-PS after TKA

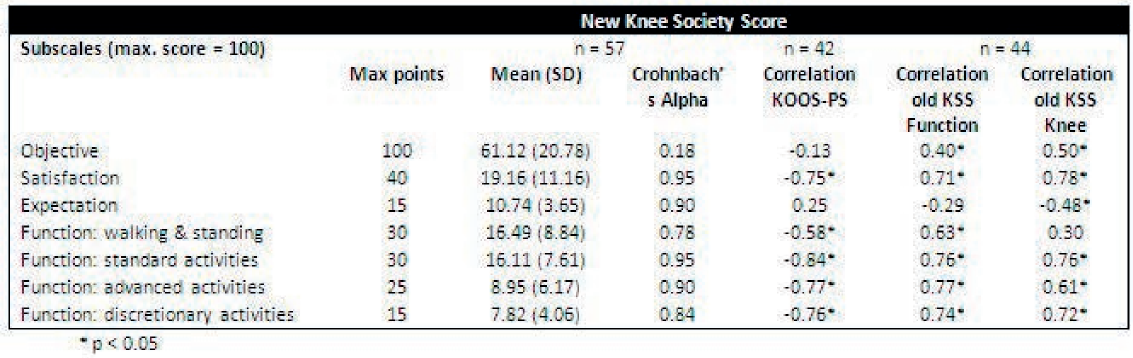

New Knee Society Score						
Subscales (max. score = 100)		n = 57		n = 42	n = 44	
	Max points	Mean (SD)	Crohnbach's Alpha	Correlation KOOS-PS	Correlation old KSS Function	Correlation old KSS Knee
Objective	100	61.12 (20.78)	0.18	-0.13	0.40*	0.50*
Satisfaction	40	19.16 (11.16)	0.95	-0.75*	0.71*	0.78*
Expectation	15	10.74 (3.65)	0.90	0.25	-0.29	-0.48*
Function: walking & standing	30	16.49 (8.84)	0.78	-0.58*	0.63*	0.30
Function: standard activities	30	16.11 (7.61)	0.95	-0.84*	0.76*	0.76*
Function: advanced activities	25	8.95 (6.17)	0.90	-0.77*	0.77*	0.61*
Function: discretionary activities	15	7.82 (4.06)	0.84	-0.76*	0.74*	0.72*

* p < 0.05

Averages, crohnbachs alfa (intern consistency) and pearson

PE.19
Is UKA a viable option for spontaneous osteonecrosis of the knee?

Danilo Bruni
Rizzoli Orthopaedic Institute, Bologna, Italy

Spontaneous osteonecrosis of the knee may be the ideal option for UKA.

Introduction:
The literature suggests a survivorship of unicompartmental knee arthroplasties (UKA) for spontaneous osteonecrosisof the knee range from 93% to 96.7% at 10 to 12 years. However, these data arise from series reporting 23 to 33 patients, jeopardizing meaningful conclusions. Our purpose is to examine a long term survivorship of UKA's in a larger group of patients with SPONK, along with their subjective, symptomatic and functional outcome; to determine the percentage of failures and the reasons for the same in an attempt to identify relevant indications, contraindications, and technical parameters in treating SPONK with a modern implant design.
ETHODS: We retrospectively evaluated 84 patients with late-stage spontaneous osteonecrosis of the knee who had a medial UKA from 1998 to 2005. All patients had preoperative MRI to confirm the diagnosis, exclude metaphyseal involvemente, and confirm the absence of major degenerative changes in the lateral and patellofermoal compartment. Mean age at surgery was 66 years and mean body mass index was 28.9. A Kaplan-Meier survival analysis was conducted using revision for any reason as the end point. The minimum followup of 63 months (mean, 98 months; range, 63-145 months).
Results:
The 10-year survivorship was 92%. Ten revisons were performed and the most common reasons for revision were subsidence of the tibial component (four) and aseptic loosening of the tibial component (three). No patient underwent revision for osteoarthritis progression in the lateral or patellofemoral compartment. There was a statistically significant difference between postoperative VAS, KSS, WOMAC,Oxford,RangeofMotionand Tibial Slope (overcorrected by 3.7 degrees, $p < 0.0023$) between the survivors and the failures.
Discussion/conclusion:
SPONK may be an optimal indication for UKA provided secondary osteonecrosis of the knee is ruled out; pre-operative MRI is performed to document involvement of other compartments, status of the ligaments and depth of lesion; and there is no over-correction in any plane.

PE.26

Analysis of different stem lengths and fixation techniques in hinged total knee arthroplasty

Susanne Fuchs-Winkelman
Dept. Of Orthopaedics, University Hospital, Marburg, Germany

To improve component stability in hinged Total Knee Arthroplasty (TKA), different stem lengths could be included during surgery. The stem, which can be either cemented or uncemented, transfers stress from the damaged proximal bone surface to the distal cortical bone.

Objective
‘To improve component stability in hinged Total Knee Arthroplasty (TKA), different stem lengths could be included during surgery. The stem, which can be either cemented or uncemented, transfers stress from the damaged proximal bone surface to the distal cortical bone.
However, no evidence-based guidelines are available to help surgeons decide on the length of stem and whether to cement it or not.
A numerical model was developed to compare different fixation techniques and stem lengths in a hinged TKA during a lunge and a squat.
Methods
‘A physiological 3D tibia model was created from Computed Tomography images of a left mechanical-equivalent Sawbone tibia. A hinged TKA (RT-PLUS, Smith&Nephew,Memphis,TN) was selected for the study. Four different configurations were considered: a short cementless stem, a long cementless stem, a short cemented stem and a long cemented stem. The short and long stems had a length of 95 and 160 mm respectively. Stem lengths and sizes were selected based on experimental tests. Loading conditions for squat and lunge motions were calculated using a validated musculoskeletal model and were applied in the finite element model.
For all the movements and configurations stresses in selected regions of interest and micromotions between the implant and the bone were computed and compared.
Results
‘Figures 1 illustrates the distribution of the average compressive stress for the four analyzed configurations in the squat movements as a function of the distance from the tibial cut. For both movements, the most stressed regions were situated around the stem tips and the presence of cement reduced the stresses along the bone-cement interface compared to the cementless configuration.
The maximal average compressive stress was higher for the cementless long stem configuration (squat 18.2 MPa, lunge 17.7 MPa) and lower for the cemented long stem configurations (squat 11.5 MPa, lunge 10.1 MPa). Also, for the short stem, the cementless configuration showed a higher average compressive stress (squat 13.3 MPa, lunge 14.6 MPa) compared to the cemented configuration (squat 9.5 MPa, lunge 10.4 MPa) in the region situated around the stem tips. However, cemented and cementless short stems showed similar maximal stresses in a region below the stem tip.
Cementless stems show higher micromotions compared to cemented stems (~50%). Long cemented stems result in lower micromotions (~50 µm) compared to short cementless stems (~120 µm).
Conclusions
‘The presence of cemented stem induces lower stresses in the tibial bone-stem interface and lower micromotions between implant and bone compared to cementless stem. A short stem shows similar maximal stresses in a region below the stem tip.

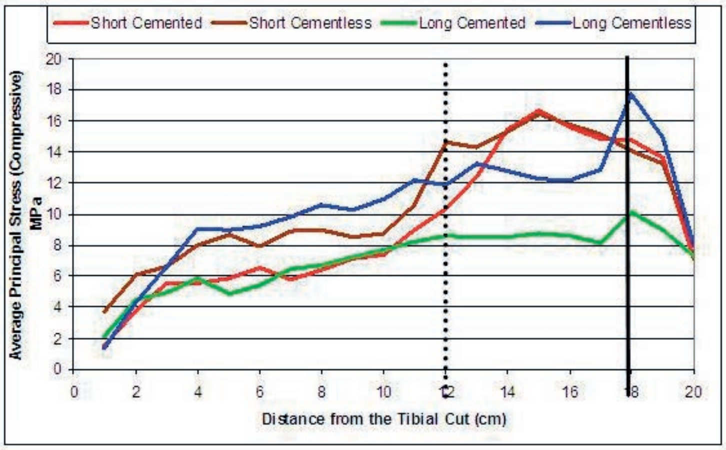

Figure 1: Average principal stress (Compressive) in the 20 region of interest analyzed during the lunge. The two vertical black lines in the figures represent the region of interest corresponding to the short stem tip (dotted line) and to the long stem tip (continuous line).

PF.01

A comparison of two reconstruction techniques for chronic type III acromio-clavicular joint injury

William Wong
Leighton Hospital, Crewe, Cheshire, UK

Both TightRope and Surgilig implants are well tolerated and have excellent functional outcomes. However, we recommend Surgicraft Surgilig procedure as the superior implant for chronic type III ACJ reconstruction.

Introduction

Treatment of symptomatic chronic Type III Acromio-Clavicular joint (ACJ) disruption remains controversial with over 100 different surgical techniques for repair or reconstruction described. There is little evidence to guide the choice of implant and surgical technique.

We present a retrospective case series comparing and describing our experience with use of Arthrex arthroscopic TightRope and Surgicraft Surgilig procedures for chronic ACJ reconstruction.

Materials and Methods

A case series of patients treated with Tightrope and Surgilig procedures during a 2-year period from 2008 to 2010 by a single surgeon at a single institution were included in this study. All presentations were confirmed on standard antero-posterior radiographs of the joint by the consultant author as type III ACJ injury.

All patients underwent surgery at 2 to 84 months after injury (mean 12.7 months). Four patients were stabilized with the Tightrope system (Arthrex). Five patients underwent ACJ reconstruction using the open Surgilig procedure (Surgicraft). Patients had a mean age of 44.9 years [range 26-69 years]. All procedures were performed by the consultant author.

Patients in both groups were treated with a shoulder sling and progressive active mobilisation of the shoulder with physiotherapy, and followed up in clinic at 6 weeks. At this point postoperative antero-posterior ACJ digital radiographs were taken and reviewed by the authors to measure clavicle position relative to the coracoid to check reduction via the Centricity PACS system measurement tool (GE Healthcare).

Patients were interviewed between 12 to 36 months postoperatively. They were asked to express satisfaction with the operation on a scale of 1-10 (1=poor, 10=excellent), whether they would consider surgery again if the need arose, and to complete the Oxford shoulder score for the operated arm. Statistical analysis was carried out using SPSS Windows version 18.0.

Results

Comparative Oxford shoulder scoring (48=excellent, 0=very poor) was not statistically dissimilar in respect to either technique. TightRope and Surgilig systems gave mean scores of 45.8 [range 41-48] and 44.2 [range 40-48] respectively ($p=0.54$). Mean satisfaction scores were lower for TightRope compared to Surgilig (7.8 vs 9), although this was not statistically significant ($p=0.31$).

6 week radiographs demonstrated a mean superior displacement of the clavicle in respect to the acromion of 12.3mm [range 7-15] using TightRope vs 3mm [range 2-5] for Surgilig ($p<0.01$). 1 patient from each group required a revision procedure. TightRope revision was performed for implant failure and further superior migration of the clavicle. Surgilig failure was secondary to new trauma resulting in ACJ displacement. At the final interview, all patients considered surgery beneficial and would be happy to undergo the procedure again if necessary. 2 patients in the TightRope group expressed some cosmetic dissatisfaction relating to undercorrection at the ACJ.

Conclusion

Both TightRope and Surgilig implants are well tolerated and have excellent functional outcomes. Better recovery is anticipated from the minimally invasive TightRope technique in the short to medium term. However, our study showed a difference between correction of ACJ deformity between both techniques, with the Surgilig procedure being the superior technique in this respect. We recommend Surgicraft Surgilig procedure as the superior implant for chronic type III ACJ reconstruction.

PF.02

Outcome assessment of 58 basal thumb joint replacements with additional vitamin C

Paul Zollinger
Ziekenhuis Rivierenland, Tiel, The Netherlands

The overall complication rate for trapeziometacarpal surgery is high and CRPS type I may occur. In our prospective cohort of 58 uncemented joint replacements no CRPS occurred under vitamin C prophylaxis (500 mg daily during 50 days).

Introduction

Basal thumb joint arthritis is known as first carpometacarpal joint (CMC I) or trapeziometacarpal arthritis and is a common site for arthritis in the hand. The prevalence is highest in women and increases with age.Any type of trapeziometacarpal surgery is known to be demanding and the overall complication rate is high. As a result complex regional pain syndrome (CRPS) type I may evolve (even up to 19%) and occurs most often in postmenopausal females. Since there is still no real cure for CRPS, the emphasis should lie on prevention. After distal radial fractures we now investigated the effect of vitamin C prophylaxis in elective standardized hand surgery (1999, 2007).

Patient & Methods

In patients with trapeziometacarpal arthritis an uncemented semi-constrained hydroxy-apatite coated prosthesis (Roseland, Depuy International Ltd. Leeds, England) was implanted.First web opening and visual analogue scale (VAS) scores (according to Huskisson; 1974) for pain, activities of daily living (ADL) and satisfaction were taken pre- and postoperatively. Two days prior to surgery 500 mg ascorbic acid was started during 50 days as prevention for CRPS. Post-operative treatment was functional.

Results

In 48 patients 58 joint replacements were performed. The group consisted of 38 females and 10 males with a mean age of 60.8 years. Operations were performed in day care under regional (plexus) anesthesia and three times under general anesthesia.There was a significant improvement in function (first web opening increased with 15 degrees) and VAS scores for pain, ADL and satisfaction ($p = 0.000$). Patient satisfaction was strongly associated with the amount of pain reduction. According to the IASP and Veldman criteria no CRPS was found (1993,1994). Complications occurred 7 times (12,1%), without any infections. Five revisions had to be performed (8,6%) for a dislocation of the cup (twice), a fractured trapezium, an aseptic loosening of the cup and for instability. As a salvage procedure a resection arthroplasty gave fairly good results in these patients (because of the intention to treat policy, these results have of course been used in the statistical analysis). Minor complications were a tenosynovitis of the thumb and an entrapment of the dorsal sensory branch of the radial nerve, which was released. Follow-up varied from 6 months to 9 years. Two patients have deceased of natural cause lately.

Discussion & Conclusion

Patients should be aware of the high complication and revision rate before they decide to undergo surgery. In case of failure, a salvage procedure can be performed.Torrededia (2006) used the same implant and reported 5 cases of CRPS after 38 implantations (13% CRPS). In our prospective cohort no CRPS occurred after 500 mg vitamin C daily (relative risk 0.87, confidence interval 0.77-0.98, $p = 0.008$). The number needed tot treat (NNT) in this study is 7.Therefore we advise vitamin C as prophylaxis against CRPS in this type of hand surgery.

PF.04

A novel combination technique in the treatment of lateral epicondylitis

Benjamin Bradley
South Devon Hospitals NHS Trust, Devon, UK

We present a new operative approach to managing lateral epicondylitis using a combination of previously described techniques. The outcome measures for this combined technique compare favourably to those for each single technique alone.

Many operative techniques have been described for the management of lateral epicondylitis with varying success. Three techniques with favourable results are radiofrequency microtenotomy, reattachment of the extensor carpi radialis brevis tendon, and post-operative wrist splinting to limit flexion.

We report the results of a single surgeon, consecutive series of 22 elbows (20 patients) treated with a combination of all three of these techniques following failed conservative measures. Each surgery was performed with an open approach, via a 4 cm incision, allowing excision of the diseased area via microtenotomy using thermoblation with a Topaz (ArthroCare, Austin, TX) wand and re-attachment of the tendon with a vicryl suture (Using the Mills manoeuvre to ensure maximum length). Patients commence self-directed elbow movement immediately with protection of the ECRB repair with a wrist splint. The splint is worn for 6 weeks. Outcomes were measured pre-operatively with the visual analogue pain score (VAS) and Disabilities of Arm, Shoulder and Hand (DASH) score. These scores were repeated post-operative at a mean follow-up time of 28 months (Range 4-57 months).

19 of 20 patients reported overall satisfaction with their procedure. VAS pain was improved from a mean of 8.2 (range 6-10) to 0.6 (range 0-3) by the procedure. Mean DASH score decreased from 60.7 (range 36.7 - 82.8) pre-operatively to 1.7 (range 0-5.8) post-operatively. Both improvements were statistically significant (P

Our results show significant improvement in both DASH and VAS scores compared to the largest published studies describing these individual techniques with no recurrence or need for further treatment. This suggests that our combination of techniques may provide improved functional results and be of benefit to surgeons treating this condition.

PF.07

Effect of post operative immobilization of thumb carpo-metacarpal arthroplasty on post operative dislocations

Priyanka Jani
Southend Hospital, Southend on Sea, UK

CMC joint arthroplasty is successful treatment option for thumb CMC joint arthritis. Dislocation/subluxation is common complication following thumb CMC joint arthroplasty.This study assesses effects of post-operative POP on dislocation rates and other functional outcomes in thumb CMC joint arthroplasty.

Introduction -There is no consencus for the treatment of isolated thumb carpometacarpal osteoarthritis. The ARPE thumb carpometacarpal arthroplasty prosthesis has been proven to have successful post operative oiutcomes [1] [2]. The results are comparable with those for trapizecomy. However, dislocation/subluxation of the prosthesis has been a commonly reported complication. Post operative immobilization with POP is a simple procedure which we integrated into the post operative regime with an aim to reduce the dislocation rates. This study aims to assess the effects of post operative POP immobilization on dislocatio nrates in patients undergoing thumb carpometacarpal (CMC) joint arthroplasty (ARPE prosthesis)

Patients & Methods -

Methodology - We conducted a retrospective comparative study which included patients that underwent thumb carpo-metacarpal arthroplassty (ARPE prosthesis) at out centre. 256 patients who underwent an ARPE thumb CMC joint arthroplasty from 2007 to 2011 were included in this study.

Participants - n=256. These patients were divided into two gruops - Group A & group B with each group having 126 patients.

Intervention - Two orthopaedic surgeons (Consultant hand surgeons)operated on the patients in the two groups. The same surgical implant was used for the thumb CMC joint arthroplasty - ARPE implant and same surgical technique was followed for both groups.

Comparators - Group A had post operative immobilization for 3 weeks in POP which holds the thumb CMC joint in an extended abducted position. Group B had no immobilization in POP and commenced physiotherapy in the immediate post operative period.

Outcomes - The primary outcome on the study included post operative dislocation rates in the two groups. The secondary outcomes included - pinch strength, tripod grip strength and pain.

Results -Follow up - The patient in the two groups were followed up for up to 60 months(maximum) at definate post op intervals.

Results -

Out of the 126 patients in Group A 7 patients had post operative dislocations whereas out of the 126 patients in Group B 16 patients had post operative dislocations. There is a significantly lower dislocation rates in patients who had post operative POP immobilization.

There is no significant difference in the pinch and tripod grip strength and pain between the two groups.

Discussion / Conclusion -The functional results of ARPE prosthesis thumb CMC joint are good and comparable to other surgical options available. Post operative POP immobilization could help reduce the incidence of dislocation following CMC joint arthroplasty. Futher prospective randmonised trials would aid to confirm the role of POP immobilization in reducing incidence of thumb CMC joint arthroplasty.

References -

[1] Brutus JP, Kinnen L. Short term results of total carpometacarpal joint replacement surgery using the ARPE implant for primary ostearthritis of the thumb. Chir Main. 2004 Oct;23(5):224-8

[2] Apard T, Saint Cast Y. MID-TERM RESULTS OF ARPE® PROSTHESIS FOR THE BASAL THUMB OSTEOARTHRITIS. J Bone Joint Surg Br 2009 vol. 91-B no. SUPP I 96

PF.08

Effect of post operative POP immobilization on incidence of dislocation in patients undergoing thumb CMC joint arthroplasty

Priyanka Jani
Southend Hospital, Southend on Sea, UK

CMC joint arthroplasty is successful treatment option for thumb CMC joint arthritis. Dislocation/subluxation is common complication following thumb CMC joint arthroplasty.This study assesses effects of post-operative POP on dislocation rates and other functional outcomes in thumb CMC joint arthroplasty.

Introduction
There is no consencus for the treatment of isolated thumb carpometacarpal osteoarthritis. The ARPE thumb carpometacarpal arthroplasty prosthesis has been proven to have successful post operative oiutcomes [1] [2]. The results are comparable with those for trapizecomy. However, dislocation/subluxation of the prosthesis has been a commonly reported complication. Post operative immobilization with POP is a simple procedure which we integrated into the post operative regime with an aim to reduce the dislocation rates. This study aims to assess the effects of post operative POP immobilization on dislocatio nrates in patients undergoing thumb carpometacarpal (CMC) joint arthroplasty (ARPE prosthesis)
Patients & Methods -
Methodology
We conducted a retrospective comparative study which included patients that underwent thumb carpo-metacarpal arthroplassty (ARPE prosthesis) at out centre. 256 patients who underwent an ARPE thumb CMC joint arthroplasty from 2007 to 2011 were included in this study.
Participants - n=256. These patients were divided into two gruops - Group A & group B with each group having 126 patients.
Intervention
Two orthopaedic surgeons (Consultant hand surgeons)operated on the patients in the two groups. The same surgical implant was used for the thumb CMC joint arthroplasty - ARPE implant and same surgical technique was followed for both groups.
Comparators
Group A had post operative immobilization for 3 weeks in POP which holds the thumb CMC joint in an extended abducted position. Group B had no immobilization in POP and commenced physiotherapy in the immediate post operative period.
Outcomes
The primary outcome on the study included post operative dislocation rates in the two groups. The secondary outcomes included - pinch strength, tripod grip strength and pain.
Results -Follow up - The patient in the two groups were followed up for up to 60 months(maximum) at definate post op intervals.
Results
Out of the 126 patients in Group A 7 patients had post operative dislocations whereas out of the 126 patients in Group B 16 patients had post operative dislocations. There is a significantly lower dislocation rates in patients who had post operative POP immobilization. POP immobilization lead to a 43% reduction in the post op dislocation rates.There is no significant difference in the pinch and tripod grip strength and pain between the two groups.
Discussion / Conclusion
The functional results of ARPE prosthesis thumb CMC joint are good and comparable to other surgical options available. Post operative POP immobilization could help reduce the incidence of dislocation following CMC joint arthroplasty. No significant differences were noted in the pain and the functional outcomes following POP immobilization. Futher prospective randmonised trials would aid to confirm the role of POP immobilization in reducing incidence of post operative dislocations in thumb CMC joint arthroplasty.

References -

[1] Brutus JP, Kinnen L. Short term results of total carpometacarpal joint replacement surgery using the ARPE implant for primary ostearthritis of the thumb. Chir Main. 2004 Oct;23(5):224-8
[2] Apard T, Saint Cast Y. MID-TERM RESULTS OF ARPE® PROSTHESIS FOR THE BASAL THUMB OSTEOARTHRITIS. J Bone Joint Surg Br 2009 vol. 91-B no. SUPP I 96

Figures & tables (Supported formats: JPG, PNG and GIF max 4MB)

PF.09

Position and Orientation of Drill Holes in Arthroscopic and Open Tightrope Fixation for Acromioclavicular Joint Reconstruction

Mohamed Hachem
King's College Health Partnerships, London, UK

Tightrope device allows nonrigid anatomic fixation of acromioclavicular joint. Our study showed adequate bone stock around coracoid in open and arthroscopic technique. Mode of failure remains unclear and we recommend biomechanical studies to assess potential factors leading to system failure.

Introduction:

Tightrope fixation is an accepted method for reconstructing the acromioclavicular joint and the presence of good bone stock around the two drill holes is probably the most important determining factor for preventing failure of the construct.

Aim:

Arthroscopic assisted tightrope stabilisation involve drilling clavicle and coracoids in a straight line. This leads to eccentric drill holes with inadequate bone around it. Open tightrope fixation involves drilling each hole under direct vision and independently and therefore has centric hole with more bone around it. The aim of our study was to assess the hypothesis of tightrope fixation in relation to location of drill holes using 3D CT scan and cadaveric models for arthroscopic and open technique for ACJ fixation.

Methods:

CT scans of normal shoulders were identified. Special software used to draw straight line from distal end of clavicle to coracoid. Bone volume around coracoid drill hole was calculated. Cadaveric shoulder specimens were dissected. The arthroscopic technique was performed under vision by drilling both clavicle and base of coracoid holes in one direction. Same specimens were used for the open technique. Base of coracoid was crossectioned above drill hole and bone volume calculated.

Results:

40 shoulders were included in the study (20 cadaveric specimens&20 CT of shoulder). Bone stock was adequate around drill holes in open and arthroscopic technique. Variable angle for insertion of drill holes using arthroscopic technique were needed depending on shape of shoulder.

Conclusion:

Tightrope device allows nonrigid anatomic fixation of acromioclavicular joint. Published studies showed high rate of fixation failure with tightrope system but with patient satisfaction and high functional results. Our study showed adequate bone stock around coracoid in both open and arthroscopic technique. Mode of fixation failure remains unclear and we recommend further biomechanical studies to assess potential factors leading to system failure.

PF.10
Morphological and mechanical 3D finite element modeling of the glenoid.

Ibrahim Kalouche
Bicetre University Hospital, Paris, France

A 3D model of the mechanical properties of the glenoid cancellous bone was determined based on mechanical testing and morphological data of the same scapulae. This model shows the heterogeneities and anisotropy of elastic properties in different parts of the scapula.

Mechanical properties of the glenoid cancellous bone are essential to understand the osteointegration and load transmission between the glenoid component and the scapular bone into which it is fixed. Previous studies with finite element models (FE) of the scapula were based on mechanical properties correlated to bone density from computed tomography or on properties not obtained from the same scapulas.

The objective of the present study was to combine mechanical properties of glenoid cancellous bone with morphological data of the same tested glenoid in order to develop a numerical three-dimensional (3D) FE model of the glenoid cancellous bone.

Mechanical properties of cancellous bone and its heterogeneities within the glenoid were determined using compression test. Then a finite element model of the scapula was developed using combination of a continuous model of the heterogeneities of the mechanical properties inside the glenoid cancellous bone and Magnetic Resonance Imaging (MRI) of the same tested scapula.

A 3D
model of the mechanical properties of the glenoid cancellous bone was obtained showing the heterogeneities of elastic properties in different parts of the scapula and the anisotropy with the three directions of loading.

The importance of this model is to give the possibility to test local loads transfer between implant and cancellous bone in different parts of the scapula, which was not done before.

PF.11

THE TRANSPEDICULAR APPROACH AS ALTERNATIVE ROUTE FOR INTERVERTEBAL DISC REGENERATION

Gianluca Vadalà
University Campus Bio-Medico, Rome, Italy

This study shows that a novel transpedicular approach represents a potential alternative route to the NP for IVD regeneration and biological spinal fusion, whilst maintaining an intacted AF.

Introduction
The present delivery approach of therapeutic agents (growth factors/cells/hydrogels) within the intervertebral disc (IVD) needs to be through injection, via the annular fibrosus (AF). However, it has recently been demonstrated that small needle puncture of the AF leads to further degeneration and disc herniation.[1] The aim of the study was to describe the alternative transpedicular approach to deliver therapeutic agents into IVDs within ovine and human cadaveric spinal segments.
Methods
Lumbar ovine and human spinal segments were used. Under fluoroscopy, a 2mm Kirschner wire was introduced in the caudal vertebra at the intersection of the horizontal line passing through the axis of the transverse process (inferior margin in human) and a vertical line passing to the lateral border of the superior facet (3mm lateral in human). The wire direction was posterior-to-anterior, lateral-to-medial and caudal-to-cranial through the pedicle and the inferior endplate to the nucleus pulposus (NP). HR-pQCT (XtremeCT) was performed to assess the right position of the wire in pedicles. Discography and nucleotomy were performed using a 14G cannula insertion or a 2 mm arthroscopic shaver blade, respectively.
Results
Fluoroscopy and HR-pQCT images showed that the NP could be approached through the endplate via the pedicle without affecting the spinal canal and the neural foramina. The contrast agent was delivered into the IVD and NP was removed from the disc by the transpedicular approach and the cavity filled with a gel of agarose and contrast agent.
Discussion
The injection of a contrast agent into the NP, demonstrated the feasibility of a drug/cell therapy to treat early disc degeneration through this approach. The tunnel might be also used to perform nucleotomy of moderate or severe IVD degeneration and allow the delivery of a hydrogel/cell construct for IVD regeneration or biological spinal fusion, respectively.
This study shows that a novel transpedicular approach represents a potential alternative route to the NP for IVD regeneration and biological spinal fusion, whilst maintaining an intacted AF.

[1] Carragee, Spine 2009

PF.12
Biomechanical investigation of augmentation in the lumbar vertebrae

Luca Cristofolini
University of Bologna, Engineering Faculty, Bologna, Italy

This in-vitro study investigated the strain distribution, stiffness and toughness of natural and augmented vertebrae. While correct augmentation significantly strengthens the vertebra, the opposite is possible in case of inadequate filling.

Introduction

Prophylactic augmentation has often been proposed to protect osteoporotic vertebrae from fracture. The aim of this in vitro study was to assess whether augmentation can actually reinforce the vertebra, and under which circumstances.

Materials and methods

Five sets of three adjacent vertebrae were obtained from elderly donors (age:70-88), who did not suffer from musculoskeletal diseases or cancer, through an ethically-approved donation program. The central vertebra was tested in the natural condition (control), while the two adjacent vertebrae were tested before and after augmentation. Augmentation was performed by injection of acrylic cement (Simplex-P) either with a mono-pedicular or bi-pedicular access. Quality of augmentation (volume and position of the cement mass) was documented by CT-scan. Axial and torsional loading was applied nondestructively to all specimens (both natural and augmented). Subsequently, all specimens were compressed to failure (either natural, or after augmentation). A subset of specimens was instrumented with 8 triaxial strain gauges to measure bone strain on the vertebral body. During nondestructive testing, the following magnitudes were measured: stiffness in torsion and compression; principal strains (only vertebrae with strain gauges). In addition, during destructive testing the first failure event was recorded, as well as the ultimate load, and the energy absorbed prior to failure.

Results

Augmentation patterns were variable and consistent with clinically observed results. When strain in the same vertebrae was compared before an after augmentation, a mild decrease of strain was found due to augmentation (-50% to +27%, Fig.1). During destructive testing, the natural vertebrae showed a first load peak, followed by abrupt failure, with a limited recovery of load when further compressive strain was delivered (A, Fig.2). Conversely, two different trends were found for the augmented vertebrae: either load decreased and then recovered similar to the natural ones (possibly with a larger ultimate load, case B), or exhibited a monotonic trend to failure (case C). Some augmented vertebrae resisted a larger load and required a larger work to failure than the adjacent natural control ones (1.2 to 45 times larger). However, other augmented vertebrae withstood a lower force and received less energy before failing than the natural ones (-5% to -43%).

Discussion

When the post-augmentation CT-scans were inspected, a correlation was found between the quality of augmentation and the strengthening/weakening effect of the treatment. The vertebrae with a better augmentation exhibited a monotonic ramp to failure (case B, Fig.2), reached a significantly larger load and withstood significantly more energy to failure than the natural ones. Conversely, the vertebrae with poorer augmentation exhibited a load-displacement curve (case C, Fig.2) that was more similar to the natural ones, with an early failure, and withstood lower loads and energy to failure than the adjacent control vertebrae.

Conclusion

While proper prophylactic augmentation can make osteoporotic vertebrae significantly stronger and tougher, suboptimal augmentation can yield the opposite effect. This finding may also explain the inconsistency in clinical outcome documented in recent vertebroplasty [1,2].

Acknowledgements:
EU-funded Osteoporotic Virtual Physiological Human Project (VPHOP FP7-ICT2008-223865)

References

1.Buchbinder et_al. NEnglJMed. 2009:557-568.
2.Kallmes et_al. NEnglJMed. 2009:569-579.

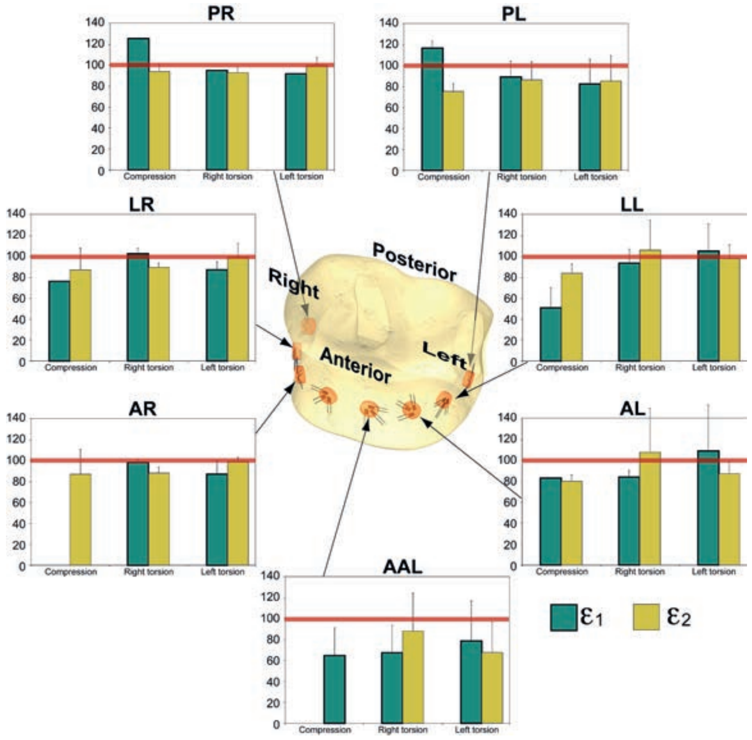

Fig. 1: Strain distribution (maximum and minimum principal strain) on the surface of the vertebral body. The strain value after augmentation is reported as a percent of the strain value in the corresponding location prior to augmentation. A value of 100% indicate no variation caused by augmentation; a value lower than 100% indicates that the augmented vertebra experiences lower strain than the natural one.

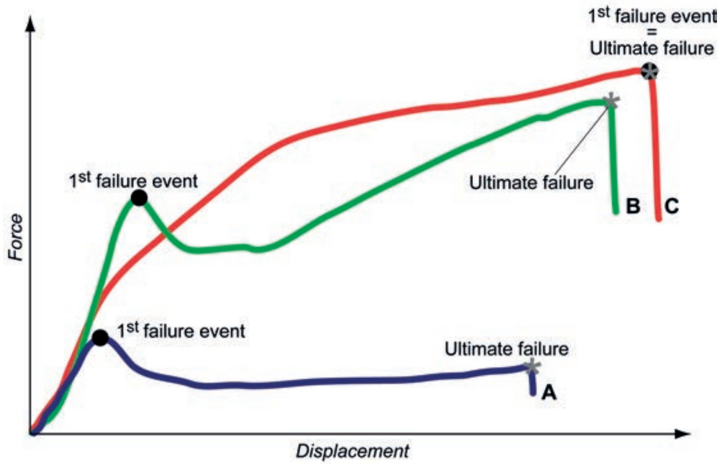

Fig. 2: Typical force displacement curve during destructive testing for (A) an unaugmented vertebra; (B) a vertebra with defective augmentation; (C) a correctly augmented vertebra.

PF.13
Dynamic Comparison of Porcine Lumbar Specimens with Intact Discs and Disc Replacements

Timothy Holsgrove
University of Bath, Bath, UK

Porcine specimens were tested with an intact disc, and after a disc arthroplasty using the DePuy In Motion disc. Some stiffness terms were significantly with the replacement device compared to the intact disc.

Introduction

Total disc replacement has emerged as a viable treatment for severely degenerated discs but the complexity of the spine is reflected in the clinical results. Short-term results are comparable with fusion but long-term results are limited in number, and are poor in terms of outcome measures. This may be due to total disc replacement procedures failing to restore the natural biomechanics of the spine.

Materials and Methods

A custom-developed six-axis spine simulator (Figure 1) was used for the dynamic stiffness matrix testing of lumbar porcine specimens with an intact disc and with a DePuy In Motion disc replacement.

Functional spinal unit (FSU) and isolated disc (ISD) specimens were tested, first without an axial preload, then with a preload of 500 N. The preload was equilibrated for 30 minutes prior to testing, and the test repeated 60 minutes after initial preload application.

Testing was completed at 0.1 Hz using amplitudes of ±4° in rotational axes, ±3 mm in anterior/posterior shear, ±1.5 mm in lateral shear, and ±0.4 mm in axial compression/extension.

Results

Comparisons were made between the stiffness of the intact disc and the disc replacement device. More terms were significantly different in the ISD specimens, due to the shielding effect of the facets and ligaments of the FSU specimens.

Four of 36 terms were significantly lower with the disc replacement in all comparisons with the intact disc. In the ISD specimens, with a preload of 500 N (Table 1), 5 of the 6 principle stiffnesses and 9 non-principal stiffnesses were significantly lower with the In Motion device compared to the natural disc.

Discussion and Conclusion

The disc replacement compared favourably with the intact porcine disc in shear and axial stiffness. However, the design of the In Motion device lacks stiffness in the three rotational axes, and is unstable in flexion/extension and lateral bending. Rotations are the primary movements in the spine, and a disc replacement should replicate the stiffness in these axes if the natural biomechanics are to be restored.

A dynamic pre-clinical testing protocol was used to quantitatively assess the efficacy of a disc replacement device. The protocol would also provide valuable data during the design stages of new disc replacements, aiding the development of the next generation of artificial discs.

References

1. Blumenthal, S., et al., 2005. A Prospective, Randomized, Multicenter FDA IDE Study of Lumbar Total Disc Replacement with the Charite Artificial Disc Versus Lumbar Fusion Part I: Evaluation of Clinical Outcomes. Spine, 30(14): p. 1565-1575.
2. Chung, S.S., Lee, C.S., and Kang, C.S., 2006. Lumbar Total Disc Replacement Using Prodisc II: A Prospective Study with a 2-Year Minimum Follow-Up. Journal of Spinal Disorders & Techniques, 19(6): p. 411-415.
3. Huang, R.C., et al., 2006. Range of Motion and Adjacent Level Degeneration after Lumbar Total Disc Replacement. The Spine Journal, 6(3): p. 242-247.
4. Putzier, M., et al., 2006. Charite Total Disc Replacement - Clinical and Radiographical Results after an Average Follow-up of 17 Years. European Spine Journal, 15(2): p. 183-195.

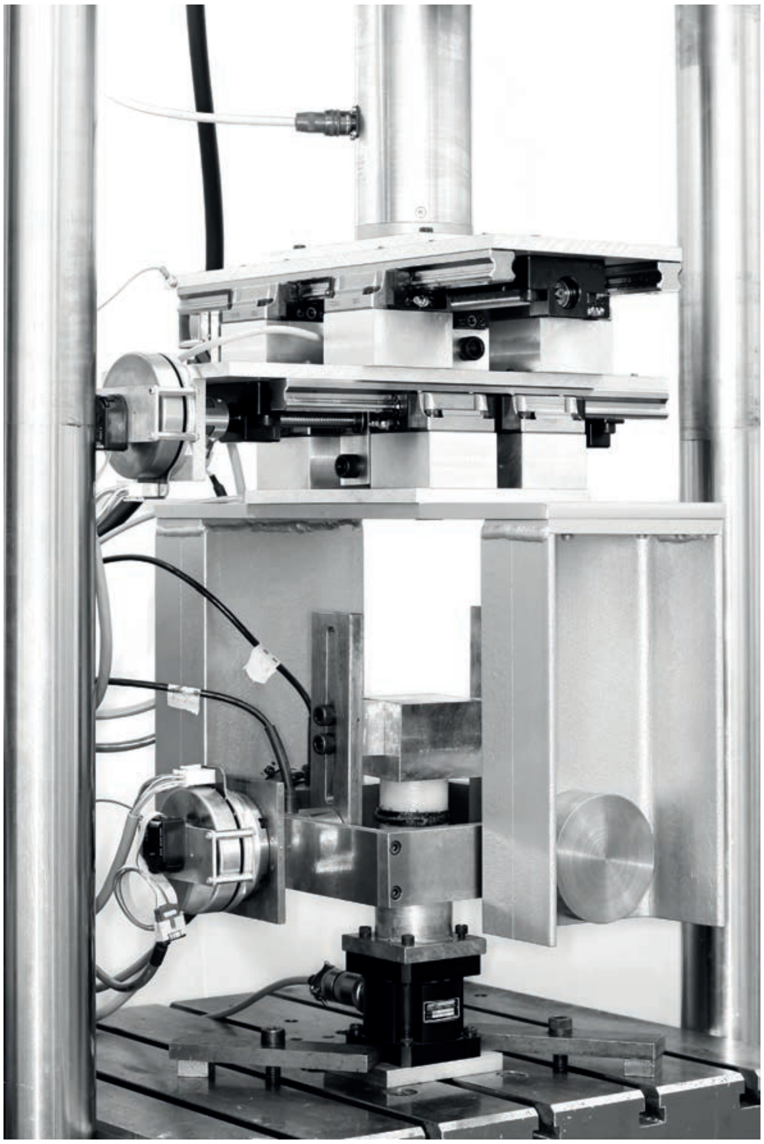

The custom spine simulator, developed at the University of Bath

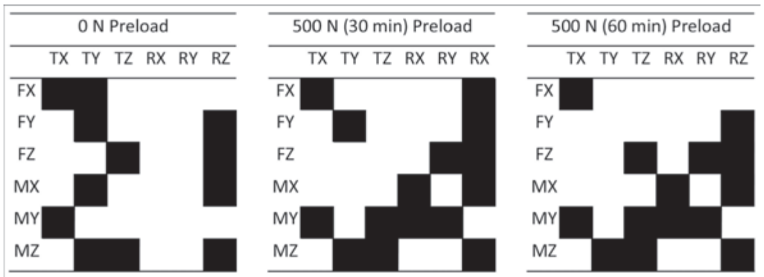

0 N Preload						
	TX	TY	TZ	RX	RY	RZ
FX	■	■				
FY		■				■
FZ			■			■
MX		■				■
MY	■					
MZ		■	■			■

500 N (30 min) Preload						
	TX	TY	TZ	RX	RY	RX
FX	■					■
FY		■				■
FZ					■	■
MX				■		■
MY	■		■	■	■	
MZ		■	■			■

500 N (60 min) Preload						
	TX	TY	TZ	RX	RY	RZ
FX	■					
FY						■
FZ			■		■	■
MX				■		■
MY	■		■	■	■	
MZ		■	■			■

Comparison of stiffness with an intact disc and the In Motion disc for ISD specimens. Black denotes a significant difference ($p<0.05$)

PF.14
How Evidence Based are Publications in Clinical Spinal Journals?

Amir Amiri
Royal National Orthopaedic Hospital, London, UK

In this study we demonstrate that majority of clinical spinal publications provide level IV evidence. Therapeutic studies demonstrate the highest proportion of level IV evidence. Spinal surgery journals with higher impact factor contain larger proportion of studies with high LOE.

Introduction:

Over the past two decades there has been a growing recognition and emphasis on evidence-based medicine (EBM) amongst clinicians, managers, funding authorities and governments. Practice of EBM is defined as the integration of the best available clinical evidence with individuals' clinical experience and patients' choice. The level of evidence (LOE) is used to classify clinical studies based on its quality and design.

There are various factors that contribute to the overall quality of a journal. Impact factor (IF) is the most widely used quality ranking measure of scientific journals. However the calculation of IF is independent of the quality or LOE of clinical papers published in a journal.

We aim to evaluate the LOE of current clinical research in spinal journals and to determine whether there is a significant correlation between the LOE and journals' IF.

Method:

All online articles published during 2010 in The Spine Journal, Spine, European Spine Journal, Journal of Neurosurgery: Spine, and Journal of Spinal Disorders and Techniques were systematically reviewed. Supplements were included.

Two reviewers independently assessed all publications. Clinical publications were ranked using the level of evidence guidelines produced by the Oxford Center for Evidence-Based Medicine.

Results:

Overall 703 articles were suitable for LOE grading. Of these 4.7% provided level I evidence, 23.2% level II, 12.5% level III, and 59.6% level IV. There was a significant association between LOE and type of study ($P<0.001$), with therapeutic studies having the largest proportion (71.8%) of level IV evidence publication. There was a statistically significant positive correlation between the proportion of level I and II evidence and journal impact factor ($\rho = 0.9$, $P = 0.037$).

Discussion:

This study revealed that almost 60% of clinical publications in spinal surgery provide level IV evidence, with only approximately one in every 20 clinical publication providing highest LOE (level I). The distribution of LOE seen in spinal surgery is similar to other surgical specialties. The majority (66.3%) of spinal research papers focused on therapy/prevention, or aetiology/harm. This group had significantly the greatest proportion of level IV evidence (71.8%), which would suggest that majority of the research available to guide therapy and management of spinal patients provides low LOE.

Every effort must be made to increase the LOE and quality of spinal research in particular therapeutic studies. However, often it is not possible to obtain high LOE studies due to multiple logistic, ethical and financial challenges associated with design and conduct of such trials. Therefore a pragmatic approach must be used when assessing the available evidence to guide clinical practice. In addition, it should be recognized that reliance on external evidence alone is not sufficient for practice of EBM. The importance of clinician's experience and patient's views should not be underestimated for successful evidence-based practice.

We also demonstrated that spinal surgery journals with higher impact factor contain larger proportion of studies with high LOE. To promote the practice of EBM in spinal surgery we would recommend editors of spinal journals to include a LOE grading for each clinical paper published.

PF.15
Does bipedality effect the morphology of the lumbar vertebrae and IVDs in mice?

Nadir Yalcin
Ataturk Training and Research Hospital, Ankara, Turkey

Demonstrating that bipedality is indeed associated with histomorphological changes in IVD suggesting accelerated degeneration may form the basis of new treatment modalities aiming to overcome the effects of bipedality, presumably by creating focal regions of "quadripedality" for early IVD degeneration.

Introduction:
Bipedality is thought to be one of the primary mechanical factors in disorders like scoliosis and spondylolisthesis. Bipedality may affect the loading mechanisims of the upright spine especially given lumbar lordosis. However, whether the shape and growth pattern of vertebral bodies is affected by bipedality is not known. There are a number of bipedal animal models (1,2) that have been developed to overcome this difficulty, i.e. spines from the same species may be compared between natural (quadripedal) and bipedal animals. Although several studies have suggested similar loading patterns in quadripedal and bipedal animals, (both in axial compression) (3-5), our hypothesis is that the vertebral bodies and or intervertebral discs (IVDs) would be affected by the altered posture.
Materials and Methods:
All procedures were approved by institutional committee of animal use for research at Hacettepe University, Ankara, Turkey. Female C57BL6 mice were used in this study. Eight mice were made bipedal according to the technique described by Machida et al (2) at 3rd week. For histomorphological analysis, the 2nd lumbar vertebra, L2-L3 discs and growth plates were analysed (Figure 1). Spines were collected at 20 and 40 weeks (n=3 quadriped, n=4 biped at each time). Total corpus volume (TCV), total trabecular volume (TTV), percentage of TTV to TCV (%TTV/TCV), total disc volume (TDV), total nucleus pulposus volume (TNPV) and total growth plate volume (TGPV) were calculated using the equation for a conical frustum.
Results:
TCV in quadrapeds and bipeds were similar at 20 and 40 weeks. Whereas TTV was increased in bipedal animals at both times, but there was no statistical significance. The proportion of TTV to TCV was higher in bipedal animals at 20 weeks (Figure 2). There was a decrease in TDV in quadripeds between 20 and 40 weeks. In contrast, the TDV of bipedals seem to be maintained at 40 weeks. The TNPV of the bipedal animals was significatly smaller than quadripeds at 20 weeks. At 40 weeks, there is no difference in TNPV between the groups, because the TNPV in quadripeds was significantly reduced at this time. Interestingly, at both times, TGPV of bipedals was significantly lower than quadripeds. By 40 weeks, the TGPV of quadripeds was reduced but remained substantially higher than bipeds which is signficant also (Figure 3).
Conclusions:
The overall morphology of the lumbar vertebral bodies of bipeds and quadripeds appears to be not significantly different. While the TCV are same, the proportion of trabecular bone increased in bipeds possibly due to higher axial loads on bone. Discs appeared to degenerate quicker in bipeds, and the growth plate in bipeds may become inactive earlier possibly due to aberrant loads on chondrocytes. In conclusion bipedalism appears to accelerate the age-related degenerative changes in the disc, but does not greatly affect the vertebral histomorphology.

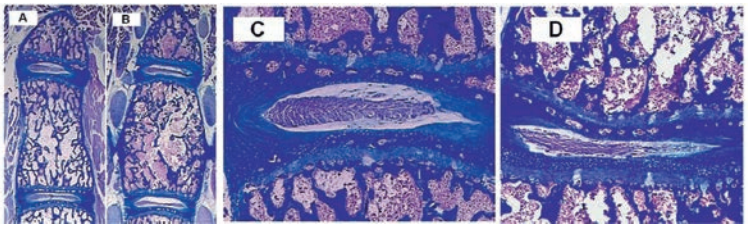

Coronal plane sections of vertebral bodies and IVDs in 40 week old quadripedal (A, C) and bipedal (B, D) mice (Trichrome, x1.5).

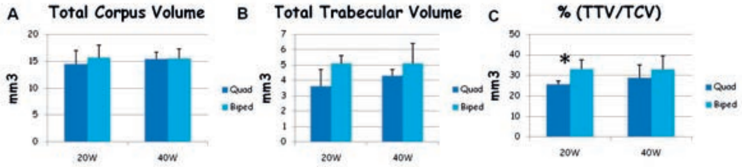

Comparisons of quadripedal and bipedal mice for Total Corpus Volume, Total Trabecular Volume and Trabecular Density (TTV/TCV) at the 20th and 40th weeks. * p<0.05.

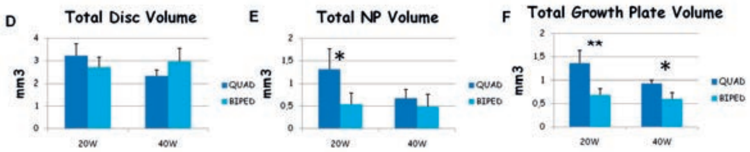

Comparisons of quadripedal and bipedal mice for Total IVD Volume, Total Nucleus Pulposus Volume and Total Growth Plate Volume at the 20th and 40th weeks. * p<0.05, ** p<0.01.

PF.16

Does the previous whiplash affect the outcome of a second whiplash injury?

Ravindra Thimmaiah
Southport Hospital, Town Lane, Southport, UK

Views of various members of the healthcare system concerning a second whiplash injury were captured using a questionnaire set up on an imaginary road traffic collision. Majority of respondents believed that whiplash injuries are cumulative in nature.

Introduction:
Neck whiplash injuries are commonly treated in medical practice. It is also one of the conditions frequently come across in medico legal practice. The aim of this study was to capture the views of various members of the healthcare system with regards to a second whiplash injury.
Methods:
A questionnaire was set up on an imaginary road traffic collision where three occupants(A,B,C) of a vehicle were injured. All three occupants had history of previous neck painfollowing previous road traffic collision. Two imaginary experts (X,Y) provided opinionregarding clinical impairment and disability. The opinion of the two experts were wide apart.This contrast was used so that respondents would only agree with one of the experts. Therespondents were requested to provide a score on a range of 0 to 10 for each of the opinionsby the experts. The disability claimed by the occupants ranged from pain and suffering fromthree months to permanent disability requiring retirement on ill health grounds. For purposesof this study we estimated scores below five as being negative and scores above five as beingpositive. The questionnaire was distributed mainly to orthopaedic surgeons, generalpractitioners and physiotherapists.
Results:
Forty five respondents participated in the study. Twenty were general practitioners, 9 orthopaedic consultants, 9 physiotherapists and 7 other health professionals. The greatest average score was 8.22 for disability of three months. The lowest average score was 3.13 for permanent disability requiring ill-health retirement. When the disability claimed was less than 18 months 4.4% of respondents disagreed with both the experts. However when disability claimed was greater than two years or permanent 17.8% of the respondents could not agree with either of the experts.
Conclusions:
Our questionnaire revealed that the majority of respondents believed that whiplash injuries are cumulative in nature. However, the large number of respondents who did not agree with one expert but on the contrary agreed or disagreed with both experts showed that answers regarding disability following a second whiplash were unknown and conjectural.

PF.17
Blinded Radiological Evaluation of OsteoAMP vs. rhBMP-2 in TLIF/LLIF Spine Procedures

Jeffrey Roh
Orthopedics International, Seattle, WA

This work shows a blinded, multi-center radiographic study evaluating and comparing fusion outcomes between rhBMP-2 (Infuse) and OsteoAMP® bone graft in transforaminal lumbar interbody fusion (TLIF)/lateral lumbar interbody fusion (LLIF) spine procedures.

Introduction
Since the introduction of rhBMP-2 for spine fusion, surgeons have had a reliable substitute to autograft. Recently, the prevalence of adverse events related to the use of rhBMP-2 has raised many concerns for surgeons. OsteoAMP® is a commercially available allograft-derived growth factor rich in osteoinductive, angiogenic, and mitogenic proteins. The fusion outcomes of OsteoAMP® and rhBMP-2 were compared to determine whether OsteoAMP® was a viable alternative to rhBMP-2.
Patients & Methods
OsteoAMP® was processed from human cadavers cleared for implant. Osteoinductive, angiogenic, and mitogenic growth factors were harvested from bone marrow. These growth factors were then bound to the cadaver bone and the bone was cleaned prior to final lyophilization and packaging. For the OsteoAMP® arm, no other biologic product was used in combination with OsteoAMP® other than the patient's own bone marrow aspirate or local autologous bone. For the rhBMP-2 arm, rhBMP-2 was loaded onto the Absorbable Collagen Sponge. RhBMP-2 was also combined with local autogenous bone (if available). All patients had been diagnosed with degenerative disc disease, stenosis and/or spondylolisthesis. Ninety patients (131 levels) underwent TLIF or LLIF between T11 and S1.Patients received X-rays and CTs at six, thirteen, twenty-six, fifty-two, and seventy-two weeks post surgery. An independent radiologist made fusion assessments blinded to intervention, product, and surgeon information. Time frame between surgical intervention and positive fusion assessment was calculated and complications reported. If a patient was not fused by 18 months, it was assumed the patient would fuse by their next annual follow-up visit for the time to fusion measurement (applied to only rhBMP-2 arm as all OsteoAMP® patients had fused).
Results
Fusion analysis showed higher fusion rates with OsteoAMP® than with rhBMP-2 at all time points (Fig. 1). RhBMP-2 did not generate any fusions at 3 months while OsteoAMP® facilitated fusion for 19.1% of patients. At 6 months, only 20.9% of rhBMP-2 patients fused while 64.4% of OsteoAMP® patients fused (Fig. 2). At 12 months, rhBMP-2 facilitated fusion for 68.4% of patients while OsteoAMP® produced fusion in 97.3% of patients. At 18 months, rhBMP-2 delivered 87.5% fusion rate while OsteoAMP® achieved 100% fusion rate. Total time for fusion for the OsteoAMP® group (191.0 days) was approximately half of the rhBMP-2 group (380.8 days). The rhBMP-2 arm had five times the reported radiographically assessed complications as the OsteoAMP® arm (Fig. 3).
Conclusion
Despite its use with an older patient population and a higher number of levels per surgery, OsteoAMP® has shown great promise as a viable alternative to rhBMP-2. Fusion rates with OsteoAMP® were statistically superior to rhBMP-2 at all time points. Time to fusion for OsteoAMP® was approximately half of rhBMP-2. Radiographically assessed complications were dramatically lower with OsteoAMP® than rhBMP-2. Further study will be required to establish OsteoAMP® as the premier bone graft substitute used in spinal fusions.

TLIF/LLIF Fusion Rates
-Fused OsteoAMP (left) and unfused rhBMP-2 (right) fusions at 6 months post surgery
-Radiographically Assessed Complications

PG.03
One year results of CHONDRON, a Gel-Type Chondrocyte Transplantation technique. A Pilot Study

Jeeshan Rahman
Royal National Orthopaedic Hospital, Stanmore Middlesex, UK

CHONDRON is a novel technique of Autologous Stem Cell Transplantation for the treatment of osteochondral defects of the knee. Our pilot study of the early results of CHONDRON shows that 76% of patients experienced an improvement of symptoms.

Background:
The Royal National Orthopaedic Hospital in Stanmore has conducted an extensive trial of ACI Vs MACI for the treatment of osteochondral defects of the knee which indicates that both are equally effective but MACI is simpler. However, both techniques are time-consuming. CHONDRON, a gel-type autologous chondrocyte implantation technique has recently been proposed as an alternative. This is quicker and easier to perform. Unfortunately there is very little data in the literature on the efficacy of CHONDRON. Consequently it was decided to determine early functional outcomes of patients who had undergone the CHONDRON procedure before establishing a full trial of this method.
Purpose:
to assess the short term functional outcome of patients who have undergone the gel-type autologous chondrocyte implantation (CHONDRON™) using validated outcome scoring questionnaires.
Study design:
A retrospective case series using standardised outcome reporting questionnaires (the Modified Cincinnati Score, the Visual Analogue Score and the Bentley Stanmore Functional Rating Score).
Methods:
From the cartilage transplantation registry, 43 patients had undergone CHONDRON™ in the assessment period. These patients were then scored using three outcome measurement tools; the Modified Cincinnati Score, the Visual Analogue Score and the Bentley Stanmore Functional Outcome Score. Six patients were lost to follow-up leaving 37 patients. The case-notes were reviewed to identify the size and number of osteo-chondral defects along with the occurrence of any previous operations on the same.
Results:
The mean age of the patients was 34.1 (range 17-49 years) with a mean follow-up of 15.2 months (Range 13-17). The male to female ratio was 25:13. The average defect size was 3.43 cm^2 (Range 1-10, SD 2.7). Three lesions did not have a size described in the notes. There were seventeen defects in the medial femoral condyle, nine defects in the patella, six in the lateral femoral condyle, two in the trochlea, two in lateral tibial plateau and one defect in the medial tibial plateau.
The mean pre-operative Modified Cincinnati Score was 39.9, which improved to a mean of 59.8 post-operatively. The mean Visual Analogue Score improved from 6.7 to 5.1 post-operatively.
The median Bentley Functional Rating Score was 3 pre-operatively and 2 post-operatively.
All mean post-operative scores demonstrated an improvement from the pre-operative scores. None of the patients had any immediate post-operative complications from the cartilage transplantation procedures. One patient sustained another osteochondral defect following a fall at home and is therefore awaiting a further transplantation procedure. Two patients required trimming of overgrown grafts. Five patients from our cohort had previously failed MACI procedures.
Conclusions:
These early results show that 76% of the patients who were treated with CHONDRON™ experienced a reduction in pain and improvement in post-operative function. In the patients in whom the symptoms were worse, the deterioration in score could be partly explained by numerous previous procedures on the same site, presence of early osteoarthritis or the presence of multiple osteochondral lesions. This highlights the importance of careful patient selection in order to gain maximum benefit from the procedure.

Picture showing defect filled with CHONDRON
-Table showing clinical outcomes following CHONDRON
-Table showing mean pre and post operative functional scores following CHONDRON

PG.05
Sustained oxygen release from PLGA microspheres

Hilde Steg
Department of Orthopedics, University Medical Center Groningen, Groningen, The Netherlands

By the production of oxygen delivering microspheres a sustained oxygen release system has been created that can serve as a side kick in large cell-scaffold constructs and is well tolerated by hMSCs.

Introduction
One of the leading causes of cell death in large cell-scaffold complexes is a lack of oxygen. The aim of this research project was to develop a material with slow oxygen release that can be used as a side kick for bone scaffold materials. By incorporation of calcium peroxide into polylactic-co-glycolic acid (PLGA) microspheres, any contact with water will release oxygen through degradation of the peroxide. This system will keep cells alive so that vascular networks can be developed after which a natural sustained oxygen supply can be achieved.

Materials and Methods
Human mesenchymal stem cells (hMSCs) were isolated with a Ficoll density gradient method from reaming debris that was collected during total hip replacement. Microspheres were produced in an oil-in-oil (o/o) solvent evaporation method out of a 10% PLGA (w/v) and 5% CaO_2 (w/w)solution. hMSCs were grown on PLGA/ CaO_2 films and in the presence of PLGA/ CaO_2 microspheres. Outcome parameters were cell growth and cell survival.

Results
Microspheres were produced that showed a reproducible oxygen release for up to 100 hours. The oxygen release profile showed a short peak at the first water contact after which a sustained oxygen release followed at approximately 0,3mg/L. hMSCs were seeded on PLGA/ CaO_2 films, but adherence to the material did not occur. The presence of microspheres was well tolerated by hMSCs grown in vitro. If high amounts of microspheres were added to tissue culture wells, cell death usually occurred due to the toxic levels of H_2O_2, a negative by-product of the reaction of CaO_2 and water.

Conclusion
A sustained oxygen release system has been created that can serve as a side kick in large cell-scaffold constructs and that is well tolerated by hMSCs.

PG.05

Sustained oxygen release from PLGA microspheres

Hilde Steg
Department of Orthopedics, University Medical Center Groningen, Groningen, The Netherlands

By the production of oxygen delivering microspheres a sustained oxygen release system has been created that can serve as a side kick in large cell-scaffold constructs and is well tolerated by hMSCs.

Introduction

One of the leading causes of cell death in large cell-scaffold complexes is a lack of oxygen. The aim of this research project was to develop a material with slow oxygen release that can be used as a side kick for bone scaffold materials. By incorporation of calcium peroxide into polylactic-co-glycolic acid (PLGA) microspheres, any contact with water will release oxygen through degradation of the peroxide. This system will keep cells alive so that vascular networks can be developed after which a natural sustained oxygen supply can be achieved.

Materials and Methods

Human mesenchymal stem cells (hMSCs) were isolated with a Ficoll density gradient method from reaming debris that was collected during total hip replacement. Microspheres were produced in an oil-in-oil (o/o) solvent evaporation method out of a 10% PLGA (w/v) and 5% CaO_2 (w/w)solution. hMSCs were grown on PLGA/ CaO_2 films and in the presence of PLGA/ CaO_2 microspheres. Outcome parameters were cell growth and cell survival.

Results

Microspheres were produced that showed a reproducible oxygen release for up to 100 hours. The oxygen release profile showed a short peak at the first water contact after which a sustained oxygen release followed at approximately 0,3mg/L. hMSCs were seeded on PLGA/ CaO_2 films, but adherence to the material did not occur. The presence of microspheres was well tolerated by hMSCs grown in vitro. If high amounts of microspheres were added to tissue culture wells, cell death usually occurred due to the toxic levels of H_2O_2, a negative by-product of the reaction of CaO_2 and water.

Conclusion

A sustained oxygen release system has been created that can serve as a side kick in large cell-scaffold constructs and that is well tolerated by hMSCs.

PG.06
A novel acellular and viroinactivated meniscus allograft

Nathalie Tan
TBF Tissue Engineering, Tissue Bank, Mions, France

We developed a ready-to-use meniscus allograft for partial and total meniscal replacement. Safety of the scaffold is conferred by decellularization and viroinactivation of the menisci while preserving structure and mechanical resistance of the tissue.

Introduction:
Meniscal tears are among the most common knee injuries. To preserve as much as possible the joint from osteoarthritis, suturing, or for larger damages, partial and total meniscal replacements are necessary. To combine the biocompatibility and mechanical resistance of meniscus allograft to the disponibility of synthetic substitutes, we developed an acellular, viroinactivated and sterile scaffold with well-preserved structure for partial and total meniscal repair.
Methods:
Human menisci were collected from living donors undergoing total knee arthroplasty and were selected on macroscopic integrity criteria. They underwent chemical treatments, freeze-drying and gamma radiation. Then, efficacy of the process and safety of the product were studied. Decelluarization of menisci was analyzed by hematoxylin-eosin staining. Preservation of the matrix structure was explored by histological studies including hematoxylin-eosin staining and Safranin O staining, and by differential scanning calorimetry. Ultrastructure of the meniscal scaffold was analyzed by scanning electron microscopy. Biomechanical studies were also conducted. Finally, viroinactivation of the scaffold was investigated by viral clearance studies on 4 selected viruses.
Results:
Histological data (figure 1) evidenced complete decellularization of the menisci. The process promoted a high level of porosity within the tissue with an homogeneous pore distribution. Glycosaminoglycans, present in the center of native menisci, were eliminated by the process. Differential scanning calorimetry showed a rather well-conserved collagen structure following the process. The meniscal surface as well as collagen circumferential and radial fibers were preserved as assessed by electron scanning microscopy (figure 2). Radial fibers ensure tissue cohesion while circumferential fibers are involved in mechanical resistance of the tissue. Ultimate tensile strengths of native and processed menisci were similar. Viral clearance studies (figure 3) showed that each viral inactivation step led to a viral load reduction compliant with the reduction factor specified in the European guidelines for viral inactivation processes (reduction factor R > 4 log₁₀).
Discussion/Conclusion: Safety of the scaffold is conferred by decellularization and viroinactivation of the menisci while preserving structure and mechanical resistance of the tissue. Freeze-drying and gamma radiation make it a ready-to-use product, with different sizes for partial and total meniscal replacement. Efficacy of this scaffold for meniscal repair will be tested in a phase II clinical trial.

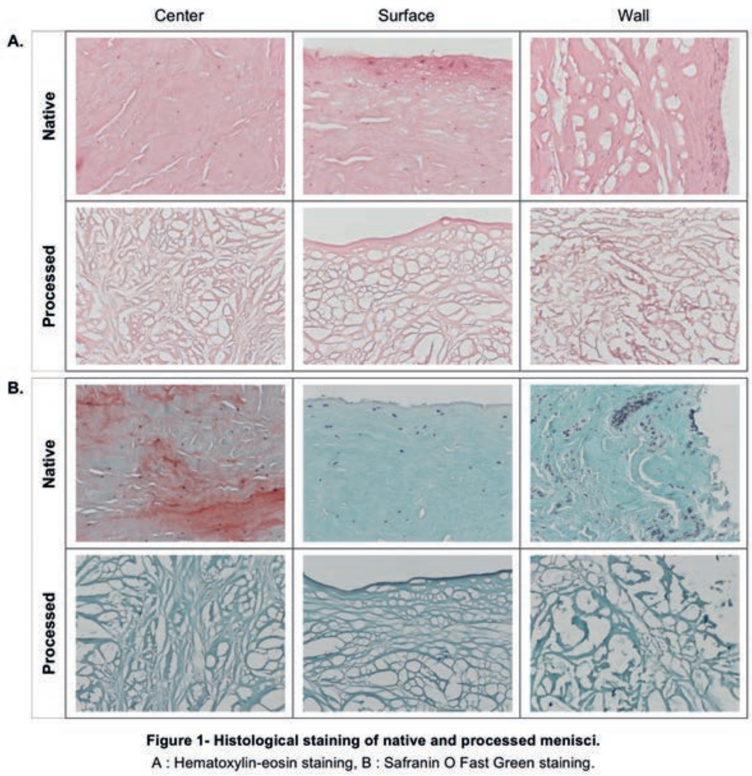

Figure 1- Histological staining of native and processed menisci. A : Hematoxylin-eosin staining, B : Safranin O Fast Green staining.

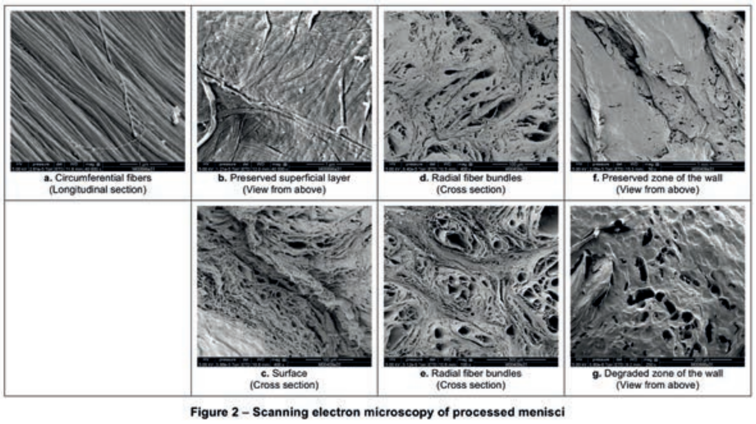
a. Circumferential fibers (Longitudinal section)
b. Preserved superficial layer (View from above)
d. Radial fiber bundles (Cross section)
f. Preserved zone of the wall (View from above)
c. Surface (Cross section)
e. Radial fiber bundles (Cross section)
g. Degraded zone of the wall (View from above)

Figure 2 - Scanning electron microscopy of processed menisci

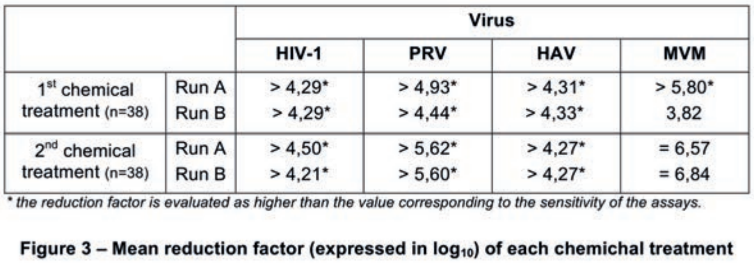

		Virus			
		HIV-1	PRV	HAV	MVM
1st chemical treatment (n=38)	Run A	> 4,29*	> 4,93*	> 4,31*	> 5,80*
	Run B	> 4,29*	> 4,44*	> 4,33*	3,82
2nd chemical treatment (n=38)	Run A	> 4,50*	> 5,62*	> 4,27*	= 6,57
	Run B	> 4,21*	> 5,60*	> 4,27*	= 6,84

* the reduction factor is evaluated as higher than the value corresponding to the sensitivity of the assays.

Figure 3 – Mean reduction factor (expressed in $\log_{10}$) of each chemichal treatment

Figure 3 - Mean reduction factor (expressed in log10) of each chemichal treatment

PG.07

Novel Bilayered Gellan gum/Gellan gum-hydroxyapatite Scaffolds for Application in Osteochondral Tissue Engineering

Joachim Oliveira
3Bs Research Group, Guimarães, Portugal

This work aims to develop and evaluate the biological performance of novel bilayered hydrogel scaffolds for application in tissue engineering of osteochondral defects

Introduction:

Bilayered scaffolds and cellular-based approaches are currently applied to solve the challenging problem of osteochondral defects [1]. This work consisted on developing novel bilayered gellan gum/gellan gum-hydroxyapatite hydrogel scaffolds and it aims to show the potential of such type of scaffolds for being used in tissue engineering (TE) of osteochondral defects. The biological performance of the bilayered scaffolds was investigated by means of culturing human chondrocytes and osteoblasts in the cartilage-like layer and bone-like layer of the scaffolds, respectively.

Patients & Methods:

The bone-like layer of the bilayered scaffolds was produced by adding low acyl gellan gum (LAGG) at 2 wt% and different amounts of hydroxyapatite powders (HAp) (5, 10, 15 and 20 wt%). The cartilage-like layer was obtained by preparing LAGG formulation at 2 wt% and formulations of LAGG at 2 wt% and high acyl gellan gum (HAGG) at 0.75 wt% at a ratio of 75:25 (v%). Solutions were subsequently transferred to a silicone mould and immersed into a PBS solution to induce the gelation. Moulds were then frozen at -80ºC and freeze-dried. The viscoelastic measurements were performed using a TRITEC8000B DMA to characterize the mechanical behaviour of the different bilayered scaffolds. The effect of the incorporation of different amount of HAp within the bone-like layer on the mechanical properties of the scaffolds was also investigated. Degradation and water uptake studies were performed by soaking the scaffolds in a phosphate buffered saline solution (pH 7.4) up to 30 days. Human chondrocytes and osteoblasts were isolated from osteochondral plugs obtained from patients that undergone total knee replacement surgery. Digestion of osteochondral plugs was carried out using standard enzymatic protocols. Then, cells were expanded until passage 5, and seeded onto the bilayered scaffolds and maintained up to 21 days of culturing.

Results:

The bilayered scaffolds were investigated using a stereo microscope to evaluate the interface between both layers. DMA analysis revealed that the storage modulus of all hydrogel formulations increased by means of increasing frequency. Through analysis of DMA data, it was possible to observe the efficient reinforcement of the bilayered scaffolds by adding 20% (w/w) of HA. In vitro studies regarding adhesion, encapsulation and viability of human chondrocytes (cartilage-like layer) and human osteoblasts (bone-like layer) cultured in the bilayered scaffolds were also carried by performing SEM analysis and LIVE/DEAD assays.

Discussion/Conclusions:

From DMA analyses, the formulation of LAGG 2% reinforced with 20% of HA presented a better performance as compared to the other bilayered scaffolds. The Calcein AM assay revealed that cells were metabolically active as observed by emission of green fluorescence. This study has shown positive results for the bilayered scaffolds, as live cells were expressing chondrogenic and osteogenic markers within the bilayered scaffolds, up to 21 days of culturing. The bilayered scaffolds showed promising biological behaviour and show potential for finding application in osteochondral TE strategies.

References

-Oliveira JM, et al., Novel hydroxyapatite/chitosan bilayered scaffold for osteochondral tissue-engineering applications: scaffold design and its performance when seeded with goat bone marrow stromal cells, Biomaterials, 2006, 27:6123-6137.

PG.09
Variation of awl geometry in microfracture does not influence the repair of osteochondral defects in the goat talus

Aimee-Claire Kok
Dept. of Orthopaedic Surgery, Academical Medical Center Amsterdam, Amsterdam, The Netherlands

The results indicate that there is no significant difference in the cartilage quality or fill of osteochondral defects treated with microfracture awls of either a conventional or a small diameter, nor between using awls creating deep and superficial holes.

Introduction:
Bone marrow stimulation treatment for osteochondral defects in the talar bone has shown satisfactory clinical results in smaller defects in 80% of patients. Risk factors for treatment failure and prognostic factors remain controversial. Literature shows high consistency in technique performance. However the effect of hole geometry on treatment outcome is not clear yet. We hypothesized that: 1) deeper holes attract more mesenchymal stem cells creating a favourable environment for hyaline cartilage repair, and 2) holes with a smaller diameter will result in a more even spreading while leaving more subchondral bone intact to act as a bony scaffold.
Methods:
In 16 goats, a Ø 6mm osteochondral defect of 3mm depth was drilled in the ankles of both hind legs. During the same procedure, one defect was treated with six Ø 0.45mm holes of either 2mm or 4mm depth. The contralateral defect in both groups was treated with three holes made by a 0.045 K-wire (Ø1.1mm) capped to a depth of 3mm to mimic with the defect area punctured in the current clinical setting. After 24 weeks the goats were sacrificed and the tali extracted. To assess cartilage quality, contrast-enhanced micro-CT scans were acquired on which an attenuation ratio between repair and healthy cartilage on the other side of the talus was calculated (the closer to 1.0, the better the repair cartilage quality). Subsequently, all tali were embedded in MMA, sectioned, stained with Masson-Goldner and Safranin-O, and scored with a modified O'Driscoll Score (scale between 0-22). We compared the effect of the different treatments using paired testing between experimental and contralateral control defects.
Results:
Micro-CT: The average attenuation ratio of defect and healthy cartilage in the 2mm group was 1.6 (range 1.5-1.8) vs. 1.6 (range 1.4-1.7) for the corresponding control defects. In the 4mm group 1.6 (range 1.3-2.1) vs. 1.5 (range 1.3-1.8). There was no significant difference in the attenuation ratio between the treatment groups ($p>0.04$). Histology: All sections contained fibrous repair tissue with variety in filling aspect. The average O'Driscoll in the 2mm treatment group was 12.5 (range 10.8-15.3) vs. 12.0 (range 9.0-13.0) in the corresponding controls. In the 4mm group 11.5 (range 9.8-16.0) vs. 12.6 (range 11.5-14.3). The median difference in O'Driscoll between treatment and control defect per goat per group was 1.3 (range -1.3 - 4.3) for the 2mm group, and -0.9 (-4.3 - 2.0) for the 4mm group. Though statistically significant ($p=0.04$), this was lower than the 15% difference considered clinically significant.
Conclusion:
All defects were filled with fibrocartilagenous tissue and integrated into the healthy tissue. However, no difference was found between Ø 0.45 mm microfracture holes and Ø 1.1 mm holes, nor between holes of 4 mm depth and 2 mm deep holes. In conclusion, geometry of microfracture holes does not influence cartilage quality or fill of osteochondral defects in the talar bone. This is contradictory to other recent animal studies in the knee. We assume this difference may be (partially) explained by the lack of a bone marrow cavity in the talus.

PH.01

Anterior Cruciate Ligament Injury Prevention Training Programs: What is the current Evidence?

Patrick Sadoghi
Harvard Medical School, Boston, USA

This meta-analysis produced strong evidence in support of a significant effect of ACL injury prevention programs. Our pooled estimates suggest a substantial beneficial effect of ACL prevention, with risk reduction of 52% in the females and 85% in males.

Purpose:
It is the objective of this study to systematically review the literature on ACL injury prevention programs and perform a meta-analysis to address three questions: First, what is the effectiveness of ACL injury prevention programs? Second, is there an evidence for a 'best' program? Third, what is the quality of the current literature on ACL injury prevention?
Methods:
We conducted a systematic review using the online databases PubMed, MEDLINE, EMBASE, CINAHL (Cumulative Index of Nursing and Allied Health), and CCTR (Cochrane Controlled Trial Register) including the search terms anterior cruciate ligament, knee, injury, prevention, control, and ACL prevention. Data on study design and clinical outcomes were extracted independently and in triplicate. After assessment of between-study heterogeneity, DerSimonian Laird random effect models were used to calculate pooled risk ratios (RR) and differences (RD). The RD was used to estimate the Number Needed to Treat (NNT), i.e. the number of patients that have to be treated to avoid one less ACL tear.
Results:
The pooled risk ratio was 0.38 (95%CI 0.20 to 0.71), showing a significant reduction of the risk of ACL ruptures in the prevention group (p=0.003). The NNT was in the range of 5 and 187. Stratified by gender the pooled RR for females was 0.48 (95%CI 0.26 to 0.89) and for males RR 0.15 (95%CI 0.08 to 0.28).
Conclusions: Our study produced strong evidence in support of a significant effect of ACL injury prevention programs. Our pooled estimates suggest a substantial beneficial effect of ACL prevention, with risk reduction of 52% in the females and 85% in males.

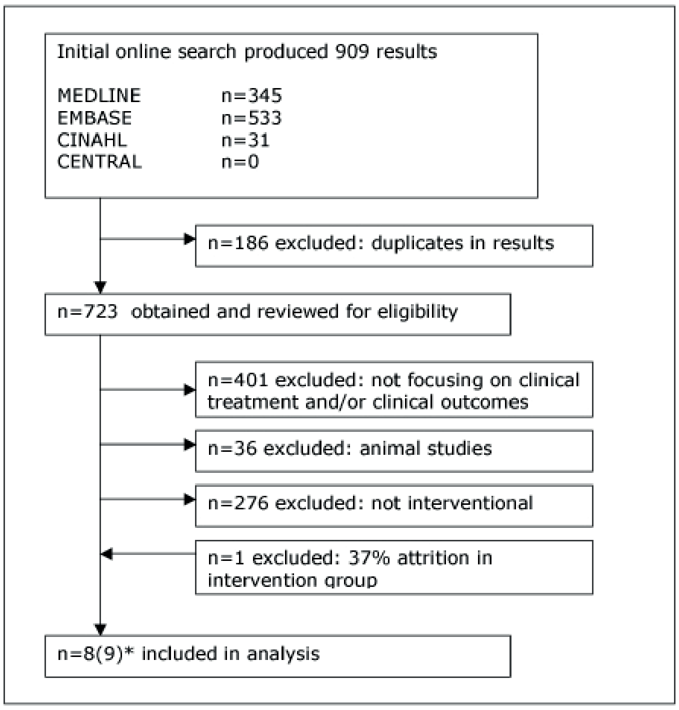

*The ninth study was only included for sensitivity analysis.

Trial flow of study identification

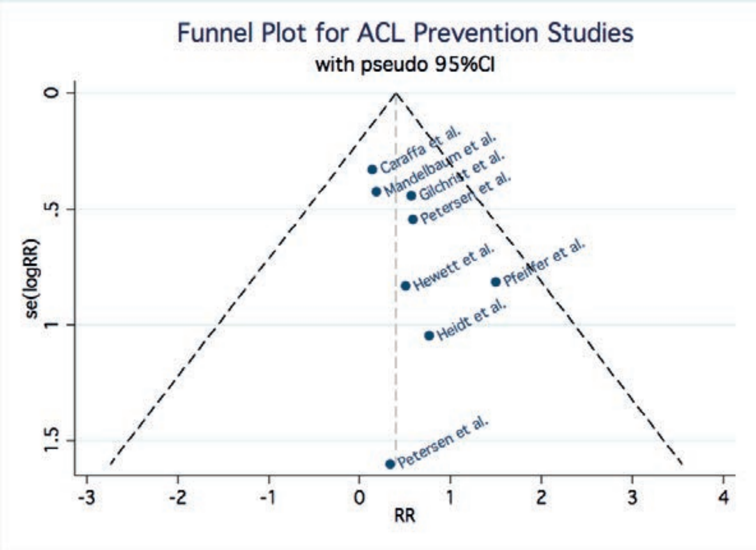

Funnel plot of included studies

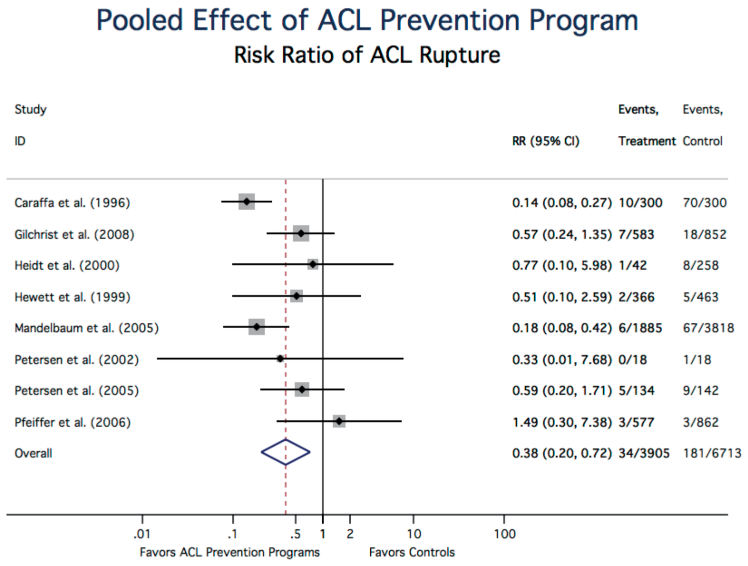

Pooled effect of ACL injury prevention programs

PH.05
Hip fracture surgery delay and cancellation: the impact of UK best practice tariffs.

Tarek Boutefnouchet
Dudley Group of Hospital NHS Trust, West Midlands, UK

According to our district general hospital experience; the implementation of national guidelines and financial incentives helped reduce time delay and rate of cancellation of hip fracture surgery. These changes were achieved despite access to the same level of resources.

Abstract

Introduction

The incidence and prevalence of neck of femur fracture carries a significant burden on patients and the health service. Delay, postponing and cancellation of hip fracture surgery leads to unnecessary starvation and adverse effects on patients and resources. Best Practice Tariffs (BPT) has been introduced to incentivise organisation into optimising the overall care for this type of injuries.

Methods

A retrospective observational analysis was carried out on all consecutive cases of hip fractures over a period of 18 months. This period spanned the introduction of BPT: 10 months before and 8 months after. Data on delay, postponing and cancellation of surgery was recorded. Cancellation is defined as postponed surgery from the original slot planned.

Results

Total number of cases was 584 and the rate of surgery cancellation 21% (n=121). Top three reasons for cancellation were: 48% medically not-fit, 32 % lack of operating time, 6% patient unprepared. The rate of surgery cancellation pre-BPT was 26% (n=85), post-BPT was 14% (n=36). The top three reasons for cancellation pre and post BPT were respectively: medically not-fit 48% vs. 47%, lack of operating time 32% vs. 33%, patient unprepared 6% vs. 8%. The mean time from admission to surgery was in pre-BPT group: 43.03 hours, in post-BPT group: 34.33 hours. In the first group surgery occurred at ≥36 hours after admission in 43.3% compared to 25% in the second group. The most significant change in reasons for delay of surgery post-BPT was lack of space in the operating theatre which dropped from 37% to 20%. In contrast, the rate of theatre list overrun increased from 7% to 16%.

Discussion/Conclusions

The introduction of best practice tariffs reduced the rate of surgery cancellation and improved the time to surgery from admission. The recorded reasons for delay and cancellation remained similar. Despite theatre and staff capacity remaining unchanged, more was achieved with the same level of resources and service improved. Additional attention is required to reduce modifiable causes of hip fracture surgery delays and cancellations.

PH.11

Mortality after fractures among elderly Japanese-American men living in Hawaii

Satona Murakami
Nagoya City University, Japan

There are less data related to fractures and mortality among elderly men comparing to women. To solve this discrepancy, we examined total mortality after hip, spine, and forearm fractures among 3845 elderly men participated in the Honolulu Heart Program.

Background

Most studies in elderly fractures have focused on postmenopausal women because of the higher incidence of fractures related to a significant decrease in bone density after menopause, combined with a longer life expectancy of women. This has resulted in limited data related to fractures and subsequent mortality among elderly men. [Purpose] The purpose of this study is to examine the relationship between hip, spine, and forearm fractures as predictors of total mortality among 3845 elderly Japanese-American men, participating in the Honolulu Heart Program

Methods

The data from the Honolulu Heart Program Exam 4 (1991-1993) was used as the baseline, with the death of subjects being tracked though the year 2000.

Results

The average age of participants was 77.9 years at baseline. A history of previous hip fracture was a predictor of total mortality, hazard ratio (1.83) was higher than being a current smoker (1.66). Anthropometric measurements including taller height, lower weight, lower BMI, higher waist-hip-ratio and lower grip strength of participants in their 70s, were associated with a higher risk of mortality after a hip fracture.

Discussion

The study suggests that interventions to retain physical strength in the elderly could be helpful in preventing fractures and related deaths.

PH.12

Open Lower Limb Fractures. Experiences from a District General Hospital.

William Carlino
Royal United Hospital, Bath, UK

All significant open lower limb fractures pose major management challenges. Contrary to traditional teaching new evidence suggests best outcomes are achieved by timely specialist surgery rather than emergency surgery by inexperienced teams.

Introduction:
The British Orthopaedic Association and the British Association of Plastic, Reconstructive and Aesthetic Surgeons reviewed their 1997 guidance on the management of open lower limb fractures and published a review of all aspects of the acute management of these injuries using an evidence-based approach. This resulted in the 'Standards for the Management of Open Lower Limb Fractures. Contrary to traditional teaching, improved outcomes for these types of injuries have been demonstrated by timely, specialist surgery rather than emergency surgery performed by less experienced teams.The aim of this audit was to review open lower limb fracture management at the Royal United Hospital and identify adherence to the British Orthopaedic Association Standards for Trauma 4 (BOAST 4).
Method:
We retrospectively collected data on all open lower limb fractures between September 2009 and January 2011. The clinical care given was rigorously assessed against the BOAST 4 criteria for open lower limb fracture management.
Results:
We identified thirteen consecutive open lower limb fractures. Antibiotics were appropriately administered on admission in 15% of patients. 62% had a photograph documented. 92% had a saline soaked dressing applied, neurovascular status documented while 85% had the fracture splinted before x-ray.
60% of patients were discussed with plastics and underwent early transfer. 80% of patients had wound debridement within 24 hours. 67% had definitive treatment within seventy two hours.
Conclusion:
The management of open lower limb fractures was suboptimal.As with all audits the areas highlighted in which teams are underperforming may reflect poor management, poor documentation or both. Clearly there it is also a priority to ensure all new Emergency Department and Orthopaedic trainees are aware of BOAST 4 standards. The antibiotics failures reflects delayed updates in local policy, the microbiology department are aware. An open fracture pro-forma and poster campaign has been initiated. A re-audit is planned.

PH.13
Myofibroblasts in posttraumatic elbow contractures

Job Doornberg

Myofibroblasts are present in elbow capsules in the early stages after trauma, but not in longstanding elbow contractures, suggesting a potential role in the early phase of posttraumatic contracture formation.

Introduction:
Elbow stiffness after elbow trauma is a common complication. When surgical release is performed the elbow capsule is often macroscopically thickened, scarred and possibly contracted. However, there is limited information on the histological aspects of these capsules. Most of these reports suggest that the capsule is contracted because of fibroblast to myofibroblast differentiation. This would be comparable with the conversion of fibroblasts in myofibroblasts is well described in various other types of fibrosis (e.g. liver, kidney, burns, Dupuytren's disease. However, the timeline is controversial and data are scarce.
We hypothesize that the number of myofibroblasts -as determined by the myofibroblast marker α-smooth muscle actin (α-SMA) is elevated in patients with posttraumatic elbow contractures compared to elbow capsules that are either normal or freshly injured. The aim of this study was to describe the temporal fibroblast to myofibroblast differentiation during the development of arthrofibrosis around the elbow after trauma to increase our understanding of posttraumatic elbow stiffness.
Patients & Methods:
We obtained thirty-seven capsules from thirty-seven patients who had operative release of posttraumatic contractures greater than five months after injury, thirteen human elbow joint capsules within fourteen days after an elbow fracture and/or dislocation and six elbow capsules from three organ donors free of contractures. Myofibroblasts in the joint capsules were quantified using immunohistochemistry. Alpha-smooth muscle actin (α-SMA) was used as a marker for myofibroblasts. Samples were characterized and scored by an independent pathologist blinded for clinical data.
Results:
The capsules obtained from uninjured elbows did not show any evidence of fibrosis with an intact and structured collagen network and stainings for α-SMA were negative. Elbow capsules from patients with acute trauma (harvested within hours to 14 days after the injury) could be divided into early- and late-phase posttrauma based on their histological appearance. Eight capsules were associated with the acute phase after trauma (hours to 9 days), and stainings for α-SMA were negative in all these eight specimens (see Fig. 1). Five specimens were histologically associated with the late phase post trauma with myofibroblasts stainings positive for α-SMA (see Fig. 2). All, but four of thirty-seven contractures showed a histological pattern consistent with fibrosis, characterized by increased fibroblast-like cell proliferation and higher cellular density of fibroblast-like cells with highly unstructured collagen. There was no staining of α-SMA in fibroblast-like cells in these longstanding contractures suggesting absence of myofibroblasts (see Fig. 3).
Discussion/Conclusion:
In conclusion, we present 'negative results' on the hypothesis that myofibroblasts and expression of the myofibroblast marker α-smooth muscle actin are elevated in the chronic stages of human posttraumatic elbow capsules. This is in contrast to most other reports in the literature. We did, however, find some presence of myofibroblasts in elbow capsule in the early stages (> 9 days) suggesting a potential role in the early phase of posttraumatic contracture formation.
The clinical relevance of this study might be that tension (early motion) in the first weeks after trauma should be prevented to avoid stimulation of myofibroblasts which are present in early phases of capsular repair, and that physical therapy and splinting exercises in chronic phase of elbow contracture formation perhaps could be applied without hesitation.

PH.16

PROCALCITONIN: IMPROVEMENT OF DIAGNOSTIC AND THERAPEUTIC STRATEGIES IN CANCER PATIENTS WITH FEBRIL NEUTROPENIA

Maria Angeles Cuadrado-Cenzual
Hospital Universitario, Salamanca, Spain

Febril Neutropenia with infection is a medical emergency that requires rapid diagnosis and intervention as soon as possible. This study was designed to determine whether PCT is useful as early diagnostic markers for bacteremia in cancer patients with febrile neutropenia

Introduction

‘Febrile Neutropenía (FN) in cancer patients is a complication related to antineoplasic therapy . Thus, 30% of the patients with cancer suffer some febrile episode throughout their disease with serious impact on their morbidity and survival. The main cause is the infectious process, but also other causes exist and the differential diagnosis is necessary for the correct therapeutic decision making. Thus early diagnosis of infection in this type of patient is of vital importance The aim of this study was to evaluate Procalcitonin (PCT) like early diagnostic marker in patient with febrile neutropenia associated with chemotherapy

Patients and methods

‘A prospective double blind study was developed in adults hospitalized cancer patients with FN chemotherapy associated. We included 78 patients with FN and with treatment to them of the fever according to clinical practice protocol. Of all of them, 61 patients completed all the study with serial studies of PCT serum levels during four days consecutive from the hospital admission, in addition to the follow-up of the clinical, microbiological and radiological variables

Results

‘Bateriemia was detected in 36 patients and PCT showed higher significantly levels (P< 0. 001) in this patients in comparision with non bacteriemia patients.

Relation between Procalcitonine values and treatment non -response was significant (p 0,999). The point of cut-off Procalcitonine level , with better Sensitivity, (74 %), and Specificity, (80%), was 0,21µg/L . The ROC curves of PCT are shown in Fig. 1.

The Multivariant Analysis showed that The value of PCT over 0,5 µg/L in patients with FN and Bacteriemia it was an independent variable like marking diagnosis of bacteriemia in patients with Febrile Neutropenia (Odss Ratio 3,5 with an interval of 95% confidence; (1.6-7.8) and p< 0.001.

Conclusion

‘Procalcitonine values in cancer patients with Febrile Neutropenia and infections; was higher and descend after restoring antibiotic treatment agreeing with clinical improvement. These data suggest it determination of PCT in cancer patients with febrile neutropenia; could be an useful early diagnostic marker for detection of bacteriemia

References

‘1. Schuttrumpf, S., et al., Utility of procalcitonin concentration in the evaluation of patients with malignant diseases and elevated C-reactive protein plasma concentrations. Clin Infect Dis, 2006.43(4): p. 468-73.
2. Giamarellou, H., et al., Potential use of procalcitonin as a diagnostic criterion in febrile neutropenia: experience from a multicentre study. Clin Microbiol Infect, 2004.10(7): p. 628-33.
3. Von Lilienfeld-Toal, M., et al., Markers of bacteremia in febrile neutropenic patients with hematological malignancies: procalcitonin and IL-6 are more reliable than C-reactive protein. Eur J Clin Microbiol Infect Dis, 2004.23(7): p. 539-44.
4. Schuttrumpf, S., et al., Procalcitonin: a useful discriminator between febrile conditions of different origin in hemato-oncological patients? Ann Hematol, 2003.82(2): p. 98-103.

PH.17

Analysis on Toll-like receptor mediating signal pathway in periprosthetic infection

Yasunobu Tamaki
Yamagata University School of Medicine, Yamagata, Japan

Periprosthetic infection is one of serious complications of joint replacements surgery. Better understanding of Toll-like receptor mediated pathomechanism is important to avoid following harmful host reactions by the bone and surrounding tissues to the implant.

Introduction

One of the serious complications in total hip arthroplasty are septic loosening caused by implant infection. The study was designed to analyze expression of Toll-like receptors (TLRs) signal pathway in septic status of loosened total hip arthroplasty (THA).

Methods

Septic (n=5) tissues from loose total hip joints, and osteoarthritic synovium (OA, n=7) was obtained. RT-PCR for mRNA expression and immunohistochemical staining (conventional and Double-immunofluorescent) were performed to analyze TLR2, 4, 5, 9 and TLR adaptor molecules (MyD88, TRIF, TRAF6). The level was compared to that of OA.

Results

Expression of TLRs and their adaptor molecules was detectable in all the samples. Their mRNA expressions of each tissue were increased than that of OA. In septic loosening, CD15+ cells were observed in focal granulocyte infiltrates, which were co-localized with each TLRs and its adaptor molecules (see Fig. 1). In osteoarthritic synovial membrane, a few scattered CD68 positive cells were observed in the synovial lining and sub-lining layers and perivascularly. Expression of TLRs in the osteoarthritic synovium was only found in vascular cells and the reactivity was weak.

Discussion

TLR is one of the key functions of innate immune system. TLRs are one of pattern recognition receptors, recognize 'danger signals' as both exogenous (PAMPs) and endogenous ligand (DAMPs). Septic tissues around loosened THAs equipped TLRs and their adaptor molecules. CD15+ granulocytes in septic tissues around THRs. mRNA and immunohistochemical analyses suggested hyper-responsiveness to exogenous PAMPs of microbial origin and/or endogenous alarmins stimuli via TLRs and their adaptor molecules in septic tissues. TLR signal pathway was highly activated than that of OA tissues. Signal pathway via TLRs and their adaptor molecules may contribute to the pathogenesis of periprosthetic septic condition.

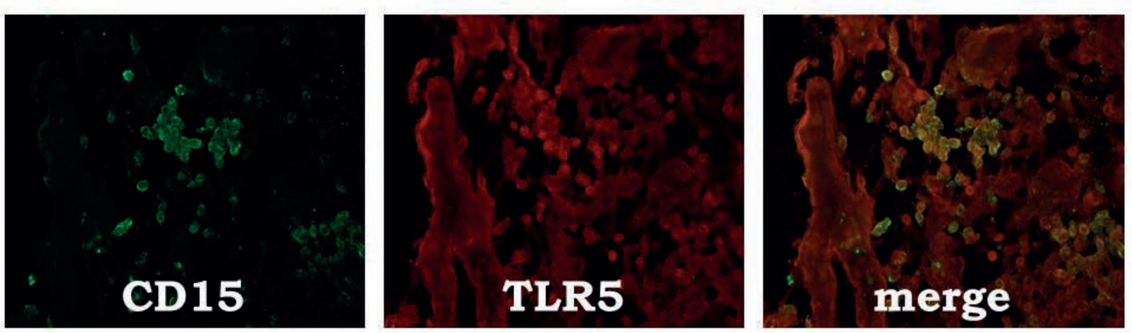

Double-immunofluorescent stainnig. Co-localization of TLR5 and CD15 in synovium around septic losening/osteolysis. A: CD15 was green, B: TLR5 was red, C; merged photo is yellow.

PH.18

Novel human biomarkers for the identification of infection in orthopedic revision-surgery patients

Mathias Glehr
Department of Orthopaedic Surgery, Medical University of Graz, Graz, Austria

Besides conventional biomarkers like CRP and leukocyte count - PCT, IL-6 and fibrinogen showed significance for detecting joint infection in revision-prosthesis.

Periprosthetic joint infection (PJI) is one of the most challenging complications after total hip and knee arthroplasty. One of the most important steps in the diagnostic process of detecting PJI remains the analysis of laboratory infection biomarkers. The aim of this study was to investigate the sensitivity and specificity of the biomarkers procalcitonin (PCT), interleukin-6 (IL-6), fibrinogen and interferon- alpha (IFN-alpha) in comparison to conventional biomarkers (CRP, leukocyte count) in the field of orthopaedic revision surgery.
Methods:
Eighty-four patients (124 operations) were prospectively included. The blood pa-rameters of interest were PCT, IL-6, fibrinogen, IFN-alpha leukocyte count and CRP. Samples were taken preoperatively and on the first, the third and the seventh post-operative days. The sensitivity and specificity of these biomarkers were calculated.
Results:
Considering all 124 operations, PCT ($p=0.038$), IL-6 ($p=0.012$), fibrinogen (p
Discussion:
This study showed that - besides conventional biomarkers like CRP and leukocyte count - PCT, IL-6 and fibrinogen showed significance for detecting joint infection. Fibrinogen is usually analysed for preoperative coagulation control anyway and gives a further hint if there is an ongoing bacterial infection. An additional analysis of the biomarkers PCT and IL-6 is worthwhile in special cases, when it is totally unclear whether there is a bacterial implant infection or an aseptic inflammation and when it is important to analyse the impact of an antibiotic therapy.

PH.19

DIAGNOSTIC VALUE PROCALCITONIN, INTERLEUKIN 6 IN COMPLICATIONS OF HIP ARTHROPLASTY

Maria Angeles Cuadrado-Cenzual
Hospital Clïnico San Carlos, Madrid, Spain

This study evaluates new laboratory markers; as serum Procalcitonin (PCT), Interleukin-6 (Il.6) and soluble intercellular adhesion molecule-1 (siCAM-1) and the diagnostic value in aseptic loosening. The determination of PCT and interleukin-6 provide excellent tests for differentiation aseptic loosening and infection

Introduction:

'Two of most relevant complications of total hip joint arthroplasty is peri-prosthetic infection and aseptic loosening. On the other hand, the diagnosis of prosthetic joint infection and its differentiation from aseptic loosening remains problematic. One of the most important steps in the diagnostic process of detecting periprosthetic joint infection remains the analysis of laboratory infection parameters.. Actually there are new laboratory markers; as serum Procalcitonin (PCT), Interleukin-6 (Il.6) and soluble intercellular adhesion molecule-1 (siCAM-1) that has been shown to be a sensitive indicator of bacterial infection, but very little is known of its behavior in periprosthetic infection. This prospective study evaluates the role of serum levels PCT, IL-6 and sICAM-1 in patients with septic and aseptic loosening as differential diagnosis markers

patients and methods

'Fifty- three patients undergoing revision hip surgery due to prosthetic joint loosening were recruited with a presumptive clinical diagnosis of either septic (11 patients) or aseptic loosening (42 patients). The diagnosis was confirmed microbiologically and levels of serum markers were determined- The white blood cell count, the erythrocyte sedimentation rate and levels of C-reactive protein, interleukin-6, procalcitonin siCAM-1 were analyzed in blood samples before operation and on days 1,3,5 and 21, The diagnostic cut-off values were determined by Received Operating Characteristic curve analysis

The sensitivity, specificity, positive predictive value (PPV), negative predictive value (NPV) and accuracy of serum markers demonstrating the potential to facilitate diagnosis of septic loosening were determined.

Results

'Forty one patients (85%) had normal PCT values (< 0.5 ng/ml) and only 5 recorded a value >1.5ng/ml. On day 5 only 1 patient had a value > 0.5ng/ml..

Serum levels of IL-6 and sICAM-1 were significantly raised in patients with septic loosening ($P = 0.001$ and $P = 0.005$, respectively). In contrast, PCT was not found to be of value in differentiating septic and aseptic loose ning. Furthermore, CRP, ESR and WBC were significantly higher ($P = 0.0001$, $P = 0.0001$ and $P = 0.003$, respectively) in patients with septic loosening

C-reactive protein (> 3.6 md/dl) and interleukin-6 (> 16 pg/ml) have the highest sensitivity (0.96). Interleukin-6 is less specific than C-reactive protein (0.87 vs 0.96). Combining C-reactive protein and interleukin-6 identifies all patients with deep infection of the implant. Procalcitonin (> 0.5 ng/ml) are very specific (0.98) but have a low sensitivity (0.41).

Discussion.

'The combination of C-reactive protein and interleukin-6 measurement provide excellent screening tests for infection of a deep implant. A highly specific marker such as procalcitonin and pre-operative aspiration of the joint might be useful in identifying patients with true positive C-reactive protein and/or interleukin-6 levels. Serum levels of IL-6, sICAM-1 may provide additional information to facilitate the diagnosis of prosthetic joint infection.

References:

1.Syed Ali, Andrew Christie, Andrew Chapel. The Pattern of Procalcitonin in Primary Total Hip and Knee Arthroplasty and its Implication in Periprosthetic Infection J Clin Med Res 2009;1(2):90-94

2, Janja Zupan, Radko Komadina and Janja Marc1The relationship between osteoclastogenic and anti-osteoclastogenic pro-inflammatory cytokines differs in human osteoporotic and osteoarthritic bone tissues Journal of Biomedical Science 2012, 19:28

PH.20

Comparable study of antibiotic release on commercially PMMA bone cements

Johannes Stadler
Medical Universitiy of Graz, Graz, Austria

A study on the release rates of bone cements and their antimicrobial activity.

Introduction

Implant associated infections are a serious complication in orthopaedic surgery. In addition to a systemic antibiotic prophylaxis/therapy it is important to release an effective dose of antibiotics at the location of the infection. Poly-methyl-methacrylate (PMMA) bone cements are known as a very good delivery system. There are many commercially available PMMA bone cements with different content of antibiotics and with different elution profiles. Many studies compare bone cements under various conditions, which make the reproducibility of the results mostly difficult. In our study we tested 10 commercially available PMMA bone cements to evaluate the antibiotic release rates under standardized conditions over a long period of time.

Methods

One unit of each bone cement brand was mixed in the laboratory according to the manufacturer instructions and applied into standardized casting moulds. The moulds were covered with PET folia and weight on top. This process resulted in 24 flat discs with 15 mm diameter and a thickness of 3.0 ±0.2 mm. PMMA discs with less deviation from each other were taken for a modified Kirby-Bauer assay (Agar Diffusion). Test bacteria (0.5 McFarland (Staphylococcus aureus, Staphylococcus epidermidis, Methicillin-resistant Staphylococcus aureus (MRSA), Methicillin-sensitive Staphylococcus aureus (MSSA)) were plated on Müller-Hinton Agar plates and discs were applied into the centre of the plates. After 24 hours at 37°C the inhibition areas were measured and the same discs were transferred on new plates daily. This step was repeated at least 6 times. All experiments were done in triplicates. Areas of inhibitions were calculated and compared to each other. Eluates of the bone cement discs were also used for the same assay (50µl of the eluates were filled in a whole in the center of the Agar plates).

Results

Antibiotic loaded PMMA bone cements showed specific differences in their elution profile. A massive reduction from day one to day two as described in literature could not be detected in our studies. Independent of the content of antibiotics in the bone cements and their elution profiles, the areas of inhibition had almost the same size.

Discussion

We measured comparable sizes of inhibition areas at the Kirby-Bauer assay over 7 days and also in a shorter exposure model over 24 hours. Experiments with eluates of the bone cement discs showed more differences. The relatively similar results in the inhibition area testing (direct application of the PMMA discs) are thus very surprising as the bone cements contain different amounts of antibiotics.

PH.21

Diagnosing neck of femur fractures on plain radiographs- who is more accurate radiologists or orthopaedic trainees?

Robert Jordan
Birmingham Heartlands Hospital, Birmingham, UK

The results from interpretation of pelvic radiographs in hip fractures by orthopaedic trainees and radiologists are comparable. We recommend that if either specialist feels initial films are equivocal that further imaging is required to ensure early diagnosis.

Introduction

The management of patients with a neck of femur fracture has a huge financial impact on the National Health Service. The diagnosis is made by obtaining a history, examining the patient and performing a plain radiograph. The ability to accurately and reliably identify these fractures on radiographs allows a prompt diagnosis, early operative intervention and avoids wasting radiological resources. However approximately 3% of patients require further imaging and are termed ‘occult’ fractures. At our centre either the emergency department or admitting orthopaedic team can request a CT scan if the radiograph is deemed equivocal and this practice has seen a sharp rise in the number of scans performed in the last five years. Our study aims to compare the sensitivity and specificity between orthopaedic trainees and radiologists in diagnosing occult hip fractures from pelvic radiographs.

Methods

All patients undergoing CT scan of the hip or pelvis for a suspected occult hip fracture between 1 November 2010 and 31October 2011 at our two centres were retrospectively identified. Two orthopaedic trainees (RJ and ED) independently reviewed the initial pelvic radiographs and if both agreed a fracture was present this was recorded. The reports from the radiologist of the initial radiograph and subsequent CT scan were recorded with the CT report used as the gold standard for comparison of performance.

Results

239 CT scans were performed for suspected neck of femur fractures during the study period with 27.2% reported as a fracture. The interpretation of radiographs by the orthopaedic trainees showed a sensitivity of 55.4% and specificity 96.6%. In comparison the radiologists had a sensitivity of 60.7% and specificity of 92.9%, this difference was shown not to be statistically significant. In 21 of the 174 cases (12.1%) where the radiologist and orthopaedic trainees agreed no fracture was present the subsequent CT revealed a fracture.

Conclusion

Orthopaedic trainees and radiologists have similar accuracy at interpreting pelvic radiographs in suspected hip fractures, so the trainee’s opinion can be relied upon. If uncertainty exists then the orthopaedic trainees or radiologists should request an urgent CT as we believe this will expedite diagnosis and treatment of hip fractures, and ensure judicious use of CT scans.

PH.23

Pantoprazole, a proton pump inhibitor, delays fracture healing in mice

Tina Histing
Department of Trauma-, Hand and Reconstructive Surgery, University of Saarland, Homburg/Saar, Germany

Pantoprazole treatment delays fracture repair most probably by affecting both bone formation and bone remodeling through down-regulation of bone formation markers and inhibition of osteoclast activity.

Background and purpose:
Proton pump inhibitors (PPIs), which are widely used in the treatment of dyspeptic problems, have been shown to reduce osteoclast activity. There is no information, however, on whether PPIs affect fracture healing. We therefore studied the effect of the PPI pantoprazole on callus formation and biomechanics during fracture repair.
Experimental approach:
Bone healing was analyzed in a murine fracture model using radiological, biomechanical, histomorphometric and protein biochemical analyses at 2 and 5 weeks after fracture. Twenty-one mice received 100mg/kg body weight pantoprazole i.p. daily. Controls (n=21) received equivalent amounts of vehicle.
Key results:
In pantoprazole-treated animals biomechanical analysis revealed a significantly reduced bending stiffness at 5 weeks after fracture compared to controls. This was associated with a significantly lower amount of bony tissue within the callus, and higher amounts of cartilaginous and fibrous tissue. Western blot analysis showed a reduced expression of the bone formation markers bone morphogenetic protein (BMP)-2, BMP-4 and cysteine-rich protein (CYR61). In addition, a significantly lower expression of proliferating cell nuclear antigen (PCNA) indicated a reduced cell proliferation after pantoprazole treatment. Of interest, the reduced expression of bone formation markers was associated with a significantly diminished expression of receptor activator of nuclear factor-κ B ligand (RANKL), indicating osteoclast inhibition.
Conclusions:
The proton pump inhibitor pantoprazole delays fracture healing by affecting both bone formation and bone remodeling.

PH.24
A new metaphyseal fracture defect model in osteoporotic rats

Seemun Ray
University of Giessen, Giessen, Germany

The new metaphyseal osteoprotic fracture model reproduces the clinical conditions of critical fracture defect in osteoporotic patients and thereby allows the targeted development of locally usable biomaterials for enhancement of fracture healing.

Introduction:
Osteoporotic fractures are a huge clinical challenge. Currently, no adequate animal model that mimics the typical clinical situation with a metaphyseal fracture defect is available. Therefore, this study aims at establishing a clinically relevant new critical size fracture in an osteoporotic rat model. The metaphyseal defect fracture used in this study represents clinically relevant situations with osteoporotic bone status and are internally fixated.
Method and Results:
Sixteen female Sprague Dawley rats were ovarectomized at fourteen week of age then treated with a calcium and vitamin-D free diet (OVX+diet). Sixteen female rats were sham operated to serve as control. Bone mineral density (BMD) was evaluated after three months of treatment using Dual X-ray absorptiometry (DEXA) scans. The OVX+diet group yielded a 20% reduction of BMD compared with the controls and a T-score of less than -2.5, thus confirming an osteoporotic status. Rats then underwent either a 3 mm (controls, n=8; OVX+diet, n=8) or a 5 mm (controls, n= 8; OVX+diet, n=8) wedge-shaped osteotomy (fracture defect) of the distal metaphyseal area of the left femur. The defect was internally stabilized with a T-shaped mini-plate. The femora were harvested six weeks post fracture defect followed by biomechanical, computer tomography and histological assessments. Biomechanical testing, using the three-point bending system revealed higher biomechanical competence in the 3 mm defect compared to the 5mm defect size in both OVX+diet and controls ($p \leq 0.05$ for all). In accordance with these findings, the micro and nano-CT evaluation as well as histological observation showed bony bridging in the 3mm fracture defect when compared to the 5 mm defect, which showed typical signs of critical size defect with clinically unstable conditions without bony consolidation.
Currently, the model is being utilized to test a variety of biomaterials with different geometries. Beside bone cement, porous and non-porous constructs are also being tested.
Discussion:
We have established a clinical relevant animal model mimicking the clinically relevant conditions of critical fracture defect in osteoporotic patients and thereby allows the scope for testing of new biomaterials for enhancement of fracture healing. Evaluation of a potential biomaterial requires a critical size model, in which no bony bridging occurs in the absence of suitable biomaterials (5mm in our case) when compared to the controls (3mm in our case). The metaphyseal fracture model presented here would not only help us to improvise surgical techniques in human conditions but also be suitable to evaluate biomaterials that would not only improve osseointegration but also stimulate bone formation in osteoporotic patients.
In conclusion, the 3mm defect model can be used for assessment of fracture healing in metaphyseal osteoporotic fractures. The 5 mm defect model with absence of fracture healing can be considered as critical size defect model in which biomaterials can be tested.

PI.02

Receptor activator of nuclear factor kappaB (RANK) expression is a prognostic factor in human osteosarcoma

Klemens Trieb
Department of Orthopedics, Wels, Austria

The expression of RANK immunohistochemically in 43 human osteosarcomas suggests that RANK is likely to provide an additional prognostic information for clinical purposes in osteosarcoma patients at the time of diagnosis.

Introduction:
The receptor activator of nuclear factor kappab (RANK), a member of the tumor necrosis factor family, is activated by its ligand and regulates the differentiation of osteoclasts and dendritic cells. Local growth of osteosarcoma involves destruction of the host bone by osteoclasts and proteolytic mechanisms. Although prognosis of osteosarcoma has been improved by chemotherapy during the last decades, the problem of non responders and the lack of prognostic markers remains. It is the aim of this study to investigate the prognostic and predictive value of RANK expression in human osteosarcoma.
Materials and Methods:
The expression of RANK was examined immunohistochemically in biopsies of 43 patients (mean age 25.7 years) with high grade osteosarcoma and the results were correlated with histologic response to chemotherapy, disease free and overall survival. Tumors with more than 40% positive osteosarcoma cells were scored positive.
Results:
In 8 of 43 (18%) osteosarcoma specimens RANK expression could be dedected, the rest were negative. RANK expression showed a statistically significant correlation with overall survival of patients. 7/8 patients with RANK expressing tumours died, whereas only one in the negative group (88% in RANK positive tumours versus 37%; $p<0.05$). No significant difference was found when comparing RANK expression status with response to chemotherapy; 50% had a poor and 50% had a good response in RANK positive and 30,3% had a good and 69,7% had a bad response in RANK negative osteosarcomas. The appearance of metastases did not correlate with RANK expression status (37,5% metastases in RANK positive tumours versus 28,6% in negative).
Discussion:
In conclusion our findings suggest that RANK is likely to provide an additional prognostic information for clinical purposes in osteosarcoma patients at the time of diagnosis.

PI.03
Prognostic factors for determining survival in patients operated for metastatic epidural spinal cord compression.

Laurens Bollen
LUMC, Leiden, The Netherlands

Introduction:
Accurate prediction of survival in patients with metastatic epidural spinal cord compression (MESCC) is of the utmost importance, in order to ensure a proper relation between extent of surgery and actual survival time.

Objectives:
In this study several prognostic factors for survival after surgical intervention are evaluated.

Methods:
All patients who were surgically treated for MESCC between January 2001 and December 2010 were included in this bi-center retrospective study (n=101). Medical records were reviewed for gender (male n=50, female n=51), age (mean 59.83 ± 10.23 years) site of primary cancer (classified according to Tomita[1]), presence of visceral and bone metastases, the number and location of spinal metastases and Frankel score. The most prevalent primary tumors were those of breast (n=23), lung (n=20), kidney (n=18) and the gastrointestinal tract (n=12). Survival time was calculated as the time difference between date of surgery and date of death and subsequently analyzed with univariate log-rank tests and multivariate Cox regression.

Results:
The overall mean survival was 16.1 ± 15.8 months with a median of 10.7 months. Minimal follow-up was 8 months and there was no loss to follow-up. Univariate log-rank tests showed primary tumor type ($p<0.001$) and the presence of visceral metastases ($p=0.012$) to be independent predictors of survival. Multivariate Cox regression analysis showed hazard ratios (HR) of 1.7 (95% confidence interval 1.2 - 2.2, $p=0.001$) for the Tomita classification and 1.746 (95% confidence interval 1.0 - 3,1, $p=0.051$) for the presence of visceral metastases.

Discussion:
When considering surgery for MESCC-related symptoms such as pain and neurologic deficit, careful weighing of patient-specific factors ensures that no needlessly extended surgery takes place in those cases that do not live long enough to fully benefit from the intervention. It would seem that the primary tumor type is the most important factor in doing so, since this also affects the visceral metastatic potential, which we demonstrated also to be a detrimental influence on survival.

Conclusion:
Primary tumor type according to the Tomita classification and the presence of visceral metastases are prognostic factors for determining survival in patients with MESCC and should be evaluated prior to considering surgery.

PI.04

Asymmetric ankle osteoarthritis - long-term effects of realignment surgery on walking

Corina Nüesch
Orthopaedic Department, University Hospital, University of Basel, Switzerland

Realignment surgery in asymmetric ankle osteoarthritis leads to less pain and improves the quality of life. However, the gait analysis, showed that restrictions in the mobility of the different foot joints remain while hip and knee joint biomechanics improve.

Introduction

In asymmetric ankle osteoarthritis (OA) the intra-articular pressure is distributed differently. If at least half of the cartilage is preserved, patients can benefit from joint preserving realignment surgery. It was seen that a minimum of three years after surgery, pain was reduced and AOFAS ankle scores were improved [1]. Contrary to ankle arthroplasty or ankle arthrodesis, knowledge of the effects of realignment surgeries on the gait biomechanics is limited. The aim of the present study was therefore to characterize the walking patterns of patients after realignment surgery and compare them to patients with asymmetric ankle OA.

Patients and Methods

10 patients suffering from asymmetric ankle OA (age: 55.4±11.0 years; BMI: 27.9±3.4; pain (VAS 0-10): 4.9±2.1; AOFAS: 62.8±15.4; SF-36: 54.6±19.1; passive plantar-/dorsiflexion range of motion (ROM): 56.0±14.7°) were measured prior to their planned realignment surgery. The postoperative patient group consisted of 8 patients (age: 44.7±7.0 years; BMI: 27.2±4.6; pain: 2.1±1.4; AOFAS: 83.5±10.8; SF-36: 80.7±18.6; passive plantar-/dorsiflexion ROM: 44.4±21.6°) following a minimum of 3 years after realignment surgery (range: 3 to 9 years).

An instrumented gait analysis with a 6 camera Vicon system (Vicon MX3+, Oxford, UK; sampling rate 120 Hz) and two force plates (Kistler, Winterthur, Switzerland; sampling rate 2400 Hz) was performed. The reflective markers were placed according to the Oxford foot model [2]. For each patient, six walking trials at a self selected walking speed were recorded and analyzed.

Results

Postoperative patients had significantly less pain (p=0.003), higher AOFAS ankle scores (p=0.001), and a higher score on the SF-36 questionnaire (p=0.004). The walking speed of the two patient groups showed no significant differences. However, the postoperative patients seemed to walk on average a little faster (1.10±0.17 m/s vs. 1.18±0.08 m/s; p=0.315). Postoperatively, the range of motion (ROM) in hip flexion tended to be higher (41.2±6.5° vs. 45.9±4.8°; p=0.068), and the knee flexion ROM was significantly higher (53.6±6.3 vs. 61.8±4.5°, p=0.004). Furthermore, the peak hip flexion moment was significantly higher in the postoperative group (0.94±0.26 Nm/kg vs. 1.11±0.22 Nm/kg; p=0.021). The other joint ROMs and peak kinetic values showed no significant differences (Table 1).

Discussion and Conclusion

The postoperative patient group only showed slight changes in the gait patterns compared to the preoperative group. The ROM of the different foot joints remained lower compared to data from healthy subjects [2]. This can be related to the already restricted passive ROM. Nevertheless, hip and knee ROM, as well as the peak hip flexion moment were increased. This could therefore lead to a slightly higher walking speed.

To conclude, this study showed that although the changes in the gait patterns were small, the postoperative patients had a higher quality of life with less pain.

References

[1]: Pagenstert et al. CORR 2007;462:156-68
[2]: Stebbins et al. Gait Posture 2006;23(4):401-10

PI.06

is the conservative treatment of achilles tendon ruptures in older patients ageist?

Amer Shoaib
Stockport NHS Foundation Trust, Stockport, UK

Achilles tendon ruptures are generally treated conservatively in older patients because of fears of wound breakdown or infection. This study shows that modern minimally invasive techniques can allow older patients to safely benefit from surgery.

Introduction

The management of Achilles Tendon rupture is controversial. Younger patients are often treated operatively but older patients are treated conservatively in plaster. The reason for non-operative management is the risk of wound breakdown in the older patient. New minimally invasive techniques involve a much smaller wound and results in a biomechanically strong repair. The use of this technique in older patients has not yet been evaluated. This study has addressed this issue.

Method

Nine patients over the age of 50 who would normally have been treated conservatively were treated with the Achillon device. The incision was 3 cm long in each case. Patients were managed postoperatively in air cell boot fully weight bearing with heel wedges. They returned to normal shoes after seven weeks. They were evaluated at three months and six months.

Results

The average age in 9 patients was 59 years. All patients were allowed home within 24 hours of surgery fully weight bearing. There were no wound breakdowns. There were no wound infections. There were no reruptures. The patients all had grade 5 power at seven weeks from surgery.

Discussion

The treatment of Achilles Tendon ruptures in older patients is controversial. The reasons for avoiding surgery are no longer valid as there exists a minimally invasive option with minimal risk of complications. The reasons for surgical treatment of younger patients are valid for older patients and we should reconsider our surgical choices in the light of these findings as they could be viewed as ageist.

PI.08

GAIT ANALYSIS OF THE EFFECT OF POSTOPERATIVE REHABILITATION SHOES

Zuned Hakim
Stockport NHS Foundation Trust, Stockport, UK

Postoperative rehabilitation shoes used in foot ankle procedures have a detrimental effect on the patients gait and can cause problems for patients. The use of specifically designed equalising device for the other foot improves gait.

Introduction

Various rehabilitation shoes are prescribed to protect the forefoot following surgery. Patients often complain of discomfort in other areas as a result of the postoperative shoe, including the knee, hip and lower back. This has never been quantified. This study aims to establish the effect on other joints using gait analysis.

Patients and Methods

11 healthy volunteers were investigated using various common types of postoperative shoe. They were studied with gait analysis equipment and the joint motion assessed with commercial software. The effect of commercial devices designed to minimise gait changes by lifting the contralateral foot were also evaluated.

Results

There was a reduction in knee flexion and extension compared to the contralateral leg in all phases of the gait cycle. This was the case with both heel wedge shoes and inflatable air boots. There was also an increase in pelvic tilt during gait with both shoes, which was more pronounced with the air boot. The foot raise device which is designed to decrease these changes was effective in minimising gait changes.

Discussion

The use of rehabilitation shoes after forefoot surgery is almost universal. Patients are rarely counselled of the risk of joint pain or back pain as a result of the postoperative shoe. Patients with pre-existing back pain or hip pain may have less symptoms if they are supplied with an equalising device to raise the other foot.

Patients are at risk of initiation or exacerbation of low back pain or lower limb joint pain from the use of postoperative shoes. Patients with a history of back or limb symptoms should be provided with an equalising device for the contralateral limb to minimise their discomfort. Patients should be warned of this risk when giving consent.

PI.10

Raman spectroscopy can identify molecular changes in osteoarthrotic subchondral bone

Jemma Kerns
UCL Institute of Orthopaedics, Royal National Orthopaedic Hospital, Stanmore, UK

The detection of osteoarthrosis using Raman spectroscopy has contributed to the understanding of the biochemical signature of subchondral bone across diseased and control tibial plateaus. This technique has the potential to shed light on the role of bone in osteoarthrosis.

Introduction

Osteoarthrotis (OA) is a common, debilitating disease of joints involving degeneration of cartilage and bone. It has been suggested that subtle changes in the molecular structure of subchondral bone may precede morphological changes in the osteoarthrotic joint [1].

There are two arguments for the mechanical initiation of osteoarthrosis:

1) An increase in the subchondral bone stiffness due to an increased load on the joint [2].

2) Changes in the bone biochemistry towards homotrimeric collagen, leading to a softening of the bone [1, 3, 4].

To explore these arguments Raman spectroscopy was employed as a novel diagnostic tool. Raman spectroscopy measures inelastic scattered laser light produced when photons interact with chemical materials. Resultant changes in wavelength form spectra representative of the chemical composition of the given sample [5].

The aim of our study is to explore the hypothesis: changes towards homotrimeric collagen in subchondral bone in osteoarthrosis can be detected with Raman spectroscopy.

Patients and Methods

Samples were acquired (ethics approval was obtained) from 10 human tibial plateaus with established medial compartment osteoarthrosis (radiographic and macroscopic diagnosis) and control tibial plateaus (n = 5) from patients undergoing surgery unrelated to OA. pQCT (Peripheral quantitative computed tomography) was employed to calculate the bone mineral density for each of the samples.

Raman

spectra were acquired from the subchondral bone with an 830 nm laser (Renishaw, Gloucester, UK).

Data processing: Raman spectra were baseline corrected and normalised to the phosphate peak (960 cm^{-1}). Ratios of phosphate : Amide I, phosphate : proline, and phosphate : carbonate were calculated. Secondly, principal component analysis was performed on the data, to assess variance across the spectral range (350 - 1800 cm^{-1}) [6].

Results

pQCT results revealed that the subchondral bone of the medial side of the OA samples had a greater volumetric density and thickness than the lateral side(p=0.001). The control specimens had the same thickness on both sides of the tibial plateau and there were some differences in density.

The initial Raman results show there is no spectral difference between the two sides of the plateau in OA or in the control samples. However, there were spectral differences between the OA and control samples.

Discussion/Conclusion

This work therefore, so far, supports the theory that there is a biochemical difference between OA and control subchondral bone.

Future efforts will assess Raman spectroscopy for both characterising and detecting osteoarthrosis during its early subclinical phase.

Acknowledgements
'We would like to thank the Royal National Orthopaedic Hospital and patients for supporting this study, and the EPSRC for funding this project.

References
Bailey AJ et al (2002). The international journal of biochemistry & cell biology, 34(2), 176-82.
Radin EL (2004). Journal of Rheumatology, 31, suppl 7.
Mansell JP et al (1998). The Journal of clinical investigation, 101(8), 1596-603.
Bailey AJ et al (2004). Biorheology, 41(3-4), 349-58.

Draper ER et al (2005). Journal of bone and mineral research 20(11), 1968-72.
Martin F et al (2010). Nature Protocols, 5(11), 1748-1760.

PI.11
MICROVASCULAR ARCHITECTURE OF IRRADIATED MANDIBLE

Arja Kullaa
SIBLabs, Kuopio, Finland

In oral cancer patients, tumour resection is usually combined with irradiation, which locally impairs bone quality and impairs the prognosis of dental implants. In the present study, three-dimensional µCT was used to evaluate the bone vascular-system in irradiated mandible.

Treatment of oral carcinomas requires surgery followed by postoperative radiotherapy or concurrent chemoradiotherapy. After cancer treatment prosthetic solutions are needed to provide patient with proper masticatory and phonetic functions and facial aesthetics. Previously implants were considered to be contraindicated in irradiated jaw because of high risk of failure, nowadays the improvement in surgical techniques and clinical protocols enable dental surgeons to plan implants on irradiated jaw with predictable success rate. The reaction of bone after irradiation is either circulatory or metabolic. Surrounding soft tissues are also altered by irradiation, with vascular damage and fibrotic phenomena that may contribute to either direct bone alteration or bone healing adaptation. The dog, because of its ability to remodel alveolar bone in ways that are similar to humans, represents the best potential animal model for study the pathogensis of irradiated bone. (1) The aim of this study was to describe the vascular system in irradiated mandible with three-dimensional (3D) morphometric µCT.

In ten skeletally mature beagle dogs, one side of mandible was irradiated in 2 sessions, lasting one week. The total dosages were 40 Gy (Group A, 5 dogs) and 50 Gy (Group B, 5 dogs). The irradiation source used was a linear accelerator (Saturne III, CGR, France) with 6 MeV electrons. The size of the treatment area was 4.5 cm x 3 cm. After the animals were sacrificed, the mandible bone blocks containing implants were dissected and fixed in 10 % formalin. Tissue segments were processed by bulk staining en bloc in basic fuchsin, which identifies the microdamage in bone and distinguishes it from the artefact caused by histological processing and sectioning (1). Basic fuchsin stains cells and empty spaces in the bone matrix - blood cells, lacunae, canaliculi, microcracks (2). The specimens were embedded routinely in polymethyl methacrylate resin without preliminary decalcification.

A series of images of the mandible bone including the implants were scanned using SkyScan 1172 Micro-Computed Tomography System (SkyScan, Kontich, Belgium) with 30 micrometer pixel resolution. After µCT, the undecalcified specimens with implants were cut with a cutting and grinding systems (Exakt, Norderstedt, Germany). Histological sections were compared with the µCT images, taking care to match specific homologous anatomical features in the bone anatomy.

The three-dimensional morphometric µCT analysis may reveal detailed and localized information (i.e. changes in volume, neovascularization etc.) about the vascular-system of irradiated mandible. Neovascularization and bone degeneration are active structures in bone healing after irradiation, and their function is of great importance in osseointegration of dental implants. Thus, determination of changes in localized neovascularization in cortical and especially in alveolar bone due to irradiation is essential.

1) Burr DB, Allen MR. Mandibular necrosis in beagle dogs treated with biphosphonates. Orthod Craniofac Res 2009: 12: 221-228.
2) Allen MR, Burr DB. Mandible matrix necrosis in beagle dogs after 3 years of daily oral biphosphonate treatment. J Oral Maxillofac Surg 2008;66: 987-994.

PI.12
Prediction of open locking in the hypermobile jaw joint

Jan Harm Koolstra
ACTA, Functional Anatomy, the Netherlands

Jaw joint hypermobility combined with a relatively steep anterior slope angle of the eminence and forwardly inclined jaw-closing muscles may predispose for locking the jaw in the wide open position.

Introduction

Patients with hypermobility of the temporomandibular joint (TMJ) may have problems closing their mouth after opening widely. In the worst case, the mandibular condyles become trapped in front of the articular eminences and the jaw muscles cannot reposition them back into the fossae (open lock), which prevents the jaw from closing. This situation is very painful and requires acute medical assistance. Presently, the aetiology of this disorder is still unknown. To explain the difference in ease of closing the jaw between patients and non-patients, we proposed that their musculo-skeletal morphology differs. It was hypothesized that a relatively steep anterior slope angle of the eminence, combined with forwardly inclined jaw-closing muscles could predispose for an open lock.

Methods

Wide opening and subsequent closing of the jaw was simulated with a dynamic biomechanical model of the human masticatory system [Tuijt, 2010]. From a reference configuration [van Eijden , 1997] the anterior slope of the articular eminence was adapted as well as the direction of the jaw-closing muscles.

Results

Combinations of backwardly oriented jaw closers and a gentle anterior slope angle allowed the mandibular condyles to travel anterior of the eminences and back into the fossae uneventfully. However, combinations of relatively forward oriented jaw closers and a steep anterior slope caused the condyle to continue travelling anteriorly upon jaw-closing attempts. This created an open lock position.

Discussion

The predicted jaw movements indicated that unfavourable combinations of muscle orientation and anterior slope angle exist that makes the masticatory system prone to open locks. Furthermore, it was demonstrated that being unsuccessful to close the jaw after being opened wide can be attributed to the failure to create sufficient jaw-closing torque by the joint reaction forces to overcome the jaw-opening torque of the jaw-closing muscles (Fig. 1). The predicted results corroborated with the hypothesis.

References

Tuijt et al, J Biomech, 43:1048-1054, 2010.
van Eijden et al, Anat Rec, 248:464-474, 1997.

PI.14

Central versus local coordination in the international HEALTH trial.

Paul Burgers
Erasmus Medical Centre, Rotterdam, The Netherlands

The organization of international multicenter trials is complex. In the HEALTH trial two different management strategies were applied. Central trial coordination can be, under certain conditions a suitable alternative for local coordination in combination with payment per patient.

Introduction:

Multicenter clinical trials can be organized in different ways. Multiple centers participated in the HEALTH trial (Hip Fracture Evaluation with ALternatives of Total Hip Arthroplasty versus Hemi-Arthroplasty). For the Dutch sites most study tasks are managed by a central trial coordinator, whereas Canadian and US sites use local study coordinators. The aim of this study was to analyze how these strategies affected trial performance.

Patients & Methods:

Design: Prospective observational study. Data related to ethics approval, trial startup time, inclusion rate and percentage of completed follow-ups were collected and compared for each hospital.

Data from pre-trial screening were compared with actual inclusion rates.

Results:

The median start-up time of the trial after obtaining ethics approval was shorter in the Netherlands than in Canada and the US (4.6 versus 11.6 weeks). The inclusion rate was similar in both groups (0.62 versus 0.64/month). The median percentage of enrolled patients in the Netherlands was 27.3% versus 17.0% in Canada and the US. The actual inclusion rates were lower than expected from pre-trial screening. The percentage of effectuated follow-up visits was > 90% in both groups.

Discussion/ Conclusion:

In this study, central trial coordination contributed to faster trial start-up and higher inclusion rates, but had no effect on the effectuated follow up visits. Central coordination is therefore a suitable alternative for appointing these tasks to local research assistants and per patient payment. Central coordination enables non-academic hospitals to participate in clinical trials. Limiting conditions for central coordination are budget availability, a manageable number of patients, and a manageable distance between participating sites.

Submitted by:Li , Lily Miss

We present the largest reported series of giant cell tumours of bone to date where we correlate clinical and histopathological features to outcome post-treatment. We aim to elucidate the unpredictable behaviour of these tumours and to evaluate treatment options.

Giant Cell Tumours of Bone : correlation of clinical and histopathological features to outcome post-surgical treatment; a single institution experience of 359 cases.

L Li[1], D Williams[1], P Gikas[1], J Jagiello[1], W Aston[1], R Pollock[1], J Skinner[1], S Cannon[1], T Briggs[1], A Flanagan[2]
[1] The Sarcoma Unit, Royal National Orthopaedic Hospital, London, UK
[2] Department of Histopathology, Royal National Orthopaedic Hospital, London, UK.

Introduction

Giant cell tumour (GCT) is one of the most controversial and discussed bone tumours. Biological behaviour can be unpredictable and there is currently no consensus as to the best treatment for these theoretically benign lesions. Surgical treatment options include intralesional excision or segmental resection. Curettage has a higher recurrence rate than resection but does preserve adjacent joint function. After curettage, the use of adjuvant therapies is still controversial.

Aim

We evaluated (1) clinical and histopathological features of patients with GCT, (2) the recurrence rate and recurrence-free Kaplan-Meier survival function post-resection or curettage, (3) Musculoskeletal Tumour Society (MSTS) functional score (1993 version), and (4) complications after treatment.

Methods

We conducted a retrospective review of 359 patients (males and females) with GCT of bone presenting to the Royal National Orthopaedic Hospital to evaluate oncological and functional results.

Results

The patients were followed up for at least 12 months. The average age of the patients was 36.9 years (range 1-89 years). Tumours were treated with extensive curettage, local adjuvant therapy (e.g. phenol), cement reconstruction or wide resection +/- use of endoprostheses. The recurrence rates, Kaplan-Meier recurrence-free survival curves, and MSTS functional scores were recorded and correlated to the clinical and histopathological features of these tumours using statistical analysis.

Conclusion

This is the largest reported series of giant cell tumours of bone to date and by correlating clinical and histopathological features to outcome post-treatment serves to elucidate the unpredictable behaviour of these tumours, evaluate current surgical treatment options and guide future therapeutic approaches.

Biomechanical investigation on distal inter-locking screw breakage in tibia nails comparing angular stable and conventional fixation.

Gueorguiev Boyko GB PhD boyko.gueorguiev@aofoundation.org AO Research Institute Davos Switzerland
Richards Robert Geoff RRG PhD geoff.richards@aofoundation.org AO Research Institute Davos Switzerland
Mückley Thomas MT MD PhD thomas.mueckley@med.uni-jena.de Dept. of Trauma, Hand and Reconstructive Surgery, Friedrich Schiller University Jena Germany
Hofmann Gunther Olaf HGO MD PhD gunther.hofmann@med.uni-jena.de Dept. of Trauma, Hand and Reconstructive Surgery Friedrich Schiller University Jena Germany
Höntzsch Dankward HD MD PhD DHoentzsch@bgu-tuebingen.de Dept of Medical Technology Development, BG Trauma Hospital Tübingen Germany
Windolf Markus WM MSc markus.windolf@aofoundation.org AO Research Institute Davos Switzerland
Submitted by:Lenz, Mark Dr.

Angle-stable locking screws (ASLS) provide a significantly longer fatigue life, compared to conventional locking screws in intramedullary nails.

Introduction:
To compare long-term performance of angular-stable locking screws and conventional locking screws for distal locking of intramedullary tibia nails under cyclic loading.
Methods:
The distal third of human tibiae surrogate bones were reamed and a 10mm intramedullary tibia nail was inserted and distally locked in the mediolateral plane with either two angle-stable locking screws (ASLS) or two conventional screws. Six specimens per group were mechanically tested under quasi-static and cyclic sinusoidal axial loading with constantly increasing load up to screw breakage.
Results:
Stiffness values of angular stable locking screw constructs were significantly higher (7809 N/mm ± 647) compared to conventional locking screw constructs (6614 N/mm ± 859), $p=0.002$. The number of cycles to failure of angle-stable locking screw constructs was significantly higher (187200 ± 18100) compared to conventional locking screw constructs (128700 ± 7000), $p<0.001$.
Conclusion:
The significantly better fatigue performance of angular stable locking screw constructs might be an interesting option in comminuted and distally located fractures to enhance the stability of fracture fixation.

Return to theatre in 30 days following hip or knee replacement: a comparison of thromboprophylaxis with enoxaparin and dabigatran

Rocos Brett Mr brettrocos@yahoo.co.uk Yeovil District Hospital Yeovil UK
Lankester Benedict JA Mr ben.lankester@ydh.nhs.uk Yeovil District Hospital Yeovil UK
Submitted by:Rocos, Brett Mr

This study suggests that a change from enoxaparin to dabigatran does not increase the incidence of early infection, or the risk of bleeding at the operative site or the gastrointestinal tract when used in elective hip or knee arthroplasty.

The introduction of direct thrombin inhibitors in arthroplasty surgery has reignited the debate on the risk of wound complications when using chemical thromboprophylaxis. It has been suggested that direct thrombin inhibitors might lead to an increased risk of systemic and operative site bleeding and wound sepsis when compared to low molecular weight heparin.

In July 2009, departmental thromboprophylaxis policy for patients undergoing hip and knee replacement surgery (including revision) was changed from subcutaneous enoxaparin for the duration of inpatient stay to dabigatran for 10 days (knees) or 28 days (hips) unless contraindicated. In the 2 years prior to policy change, 1091 patients underwent hip or knee arthroplasty (Group A), with1150 patients undergoing the same procedures in the 2 years following July 2009 (Group B). A minority of patients were already on warfarin (2% in group 1, 3% in group 2).

This study presents a retrospective analysis of all patients who returned to theatre within 30 days of joint replacement surgery to assess whether the change in unit policy caused any discernible increase in bleeding-related complications.

In group A, 20 / 1091 patients (1.8%) returned to theatre within 30 days. 9 were for reasons unrelated to thromboprophylaxis (mainly dislocated hips), 4 for gastrointestinal bleeding and 7 for wound complications (haematoma, wound breakdown, or infection).

In group B, 22 / 1150 patients (1.9%) returned to theatre within 30 days. 13 were for unrelated reasons, 4 for gastrointestinal bleeding, and 5 for wound complications. One patient with a wound complication was on warfarin and therefore did not receive dabigatran.

The lower wound complication rate in group B was not statistically different.

This study, in a large heterogeneous group of patients, suggests that a change from enoxaparin to dabigatran does not increase the incidence of early infection, or the risk of bleeding at the operative site or the gastrointestinal tract.

The influence of interprosthetic gap on single-plate fracture reconstruction with or without anterior strut allorgraft. A biomechanical evaluation.

Segal Olivier O MD olivier_segal@hotmail.com Orthopaedic Surgery Department, University Hospital Pellenberg Pellenberg Belgium
Vander Sloten Jos J Prof. PhD, Eng jos.vandersloten@mech.kuleuven.be BMe - Biomechanics Section, Faculty of Engineering, KU Leuven Heverlee Belgium
Bellemans Johan J Prof. PhD, MD johan.bellemans@uzleuven.be Orthopaedic Surgery Department, University Hospital Pellenberg Pellenberg Belgium
Corten Kristoff K MD kristoff.corten@uzleuven.be Orthopaedic Surgery Department, University Hospital Pellenberg Pellenberg Belgium
Submitted by:Quirynen, Thomas MSc, Eng

Single-plate fixation, combined with a good interprosthetic gap fracture reduction, succeeds in reconstructing the femur to its initial values, regardless of the gap distance. Addition of an anterior strut did not show a significant biomechanical benefit.

Introduction

Interprosthetic gaps between the tip of a total hip (THA) or total knee (TKA) replacement stem influence the biomechanical properties of the femur. Gaps between 5 and 15cm should be avoided but these gaps are predominantly present. It remains unclear whether this gap distance influences the stability of plate constructs with or without an anterior strut allograft.

Objectives

It was our aim (1) to evaluate the effect of the interprosthetic gap distance on the biomechanical properties of the femur and (2) to define the optimal reconstruction technique to treat these fractures.

Methods

The maximal load to failure (Fmax), the compression at failure (Cmax), stiffness and the absorbed energy at failure of 3 inter-prosthetic gaps between a cemented THA and TKA stem in 18 validated sawbone specimens were evaluated. Similarly, these specimens were tested after single-plate reconstruction with and without (cortical) strut onlay.

Results

A mean Fmax of 7700N was noted for gaps between 5 to 15 cm. There was no significant change of Fmax between the different gaps. A lower Cmax was present with a gap distance of 10 and 15cm and the absorption of energy prior to failure was lowest with gap distances between 10 and 15 cm. The femur fractured with a butterfly fragment at the site of the gap. The stability of lateral plate constructs was highly influenced by the reduction quality of the fracture fragments. Addition of an anterior strut did not significantly improve the stability.

Conclusions

Single-plate fixation succeeds in reconstructing the femur to its initial values, regardless of the gap distance. Addition of an anterior strut did not show a significant biomechanical benefit. When confronted with interprosthetic gap fractures, single-plate constructs in combination with a good reduction restore the femur to initial strength.

Tantalum : Is it the final frontier for managing extreme osteolysis in Revision Knee Arthroplasty?

Moss Michael M C Mr michael.moss@wsht.nhs.uk St.Richards Hospital Chichester UK
Vafaye John J V Mr john.va.faye@me.com UK Specialist Hospitals LONDON UK
Kamal Tamer T Mr tamer.kamal@yahoo.com St.Richards Hospital Chichester UK

Submitted by:Rao, Biyyam Madhusudhan Mr.

Management of major osteolysis in revision knee arthroplasty still remains a challenge. In this prospective study we evaluate results of the porous tantalum metaphyseal cones in treatment of severe tibial and femoral bone loss encountered during revision knee arthroplasty.

Introduction

Management of large osteolytic defects in a revision total knee arthroplasty still remains a challenge. To date there has been no established way of treating this complex problem. Several options are available for reconstruction including impaction bone grafting, Structural or bulk allograft, custom-made prostheses, polyethylene augments, modular metal augmentation of prostheses and mega prosthesis. In this prospective study we evaluate results of porous tantalum metaphyseal cones, designed and used specifically for the treatment of severe tibial and femoral bone loss encountered during revision total knee arthroplasty.

Patients and Methods

In this prospective study of consecutive 123 revision knee arthroplasties, 34 (30 Tibial, 4 Femoral) metaphyseal Trabecular metal cones (Zimmer Inc. Warsaw, Indiana) in 32 patients were used along with Rotating hinged total knee prostheses (Zimmer Inc. Warsaw, Indiana) to address major osteolysis in the proximal tibia and distal femur. The osteolytic defects were classified according to Anderson Orthopaedic Research Institute (AORI) classification and tantalum cones were used in either type II or III defects (See Fig 1,2). Indications were 12 patients for periprosthetic infections, 15 for aseptic loosening and 4 for periprosthetic fractures.

Results

At average follow up of 28 months (range 48-18 months), the mean Oxford scores improved from 12.90 to 33.40 (p value 0.001), American Knee society scores improved from 33.15 to 75.28 (P value < 0.55). There was improvement of mean functional range of movement to 2.53°- 91.09° of flexion (P value < 0.55) (See Fig 3). No radiolucent lines suggestive of loosening were seen around the trabecular metal cones and all the radiographs showed good Osteo-integration. There was no evidence of any collapse or implant migration. As complications we had 2 reinfections, 2 deaths due to unrelated causes, 1 femoral stem-disengagement, 2 non progressive tibial and femoral stem radiolucent lines and 2 patients with shin.

Conclusions

Till now there is no established method for treatment of large bony defects during revision knee arthroplasty. Large quantities of allografts difficult to procure, expensive, can collapse or resorb and have risk of transmitting diseases. Modular metal augments are rigid and do not seem to integrate with host bone or effectively address severe bone loss and the instability and have potential for early loosening and failure.

As opposed to these problems, the mechanical properties and recent designs of tantalum cones have made them very promising, versatile and user friendly in managing the major osteolysis. Like mid-term studies documented in literature [1], we have also had encouraging results in using these tantalum cones in revision knee arthroplast with large osteolytic defects.

References

1. Meneghini RM et al. Use of porous tantalum metaphyseal cones for severe tibial bone loss during revision total knee replacement. J Bone Joint Surg Am 2008; 90:78.
2. James L. Howard et al. Early Results of the Use of Tantalum Femoral Cones for Revision Total Knee Arthroplasty. J Bone Joint Surg Am. 2011 Mar 2; 93(5):478-84.
3. Meneghini RM et al. Use of porous tantalum metaphyseal cones for severe tibial bone loss during revision total knee replacement. Surgical technique. J Bone Joint Surg Am. 2009 Mar 1; 91 Suppl 2 Pt 1:131-8.
4. Lachiewicz PF et al. Can tantalum cones provide fixation in complex revision knee arthroplasty? Clin Orthop Relat

Tip-apex distance (TAD): a comparison between dynamic hip screw (DHS) and Cephalo medullary nail fixation of extracapsular fractures of the hip

Kiew SiehYean SY Foundation 1 doctor siehyean@gmail.com Mersey Foundation School Liverpool United Kingdom
Kumar Gunasekaran G Consultant Trauma and Orthopaedic Surgeon gunasekaran.kumar@rlbuht.nhs.uk Royal Liverpool and Broadgreen University Hospitals NHS Trust Liverpool United Kingdom
Submitted by:Kiew, SiehYean Dr

Selective MR imaging of rabbit knee cartilage by using a mixture which contains both positively and negatively charged ionic contrast agents

Kazuya IKOMA K.I. kazuya@koto.kpu-m.ac.jp Kyoto Prefectural University of Medicine Kajii-cho, Kamigyo-ku, Kyoto-city, Kyoto Japan
Yusuke HARA Y.H. yhara@koto.kpu-m.ac.jp Kyoto Prefectural University of Medicine Kajii-cho, Kamigyo-ku, Kyoto-city, Kyoto Japan
Ken-ichi MATSUDA K.M. matsuken@koto.kpu-m.ac.jp Kyoto Prefectural University of Medicine Kajii-cho, Kamigyo-ku, Kyoto-city, Kyoto Japan
Mitsuhiro KAWATA M.K. mkawata@koto.kpu-m.ac.jp Kyoto Prefectural University of Medicine Kajii-cho, Kamigyo-ku, Kyoto-city, Kyoto Japan
Masahiro UMEDA M.U. ume@meiji-u.ac.jp Meiji University of Integrative Medicine Hiyoshi-cho, Nantan-city, Kyoto Japan
Toshikazu KUBO T.K. tkubo@koto.kpu-m.ac.jp Kyoto Prefectural University of Medicine Kajii-cho, Kamigyo-ku, Kyoto-city, Kyoto Japan

Submitted by:KIDO, Masamitsu Efficacy of a clinical trace element mixture as an MR enhancing agent in rabbit knee

A clinical trace element mixture was first used as a mixture which contains both positively and negatively charged ionic contrast agents. It has a selective MR imaging ability in articular cartilage.

Introduction:
Since the early degenerative changes of cartilage cannot be evaluated by using X-rays, the evaluation method using MRI has been developed. Negatively charged ionic contrast agents (e.g. Gd-DTPA) has been clinically applied to MR imaging of articular cartilage. Although positively charged manganese was reported to enhance the MR imaging of articular cartilage in animals, it has not been clinically applied to those in human beings. The aim of this study is to analyse the efficacy of selective MR imaging of rabbit knee cartilage by using a mixture which contains both positively and negatively charged ionic contrast agents (Mineric).
Methods:
A trace element mixture (Mineric®, Nipro Pharma Corp., Japan), a typical trace element replenisher used in clinical practice, was employed in this study. It contains both positively and negatively charged ions (0.5 mmol/l manganese chloride, 17.5 mmol/l colloid-mediated ferric chloride, 30.0 mmol/l zinc sulfate, 2.5 mmol/l cupric sulfate, and 0.5 mmol/l potassium iodide). Straight Mineric, 1.0 mmol/l Gd-DTPA (Magnevist®, Schering, Germany), and normal saline were used. Eighteen knees of 9 rabbits were used for this study. MRI measurements were recorded on an Anova 300 WB spectrometers (7.05T).
As the experimental protocol, the MR-enhancing agents were injected every 0.3 ml into bilateral knee joints, and the rabbits were sacrificed five minutes after the injections. The whole block of each knee joint was set parallel to static magnetic field, keeping the knee in a straight position. The calculated T_1 and T_2 images were obtained by the inversion recovery method and spin-echo method (FOV 25.6x25.6 mm, matrix 256x512, slice thickness 2 mm). Signal intensities were read from the region of interest (ROI) set as entire articular cartilage in the lateral condyle of the femur. The mean values of T_1 and T_2 were obtained from these ROIs. The T_1 and T_2 values of the fluid were evaluated similarly. Side effects in 4 knee joints of 2 rabbits were investigated. The histological evaluations were performed lastly with HE stains. The data were analysed using an unpaired t-test. The results were presented as the mean ± standard deviation (SD). A significant difference was defined as p value less than 0.05.
Results:
Proton density weighted images of femoral articular cartilages were visualized well when both agents were used (Figure). The T_1 values of the cartilage and fluid were significantly decreased in the cases of Gd-DTPA and Mineric in comparison with that of saline (Table 1). The T_1 value of the fluid was significantly decreased in the case of Mineric in comparison with that of Gd-DTPA. The T_2 value of fluid was significantly decreased in the case of Mineric in comparison with both of Gd-DTPA and saline, but no significant difference was observed in the T_2 value of the cartilage in all the cases (Table 2). Morphological analogy between MR imaging and the histology was well confirmed. No obvious side effects were observed.

Conclusion:

It has a selective MR imaging ability in articular cartilage with a mixture which contains both negatively and positively charged ionic contrast agents.

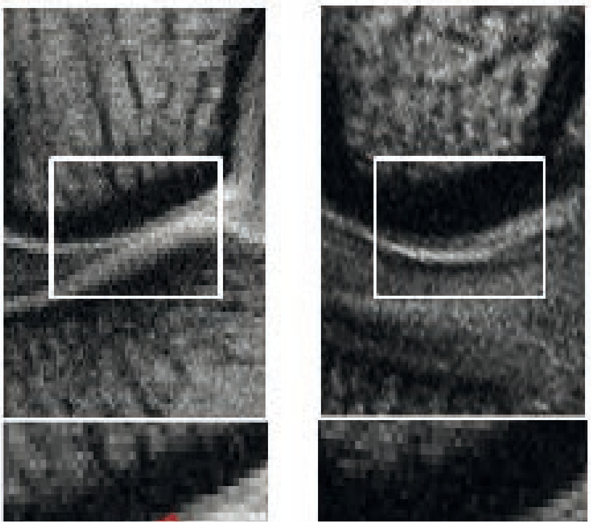

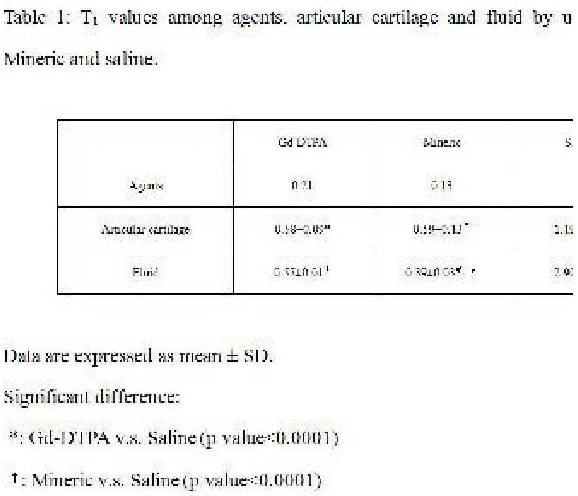

Table 1: T_1 values among agents, articular cartilage and fluid by u

Mineric and saline.

	Gd-DTPA	Mineric	S
Agents	0.21	0.13	
Articular cartilage	0.38±0.05*	0.39±0.12†	1.1
Fluid	0.37±0.01†	0.39±0.03*,†	2.9

Data are expressed as mean ± SD.

Significant difference:

*: Gd-DTPA v.s. Saline (p value<0.0001)

†: Mineric v.s. Saline (p value<0.0001)

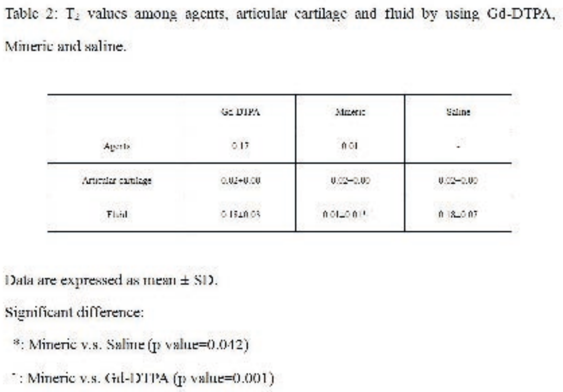

Table 2: T_2 values among agents, articular cartilage and fluid by using Gd-DTPA, Mineric and saline.

	Gd-DTPA	Mineric	Saline
Agents	0.17	0.01	-
Articular cartilage	0.02±0.00	0.02±0.00	0.02±0.00
Fluid	0.15±0.03	0.01±0.01†	0.18±0.07

Data are expressed as mean ± SD.

Significant difference:

*: Mineric v.s. Saline (p value=0.042)

†: Mineric v.s. Gd-DTPA (p value=0.001)

-Entire articular cartilage in the lateral condyle of the femur was analysed. The area of red square was selected as region of interest (ROI).

-Table 1

-Table 2

Submitted by:Imai, Kan

We quantified and compared the relative bone positions of the hindfoot in normal and flat feet using the 3D CT images. This study allows for more information to be provided in diagnosing the flat foot and selecting surgical procedures.

Background:
It is important to understand the relative bone position of the hindfoot in order to understand flat foot pathologies as well as to make an accurate diagnosis; the 3D bone position is not yet completely understood. The aim of this study is to quantify and compare the relative bone positions that constitute the hindfoot in the neutral position of the ankle joint in normal and flat feet using the 3D CT reconstruction images.

Methods:
CT images were taken of the 22 normal feet and 29 feet with flat foot deformity in neutral position, from which 3D virtual models were made of each mid-hind foot bone. The eigen vector of the talus, the calcaneus, and the navicular bone relative to the tibia was calculated. The eigen vector of the calcaneus, the navicular bone, and the first metatarsal bone relative to the talus was calculated (Figure 1). We compared the 3D relative bone position between normal and flat feet in neutral position.

Results:
The relative bone position of the talus in flat foot was wider relative to the tibia (normal foot: -79.6° [SD 4.8°]; flat foot: -77.1° [SD 3.2°]; $P < 0.05$) in sagittal plane as well as wider (normal foot: 11.9° [SD 22.4°]; flat foot: -0.7° [SD 15.6°]; $P < 0.05$) than in normal foot in transverse plane. The relative bone position of the calcaneus in flat foot was wider relative to the tibia (normal foot: -14.6° [SD 8.1°]; flat foot: 29.2° [SD 11.1°]; $P < 0.01$) in transverse plane as well as wider in coronal plane (normal foot: 5.1° [SD 2.6°]; flat foot: 11.0° [SD 2.6°]; $P < 0.01$) in comparison to normal foot. The difference in the relative bone position of the navicular bone relative to the tibia between the flat foot and normal foot was not significant (Table 1).

The relative bone position of the first metatalsal bone in flat foot was wider relative to the talus in sagittal plane (normal foot: -29.8° [SD 5.4°]; flat foot: -21.4° [SD 4.3°]; $P < 0.01$) as well as wider in transverse plane (normal foot: -11.7° [SD 4.5°]; flat foot: -3.9° [SD 16.5°]; $P < 0.05$) than in normal foot (Figure 2). The relative bone position of the calcaneus in flat foot was wider relative to the talus in sagittal plane (normal foot: -51.8° [SD 5.0°]; flat foot: -45.7° [SD 7.1°]; $P < 0.01$), wider in transverse plane (normal foot: 10.8° [SD 5.4°]; flat foot: 22.6° [SD 9.2°]; $P < 0.01$) as well as wider in coronal plane (normal foot: 8.5° [SD 4.0°]; flat foot: 22.9° [SD 12.7°]; $P < 0.01$) in comparison to normal foot. The relative bone position of the navicular bone in flat foot was wider in sagittal plane compared to the talus (normal foot: -51.8° [SD 4.6°]; flat foot: -46.7° [SD 7.1°]; $P < 0.01$) (Table 2).

Conclusions:
This study allows for more information to be provided in diagnosing the flat foot and selecting surgical procedures about flat foot.

Long term morbidity from All Terrain vehicles (ATV) accidents.

Arumilli Buchi Mr. rajjuorth@gmail.com Manchester Royal Infirmary Hospital. Manchester UK.
Messmer Peter Prof. pmessmer@aotrauma.org Basal University Basal Switzerland.
Submitted by:Khawaja, Sajid Aslam Mr.

Use of All Terrain Vehicles as they are commonly known in the United Kingdom is increasing as a result of tourism and encouragement to partake of outdoor activities. The law governing their use is in place, but often not adhered to. This paper analyses the epidemiology and long-term morbidity in patients admitted following ATV accidents in a busy trauma unit in Middle East.

Background:
Use of All Terrain Vehicles (ATVs) or Quad Bikes as they are commonly known in the United Kingdom is increasing as a result of tourism and encouragement to partake of outdoor activities. The law governing their use is in place, but often not adhered to. This paper analyses the epidemiology and long-term morbidity in patients admitted following ATV accidents in a busy trauma unit inMiddle East.
Methodology:
The data were collected over a period of 12 months from February 2009 to February 2010. The parameters noted were the demographics of the patients, hospital stay and long term morbidities. The investigation took place at theRashidHospitalinDubai.
Results:
A total of 34 patients were admitted following ATV accidents. 88% were male. The average age at admission was 27 (range: 14 to 47) years. 20% of patients had polytrauma. The hospital stay ranged from3to 33 days (mean 9.7). Only 6% of patients were wearing a helmet at the time of the accident.
The most common group of injuries were limb injuries, with 26% of patients suffering injuries to the lower limb. A wide spectrum of injury patterns was recorded. 17.6% of cases had spinal injuries, 9% facial injuries, 6% pelvic and 5.8% a head injury. Two patients were paraplegic on presentation. One patient had a wrist drop, one foot drop and one had brachial plexus palsy. Persistent faecal incontinence was a problem in one patient.
Conclusions:
ATV use can be potentially lethal if not used safely. There appears to be a significant incidence of and morbidity (17.6%) from neurological injuries.Adhering to safety guidance or putting these on a legal footing could prevent mortality and morbidity in patients following recreational or occupational use of ATVs.

In vitro assessment of primary human chondrocyte viability following treatment with intra-articular contrast media and local anaesthetic

Baker Joe JF Mater Misericordiae University Hospital Dublin Ireland
Walsh Pauline PM School of Medicine & Medical Sciences, University College Dublin Dublin Ireland
Mulhall Kevin KJ Professor Mater Misericordiae University Hospital Dublin Ireland
Submitted by:Broderick, James

Gadolinium and iodine-based contrast agents are safe for intra-articular injection. However, addition of local anaesthetic to injection solutions causes a statistically significant reduction in chondrocyte viability, suggesting that local anaesthetics should not be routinely added to intra-articular contrast media

Introduction:

MR and CT arthrography, procedures in which either gadolinium or iodine-based contrast agents are administered intra-articularly, have become commonly used tools in musculoskeletal diagnosis. Although considered safe for systemic use, toxicities have been identified for these agents in some tissues, yet, there have been few studies examining their toxicity on the joint. The aims of this study were to (1) investigate the effects of four routinely used intra-articular contrast agents on human chondrocyte viability in both a time-dependent and dose-dependent fashion, and (2) determine the additive effect of local anaesthetic agents to the contrast media.

Methods:

Primary human chondrocytes, isolated from femoral heads obtained at the time of hemiarthroplasty performed for femoral neck fracture, were grown in monolayer culture and exposed to one of the intra-articular contrast agents (Magnevist or Multihance 1.7, 2.5, 5, 10 and 20 mmol gadolinium/L; Omnipaque or Ultravist 50, 100 and 200 mg iodine/ml). Chondrocytes were exposed to these agents either in isolation, or, as part of an arthrogram injection cocktail routinely used in clinical practice (saline-diluted Magnevist 2.5 mmol/L with/without 1% lidocaine; saline-diluted Omnipaque 300 mg/ml with/without 1% lidocaine) for a treatment duration period of 15 minutes, 30 minutes, 1, 4, 16 or 24 hours. Cells exposed to cell culture media or saline served as controls. Twenty-four hours after exposure, cell viability was assessed using the CellTiter96®AQ$_{ueous}$One Solution Cell Proliferation Assay. Chondrocyte phenotype was confirmed with Collagen 2 expression.

Results:

Iodine-based contrast agents did not cause a significant difference in chondrocyte viability in either a time or dose-dependent fashion. A significant decrease in cell viability was only noted for gadolinium-based agents at a supra-therapeutic concentration of 20 mmol/L ($P = 0.03$). However, the addition of local anaesthetic, to both CT and MRI arthrogram solutions, caused a statistically significant decrease in chondrocyte viability ($P < 0.05$), which occurred in a time-dependent fashion ($P < 0.05$).

Conclusions:

Gadolinium and iodine-based contrast agents are safe for intra-articular injection at the concentrations routinely used in clinical practice. However, a time-dependent reduction in chondrocyte viability was confirmed with the addition of local anaesthetic to the injection solutions. These in vitro findings suggest that local anaesthetic agents should not be routinely added to intra-articular radiographic contrast media.

Hypoxia mimicking small molecules induce an angiogenic trophic profile in human mesenchymal stromal cells

Fernandes Hugo
Doorn Joyce
Jeroen van de Peppel
Hans van Leeuwen
Margreet de Vries
Zeen Aref
Paul Quax
Ola Myklebost
Clemens van Blitterswijk
Jan de Boer

Submitted by:Fernandes, Hugo

The discovery of new molecules with pro-angiogenic potential can overcome one of the major limitations in cell-based therapies: tissue necrosis upon implantation. Here we present a new molecule that can be used to control stem cell´s pro-angiogenic profile.

The repertoire of trophic factors determines the biological engagement of human mesenchymal stromal cells (hMSCs) in processes such as immunomodulation and tissue repair. For instance, we previously identified small molecules which could induce a pro-osteogenic panel of trophic factors, resulting in improved bone formation. The pro-angiogenic response of hMSCs, in contrast, is mediated by vascular endothelial growth factor (VEGF). In this manuscript, we employed a high throughput assay on a hMSCs cell line containing a hypoxia responsive element from the VEGF promoter to identify novel small molecules which mimic the natural hypoxic response. The effect of several of these small molecules was cell type/species dependent, but we identified phenanthroline as a robust hit and show that this compound induces high expression of HIF-1 target genes in hMSCs compared with desferoxamine (DFO, a known hypoxia mimic) (Figure 1). Moreover, terminally exposure of terminally differentiated osteoblasts and ligamente-derived cells to Phenanthroline led to a robust up-regulation of VEGF indicating the potential to elicit a pro-angiogenic profile when transplanting such cells in vivo. Furthermore, we demonstrate that conditioned medium derived from cells treated with hypoxia, DFO or phenanthroline has similar effects on proliferation and differentiation of primary cells. Interestingly, only phenanthroline induced high expression and secretion of another angiogenic cytokine, interleukin-8, suggesting that the mechanism of phenanthroline-induced hypoxia is distinct from DFO and hypoxia and might involve the activation of other, until now unknown, signalling pathways (Figure 2). Importantly, phenanthroline alone was sufficient to induce vascular invasion of a Matrigel plug in vivo, making it a highly promising molecule for future revascularization strategies (Figure 3).
Primary hMSCs were cultured in the presence of 150 μM DFO, 200 μM Phen or in an hypoxia chamber (2% O2). After 2 days, whole genome expression analysis was performed and the expression of known HRE-containing genes was examined. Of the three culture methods, most genes were strongest induced using Phen. Heatmaps show the relative expression of denoted genes compared to cells in basic medium, with all genes statistically significant regulated compared to cells in basic medium ($P<0.05$).- hMSCs were cultured in the presence of 150 μM DFO, 200 μM Phen or in hypoxia (2% O2) for 2 days, after which cells were lysed. Protein concentrations of IL-8, VEGF, bFGF and G-CSF were determined in cell lysates and as shown, only Phen induced secretion of high levels of Il-8, which were not affected by DFO or hypoxia. In contrast, VEGF secretion was increased by all three culture methods, but highest by DFO.- Matrigel plugs (0.5 ml) containing either PBS , DFO (150 μM) or Phen (200 μM) were injected subcutaneously and analyzed for capillary ingrowth after 7 days. a, vessel ingrowth was scored in a categorical way and expressed as mean ± SEM per group (n=7) in arbitrary units (AU). b, the endothelial nature of the ingrowing cells structures is confirmed by CD31 staining. c, in two plugs in the Phen treated group extraordinary ingrowth of capillary like structures throughout the total plug could be observed, demonstrated a clear lumen surrounded by CD31 positive cells.

Ligament-derived cells for regenerative medicine applications

Fernandes Hugo
Saris Daniel
Kelder Cindy
Barata Tânia
Ferreira Lino
Vazão Helena
Corina Ghebes

Submitted by:Fernandes, Hugo

Mesenchymal stromal cells (MSC) are multipotent cells usually isolated from bone marrow aspirates and hold great potential for regenerative medicine. However, because large number of cells are needed to regenerate worn-out tissues, extensive in vitro expansion is needed prior to in vivo use. Tendons and ligaments (T/L) are often injured in young active people as well as in old people suffering from osteoarthritis. Currently, surgeons use autografts or allografts to replace the damaged T/L. Upon replacement, the new T/L will be remodeled and integrate into the bone. However, due to poor vascularization during the initial stage, loss of extracellular matrix and poor cell survival the graft can be compromised. In order to accelerate the remodeling stage and the integration with the bone - therefore decreasing the recovery time of patients - MSCs, or other multpotent cell source with similar characteristics, can be co-delivered during the surgical procedure. Here we show that ligament-derived cells are multipotent cells with phenotypical resemblance to MSCs (Figure 1). Interestingly, and in contrast with MSCs, they can be expanded in vitro, without loss of pluripotentcy, for longer than MSCs (at passage 5 MSCs loose multipotentcy whereas ligament-derived cells maintain pluripotentcy up to passage 10) (Figure 2). Moreover, using high-throughput screening we were able to find molecules that can increase proliferation of ligament-derived cells as well as endothelial cells. We believe these different cell populations can play a key role in cell-based therapy for T/L regeneration and other applications in the field of regenerative medicine.

DEPOSITION OF ZIRCONIA THIN FILM ON THE PLASTIC COMPONENT FOR LOW WEAR JOINT PROSTHESES: A PILOT STUDY OF A CHALLENGING APPROACH

BIANCHI MICHELE MB Dr. m.bianchi@biomec.ior.it ISTITUTO ORTOPEDICO RIZZOLI Bologna Italy
LOPOMO NICOLA NL Dr. n.lopomo@biomec.ior.it ISTITUTO ORTOPEDICO RIZZOLI Bologna Italy
MALTARELLO MARIA CRISTINA MCM Dr. mariacristina.maltarello@ior.it ISTITUTO ORTOPEDICO RIZZOLI Bologna Italy
BOI MARCO MB Dott. m.boi@biomec.ior.it ISTITUTO ORTOPEDICO RIZZOLI Bologna Italy
MARCACCI MAURILIO MM Prof. MD m.marcacci@biomec.ior.it ISTITUTO ORTOPEDICO RIZZOLI Bologna Italy
RUSSO ALESSANDRO AR Dr. MD a.russo@biomec.ior.it ISTITUTO ORTOPEDICO RIZZOLI Bologna Italy
Submitted by:Bianchi, Michele Dr.

In order to reduce wear, zirconia thin films with optimal charachteristics of hardness and adhesion have been deposited by Pulsed Plasma Deposition technique on medical grade UHMWPE. Film mechanical properties have been characterized by nanoindentation, scratch and tribological tests.

Introduction

Joint replacement is the most frequent treatment when joints are severely damaged by traumatic or degenerative conditions of the joint cartilage. One main reason for long-term implant failure is the release of debris especially from the plastic component, as a consequence of the cyclic loading against the metallic or ceramic counterface [Dumbleton, 2002]. Wear debris can bring to chronic inflammation of the periprosthetic tissues, bone reabsorption, aseptic loosening up to implant failure [Holt 2007]. Different bearing materials and surface modifications have been proposed to reduce wear debris production [Piconi, 1999; Lappallainen, 2005;]. However, a common agreement on the best solution has not achieved yet, keeping the road open to new solutions.

The proposed challenging approach prefigures the direct coating of the material commonly used in the prosthetic plastic inlay with a hard and well-adherent ceramic film, in order to drastically reduce wear while preserving the well-established bulk mechanical properties of the substrate.

Results

Nanostructured zirconia (ZrO2) films (thickness up to a few micron, see Figure 1) have been deposited on the surface of medical grade plastic materials by a novel technique called Pulsed Plasma Deposition (PPD) .

PPD is a new vapour deposition technique based on the ablation of a target material as a consequence of the impact of a high-energy electron beam. The plasma plume of the ablated material is directed toward and deposited onto the substrate positioned at the right distance. Thank to the possibility to deposit hard films even at room temperature, PPD is suitable for coating heat sensitive materials like plastics.

X-ray diffraction measurements revealed that zirconia films grew in cubic phase, while scanning electron microscopy images showed a dense, columnar film microstructure, exhibiting a nanostructured top surface (grain size < 500nm). Films showed very high hardness values (~20GPa) and an excellent adhesion degree to the substrate, despite the large mechanical mismatch between the two materials. Finally, preliminary results of tribological tests revealed very low wear rate of the films under different work conditions.

Conclusions

We presented the preliminary results of a novel approach aiming to the drastic reduction of wear of common joint prostheses. Hard and well-adherent ceramic thin films deposited directly on the surface of the plastic inlay through a state-of-the-art physical vapour deposition technique, are envisaged to drastically reduce implant joint wear, thus lengthening the implant life.

References

Dumbleton et al, J Arthrop, 17:649-661, 2002.
Holt et al, Clin Orthop Rel Res, 460:240-252, 2007.
Lappallainen et al, Clinic Orthop Rel Res, 430:72-79, 2005.
Piconi et al, Biomater, 20:1-25, 1999.

SEM image of the cross section of a 3 micron thick ZrO2 film.

Structural Tissue Changes and Prolonged Clinical Improvement by Joint Distraction in Treatment of End-stage Knee Osteoarthritis; the Two Years Follow-up

van Roermund Peter P.M. MD, PhD k.wiegant@umcutrecht.nl University Medical Center Utrecht Utrecht The Netherlands
Intema Femke F. MD, PhD k.wiegant@umcutrecht.nl University Medical Center Utrecht Utrecht The Netherlands
Cotofana Sebastian S. PhD k.wiegant@umcutrecht.nl Paracelsus Medical University Salzburg Austria
Eckstein Felix F. PhD k.wiegant@umcutrecht.nl Paracelsus Medical University Salzburg Austria
Mastbergen Simon S.C. PhD k.wiegant@umcutrecht.nl University Medical Center Utrecht Utrecht The Netherlands
Lafeber Floris F.P.J.G. PhD f.lafeber@umcutrecht.nl University Medical Center Utrecht Utrecht The Netherlands
Submitted by:Wiegant, Karen MD

Distraction therapy is the first and only treatment for end-stage OA resulting in not just prolonged clinical but also prolonged structural cartilage changes. This gives for the first time the opportunity to study the mechanisms involved in cartilage repair.

Introduction:
For young patients with end-stage knee osteoarthritis (OA), treatment options are limited. Knee joint distraction (KJD) is a new treatment for end-stage knee OA that temporarily unloads the femorotibial cartilage and subchondral bone and preserves the joint as a alternative for joint replacement. The present study evaluates the 2 years follow-up results on both clinical and structural improvement.

Methods:
An open, uncontrolled study was performed including 20 patients (age 49±6 years; 11 females) with end-stage knee OA, considered for total knee replacement.Patients were treated with KJD for 2 months. The study was approved by the medical ethical committee (METC) of the University of Utrecht and all patients gave written informed consent.
An external fixation frame was placed, bridging the knee joint and creating a distance of 5 mm (fig 1). During the treatment most patients (n=17) suffered from single or multiple pin-tract infections, all being successfully treated with antibiotics.
The primary clinical outcome parameter was pain and function by use of the 'Western Ontario McMasters University Index' (WOMAC) questionnaire, with a visual analogue pain score (VAS) as secondary outcome. The primary structural outcome was minimal joint space width (JSW) on weight bearing radiographs. Secondary structural outcomes were quantitative MRI cartilage morphology parameters. Additionally, biomarkers for synthesis (sPIIANP) and breakdown (uCTXII) of collagen type II were evaluated. All structural parameters were analyzed blinded.

Results:
Total WOMAC score increased from 45%±3.6 at baseline to 77%±4.8 at 1 year and sustained at 78%±4.8 at 2 years ($p=0.001$). In parallel, VAS pain score decreased from 73±2.1 at baseline to 31±5.8 at 1 year and 28±6.0 mm at 2 years ($p=0.000$). The clinical improvement coincided with structural tissue changes: the minimum JSW increased from 1.1±0.3 at baseline to 1.6±0.3 at 1 year and 1.8±0.3 mm ($p=0.03$) at 2 years follow-up. The mean JSW showed a similar pattern (fig 2).
Quantitative MRI analysis corroborated these results by an increase in cartilage thickness over total subchondral bone area (ThCtAB) (from 2.4±0.1 at baseline to 3.0±0.5 at 1 year and 2.8±0.1 mm at 2 years; $p=0.05$) and a decrease of the percentage of subchondral bone area that was denuded (dABp: change from 22±5 at baseline to 4.5±8.7 at 1 year and 8±2 % at 2 years; $p=0.004$) (fig3). Comparisons of the MRI and X-ray changes showed clear correlations ($R=0.67$ $p=0.000$, $R=-0.66$ $p=0.005$ for ThCtAB and dABp vs X-ray mean JSW, respectively).
Biomarker analysis showed a PIIANP/CTXII ratio in favour of synthesis for every patient at every timepoint and a trent to increase from 6 months to 2 years follow-up, indicating a net increase in collagen synthesis.

Discussion:
Joint distraction results in significant improvement in both the clinical and structural status that is sustained for at least 2 years. MRIs suggest an increase in cartilage thickness and covering of denuded areas. The mechanical competence of the formed tissue is suggested by increased JSW on weight-bearing X-rays, and the hyaline nature by collagen type II biomarker analysis.

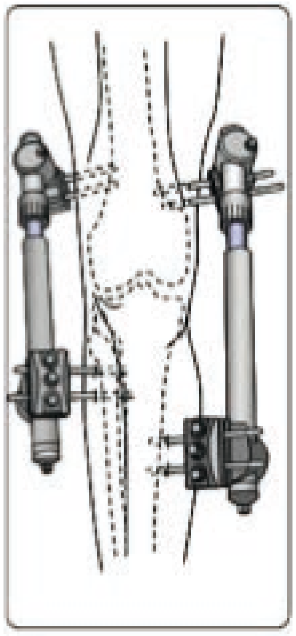

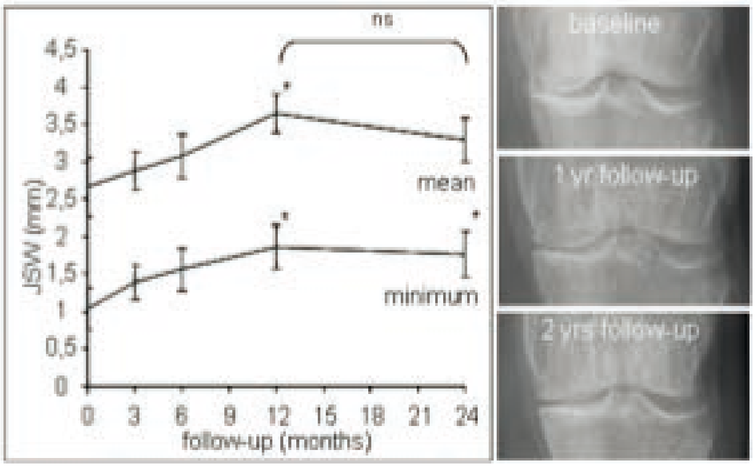

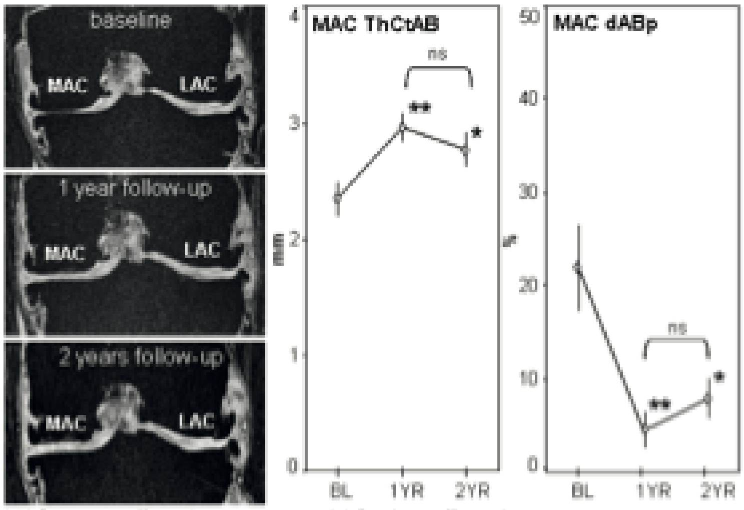

MAC = most affected compartment; LAC = less affected compartment.

-KJD external fixation frame.

-X-rays are representative for a participant of the trial. X-ray mean and minimal JSW. * $p<0.05$

--MRI images are representative for a participant of the trial. MRI ThCtAB and dABp. * $p<0.05$

Joint Distraction in Treatment of Canine Experimentally Induced Osteoarthritis leads to Cartilage Repair accompanied by Sustained Relieve of Pain

Mastbergen Simon S.C. PhD k.wiegant@umcutrecht.nl University Medical Center Utrecht Utrecht The Netherlands
Intema Femke F. MD, PhD k.wiegant@umcutrecht.nl University Medical Center Utrecht Utrecht The Netherlands
van Roermund Peter P.M. MD, PhD k.wiegant@umcutrecht.nl University Medical Center Utrecht Utrecht The Netherlands
Hazewinkel Herman H.A.W. PhD k.wiegant@umcutrecht.nl University of Utrecht Utrecht The Netherlands
Lafeber Floris F.P.J.G. PhD f.lafeber@umcutrecht.nl University Medical Center Utrecht Utrecht The Netherlands

Submitted by:Wiegant, Karen MD

Knee Joint Distraction (KJD) in humans is the only treatment, at the moment, for end-stage OA resulting in not just clinical but also structural cartilage changes. These changes and possible responsible mechanisms are investigated in this canine KJD model.

Introduction:
Knee Joint Distraction (KJD) might be an alternative treatment instead of a total knee prosthesis, especially in relatively young patients with end-stage knee OA. KJD in humans results in long-term clinical benefit and tissue structure modifications. The exact mechanism responsible for this structure modification is unclear. Therefore, joint distraction was applied in a canine experimental model of OA to study the involvement of tissue repair.
Methods:
In 16, skeletally mature, female mixed-breed dogs (mean age 1.6±0.5 years, weighing 18.0±1.3kg), OA was induced in the right knee joint according to the Groove model (condylar surgical applied damage, fig 1). The depth of the applied grooves was restricted to 0.5mm, ensuring an untouched subchondral bone plate. The dogs were randomly divided into two groups. Distraction therapy was performed in 9 dogs. Ten weeks post-surgery, the right knee joint was distracted for 3-5 mm by use of a hinged external fixator for 8 weeks (fig 1). Seven dogs were left untreated. Twenty-five weeks after removal of the external fixation frame, cartilage integrity of the tibial plateau was analyzed macroscopically, histologically and biochemically (collagen damage, proteoglycan content and release). Pain was studied by (un)loading of the joint using force plate analysis (FPA) frequently every 5-10 weeks throughout the study. The study was approved by the University of Utrecht Medical Ethical Committee for animal studies.
Results:
In all with KJD treated animals, macroscopic cartilage damage of the tibial plateau was statistically significant less severe than observed in the control OA dogs (p=0.04). These macroscopic observations were confirmed by histological analysis (fig 2). This improvement of cartilage integrity was even more clearly in the biochemical analysis of the proteoglycan content. Significantly less loss of proteoglycans was seen in the treated dogs compared to the control OA dogs (-8±3% vs. -18±3%; p=0.03; fig 2). Additionally, collagen damage after distraction was diminished, although not statistically significant (+0.3±1%, fig2). Compared to the chondrocyte activity of the OA dogs, the treated animals showed on average a normalization of the newly formed proteoglycan release and total proteoglycan release (-5±3% vs. 9±4%; p=0.05 and 6±6% vs. 20±7%; ns, respectively).
The improvement of cartilage integrity and chondrocyte activity is accompanied with a clear improvement of gait pattern, i.e. improvement in function/pain of the treated joint. Both the brake force as the stance force normalized completely in the treated dogs compared to the OA dogs(-0.05N vs. -0.35N and -0.005N vs. -0.70N, respectively, both p=0.04; fig 3).
Discussion:
Joint distraction results in less cartilage damage and less pain (based on normalization of loading of the affected knee) in a canine model of experimentally induced osteoarthritis. The results of this animal in vivo study corroborate the observed cartilage repair and clinical benefit in human studies.

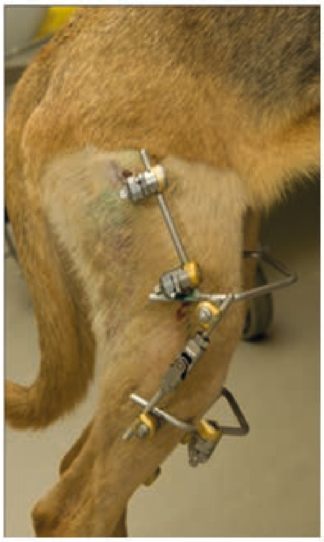

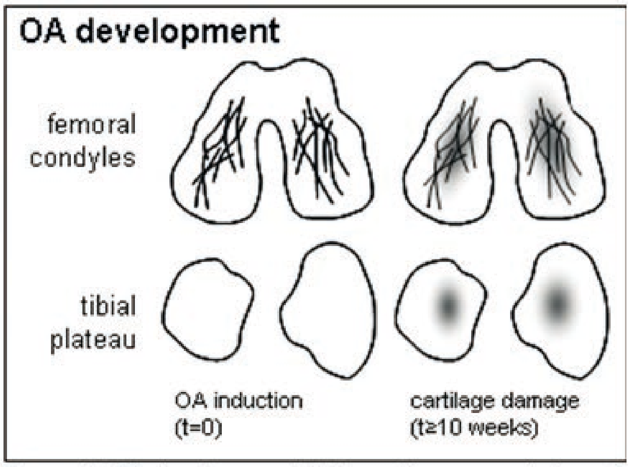

Figure 1. OA development: Schematic representation of location of the grooves on the weight-bearing area of the femoral condyles. The tibial plateau was left untouched.

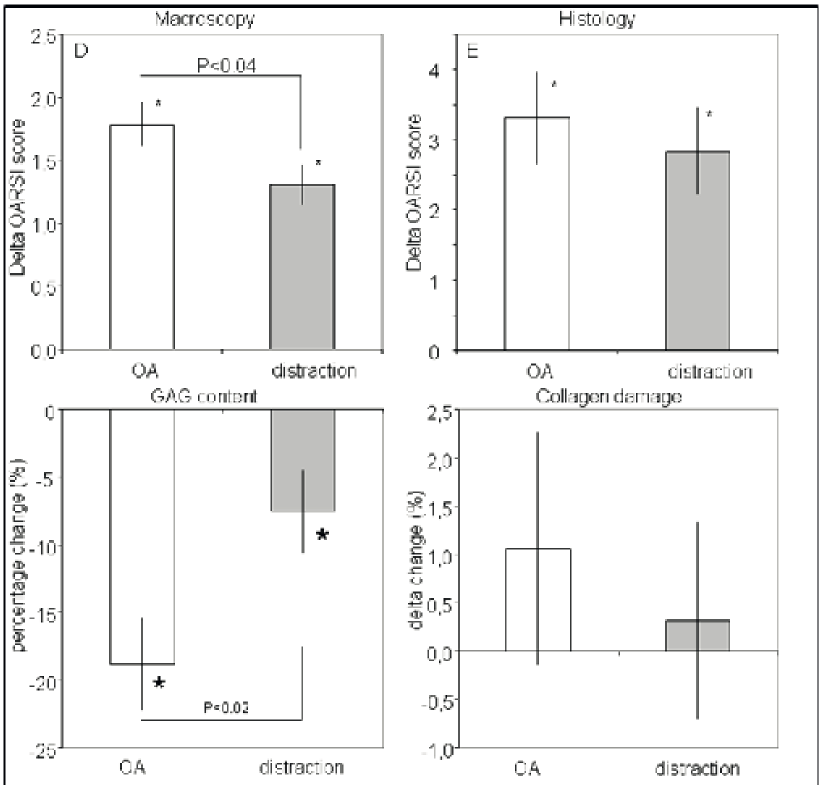

Fig 2. Mean values ±SEM of both the untreated and treated dogs expressed as delta change of the exp. joint compared to the contralateral control joint.

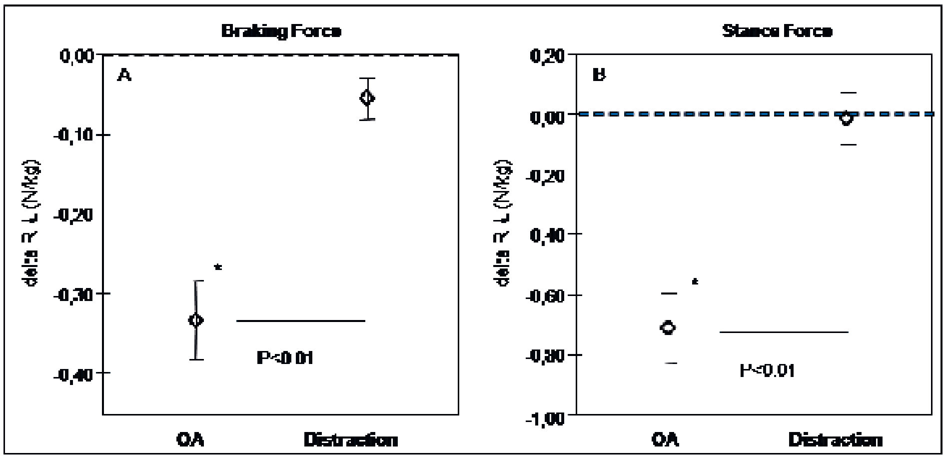

Fig 3. Load distribution between hind legs for FPA (braking and stance force) between untreatd (OA) and treated (distraction)dogs.

-Canine knee joint distraction frame and schematic overview of the Groove model.

-Cartilage outcome parameters.

-Change in load distribution after KJD treatment.

Clarifying the three-dimensional position and the size of the Bennett's lesion (thrower's exostosis) using three-dimensional computed tomography

Goto Hideyuki H.G Nagoya City University Japan
Sugimoto Katsumasa K.S Nagoya Sports Clinic Japan
Kobayashi Masaaki M.K Nagoya City University Japan
Nagaya Yuko Y.N Nagoya City University Japan
Iguchi Hirotaka H.I Nagoya City University Japan
Nozaki Masahiro M.N Nagoya City University Japan
Yoshida Masahito M.Y Nagoya City University Japan
Nishimori Yasuhiro Y.N Nagoya City University Japan
Murase Atsunori M.A Nagoya City University Japan
Otsuka Takanobu T.O Nagoya City University Japan

Submitted by:Takenaga, Tetsuya

This study clarified the etiology of the Bennett's lesion resulting from traction force of the long head of the triceps brachii using 3DCT.

Introduction:
Since Bennett first described bone deposits at the posteroinferior part of the glenoid (Bennett's lesion or thrower's exostosis) in professional baseball pitchers in 1941 [1], a symptomatic Bennett's lesion has often been treated conservatively and surgically. However, the etiology of Bennett's lesion remains controversial owing to the lack of precise anatomical information about the location and morphology of the bony spur. The purpose of the present study is to analyze the location and size of the Bennett's lesion using three-dimensional computed tomography (3DCT) and to clarify the etiology of it.
Patients & methods:
Nine right and two left shoulders of 11 baseball players (all males; mean age, 26.1 years, range 16 to 32 years) with posterior shoulder pain during throwing were evaluated and diagnosed as having symptomatic Bennett's lesion by radiography or ultrasonography. A CT scan was performed with these patients. The GE Proseed SA Libra CT device was used. Image slices 3 mm thick were reconstructed on 3DCT. The location of the Bennett's osteophytes was recorded according to the clock face on the reconstructed image. The thicknesses of the osteophytes were measured at the cranial, center, and caudal positions (see Fig. 1). The length, width, and the distance from the glenoid edge of the bony spurs were measured (see Fig. 2). Seven cases were treated conservatively and four cases treated surgically. All players returned to their previous level of sports activity.
Results:
Bennett's osteophytes were located from the 6:30 to the 8:30 position of the glenoid. The mean cranial, center and caudal distances from the edge of the glenoid were 2.0, 1.5 and 2.9 mm, respectively. The mean length of the bony prominence was 20.3 mm, and the mean cranial, center and caudal widths were 4.3, 9.1 and 6.8 mm, respectively. The mean thicknesses of the bony spurs were 1.8, 6.5 and 4.2 mm, respectively.
Discussion/conslusion:
Bennett described the osteophytes had developed because of excessive use of the arm along with the tremendous pull on the posterior capsule and the triceps tendon[1]. However, several hypotheses have been proposed such as reactive bone formation resulting from capsular traction, or the impaction of the humeral head on the posterior glenoid. An anatomical study of the posteroinferior part of the glenoid revealed that the posterior capsule was attached to the edge of the glenoid rim; that study also demonstrated that the long head of the triceps brachii originated from the 7:30 to the 9 o'clock position of the glenoid with a wide insertion site ranging from 20 to 30 mm, which was consistent with the size and the location of the Bennett's lesion [2]. The present study show that the Bennett's lesion is located closer to the long head of the triceps brachii than to the posterior capsule, supporting the theory of traction force by the long head of the triceps brachii as the main cause of these bony spurs.

References:
1. Bennett GE, et al. JAMA. 1941; 117: 510-514.
2. Sugimoto K, et al. The Shoulder Joint. 2005; 29: 239-242.

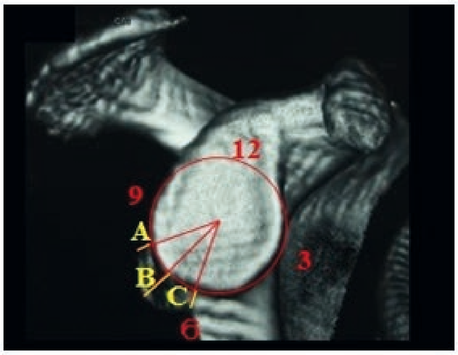

Figure 1. The location of the Bennett's osteophytes was recorded according to the clock face on the reconstructed image (e.g. from the 6 o'clock to the 8 o'clock position). The thicknesses of the osteophytes were measured at the cranial, center, and caudal positions (yellow A,B,C).

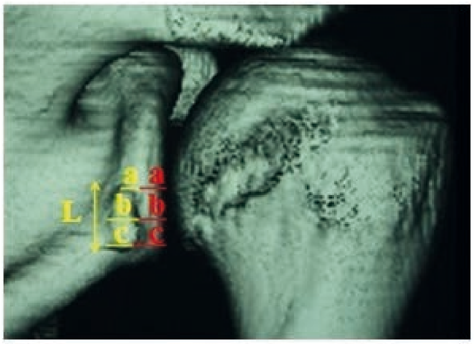

Figure 2. The length (yellow L), widths (yellow a,b,c), and the distances from the glenoid edge (red a,b,c) of the Bennett's osteophytes were measured.

The Functional Flexion Axis of the Knee Corresponds to the Clinical Epicondyle Axis in Posterior-Stabilized Total Knee Arthroplasties

Abe Satomi SA Dr Asahikawa Medical University Japan
Ruike Takuya TR Dr Asahikawa Medical University Japan
Kobayashi Hiroshi HK Dr Asahikawa Medical University Japan
Ito Hiroshi HI Prof., Asahikawa Medical University Japan
Submitted by:Nochi, Hitoshi Dr.,Ph.D

We investigated the femoral rotational alignment in relation to the tibial mechanical axis in patients when implanted using a balanced gap technique. Our study indicates that the functional flexion axis is close to the CEA in PS-TKA.

Introduction:
The assumption that symmetric extension-flexion gaps improve the femoral condyle lift-off phenomenon and the patellofemoral joint congruity in total knee arthroplasty (TKA) is now widely accepted. Conventional understanding of knee kinematics suggests that the femoral component should be rotationally aligned parallel to the surgical epicondylar axis (SEA). On the other hand, the theory of the balanced gap technique suggests the knee be balanced in extension and flexion to achieve proper kinematics and stability of the knee without reference to fixed bony landmarks. The purpose of our study was to evaluate the relationship among rotation alignment of the femoral component and postoperative flexion gap balance, and the femoral rotational alignment in relation to the tibial mechanical axis in patients when implanted using a balanced gap technique.
Materials and Methods:
We studied 53 consecutive primary osteoarthritic (OA) knees that underwent primary Posterior-Stabilized (PS) -TKA (NexGen LPS-flex, Zimmer). All subjects completed written informed consent. The patient population was composed of 7 men and 35 women with a mean age of 72.5 ± 8.3 years. The average height, weight, BMI, weight-bearing FTA, and the patella height (T/P ratio) were 151.7 ± 7.7cm, 62.6 ± 11.8 kg, 27.2 ± 4.5, 184.9 ± 5.9° and 0.93 ± 0.14 respectively. All procedures were performed through a medial parapatellar approach and a balanced gap technique used a newly developed versatile tensor device which can measure the medial and lateral gaps individually and makes use of the balanced gap technique guide with patellofemoral joint reduction introduced in the 56th ORS 2010. Pre- and post-operatively, a condylar twist angle (CTA) was evaluated using computed tomography (CT). To assess the postoperative flexion gap balance, the condylar lift-off angle (LOA) was evaluated using epicondylar view radiographs by adding a 1.5 kg weight at the ankle. Coronal alignment of the tibial component in reference to the tibial mechanical axis (angle θ) was evaluated using plain AP radiography. Data were expressed as mean ± SD and analyzed with Stat View version 5.0.
Results:
The extension gap was well balanced; it was within 3 mm in all cases. The average of the preoperative CTA, the postoperative CTA, the LOA and the angle θ were 6.0 ± 1.5°, 1.2 ± 2.4°, 0.8 ± 1.4° (varus) and 89.7 ± 1.2° respectively. No significant correlation was observed between the postoperative CTA, the LOA and the angle θ. The degree of the clinical epicondylar axis (CEA) to the tibial mechanical axis was 90.1 ± 2.9°. Only one knee needed lateral retinaculum release, because of poor patella tracking when evaluated by the one stitch method.
Discussion:
This study demonstrates that our balanced gap technique, using a newly developed tensor device, achieved good patellofemoral joint congruity and balanced flexion gaps postoperatively. The CEA was perpendicular to the tibial mechanical axis in PS-TKA with well balanced extension-flexion gap achieved by a balanced gap technique. In conclusion, this study indicates that the functional flexion axis is close to the CEA in the knee that underwent PS-TKA.

Innate immune sensors enhanced macrophagic reaction after phagocytosis of wear debris in so-called ‘aseptic‘ condition

Hirayama Tomoyuki TH M.D., Ph.D. t.hirayama@med.id.yamagata-u.ac.jp Yamagata University School of Medicine Department of Orthopaedic Surgery Yamagata-city, Yamagata Japan
Tamaki Yasunobu TY M.D., Ph.D. tamaki@med.id.yamagata-u.ac.jp Yamagata University School of Medicine Department of Orthopaedic Surgery Yamagata-city, Yamagata Japan
Takakubo Yuya YT M.D., Ph.D. takakubo-y@med.id.yamagata-u.ac.jp Yamagata University School of Medicine Department of Orthopaedic Surgery Yamagata-city, Yamagata Japan
Sasaki Kan KS Professor s-kan@msb.biglobe.ne.jp Yamagata University School of Medicine Department of Orthopaedic Surgery Yamagata-city, Yamagata Japan
Takagi Michiaki MT Professor mtakagi@med.id.yamagata-u.ac.jp Yamagata University School of Medicine Department of Orthopaedic Surgery Yamagata-city, Yamagata Japan

Submitted by:Naganuma, Yasushi

Implant wear debris exposed by PAMPs could enhance so-called ‘aseptic‘ local host response initially followed by phagocytosis of macrophages via innate immune sensors.

Introduction
Aseptic loosening of total joints replacement is a one of complications to loss for more times and economics [1]. Toll like receptors (TLR) and NOD like receptors (NLR) are the member of pattern recognition receptors (PRRs). It was reported that pathogen-associated molecular patterns (PAMPs) and damage-associated molecular patterns (DAMPs) were recognized by PRRs and could induce some of immune responses resulting osteolysis [2]. TLR2 recognize lipoteichoic acid (LTA), which is a lipoprotein of consistsing the gram positive coccus cell walls, and NALP3 recognize phagocytosed PAMPs including implant wear debris [1,2]. We analyze patterns of mRNA expression levels in inflammatory cytokines, TLR2 and NALP3 in phagocyte stimulating by titanium (Ti) and Ti with LTA (Ti+LTA).
Materials and Methods
1. Culture of RAW264.7:
RAW264.7 cultured under the condition of humidified 95% air admixed 5% CO2 for 96 hours at 37°C in the media of consisting 90% high glucose DMEM, 10% fetal bovine serum. The cells were passaged over three times. Adherent cells were collected and the adherent cell fraction (2×10^5 cells/ml) was harvested. After 24 hours cultivation, supernate containing non-adherent cells was removed, and DMEM was added [3].
2. Quantitative real-time polymerase chain reaction (qRT-PCR) analysis on mRNA level after exposure of Ti particles coating with LTA to macrophages: 0.15 % Ti particles (Ti) or 0.15 % Ti with 100 ng/ml LTA (Ti+LTA) were added to culture plate. Unstimulated macrophages were cultured as negative control cells. Total RNA was isolated after 0, 1, 3, 6, 12 hours of exposure and reverse transcription was performed. Total RNA was converted into cDNA and enzymatic amplification of the specific cDNA sequences was performed of LightCycler system. Quantitative analysis was performed with the use of LightCycler Software. mRNA of TNF-α, IL-1ß, TLR2 and NALP3 was amplified with the use of its primer at each times. To compare mRNA expression levels, GAPDH was used as control. Statistical analysis was performed by Student’s T test [4].
Results qRT- PCR
1. Accuracy of PCR analysis:
TNF-α, IL-1ß, TLR2, NALP3 and GAPDH were detected in all samples. Each PCR performance was estimated by two types of analysis, which were melting curve and quantification analysis. Each melting curve analysis showed only single peak, which revealed the accurate PCR performance without nonspecific products.
2. Response of macrophages to Ti or Ti+LTA
mRNAs of inflammatory cytokines, TLR2, and NALP3 were detected in RAW264.7 stimulating with Ti and Ti+LTA. Ti+LTA increased significantly mRNA levels of TNF-α at 1 hour and IL-1ß at 3 and 6 hours standardized by GAPDH ($p > 0.05$). mRNA levels of TLR2 were upregurated in Ti and Ti+LTA at 1hour and mRNA levels of NALP3 in Ti+LTA were higer than in Ti at 1 hour .
Discussion

Inflammatory cytokines were increased by stimulating macrophage with Ti+LTA via TLR2 and NALP3-mediated inflammatory signal pathways. The results indicated wear debris exposed by PAMPs could enhance so-called ‘aseptic‘ local host response initially followed by phagocytosis of macrophages via innate immune sensors.

References

[1] Cobelli N, et al: Nat Rheum 2011;7:600-608

[2] Takagi M, et al: J Clin Exp Hematopathol 2011;51:77-92.

[3] Tamaki Y, et al: J Biomed Mater Res B Appl Biomater 2008;84:191-204.

[4] Hirayama T, et al: J Orthop Res 2011;29:984-992

The Effect of Processing, Sterilization and Carrier on the Osteoinductivity of Ovine Demineralized Bone Matrix in an Ectopic Athymic Rat Model

Russell Nicholas Mr n.russell@unsw.edu.au UNSW Sydney Australia
Lovric Vedran Mr v.lovric@unsw.edu.au UNSW Sydney Australia
Yu Yan Associate Professor y.yu@unsw.edu.au UNSW Sydney Australia
Rives Alain Dr a.rives@unsw.edu.au UNSW Sydney Australia
Pelletier Matthew Dr m.pelletier@unsw.edu.au UNSW Sydney Australia
Walsh William Professor w.walsh@unsw.edu.au UNSW Sydney Australia
Submitted by:Russell, Nicholas

Supercritical CO2 sterilization preserves the osteoinductivity of DBM. Ethanol was found to be a superior defatting agent compared to hydrogen peroxide; while saline used as the carrier preserved the grafts osteoinductive potential better compared to pluronic.

Introduction:

Allogeneic demineralized bone matrix (DBM) has been used extensively as a clinical graft material for defects as well as fusion because of its osteoinductive and osteoconductive properties. However, there are concerns over the optimal processing and sterilization methods to eliminate immunological risks whilst maintaining the biological efficacy of the graft. This pilot study aimed to evaluate the effect of Supercritical Carbon Dioxide ($SCCO_2$) treatment on the osteoinductivity of ovine DBM using an ectopic nude rat model.

Patients & Methods:

Cortical bone was milled to a 250-710µm particle size and randomly assigned to a treatment group (Figure 1). Depending on the group, the bone was then defatted (Ethanol or Hydrogen Peroxide), demineralized (HCl), and then terminally sterilized using either gamma irradiation or $SCCO_2$ treatment. Prior to surgery the different DBM preparations (Groups 1-8) were mixed with either sterile saline or Pluronic F-127 and loaded into sterile syringes for surgery. During all procedures aseptic conditions and practices were maintained. Sixteen 8 week old nude rats were anaesthetized and 0.2cc of each DBM preparation was implanted bilaterally into a muscle pocket in each leg (n=4 per group). The rats were euthanized 6 weeks post-operatively and the legs disarticulated. X-ray, µ-CT (Surface Area, Volume and Bone mineral Density) and Haemotoxylin & Eosin histology (qualitative and quantitative) were used as experimental endpoints to determine the amount and quality of new bone formation.

Results:

Groups 1-4 tested the effect of sterilization method (gamma irradiation vs $SCCO_2$)and carrier (Saline vs Pluronic) on the osteoinductivity of the DBM. X-ray results (Figure 2) suggested that sterilization with gamma irradiation (Groups 3-4) inhibited ectopic bone formation compared to $SCCO_2$ (Groups 1-2), with no effect of carrier. However, micro-CT results (Figure 3) showed that despite substantially more bone volume in group 1 ($SCCO_2$ saline), it was not statistically significant ($p < 0.05$). There was no significant difference between either group using pluronic as a carrier (Groups 2 and 4). Histomorphometric analysis confirmed the micro-CT results with substantially more residual DBM/ new bone in group 1compared to groups 2-4.

Groups 5-8 introduced defatting agent (ethanol vs hydrogen peroxide) as an experimental variable. X-ray results (Figure 2) indicated that DBM treated with hydrogen peroxide (Groups 5-6) was resorbed when implanted regardless of sterilization method; whereas ethanol treatment (Groups 7-8) resulted in substantial bone formation. Micro-CT results (Figure 3) confirmed this finding with statistically higher amounts of bone volume in the ethanol groups. Quantitative histology revealed the DBM in groups 5-6 was still present in the muscle pocket, however there was no evidence of remineralization or osteoinductivity. In Groups 7-8 there was substantial biological activity present as indicated by de novo bone, osteoclastic activity and bone marrow formation. There was no statistically significant effect of terminal sterilization method between the ethanol groups (Groups 7-8) for any measured parameter.

Discussion/conclusion:

The results of this pilot study showed that terminal sterilization using $SCCO_2$ did not significantly affect the osteoinductivity of DBM compared to gamma irradiation. Ethanol was found to be a superior defatting agent compared to hydrogen peroxide; while saline used as the carrier preserved the osteoinductive potential of the graft better compared to pluronic.

Group	Defatting	Sterilization	Carrier	Implants
1	Ethanol	$SCCO_2$	Saline	4
2	Ethanol	$SCCO_2$	Pluronic	4
3	Ethanol	Gamma	Saline	4
4	Ethanol	Gamma	Pluronic	4
5	Hydrogen Peroxide	$SCCO_2$	Saline	4
6	Hydrogen Peroxide	Gamma	Saline	4
7	Ethanol	$SCCO_2$	Saline	4
8	Ethanol	Gamma	Saline	4

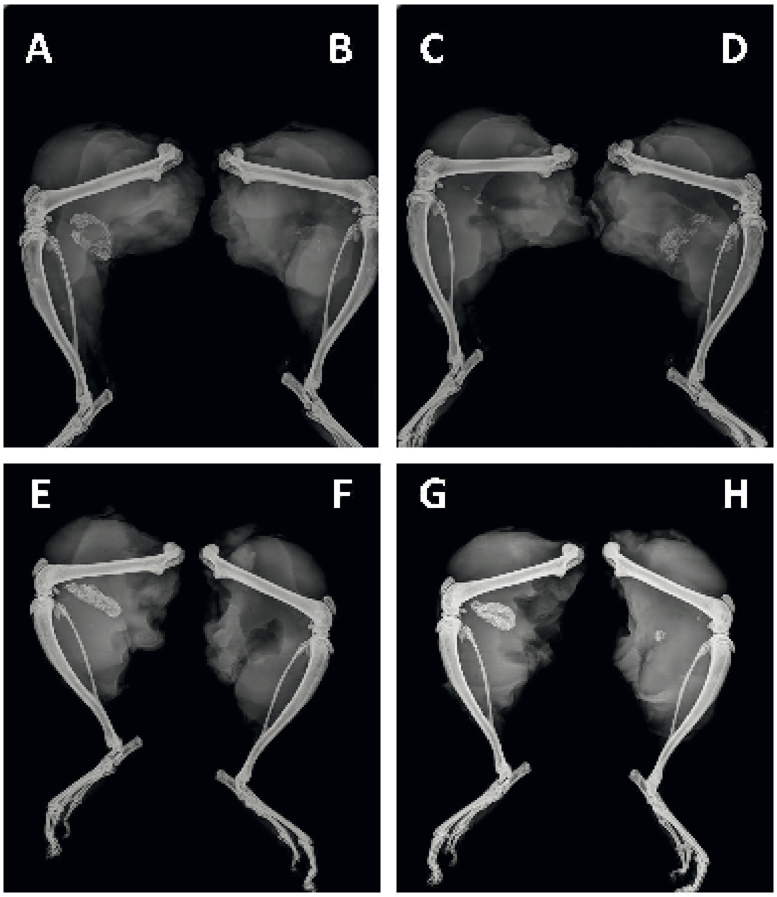

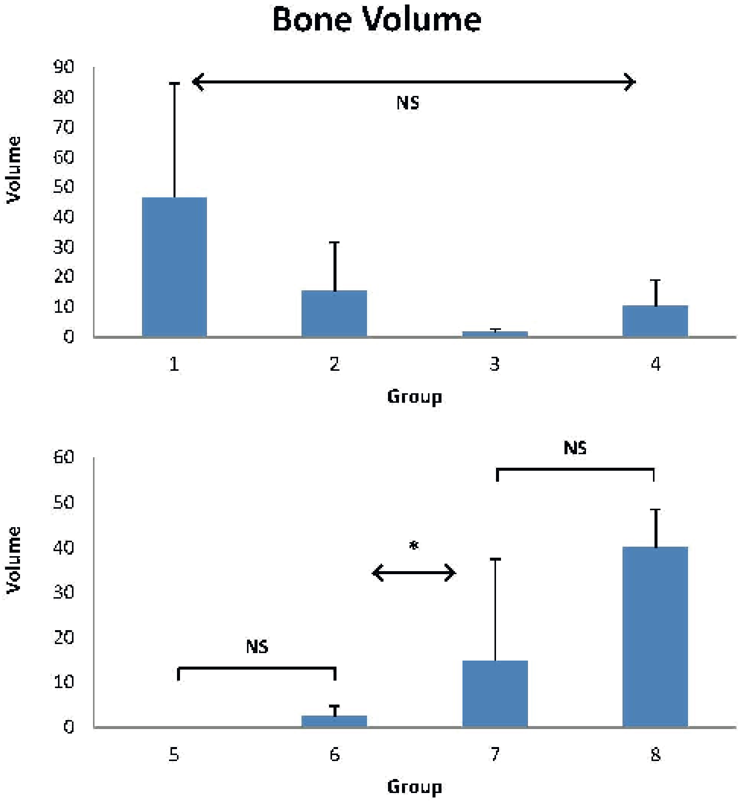

-Figure 1. Summary of processing methods and number of implants for each experimental group

-Figure 2. Representative x-rays comparing ectopic bone formation following ethanol or hydrogen peroxide defatting and SCCO2 or Gamma sterilization: A) SCCO2 Saline (group 1); B) Gamma Pluronic (group 4); C) Gamma Saline (group 3); D) SCCO2 Pluronic (group 2); E) SCCO2 Ethanol (group 7); F) SCCO2 Hydrogen Peroxide (group 5); G) Gamma Ethanol (group 8); H) Gamma Hydrogen Peroxide (group 6).

-Figure 3. Bone volume measured by thresholding Micro-CT scans and 3D image analysis; There was no significant difference between groups 1-4;There was statistically significant more bone volume in groups 7 and 8 compared to groups 5 and 6; * denotes statistical significance at $p < 0.05$, while NS is not statistically significant.

Tip-apex distance (TAD): a comparison between dynamic hip screw (DHS) and Cephalomedullary nail fixation of extracapsular fractures of the hip.

Kiew SiehYean Dr siehyean@gmail.com Royal Liverpool University Hospital Liverpool United Kingdom
Kumar Gunasekaran Mr gunasekaran.kumar@rlbuht.nhs.uk Royal Liverpool University Hospital Liverpool United Kingdom
Submitted by:Kiew, SiehYean Dr

Tip-apex distance (TAD) is a known predictive marker of screw cut-out in fixation of extracapsular hip fractures. In our study we found that cephalomedullary device fixation yields a TAD comparable to that obtained using the dynamic hip screw.

Introduction:
Tip-apex distance (TAD) of >25mm is a known predictive marker for screw cut-out in fixation of extracapsular hip fractures. TAD also allows intra-operative estimation of optimal lag screw placement within the femoral head. The purpose of this study was to compare TAD achieved using a Dynamic Hip Screw (DHS) to that obtained using a Cephalomedullary nail for stabilisation of extracapsular hip fractures.
Methods:
From Oct 2009-Dec 2011, 246 patients underwent stabilisation of extracapsular fractures of the hip using either a DHS or a Cephalomedullary device [Intra-medullary Hip Screw (IMHS) or Intertan nail using one proximal screw]. TAD was measured on intra-operative images, mean TAD was calculated and statistical analysis performed using a one-way ANOVA to look for any significant difference between the devices. Median follow-up duration was 12 months (range 2-27 months). Implant-related complications and revision surgery were used as markers of fixation failure.
Results: (Fig 1) Of the 246 patients, 87 were males, 159 were females; mean age 78 years (26 to 101). The implant used was as per surgeon's choice but the more unstable fractures were stabilised with a Cephalomedullary device. Most of the procedures were performed by trainee surgeons under supervision. In the 150 patients whose fractures were stabilised using a DHS, mean TAD was 17.1mm(±6.5mm). Mean TAD in 81 fractures stabilised with an IMHS was 15.3mm(±5.2mm), whilst in the 15 fractures stabilised with an Intertan nail, mean TAD was 19.2mm(±6.3mm). TAD was suboptimal (>25mm) in 9.3%, 4.9% and 13.3% in the DHS, IMHS and Intertan groups respectively. These results imply that lag screw position achieved using an IMHS is better than that using a DHS ($p=0.084$) or an Intertan femoral nail ($p=0.067$). Complication rates were similar in all groups.
Discussion:
Biomechanical studies have shown the advantage of intramedullary over extramedullary stabilisation of proximal femoral fractures. However, stabilisation of extracapsular hip fractures with a Cephalomedullary nail is more technically demanding than a DHS as the most crucial step (lag screw introduction) is performed during the later part of the surgery. Position of the lag screw in a Cephalomedullary device is constrained by the entry point of the nail, loss of fracture reduction during nail insertion, lag screw guide wire 'skiving' off the lateral cortex and ending up higher in the femoral head. Cochrane review in 2008 recommended use of sliding hip screw for extracapsular hip fractures due to higher complication rates in Cephalomedullary fixation of these fractures. In our series with a heterogeneous surgeon group in various stages of career progression, TAD using Cephalomedullary devices were better than DHS although this did not achieve statistical significance. We propose that if fracture reduction is adequate and maintained during the procedure with no technical issues during surgery, Cephalomedullary device fixation can be of similar or higher standards than DHS fixation.
Conclusion:
Cephalomedullary stabilisation of extracapsular hip fractures though technically demanding is safe and reliable. Newer implants should be used with caution due to learning curve as shown by a higher TAD in the group with Intertan nail fixation.

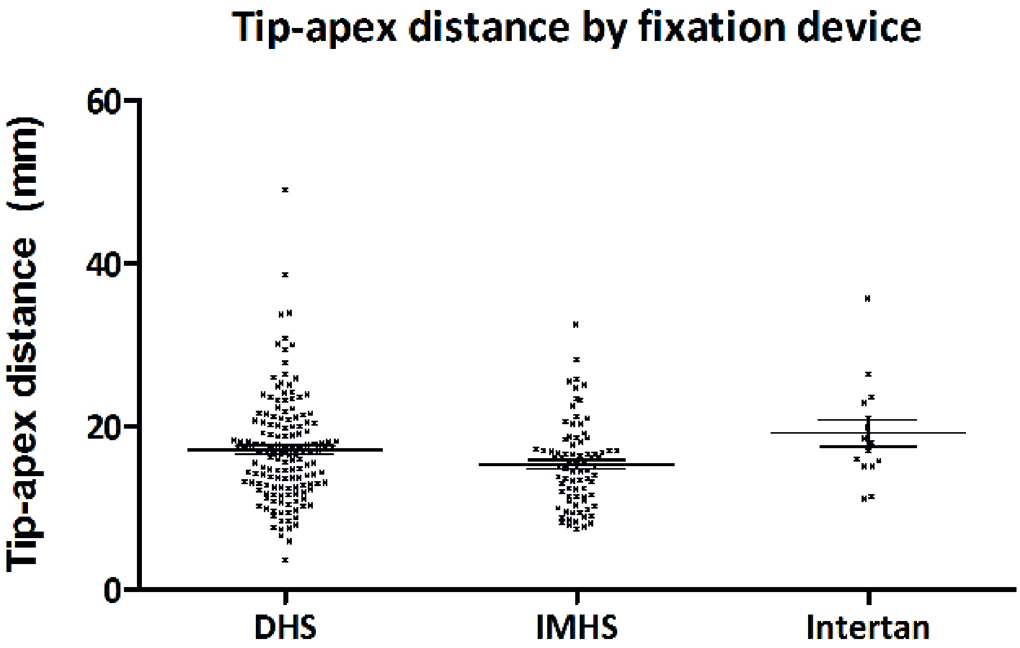

-

-Tip-apex distance by fixation device

Elevated Lysyl hydroxylase 2b expression during experimental OA; the potential cause of persistent synovial fibrosis

Remst Dennis D.F.G. MSc D.Remst@reuma.umcn.nl Radboud University Nijmegen Medical Centre Nijmegen The Netherlands
Blaney Davidson Esmeralda E.N. PhD E.BlaneyDavidson@reuma.umcn.nl Radboud University Nijmegen Medical Centre Nijmegen The Netherlands
Vitters Elly E.L. BSc E.Vitters@reuma.umcn.nl Radboud University Nijmegen Medical Centre Nijmegen The Netherlands
Blom Arjen A.B. PhD A.Blom@reuma.umcn.nl Radboud University Nijmegen Medical Centre Nijmegen The Netherlands
Stoop Reinout R PhD reinout.stoop@tno.nl TNO, Metabolic Health Research Leiden The Netherlands
Snabel Jessica J.M. BSc jessica.snabel@tno.nl TNO, Metabolic Health Research Leiden The Netherlands
Bank Ruud R.A. PhD r.a.bank@med.umcg.nl University Medical Center Groningen Groningen The Netherlands
van den Berg Wim W.B. PhD W.vandenBerg@reuma.umcn.nl Radboud University Nijmegen Medical Centre Nijmegen The Netherlands
van der Kraan Peter P.M. PhD P.vanderKraan@reuma.umcn.nl Radboud University Nijmegen Medical Centre Nijmegen The Netherlands

Submitted by:Remst, Dennis

LH2b expression and the number of pyridinoline cross-links per collagen triple helix are both significantly induced in the synovium of mice with experimental OA. Indicating LH2b is a key factor in OA-related fibrosis.

Introduction:
Fibrosis is a major contributor to joint stiffness in osteoarthritis (OA) and associated with joint pain. In different fibrotic diseases the number of pyridinoline cross-links is increased, resulting in harder to degrade collagen. The enzyme responsible for pyridinoline cross-link formation is Lysyl hydroxylase 2b (LH2b). We examined whether LH2b expression and the number of pyridinoline cross-links per collagen triple helix was elevated in the synovium of mice with collagenase-induced OA, an OA model which is accompanied by fibrosis. In addition, to elucidate the mechanisms by which LH2b is regulated, we investigated whether TGF-ß-induced LH2b was Smad2P or Smad3P dependent in human synovial OA fibroblasts.
Methods:
We induced OA by intra articular injection of collagenase into the right knee joint of C57Bl/6J mice. Mice were sacrificed 7, 21, 28 and 42 days after collagenase injection and mRNA was isolated from the synovium for Q-PCR analysis. Paraffin sections of the murine knee joints were stained immunohistochemically for LH2 to determine the LH2 expression. The number of pyridinoline cross-links per triple helix in synovium was determined with HPCL. All animal experiments were approved by the local animal ethics committee. Human fibroblasts (hSF) were isolated from synovial tissue of knee joints of OA patients undergoing arthroplasty. The hSF were stimulated with TGF-ß alone or in combination with the Smad3P inhibitor SIS3 or the ALK5 kinase inhibitor SB-505124 (SB-5). RNA was isolated and the gene expression for LH2b and collagen type 1 (COL1A1) was analyzed with Q-PCR.
Results:
On al measured time points LH2b mRNA expression was significantly upregulated in the synovium of OA-affected knee joints compared to healthy joints. Histological sections of murine knee joints with collagenase-induced OA showed a large increase in the thickness of the synovial membrane in time (Fig 1). Day 7 showed a strong increase in LH2 staining, at later time points there was still a clear increase but less intense than at day 7. The number of pyridinoline cross-links per triple helix was significant increased after day 7 compared to control knee joints. TGF-ß upregulated both LH2b and Col1A1 gene expression in hSF. SIS3, the Smad3P inhibitorstrongly down-regulated Col1A1in both the presence as absence of TGF-ß. In contrast to Col1A1, LH2b was still induced by TGF-ß in the presence of SIS3. SB-5 blocked both TGF-ß-induced LH2b and Col1A1.

Discussion/Conclusions:

We show a strong upregulation of LH2(b) expression and more than a doubling in pyridinoline cross-links per triple helix in the synovium of murine knee joints with collagenase-induced OA. Suggesting that LH2b is responsible for OA-related fibrosis. TGF-ß, that is elevated during OA, is most likely the driving force of enhanced LH2b expression. We showed previously that TGF-ß-induced LH2b relies onALK5 (Smad2/3) and not ALK1signaling. Blocking both Smad2 and Smad3 signaling prevented TGF-ß-induced LH2b, whereas LH2b was still induced by TGF-ß when only Smad3P was inhibited. Indicating that LH2b is mediated through ALK5/Smad2P. Blocking LH2b directly or via Smad2P may therefore be an interesting intervention to prevent OA-related fibrosis and therefore joint stiffness.

Strontium ranelate treatment for one year did not prevent a new- the third one- atypical femoral fracture in a patient who had been receiving bisphosphonates for 12 years. A case report.

Paganias Christos CG MD, MSc christospaganias@gmail.com KAT Hospital Kifissia, Athens Greece
Schizas Nikitas N MD KAT Hospital Kifissia, Athens Greece
Tilentzoglou Anastasia A MD, PhD KAT Hospital Kifissia, Athens Greece
Anastasopoulos Panagiotis P MD KAT Hospital Kifissia, Athens Greece
Koutroufinis-Tatatsis Anastasios A MD KAT Hospital Kifissia, Athens Greece
Koutsostathis Stefanos SD MD, PhD KAT Hospital Kifissia, Athens Greece
Macheras George GA MD, PhD KAT Hospital Kifissia, Athens Greece

Submitted by:Christos, Paganias MD, MSc

We report the case of a 73 year-old woman that suffered a new- the third one- atypical femoral fracture, probably as a result of 12 years bisphosphonate treatment, even though she was receiving strontium ranelate during the last year.

Introduction

The presence of atypical femoral fractures in patients receiving long-lasting bisphosphonate treatment is wide in the recent literature. In the majority of these cases, the fracture occurs during the period that the patient is receiving the antiresorptive treatment.

Case presentation

A 73 year-old female patient suffering a dull pain at the left subtrochanteric region during the last two months, presented at the emergency department because of acute deterioration of this pain. The patient was not able to walk. According to her medical record, she has been receiving treatment for osteoporosis during the last 13 years and, at the same time, calcium and vitamin D supplementation. During the first 7 years she was receiving alendronate, for the next 5 years risendronate and, during the last year, strontium ranelate. She suffered a low energy subtrochanteric fracture at the right femur 8 years ago and a low energy fracture of the diaphysis of the left femur, 6 years ago. Both of them were fixed with intramedullary nailing. Two months before the occurence of both fractures, the patient reported onset of pain resembling the pain she was suffering the last two months.

X-rays were taken and the presence of an atypical subtrochanteric fracture was revealed. The fracture was located at the lateral cortex of the left femur, without an extension to the medial cortex, probably because of the existence of the intramedullary nail. Apart from this, bone turnover markers were examined, and osteocalcin and CTX serum levels were found to be low. After reviewing patient's older X-rays, we concluded that the pattern of previous fractures was also that of atypical fractures, probably because of the long-lasting bisphosphonate treatment.

The patient was treated conservatively. The already existing intramedullary nail was retained and the patient was advised to walk partially weight- bearing. Strontium ranelate treatment was continued, as it is considered to act both as an anabolic and anticatabolic agent.

Conlusion

This case reflects the ongoing act of bisphosphonates and the existing possibility of the appearance of side effects related to them, even one year after ceasing their administration, no matter if the patient immediately starts receiving an agent that is thought to have an anabolic effect to bone metabolism.

Critical time point for MSCs implantation in Atrophic non-union Determining bone regeneration potential of mesenchymal stem cells implantation between early and late stage of the fracture healing process in atrophic non-union

Tawonsawatruk Tulyapruek Mr. Tulyapruek@gmail.com The university of Edinburgh Edinburgh UK
Spacido Antonello Mr. aspadacc@staffmail.ed.ac.uk The university of Edinburgh Edinburgh UK
Péault Bruno Dr. bruno.peault@ed.ac.uk The University of Edinburgh,University of California at Los Angeles Edinburgh, Los Angeles UK, USA
Simpson Hamish Dr. Hamish.Simpson@ed.ac.uk The university of Edinburgh Edinburgh UK
Submitted by:Tawonsawatruk, Tulyapruek

MSCs implantation can be used as a minimally invasive technique to improve bone regeneration in atrophic non-union model at the early stage of the fracture healing process, not in established atrophic non-union.

Introduction
Diaphyseal atrophic non-unions demonstrate biological impairment of healing. This pathological condition causes patients' disability. MSCs are capable of osteogenesis and they represent a promising alternative approach as a minimally invasive therapy to enhance bone regeneration. However, it has been reported that beneficial effects of MSCs in bone regeneration showed inconsistent results. Recent evidence suggests that the yield and source of MSCs are important factors to determine the successful outcome. In this study we had the hypothesis that stage of the fracture healing process might affect MSC treatment outcome. The aim of this study were to determine the therapeutic effects of MSCs in the atrophic non-union model using a percutaneous injection minimally invasive technique compared between early (3weeks) and late (8 weeks) periods after induced atrophic non-union model.

Materials and methods
30 male, 4-5 month old Wistar rats were used in this study. All the procedures were conducted following approval by the Local Research Ethics Committee and the Home Office, UK according to the animal (Scientific Procedure) Act 1986. An atrophic non-union was created at the tibial mid shaft by stripping the periosteum and endosteum as well as creating a small (1.0 mm) non-critical gap. The tibia was then stabilised with an external fixator. This technique was validated in 11 animals using clinical diagnosis, serial X-rays, histology and micro-CT (see Fig.1). 19 animals were randomly allocated into four groups according to treatment and time point after induced atrophic non-union; Group 1 PBS injection at 3 weeks (n=3), Group 2 rMSCs injection at 3 weeks (n=6), Group 3 PBS injection at 8 weeks (n=5) and Group 4 rMSC injection at 8 weeks (n=5). Either cells or PBS was administered using percutaneous injection technique (see Fig.2). The progression of fracture healing was evaluated using serial X-rays every 2 weeks. Histology and micro-CT were used to assess the fracture healing 8 weeks after cell implantation.

Results
The percutaneous injection of MSCs locally into the atrophic non-union in the early 'post-injury' period (3 weeks) significantly improved the fracture healing process ($p= 0.048$): Five out of six MSC-injected rats demonstrated improvement in fracture healing, whereas none of the PBS-injected rats (0 of 3) showed improvement on serial radiographs. Atrophic non-union with MSCs implantation in the late 'post-injury' period (8 weeks) showed not significant improvement of fracture healing. (2 of 5) ($p> 0.05$) (see Fig.3). Bone union was confirmed using radiographic image, histology and micro-CT (3D image).The bone volume per total volume (BV/TV) from micro-CT in the MSC treatment group at 3 weeks showed significant higher than later treated group and control.

Discussion/Conclusion
Percutaneous local implantation of mesenchymal progenitor cells rescued the fracture healing process in cases destined to progress to non-union. However, the timing after fracture is considerable factor that should be taken into account for MSCs treatment.

Reference
1. HERNIGOU, P., POIGNARD, A., BEAUJEAN, F. & ROUARD, H. 2005. Percutaneous autologous bone-marrow grafting for nonunions. Influence of the number and concentration of progenitor cells. J Bone Joint Surg Am, 87, 1430-7.
2. REED, A. A., JOYNER, C. J., ISEFUKU, S., BROWNLOW, H. C. & SIMPSON, A. H. 2003. Vascularity in a new model of atrophic nonunion. J Bone Joint Surg Br, 85, 604-10.

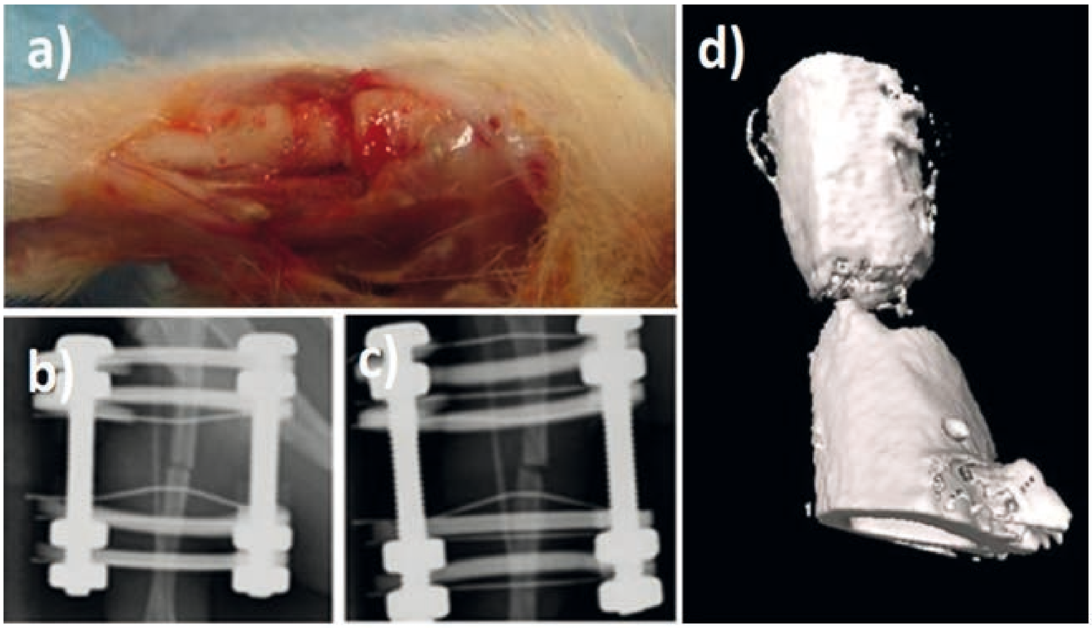

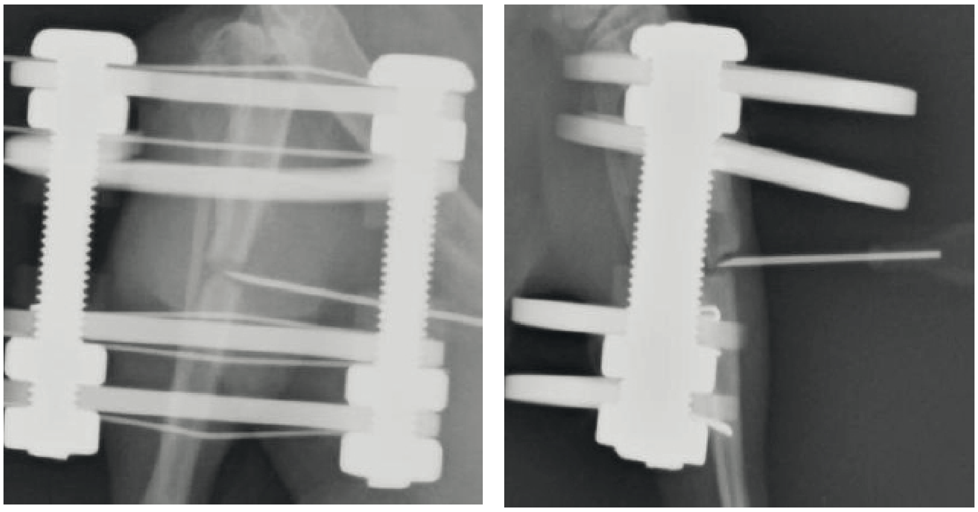

Treatment/weeks after injection cells	At injection time	2 weeks	4 weeks	6 weeks	8 weeks
PBS injection at 3 weeks "control"	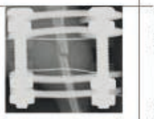	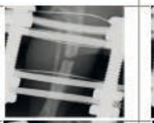	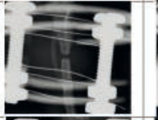		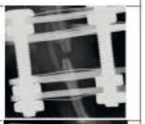
Rat MSCs injection at 3 weeks	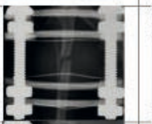	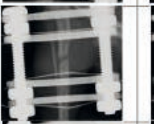	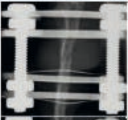	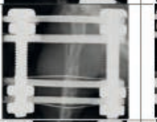	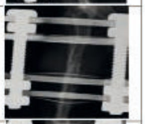
PBS injection at 8 weeks "control"	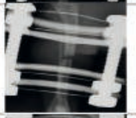	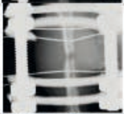	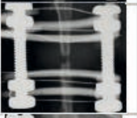	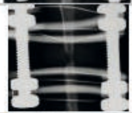	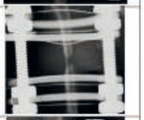
Rat MSCs injection at 8 weeks	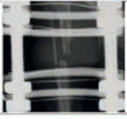			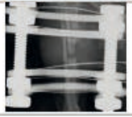	

-Atrophic non-union model:a) Gross appearance at the fracture gap; b) and c) Radiography (AP and Oblique) at 8 weeks post operation showing the typical atrophic non-union d) 3-dimensional image from micro-CT scan showing clearly the rounded ends, both proximal and distal and no bone formation at fracture gap
-Radiographic images of percutaneous injection: The rat MSCs were implantation at the local site of the atrophic non-union model by percutaneous injection technique. Antero-posterior view (left) and lateral view (right)
-The serial radiographic assessment: The serial radiographic of fracture shows progression of healing in rat MSCs treatment group at 3 weeks post injection, whereas in other groups show no sign of fracture healing.

Submitted by:Hua, Jia Dr

Introduction:

This study uses bone tissue engineering (BTE) construct to enhance new bone formation in revision total hip replacement (rTHR) situation. The hypothesis was that the addition of autologous mesenchymal stem cells (MSCs) to a porous metal scaffold coated with a calcium phosphate (CaP) layer will enhance rapid formation of bone within the implant, thus repairing adjacent defect areas and increasing fixation strength.

Methods:

20 sheep were used with two different models: a direct contact model in which the constructs were in direct contact with the host bone and a gap model in which a 2.5mm gap was created between the constructs and the host bone. For the direct contact model, ten female sheep were implanted with CaP coated(1) porous TiAl6V4 cylinders either with no cells or with $1x10^6$ autologous MSCs in a perfusion bioreactor(2) for 7 days. On both right and left sides of the sheep, defects of 10mm diameter were created in the medial femoral condyle and the constructs inserted. For the gap model, 2.5 mm gap was created to simulate bone defects in rTHRs, The animals were euthanized at 6 weeks. The femoral condyles were removed and processed for either undecalcified histology (Toluidine Blue/Paragon stains) and histomorphometric analysis or mechanical push-out tests.

Results:

Mechanical push-out tests There were no statistical differences between both types of implants. The forces required to push the implants out in the gap model were significantly lower than in the direct contact model (Fig. 1). New bone formation: No significant differences in new bone formation between the tissue-engineered and the non tissue-engineered implants ($p>0.05$) were found. New bone formation was between 40% and 50% for the direct contact model. For the gap model, new bone formation was over 20% for both types of implants.

Bone-implant contact: Both implants showed similar results with bone attached to over 50% of the implants' surface ($p>0.05$) (Fig. 2). In the gap model, the tissue-engineered implants showed slightly more bone contact than the non tissue-engineered ones but the difference was still insignificant ($p=0.917$). Overall, the new bone formation occurred more on the periphery of the implant than in the centre.

Histological analysis: For all the samples bone ingrowth into the pores was observed as well as direct bone-implant contact. The new bone tissue was well vascularised.

Discussion:

Bone ingrowth into the porous implants was demonstrated by histology. Location and vascularisation of the constructs, a 20% reduction in pore size exhibited by the tissue-engineered implants compared to the non-tissue engineered ones and the length of the study may be accounted for the slight decrease in new bone formation shown by the tissue-engineered constructs.

Histological evidence of direct bonding between the implant and bone was found, thus demonstrating the osteoconductive potential of the CaP coating. In the defects with gap the MSCs added to the scaffolds differentiated to osteoblasts with concomitant bone tissue formation on the surface of the implant taking place, thus showing a higher implant-bone contact area. Therefore, the forces necessary to push the tissue-engineered implants out of the bone were higher.

Since the gap model is representative of the bone defects found in rTHRs the results indicate that the addition of MSCs to porous CaP coated TiAl6V4 scaffolds for the regeneration of the bone stock at rTHRs may be beneficial.

Comparison Of Different Techniques For Flexible Fixation Of Open Book Type Pelvic Injuries With Two Leg Alternate Loading. A Biomechanical Study

Agarwal Yash Y Mr. yash.agarwal@aofoundation.org AO Research Institute Davos Davos Switzerland
Stuby Stuby S Dr. med. fabian.stuby@uni-tuebingen.de Ebrherd Karls University Tuebingen Germany
Windolf Markus M Mr. markus.windolf@aofoundation.org AO Research Institute Davos Davos Switzerland
Shiozawa Thomas T Dr. med. Thomas.shiozawa@uni-tuebingen.de Ebrherd Karls University Tuebingen Germany
Ochs Björn BG Dr. med. gochs@bgu-tuebingen.de Ebrherd Karls University Tuebingen Germany
Gonser Christoph CE Dr. med. cgonser@bgu-tuebingen.de Ebrherd Karls University Tuebingen Germany
Stöckle Ulrich U Dr. med. ustoeckle@bgu-tuebingen.de Ebrherd Karls University Tuebingen Germany
Gueorguiev Boyko B Dr. Boyko.gueorguiev@aofoundation.org AO Research Institute Davos Davos Switzerland

Submitted by:Agarwal, Yash

Pubic symphysis injuries are stabilized with plates, bridging the symphysis. The technique results in screw loosening or plate breakage. The aim of this study was to investigate the effect of the rigidity in fixation of pubic symphysis on implant performance.

Background

The biomechanical stability of the pelvic ring is essential for the entire musculoskeletal function [1]. Open Book injuries (AO 32 B1.1 and B1.2) are usually stabilized with plates, bridging the pubic symphysis. The technique results in screw loosening or plate breakage, leading to implant removal. The aim of this study was to investigate the effect of the rigidity in fixation of pubic symphysis on implant performance.

Methods

Six human cadaver pelvises with proximal femora and intact ligaments were used in this study. They were firstly tested in intact state, applying non-destructive two leg alternate cyclic sinusoidal loading through the proximal femora, increased from 170 N to 340 N over 1000 cycles (1 Hz, increase 0.17 N/cycle) [2]. The relative movements at the pubic symphysis in all six degrees of freedom were measured and calculated in terms of translations and rotations [3] via Motion Tracking. An Open Book injury was then simulated and stabilized with a modular LCP-based implant system, fixed with two locking screws on each symphysis side, both sides connected with a variable number of rods. The stabilization was consecutively performed with 1-rod (flexible in the symphyseal transversal plane), 2-rod (fixed parallel to the plain of the rods) and 4-rod (rigid) configurations and tested non-destructively in a randomized sequence using the same test protocol as before. Finally, a destructive cyclic test with increasing load, starting from 340 N (1 Hz, increase 0.17 N/cycle) was performed until construct failure occurred, which was defined as at least 2 mm translation along the symphyseal transversal axis. Statistical analysis was performed with Shapiro Wilk Test, paired T-Test and General Linear Model Repeated Measures using SPSS software package.

Results

Increasing number of connecting rods generally results in decline of symphysis movements. The 1-rod shear translational movement along the symphyseal vertical axis at 170 N was significantly bigger compared to the 2-rod and 4-rod configurations (pthe symphyseal transversal axis at 340 N was significantly larger compared to the 2-rod and 4-rod configurations (p

Conclusion

The biomechanical performance of the stabilization with the 2-rod configuration was superior compared to the 1-rod and 4-rod constructions, considering its similarity to physiological pubic symphysis movements, and showed the lowest implant loosening and highest stability of fixation with potential to resist more than 1.5 times body weight until implant failure occurs.

References

[1] Denton, Biomechanics of the Pelvis, 1980, 211-21, Basal Facts
[2] Agarwal Y, Stuby F, Gueorguiev B, et al. Biomechanical Invesitgation of pubic symphysis movements with two leg alternate loading, 2012, Proceedings of European Society of Biomechanics, Lisbon2012
[3] Walheim and Selvik, Mobility of the Pubic Symphysis: In vivo Measurements with an Electromechanical Method and a Roentgen Stereo Photogrammetric Method, 1984, 203-08, Acta Orthopaedica

Standardized synthetic femur models : a biomechanical comparison

Jakubowitz Eike E.J. Dr. Jakubowitz@implantatforschung.de University Hospital Giessen and Marburg GmbH Giessen Germany
Heisel Christian C.H. Prof. Heisel@implantatforschung.de ARCUS-Sportklinik Pforzheim Germany
Reinders Jörn J.R. Dipl.-Ing.(FH) Reinders@implantatforschung.de University Hospital Heidelberg Heidelberg Germany
Sonntag Robert R.S. Dipl.-Ing. Sonntag@implantatforschung.de University Hospital Heidelberg Heidelberg Germany
Kretzer Jan Philippe J.P.K. Dr. Kretzer@implantatforschung.de University Hospital Heidelberg Heidelberg Germany

Submitted by:Nadorf, Jan Dipl.-Ing.(FH)

Within this study we could show that the new 4th generation synthetic femur designs could qualitatively give comparable results to older synthetic bone models regarding biomechanical tests, like primary stability measurements on cementless hip stems.

Introduction:
Concerning biomechanical research, human specimens are preferred to achieve conditions that are close to the clinical situation. On the other hand, synthetic femurs are used for biomechanical testing instead of fresh-frozen human femurs, to create standardized and comparable conditions. A new generation of synthetic femurs is currently available aiming to substitute the validated traditional one. Structural femoral properties of the new generation have already been validated, yet a biomechanical validation is missing.
The aim of our study was to analyse potential differences in the biomechanical behaviour of two different synthetic femoral designs by measuring the primary rotational stability of a cementless femoral hip stem.
Methods:
The cementless SL-PLUS® standard stem (size 6, Smith&Nephew Orthopaedics AG, Rotkreuz, Swizerland) was implanted in two groups of synthetic femurs. Group A consists of three 2nd generation femurs and group B consists of three 4th generation femurs (both: size large, composite bone, Sawbones® Europe, Malmö, Sweden). Using an established method to analyse the rotational stability, a cyclic axial torque of ±7.0Nm along the longitudinal stem axis was applied. Micromotions were measured at defined levels of the bone and the implant. The calculation of relative micromotions at the bone-implant interface allowed classifying the rotational implant stability.
Results:
Lowest relative micromotions were located near the isthmus for both designs (2nd 3.47 ± 1.43mdeg/Nm and 4th 5.97 ± 0.39mdeg/Nm), whereas highest relative micromotions were located at distal tip for both designs (2nd 8.42 ± 1.38mdeg/Nm and 4th 8.40 ± 0.39mdeg/Nm). No statistically significant differences were found between 2nd and 4th generation femurs in the distal part (2nd 8.42 ± 1.38mdeg/Nm and 4th 8.40 ± 0.39mdeg/Nm; $p>0.05$), but proximally (2nd 3.63 ± 1.10mdeg/Nm vs. 4th 6.55 ± 1.27mdeg/Nm; $p<0.05$). Compared to the 2nd generation, the 4th generation femur resulted in less absolute micromotions and less standard deviation of micromotions.
Discussion:
Compared to other implant designs, the SL-PLUS® stem resulted in low relative motions regardless the used synthetic femur. Within the two distal measuring levels, no significant differences could be observed. Proximally, at the level of the Trochanter minor, mean relative motions nearly doubled from group A to B. However, the anchorage principle of the SL-PLUS® stem was still similar in both synthetic femurs. Qualitatively, both synthetic femurs revealed a proximal fixation of the stem. Although the values of relative motion slightly differs, 4th generation synthetic femurs are suitable to achieve similar results for measuring the primary stability of cementless femoral hip stems compared to 2th generation synthetic femurs.
Future measurements with human specimens should validate weather one of the synthetic bone models is closer to the human situation.
Within this study we could show that the new 4th generation synthetic femur designs could qualitatively give comparable results to older synthetic bone models regarding biomechanical tests, like primary stability measurements on cementless hip stems.

A simplified method to determine joint loading as a surrogate marker of pain/disability in a canine model of osteoarthritis, validated using force plate analyses as a gold standard

Hazewinkel Herman H.A.W. PhD k.wiegant@umcutrecht.nl University of Utrecht Utrecht The Netherlands
Doornebal Arie A. PhD k.wiegant@umcutrecht.nl University of Utrecht Utrecht The Netherlands
Barten-van Rijbroek Angelique A.D. k.wiegant@umcutrecht.nl University Medical Center Utrecht Utrecht The Netherlands
Mastbergen Simon S.C. PhD k.wiegant@umcutrecht.nl University Medical Center Utrecht Utrecht The Netherlands
Lafeber Floris F.P.J.G. PhD f.lafeber@umcutrecht.nl University Medical Center Utrecht Utrecht The Netherlands

Submitted by:Wiegant, Karen MD

Advantages of the 4P-balance vs force plate analysis: less time consuming, no intensive training of dogs or personnel required, and can be performed at any location. This makes the 4P-balance a useful complementary method for measuring disability in dogs.

Introduction

For dogs, force plate analysis (FPA) is a widely used method for joint loading as surrogate markers of pain and (dis) ability, a time consuming technique which needs prolonged training for the dogs as well as the dog-trainers. A simplified method to analyse joint loading was developed; a mobile weighing platform with four individual scales (4-plates-balance: 4P-balance). Loading of the stifle joints was evaluated during progression of OA.

Methods

In twelve skeletally mature dogs (mixed breed, mean age 1.2±0.1 years, weighing 16.6±0.3 kg) experimental OA was induced in the right stifle joint according to the Groove model (condylar surgical applied damage, fig 1). The depth of the applied grooves was restricted to 0.5mm, ensuring an untouched subchondral plate. Earlier experiments established that in this model OA is developed at both the femoral condyles and at the surgically untouched tibia plateaus at 10 weeks post-surgery.

FPA (in N/kg total), and weighing on the 4P-balance (in kg/kg total) was performed twice at baseline and at every 5 weeks. At the 4P-balance five measurements of 10 seconds were performed, analysed and compared to all degrees of freedom of the FPA (stance (Fz), brake (Fy-max) and propulsion force (Fy-min)).

Results

A statistical significant correlation between measurements on the 4P-balance and the FPA for the experimental right hind leg is found, except for the Fy-min (R=+0.52, p=0.000; R=+0.52, p=0.000; R=+0.30, p=0.786 for respectively Fz, Fy-max and Fy-min).

Additionally, when expressed as a change between the right and left joint, again a statistical significant correlation was found between the 4P-balance and the FPA (R=+0.71, p=0.000; R=+0.70, p=0,000; R=+0.61, p=0,001 for respectively Fz, Fy-max and Fy-min).

During development of OA similar changes are seen for both methods. From baseline to 10 weeks follow-up there is a significant decrease in load of the right hind leg (4Pb p=0.02; FPA-Fz p=0.02; FPA-Fymax p=0.006 and FPA-Fymin ns) and at 10 weeks follow-up there is a significant difference in load distribution of both hind legs (4Pb p=0.008; FPA-Fz p=0.005; FPA-Fymax p=0.01 and Fymin ns).

Discussion

Pain/disability, due to OA in the extremities is difficult to measure in animal models, including dogs. FPA (force plate analyses) is the gold standard to evaluate (un)loading/(dis)ability of the extremities in dogs. The present study clearly demonstrates that the use of this novel designed mobile weighing platform with four individual scales with parallel computer controlled registration is a sufficient surrogate for FPA as a measure for pain disability due to development of OA. The technique is less expensive, less time-consuming and simpler to accomplish, because it can be performed at any location. Although, FPA is clearly a more elaborated technique and provides more information about gait and different forces and the 4-plates balance is a more static measurement, the latter may be of good additional value in studies evaluating pain/disability in canine models of OA.

Mechanical factors dominate over the influence of the joint homeostasis in trauma induced experimental osteoarthritis in the goat

Beekhuizen Michiel M. MD k.wiegant@umcutrecht.nl University Medical Center Utrecht Utrecht The Netherlands
Mastbergen Simon S.C. PhD k.wiegant@umcutrecht.nl University Medical Center Utrecht Utrecht The Netherlands
Barten-van Rijbroek Angelique A.D. k.wiegant@umcutrecht.nl University Medical Center Utrecht Utrecht The Netherlands
Custers Roel R.J. MD, PhD k.wiegant@umcutrecht.nl University Medical Center Utrecht Utrecht The Netherlands
Creemers Laura L.B. PhD k.wiegant@umcutrecht.nl University Medical Center Utrecht Utrecht The Netherlands
Saris Daniel D.B.F. MD, PhD k.wiegant@umcutrecht.nl University Medical Center Utrecht Utrecht The Netherlands
Lafeber Floris F.P.J.G. PhD f.lafeber@umcutrecht.nl University Medical Center Utrecht Utrecht The Netherlands

Submitted by:Wiegant, Karen MD

These data suggest that the development of OA is more dependent on the biomechanical component, as cartilage integrity is mostly affected in the medial compartment. In this model unilateral surgical damage does not result in generalized OA.

Introduction
At the moment osteoarthritis (OA) is seen as a multifactorial disease and develops due to several risk factors. In the present study we investigated the role of biomechanical loading and disturbed biochemical joint homeostasis in the development of osteoarthritis, in an experimental caprine model of joint damage.
Methods
In nine skeletally mature female milk goats (72.9±2.9 kg, age is unknown), cartilage damage was introduced in the right stifle joint according to the Groove model. Grooves were made with a K-wire with a bend tip, only on the medial femoral condyle and maximally 0.5mm deep to preserve the subchondral bone plate from damage (fig1). The left stifle joint served as a control. After 20 weeks the goats were euthanized and the cartilage and synovial tissue was analyzed on macroscopical, histological (both OARSI goat score) and biochemical (proteoglycan (PG) turnover) OA characteristics.
Results
Macroscopic analysis showed a significant increase in the OARSI goat cartilage damage score for both the femoral and tibial experimental medial compartment compared to control (femur and tibia; +170% p=0.004 and +43% p=0.05 respectively). No effect on the ungrooved lateral compartment was seen. The histological analysis of the cartilage corroborated these results. A significant increase in the OARSI score for the experimental medial compartment (+226% p=0.000 and +82% p=0.007, respectively for femur and tibia) was seen. Biochemical analysis showed a decreased PG content in the medial experimental compartment compared to control (femur -12% p=0.04 and tibia -7% p=0.04). Delta-changes for macroscopic and histological analysis and percentage-change for biochemical analysis between experimental and control compartment are summarized in figure 1. There was a slight increase in synovial inflammation in the experimental joint (p=0.003). For all previous mentioned analyses, no changes in the experimental lateral compartment or the control joint were found.
Discussion
The present study shows clearly that the development of joint damage is much more dependent on the biomechanical component, since all detectable damage is in the medial compartment of the experimental stifle joint; at the femoral condyle where damage was surgically induced and at the opposite tibial plateau. Joint homeostasis is somewhat disturbed, indicated by moderate synovial inflammation. However, this did not lead to generalised OA within this time period.

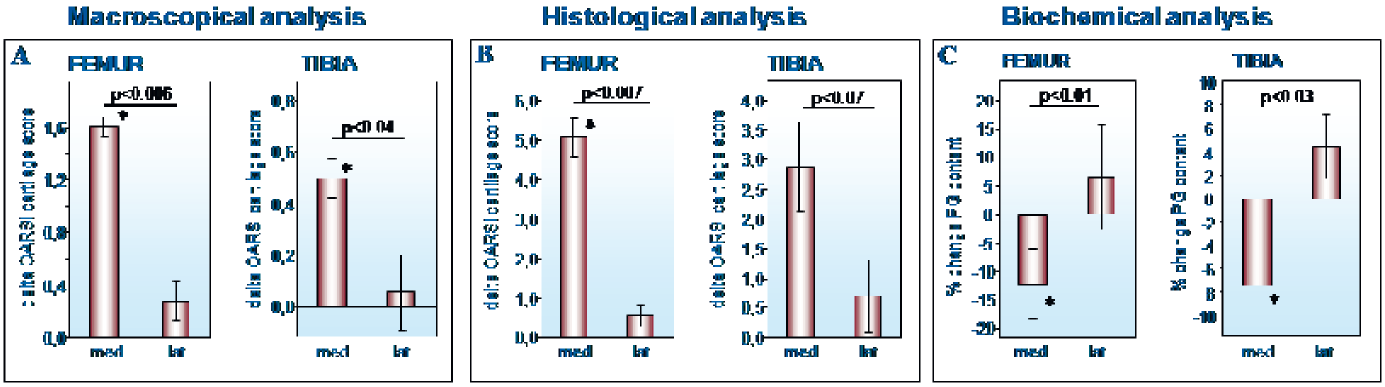

Fig 1. Macroscopical (a), histological (b) and biochemical (c) evaluation of cartilage. Delta change for macroscopical and histological analysis. Percentage change for biochemical analysis. Changes are expressed as experimental versus control compartment. med = medial, lat = lateral.

-Cartilage outcome parameters.

Role of Rotating Hinge Knee in Revision Arthroplasty

Rao Biyyam B M Mr madhu.rao@nhs.net St.Richard's Hospital, Western Sussex Hospitals NHS Trust Chichester UK
Moss Michael M C M Mr michael.moss@wsht.nhs.net St.Richard's Hospital, Western Sussex Hospitals NHS Trust Chichester UK
Taylor Lee L J T Mr lee.taylor@wsht.nhs.net St.Richard's Hospital, Western Sussex Hospitals NHS Trust Chichester UK
Vafaye John J V F Mr john.vafaye@me.com UK Specialist Hospitals London UK
Submitted by:Rao, Biyyam Mr

Prospective study to evaluate the clinical and radiographic outcomes of a newer generation Rotating hinged total knee in a large cohort of patients of revision knee arthroplasty with major bone loss and soft tissue deficiencies.

Introduction
Historically older generation of hinged knee replacements have been known to have inferior results. The aim of this prospective study is to evaluate the clinical and radiographic outcomes of a newer generation hinged total knee in a large cohort of patients of revision knee arthroplasty with major bone loss and soft tissue deficiencies.
Methods and Materials
In this prospective study we include 108 patients undergoing Revision knee arthroplasty using modern Rotating Hinged knee (RHK) prosthesis (Zimmer Inc., Warsaw, Indiana). Indications for revision knee arthroplasty included periprosthetic infections with major bone loss (39 patients), aseptic loosening with major osteolysis (32 patients), periprosthetic fractures around knee (04 patients), failed Unicompartmental knee replacements with major bone defects (04 patients), mal-alignment of prosthesis (6 patients), unexplained painful knees (04 patients) and ligamentous instability (19 patients). To address the combined bone loss and collateral instability, we used the Rotating Hinged total knee prosthesis in all 108 patients(Fig.1). Associated bony defects were classified according to Anderson Orthopaedic research institute (AORI) classification. We used 30 tibial and 4 femoral trabecular metal cones (Zimmer Inc., Warsaw, Indiana) in type 2 and type 3 AORI defects (Fig.2) to address the bone loss along with RHK. The mean age of patients was 76 years (range 56-92 years) with 64 men and 44 women. The mean follow up of this study is of 34 months (range 18 : 48 months).
Results
The mean Oxford scores improved from 21 to 32 (p value : 0.006) and mean American knee society scores (KSS) improved from 32 to 76 (p value 0.001). Based on KSS results we had 52% excellent results, 32% good, 14% fair and 6% poor results. The SF-36 mean physical functioning score was 46.09 points (SD : 3.34), and the SF-36 mean mental functioning score was 51.57 points (SD - 17.73). Radiographic analysis showed non progressive radiolucent lines around tibial stems and femoral stems in 2 patients but no subsidence of implant was noticed in any patient. Of these one had to be re-revised for continual pain. Complications included 4 deaths from unrelated causes, 1 above knee amputation for recurrent infection, 3 re-revisions for infections and 2 infections on long term suppressive antibiotics. There was one periprosthetic fracture around tibial stem treated conservatively and one femoral stem disengagement (Fig.3) with no untoward knee functional results.
Conclusions
With advent of modern rotating hinge devices there appears to be place for them in revision knee arthroplasty especially with major bone loss and gross ligamentous instability. The newer generation rotating hinge knee prosthesis are 95% condylar weight bearing (Zimmer Inc., Warsaw, Indiana), which appear to have better functional outcome in revision knee arthroplasties compared to the previous designs and studies. Still use of these hinge prostheses should be reserved for extreme circumstances, such as for gross instability, massive bone loss, periprosthetic fractures, and chronic dysfunction of the extensor mechanism. Use of less constrained devices is recommended whenever possible, and revision surgery should be performed as soon as failure is diagnosed to avoid massive bone loss.

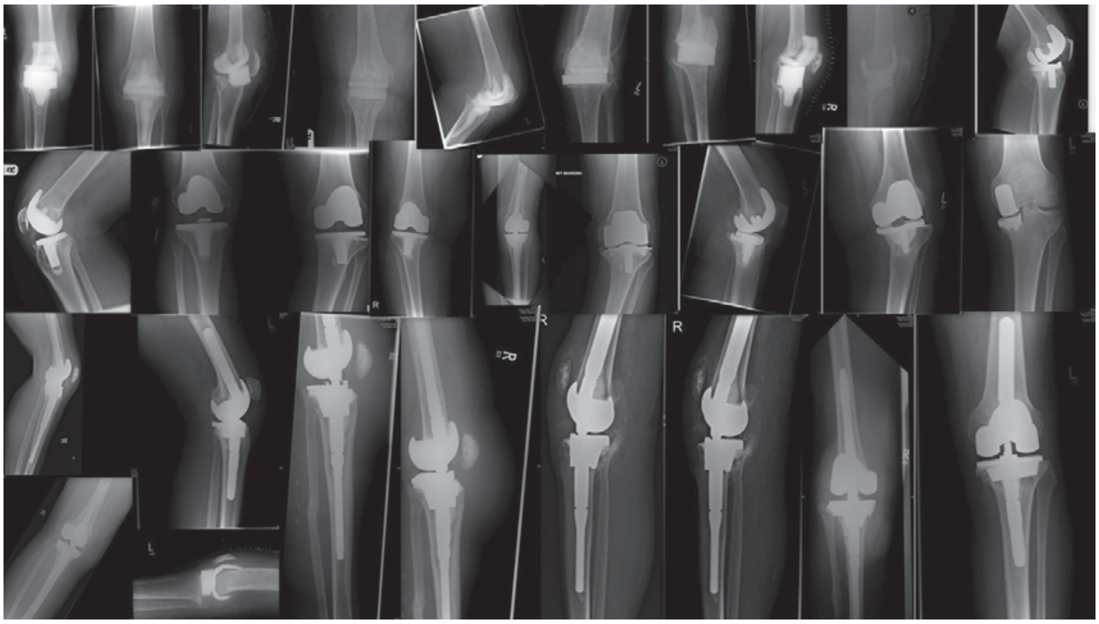

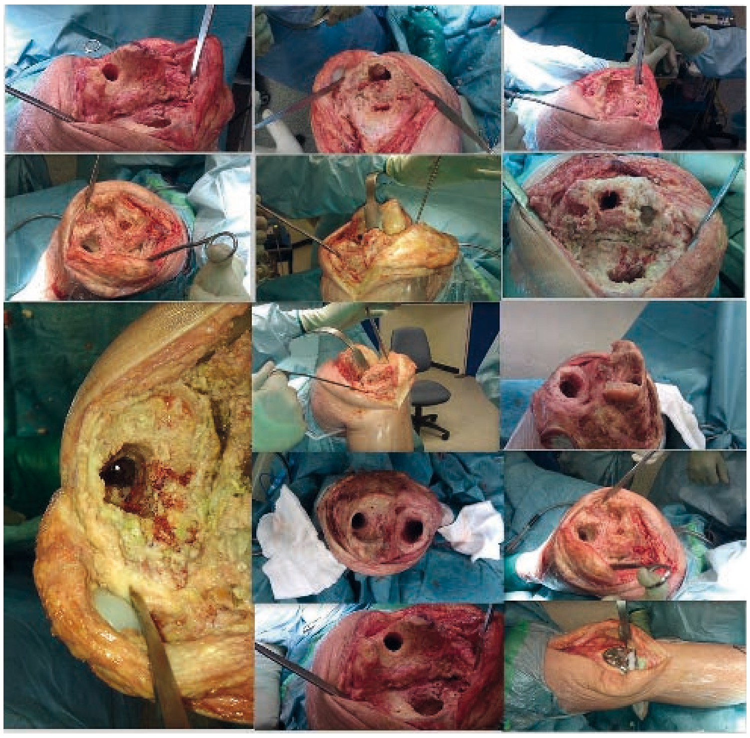

-Pre and post operative radiographs of Rotating Hinge Knee
-AORI Type 2 and 3 defects
-Case examples with few Tantalum cones and One complication of Femoral stem Disengagement

Monitoring of cement injection during a verterbroplasty by time-lapsed computed tomography and micro-finite element modelling reveals the migration of high stresses concentration in the bone structure.

Zderic Ivan I MSc Ivan.Zderic@aofoundation.org AO Research Institute Davos Switzerland
Boger Andreas A PhD andreas.boger@hs-ansbach.de HS-Ansbach Ansbach Germany
Windolf Markus M MSc markus.windolf@aofoundation.org AO Research Institute Davos Switzerland

Submitted by:Stadelmann, Vincent PhD

Incremental cement injection under time-lapsed CT offers new opportunities for the characterization of cement flow and associated mechanical effects during vertebroplasty procedures.

Background

Prophylactic vertebroplasty, the percutaneous injection of bone cement into a weak vertebral body (VB), has been shown to reinforce the bone and possibly to minimize fracture risks[1]. Cement leakage is still causing severe complications, and smaller volumes of cement can reduce its occurrence[2]. But a significant mechanical benefit is only obtained when the cement filling connects both endplates[3] , which inevitably increases the leakage risk. A better understanding of the cement flow into bone is thus required to develop vertebroplasty with minimized leakage risks. In this regard, the present study aimed at developing tools to monitor the cement filling and its mechanical impact during a stepwise injection.

Methods

A fresh frozen human cadaveric L1 vertebra was prepared for augmentation: two vertebroplasty needles were inserted transpedicularly into both pedicles to irrigate the VB with 100 ml of water. Prior to augmentation, the VB was XtremeCT-scanned (Scanco, Switzerland) at 82µm nominal resolution. The VB was then fixed on a custom carbon holder in the center of a CT bore (Siemens Emotion6). An injection device was connected to a PEEK cannula inserted through the left pedicle (Fig. 1a) for the injection of 10ml VertecemV+ cement (Synthes, Switzerland). After each millilitre of injection, the VB was CT-scanned (0.63mm resolution). Each CT image was then registered and remeshed to the original XtremeCT image, and the cement cloud was segmented. Image data for each incremental step was then prepared for micro finite element modelling (microFE) through voxel conversion approach[4]. The endplates were virtually embedded to apply the boundary conditions of a uniaxial compression. The models were solved for stiffness, failure load[5] and Von Mises stress (VMS) distribution.

Results

The endplate contact was established at 5ml of cement. A leakage was observed at 6ml (Fig1b). MicroFE modelling showed a linear increase of the apparent stiffness, from 4640 N/mm at 0ml to 9440 N/mm at 6ml of cement (+103%); and the failure load, from 650N to 1040N (+60%). The highest VMS in bone elements were observed between the cement and the endplates (Fig. 2). Under a constant load, the mean VMS in bone decreased linearly from 35MPa to 20MPa. But the mean of the top 100 VMS did not change significantly between 0 and 4ml of cement (325±65MPa), and then decreased by 20% and 30% for 5ml and 6ml respectively.

Discussion

The time-lapsed CT approach reveals precisely the distribution of cement within the bone structure at each increment. Combined with microFE modelling, this approach allows monitoring of the mechanical properties of the augmented bone during injection. Our data suggests that stopping the procedure at a partial filling would induce a risk of failure for the trabecular bone immediately below or above the cement cloud, which agrees closely with other studies[6]. Further investigation is in progress.

References

1. Sun, Spine (2004).
2. Laredo, Semin. Ultrasound CT MR (2005).
3. Hulme et al. J Biomech (2008).
4. Müller & Rüegsegger, Med Eng Phys (1995).
5. Pistoia et al. J Biomech Eng (2001).
6. Chevalier et al. Spine (2008).

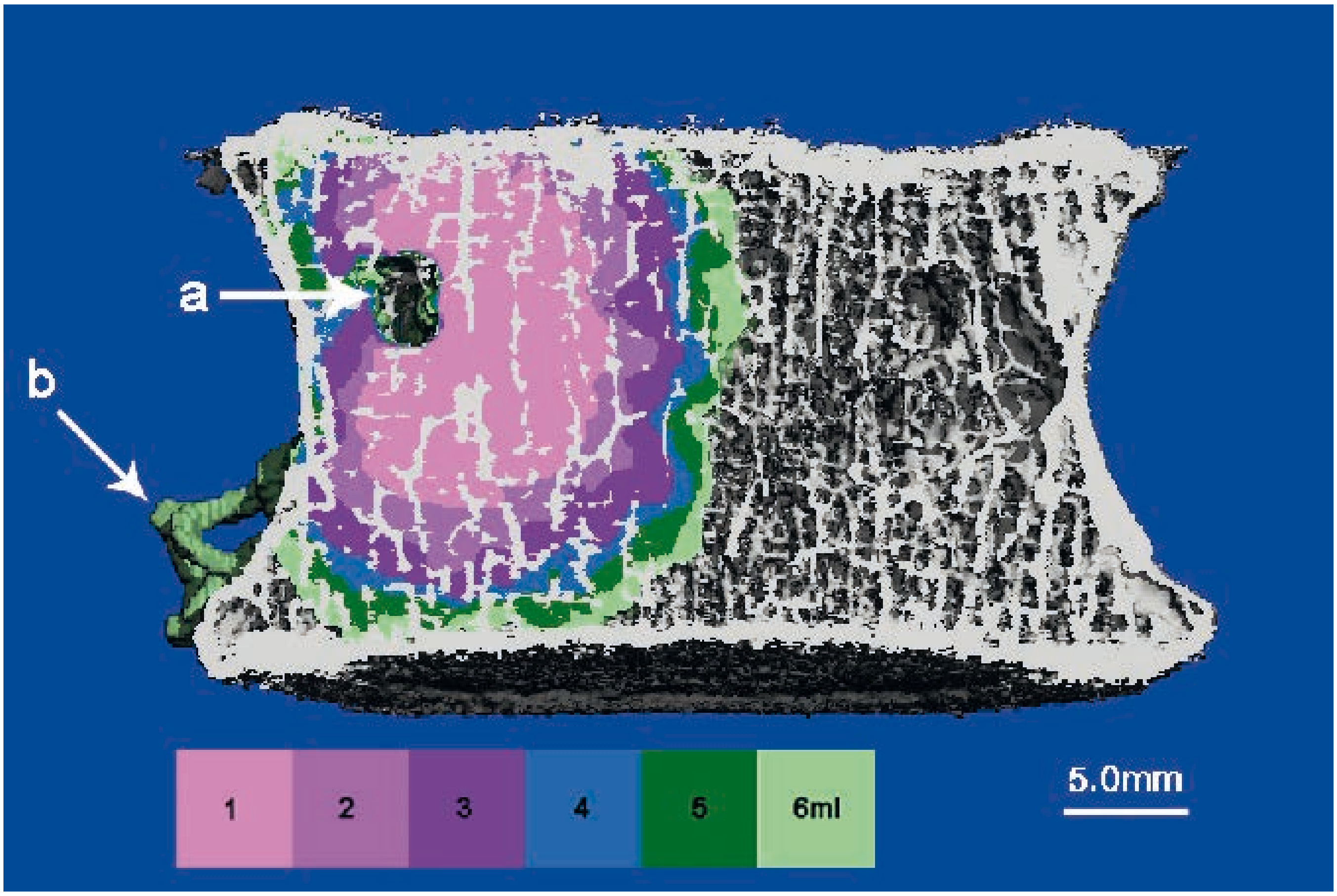

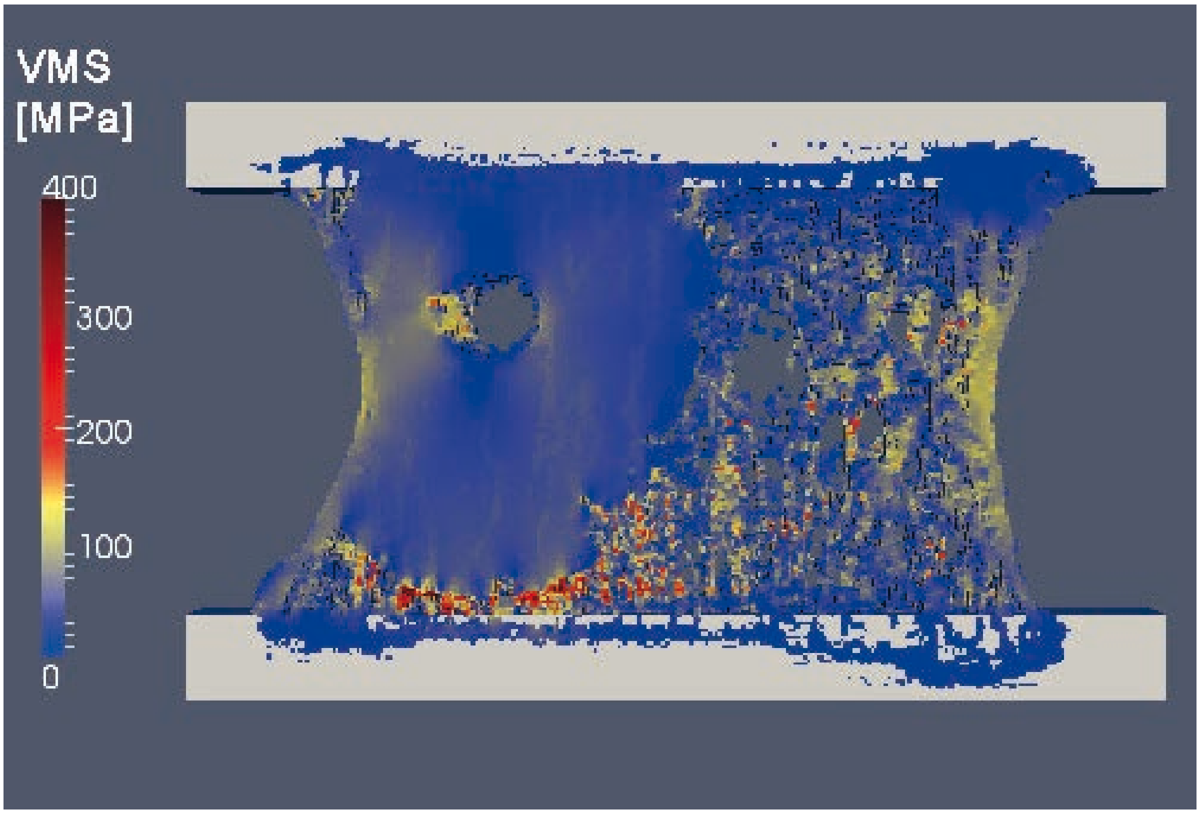

-Cement distribution at each increment of injected volume within the bone structure. (a: point of entry, b: leakage of cement)

-Stress distribution within bone structure with 4ml cement. High VMS are concentrated under the cement mass.

Impaction Bone Grafting in Primary Total Hip Arthroplasty in Absence of Acetabular Defects: the Results after 2 Years Follow-up.

Schmitz Marloes M.W.J.L. M.D. m.schmitz@orthop.umcn.nl Radboud University Nijmegen Medical Centre Nijmegen Netherlands
Colo Ena E. Medical student e.colo@orthop.umcn.nl Radboud University Nijmegen Medical Centre Nijmegen Netherlands
Rijnen Wim W.H.C. MD, PhD w.rijnen@orthop.umcn.nl Radboud University Nijmegen Medical Centre Nijmegen Netherlands
Gardeniers Jean J.W.M. MD, PhD j.gardeniers@orthop.umcn.nl Radboud University Nijmegen Medical Centre Nijmegen Netherlands
Scheurs Wim B.W. MD, PhD b.schreurs@orthop.umcn.nl Radboud University Nijmegen Medical Centre Nijmegen Netherlands

Submitted by:Schmitz, Marloes MD

IBG in primary cemented THA's in young patients without an acetabular defect shows satisfying results including a 100% survival for aseptic loosening after a minimum follow-up of 2 years. This creates an optimal situation for possible future revisions.

Introduction
The long-term survival of total hip arthroplasties (THA) among younger patients is still less favorable, mostly due to a high activity level and underlying disorders. Frequently, due to the pathology an acetabular bone stock deficiency in this group is seen. The impaction bone grafting (IBG) technique has been described as a biological attractive solution to reconstruct these defects. However, even in absence of acetabular bone stock deficiency, a young patient still might benefit from IBG which enhances the fixation of the cemented cup component and in the long term supports future revision as the bone stock has been expedited. Therefore weevaluate the difference in revision rate and early complications between patients under the age of 50 years, who had a primary cemented THA versus a cemented THA with acetabular IBG.
Patients and Methods
In 2008 all our consecutive patients younger than 50 received a cemented THA with IBG regardless of the presence or absence of an acetabular bone stock defect (n=28). We compared them to all our patients younger than 50 without an acetabular bone stock deficiency who received a primary THA without IBG in the period 2006-2007 (n=26). Radiological and clinical parameters were assessed.
Results
Mean follow-up was 3.5 years (range 2.0-5.8) with no patient being lost to follow-up. Mean age at index surgery was 36.1 years (range 12.6-49.2). Survival of the THA with and without IBG regarding aseptic loosening was 100%. One THA with IBG was revised for septic loosening after 0.53 years. Another THA with IBG was completely revised for recurrent dislocations after 3.45 years. Radiological acetabular loosening was seen in two IBG cups and one non-IBG cup. No radiological femoral loosening occurred. Osteolysis was seen in one stem in the non-IBG group.
Discussion/Conclusion
IBG in primary cemented THA's shows satisfying results including a 100% survival for aseptic loosening after a minimum follow-up of 2 years.

Cell deformation behavior in rabbit model of early OA

Han Sang Kuy S-K PhD sangkuyhan@hotmail.com University of Calgary Calgary Canada
Herzog Walter W PhD Walter@kin.ucalgary.ca University of Calgary Calgary Canada
Korhonen Rami RK PhD rami.korhonen@uef.fi University of Eastern Finland Kuopio Finland

Submitted by:Turunen, Siru

Chondrocyte mechanics changed in a very early stage of OA. Changes were mainly explained by fibrillation of the collagen network and reduction in the amount of proteoglycans.

Introduction

Chondrocytes produce and maintain articular cartilage extracellular matrix (ECM). Chondrocyte volume and morphology change under mechanical stress and during the progression of osteoarthritis (OA). These changes might lead to severe alterations in cell biosynthesis, yet cell responses to mechanical loading in early OA still remain unknown.

In this study our aim was to reveal cell responses to mechanical loading four weeks after anterior cruciate ligament transaction (ACLT) in rabbits (a widely used model of OA) and compare them with the structural changes in the tissue.

Materials and Methods

Eight New Zealand white rabbits underwent unilateral ACLT. Patellae from both knees were harvested 4 weeks after the operation.

Dextran labeled samples were imaged with a dual photon microscope coupled with a Chameleon XR infrared laser simultaneously with a 2 MPa mechanical loading (20 min).

Cell volume and morphology were analyzed before and after the loading, and local tissue strain was analyzed by measuring the distance between centroids of paired cells.

Collagen fibril orientation was analyzed with polarized light microscopy (PLM) as a function of tissue depth. Digital densitometry was used to reveal the spatial proteoglycan (PG) content of the samples. Depth-dependent collagen content was analyzed with Fourier Transform Infrared (FTIR) microspectroscopy.

Results

The average change in cell volume as a result of the mechanical loading was significantly different between the groups (increased in ACLT group vs. diminished in contralateral group). Also, changes in the width and depth of the cells were significantly larger in the ACLT than in the contralateral group.

Collagen orientation angle increased significantly in the ACLT group compared to contralateral group, while collagen content in both groups remained the same. PG content was significantly lower in the ACLT group than in the contralateral group.

Discussion

Chondrocyte response to mechanical loading of cartilage was studied with a rabbit ACLT model 4 weeks after intervention. Changes in chondrocyte volume, width and depth in response to mechanical loading were different in the ACL transected joint cartilage compared to the contralateral joint cartilage. Collagen orientation angle and PG content were altered in the ACLT group compared to the contralateral group, while collagen content remained the same in both groups. Our results suggest that cell deformation behaviour is already altered in early OA, and can be explained by decrease in the PG content and fibrillation of the superficial collagen network. It is speculated that in ACLT cartilage the support from the collagen network is diminished and might not limit cell width increase in response to mechanical loading. Also, the smaller amount of PGs might result in softener cell environment, and thus, an increase in cell volume during mechanical loading.

In conclusion, our results suggest that changes in articular cartilage structure, especially increase in collagen fibrillation and reduction in the PG content, affect chondrocyte biomechanics at very early stage of OA.

Low incidence of greater trochanter fractures after cemented total hip arthroplasty in young patients

Schmitz Marloes M.W.J.L. MD m.schmitz@orthop.umcn.nl Radboud University Nijmegen Medical Centre Nijmegen Netherlands
de Kam Daniel D.C.J. MD, PhD D.dekam@chir.umcn.nl Radboud University Nijmegen Medical Centre Nijmegen Netherlands
Rijnen Wim W.H.C. MD, PhD w.rijnen@orthop.umcn.nl Radboud University Nijmegen Medical Centre Nijmegen Netherlands
Gardeniers Jean J.W.M. MD, PhD j.gardeniers@orthop.umcn.nl Radboud University Nijmegen Medical Centre Nijmegen Netherlands
Schreurs Wim B.W. MD, PhD b.schreurs@orthop.umcn.nl Radboud University Nijmegen Medical Centre Nijmegen Netherlands

Submitted by:Schmitz, Marloes MD

Fractures of the greater trochanter can results in persisting pain and limping. We saw a low incidence of fractures of the greater trochanter after a cemented THA and no relation between femoral osteolysis and the presence of a femoral fracture.

Introduction
Young patients will inevitably face revisions of their total hip arthroplasty. In revisions the focus is on bone loss repair, however attention should be given to the incidence of loss of the abductor mechanism, which can result in persisting pain and limping. Recently, an increasing number of reports have pointed out osteolysis as a risk factor for fractures of the greater trochanter, resulting in abductor loss. In this study we want to investigate the incidence of greater trochanter fractures in 343 consecutive cemented total hips in 267 patients. In addition, we report the radiological osteolysis in order to discover a possible relationship between the occurrence of osteolysis in different areas of the femur after a cemented THA and the prevalence of greater trochanter fractures.
Patients and Methods
We reviewed historical prospectively collected data of 343 total hips in 267 consecutive patients who received a primary cemented THA between 1988 and 2004 in our centre. We evaluated all available preoperative and postoperative anterior-posterior and lateral radiographs for presence of a greater trochanter fracture and osteolysis. Fractures were classified according to the Vancouver Classification. Radiographic signs like radiolucent lines and osteolysis in accordance to the 7 Gruen zones were described.
Results
Mean age at time of surgery was 38,3 years (range 16,4-50,0). Mean follow-up time was 8,9 years (range 2 : 19 yrs). Two fractures of the greater trochanter 6 and 9 years after surgery were seen, resulting in a 0.6 % fracture rate. None of these fractures showed signs of osteolysis. However, osteolysis of the trochanteric area was seen in 11 cases.
Conclusions
We saw a low incidence of fractures of the greater trochanter after a cemented THA and no relation between osteolysis and the presence of a femoral fracture.

Possibilities of using digital fracture reduction and customization of bone plates in preplanning and during surgery

Rännar Lars-Erik Ph.D. lars-erik.rannar@miun.se Mid Sweden University Östersund Sweden
Bäckström Mikael Ph.D. mikael.backstrom@miun.se Mid Sweden University Östersund Sweden
Submitted by:Cronskär, Marie PhD student

The technology of digital design and direct additive manufacturing of customized implants are progressing rapidly. This case study examines the possibilities of using such technology for a bone plate, used for fixation of a clavicle fracture.

Introduction:

The technology of digital design and direct manufacturing is progressing rapidly. Digital 3D-models can be created from CT-data and used as a basis for the individually designed implants. The implants can then be directly manufactured with additive manufacturing (AM) methods. To investigate the use of this technology in both preplanning and performance of fracture fixation, a case study on a customized plate for repairing a fractured clavicle was carried out.

Methods:

Digital 3D-models of the left fractured and right non-fractured, clavicles were generated from CT-data of a 24 year old man. The 3D-model of the right clavicle was mirrored and used as a basis for the design of the customized plates, which were then directly manufactured using AM methods, first as prototypes in ABS plastic, then finally in medical grade Ti6Al4V. Grinding and polishing of two of the Ti-plates were performed to achieve a surface finish which counteracts tissue in-growth. In order to know where to position the plates, according to the fracture, the 3D-model of the fractured bone (fig 1a) was virtually reduced and used as guidance (fig 1b). The process of digital design and direct additive manufacturing routine was thoroughly described earlier. The mirrored computer model of the non-fractured bone was manufactured in ABS-plastic and later used as template during surgery, for the reshaping of an anatomical ‘LCP SA-ClavPl. 3.5’ plate to fit the patient.

Results:

The customized plate wrapped in a sterilized plastic bag was tried out in the wound and have shown a very good fit and according to the surgeon would be the best choice in this case. The anatomical plate had a poorer fit with big gaps, and about 40 minutes of surgery time was used for the reshaping of this plate. Also the plastic model provided good help in the anatomical plate reshaping. During the pre-operative planning and the course of the surgery more ideas on the utilization of AM benefits for customized implant manufacturing have been formulated. For example, the screw positioning can be planned in advance using the repositioned bone model and the individually designed plate can be used as support of easier handling of the fracture reduction. In order to further improve the plate design, three plates with some different shapes were manufactured (fig 2). One of them is twisted, medially starting in an anterior position and ending in a superior position, to smoothly pass by the coraco-clavicular ligament (fig 1c).

Discussion/conclusion

Our case study indicates that customized plates assure a better fit to the patient and the fracture and also help to reduce surgery time. Furthermore, there is no need for tapering reconstruction-segments used for final plate reshaping, and by excluding those, the plate can be thinner and still withstand the same loads. Unfortunately such factors as the time needed for the design and manufacturing and the cost of customized implants were so far preventing wider applications of these plates for the trauma fracture fixation. But as the technologies advance, the influence of these factors gradually diminishes.

1. Emmelmann, C., et al., Laser Additive Manufacturing of Modified Implant Surfaces with Osseointegrative Characteristics. Physics Procedia, 2011. 12, Part A(0): p. 375-384.
2. Salmi, M., et al., Patient-specific reconstruction with 3D modeling and DMLS additive manufacturing. Rapid Prototyping Journal, 2012. 18(3): p. 209-214.
3. Cronskar, M., L.-E. Rännar, and M. Backstrom, Implementation of Digital Design and Solid Free-Form Fabrication for customization of Implants in Trauma Orthopaedics. Journal of Medical and Biological Engineering, 2012. 32(2): p. 91-96.

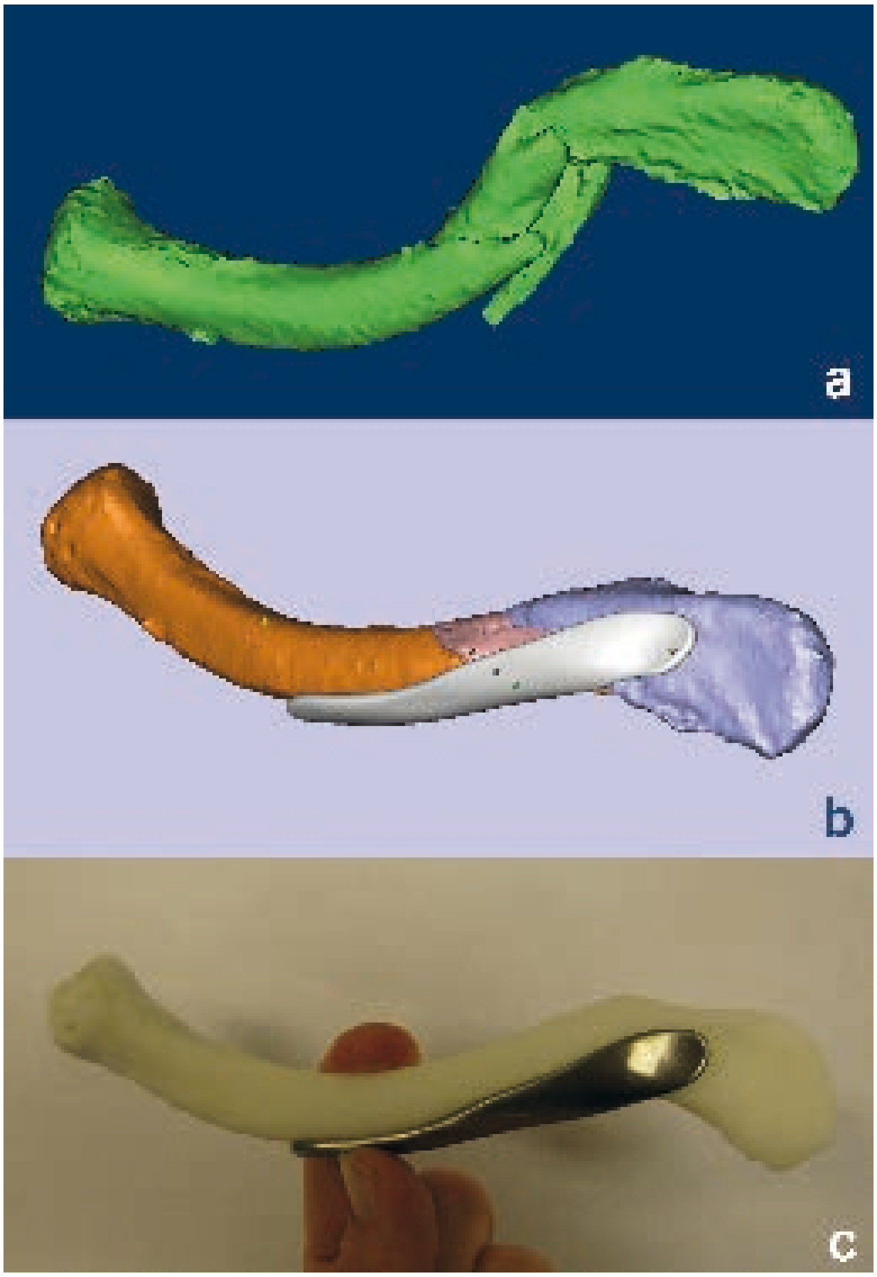

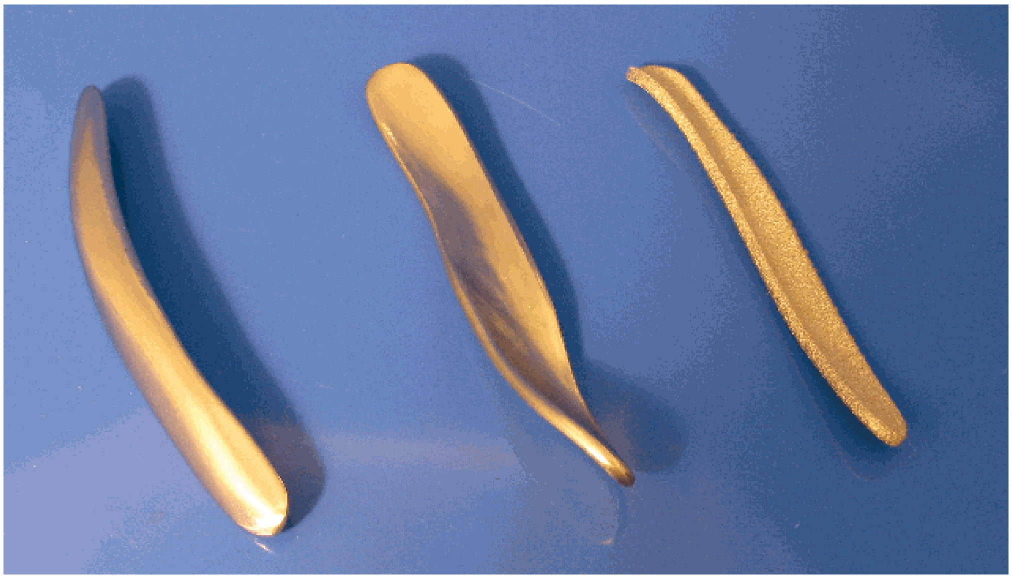

-a) Digital model of fractured clavicle, b) reduced clavicle model with customized plate and c) plastic model of the mirrored non-fractured clavicle with a customized plate.

-Three different designs of customized clavicle plates. The two to the left are finished with grinding and polishing and the one to the right has a raw surface.

Human End-Stage Osteoarthritic Cartilage is Responsive to Transforming Growth Factor Beta and Contains a Population of Cells that Expresses SMAD2/3P and SMAD1/5/8P

van Caam Arjan APM MSc a.vancaam@reuma.umcn.nl Radboud University Nijmegen Medical Centre Nijmegen Netherlands
Blaney Davidson Esmeralda EN. PhD E.BlaneyDavidson@reuma.umcn.nl Radboud University Nijmegen Medical Centre Nijmegen Netherlands
Vitters Elly EL BSc e.vitters@reuma.umcn.nl Radboud University Nijmegen Medical Centre Nijmegen Netherlands
van den Berg Wim WB PhD w.vandenberg@reuma.umcn.nl Radboud University Nijmegen Medical Centre Nijmegen Netherlands
van der Kraan Peter PM PhD P.vanderKraan@reuma.umcn.nl Radboud University Nijmegen Medical Centre Nijmegen Netherlands

Submitted by:van Caam, Arjan MSc

In human end-stage Osteoarthritic cartilage, TGF-beta is able to down regulate MMP13 expression via Smad2/3 phosphorylation. Modulation of this pathway can contribute to decreased damage in OA

Introduction:

Joint diseases such as osteoarthritis (OA) result in destruction of articular cartilage. Transforming Growth factor beta (TGF-beta) is considered as a protective factor in young cartilage while this function is lost upon aging. In chondrocytes, TGF-beta can signal via phosphorylation of SMAD2/3 (via ALK5) or SMAD1/5/8 (via ALK1). In earlier studies we have found that in young healthy human cartilage (age < 10 years) only SMAD2/3 phosphorylation (SMAD2/3P) was detectable and no SMAD1/5/8 phosphorylation (SMAD1/5/8P). Moreover, in human OA cartilage we showed a significant correlation between ALK1 and MMP13 expression. Our goal was to study the expression of SMAD2/3P and SMAD1/5/8P in chondrocyte populations in end-stage human OA cartilage and whether addition of exogenous TGF-beta modulates the expression of MMP13, ALK5 and ALK1 in this cartilage.

Methods:

Human OA articular cartilage was obtained during knee joint replacement (n=20) and processed for histology. Cartilage sections were stained for SMAD2/3P and SMAD1/5/8P using specific antibodies. In addition, human OA cartilage was incubated with 10 ng/ml TGF-beta for 24h with or without pre-incubation with the ALK5 inhibitor SB-505124 (50µM) for 6 hours. Expression of MMP13, ALK5 and ALK1 was analyzedbyquantitativePCR. Data was analyzed for significance by one way ANOVA. These experiments were approved by the local ethical committee, and samples were obtained after informed consent.

Results:

We found both SMAD2/3P and SMAD1/5/8P positive cells in human OA cartilage (fig. 1). Strikingly, SMAD2/3P staining was mostly negative in histological intact cartilage areas while cells in damaged areas, mainly in chondrocyte clusters, were often strongly positive. Staining for SMAD1/5/8P was most intense in cells surrounding damaged regions and chondrocyte clusters. Incubation of human OA cartilage with TGF-beta significantly down regulated MMP13 expression (fig. 2). This effect was totally abolished by the ALK5 inhibitor SB-505124, indicating that the effect of TGF-beta on MMP13 runs via Smad2/3 signaling. Moreover, TGF-beta significantly elevated ALK5 expression while decreasing ALK1 expression, and both these effects were completely blocked by pre-incubation with SB-505124.

Discussion:

Stimulation of human end-stage OA cartilage with high TGF-beta concentrations down regulates MMP13 expression and modulates TGF-beta type I receptors. The latter results in an increased ALK5/ALK1 ratio, favouring TGF-beta signaling via ALK5. All these effects run via SMAD2/3 (ALK5). We propose, based on these results and earlier findings, that during aging TGF-beta loses its protective role due to the loss of SMAD2/3 signaling in articular chondrocytes. This loss plays a role in the initiation of cartilage degradation. However, human end-stage OA cartilage contains a population of chondrocytes in the highly damaged areas that is still capable of responding to TGF-beta. In contrast to intact areas that are devoid of SMAD2/3P and SMAD1/5/8P postive cells, the cells in the damaged areas stain highly positive and are most likely involved in (unsuccessful) repair. This study demonstrates that TGF-beta, via SMAD2/3, is able to down-regulate MMP13 expression in a cell population in human end-stage OA cartilage. Modulation of this pathway could contribute to decreased MMP13 expression, and thus damage, in OA cartilage.

Potential of osteoblastic differentiated Adipose Mesenchymal Stem Cells for bone tissue engineering in a porcine pre-clinical model.

Schubert Thomas MD Thomas.schubert@uclouvain.be Center of Tissue and Cell Therapy Brussels Belgium
Lafont Sébastien Laboratory of experimental Surgery Brussels Belgium
Beaurin Gwen Laboratory of experimental Surgery Brussels Belgium
Delloye Christian MD, PhD Center of Tissue and Cell Therapy Brussels Belgium
Gianello Pierre MD, PhD Laboratory of experimental Surgery Brussels Belgium
Dufrane Denis MD, PhD denis.dufrane@uclouvain.be Center of Tissue and Cell Therapy Brussels Belgium
Submitted by:Schubert, Thomas Dr.

An autograft made of 3D osteogenic differentiated Adipose Mesenchymal Stem Cells has the potential to form bone in spine fusion and femoral non-union porcine pre-clinical models.

Introduction:
Osteoblastic differentiated Adipose Mesenchymal Stem Cells (AMSCs) may be proposed for bone tissue engineering. Two surgical models were developed in pigs to assess the potential of a three dimensionally osteogenic differentiated AMSCs autograft: (i) a multi-level spinal fusion and (ii) a femoral non-union.
Methods:
(i) Spine fusion (n=6): to assess the early phase of ossification, a 4 levels Anterior Lumbar Interbody Fusion procedure was achieved using Intervertebral PEEK cages. Four pigs were sacrificed at 8w and the two remaining at 12w post implantation. Four experimental groups were randomly assigned as: 1 empty cage, 1 space filled with freeze-dried (FD) irradiated cancellous bone graft, one with autologous bone graft and one with a 3D osteogenic differentiated AMSCs autograft, respectively.
(ii) Femoral non-union (n=4): a critical femoral defect of 1,5 folds the diameter of the femur stabilized by two 4,5mm titanium Locking Compression Plates (LCP) was used to achieve a non-union at 6 months post-surgery. An autologous 3D osteogenic differentiated AMSCs autograft was then implanted after removing of all fibrous tissues and heightening of bone stumps.
Animals were followed in vivo by CT-scan every 4 weeks. After sacrifice, explanted tissues were analyzed by micro CT-Scan (µCT), micro radiography (µRX), histomorphometry (Hemalun-Eosin, Masson's trichrom, Methylene Blue-Fuchsin) and immunohistochemistry for Osteocalcin.
Results:
(i) Spine fusion: at 12w, no spontaneous fusions were observed. FD grafts showed bone resorption between 8 and 12w as demonstrated by µCT (194.3 ± 62.9 mg/cm³ vs 141.1 ± 53.3 mg/cm³, PPP
(ii) Femoral non-union: loss of stabilization was observed with 1 LCP before 8 weeks. Four non-unions of the femoral shaft were obtained at >6months with 2 plates, demonstrated by CT-scan and the presence of fibrotic / poorly vascularized tissue in the defect. In the 4 pigs implanted with osteogenic differentiated AMSCs, one demonstrated bone fusion at 5 months. Explanted tissue showed bone bridging on µCT and µRX. Bone and chondrocyte-like tissue found at the implantation site demonstrated endochondral ossification (Figure 2). In one pig, loss of stabilization was observed 3 month after implantation. Two other pigs implanted with 3D differentiated autologous AMSCs are currently in progress of consolidation at 3 months post implantation.
Discussion & conclusion:
To assess the potential of a 3D autologous AMSCs bone graft, two surgical models were developed on pigs. We observed no spontaneous fusion in both models. Three-D differentiated AMSCs demonstrated bone formation in the vertebral model. Our femoral non-union model demonstrates the potential of our 3D engineered graft to induce bone fusion in a fibrotic unfavourable environment.

Acknowledgements: This work was supported by grants of the Saint-Luc and Salus Sanguinis Foundations.

Restoration of large acetabular bone defects in hip arthroplasty with impaction grafting and coated porous titanium particles as a full bone substitute.

Aquarius René R MSc R.Aquarius@orthop.umcn.nl Radboud University Nijmegen Medical Centre, Orthopaedic Research Lab Nijmegen Netherlands
Verdonschot Nico N MSc, PhD n.verdonschot@orthop.umcn.nl University of Twente, Laboratory of Biomechanical Engineering Enschede Netherlands
Schreurs Barend BW MD, PhD b.schreurs@orthop.umcn.nl Radboud University Nijmegen Medical Centre, Department of Orthopaedics Nijmegen Netherlands
Buma Pieter P MSc, PhD p.buma@orthop.umcn.nl Radboud University Nijmegen Medical Centre, Orthopaedic Research Lab Nijmegen Netherlands
Submitted by:Walschot, Lucas MD

Reconstructions with impacted, coated porous titanium particles (TiP) show good osteoconduction without osteolysis or metallosis. Wear patterns were variable and systemic titanium concentrations very low. A human pilot study should prove that application of TiP is safe in the long-term.

<p>Introduction: Impaction grafting restores bone defects in hip arthroplasty with bone particles. Drawbacks have led to the search for bone substitutes. Porous titanium particles (TiP) are deformable and osteoconductive like bone particles. TiP were applied in a realistic in-vivo model to answer the following questions: are impacted, coated TiP armored by host bone under loaded conditions, do micro-particles lead to wear and does the large surface of the implanted TiP cause elevated systemic titanium levels?

Animals and Methods: The right acetabulum of ten mature milk goats (63 (6) kg) was excavated to create a large defect (AAOS type 3A-B). TiP with a carbonated apatite coating were used with a cemented polyethylene cup and a mesh to reconstruct the original acetabulum. A stem with a metal head was cemented in the femur. Goats were killed after fifteen weeks for histologic evaluation (light microscopy) and wear characterization (scanning electron microscopy). Blood samples were taken pre- and post-operatively. Results were expressed as mean (standard deviation).

Results: One goat suffered from a contralateral femoral fracture. Bone ingrowth distance and graft layer thickness in the remaining nine goats measured 2.8 (0.8) mm and 5.6 (0.8) mm respectively. TiP showed osseointegration at the bone interface and only limited cement penetration with no signs of metallosis or osteolysis (Figure 1). Wear patterns were mixed (Figure 2). Titanium concentrations increased from 0.6 (0.3) to 1.1 (0.7) ppb (p

Conclusion: A reconstructive layer of impacted TiP with a carbonated apatite coating shows good osteoconduction and is stable under loaded conditions. Wear patterns were variable like observed after application of calcium-phosphate particles. Systemic titanium concentrations remained very low. A clinical pilot study should prove that application in humans is safe in the long-term.

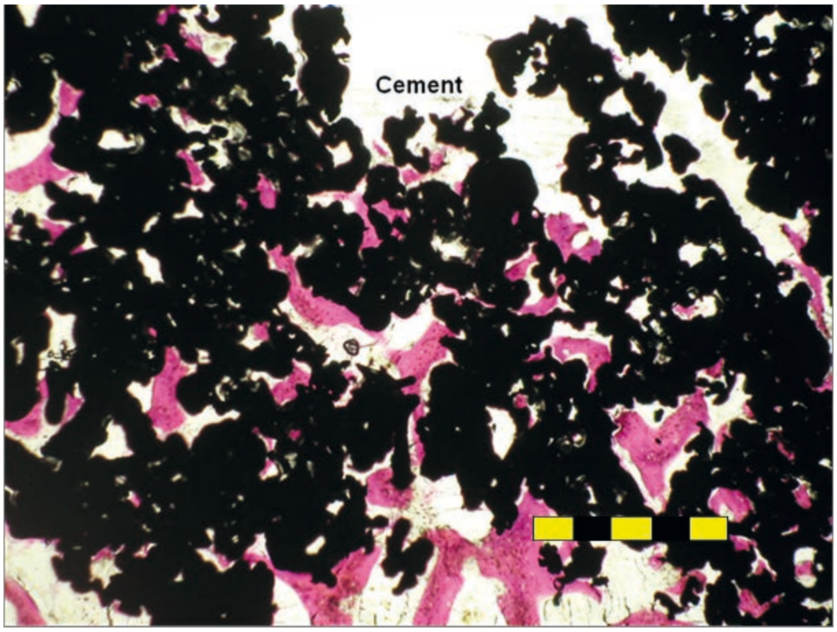

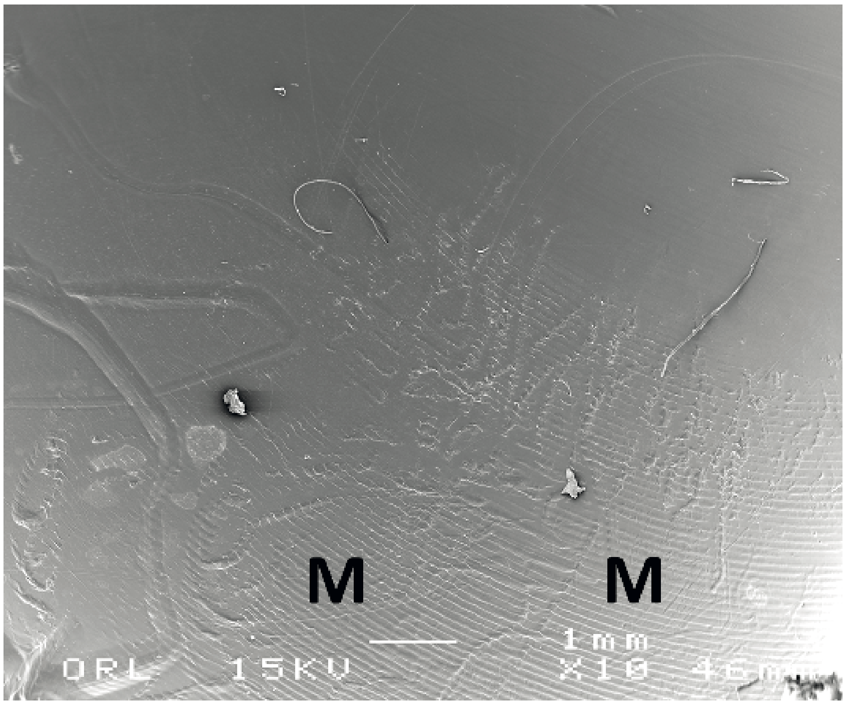

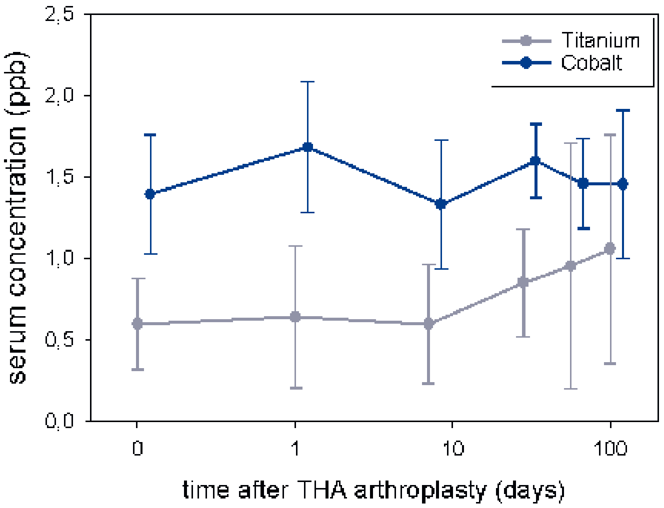

-Figure 1. Black=TiP, pink=bone. Bar indicates 0.2 mm.
-Figure 2. Wear of the cup. M=original machinery marks.
-Figure 3. Systemic titanium concentrations (control: cobalt).

The role of the hydroxiapatite coating in the progression of osteolisis after total hip replacements. The sealing effect in the proximal femur.

Pérez-Coto Iván Dr. Hospital San Agustín Avilés Spain
Escandón Ana Dra. Hospital San Agustín Avilés Spain
Hernández-Vaquero Daniel Prof. school of Medicine Oviedo Spain

Submitted by:Sandoval García, Manuel Ángel Dr.

The circunferencial hydroxiapatite coating at the femoral stem prevent the migration of wear particles and provide an effective sealing effect against the progression of the wear particle-induced disease.

Introduction:
The wear particle-induced disease is the main problem facing the longevity of total hip arthroplasty (THA) due to the loosening of the components caused by the lysis. The hydroxiapatite (HA) porous coating in the proximal femoral stem of a total hip arthroplasty enhanced the bone ingrowth and prevent the migration of the component.
Objectives:
Our objectives were to know what is the role of the HA-coating in resisting wear particle migration. Secondly, to study if there is a sealing effect in the interface bone:HA coating of the proximal femoral stem.
Methods:
Our study included 62 cementless THA with a circunferencial porous HA-coating in the proximal femoral stem. All cases were studied with magnetic resonance, using special protocols in order to reduce artifacts. We evaluated the presence, severity and location of the osteolytic lesions in femur, according to the distribution of the circunferencial HA-coating.
Results:
Osteolysis was visible in 46 hips, 25 of which in femur. When we evaluated the location by Gruen zones, most of the lytic lesions were found in the area 1 (22) and in the area 7 of Gruen (10). No lesions were found in zones 2 and 6, where the HA-coating contact with the bone, neither in zones 3,4 and 5, distal to the circunferencial coating of HA.
Conclusion:
In our series, all the osteolytic lesions were detected in non HA-coated areas or in areas proximal to this coating. However no lesions were found in areas where the HA-coating contact with bone or distal to this interface. Our results demonstrate that the circunferencial HA-coating at the femoral stem prevent the migration of wear particles and provide an effective sealing effect against the progression of the wear particle-induced disease.
(*)This study is promoted and funded by De Puy Jonhson and Jonhson

Suppression of Toll-like receptor (TLR)4, and IRAK1, 4 in macrophages after phagocytosis of lipopolysaccharide-coated titanium particles

Yasunobu Tamaki YT MD, PhD ytamaki@med.id.yamagata-u.ac.jp Yamagata University Yamagata Japan
Yuya Takakubo YT MD, PhD takakubo-y@med.id.yamagata-u.ac.j Yamagata University Yamagata Japan
Tomoyuki Hirayama TH MD, PhD t.hirayama@med.id.yamagata-u.ac.jp Yamagata University Yamagata Japan
Yasushi Naganuma YN MF yasushi804@msn.com Yamagata University Yamagata Japan
Kan Sasaki KS Professor s-kan@msb.biglos-kan@msb.biglobe.ne.jp Yamagata University Yamagata Japan
Konttinen Yrjö YTK Professor yrjo.konttinen@helsinki.fi University of Helsinki Helsinki Finland
Submitted by:Michiaki, Takagi Professor

Self-protective mechanism of down-regulated TLR4, IRAK1 and IRAK4 expressions were found in the process of phagocytosis of LPS-coated titanium particles. These phenomena may explain the nature of slow disease progression in periprosthetic osteolysis related to microbial products, when compered with the phenomena caused by acute and direct microbial stimuli.

Introduction

Adherent lipopolysaccharide (LPS) on particles can induce macrophage activation via Toll-like receptor (TLR) 4 [1]. Recently, abundant expression of TLRs in macrophages was found in periprosthetic tissues [2]. However, the precise role of TLRs and their adaptor molecules in the process of aseptic loose connective tissues is still unclear. Expression of TLRs, their adaptor molecules and cytokines in macrophages stimulated by titanium particles (Ti) with or without LPS coating was examined to clarify the TLR-mediated signal pathway under adherent endotoxins to wear particles.

Materials and Methods

1. Cells: The bone marrow cell suspension of Wister rats was incubated with 10 ng/ml M-CSF. Adherent cells were collected by exposure to tripsin-EDTA solution. The adherent cell fraction was obtained after enzyme treatment.
2. Titanium particles (Ti) preparation: Endotoxin-free Ti were prepared by five cycles of alternating treatment with 25% nitric acid and alkali/ethanol. LPS-coated Ti was prepared by exposure of 10 ng/ml LPS [3].
3. Double-immunofluorescent staining: After fixation by acetone, colocalization of cytokines, TLRs and their adaptor molecules were examined using Alexa Fluorescent system for CD68, TNF-α, IL-1ß, IL-6, TLR4, MyD88, IRAK1, IRAK4 and TRAF6.
4. Quantitative PCR analysis: Particles coated by LPS (Ti/LPS+) and endotoxin-free control Ti particles (Ti/LPS-) were added to cultured plates. Unstimulated macrophages were cultured as negative control cells for Ti/LPS+ and Ti/LPS- experiments. Total RNA was converted into cDNA and enzymatic amplification of the specific cDNA sequences followed by quantitative analysis. mRNA of TNF-α, IL-1ß, IL-6, TLR4, MyD88, IRAK1, IRAK4 and TRAF6 was amplified with the use of its primer at each times.

Results

1. Double-immunofluorescent staining: Colocalization of CD68 with TNF-α, IL-1ß, IL-6, TLR4, MyD88, IRAK1, IRAK4 and TRAF6 was detected in adherent cells from bone marrow, which indicated the cells macrophages with expression of the receptor and related molecules.
2. Quantitative PCR: mRNA levels of TNF-α, IL-1ß and IL-6 standardized by GAPDH, were significantly higher in Ti/LPS+ than Ti/LPS-. In contrast, mRNA levels of TLR4 decreased significantly in Ti/LPS+ compared with Ti/LPS-. mRNA level of IRAK1 and IRAK4 decreased significantly in Ti/LPS+ , whereas that of Myd88 was unchanged followed by later decrease and TRAF6 was suppressed after transient increase in Ti/LPS+DiscussionProinflammatory cytokines increased by contact with and/or phagocytosis of LPS-coated foreign metallic materials via TLR4-mediated inflammatory signal pathways. Subsequent down-regulation of TLR4 at the receptor level, and of IRAK1 and IRAK4 at the post-receptor level, suggests that self-protective anti-inflammatory mechanisms are activated in macrophages and injury to innocent bystander cells/tissues after initiation of the host responses. These phenomena may explain the nature of slow disease progression in periprosthetic osteolysis, when compered with the phenomena caused by acute microbial stimuli.

References: [1] Bi Y: J Bone Miner Res 2001;16:2082-2091. [2] Takagi M: J Biomed Mater Res A 2007;81:1017-1026. [3] Greenfield EM: J Biomed Mater Res B Appl Biomater 2005;72:179-185.

Submitted by:Rutten, Sjoerd

Randomized clinical trial showing that low-intensity pulsed ultrasound is effective in accelerating delayed fracture healing, but as a single treatment option does not improve fracture union when sufficient stability is absent as in the non-fixated delayed union of the fibula.

Introduction:
Low-intensity pulsed ultrasound (LIPUS) is frequently used in clinical practice to treat impaired and/or delayed fracture healing, but its effectiveness is unclear. Therefore we aimed to investigate the effectiveness of LIPUS as a single treatment option to accelerate and/or enhance fracture union in patients with a delayed union of the fibula enrolled in a randomized clinical trial.
Patients & Methods:
The delayed union of the non-fixated osteotomized fibula after a standard high tibial osteotomy was used as model to compare fractures of similar type and nature. In total 20 patients (6 male, 14 female; age 41-63 years) with an average fracture age of 7 months (range 6 to 11 months) showing a delayed union of the fibula were enrolled, and assigned to the double-blinded allocated treatment intervention (10 LIPUS, 10 controls). Patient received 20 minutes of daily LIPUS- or sham-treatment over a period of 5 months. Fracture healing was assessed by radiographical and physical examination at scheduled monthly outpatient follow-up visits in 7 LIPUS-treated patients and 8 controls. Both groups of patients were similar with regard to gender, age, medication use, and co-morbidity. In total 5 delayed unions were excluded from the primary analysis (3 LIPUS, 2 Controls), 3 patients were non-compliant, 1 consent was withdrawn, and 1 patient was falsely included. Statistical analysis of the data was performed using Mann:Whitney U test for non-parametric analysis.
Results:
The primary analysis did not show a difference in number of healed cases between LIPUS-treated and sham-treated controls (Fig 1). Independent radiographical assessment showed that LIPUS decreased healing time by 29% (not significant) at 5 months (4 LIPUS, 4 controls; Fig 2A), and by 57% (p=0.023) at 1 year after the start of LIPUS-treatment (4 LIPUS, 7 controls; Fig 2B). Subjective clinical signs of fracture healing, i.e. pain at weight-bearing and manual stressing of the delayed union site, were similar in LIPUS-treated patients and controls. No direct relation was seen between the variables evaluated (age, gender, co-morbidity, use of medication) and final clinical outcome.
Conclusion:
Our data shows that LIPUS-treatment is effective in accelerating delayed and/or impaired fracture healing. However, as a single treatment option LIPUS does not directly contribute to improved fracture union when sufficient stability is absent as in the non-fixated delayed union of the fibula.

A 3-Dimensional osteogenic-like structure from human autologous adipose mesenchymal stem cells: Reproducibility, Genetic stability, clinical safety/efficacy.

Dufrane Denis DD MD,PhD denis.dufrane@uclouvain.be Endocrine Cell Therapy Unit/University clinical Hospital St-Luc Tour Franklin +1 Avneue Mounier, B1200 Belgium
Antoine-Poirel Hélène APH MD,PhD Centre of Human Genetics/University clinical Hospital St-Luc
Docquier Pierre-Louis DPL MD,PhD Orthopaedic surgery service/ University clinical Hospital St-Luc
Aouassar Najima AN BSc Endocrine Cell Therapy Unit/University clinical Hospital St-Luc
Ameye Geneviève AG BSc Centre of Human Genetics/University clinical Hospital St-Luc
Verhaeghe Line VL BSc Centre of Human Genetics/University clinical Hospital St-Luc
Nonckreman Sandrine NS BSc Centre of Human Genetics/University clinical Hospital St-Luc
Andre Wivine AW MSc Endocrine Cell Therapy Unit/University clinical Hospital St-Luc
Delloye Christian DC MD,PhD Orthopaedic surgery service/ University clinical Hospital St-Luc

Submitted by:Dufrane, Denis MD,PhD

Bone non-consolidation is a serious complication after bone tumour resection and congenital pseudarthrosis syndrome which affect the spontaneous bone repair. This study investigates an autologous 3-dimensional grafts made of osteogenic adipose mesenchymal stem cells to improve the osteogenesis.

Introduction:

This study proposes to investigate the osteogenic-differentiation of autologous human AMSCs in 3D (without any scaffold) to cure a bone defect. This work studied the safety/efficacy of this procedure in term ofhuman AMSCs isolation/expansion/differentiation, genetic stability and clinical safety/efficacy in oncogenic and congenital pseudarthrosis contexts.

Methods:

AMSCs isolation (collagenase digestion of subcutaneous adipose tissue) /differentiation into an original 3D «bone-like» structure were performed from 8 patients following the patented process 'DUFRANE et al., WO/2010/139792' (Fig. 1). The subcutaneous adipose tissue (1-2ml) was easily procured by a small lipoaspiration following a local anesthesiae. Group 1: Five patients with bone tumour (3 osteosarcomas/1 chondroblastoma/1 Ewing's sarcoma) characterized by several clonal cytogenetic alterations (Karyotyping /FISH study of tumor suppressor gene loci such as TP53/17p13, CDKN2/9p21, RB1/13q14) of the original tumour and Group 2: Three patients with pseudarthrosis (Neurofibromatosis/ Diamond Blackfan syndrome) were included in this study. Graft characterization (Osteocalcin/Von Kossa staining) and genetic analysis were performed on AMSCs proliferation/differentiation phases. Microarrays analysis studied the gene expression for osteogenic (RUNX2,BMP2, OPN3, FGF2,ALPL,SP7,FGF23,SMAD9,MEN1) and senescence/tumorogenic (c-Myc,TP53,NFKB,Cyclin D) development between un-/and osteogenic-differentiated states of AMSCs. Endotoxin content and mycoplasm contamination were assessed for all grafts. Autologous graft was implanted at the junction of native bone/bone allograft (Fig.2) and in the bone defect (Fig.3) after tumour resection and congenital pseudarthrosis, respectively. Patients were followed by biological (C-Reactive Protein/fibrinogen) and radiological (radiography/CT-Scan) investigations.

Results:

A mean of 65 ± 22 days was required to achieve the Passage 4th (in view to induce differentiation) and a mean of 9.6 ± 4.4 x 10^6 cells. In view to obtain 3-D osteogenic structure (confirmed by osteocalcin expression/collagen deposition/ mineralization), 59 ± 17 days were required after the proliferation phase. The microarrays analysis demonstrated the up-regulation of osteogenic genes for differentiated cells (p'0.05) and no sign of upregulation for TP53/NFKB/ Cyclin D/c-Myc for both un-/differentiated AMSCs. In Group 1, no native tumour anomalies were found prior/after osteogenic differentiation of AMSCs. However, AMSCs culture (up to Passage 4) can induced, in both Group 1 and 2, tri-/tetraploidies (0,5-14% of cells), recurrent clonal alterations as trisomy 7 (in 6-20% of cells for 3 patients) and chromosomal breakage cht(3)(q13.3) (for 4 patients) for undifferentiated AMSCs in proliferation phase. Interestingly, the osteogenic differentiation reduced significantly anomalies found in proliferation state (trisomy 7: '2-5.5% of cells). No sign of inflammatory reaction was acutely ('1 week post-implantation) and chronically ('1 month) observed for all patients. A significant improvement of bone union was found at 3 and 6 months post-implantation for tumour and congenital pseudarthrosis contexts, respectively.

Discussion &nconclusion

These preliminary results demonstrated: (i) the reproducibility to obtain the 3D structure from all autologous AMSCs; (ii) the impact of proliferation/differentiation on the genetic stability of human AMSCs and (iii) the safety and efficacy of this clinical procedure.

Acknowledgements:
This work was supported by grant of the Salus Sanguinis Foundation.

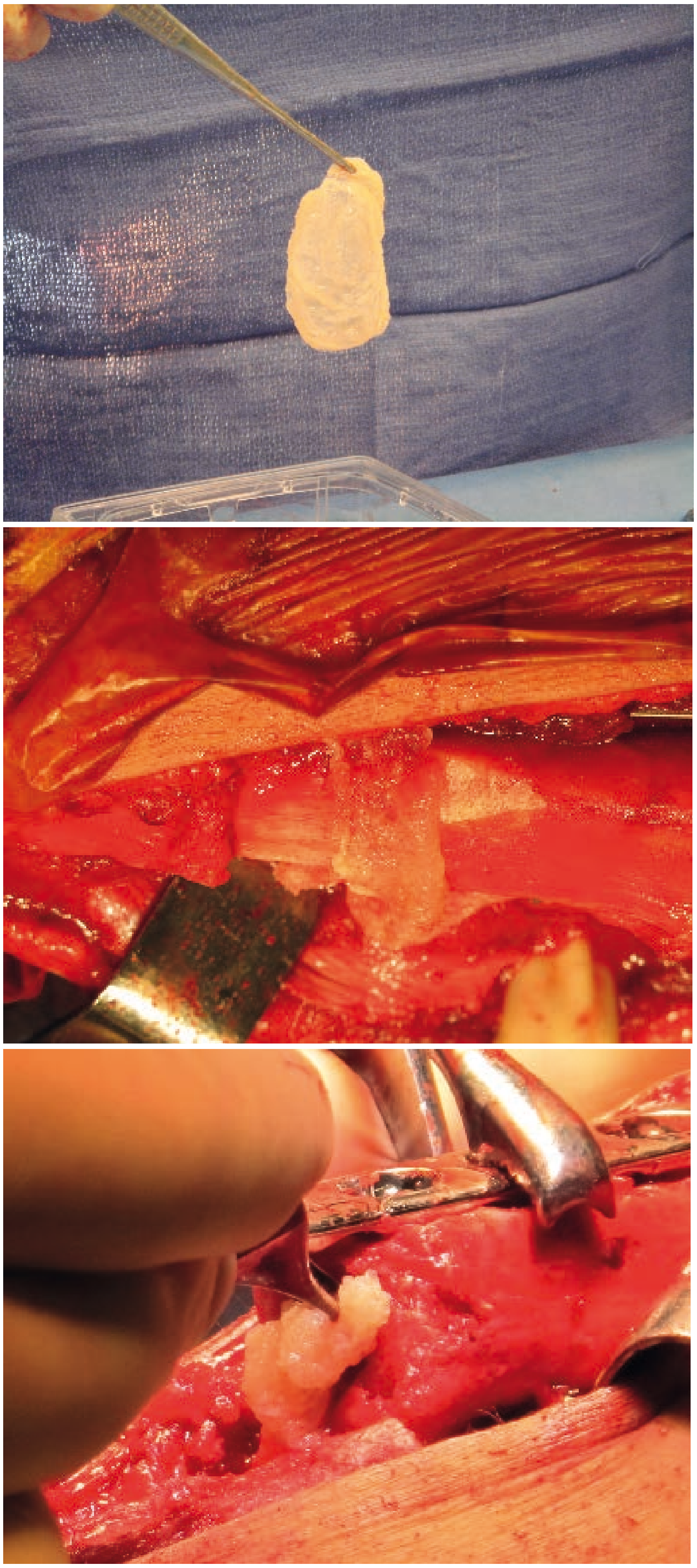

TLEMsafe: A EUROPEAN PROJECT TO IMPROVE PREDICTABILITY OF FUNCTIONAL RECOVERY OF PATIENTS REQUIRING SEVERY MUSCULOSKELETAL SURGERY

Verdonschot Nico N PhD n.verdonschot@orthop.umcn.nl University of Twente Enschede Netherlands
Koopman Bart HFJM PhD University of Twente Enschede Netherlands
Wirix-Speetjens Roel R PhD Materialise NV Leuven Belgium
Torholm Soren S PhD Anybody Aalborg Denmark
Feilkas Thomas T PhD Brainlab Munich Germany
Krogt van der Marjolein MM PhD University of Twente Enschede Netherlands
Submitted by:Verdonschot, Nico Prof.dr.ir.

We report on the European TLEMsafe project which is aimed to predict functional recovery of patients who undergo severy musculoskeletal surgery. We combine MRI-based personalized musculoskeletal models to reach this goal.

Introduction
The goal of the European project TLEMsafe is to create an ICT-based patient-specific surgical navigation system that helps the surgeon safely reaching the optimal functional result for the patient and is a user friendly training facility for the surgeons.
Methods
TLEMsafe is developed by generating semi-automated 3-D image-analyzing tools to parameterize the M-S system. The patient-specific parameters are fed into a recently developed M-S model with which the patient-specific functional outcome can be predicted. This consists of a direct effect (e.g. due to the removal of a muscle in a tumor patient), but has also a secondary effect in the sense that the patient will generate adaptive behaviour to the altered M-S system. Implementation of the adaptive capacity will be a unique (but essential) feature which allows valid predictions of the functional effects of surgical interventions. The next step is that the surgeon can virtually operate on the patient-specific model after which the model predicts the functional effects. Once the optimal plan is selected, this is fed into a system that allows the surgeon to reproduce the selected surgical plan during the actual surgery. TLEMsafe is a navigation system based on innovative ICT tools for training and pre-operative planning. Extensive, innovative validation techniques including quantitative indicators to improve safety (of surgical operation) and quality (highly predictable effects of complex surgery) are included.
Results
During the first 24 months of the project MRI scans were made of ten healthy subjects and of one pilot patient. These scans are currently analyzed and software is developed to extract personalized parameters from the images. Cadaver experiments in which muscle attachment points and muscle volumes are measured are performed to enable validation of MRI-based personification of musculoskeletal modelling.
Subsequently, the extracted personalized parameters are fed into the Anybody software package to generate personalized musculoskeletal models. A workflow is generated to allow for fast generation of these models. To enable a faster generation of these models, extensive sensitivity analyses are performed to assess which musculoskeletal parameters should be personalized in high detail and which parameters do not affect functional predictions and, hence, can be estimated more grossly. To feed the simulations functional measurements have been performed on the same 10 healthy subjects who were MRI scanned. Isokinetic, isometric strength measurements were recorded to further personalize the models. Functional measurements of daily activities (walking, negotiating stairs, squatting, initiating/terminating gait, getting up/sitting down on a chair) will allow for estimation of the muscle forces during these activities in a personalized manner.
Furthermore, a virtual pre-planning toolbox is generated which allows the surgeon to operate on the virtual patient. The input and output of the virtual toolbox is being made more compatible with Anybody software and the output is coupled to the Brainlab computer navigation system. Next steps are to focus on the validity of personalized musculoskeletal models and to assess the pre-and post-operative functionality of patients and their adaptive capacity during the recovery period after severe musculoskeletal surgery.

Acknowledgements
Funded by the European Commission FP7-ICT-2009.

Lysophosphatidic Acid (LPA)-functionalised titanium; a superior implant material for supporting human osteoblast differentiation.

Blackburn Julia Miss jlrkblackburn@doctors.org.uk Musculoskeletal Research Unit Avon Orthopaedic Centre England
Mansell Jason P Dr J.P.Mansell@bristol.ac.uk Musculoskeletal Research Unit Avon Orthopaedic Centre England
Blom Ashley W Mr ashley.blom@nbt.nhs.uk Musculoskeletal Research Unit Avon Orthopaedic Centre England
Knapp Jonathan G Mr j.g.knapp2003@gmail.com Department of Chemistry University of Bristol England
Faul Charl FJ Dr charl.faul@bristol.ac.uk Department of Chemistry University of Bristol England

Submitted by:Blackburn, Julia Miss

This study is the first to describe the fabrication of covalent LPA-functionalised titanium that is better suited to support calcitriol-induced human osteoblast maturation. Our research provides an important first step in realising the development of superior, next-generation, functional biomaterials.

Introduction
160,000 total hip and knee replacements are performed in the UK every year. 10% will fail due to aseptic loosening and require revision surgery costing an estimated £300m per year. Successful osseointegration requires the production of a mechanically competent collagenous matrix, by osteoblasts, at the implant site. Numerous studies have described non-covalent interactions of various agents to biomaterials to enhance osseointegration, but covalent biomaterial modifications are more likely to produce surfaces capable of withstanding the rigors of the implantation process. Furthermore the growth factors selected are typically large molecules, e.g., bone morphogenic proteins, which are more likely to pose steric hindrances to target cell surface receptors. Lysophosphatidic acid (LPA) is a small bioactive lipid which we discovered interacts with vitamin D3 (D3) to secure human osteoblast (hOB) maturation at both titanium (Ti) and hydroxyapatite surfaces.
Methods
We therefore covalently attached LPA and a related compound, (3S) 1-fluoro-3-hydroxy-4-butyl-1-phosphate (FHBP), to both solid and porous Ti discs. Four methods of attachment were assessed. Either piranha solution or hot (60⁰C) concentrated sodium hydroxide (10M) were used prior to attachment of one of two linker molecules (3-mercaptopropyl trimethoxysilane(MTPMS) or vinyl trimethoxysilane(VTMS) in anhydrous toluene) over 24 hours. With VTMS, 1,8 octanedithiol was added prior to the final step for all methods in which LPA or FHBP were added with the radical initiator azobisisobutyronitrile (AIBN) at 60⁰C overnight.
Discs were seeded with hOBs, and after 3 days of culture, cell number and total alkaline phosphatase (ALP) activity were quantified to assess the ability of lipid-functionalised Ti to support D3-induced cell maturation. Solid functionalised discs were washed and reused a further two times, whilst other discs were stored for 6 months to ascertain LPA survival to irrigation and longer-term storage respectively. All experiments were performed three times and all data were subject to a one-way analysis of variance (ANOVA) to test for statistical significance. For p values of
Results
The method which best supported D3-induced osteoblast maturation involved piranha solution and MTPMS. Increased alkaline phosphatase (ALP) activity, independent of cell number, indicated that both LPA and FHBP-modified Ti serve as superior substrates for securing D3-induced hOB maturation compared to unmodified metal (p
Discussion
Covalent attachment ensures that the lipids are more likely to remain bound when subject to the forces encountered during implant insertion. Using a small molecule such as LPA, rather than larger growth factors, allows greater surface coverage and reduces potential steric hindrance to their cell surface receptor proteins. Research is ongoing to evaluate the efficacy of our modified Ti surfaces to secure hOB formation from their stem cell progenitors.

MANAGEMENT OF INFECTED NON UNION OF TIBIA BY ILIZAROV CIRCULAR FIXATOR- a study of 41 cases.

Submitted by:Chandrasekaran, Annamalai Professor

the circular external fixator has a biomechanical advantage, single procedure, percutaneous and no bone graft was used when the techniques improved. 100% union was achieved.

the circular external fixator has a biomechanical advantage, single procedure, percutaneous and no bone graft was used when the techniques improved. 100% union was achieved.

Aim

To study the outcome of infected non union of both bones of leg treated with Ilizarov circular fixator system.

Introduction

Acute and delayed open fractures of tibia are one of the common Orthopaedic problems in a busy trauma unit. They are either brought in immediately or delayed according to the place the injury had happened either near by or from far off places. Many factors play. The delayed fractures more than six hours are attended earlier in some centers and a proper initial management would not have been possible, invariably leading on to infection. Some patients with multiple skeletal problems are resuscitated from distant places, operated elsewhere come with already infected fractures. All these fractures pose difficulties in their management in the form of preventing or eliminating infection, stabilisation of the fracture, skin cover, bony union, functional rehabilitation, time taken and finally the cost factor. With earlier experience of different modalities of management of this problem, we have used Ilizarov circular external fixator which is helpful in solving almost all the problems because of biomechanical advantage.

This study was done in Sri Ramachandra Medical University, between May, 1995-April2012.41 cases were treated in a single unit and followed up periodically

All the cases were of trauma origin and infected during the course of treatment elsewhere presented to us with an intra medullary device and screws, external fixators :tubular/ring, plaster of paris casts or native bandages. Invariably they had discharging sinus or healed ones during the course of treatment. Few discharges from sinuses grew organism. Blood investigations occasionally normal, few with raised ESR and CRP.

The non unions were classified according to Czech and Weber. When a culture is positive appropriate antibiotics were given for 3 days, and when no organism was grown routine prophylactic antibiotics were given. Procedures and results are shown in chart.

This study proves the circular external fixator has a biomechanical advantage, single procedure, percutaneous and no bone graft was used when the techniques improved. 100% union was achieved.

MANAGEMENT OF LARGE BONE DEFECT : A STUDY OF 41 CASES USING MECHANICAL PRINCIPLES OF ILIZAROV CIRCULAR FIXATOR

Submitted by:Chandrasekaran, Annamalai Professor

Distraction osteogenesis using circular ilizarov fixator is a rewarding procedure as it gives back a sensitive feet by preventing amputation.

AIM
There are various methods to treat a bone defect more than 3 cm. This study of 41 cases of different aetiology is treated by using mechanical principles of Ilizarov Circular fixator.
Trauma -33
Osteomyelitis -01
Tumour -02
Congenital -02
APM stage iii -02
Post infective - 01

Introduction
Large bone defects of bone are difficult to treat for the reason, the regenerated bone has to restore its anatomical structure, able to withstand for the routine daily activity and physiologically restore the normal functions.
This work was done in Sri Ramachandra Medical University, Chennai; India from June 1995 to April 2012.The age group was between 3years to 70 years, Males 34 and females 8. The gap measured from 3 am to 20 cm. Up to 5 cm external bone transport is useful. Double osteotomy will be required for a 5-10 cm gap. More than 10 cm internal bone transportation is useful. Normally it takes almost a year up to 10cm. A very large defect of 20 cm the distraction time and consolidation time is very prolonged and may require staged procedure and other enhancing factors like bone marrow aspirate concentrate.
Procedures
Resection, bifocal distraction : compression osteosynthesis, arthrodesis - 03
Closed distractional osteosynthesis - 06
Tibiofibular synostosis -03
Bifocal distraction- compression osteosynthesis -24
Osteotomy and lengthening -05
Trifocal distraction :compression osteosynthesis -01
Some patients required more than 2, 3 procedures, consolidation time is variable almost 3 to 5 times the distraction period, patient education for a proper follow up does not work. The desired length may not be achieved due to different causes.Complication rates are high and can be prevented by good preoperative planning, proper follow up, identification of complications, revision if necessary. But finally it is a rewarding procedure as it gives back a sensitive feet by preventing amputation.

Periprosthetic acetabular bone density and metal ion levels after large head metal-on-metal total hip arthroplasty, short-term results from a randomized controlled trial

Van der Veen Hugo HC MD hcvanderveen@hotmail.com Martini Hospital Groningen Netherlands
Van den Akker-Scheek Inge I MSc PhD ingescheek@hotmail.com Martini Hospital Groningen Netherlands
Zee Mark MJM MD m.j.m.zee@gmail.com Martini Hospital Groningen Netherlands
Bulstra Sjoerd SK MD PhD s.k.bulstra@orth.umcg.nl University Medical Centre Groningen Groningen Netherlands
Van Raay Jos JJAM MD PhD raayjjam@mzh.nl Martini Hospital Groningen Netherlands

Submitted by:Zijlstra, Wierd MD PhD

We compared large head metal-on-metal to metal-on-polyethylene total hip arthroplasty in a randomized trial. Bone density superior to the cup was retained in metal-on-metal patients, but not in metal-on-polyethylene patients, after 1 year, irrespective of metal ion levels.

Information on periprosthetic acetabular bone density is lacking for large head metal-on-metal total hip arthroplasties. We aimed to evaluate periprosthetic acetabular bone density, clinical results and serum metal ion levels after large head metal-on-metal total hip arthroplasty . We describe the short term results, at 1 year postoperatively, in an ongoing trial.

We compared cementless large femoral head (mean 48mm) metal-on-metal total hip arthroplasties (M2a-Magnum, Biomet) to cementless 28mm metal-on-polyethylene total hip arthroplasties (Mallory-Head, Biomet) in a randomized clinical trial. Periprosthetic acetabular bone density was analyzed with dual energy x-ray absorptiometry in four periprosthetic acetabular regions of interest in 70 patients. Baseline bone density at 6 weeks postoperatively did nof differ between groups, using the native contralateral hip.

After 1 year, bone density decreased (-3.5% to -7.8%) in 3 of 4 regions of interest in metal-on-polyethylene patients, but was retained in all regions in metal-on-metal patients. Bone density preservation was most pronounced superior to the cup (+1% versus -3.7%). Serum cobalt and chromium ion levels were elevated in the metal-on-metal patients (median 1.7, resp. 2.1 µg/L); titanium levels were equal in both groups (5.3-5.7 µg/L). Ion levels were not related to bone density, acetabular inclination or femoral head size. Oxford and Harris hip scores improved in both groups, and were similar.Radiological analysis revealed no subsidence, pedestals, bone densification, periprosthetic osteolysis, interface deterioration or reactive line formation.Cumulative survival at 1 year, with revision for any reason as the endpoint, was 100% for the metal-on-polyethylene and 96% for the metal-on-metal group (95%-CI 90.5-100%). At 3 years, these rates were 100% and 94% (3 revisions; 95%-CI 87-100%), respectively. The two survival curves were not statistically different. CT-scanning of all patients is under way.

Periprosthetic acetabular bone mass density was retained with large head metal-on-metal total hip arthroplasty, compared to 28mm metal-on-polyethylene arthroplasty. Allthough preliminary, this may support better bone loading and preservation with large head hard-on-hard bearings. Large head metal-on-metal bearings are not forgiving and warrant careful surveillance.

Periprosthetic acetabular regions of interest (ROI) used for the bone mass density (BMD) measurements with dual energy x-ray absorptiometry (DEXA).

Weil

shoaib amer as mr amershoaib@doctors.org.uk stockport nhs foundation trust stockport united kingdom
hakim zuned zh mr zhakim@doctors.org.uk stockport nhs foundation trust stockport united kingdom
lattouf gerard gl mr gerardlattouf@yahoo.com stockport nhs foundation trust stockport united kingdom
omar alsawaf oa mr omar.alsawaf@stockport.nhs.uk stockport nhs foundation trust stockport united kingdom
Submitted by:shoaib, amer mr

Basic science studies has indicated that Morton’s Neuroma may be a result of a compression neuropathy. This study details the clinical results of decompression rather than excision of the interdigital nerve.

Introduction

Morton’s Neuroma is routinely treated by excision of the interdigital nerve. . Traditional surgery works by denervation, but the results are variable, and recurrence is common. Multiple Morton’s Neuromas present a difficult clinical challenge. MR and ultrasound often demonstrate a normal nerve or an interdigital bursa. Some experts advise division of the intermetatarsal ligament rather than excision. This case series evaluates an alternative method of treatment.

Methods

Patients with a clinical diagnosis of Morton’s Neuroma, with symptoms only on weight bearing, were treated with division of the intermetatarsal ligaments and Weil’s osteotomies. The nerve was not excised. Patients wore a postoperative shoe for six weeks. If radiographs were satisfactory, they returned to weight bearing in a normal shoe. They were evaluated at 12 weeks with AOFAS scoring, as part of the routine clinical pathway.

Results

14 patients were treated with Weil’s osteotomy, including one who had recurrence of symptoms following traditional surgery. The mean AOFAS score rose from 71 to 91. No patient had recurrent symptoms after surgery. The patient who had previously been treated with excision of the nerve also had some improvement.

Discussion

The success of this surgery in relief of symptoms in this case series raises questions about the pathology, diagnosis and treatment of Morton’s Neuroma. Many MR studies find abnormal nerves in asymptomatic patients, and no neuroma in symptomatic patients. Patients have symptoms exacerbated by weight bearing, and nerve compression may play an important part in the pathophysiology. Weil’s osteotomy works by decreasing the effective weight bearing in the involved rays. It is particularly useful if symptoms exist in multiple intermetatarsal areas.

Conclusions

Multiple Weil’s osteotomies are an effective method for treatment of Morton’s Neuroma. The basis for the traditional approach of excision of the nerve may be flawed and merits further study.

Changes In Foot Dimensions After Forefoot Surgery : Why Does The Shoe Still Not Fit.

Hakim Zuned ZH Mr Zhakim@doctors.org.uk Stockport NHS Foundation Trust Stockport UK
Heire Priam PH Dr priam-heire@doctors.org.uk Stockport NHS Foundation Trust Stockport UK
Lattouf Gerard GL Mr GerardLattouf @yahoo.com Stockport NHS Foundation Trust Stockport UK
Shoaib

Introduction

Patients with hallux valgus often complain of difficulty in finding suitably sized footwear both preoperatively and postoperatively. The deformity leads to increased forefoot width that patients expect to be reversed with surgery. There is little data on the quantification of the changes in foot dimensions and why patients continue to have problems with footwear.

Patients and Methods

91 feet were identified in 85 patients operated upon for hallux valgus surgery, hallux valgus and lesser ray procedures or lesser ray procedures alone. Preoperative and postoperative weight bearing AP radiographs were analysed to measure the soft tissue and bony forefoot width and the soft tissue height. The percentage and absolute changes in bony and soft tissue dimensions were calculated.

Results

There was a mean reduction of 2.7% in soft tissues after lesser ray surgery alone. There was a mean reduction of 8.6% in bony width after scarf or chevron osteotomies alone. There was a mean reduction of 8.3% in bony width after scarf or chevron osteotomy with lesser ray procedures. Bony reductions were statistically significant.

The soft tissue height of the foot increased 1.8% in lesser ray surgery, 26% in chevron and lesser ray surgery and 30% in scarf and lesser ray surgery. These were statistically significant.

Discussion

A consistent reduction in forefoot width following hallux valgus surgery occurs. This does not explain why patients continue to have footwear problems, but the significant soft tissue change in vertical height does. The type of osteotomy and extent of surgery affect the degree of increase in vertical height.

This study has identified that the reason that patients continue to have footwear difficulties after forefoot surgery is the change in vertical height of the forefoot. Patients should be informed of this preoperatively to ensure realistic expectations.

Amer AS Mr amershoaib@doctors.org.uk Stockport NHS Foundation Trust Stockport UK

Forefoot surgery results in a change in the dimensions of the foot. Although bony width of the foot decreases with procedures involving the hallux the soft tissue height increases which can account for on-going footwear difficulties.

DISTAL TIBIAL LOCKING PLATES : NOT AN EASY OPTION FOR SURGEON OR PATIENT

Hakim Zuned ZH Mr zhakim@doctors.org.uk Stockport NHS Foundation Trust Stockport UK
Choi Cameron CC Dr Stockport NHS Foundation Trust Stockport UK
Lattouf Gerard GL MR GerardLattouf @yahoo.com Stockport NHS Foundation Trust Stockport UK
Shoaib Amer AS MR amershoaib@doctors.org.uk Stockport NHS Foundation Trust Stockport UK
Submitted by:Hakim, Zuned Mr

Distal tibial fractures are difficult and challenging fractures to manage. Locking plates are a good method of treatment when used appropriately, particularly given the alternative is external fixation. Complications rates are low but potentially serious.

Introduction

The treatment of very distal tibial fractures and pilon fractures is difficult. There is a wide variation in the severity of injury and the options for surgical management. Plates and external fixation each have their advantages. This retrospective study looks at complications and technical tips for anterolateral plating.

Materials and Methods

35 consecutive distal tibial platings were evaluated. The AO classification for each fracture was determined and any patient factors affecting outcome. Outcome variables included time to radiological union, infection rate, wound breakdown rate, and joint movement after treatment.

Results

There were 32 anterolateral platings and 3 medial platings. The union rate was 95%. There were two deep infections which required surgical treatment. There were two wound breakdowns, one of which required plastic surgical intervention. Two patients had prominent metalwork, requiring removal. Other complications included deep peroneal nerve palsy, stiffness, and vascular compromise. The complication rates were lower for surgeons operating more frequently on these fractures. Two patients subsequently required bone transport and one required an amputation.

Discussion

The complication rate found was similar to that reported in the literature. The few complications were however very significant for the patient and also for the surgeon as they required bone transport. Complications other than infection occurred in the few cases performed by surgeons low on their learning curve. We present technical tips for surgery. The presence of callus only after mobilisation indicates that union is slow.

Anterolateral plating is a viable option for distal tibial fractures, especially 43B fractures. There is a learning curve associated with their use. Complication rates are low overall, but significant consequences can accompany complications. As an alternative to external fixation, distal locking plates are not a pain free option for the surgeon, as well as for the patient.

Assessment of Rehabilitation Programme for Joint Hypermobility Syndrome using Postural Stability as a Quantitative Outcome Measure

Hu Xiaoyang Ms huxy1119@gmail.com UCL Institute of Orthopaedics and Musculoskeletal Science London UK
Kostic Daniella Ms d.kostic@ucl.ac.uk UCL Institute of Orthopaedics and Musculoskeletal Science London UK
Tan Wang Sin Dr gina.tan.ws@gmail.com Royal National Orthopaedic Hospital London UK
Sathiananda Sobitha Dr sobitha.sathiananda@rnoh.nhs.uk Royal National Orthopaedic Hospital London UK
Cohen Helen Dr helen.cohen@rnoh.nhs.uk Royal National Orthopaedic Hospital London UK
Wolman Roger Dr roger.wolman@rnoh.nhs.uk Royal National Orthopaedic Hospital London UK
Submitted by:McCarthy, Ian Dr

Analysis of postural stability using a force plate was shown to be a simple and precise way of assessing patients with joint hypermobility syndrome, and could demonstrate the effectiveness of an exercise-based rehabilitation programme.

Introduction:

Joint Hypermobility Syndrome (JHS) patients have been shown to exhibit proprioceptive deficit, which may lead to inappropriate loading of joints and contribute to subsequent joint damage. However, at present there is no standard objective outcome measurement. As there is a large proprioceptive contribution to postural control, the use of a force plate is one possible method to provide a precise measurement of postural stability and also proprioceptive acuity. The objectives of our study are: 1) to quantify postural stability measurements as well as the physical activity levels in patients with JHS and in normal subjects, and 2) to use postural stability measurement to evaluate the effectiveness of a three-week in-patient rehabilitation programme for patients with JHS.

Patients and Methods:

25 JHS patients and 25 age- and gender-matched controls were recruited and asked to stand for 30 seconds on a force plate (Leonardo Mechanography®, Novotec, Pforzheim, Germany). Tests were performed with two legs feet together (Romberg test), with eyes open (RomEO) and then with eyes closed (RomEC). The standard Ellipse Area (EA) containing 90% of the path of the Centre of Force was measured. Patients' and controls' age, height and Beighton score were also recorded. An International Physical Activity Questionnaire assessing the time they spent on vigorous activity, moderate activity, sitting and walking for last seven days was also completed by the subjects. Ethical approval was obtained from the NHS National Research Ethics Service, and all participants gave written informed consent. In the second part of the study, ten patients with severe clinical symptoms who had been admitted to our institution for an intense three-week rehabilitation programme were studied. Measurements of postural stability were performed at the start and end of their rehabilitation; these patients also completed the IPAQ questionnaire.

Results:

Patients with JHS had worse postural stability (EA = 8.69 + 7.13 cm^2) than controls (EA = 3.17 + 2.30 cm^2) for the RomEC test (P=0.02); they also spent much less time on physical activities than a comparable control population (P=0.001). Moreover, vision contributed more to postural stability in patients than in the control population (P=0.001). For patients undergoing the in-patient rehabilitation programme, there was a statistically significant improvement in their postural stability from a mean EA of 21.49 + 14.78 to 9.02 + 11.54 cm^2 (p = 0.005).

Discussion:

We were able to show that, as a group, JHS patients have worse postural stability than control subjects. The study was able to develop a standardized clinical measurement method. Using this method, we have shown a significant improvement in postural stability for patients in a rehabilitation programme, though their stability was still outside the normal range.

In vivo Measurement of the Stiffness of Regenerate Bone in Distraction Osteogenesis of the Tibia using RSA, Load Measurement and CT

Reina Romo Esther Dr erreina@us.es University of Seville Seville Spain
Calder Peter Mr peter.calder@rnoh.nhs.uk Royal National Orthopaedic Hospital London UK
Marsh David Prof d.marsh@ucl.ac.uk UCL Institute of Orthopaedics and Musculoskeletal Science London UK

Submitted by:McCarthy, Ian Dr

The decision about the time point to remove the external frame in limb reconstruction surgery is difficult. Quantitative analysis may provide a more objective means of assessment that can aid clinical decision-making.

Introduction:
Patients must spend a significant period of time in an external frame during distraction osteogenesis. This has driven research efforts into new therapies to increase the rate of repair. Objective measurements of the maturation of regenerate are required to evaluate adjunct therapies such as low amplitude high frequency vibration or the use of stem cells. It is proposed that i) Load measurements combined with roentgen stereophotogrammetric analysis (RSA) can be used to calculate the stiffness of the regenerate in distraction osteogenesis of the tibia; ii) Patient-specific finite element (FE) analysis derived from CT images can predict the stiffness of the regenerate.
Material & Methods:
To validate the technique, the accuracy and precision of RSA to assess movement at the osteotomy site was performed using synthetic bones into which tantalum markers were implanted. Controlled movement was applied using a precision x-y-z stage. Movement resulting from applied load was measured, together with the load transmitted through the regenerate, which was simulated by materials of differing stiffness. In the clinical application, tantalum RSA marker beads were inserted into the bone either side of the osteotomy site during surgery. On two or three occasions during maturation of the regenerate stiffness measurements were performed. The longitudinal struts of the external circular frame were replaced by aluminium rods containing tension-compression load cells. Two pairs of RSA x-rays were taken, the first with the limb unloaded and the second with a load of 20% body weight applied to the limb. Simultaneously, the load cells attached to the external frame measured the load transmitted through the frame. After these measurements, CT scans were performed with an orthogonal resolution of 0.3 mm. The scans of the regenerate were segmented into mineralised and non-mineralised tissue, which were then meshed and converted into FE models.
Results:
RSA was shown to measure accurately and precisely the displacement of the regenerate under load. Clinically, axial displacement of the regenerate decreased during the maturation phase, though RSA demonstrated complex relative 3D movement between the bone ends. Load share through bone increased during maturation. Mineralisation of the regenerate initiated close to the bone ends, and increased with time. Isolated islands of mineralisation can also be seen in the centre of the regenerate. FE analysis demonstrated the heterogeneity of mechanical properties within the regenerate. Comparison of RSA measurements with FE analysis has so far been performed in two patients. Initial axial displacements under load were 4.16 mm and 0.88 mm, decreasing to 0.13 and 0.04 mm respectively at the time at which removal of the frame was being considered. These latter values are comparable to or less than the measurement error for RSA. From these measurements, estimates of axial stiffness for the regenerate at the end of maturation were 1488 N/mm and 3536 N/mm, compared with 1347 N/mm and 2026 N/mm respectively estimated from FE analysis.
Discussion & Conclusion:
We conclude that it feasible to monitor the early progression of regeneratematuration using a combination of imaging RSA and direct load measurement. RSA is a research technique that is only available in a small number of centres, but quantitative analysis of CT scans is a promising approach to estimation of regenerate stiffness that may be more generally applicable.

A combined clinical and biomechanical look on early femoral component loosening in high flexion total knee arthroplasty: what about the cement-bone interface?

Groes van der Sebastiaan S Drs.Msc. svandegroes@gmail.com RUNMC Nijmegen Netherlands
Waal Malefijt de Maarten MC MD PhD M.deWaalMalefijt@orthop.umcn.nl RUNMC Nijmegen Netherlands
Verdonschot Nico N PhD n.verdonschot@orthop.umcn.nl RUNMC Nijmegen Netherlands

Submitted by:Verdonschot, Nico Prof.dr.ir.

The femoral component of high flex TKA's may loosen at high flexion. We analyzed the strength of the metal-cement and bone-cement interface and indicate how the bone can be prepared in order to reduce the probability of failure.

Introduction

A few follow-up studies of high flexion total knee arthoplasties report disturbingly high incidences of femoral loosening. Finite element analysis showed a high risk for early loosening at the cement-implant interface at the anterior flange. However, femoral implant fixation is depending on two interfaces: cement-implant interface and the cement-bone interface. Due to the geometry of the distal femur, a part of the cement-bone interface consists of cement-cortical bone interface. The strength of the cement-bone interface is lower than the strength of the cement-implant interface.

The research questions addressed in this study were: 1) which interface is more prone to loosening and 2) what is the effect of different surgical preparation techniques on the risk for early loosening.

Materials & methods

To achieve data for the cement-(cortical)bone interface strength and the effects of different preparation techniques on interfacial strength, human cadaver interface stress tests were performed for different preparation techniques of the bony surface and the results were implemented in a finite element (FE) model as described before. The FE model consisted of a proximal tibia and fibula, TKA components, a quadriceps and patella tendon and a non-resurfaced patella. For use in this study, the distal femur was integrated in the FE model including cohesive interface elements and a 1 mm bone cement layer. In the model, the cement-bone interface was divided into two areas, representing cortical and cancellous bone. The posterior-stabilised PFC Sigma RP-F (DePuy, J&J, USA) was incorporated in the FE knee model following the surgical procedure provided by the manufacturer. A full weight-bearing squatting cycle was simulated (ROM = 50°-155°). The interface failure index was calculated.

Results

Overall, the highest stresses were found at the proximo-medial part beneath the anterior flange of the femoral component. Highest shear stresses were found at the cement-implant interface (peak shear stress of 3.33 MPa at 150° of flexion). Highest tensile stresses were found at the cement-cortical bone interface (peak tensile stress of 1.30 MPa at 150° of flexion).

The failure index was highest at the cement-bone interface. When the total anterior flange was covering cancellous bone, 0.4% of the cement-bone interface would fail and 0% of the cement-implant interface at 145° of flexion. In the more realistic simulation of cortical bone with periost, almost 31.3% of the complete cement-bone interface would fail even within normal range of motion (<120°). This can be reduced by drilling holes through the cortex to 2.6%.

Discussion

Obviously, the FE knee model utilized in this study contains limitations which may have affected the interface stresses calculated. However, the results presented here clearly demonstrate high risk of early loosening at the cement-bone interface. This risk can be reduced by some simple preparation techniques of the cortex behind the anterior flange. Proper anterior fixation of the femoral component, and thus adequate surgical technique, is essential to reduce the risk of femoral loosening for high-flexion TKA.

Refixation of osteochondral fractures by ultrasound-activated, resorbable pins - an ovine in-vivo study

Kienast Benjamin JW Dr. bekienast@web.de BG Trauma Center Hamburg Germany
Neumann Hanjo hanjo@biomechatronics.de BG Trauma Center Hamburg Germany
Schulz Arndt P PD Dr. mail@apschulz.de University of Luebeck Medical Center Luebeck Germany
Gille Justus PD Dr. justus_gille@usa.net University of Luebeck Medical Center Luebeck Germany
Klinger Matthias PD Dr. klinger@anat.uni-luebeck.de University of Luebeck Medical Center University of Luebeck Medical Center Germany
Juergens Christian Prof. Dr. c.juergens@buk-hamburg.de BG Trauma Center Hamburg Germany
Submitted by:Kienast, Benjamin Dr.

Refixation of osteochondral fracture fragments with conventional and bioresorbable materials was evaluated in a sheep model. The new SonicPin showed promising results compared to the established Ethipins and Microsrews.

Ostecohondral injuries, if not treated adequately, often lead to sever osteoarthritis. Possible treatment options of these injuries are the refixation of the fragment or replacement therapies like pridie drilling, microfracturing or osteochondral grafts. They all have certain disadvantages. Only refixation of the fragment can lead to a smooth and resilient joint surface. Aim of this study was the evaluation of an ultrasound-activated bioresorbable pin (SonicPin™, Stryker) for the Refixation of osteochondral fragments under physiological conditions. In 16 Merino sheep defined osteochondral fragments of the medial femoral condyle were produced and refixated with either SonicPins™, Ethipins® or conventional titanium microscrews. Macroscopic and microscopic scoring was accomplished after three months. The SonicPin™ system is qualified for the refixation of osteochondral fractures. The healing ratio is higher than in the Ethipin®-group and lower than in the screw-group. A negative influence on the cartilage by the induced heat through the SonicPin™ system is not proved. No further operation for the removal of the implant is necessary. The imaging by MRI is not compromised, as it is with implanted screws.

EQUIVALENT CHANGES IN GENE EXPRESSION IN ARTICULAR CARTILAGE AFTER PHYSIOLOGICAL AND EXCESSIVE LOADING. Activation of protective TGF-beta signaling.

van Caam Arjan APM MSc. A.vanCaam@reuma.umcn.nl Nijmegen Centre for Molecular Life Sciences, Radboud University Nijmegen Medical Centre Nijmegen Netherlands
de Mulder Eric ELW MSc. E.deMulder@orthop.umcn.nl Nijmege Radboud University Nijmegen Medical Centre Nijmegen Netherlands
van der Kraan Peter PM Dr. P.vanderKraan@reuma.umcn.nl Nijmegen Centre for Molecular Life Sciences, Radboud University Nijmegen Medical Centre Nijmegen Netherlands
Buma Pieter P Prof. Dr. P.Buma@orthop.umcn.nl Nijmegen Centre for Molecular Life Sciences, Radboud University Nijmegen Medical Centre Nijmegen Netherlands
Submitted by:Madej, Wojciech MSc

Physiologically loaded and excessive loaded chondrocytes activate similar genes involved in cartilage homeostasis. Furthermore, repetitive compression activate protective TGF-beta signaling which can suppress the chondrocytes terminal differentiation.

Introduction:
(Partial) Meniscectomy causes dramatic changes in knee joint biomechanics. This frequently leads to development of osteoarthritis (OA). However, the mechanism how changed loading patterns leads to OA remains unknown.During early stages of OA, chondrocytes undergo changes analogous to the terminal differentiation of chondrocytes. Terminal differentiation can be repressed by TGF-ß and Smad2/3 signaling is the key route of mediation of this inhibitory effect.
Objective:
To test the effect of physiological and excessive loading of cartilage on the expression levels of genes involved in cartilage metabolism and chondrocyte differentiation.
Materials and methods:
Full-thickness articular cartilage specimens were cored from metacarpophalangeal joint surface of skeletally mature cows. Explants were divided into two stimulation groups: 30 min stimulation with 3 MPa (physiological) and 30 min stimulation with 12 MPa (excessive). Unloaded cartilage was used as control. Groups were subjected to sinusoidal compression (1Hz) using BOSE ElectroForce®BioDynamic® test system, in culture conditions. After two different time intervals (2 and 6 hours) samples were frozen, total RNA was isolated and cDNA produced. The expression of selected genes was examined using real-time PCR.
Results:
Mechanical compression caused significant changes in expression of genes involved in cartilage metabolism. There was significant up regulation of TGF-ß1 and COX-2 in both mechanically stimulated groups when compared to static control. However there were no significant differences in TGF-ß and COX-2 expression levels between 3MPa and 12MPa stimulation groups. In addition, there was no difference in expression levels of TGF-ß and COX-2 between the two time intervals. Furthermore, mechanical compression modulated the expression of markers for TGF-ß signaling pathways. Stimulation with both; physiological loading (3MPa) and overloading (12MPa) resulted in up regulation of PAI-1 expression, indicating of activated Smad2/3. In contrast, ID1 expression was significantly down regulated. Mechanical compression caused non-significant changes in the expression levels for ECM compounds (COL2A1, ACAN) and for iNOS. Gene expression of IL-1ß, MMP-3, 9 and 13, ADAMTS4 and 5, IL-10 was not detectable in any experimental group.
Discussion:
Physiologically loaded and excessive loaded chondrocytes in articular cartilage specimens activate similar genes involved in cartilage homeostasis. Changes in expression of genes by repetitive loading do not depend on the amount of force that was applied in our experiments. In physiologically loaded and excessive loaded articular chondrocytes, TGF-ß signals via ALK5 and cause activation of the Smad2/3 pathways. This activation might be involved in the suppression of the chondrocytes terminal differentiation.

Submitted by:Schulz, Arndt P. MD, PhD, MRCS (Glasgow)

The biomechanical properties of Titanium oesteosynthesis plates can in theory be improved by plasma polishing. We compared different implantsn an endurance test for interaction with simulated soft tissues. We could show that surface energy of polished titanium plates is reduced.

Introduction:

Bone plates for fracture fixation are commonly made from stainless steel, titanium alloy or pure titanium. Electrochemical polishing can improve corrosion resistance of stainless steel as well as fatigue resistance of titanium implants. The good biocompatibility and osteointegrability of titanium is favorable for long-term implants like total joint arthroplasty yet renders removal of titanium bone plates difficult. Soft tissue irritations are also a side effect of titanium bone plates.

The aim of this study was therefore to evaluate the influence of electrolyte-plasma polishing on mechanical soft tissue interaction of pure titanium and titanium alloy bone plates.

Materials and Methods:

Test samples of stainless steel (DIN ISO 5832-1), grade 2 titanium (DIN ISO 5832-2) and Ti-6Al-4V (DIN ISO 5832-3) were tested for Vickers hardness, contact angle and surface roughness. An endurance test for the mechanical interaction between sample surface and soft tissue was carried out with a custom made testing machine (Figure 1). This machine simulates sliding of tendons on the surface of the sample with five parallel strings of non-resorbable suture in saline solution. The strings are driven cyclic with a frequency of 5Hz by a DC motor and are held in tension with individual pull-springs. The number of cycles until rupture of the individual strings is counted with camera control.

Results:

No difference of Vickers hardness of the samples was found before and after plasma polishing.

Surface energy of stainless steel is 33.5mN/m, for grade 2 titanium 46.4mN/m and 39.5mN/m after polishing and for Ti-6Al-4V 60.7mN/m and 45.2mN/m after polishing.

Roughness (Ra) is 0.12µm for stainless steel, for grade 2 titanium 0.8µm and 0.26µm after polishing and for Ti-6Al-4V 0.34µm and 0.3µm after polishing.

Mean sliding cyles until rupture was 31336 for stainless steel, 2775 for unpolished and 16833 for polished grade 2 titanium and for unpolished Ti-6Al-4V 2696 and 17286 for the polished sample.

Discussion:

Electrolyte-plasma polishing clearly reduces the surface roughness by a factor of 2 for grade 2 titanium. For Ti-6Al-4V it is only reduced by a factor of 0.13. The surface of stainless steel, however, is smoother than the polished titanium. Regardless of the small improvement in surface quality measured for the polished Ti-6Al-4V the endurance of sliding cycles for the titanium and titanium alloy samples is increased comparably. Stainless steel exhibits the best endurance with a factor of 2 in comparison to the polished titanium surfaces.

The surface energy of titanium is reduced by the electrolyte-plasma polishing thus adhesion of cells and bimolecules can be reduced. This effect is also described in literature; higher surface energies of rough titanium surfaces improve expression of bone specific extracellular matrix thus aiding osteointegration.

Investigation on Poisson's ratio of human cortical bone determined via LED-Micrometer : a feasibility study

Sitzer Annette A. M. Sc. sitzer@biomechatronics.de University Hospital Schleswig-Holstein, Biomechanics Laboratory Lübeck Germany
Waizner Klaus K. Dipl.-Ing. (FH) klaus.waizner@uksh.de University Hospital Schleswig-Holstein, Biomechanics Laboratory Lübeck Germany
Wendlandt Robert R. Dipl.-Ing. wendlandt@biomechatronics.de University Hospital Schleswig-Holstein, Biomechanics Laboratory Lübeck Germany
Handels Heinz H. Prof. Dr. rer. nat. habil. handels@imi.uni-luebeck.de University of Lübeck, Institute of Medical Informatics Lübeck Germany
Weyers Imke I. Dr. med. weyers@anat.uni-luebeck.de University of Lübeck, Institute of Anatomy Lübeck Germany
Jürgens Christian C. Prof. Dr. med. C.juergens@buk-hamburg.de Berufsgenossenschaftliches Unfallkrankenhaus Hamburg Hamburg Germany
Schulz Arndt-Peter A. P. PD Dr. med. schulz@biomechatronics.de Berufsgenossenschaftliches Unfallkrankenhaus Hamburg Hamburg Germany

Submitted by:Sitzer, Annette M. Sc.

After verification of a new test method determining the transverse stiffness of simulated cortical bone via LED-Micrometer, Poisson's ratio of human cortical bone was measured. Due to the rough surface of human bone after lathing the results were not reproducible.

Introduction

Up to now it is challenging to measure Poisson's ratio of human bone mechanically in each anatomic direction. Considering the human femur this is especially true for cortical bone of the diaphysis. Due to limited dimensions of samples extracted from the transverse plane and the applied force limited by the strength of bone, only small deformations of a few microns occur when mechanically loaded. Linear encoders showed a high inaccuracy when measuring the transverse expansion of small bone samples [1]. This study intended to verify a test method using a LED-Micrometer for the determination of Poisson's ratio.

Methods

In order to verify the reproducibility of the method, simulated cortical bone samples were measured with a varying position of the LED-micrometer after each second measurement. A transverse cuboid was extracted and turned down to a diameter of 3mm at a length of 3.4mm. The test setup design ensured uniaxial force application. The investigated LED-Micrometer allows the detection of sample expansion with a resolution of 0.1µm. The sample was loaded and expansion was measured four times in transverse and proximal-distal direction each. Afterwards stiffness was determined and investigated pairwise. Furthermore, three cadaveric human cortical bone samples were extracted from the femoral diaphysis, post-processed and loaded according to the previous artificial sample. The position of the LED-Micrometer was centrically readjusted after each measurement, in order to investigate the reproducibility of the method. Then Poisson's ratios were determined and investigated.

Results

The signal of the LED-Micrometer, describing transverse expansion of the artificial sample, showed positive curve linearity ($R^2=0.9871 \pm 0.0071$). Although different adjusted heights the transverse stiffness varied strongly the pairwise comparison showed small standard deviations below 2% with one outlier of 4.7%. In contrast, some signals describing expansion of the cadaveric bone samples were non-linear ($R^2=0.9177 \pm 0.1543$). Some even showed a negative progress resulting in negative Poisson's ratios. In general results were in a range of 0.14 ± 0.18 - 0.79 ± 0.57. High standard deviations are linked to the porosity of the samples.

Discussion/Conclusion

Although the reproducible results gained with simulated bone were promising, the investigation of cadaveric cortical bone could not verify the described test-method. The signal was susceptible to grooves in the surface. The LED-beam is too narrow to compensate for uneven surfaces of bone samples after lathing. Poisson's ratios of 0.2-0.5 were reported in literature [2]. The herein determined results yielding higher than 0.5 are unrealistic due to incompressibility of bone. Negative results are also impossible, since cortical bone shows no constriction when mechanically loaded. Conclusively, the LED-Micrometer is inadequate for the intended purpose.

References

[1] Sitzer, A.: Determination and verification of material properties related to CT data in human cortical bone, Master's Thesis, University of Lübeck/Lübeck University of Applied Sciences, 2010.
[2] Wirtz D., et al.: Critical evaluation of known bone material properties to realize anisotropic FE-simulation of the proximal femur. Journal of biomechanics, 2000. 33(10): p. 1325-1330.

The effect of a biphasic injectable bone substitute of the interface strength in a rabbit knee prosthesis model

Wang Jian-Sheng JS Wang Dr. jian-sheng.wang@med.lu.se Lund University Lund Sweden
Zampelis Vasilis V Zampelis Dr. Vasileios.Zampelis@med.lu.se Lund University Lund Sweden
Lidgren Lars L Lidgren Dr. lars.lidgren@med.lu.se Lund University Lund Sweden
Isaksson Hanna H Isaksson Researcher Hanna.Isaksson@solid.lth.se Lund University Lund Sweden
Tägil Magnus M Tägil Dr. magnus.tagil@med.lu.se Lund University Lund Sweden

Submitted by:Wang, Jian-Sheng Doctor

Summary

A biphasic injectable bone substitute can provide prosthetic stability in a rabbit tibia model and may increase the prosthetic interface strength in a later stage.

Introduction

Periprosthetic osteolysis is one of the most common causes leading to revision arthroplasty. Morselized cancellous bone graft is often used to reconstruct bone loss. Its limited availability and risk of blood borne disease such as hepatitis and HIV has led to use of injectable bone substitutes. In the present study a combination of both calcium sulphate and hydroxyapatite were used as bone void filler. Our aim was to investigate the prosthetic stabilisation and tissue integration with or without the use of an injectable bone substitute in a rabbit knee model.

Materials & Methods

Sixteen rabbits were used in the study. Bone marrow cavity in tibia was reamed with a3.6 mmdrill and a round tibia prosthesis stem of3.5 mmin diameter and8 mmin length was inserted in the proximal tibia. The rabbits were operated with bilateral prosthesis and the marrow was filled with or without injectable bone substitute (Cerament ®, Bonesupport, Sweden) consisting of 60% α-calcium sulphate hemihydrate and 40% hydroxyapatite with a radiocontrast agent, iohexol. The rabbits were euthanized after 6 and 12 weeks. Six rabbits in each period were analyzed by a mechanical pull out test and histology. The pull out test was performed under an Instron/MTS machine with displacement control at2 mmmin-1 and the pull out force was analyzed. Thereafter, histological and histomorphometric analysis of the specimens was performed using a microscope. The percentage of bone contact for each cross section was calculated by measuring the bone contact length divided by total prosthesis length. Micro-CT was used to analyze the total bone volume (1 mmaround the prosthesis) from 2 rabbits in each period.

Results

The interface strength between the prostheses fixed with or without Cerament® showed no significant difference, however, at 12 weeks the strength increased by 46% in the group using Cerament compared to 32% without ($p=0.05$). Histology showed a homogenous bone/ prosthetic contact. The remaining hydroxyapatite particles were integrated in the new-formed bone. Histomophometry and micro-CT showed similar bone contact in percent and bone volume around the prosthesis in the two groups.

Conclusion

In the present study, the bone substitute provided both initial and later prosthetic stabilization. As shown in histology and micro-CT, the proportion of new-formed bone in the interface was similar in the two groups. The new formed bone in the Cerament group contained hydroxyapatite particles and a different bone quality which in turn may give additional stability to the prosthetic component. We suggest that Cerament® can be used as bone void filler in prosthetic fixation.

Effect of electrolyte-plasma polishing on the surface properties of titanium bone plates - an in-vitro study with a novel testing device mimicking tendon properties

Wendlandt Robert RW Dipl. Ing. wendlandt@biomechatronics.de University Lübeck, Biomechanics Lübeck Germany
Jürgens Christian CJ Prof. Dr. juergens@apschulz.de BG Trauma Hospital Hamburg Hamburg Germany
Schulz Arndt P. APS PD Dr. aps77@web.de University Hospital Lübeck, Trauma and Orthopaedics Lübeck Germany

Submitted by:Schulz, Arndt P. MD, PhD, MRCS (Glasgow)

The biomechanical properties of Titanium oesteosynthesis plates can in theory be improved by plasma polishing. We compared different implants in endurance testing for interaction with simulated soft tissues. We could show that surface energy of polished titanium plates is reduced.

Introduction:
Bone plates for fracture fixation are commonly made from stainless steel, titanium alloy or pure titanium. Electrochemical polishing can improve corrosion resistance of stainless steel as well as fatigue resistance of titanium implants. The good biocompatibility and osteointegrability of titanium is favorable for long-term implants like total joint arthroplasty yet renders removal of titanium bone plates difficult. Soft tissue irritations are also a side effect of titanium bone plates.
The aim of this study was therefore to evaluate the influence of electrolyte-plasma polishing on mechanical soft tissue interaction of pure titanium and titanium alloy bone plates.
Materials and Methods:
Test samples of stainless steel (DIN ISO 5832-1), grade 2 titanium (DIN ISO 5832-2) and Ti-6Al-4V (DIN ISO 5832-3) were tested for Vickers hardness, contact angle and surface roughness. An endurance test for the mechanical interaction between sample surface and soft tissue was carried out with a custom made testing machine. This machine simulates sliding of tendons on the surface of the sample with five parallel strings of non-resorbable suture in saline solution. The strings are driven cyclic with a frequency of 5Hz by a DC motor and are held in tension with individual pull-springs. The number of cycles until rupture of the individual strings is counted with camera control.
Results:
No difference of Vickers hardness of the samples was found before and after plasma polishing.
Surface energy of stainless steel is 33.5mN/m, for grade 2 titanium 46.4mN/m and 39.5mN/m after polishing and for Ti-6Al-4V 60.7mN/m and 45.2mN/m after polishing.
Roughness (Ra) is 0.12µm for stainless steel, for grade 2 titanium 0.8µm and 0.26µm after polishing and for Ti-6Al-4V 0.34µm and 0.3µm after polishing.
Mean sliding cyles until rupture was 31336 for stainless steel, 2775 for unpolished and 16833 for polished grade 2 titanium and for unpolished Ti-6Al-4V 2696 and 17286 for the polished sample.
Discussion:
Electrolyte-plasma polishing clearly reduces the surface roughness by a factor of 2 for grade 2 titanium. For Ti-6Al-4V it is only reduced by a factor of 0.13. The surface of stainless steel, however, is smoother than the polished titanium. Regardless of the small improvement in surface quality measured for the polished Ti-6Al-4V the endurance of sliding cycles for the titanium and titanium alloy samples is increased comparably. Stainless steel exhibits the best endurance with a factor of 2 in comparison to the polished titanium surfaces.
The surface energy of titanium is reduced by the electrolyte-plasma polishing thus adhesion of cells and bimolecules can be reduced. This effect is also described in literature; higher surface energies of rough titanium surfaces improve expression of bone specific extracellular matrix thus aiding osteointegration.
Altogether, stainless steel shows the best surface properties for bone plates in terms of surface energy and mechanical soft tissue interaction and electrolyte-plasma polishing of titanium can only narrow this gap.

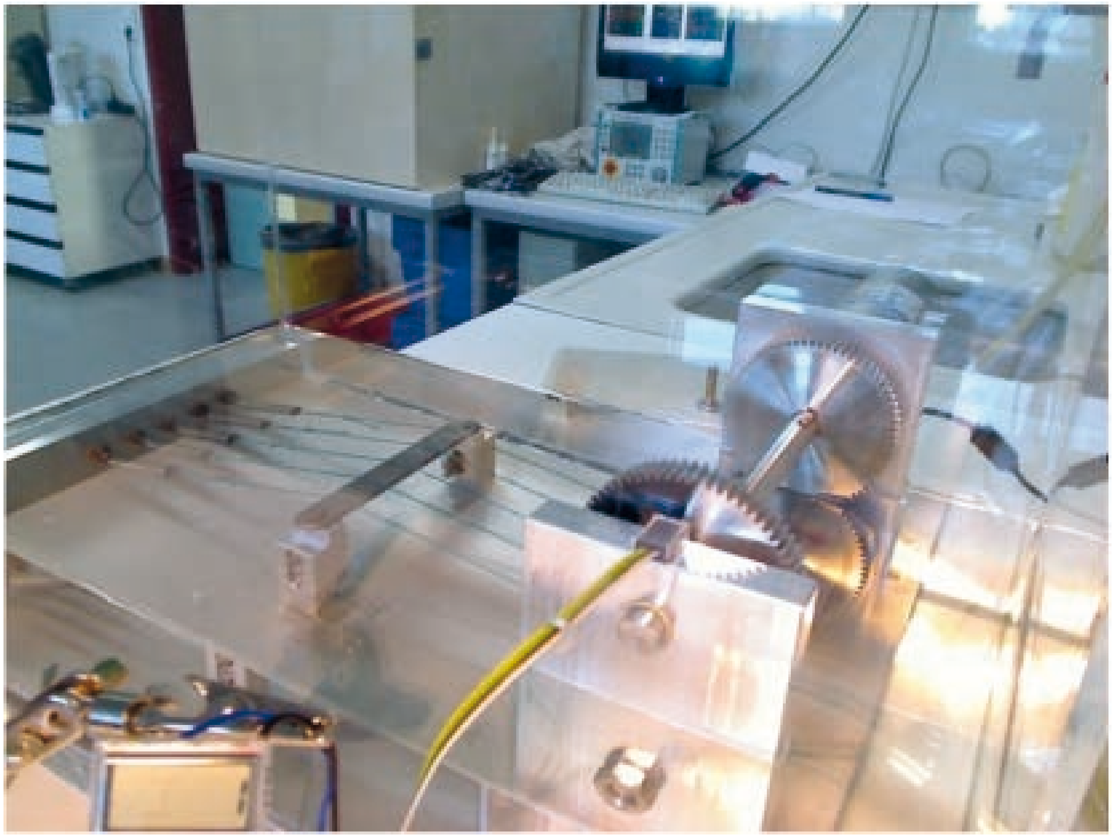

-Novel apparatus mimicking tendons sliding over an osteosynthesis plate.

Submitted by:del Prado, Gema PhD

The adherence of seven bacterial species to UHMWPE reinforced with carbon nanotubes was evaluated in this study. Adherence of five strains was significantly reduced ($p \leq 0.001$) when compared to that found on raw UHMWPE.

Introduction

Bacterial adherence has high clinical importance (1), being of particular concern in implant- related infections (2). Molecular functionalization using carbon nanotubes has recently shown some potential applications in biomedicine (3). Searching new biomaterials for prostheses engineering, this study has evaluated the adherence of seven bacterial species to a MWCNT reinforced polyethylene versus the raw material.

Material and Methods

The collection strain Staphylococcus aureus 15981 (4), and the reference strains Staphylococcus epidermidis ATCC 35984, Escherichia coli ATCC 29225, Pseudomonas aeruginosa ATCC 27853, Corynebacterium urealyticum ATCC 43044, Enterococcus faecalis ATCC 29212 and Mycobacterium fortuitum ATCC 6841, were included in the study. UHMWPE (GUR 1050®, Orthoplastic Ltd., Lancashire UK) discs with a diameter of 8 mm and 2 mm thick, containing or not 3 % wt multi wall carbon nanotubes, (NANOCYL® Nanocyl, Sambreville, Belgium) were tested as accretion surfaces.

For adherence studies, methodology of Pérez-Tanoira et al. (5) was applied, with minor modifications. Bacterial inoculum was prepared from an overnight culture in TSB-T at 37º C excepting for C. urealyticum and M. fortuitum, which were incubated in TSB-T plus Tween 80 for 72 hours. The sterilized surfaces were exposed to $\approx 10^8$ colony forming units (CFU)/mL during 90 minutes at 35º, washed with PBS (X 3) and incubated 24 hours at 4ºC. Finally, surfaces were stained with Acridine Orange for 2 min. Adhered bacteria were visualized by fluorescence microscopy. Images of 10-20 fields/ surface were photographed at 40x magnification. Assays were always made in triplicates. The percentage of bacterial coverage was determined by ImageJ software. Differences in bacterial adherence among surfaces as well as strains were individually analysed by unpaired t tests. Statistical significance was considered for $p \leq 0.001$.

Results

Figure shows the percentage of bacterial coverage per surface type (mean ± S.D). Significant reduction was observed in five bacterial species (S. aureus, P. aeruginosa, E. coli, C. urealyticum, and E. faecalis) when compared UHMWPE to the composite material.

E. coli registered the lowest adherence toUHMWPE compared to all the strains ($p \leq 0.001$) and equaled that S. aureus to MWCNT/UHMWPE. S. epidermidis and E. faecalis were the most adherent strains, finding significant differences respect all the other strains in MWCNT/ UHMWPE composites and raw UHMWPE, respectively.

Discusion / Conclusions

Regarding to the experimental data, the capability of MWCNT/UHMWPE in diminishing bacterial adherence seems to be species-dependent. Although neither the adherence of S. epidermidis or M. fortuitum was significantly reduced, the use of composite reinforced with MWCNT could be interesting against S. aureus (a leading cause of biomaterial-related infection) and other pathogens, with several applications. Since differences between laboratory and clinical strains could be found, further studies must be performed using clinical isolates.

References

1 Donlan et al.Clin Microbiol Rev (2002) 15:167-193
2. Kurtz et al. J Arthroplasty (2008) 23: 984-91
3. Wenrong-Yang et al. Nanotechnology (2007) 41: 412011 (12pp)
4. Valle et al. Mol Microbiol (2003) 48: 1075-87
5. Pérez-Tanoira et al. J Biomed Mat Research A (2012).100:1521:1528

Biomechanical testing of conventional vs. angular stable osteosynthesis plates with a synthetical fracture model of the osteopenic distal humerus

Wendlandt Robert wendlandt@gmail.com University medical center Schleswig-Holstein, Biomechanics Laboratory Luebeck Germany
Waizner Klaus klaus.waizner@uksh.de University medical center Schleswig-Holstein, Biomechanics Laboratory Luebeck Germany
Rank Christina University medical center Schleswig-Holstein, Biomechanics Laboratory Luebeck Germany
Renken Felix Dr. med University medical center Schleswig-Holstein, Trauma surgery Luebeck Germany
Schulz Arndt-Peter Dr. med schulz@biomechatronics.de University medical center Schleswig-Holstein, Trauma surgery Luebeck Germany

Submitted by:Wendlandt, Robert

Osteosynthesis plates were tested dynamically on a synthetic fracture model of the osteopenic distal humerus showing superior performance for angular stable plates as opposed to conventional plates.

Introduction:
Fractures of the distal Humerus account for approximately 2% of all fractures, the incidence increases sharply with age. The treatment of intra-articular transcondylar fractures of the distal humerus is very demanding as good stability is required to start physical therapy postoperatively. Traditionally biomechanical testing in this area has been performed with cadaveric specimen. Although realistic results can be gained, this model is problematic due to specimen shortage, preparation and reproducibility. In this study the testing is performed on a synthetic fracture model of the osteopenic distal humerus based on an artificial composite bone and polyurethane foam.
Methods:
For the development of the fracture model, composite artificial humeri were used for the proximal part of the fracture model and polyurethane (PU) foam with a density of 0.13g/cm³ was used for the articular fragments (both: Sawbones, Malmo, Sweden). The density of the PU foam was determined in repetitive pre-tests to produce a failure rate similar to failure rates in the literature. With a diamond saw (Exakt, Germany) a reproducible C2 fracture with a 5mm metaphyseal and a 0.7mm articular fragmental fracture gap was created. The fragments are fixed to the humeral diaphysis using an exact 90 degree formation of 2 locked small fragment reconstruction plates (Litos, Germany) or 2 conventional plates (Marquardt, Germany). Three specimens were assembled per group for testing. The distal part of the humerus was counterforced on a specificallly constructed rocker mechanism thereby realizing a physiological force transmission relation of 40/60 between the capitulum and trochlea. Sinusoidal forces were applied with an angle of 5° to the mechanical axis of the shaft to simulate a flexion movement of the elbow joint using a pneumatic testing machine (DHM 100824, Clausthal-Zellerfeld, Germany). Starting with a compressive force of 20N to 150N at a frequency of 1Hz the maximum force was increased every 5000 cycles by 10N. Every 1000cycles an image of the fracture gap without load is taken with a microscopy camera (DNT, Germany). When the gap is closed the test is finished. Also the failure mode is analyzed via the images.
Results:
The mean cycles until failure for the conventional plates are 12700 (5600 : 21500) and 57000 (54000 : 61000) for the angular stable plates. The failure mode for both types of osteosynthesis plates is screw loosening in the PU foam. Mechanical failure of the plates was not visible.
Discussion:
Construction of the setup was orientated at the works of Schuster et al. (J Orthp Trauma 2008). Though human cadaveric bones where used as compared to the synthetic fracture model in the current study, the results show a superior performance of the angular stable plates in the treatment of complex fractures of the distal humerus when bone quality is low. The specific evaluation of the test results are not completely equal, yet the results of Schuster et al. exhibit a failure ratio between conventional/angular stable of 0.25 similar to the ration of endured cycles of 0.22 in this study.

Submitted by:del Prado, Gema PhD

The adherence of seven bacterial species to UHMWPE reinforced with carbon nanotubes was evaluated in this study. Adherence of five strains was significantly reduced ($p \leq 0.001$) when compared to that found on raw UHMWPE.

Introduction

Bacterial adherence has high clinical importance (1), being of particular concern in implant- related infections (2). Molecular functionalization using carbon nanotubes has recently shown some potential applications in biomedicine (3). Searching new biomaterials for prostheses engineering, this study has evaluated the adherence of seven bacterial species to a MWCNT reinforced polyethylene versus the raw material.

Material and Methods

The collection strain Staphylococcus aureus 15981 (4), and the reference strains Staphylococcus epidermidis ATCC 35984, Escherichia coli ATCC 29225, Pseudomonas aeruginosa ATCC 27853, Corynebacterium urealyticum ATCC 43044, Enterococcus faecalis ATCC 29212 and Mycobacterium fortuitum ATCC 6841, were included in the study. UHMWPE (GUR 1050®, Orthoplastic Ltd., Lancashire UK) discs with a diameter of 8 mm and 2 mm thick, containing or not 3 % wt multi wall carbon nanotubes, (NANOCYL® Nanocyl, Sambreville, Belgium) were tested as accretion surfaces.

For adherence studies, methodology of Pérez-Tanoira et al. (5) was applied, with minor modifications. Bacterial inoculum was prepared from an overnight culture in TSB-T at 37º C excepting for C. urealyticum and M. fortuitum, which were incubated in TSB-T plus Tween 80 for 72 hours. The sterilized surfaces were exposed to $\approx 10^8$ colony forming units (CFU)/mL during 90 minutes at 35º, washed with PBS (X 3) and incubated 24 hours at 4ºC. Finally, surfaces were stained with Acridine Orange for 2 min. Adhered bacteria were visualized by fluorescence microscopy. Images of 10-20 fields/ surface were photographed at 40x magnification. Assays were always made in triplicates. The percentage of bacterial coverage was determined by ImageJ software. Differences in bacterial adherence among surfaces as well as strains were individually analysed by unpaired t tests. Statistical significance was considered for $p \leq 0.001$.

Results

Figure shows the percentage of bacterial coverage per surface type (mean ± S.D). Significant reduction was observed in five bacterial species (S. aureus, P. aeruginosa, E. coli, C. urealyticum, and E. faecalis) when compared UHMWPE to the composite material.

E. coli registered the lowest adherence toUHMWPE compared to all the strains ($p \leq 0.001$) and equaled that S. aureus to MWCNT/UHMWPE. S. epidermidis and E. faecalis were the most adherent strains, finding significant differences respect all the other strains in MWCNT/ UHMWPE composites and raw UHMWPE, respectively.

Discusion / Conclusions

Regarding to the experimental data, the capability of MWCNT/UHMWPE in diminishing bacterial adherence seems to be species-dependent. Although neither the adherence of S. epidermidis or M. fortuitum was significantly reduced, the use of composite reinforced with MWCNT could be interesting against S. aureus (a leading cause of biomaterial-related infection) and other pathogens, with several applications. Since differences between laboratory and clinical strains could be found, further studies must be performed using clinical isolates.

References

1 Donlan et al.Clin Microbiol Rev (2002) 15:167-193
2. Kurtz et al. J Arthroplasty (2008) 23: 984-91
3. Wenrong-Yang et al. Nanotechnology (2007) 41: 412011 (12pp)
4. Valle et al. Mol Microbiol (2003) 48: 1075-87
5. Pérez-Tanoira et al. J Biomed Mat Research A (2012).100:1521:1528

Submitted by:Walsh, Pauline

Patients who received preconditioning before surgery were found to have reduced serum levels of TNF-alpha, IL-6 and IL-10 at 24h after surgery compared to controls, and this was coupled with induction of oxidative stress gene expression following 1h of surgery.

Introduction:
Ischaemic preconditioning (IPC) is a phenomenon whereby a tissue becomes more tolerant to a period of prolonged ischaemia when it is first subjected to short bursts of ischaemia and reperfusion. It has been shown to limit myocardial injury in both animal and human studies, however, its application to orthopaedic surgery remains limited to date. The aim of this study was to investigate the ability of IPC to reduce the post-operative systemic inflammatory response in total knee arthroplasty patients, and also to investigate the induction of oxidative stress defence gene expression as part of the preconditioning mechanism.

Patients & methods:
Ethical approval for this study was granted by the local ethics committee and informed consent was obtained from each patient before enrolment in the study. Patients were randomised to control ($n = 10$) and IPC ($n = 10$) groups. The IPC protocol consisted of three five-minute periods of tourniquet insufflation on the upper thigh of the operative limb, interrupted by five minute periods of reperfusion. The control group simply had tourniquet insufflation as normal prior to the start of surgery.

Peripheral blood was collected from patients pre- and post-operatively, and analysed for cytokine expression (TNF-alpha, IL-6, IL-10, IL-8). Muscle biopsies were taken from the quadriceps muscle of the operative leg at the immediate onset of surgery and at one hour into the surgery, and analysed for oxidative stress defense gene expression by real time PCR. Clinical evaluation was performed using WOMAC, SF36 and knee society scoring systems. Statistical analyses were performed with MiniTab15 using the paired t-test.

Results:
Following reperfusion, serum TNF-alpha, IL-6 and IL-10 concentrations increased significantly compared with baseline levels in both control and preconditioned patients ($p < 0.05$). However, 24 hours after surgery the levels of these cytokines were found to be reduced (~ 20%)in preconditioned patients, as compared to control patients.

In addition, gene expression analysis revealed a >2-fold increase in the expression of a number of important oxidative stress defense genes in muscle biopsies taken from preconditioned patients following one hour of surgery including catalase, glutathione-S-transferase and seqestosome 1 ($p < 0.05$). There was no significant difference between the two groups in terms of functional knee score, time to discharge or adverse events.

Discussion:
The release of pro-inflammatory mediators such as cytokines and reactive oxygen species is a key element of the post-operative inflammatory response. The modulation of these systemic effects has the potential to limit reperfusion injury, which may in turn, lead to improvements in patient outcome following surgery. In this study, preconditioned patients were found to have reduced serum levels of TNF-alpha, IL-6 and IL-10 at 24 hours after surgery, and this was coupled withincreased oxidative stress gene expression (CAT, GST, SQSTM1) following 1 hour of surgery. These findings indicate that IPC can indeed suppress the post-operative inflammatory response in these patients with the requirement for an anti-inflammatory stimulus (IL-10) being lessened in these patients. Furthermore, the induction of an oxidative stress response may play an important role in the protection provided by ischaemic preconditioning.

Submitted by:Wang, Haili

The quantitative sensory testing (QST) is an objective measurement method for the somatosensory nerval system. This study aimed to investigate pain thresholds in hip osteoarthritis patients before a total hip replacement.

Introduction

More than 100.000 total hip replacement(TKR)operations are performed inGermanyevery year. The outcome is generally evaluated by scores with subjective pain scales. The quantitative sensory testing is an objective measurement method for the somatosensory nerval system. The aim of this study was to investigate preoperatively pain thresholds in hip osteoarthritis patients and to compare these with healthy subject's data.

Patients and Methods

Forty-ninePatients with unilateral hip osteoarthritis, which were scheduled for a total hip replacement, and 50 healthy subjects were included. The pain history and intensity, the medication, the Harris Scores, Merle Scores and FFbH OA Scores were completed. The QST was performed on the non-dominant palm, and on both Great Trochanters in order to measure the thermal and pressure pain thresholds. The results were statistically analysed with non-parametric tests and correlation coefficient after Pearson and Spearman-Rho (SPSS 17 for Windows).

Results

Patients with Hip Osteoarthritis showed a lower pressure pain threshold at the Greater Trochanter on the sick site than those of the control subjects ($p=0.002$) but not than those on the healthy side. The heat pain threshold of the sick side was significantly lower than those of the healthy side ($p=0.005$).

The pain intensity as age, sex, and weight influenced significantly the pressure pain threshold. The mean of Harris Scores of patients was 54.27 ± 17.58 and correlated significantly with the sensitivity to cold stimuli ($p<0.001$)

Discussion and conclusion

Hip Osteoarthritis patients are more sensitive for pressure pain compared to healthy subjects. As cold pain threshold was shown in the current study to correlate with Harris scores, it may be used as a predictor for the therapy outcomes.

Key words: hip osteoarthritis, pain threshold, quantitative sensory testing

Submitted by:Crisan, Dan Dr.

Tibial plateau fractures are a realtively common traumatic event with more than half of the patients being over 50 years of age and typically women who sustain low energy trauma.

With the routine use of preoperative CT and MRI imaging there is a more accurate classification of the tibial plateau fractures, leading to improved indication of surgical treatment. However, the indication for operative treatment should be individulalised considering not only fracture pattern but other factors such as soft tissue status and patient characteristics, such that even for complex fractures a lateral locked angle plate can be indicated. Our aim is to verify in an experimental study if this ostheosyntesis method provides sufficient fixation for complex proximal tibial fractures with a medial component (Shatzker IV,V,VI).

Patients & Methods

A finite element model analysis of the bone-plate construct will determine the strength and stability of the construct under the forces that have been proven experimentally to act on the tibial plateau in weight bearing. A three dimensional nonlinear finite element model was developed to investigate tibial fixation designs of 3 patients with tibial plateau fractures that had undergone internal fixation of the fracture with locked angle lateral plates (anterolateral approach, no fibular osteotomy) based on preoperative and postoperative CT examination.

Results

The axial loads applied equaled up to 2000N, the cortical and cancellous bones carried, respectively, 12-13% and 75-82% of the axial load while the remainder was carried trough the screw/plate construct. The results were processed using the three way ANOVA system.

Conclusion

The pourpouse of this study is to help prove the in vivo limitations of the lateral locked angle plate ostheosynthesis when subjected to the normal gait forces. The data shows that even if the medial tibial condyle is not rigidly suported a unilateral plate can provide a good fixation fo theese fractures. Midterm clinical evidence also supports this fact.

References

Cift et al. Biomechanical comparison of plate-screw and screw fixation in medial tibial plateau fractures (Schatzker 4). A model study. Orthop Traumatol Surg Res (2010) vol. 96 (3) pp. 263-7

Gray et al. Experimental validation of a finite element model of a human cadaveric tibia. J Biomech Eng (2008) vol. 130 (3) pp. 031016

Hashemi and Shirazi-Adl. Finite Element Analysis of Tibial Implants - Effect of Fixation Design and Friction Model. Comput Methods Biomech Biomed Engin (2000) vol. 3 (3) pp. 183-201

Papagelopoulos et al. Complications after tibia plateau fracture surgery. Injury (2006) vol. 37 (6) pp. 475-84

Lindeque and Baldini. A biomechanical comparison of three different lateral tibia locking plates. Orthopedics (2010) vol. 33 (1) pp. 18-21

Fluid flow induced osteoclast differentiation is associated with alterations in genes regulating IL-6 signaling, cell death and osteoblast differentiation

Madsen Rune B.A Hospital for Special Surgery New York USA
Dvorzhinskiy Aleksey B.A Hospital for Special Surgery New York USA
McArthur Benjamin M.D Hospital for Special Surgery New York USA
Andersson Göran Ph.D. Karolinska University Hospital Stockholm Sweden
Ross Patrick F Ph.D. Hospital for Special Surgery New York USA
Bostrom Mathias P M.D Hospital for Special Surgery New York USA
Submitted by:Fahlgren, Anna PhD

In an animal model for prosthetic loosening, pressurized fluid flow of cortical bone stimulates complex, time-dependent changes in expression of genes regulating the survival, necrosis and differentiation of myeloid and mesenchymal cell lineages, leading to rapid increase of osteoclast differentiation.

Introduction:
Mechanical loading of bone is anabolic, while aseptic loosening of implants is catabolic. In our established rat model of mechanically induced prosthetic loosening^{1, 2}, osteoclast differentiation is increased dramatically after 3 days[3] but little is known about the underlying mechanism(s). The objective of this study was to profile signal transduction pathways in our model.
Material and Methods:
42 male rats were used in an animal model for mechanically induced prosthetic loosening. A titanium plate with a central screw was inserted on the proximal tibia into a milled depression on the surface of the cortex. The screw and plate were allowed to osseointegrate for 5 weeks. Thereafter, the central screw was replaced by a piston, which was moved perpendicular to the bone surface and Titanium plate (Figure 1). Microarrays on cortical bone samples exposed to pressurized fluid flow were performed 3, 6, 12, 24 and 36 hrs after the pressure cycle, using time zero samples as controls.
Results:
Of a total of 5640 genes that underwent a 1.25-fold change or greater(p-value less than 0.05) due to fluid flow only 30, mostly related to cell metabolism, were common for all time points. Gene ontology also identified significant changes in genes mediating cell death, growth and proliferation and cell-to-cell signaling. Signals linked to inflammation and apoptosis were significant up-regulated in a biphasic manner at 3 and 12 and/or 24 hrs. Out of the 4384 genes that were regulated at these timepoints, 119 were common for all three time-points. At the cellular level, genes associated with macrophage, osteoclast and osteoblast formation and/or function were affected at the same time points. The strongest inflammatory gene expression was seen after 3 hrs with increases in the interleukin (IL) family cytokines IL-6, IL-11 and leukemia inhibitory factor (LIF) and the transcription factors STAT3 and STAT4. In addition, levels of the pro-apoptotic factor TWEAK were higher while those of BOK, a second pro-survival molecule, were lower. There is an early and late rise in RIPK3, which stimulates a form of programmed necrosis that is suppressed by caspase 8 in response to TNFa. At later time points, osteoblast-related genes were clearly suppressed (osteocalcin, Col1a, PTHr1), while a number of those regulating macrophage and osteoclast differentiation (CSF-1, Bach1, HO-1, RANKL, RANK, OPG) were enhanced (Table 1).
Discussion and Conclusion:
These data suggest that mechanical loading of cortical bone stimulates complex, time-dependent changes in expression of genes regulating the survival, necrosis and/or differentiation of cells of both the myeloid and mesenchymal lineages. The IL-6 cytokine family[4], also associated with increased risk of osteolysis[5], might be highly involved in the initiation of the process. The net outcome, increased matrix destruction, reflects an integrated response that leads to a rapid increase in the numbers of bone-degrading osteoclasts.
References: 1) Skripitz et al. J Orthop Res. 2000, 2) Fahlgren et al. Acta Orthop. 2010; 3) Nilsson et al. Journal of Cell. Biochem. 2012,) O´Shea et al. Immunity Review 2012, 5) Gordon et al. Arthritis and Rheumatism 2008

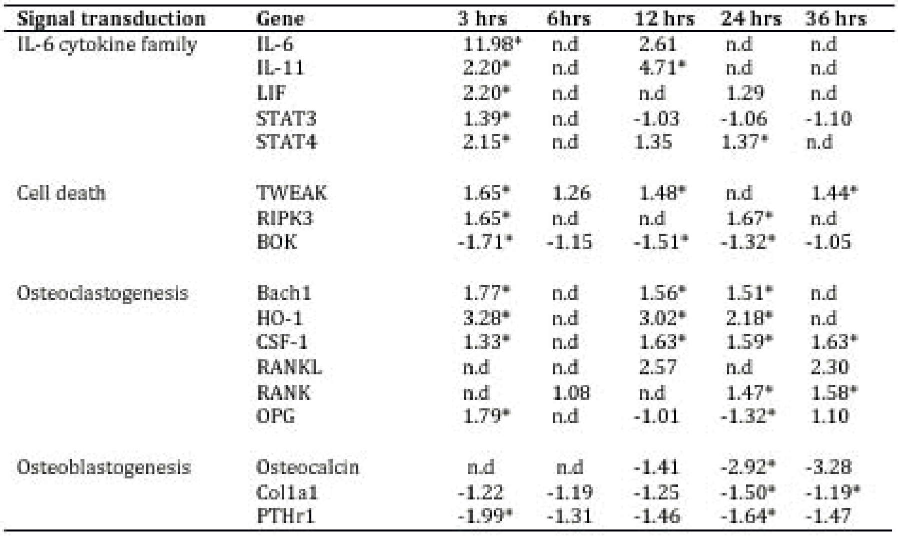

Signal transduction	Gene	3 hrs	6hrs	12 hrs	24 hrs	36 hrs
IL-6 cytokine family	IL-6	11.98*	n.d	2.61	n.d	n.d
	IL-11	2.20*	n.d	4.71*	n.d	n.d
	LIF	2.20*	n.d	n.d	1.29	n.d
	STAT3	1.39*	n.d	-1.03	-1.06	-1.10
	STAT4	2.15*	n.d	1.35	1.37*	n.d
Cell death	TWEAK	1.65*	1.26	1.48*	n.d	1.44*
	RIPK3	1.65*	n.d	n.d	1.67*	n.d
	BOK	-1.71*	-1.15	-1.51*	-1.32*	-1.05
Osteoclastogenesis	Bach1	1.77*	n.d	1.56*	1.51*	n.d
	HO-1	3.28*	n.d	3.02*	2.18*	n.d
	CSF-1	1.33*	n.d	1.63*	1.59*	1.63*
	RANKL	n.d	n.d	2.57	n.d	2.30
	RANK	n.d	1.08	n.d	1.47*	1.58*
	OPG	1.79*	n.d	-1.01	-1.32*	1.10
Osteoblastogenesis	Osteocalcin	n.d	n.d	-1.41	-2.92*	-3.28
	Col1a1	-1.22	-1.19	-1.25	-1.50*	-1.19*
	PTHr1	-1.99*	-1.31	-1.46	-1.64*	-1.47

-Figure 1. Fluid pressure is applied at 0.17 Hz, 2 minutes twice daily. Ti (Titanium), FT (Fibrous Tissue), B (Cortical Bone)

-Table 1. Fold change of selected genes of interests. *= Significant fold change versus non-pressurized control ($p<0.05$). n.d= not detectable in the microarray.

Stem cells transplantation and core decompression therapies for avascular necrosis of femoral head Stem cells transplantation and core decompression therapies for avascular necrosis of femoral head Stem cells transplantation and core decompression thera

Fei Chang Vice Professor ccfei_cn@hotmail.com CJUH Changchun China

Submitted by:MENGYAO, SUN

The article summarized our retrospective study of early stage avascular necrosis of the femoral head (stage I and II) treated with stem cells transplantation and core decompression.

Introduction

The article summarized our retrospective study of early stage avascular necrosis of the femoral head (stage I and II) treated with stem cells transplantation and core decompression.

Subjects & Methods

From July 2008 to February 2010, eleven patients (10 male, 1 female, 13 symptomatic hips) were diagnosed as avascular necrosis of the femoral head with MRI. The number of hips affected by avascular necrosis in current series of 13 hips was 3 in patients taking corticosteroids, 5 in patients with excessive alcohol intake, and 5 in patients withidiopathic osteonecrosis. The mean age of the patients was 44 (range: 23-52). Hips were graded for severity according to ARCO's system. Five hips in 4 patients were stage I, and 8 hips in 7 patients were stage II. The patient were underwent with stem cells transplantation and core decompression in our hospital. All patients were permitted to move without any help one month post-operation, and the follow-up period was from 15 to 36 months, average 18.5 months.

Results

Follow-up visits were scheduled at the 1st, 3rd, 6thmonth, 1 year, and annually thereafter. The outcome was demonstrated according to the changes in the Harris' hip score. The average Harris' hip score was 78.5 ± 11.2 at 6thmonth post-operation, significantly higher than the score pre-operation (53 ± 10.7, $P<0.05$). But 7 of 10 patients (6 in stage II) complained of an improving aggravation of pain from 6 months post-operation, proving by a reduction of the pain part of Harris' hip score which showed an average of 15 at pre-operation, 40.2 at 3rdmonth post-operation and 21.8 at 6thmonth. The Harris' hip score at 12thmonth post-operation was 64.5 ± 8.8. Three patients in stage II were treated with total hip arthroplasty at 10thand 20thmonth post-operation due to unbearable pain and movement disability

Conclusion

The patients felt great improvement post-operation, proving by a statistical comparison between the Harris' hip scores of pre-operation and post-operation. An aggravation of pain was found at the 6thmonth post-operation in patients most from stage of ARCO II. It might be somehow the sign of increased pressure in femoral head.

Stem cells transplantation and core decompression therapies for avascular necrosis of femoral head

Fei Chang Vice Professor ccfei_cn@hotmail.com CJUH Changchun China

Submitted by:MENGYAO, SUN

The article summarized our retrospective study of early stage avascular necrosis of the femoral head (stage I and II) treated with stem cells transplantation and core decompression.

Introduction

The article summarized our retrospective study of early stage avascular necrosis of the femoral head (stage I and II) treated with stem cells transplantation and core decompression.

Subjects & Methods

From July 2008 to February 2010, eleven patients (10 male, 1 female, 13 symptomatic hips) were diagnosed as avascular necrosis of the femoral head with MRI. The number of hips affected by avascular necrosis in current series of 13 hips was 3 in patients taking corticosteroids, 5 in patients with excessive alcohol intake, and 5 in patients withidiopathic osteonecrosis. The mean age of the patients was 44 (range: 23-52). Hips were graded for severity according to ARCO's system. Five hips in 4 patients were stage I, and 8 hips in 7 patients were stage II. The patient were underwent with stem cells transplantation and core decompression in our hospital. All patients were permitted to move without any help one month post-operation, and the follow-up period was from 15 to 36 months, average 18.5 months.

Results

Follow-up visits were scheduled at the 1st, 3rd, 6thmonth, 1 year, and annually thereafter. The outcome was demonstrated according to the changes in the Harris' hip score. The average Harris' hip score was 78.5 ± 11.2 at 6thmonth post-operation, significantly higher than the score pre-operation (53 ± 10.7, $P<0.0?$). But 7 of 10 patients (6 in stage II) complained of an improving aggravation of pain from 6 months post-operation, proving by a reduction of the pain part of Harris' hip score which showed an average of 15 at pre-operation, 40.2 at 3rdmonth post-operation and 21.8 at 6thmonth. The Harris' hip score at 12thmonth post-operation was 64.5 ± 8.8. Three patients in stage II were treated with total hip arthroplasty at 10thand 20thmonth post-operation due to unbearable pain and movement disability

Conclusion

The patients felt great improvement post-operation, proving by a statistical comparison between the Harris' hip scores of pre-operation and post-operation. An aggravation of pain was found at the 6thmonth post-operation in patients most from stage of ARCO II. It might be somehow the sign of increased pressure in femoral head.

Quad-Snip or TTO for revision of septic knee arthroplasty? Prospective randomized comparison at 8 years mean follow-up

Iacono Francesco FI MD. PhD f.iacono@biomec.ior.it Rizzoli Orthopaedic Institute Bologna Italy
Lo Presti Mirco MLP MD, Ph D m.lopresti@biomec.ior.it Rizzoli Orthopaedic Institute Bologna Italy
Raspugli Giovanni GR MD g.raspugli@biomec.ior.it Rizzoli Orthopaedic Institute Bologna Italy
Sharma Bharat BS MD medrite@gmail.com Rizzoli Orthopaedic Institute Bologna Italy
Marcacci Maurilio MM MD. Chair, Full Professor, PhD m.marcacci@biomec.ior.it Rizzoli Orthopaedic Institute Bologna Italy

Submitted by:Bruni, Danilo Dr

Tibial tubercle osteotomy is a safe and effective procedure for revision of infected knee arthroplasty.

Introduction:
Conventional surgical exposures are usually inadequate for 2-stage revision knee replacement of infected implants. Reduced range of motion, extensor mechanism stiffness, peripatellar contracture and soft tissue scarring make patellar eversion difficult and forced eversion places the integrity of the extensor mechanism at risk. On the contrary, a wide exposure is fundamental to allow complete cement spacer removal, soft tissue balancing, management of bone loss and reimplantation without damaging periarticular soft tissues.Our purpose is to compare the long-term clinical, functional and radiographic results and the reinfection rate of the quadriceps snip approach and the tibial tubercle osteotomy in 2-stage revision knee replacement performed for septic loosening of the primary implant.
Patients & Methods:
In our department, 87 patients had a 2 stage revision knee replacement for septic loosening of the primary implant between 1996 and2008. Inall patients, first stage consisted of primary implant removal, extensive soft tissue debridement and positioning of a static antibiotic loaded cement spacer. The timing for reimplantation was decided basing on negative clinical and laboratory (ESR, CRP) signs and negative Leukoscan results. For reimplantation, a quadriceps snip was used in patients with an intraoperative flexion >90° (Group A) while a tibial tubercle osteotomy (Group B) was used in patients with an intraoperative flexion <90°.
Results:
At observation point, 4 patients died for reasons unrelated to surgery, leaving 42 patients in Group A and 41 in Group B. We had a total amount of 10 recurrent infections (11%) after reimplantation, 7 patients in Group A and 3 patients in Group B ($p<0.005$). Patients with a reinfection in Group A were treated with a knee fusion in 4 cases, a re-revision in 2 cases and an amputation above the knee in 1 case, while all those with a reinfection in Group B had a knee fusion. According to HSS score, 11 patients were rated as Excelent/Good in Group A and 9 patients in Group B (p=n.s.). Three patients had a major complication in Group A and 0 patients in Group B ($p=0.0005$). No differences were found between the two groups regarding range of motion and subjective satisfaction.
Discussion/conclusion:
Tibial tubercle osteotomy is a safe procedure to obtain a wide exposure in 2-stage revision knee replacement performed for septic loosening of the primary implant and it is effective in reducing reinfection rate without compromising clinical results and range of motion.

Differences in expression profiles of osteolysis-related cytokines in tissues retrieved from aseptically failed hip and knee arthroplasties

withdrawn

Quantification of training effects on femoral bone quality: the surplus value of stiffness evaluation under stance and fall conditions

Lenaerts Leen Leen.Lenaerts@mech.kuleuven.be Biomechanics Section, KU Leuven Leuven Belgium
Verschueren Sabine Sabine.Verschueren@faber.kuleuven.be Research Unit for Musculoskeletal Rehabilitation, KU Leuven Leuven Belgium
Bogaerts An An.Bogaerts@faber.kuleuven.be Research Unit for Musculoskeletal Rehabilitation, KU Leuven Leuven Belgium
Boonen Steven Steven.Boonen@med.kuleuven.be Division of Geriatric Medicine, KU Leuven Leuven Belgium
Delecluse Christophe Christophe.Delecluse@faber.kuleuven.be Research Center for Exercise and Health, KU Leuven Leuven Belgium
Fritscher Karl karl.fritscher@umit.at Institute for Biomedical Image Analysis, UMIT Hall in Tirol Austria
van Lenthe Harry Harry.vanLenthe@mech.kuleuven.be Biomechanics Section, KU Leuven Leuven Belgium

Submitted by: Lenaerts, Leen

Bone stiffness, measured under stance and fall loading conditions, appears to be a sensitive parameter to pick up bone adaptive responses to training that go unnoticed with the analysis of bone mineral density (BMD).

Introduction

Up to date, effects of osteoporosis treatments on bone quality have mainly been assessed by means of BMD measurements. However, bone quality does not depend on BMD alone; other aspects such as bone geometry and internal architecture are important too. Therefore, the aim of this study was to quantify effects of training in postmenopausal women on bone quality in terms of bone stiffness and on total hip BMD. As results found for one loading configuration are not necessarily indicative for results found for another loading configuration [Keyak, 2000] bone stiffness was evaluated under stance and fall loading conditions using CT-based finite element analyses (FE).

Patients and methods

Eighty-one postmenopausal women (age=60-81years) volunteered to participate. Subjects were randomly assigned to one of three groups: a control group (CON, n=23), a fitness training group (FIT, n=21) and a WBV training group (WBV, n=37). The training groups participated in a one-year training program as described by Bogaerts et al (2007). The control group did not participate in any training. At baseline (PRE) and after one year of training (POST), DXA and CT scans (resolution 0.98mm x 0.98mm x 1mm) were obtained of the proximal femora of every volunteer.
For each CT-scan, the right femur was segmented [Fritscher, 2007] and used to build a patient-specific FE model consisting of hexahedral elements. PRE and POST femora were registered such that identical loading conditions could be applied. Linear elastic material properties were assigned to every element, based on the grayvalue of the corresponding voxel in the CT images [Morgan, 2003]. The length of all models was set to 150mm. Boundary conditions simulating stance and sideways fall loading were applied (Fig. 1). The FE models were solved using MARC (MSC Software,Santa Ana,CA) and the stiffness of every proximal femur was calculated under both loading conditions, as the total reaction force on the femur head divided by the applied displacement. The average PRE-POST differences in BMD, STANCE stiffness and FALL stiffness were calculated for each of the three groups. Results were analyzed by repeated measures ANOVA and contrast analysis.

Results

Stiffness decreased significantly in CON but was unaffected in FIT and WBV for both loading conditions (Table 1). The change in stiffness over time in CON was significantly different than in WBV (Table 2). BMD declined significantly in all three groups. No differences were found in PRE-POST stiffness changes between the two loading conditions.

Discussion

Our findings suggest that due to training bone stiffness can be preserved even when BMD is decreasing. Where BMD was lost in all three groups, bone stiffness decreased only in CON compared to the training groups that maintained stiffness. We conclude that bone stiffness appears to be a sensitive parameter picking up bone adaptive responses that go unnoticed with the analysis of BMD.

References
Bogaerts et al, Gaitpost, 26:309-316, 2007.
Fritscher et al, Int J CARS, 1(6):341-350, 2007.
Keyak, J Biomech, 33:499-502, 2000.
Morgan et al, J Biomech, 36:897-904, 2003.

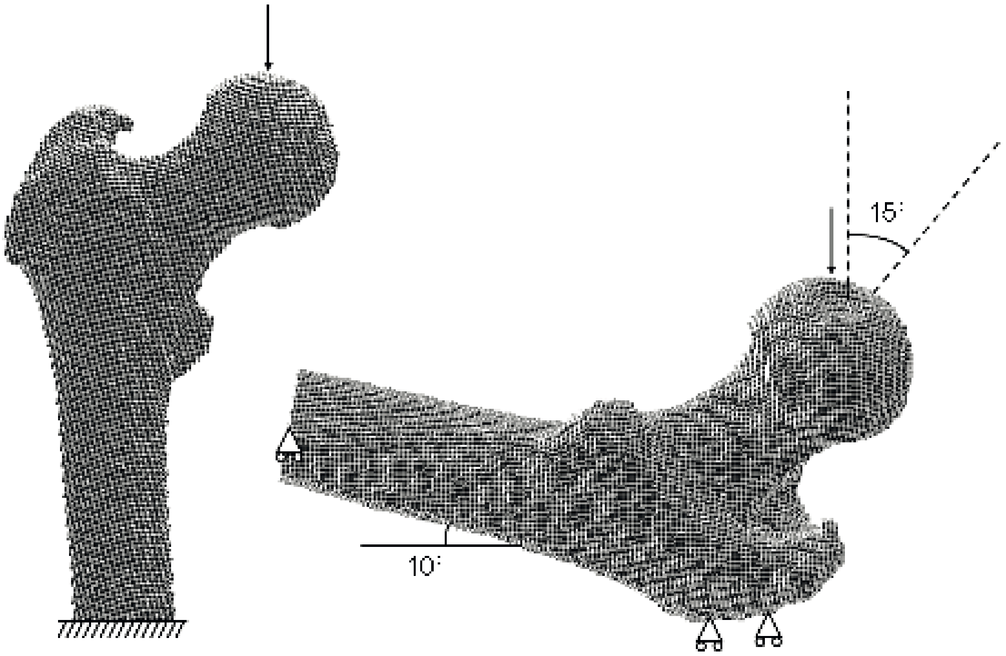

	CON	FIT	WBV
BMD	*-1.56 ± 2.04	*-1.50 ± 2.87	*-1.01 ± 2.27
STANCE stiffness	*-1.85 ± 3.23	0.09 ± 4.52	1.14 ± 4.01
FALL stiffness	*-2.92 ± 4.17	0.47 ± 6.97	1.12 ± 5.76

	CON vs FIT	CON vs WBV	FIT vs WBV
STANCE stiffness	0.106	*0.005	0.314
FALL stiffness	0.060	*0.009	0.632

-Figure 1: Left: Boundary conditions to simulate stance. The distal end of the femur is fixed and a displacement of 0.2mm is applied to the femur head parallel to the shaft axis. Right: Boundary conditions to simulate sideways fall. The angle between the shaft axis and the horizontal is 10°. The femur head was rotated internally by 15°. A vertical displacement of 0.2mm was applied to the femur head.
-Table 1: One-year changes (%) in BMD and in stiffness under stance and fall loading conditions for the control group (CON), the FIT training group (FIT) and the whole body vibration training group (WBV). (* Significant PRE-POST difference within group, $p < 0.05$)
-Table 2: Resulting p-values of a post-hoc analysis investigating the interaction between CON and FIT, CON and WBV and FIT and WBV. (* Significant PRE-POST difference between groups, $p < 0.05$)

Healing of segmental femoral defect in nude rats using human bone marrow mesenchymal stem cell (hMSC) cultured on HA/TCP scaffold

STANOVICI Julien J MD julien.stanovici@gmail.com INSERM, UMR957 Nantes France
ROSSET Philippe P Pr rosset@med.univ-tours.fr INSERM, UMR957 Nantes France
HEYMANN Dominique D Pr domnique.heymann@univ-nantes.fr INSERM, UMR957 Nantes France
LAYROLLE Pierre P DR pierre.layrolle@univ-nantes.fr INSERM, UMR957 Nantes France
Submitted by:Stanovici, Julien Dr

We conducted a preclinical study analysing bone healing in a femoral critical size bone defect in a nude rat model. hMSC enhance repair of bone defect compared to biomaterials alone.

Introduction:
Bone tissue engineering is a recent alternative in orthopaedic surgery to repair bone defect and non union fracture. More preclinical study are required for efficiency and safety assesment in cell therapy.
Materials and methods:
We conducted a preclinical study analysing bone healing in a femoral critical size bone defect in a nude rat model.Segmental defects (5 mm) were created and stabilized by using custom-made external fixators (Fig 1), in 30 rats (6 per group). Defects were filled with HA/TCP granules of different sizes (group I et II), associated with human mesenchymal stem cells (hMSCs) on HA/TCP (group III), or with hMSCs cultured on HA/TCP in vitro before implantation(group IV). Control group was left empty. Healing was evaluated by serial radiography, microcomputed tomography (Fig 2) and decalcified histology at 16 weeks. We conducted in situ hybridation using the alu sequence to highlight the contribution of human cells to bone healing in the host.
Results:
We did not observe complete healing but we found significant new bone formation in hMSCs blended extemporaneously and cultured with HA/TCP compared to the other group without MSC. MicroTDM of explants and histology showed similar results.
Conclusion:
hMSC cultured on HA/TCP or blended extemporaneously enhance repair of bone defect and may be a potent alternative to autologous bone grafting.

Surgical procedure
-MicroTDM: 1:Control, 2: hMSC cultured on HA/TCP, 3:HA/TCP. White:bone/Blue:HA/TCP

The Effect of Ischaemic Preconditioning in Total Knee Arthroplasty

Broderick James University College Dublin Dublin Ireland
Mulhall Kevin J University College Dublin Dublin Ireland
Submitted by:Walsh, Pauline Dr.

Patients who received preconditioning before surgery were found to have reduced serum levels of TNF-alpha, IL-6 and IL-10 at 24h after surgery compared to controls, and this was coupled with induction of oxidative stress gene expression following 1h of surgery.

Introduction

Ischaemic preconditioning (IPC) is a phenomenon whereby a tissue becomes more tolerant to a period of prolonged ischaemia when it is first subjected to short bursts of ischaemia and reperfusion. It has been shown to limit myocardial injury in both animal and human studies, however, its application to orthopaedic surgery remains limited to date. The aim of this study was to investigate the ability of IPC to reduce the post-operative systemic inflammatory response in total knee arthroplasty patients, and also to investigate the induction of oxidative stress defence gene expression as part of the preconditioning mechanism.

Patients & Methods

Ethical approval for this study was granted by the local ethics committee and informed consent was obtained from each patient before enrolment in the study. Patients were randomised to control (n = 10) and IPC (n = 10) groups. The IPC protocol consisted of three five-minute periods of tourniquet insufflation on the upper thigh of the operative limb, interrupted by five minute periods of reperfusion. The control group simply had tourniquet insufflation as normal prior to the start of surgery.

Peripheral blood was collected from patients pre- and post-operatively, and analysed for cytokine expression (TNF-alpha, IL-6, IL-10, IL-8). Muscle biopsies were taken from the quadriceps muscle of the operative leg at the immediate onset of surgery and at 1h into the surgery, and analysed for oxidative stress defense gene expression by real time PCR. Clinical evaluation was performed using WOMAC, SF36 and knee society scoring systems. Statistical analyses were performed with MiniTab15 using the paired t-test.

Results

Following reperfusion, serum TNF-alpha, IL-6 and IL-10 concentrations increased significantly compared with baseline levels in both control and preconditioned patients ($p<0.05$). However, 24h after surgery the levels of these cytokines were found to be reduced by >20% in preconditioned patients, as compared to control patients.

In addition, gene expression analysis revealed a >2-fold increase in the expression of a number of important oxidative stress defense genes in muscle biopsies taken from preconditioned patients following 1h of surgery including catalase, glutathione-S-transferase and seqestosome 1 ($p<0.05$). There was no significant difference between the two groups in terms of functional knee score, time to discharge or adverse events.

Discussion

The release of pro-inflammatory mediators such as cytokines and reactive oxygen species is a key element of the post-operative inflammatory response. The modulation of these systemic effects has the potential to limit reperfusion injury, which may in turn, lead to improvements in patient outcome following surgery. In this study, preconditioned patients were found to have reduced serum levels of TNF-alpha, IL-6 and IL-10 at 24h after surgery, and this was coupled with increased oxidative stress gene expression following 1h of surgery. These findings indicate that IPC can indeed suppress the post-operative inflammatory response in these patients with the requirement for an anti-inflammatory stimulus (IL-10) being lessened in these patients. Furthermore, the induction of an oxidative stress response may play an important role in the protection provided by IPC.

Osteochondral regeneration of a critical size defect in a minipig model using Adipose-derived Stem Cells in association with an hydrogel of oligo(polyethylene glycol) fumarate

Arrigoni Elena E PhD elena.arrigoni@unimi.it Department Of Medical Pharmacology - Università Degli Studi Di Milano Milan Italy
de Girolamo Laura L PhD laura.degirolamo@grupposandonato.it IRCCS Galeazzi Orthopaedic Institute Milan Italy
Niada Stefania S Dr stefania.niada@unimi.it Department Of Medical Pharmacology - Università Degli Studi Di Milano; IRCCS Galeazzi Orthopaedic Institute Milan Italy
Di Giancamillo Alessia A DVM alessia.digiancamillo@unimi.it Department Of Veterinary Sciences And Technology For Food Safety - Università Degli Studi Di Milano Milan Italy
Domeneghini Cinzia C DVM cinzia.domeneghini@unimi.it Department Of Veterinary Sciences And Technology For Food Safety - Università Degli Studi Di Milano Milan Italy
Dadsetan Mahrokh M PhD Department Of Orthopedic Surgery - Mayo Clinic College Of Medicine Rochester USA
Yaszemski Michael M MD Department Of Orthopedic Surgery - Mayo Clinic College Of Medicine Rochester USA
Vena Pasquale P Med Eng LaBS - Laboratory of Biological Structure Mechanics, Structural Engineering Department, Politecnico di Milano Milan Italy
Peretti Giuseppe M GM MD giuseppe.peretti@unimi.it Department Of Orthopaedics And Traumatology - San Raffaele Scientific Institute Milan Italy
Brini Anna T AT PhD anna.brini@unimi.it Department Of Medical Pharmacology - Università Degli Studi Di Milano; IRCCS Galeazzi Orthopaedic Institute Milan Italy

Submitted by:Arrigoni, Elena PhD

Adipose-derived Stem Cells (ASCs) in association with an hydrogel of oligo(polyethylene glycol) fumarate (OPF) are able to improve the repair of a critical osteochondral defects in a minipig model

Introduction
Osteochondral tissue loss caused by high-energy trauma, disease, and tumor resection have always been a very troublesome problem for orthopedic surgeons. During normal bone defect healing, undifferentiated mesenchymal stem cells, in the presence of suitable stimuli, proliferate and differentiate into osteoblasts and chondrocytes forming bone tissue and cartilage, and repairing the injury. However, in some cases, defects fail to healing and surgical intervention is often required. Tissue engineering is an innovative approach that overcome the standard surgical procedures, to achieve the regeneration of bone and cartilage tissues. Adipose-derived Stem Cells (ASCs), isolated from the stromal vascular fraction derived from subcutaneous fat tissue, show a multi-differentiative ability which may be exploited, alone or in association with suitable scaffolds, as novel and efficient tools for bone and cartilage regeneration.
Methods.
ASCs, isolated from seven adult male minipigs, expanded in culture, were used to repair a critical femoral osteochondral defect in association with an hydrogel scaffold of oligo(polyethylene glycol) fumarate (OPF). In the peripheral part of the trochlea of each animals were created four defects (diameter 9mm, depth 8mm), that were then treated with constructs made of OPF scaffold pre-seeded with either autologous or heterologous ASCs. Untreated defects and defects filled by just scaffold were included as controls.
Results.
ASCs were rapidly isolated with an average of $6.45x10^4 \pm 4.34x10^4$ per ml of processed adipose tissue. All the suine ASCs populations were analyzed in vitro: their doubling times were of 59.2±16.6 hours and their clonogenic ability was stable and greater than human ASCs (15.7±8.2%). Their osteogenic differentiation ability was shown by collagen production and extracellular calcified matrix deposition (+136% and +70% of osteo- vs undifferentiated ASCs, respectively). 4 weeks after subcutaneous fat withdrawal, constructs made with $3x10^6$ of either autologous or heterologous undifferentiated ASCs were implanted in the bone defects. No side-effects have been observed during the follow up and 6 months later, animals were sacrificed and knees explanted. Gross appearance analyses showed quite satisfactory filling of the lesions in all the samples, with the exception of one animal, whose joint appeared infected and not healed. Good osteointegration was observed by MRI evaluation. Histological and

immunohistochemical analyses revealed an increased expression of collagen type II in the ASCs+OPF treated groups compared to the groups treated with the OPF hydrogel alone. In addition, biomechanical analyses confirmed the histological results showing an improved elastic module of the new formed cartilage tissue.

Conclusions.

ASCs were able to promote a quite complete regeneration of the subchondral bone and a cartilage-like tissue and might be considered a treatment option for the regeneration of osteochondral defects. Moreover, since no differences were observed between autologous and heterologous constructs, the possibility of an allogeneic use of these cells is also supported and encouraging for a future clinical practice.

Biological effects of clinically relevant CoCr nanoparticles on the cells of the Dura Mater. Phenotypic analysis of the porcine model and establishment of the phagocytotic potential of each type of dural cells.

Bhel Bharat MSc IMBE Leeds University UK
Brown Chris Dr IMBE Leeds University UK
Hall Richard M Professor IMBE Leeds University UK
Tipper Joanne L Dr IMBE Leeds University UK
Fisher John Professor IMBE Leeds University UK
Ingham Eileen Professor IMBE Leeds University UK
Submitted by:Papageorgiou, Iraklis Dr

This study revealed the capacity of dural cells to take up model particles was dependent on the size of the particles. Also, there are novel differences in the resistance of the two dural cell types to metal nanoparticle-induced toxicity. The results generated from this study contribute to a greater understanding of the potential risks associated with the use of MOM total disc prostheses.

Introduction

The increased use of metal-on-metal (MOM) hip implants resulted in the emergence of similar MOM prostheses for use in total disc replacement (TDR). However, wear debris generated from metal prostheses can lead to adverse tissue reactions. Consequently, adequate evaluation of the cellular responses to metal wear debris generated by TDR is warranted especially in the para-spinal tissues such as the dura mater. The aims of this study were to utilize a porcine model system and to investigate the effects of clinically relevant metal nanoparticles on cells of the dura mater.

Material/Methods

Dural epithelial and fibroblasts were isolated from the porcine dural membrane. Cells were characterised by immunocytochemistry using a range of antibodies. Cells were cultured with micron-sized (1µm) and nanometer-sized (40nm) fluorescent polystyrene particles for 24h, 2 and 3 days. The cells were then stained with rhodamine-phalloidin [actin] and Hoechst 33342 [nuclei], visualised using confocal and deconvolution microscopy and 200 of each cell type were assessed for particle uptake.

Clinically-relevant CoCr wear particles were generated in a 6 station pin-on-plate wear rig and were characterized using FEGSEM. Porcine dural fibroblasts and dural epithelial cells were cultured with Co-Cr nanoparticles at particle volumes ranging from 0.06 μm^3 to 121 μm^3 per cell. The resulting biological effects were evaluated using the ATP-lite™ assay (viability), ELISA (cytokines) and carboxy - H2DCFDA (oxidative stress).

Results

Both dural epithelial and fibroblast cells expressed fibronectin, tenascin, collagen I and collagen III. The epithelial cells also had characteristics of typical endothelial cells since they expressed von Willebrand factor, CD31 and E-Cadherin. The fibroblasts did not express these markers.

With regard to micron sized particle uptake, the epithelial cells failed to uptake significant numbers over 24 hours, whereas the fibroblasts engulfed large numbers of the particles. (Fig. 1A). The inability of the epithelial cells to engulf micron sized particles was a temporal phenomenon and after 2 days, particles were taken up (Fig 1B). This pattern of particle engulfment was not repeated for the nano-sized particles. Both epithelial and fibroblast cells ingested high numbers of nano-particles following 24h exposure.

Differential effects of the Co-Cr nanoparticles were observed on fibroblasts and epithelial cells. The particles significantly reduced the viability of the epithelial cells in a dose and time-dependent manner but did not affect fibroblast viability (Figures 2 & 3). Both the fibroblasts and epithelial cells were induced to secrete IL-8 when cultured with the particles. Evaluation of wear particle-induced oxidative stress revealed the generation of reactive oxygen species in both cell types at a dose of 50 μm^3 per cell after 24 hour exposure.

Discussion

This study revealed the capacity of dural cells to take up model particles was dependent on the size of the particles. Nanometer size particles were able to penetrate both types of cells. However, dural fibroblasts engulfed micron-sized particles at a much higher rate than epithelial cells. This suggested that epithelial cells create some barrier to the penetration of larger particles. Also, the survival of the fibroblasts at doses cytotoxic to the epithelial cells suggests novel differences in the resistance of the two cell types to metal nanoparticle-induced toxicity which may be regulated by a difference in their susceptibility to reactive oxygen species. Moreover, secretion of IL-8 by the epithelial cells and fibroblasts upon culture with CoCr nanoparticles indicated the inflammatory potential of the wear particles.

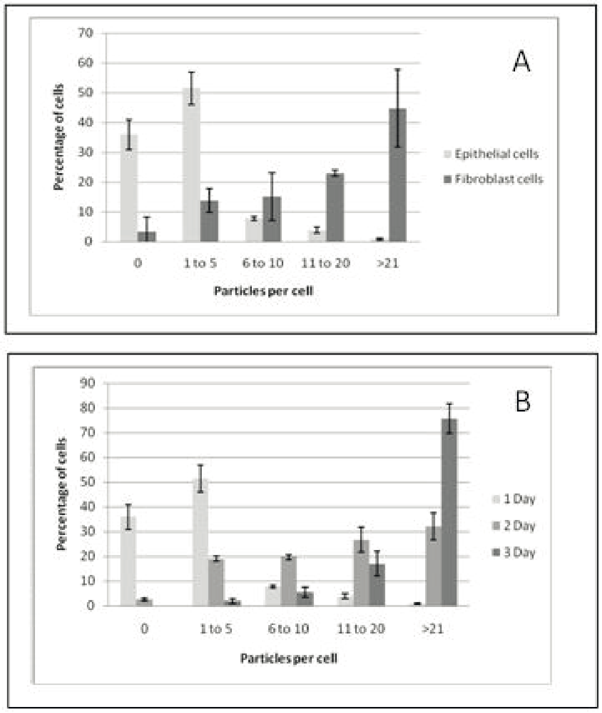

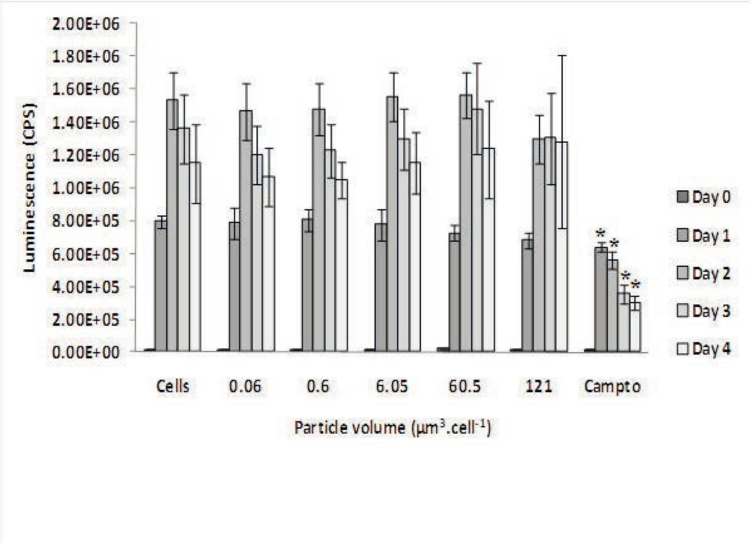

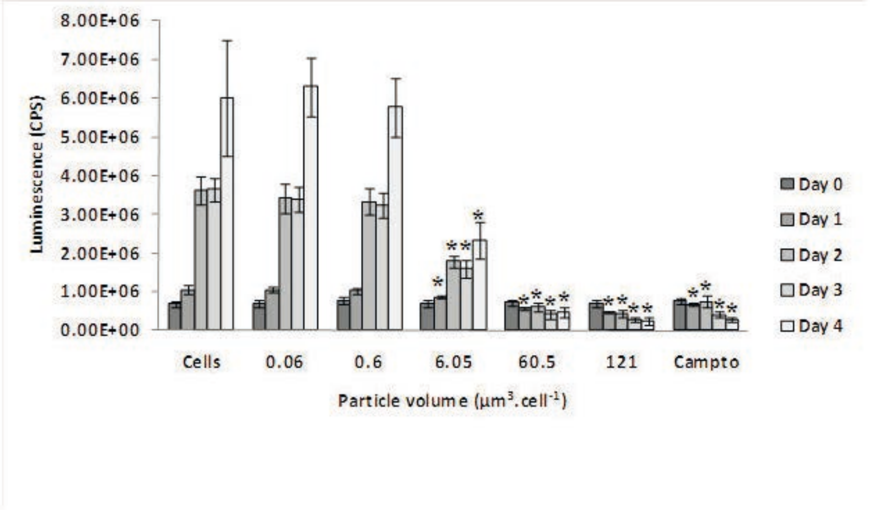

-Figure 1. Cellular uptake of fluorescent microspheres. (A) Percentage of dural fibroblasts and dural epithelial cells that had phagocytosed a given number of particles after 24 h exposure (B) Percentage of dural epithelial cells that had phagocytosed a given number of particles after 24h, 2 and 3 day exposure

-Figure 2: Effect of Co-Cr nanoparticles on viability of porcine dural fibroblasts. Data is expressed as the mean (n=6) ± 95% confidence limits. *$p<0.05$ ANOVA.

-Figure 3: Effect of Co-Cr nanoparticles on viability of porcine dural enothelial cells. Data is expressed as the mean (n=6) ± 95% confidence limits. *$p<0.05$ ANOVA.

3D Morphology of the Sacrum and its Impact on Treating Sacral Insufficiency Fractures. A Workflow using CT based 3D Statistical Modeling

Rommens Pol M. PMR MD, Prof. pol.rommens@unimedizin-mainz.de Department of Trauma Surgery, Centre for Musculoskeletal Surgery, University Medical Center of Johannes Gutenberg-University Mainz Germany
Sawaguchi Takeshi TS MD, Prof. sawaguch@mxq.mesh.ne.jp Department of Orthopedics & Joint Reconstructive Surgery, Toyama Municipal Hospital Toyama Japan
Kamer Lukas LK MD, DDS lukas.kamer@aofoundation.org AO Research Institute Davos Davos Switzerland
Noser Hansrudi HN PhD, Prof. hansrudi.noser@aofoundation.org AO Research Institute Davos Davos Switzerland
Submitted by:Wagner, Daniel MD

In order to establish an anatomical background for new fixation concepts in sacral insufficiency fractures, we developed a computerized workflow to analyze CT data of intact sacra using a three-dimensional (3D) statistical modeling approach.

Introduction:
Within the rapidly growing population of elderly people, osteoporotic fractures, and among them sacral insufficiency fractures, are getting common. Conservative treatment of sacral insufficiency fractures often ends in chronic pain and nonunion. Surgery includes positioning of sacro-iliac screws, trans-sacral bars or performing sacroplasty. However adequate fracture fixation remains a clinical challenge especially in conditions with significant bone loss or due to the complex and largely variable anatomy of the sacrum. To facilitate the development of efficient treatment strategies in this complex bone we present our technique for computerized 3D statistical modeling and analysis in order to evaluate the morphological variation of the sacrum including S1 and S2 level and the distribution of bone stock using CT data of unaffected pelves.
Materials and Methods:
To develop the workflow, we selected a series of 20 routine CT scans of elderly patients (≥ 65 years) without bone pathology otherwise than bone loss and processed them in Amira software. After producing 3D computer models of the sacra we defined anatomically corresponding landmarks. We developed a computer tool to generate a 3D statistical model to analyze the entire sacrum or parts of it.
Results:
We developed a workflow and computer tools to generate a 3D statistical model of the sacrum. This included the computation of 50`000 anatomically corresponding points and 3D modeling of the medullary channel and neuroforamens. The approach allows creating 3D statistical submodels such as corridors of S1 and S2 for safe screw positioning in a mean shape or any other shape of the statistical model. Then the model was used to performing shape and size analysis, to measure morphological parameters like distances or angles and to analyze the bone stock distribution, given in Hounsfield Units. With this we are able to compare the relative bone density within the sacrum between subgroups such as genders or different stages of bone loss.
Discussion/Conclusion:
This model will help in efficient evaluation of new treatment options in insufficiency fractures of the sacrum, as these are a challenge in treatment and increasing in incidence. The workflow will allow us to assess subgroups such as male and female or different ethnicities, to identify dysmorphias and to compare these groups to enhance the development in new ways of clinical treatment of insufficiency fractures. Important for new therapeutic approaches is the relative bone stock within the sacrum to provide a good anchorage of implants.

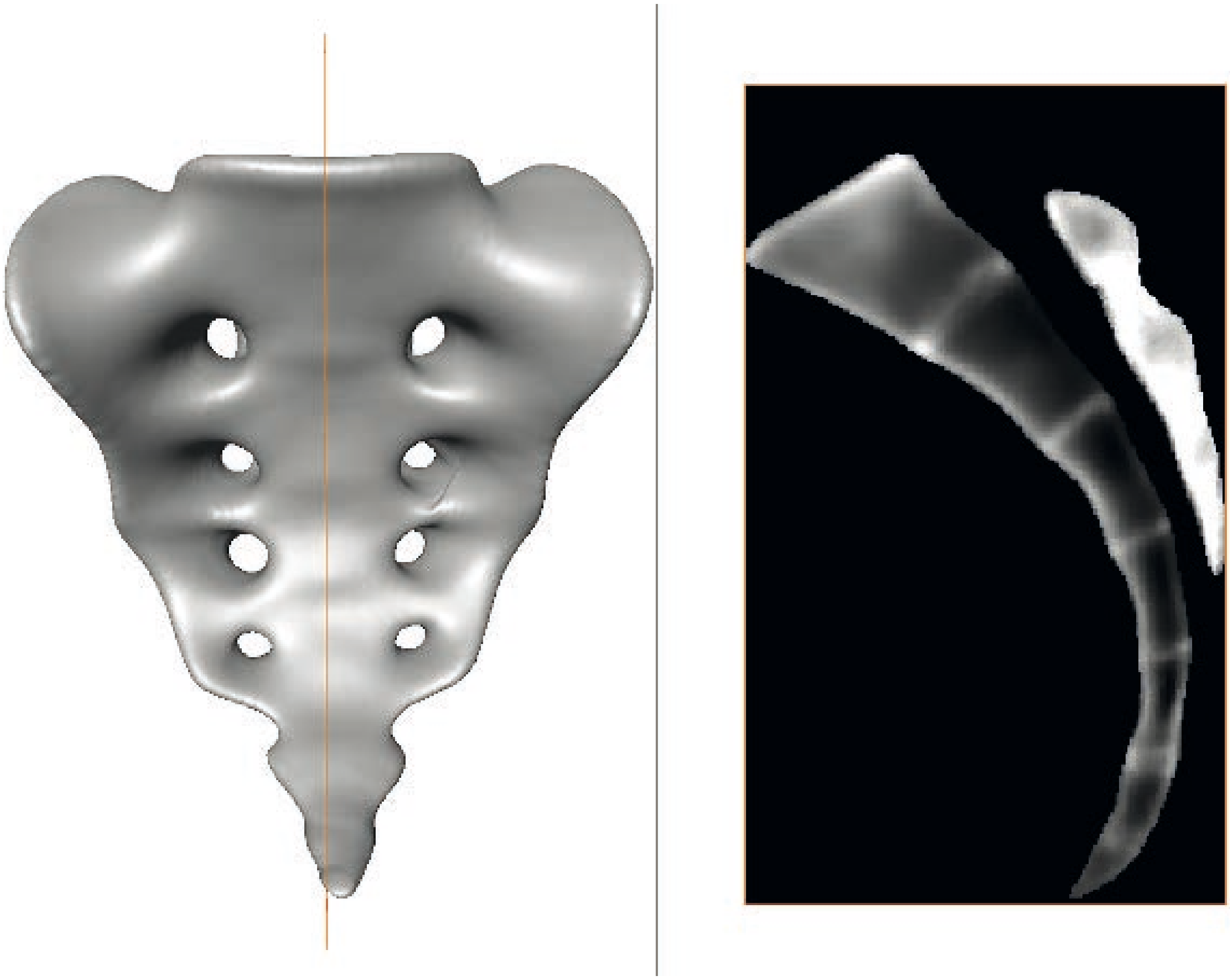

Figure: 3D mean shape of a sacral model (left) and its sagittal reconstruction illustrating the statistical distribution of the bone mass given in Hounsfield Units (right) computed from 20 CTs.

ISOPROSTANE LEVELS ARE ALTERED IN RHEUMATOID ARTHRITIS AND SUPPRESS NFκB ACTIVITY TO INHIBIT OSTEOCLAST FORMATION

Lwin Seint Ms University of Oxford UK
Brooks Joshua Dr Vanderbilt University Medical Center US
Danks Lynett Dr Kennedy Institute of Rheumatology UK
Lundberg Karen Dr Kennedy Institute of Rheumatology UK
Morrow Jason Dr Vanderbilt University Medical Center US
Milne Ginger Dr Vanderbilt University Medical Center US
Edwards James R Dr james.edwards@ndorms.ox.ac.uk University of Oxford UK

Submitted by:Edwards, James Dr

Our findings indicate that the detection and monitoring of Omega 3 fatty acid breakdown products (Isoprostanes) may reflect disease development and progression in RA, along with highlighting a novel mechanism regulating osteoclastogenesis in inflammatory bone disease.

Excessive osteoclastic resorption is a defining feature of rheumatoid arthritis (RA), resulting in devastating tissue damage and pain. Omega-3 fatty acids (Ω3-FA) protect against RA and reduce bone pain, however the mechanism through which this occurs remains unknown.The breakdown of Ω3-FA occurs by either i)enzymatic action by cyclooxygenase enzymes (Cox) to form prostaglandins, or ii) via non-enzymatic oxidation mediated by circulating free radicals. Cyclopentenone isoprostanes (IsoPs) form in situ as oxidation products of Ω3-FA.
We hypothesize that a beneficial effect of Ω3-FA in RA occurs following the formation of IsoPs, to suppress osteoclast formation.
To test this, we used Gas Chromatography-Mass Spectometry to analyze the IsoP profile in serum from age-, sex-matched RA patients or controls ($n=7$). The consented collection of all samples was performed under national and institutional guidelines. RA patient samples were confirmed as CEP1 and CCP positive. In addition we employed osteoclast formation assays using RAW 264.7 cells treated with 15-A3-IsoP in addition to RANKL and M-CSF. The molecular mechanism through which IsoP may affect osteoclast formation was assessed using an NFκB-reporter macrophage cell line, to recapitulate and quantify NFκB signaling in osteoclast precursor cells. These studies were supported by immunofluorescent staining for nuclear/cytoplasmic p65 and western blot analysis for phosphorylated IκBα. To confirm the role of NFκB in IsoP mediated osteoclast inhibition, site-directed mutagenesis was employed to alter a putative IsoP binding region of IKK (C179). Mutated RAW 264.7 cells were assessed for osteoclast formation capacity and NFκB activation status, compared to unmodified cells.Our studies show that the IsoP levels within RA serum are significantly altered, compared to normal control patients. In addition, osteoclast precursor cells treated with 15-A3-IsoP (15uM) formed fewer TRAP+ multinucleated cells (26.3±5.3) compared to vehicle treated controls (46.3±4.3, $p<0.05$).Moreover, osteoclast precursor cells treated with 15-A3-IsoP demonstrated up to 60% decrease in NFkB reporter activity (25uM, $p<0.01$), phosphorylated IκBα protein levels and nuclear localization of the p65 protein.Mutation of C179 on IKK resulted in a loss of inhibition of NFκB activity and osteoclast formation, following 15-A3-IsoP treatment compared to WT cells ($p<0.01$).
These findings show that the 15-A3-IsoP molecule inhibits osteoclast formation through interactions with C179 on the IKK molecule, to reduce IκBα phosphorylation and suppress NFκB activation. Moreover, we identified a significant change in IsoP levels in RA patients compared to controls, suggesting that reduced IsoP levels may contribute in part, to the increased osteoclastic resorption of RA.

Biotribology of a vitamin E stabilised polyethylene for hip arthroplasty : influence of bearing material, surface roughness, ageing and third-body particles

Holderied Melanie M.Sc. Aesculap AG Tuttlingen Germany
Mulliez Marie-Anne M.Sc. Aesculap AG Tuttlingen Germany
Streller Rouven Ph.D. Aesculap AG Tuttlingen Germany
Hermle Thomas M.Sc. Aesculap AG Tuttlingen Germany
Blömer Wilhelm M.Sc. Aesculap AG Tuttlingen Germany

The objective of the study was to analyse the biotribological behaviour of a newly developed vitamin E stabilised polyethylene for hip arthroplasty. In comparison to a standard and a highlycrosslinked polyethylene the influence of ageing and third-body particles was evaluated.

Introduction

Total hip arthroplasty (THA) with articulations made of polyethylene liners and cobalt-chromium or ceramic heads has become a successful clinical treatment for patients with coxarthrosis or rheumatoid arthritis.Highly crosslinked (XPE) acetabular liners have shown significant improvements in decreasing wear and osteolysis [1,2].To improve the oxidation resistance highly crosslinked polyethylenes have to be thermally treated after irradiation. Due to a loss of crystallinity after remelting the mechanical properties of XPE are substantially reduced, a possible reason for structural material fatigue, pitting and crack initiation in vivo [3,4,5].Therefore, the stabilisation of XPE by blending of the antioxidant vitamin E in the polyethylene powder was introduced to enhance oxidation resistance and fatigue strength by avoiding post-irradiation melting [6,7].

Materials & Methods

In vitro wear simulation was performed for 5 million cycles according to ISO 14242-1 on a 6+2 station EndoLab hip simulator. Three groups of polyethylene inserts were made out of GUR 1020:

$PE_{std.}$(-irradiated 30kGy, N_2)

$XPE_{rem.}$(-irradiated 75kGy, remelted, EO)

XPE_{VitE}(e-beam 80kGy, 0.1% vitamin E, EO)

As counterparts femoral heads made out of CoCr29Mo6 (CoCr) and Ceramic (Biolox)(AesculapAG, Tuttlingen) were tested in a diameter 36mm articulation.

The polyethylene inserts were used unaged and after artificial ageing (70°C pure oxygen at 5 bar, duration 14 days) and soaked prior to wear simulation to allow for saturated fluid absorption. The amount of wear was measured gravimetrically with loaded references according to ISO 14242-2.

Subsequently a third-body particulate debris configuration was simulated by adding bone cement particles (Palacos R, size125-150µm) in a concentration of 5g/l.

Results

For the ceramic-polyethylene articulations under aged conditions the clinical reference material $PE_{std.}$ demonstrated an average wear rate of 30.3 ± 3.1 mg/mc compared to 1.5 ± 0.5 mg/mc ($XPE_{rem.}$) and 3.4 ± 0.5 mg/mc (XPE_{VitE}). Versus the aged inserts a decrease of approximately 60% was measured for the standard polyethylene in an unaged condition with a mean wear rate of 19.0 ± 0.6 mg/mc (PE_{std.unaged}), but no substantial change was given for the vitamin E stabilised inserts with 3.3 ± 0.1 mg/mc (XPE_{VitEunaged}).

The cobalt-chromium-polyethylene couplings demonstrated average wear rates of 2.1 ± 0.4 mg/mc ($XPE_{rem.}$) and 4.4 ± 0.4 mg/mc (XPE_{VitE}).

By adding bone cement as third-body particulate debris the mean wear rate of XPE_{VitE} inserts increased in articulation with Biolox delta by 2.3-fold (7.8 ± 0.5 mg/mc) and with CoCr heads by 10.7-fold (47.0 ± 36.1 mg/mc), respectively.

Conclusion

Vitamin E stabilised polyethylene is promising in decreasing oxidation after irradiation and demonstrates low wear, even under artificial ageing conditions in total arthroplasty.

References

1. Oral E, Muratoglu OK: Vitamin E diffused, highly crosslinked UHMWPE: a review. Int.Orthopaedics Vol.35, pp.215-223,2011.
2. Kurtz SM, Gawel HA,Patel JD: History and systematic review of wear and osteolysis outcomes for first-generation highly crosslinked polyethylene. Clin. Orth. Rel. Res. Vol. 469 No.4, pp. 2262-2277, 2011.
3. Bradford L, Baker DA, Graham J, Chawan A, Ries MD, Pruitt LA: Wear and surface cracking in early retrieved highly cross-linked polyethylene acetabular liners. JBJS 86-A No.6, pp.1271-1282, 2004.
4. Kurtz SM, Austin M, Azzam K et al.: Mechanical properties, oxidation and clinical performance of retrieved highly crosslinked Crossfire liners after intermediate-term implantation. J Arthroplasty Vol. 25 No.4, pp.<span s

Submitted by:Leigheb, Massimiliano MD, PhD, MSc

Introduction:

Even if the autogenous bone still remains the gold standard to augment or bridge osseous defects, bone substitute materials of natural or synthetic origin are becoming more and more used to avoid the risks associated with autogenous bone grafting such as perioperative morbidity and complications. The literature reports only few comparative studies on these materials, and most of them are histologic and morphometric evaluations, or microradiograph measurements obtained from in vivo explants. Moreover, we do not find in vitro studies on bone cells that compare their behavior when cultured in contact with these bone substitutes.

Purpose of this work is to study and compare the behavior of macrophages and human osteoclasts cultured in contact with different bone substitutes used in orthopaedic surgery for non-unions, traumatic loss of substance, after oncological resections and whenever a graft is needed to fill bone defects.

Materials & Methods:

Bone substitutes of natural and synthetic origin were used: human, bovine, hydroxyapatite and hydroxyapatite + b-tricalcium phosphate. Macrophage activation and cytokine release were evaluated using SEM analysis and a sandwich ELISA kit while the activity of human osteoclast-like cells was studied quantifying Calcium released from the studied substrata together with SEM analysis of cell morphology and of pit formation on the bone substitutes.

Results:

Hydroxyapatite resulted to be the greatest macrophage activator, while the bovine derived material resulted to be the only bone substitute that doesn’t induce macrophages to release IFNg. No material had direct induction of osteoclast precursor differentiation even if mature osteoclasts showed the greater activity on the human derived material, while the bovine one was the substrate with the minor osteoclast’s activity.

Discussion: The strategies involved in the repair of bone defects include the use of autogenous bone, bone cement, metals, polymers and ceramics. Local and systemic factors are involved in favoring or inhibiting bone repair, and a fundamental role is played by the cells of macrophage lineage, which, producing cytokines, mediate inflammation, bone cells differentiation, and bone cells activity. A growing body of evidence suggests that inflammatory signals are critical for the initiation of the fracture healing response, and the effect of inflammatory cytokines on bone depends on the timing and context of their expression.

Conclusions:

The four tested materials reacted differently with the tested cells and between them, the bovine derived bone, being the lower macrophages and osteoclasts activator may be considered a good bone substitute for clinical situations requiring greater time of permanence of the material in the site of implantation while the human derived bone will be better suitable for clinical applications that require lower time of permanence. Compared to bone autograft, all these osteo-conductive biomaterials combined with proper osteo-inductive agents can provide better regenerative effects with less undesired effects.

Effects of costunolide and dehydrocostus lactone on viability, matrix metalloproteinases and apoptosis in human soft tissue sarcoma cells

Rinner Beate RB Dr beate.rinner@linikum-graz.at Center for Medical Research, Medical University of Graz Graz Austria
Stuendl Nicole NS nicole.stuendl@klinikum-graz.at Department of Orthopaedic Surgery, Medical University of Graz Graz Austria
Kunert Olaf OK Dr olaf.kunert@uni-graz.at Institute of Pharmaceutical Sciences, Department of Pharmaceutical Chemistry, Karl-Franzens-University Graz Austria
Boechzelt Herbert HB Dr Boechzelt, Herbert [herbert.boechzelt@joanneum.at] Department of Plant Materials Sciences and Utilisation, Joanneum Research Forschungsgesellschaft mbH Graz Austria
Leithner Andreas AL Prof. Dr andreas.leithner@linikum-graz.at Department of Orthopaedic Surgery, Medical University of Graz Graz Austria
Bauer Rudolf RB Prof. Dr rudolf.bauer@ni-graz.at Institute of Pharmaceutical Sciences, Department of Pharmacognosy, Karl-Franzens- University Graz Austria
Kretschmer Nadine NK Dr nadine.kretschmer@uni-graz.at Institute of Pharmaceutical Sciences, Department of Pharmacognosy, Karl-Franzens- University Graz Austria

Submitted by:Lohberger, Birgit Dr.

The present study investigated the anti-tumor effects of costunolide and dehydrocostus lactone isolated from Saussurea lappa in three human soft tissue sarcoma (STS) cell lines of various origins.

Introduction:
Uncontrolled proliferation, metastasis and failure in apoptosis constitute crucial elements in the development and progression of tumors. Several studies have demonstrated the efficacy of plant-derived agents in the treatment of various malignant entities. The present study investigated the anti-tumor effects of costunolide and dehydrocostus lactone isolated from Saussurea lappa in three human soft tissue sarcoma (STS) cell lines of various origins. STS represent a rare group of malignant tumors that frequently exhibit chemotherapeutic resistance and increased metastatic potential following unsuccessful treatment.
Material and Methods:
Cell viability was determined using the MTS assay. Cell cycle distribution, cleaved caspase-3, and Annexin V/PI were analysed by FACS analysis. The protein expression level of PARP and cleaved-PARP were analysed using western blotting. In addition, the expression levels of matrix metalloproteinases (MMPs), which play a crucial role in extracellular matrix degradation and, therefore, metastasis, were investigated using Luminex® technology and real-time RT-PCR.
Results:
Both compounds inhibited cell proliferation of STS cell lines at concentrations ranging from 0.5 to 100 µg/ml and incubation periods from 24 to 72 h. Dehydrocostus lactone caused a significant reduction of the G1 phase and an increase in S and G2/M phases, as well as high levels of cleaved caspase-3 and PARP cleavage.
Our results indicate that MMP-1 expression tends to be upregulated in the presence of costunolide or dehydrocostus lactone. MMP-2 were downregulated significantly in all STS cell lines after dehydrocostus-lactone treatment, and the MMP-9 expression were downregulated significantly in dehydrocostus-lactone-treated TE-671 cells and costunolide-treated SW-872 and SW-982 cells.
Conclusions:
From our data, especially the inhibition of MMP-2 and MMP-9 could be an interesting approach toward a biological therapy of sarcoma. Therefore, it may provide a promising lead candidate for the development of therapeutic agents against drug-resistant tumours.

Bone Augmentation with Adipose Stem Cells and Calcium Phosphate Carriers for Human Maxillary Sinus Floor Elevation: An Ongoing Phase I Clinical Trial.

Helder Marco MN Ph.D. m.helder@vumc.nl VU University Medical Center Amsterdam The Netherlands
Overman Janice JR M.D. j.overman@acta.nl Academic Centre for Dentistry Amsterdam Amsterdam The Netherlands
ten Bruggenkate Christiaan CM D.D.S., M.D., Ph.D. C.t.Bruggenkate@rijnland.nl VU University Medical Center Amsterdam The Netherlands
Schulten Engelbert EAJM D.D.S., M.D., Ph.D. eajm.schulten@vumc.nl VU University Medical Center Amsterdam The Netherlands
Klein-Nulend Jenneke J Ph.D. j.kleinnulend@acta.nl VU University Medical Center Amsterdam The Netherlands

Submitted by:Prins, Henk-Jan PhD

In this phase I clinical trial the feasibility and safety of bioactive implants, consisting of a calcium phosphate carrier seeded with freshly isolated adipose stem cells in a one-step surgical procedure, are investigated. Furthermore, the bone forming capacity is studied.

Introduction

For patients with insufficient maxillary bone height, maxillary sinus floor elevation (MSFE) with autologous bone enables the insertion of dental implants. Autografting, however, has disadvantages, such as limited graft availability and donor site morbidity. Synthetic bone substitutes can be used as an alternative transplant material, but these only have osteoconductive properties and lack osteoinductive potential. The stromal vascular fraction, which can be freshly isolated from adipose tissue, contains stem cells that are able to attach rapidly to calcium phosphate (CaP) carriers, proliferate, and differentiate towards the osteogenic lineage. In this phase I clinical trial the feasibility of generating osteoinductive implants, consisting of a CaP carrier seeded with freshly isolated adipose stem cells, are investigated, and their bone forming capacity is studied.

Patients &Methods

The following three patient groups (n=5) are distinguished using CaP carriers with different resorption rates: 1) Ceros ß-tricalcium phosphate (TCP); 2) Straumann Bone Ceramic biphasic calcium phosphate (SBC-BCP; 60% hydroxyapatite (HA)/40% TCP); and 3) SBC-BCP (20% HA/80% TCP). CaP carriers were seeded with $10x10^6$ viable nucleated cells per gram of CaP carrier. These hybrid constructs are generated using an innovative one-step surgical procedure, which can be performed within hours in the OR-complex using a Celution 800/CRS device (Figure 1). Occurrence of any adverse events related to the product and/or procedure are monitored. After six months biopsies from the grafted area are obtained during dental implant surgery and evaluatedfor bone formation by histomorphometrical and µCT analysis. Clinical, radiographic, and cone-beam CT data are collected and evaluated pre- and postoperatively, and at regular intervals during follow-up.

Results

Currently (May, 2012), ten patients (6 females, 4 males) uneventfully underwent either an unilateral MSFE procedure, or a bilateral MSFE procedure using a ‘split mouth design' with CaP carrier combined with stem cells on the test-side and CaP carrier only on the control-side (Table 1). Mean viability of the harvested cells was 83±6% with a average cell yield of 184,000±47,000 viable cells per ml of adipose tissue (Table 2). All patients showed normal wound healing on both sides. During follow-up no adverse effects were reported. Bone biopsies are currently being evaluated.

Discussion/conclusion

This study demonstrates that a one step-surgical procedure is feasible for an MSFE procedure. It is hypothesized that the bioactive carrier combined with stem cells will improve the quality and quantity of bone formation in an MSFE procedure as compared with the use of a CaP carrier only, and that efficacy might be influenced by the properties of the CaP carrier. If successful, this novel treatment concept offers broad potential for other bone tissue engineering applications.

Concept of a maxillary sinus floor elevation with freshly isolated adipose-derived stem cells in a one-step surgical procedure. The plastic surgeon starts harvesting adipose tissue by liposuction. The oral and maxillofacial surgeon starts the maxillary sinus floor elevation procedure, whereas the tissue engineer isolates the adipose stem cells from the adipose tissue and seeds the cells onto the bone substitute. The oral and maxillofacial surgeon inserts the bone

substitute combined with stem cells into the maxillary sinus floor, and finally the wound is closed.
-Patient data. Table indicates the gender and age (years) of the ten patients included; whether the patient was treated unilaterally or bilaterally ('split-mouth design'); graft material used as carrier; and the dental implant sites according to the Fédération Dentaire Internationale (FDI) system.
-Cell yield and viability. Table indicates the adipose tissue volume harvested and processed using a Celution 800/CRS device; the total viable cell yield (x106); number of viable cells per ml of adipose tissue; and the viability of the total cell number.

Submitted by:Abdelbadie, Ahmed

The midvastus approach is a less invasive approach having the merit of wide exposure and simplicity of the standard approach. It represents a compromise between the standard approach and MIS TKA.

Introduction: The medial parapatellar approach, originally described by von Langenbeck in 1879, remained as the working horse in total knee replacement surgery. The major problems in this technique remained in the reduction of patellar blood flow, extensor mechanism imbalance, and the need to lateral retinacular release in some cases. The mid-vastus approach appeared as an alternative to the problems detected with the traditional medial parapatellar incision to minimize the risks of extensor mechanism imbalance. While using this approach, no special instruments, as in the case of minimally invasive surgery, will be needed. The same benefits could be reached with proper visualization during surgery and shorter operative time.

Patients and methods: This is a prospective study of 29 primary knee arthroplasties done by the midvastus approach without patellar eversion (see figure 1). All cases were done in Suez Canal University hospital between May 2008 and June 2010. Mobile-bearing cruciate-substituting total knee prosthesis was used in all cases.

Results: Operative data showed no increase in the operative time with no significant increase in the blood loss. No lateral retinacular release was needed. The bone defects can be treated easily through this approach (see Table 1). No serious complications encountered in all patients except one case of infected prosthesis (see figure 2).

Conclusions: The approach is universal and can be recommended for all patients (except for revision cases and severe deformities). No need for special instrumentation. The results are better than the standard approach with earlier return to SLR, faster pain relief and shorter hospital stay.

References:

-Bramlett K: Trivector retaining arthrotomy for total knee arthroplasty. Orthop Trans 1993 ;17: 1174-1184.
-Engh GA, Holt BT and Parks NL: A midvastus muscle-splitting approach for total knee arthroplasty. J Arthroplasty 1997;12: 322-331.
-Marson BM and Toklish JT: The effect of a tourniquet on intraoperative patellofemoral tracking during total knee arthroplasty. J Arthroplasty 1999 ; 14:197-199.
-Komatsu T, Ishibashi Y, Otsuka H et al: The effect of surgical approaches and tourniquet application on patellofemoral tracking in total knee arthroplasty. J Arthroplasty2003;18: 308-312.
-Huang HT, Su JY, Chang JK et al: The early clinical outcome of minimally invasive quadriceps-sparing total knee arthroplasty: report of a 2-year follow-up. J Arthroplasty 2007;22:1007-12.
-Kolisek FR, Bonutti PM, Hozack WJ et al : Clinical experience using a minimally invasive surgical approach for total knee arthroplasty: early results of a prospective randomized study compared to a standard approach. J Arthroplasty 2007; 22:8-13.
-Cushner FD and Friedman RJ: Blood loss in total knee arthroplasty, Clin Orthop Relat Res 1991; 269.
-Jämsen E, Huhtala H, Puolakka T et al: Risk factors for infection after knee arthroplasty: a register-based analysis of 43,149 cases. J Bone Joint Surg Am 2009;91:38- 47.
-Hube R, Keim M and Mayr HO: The mini-midvastus approach for total knee arthroplasty, Oper Orthop Traumatol 2009;21(1):3-13.

Short (15 Minutes) BMP-2 Treatment Stimulates Osteogenic Differentiation of Human Adipose Stem Cells Seeded on Calcium Phosphate Scaffolds

Farré-Guasch Elisabet E. D.D.S., Ph.D. efarre@csc.uic.es ACTA-University of Amsterdam and VU University Amsterdam, Research Institute MOVE, Dept Oral Cell Biology Amsterdam The Netherlands
Helder Marco M.N. Ph.D. m.helder@vumc.nl VU University Medical Center, Research Institute MOVE, Dept Orthopaedic Surgery Amsterdam The Netherlands
ten Bruggenkate Christiaan C.M. D.D.S., M.D., Ph.D. chr.bruggenkate@vumc.nl VU University Medical Center, Research Institute MOVE, Dept Oral and Maxillofacial Surgery Amsterdam The Netherlands
Schulten Engelbert E.A.J.M. D.D.S., M.D., Ph.D. eajm.schulten@vumc.nl VU University Medical Center, Research Institute MOVE, Dept Oral and Maxillofacial Surgery Amsterdam The Netherlands
Klein-Nulend Jenneke J. Ph.D. j.kleinnulend@acta.nl ACTA-University of Amsterdam and VU University Amsterdam, Research Institute MOVE, Dept Oral Cell Biology Amsterdam The Netherlands

Submitted by:Overman, Janice MD

Fifteen-minutes incubation with a physiological dose BMP-2 had a long-lasting stimulating effect on osteogenic differentiation of hASCs after culturing on BCP/ ß-TCP scaffolds. This indicates that short pre-treatment with BMP-2 fits in a clinical one-step surgical procedure for bone regeneration.

A one-step concept for bone regeneration has been postulated in which human adipose tissue-derived mesenchymal stem cells (hASCs) are harvested, triggered to differentiate, seeded on biosynthetic substitute carriers, and implanted in the same operative procedure. Toward this goal it was investigated whether short (minutes) incubation with a physiological dose of BMP-2 suffices to trigger osteogenic differentiation of hASCs seeded on calcium phosphate carriers.

hASCs were isolated fromsubcutaneous abdominal wall adipose tissue. hASCs were treated with/without BMP-2 (10 ng/ml) for 15 min, and seeded on ß-tricalcium phosphate granules (ß-TCP; sized 0.7 mm) or biphasic calcium phosphate (BCP; 60%/40% or 20%/80% hydroxyapatite/ß-TCP). Attachment was determined after 10-30 min. After 4, 14, and 21 days of culture, proliferation (DNA content), and osteogenic differentiation (alkaline phosphatase (ALP) activity; osteogenic gene expression of CBFA1, collagen-1, osteonectin, and osteocalcin), as well as expression of the adipogenic marker PPAR-γ were analyzed. Gene expression was determined by real-time PCR.

hASC attachment to the different ß-TCP and BCP scaffolds was similar, and unaffected by BMP-2. BMP-2 increased the DNA content of hASCs seeded on the scaffolds by 2.1-fold (day 14) and 2.7-fold (day 21) compared to untreated controls. ALP activity increased in time on both scaffold types, but this was not affected by BMP-2. ALP gene expression was increased (3.0-fold) by BMP-2 on BCP scaffolds only at day 14. In hASCs seeded on BCP and ß-TCP, BMP-2 also stimulated gene expression of the osteogenic markers CBFA1 by 4.9-fold (BCP) and 3.7-fold (ß-TCP), collagen-1 by 6.8-fold (BCP) and 8.9-fold (ß-TCP), osteonectin by 8.6-fold (BCP) and 7.3-fold (ß-TCP), and osteocalcin by 1.9-fold (BCP) and 2.2-fold (ß-TCP) at day 21. In contrast, BMP-2 treatment inhibitedexpression of the adipogenic marker PPAR-γ by 4.5-fold (BCP) and 4.0-fold (ß-TCP) at day 21.

In conclusion, this study revealed that 15 minutes incubation with a physiological dose BMP-2 had a long-lasting stimulating effect on osteogenic differentiation of hASCs after culturing onBCP or ß-TCP scaffolds. Our findings indicate that this short pre-treatment with BMP-2 is a very promising tool for its use in a clinical one-step surgical procedure, and strongly support a one-step clinical concept for bone regeneration.

Sociodemographic Factors Influence the Risk for Femur Shaft Fractures in Children: A Swedish Case Control Study from 1997 : 2005

von Heideken Johan MD johan.von.heideken@ki.se Department of Women's and Children's Health, Karolinska Institutet Stockholm Sweden
Svensson Tobias MSc tobias.svensson@ki.se Department of Medicine, Solna, Clinical Epidemiology Unit, Karolinska Institutet Stockholm Sweden
Iversen Maura PT, MPH, DPT, SD M.Iversen@neu.edu Department of Physical Therapy, Northeastern University Boston United States of America
Blomqvist Paul MD, PhD paul.blomqvist@ki.se Department of Medicine, Solna, Clinical Epidemiology Unit, Karolinska Institutet Stockholm Sweden
Haglund-Åkerlind Yvonne MD, PhD yvonne.haglund-akerlind@aleris.se Department of Women's and Children's Health, Karolinska Institutet Stockholm Sweden
Janarv Per-Mats MD, PhD per-mats.janarv@capio.se Department of Women's and Children's Health, Karolinska Institutet Stockholm Sweden
Submitted by:von Heideken , Johan MD

Socioeconomic variables do influence the rate of femur shaft fractures in children (0-14 years of age) and the cause of fracture. The magnitude of the association differs between boys and girls especially in children age 7-14 years of age.

Background:
To investigate gender and age differences in sociodemographic risk factors and their relationship with femur shaft fractures and injury mechanisms in children.
Methods:
Population based case-control study. Swedish children (N=1,874), aged 0 : 14 years, with a femur shaft fracture diagnostic code between 1987 to 2005 were selected from the Swedish National Hospital Discharge Registry and compared to matched controls (N=18,740). Demographic, socioeconomic, and injury data were based on record linkage between six Swedish registers. Adjusted Odds Ratios were calculated.
Results:
In children 0 : 14 years of age, parental age < 25 years old increased the risk for femur fracture by 26%, compared to parents with an average age of 25 : 37 years. If parents' total income was among the 25th percentile, the risk increased by 20%, compared to parents with an income in the 50th percentile. Children with at least one university-educated parent reduced their fracture risk by 15%, compared to children whose parents had 10 : 12 years of education. Boys with younger parents or who lived in low-income households had an increased fracture risk. Girls had a higher risk if they lived in high-income households but having parents with higher education was protective. Boys' risk for sports accidents decreased if one or both parents received social welfare. Having an educated parent reduced the risk of a traffic-related fracture in boys. Girls had an increased risk for falls of < 1 meter if they lived in a one adult household. There was an increased risk for sports accidents among girls if they had two or more older siblings or parents with elementary school education. In girls, three traffic-related risk factors were identified: having younger parents; having more than two older siblings; and living in low income-households.
Conclusions:
Sociodemographic differences related to cause of injury and femur shaft fracture rate among children differ between boys and girls in different age groups. These data have implications for parental education and counselling.

Guided bone regeneration in critical defects using porous titanium scaffolds loaded with gelatin nanosphere-based gels for controlled release of BMP-2 and FGF-2

van der Stok Johan J. MD j.vanderstok@erasmusmc.nl Erasmus University Rotterdam The Netherlands
Wang Huanan H. Radboud University Nijmegen The Netherlands
Verhaar Jan J. A. N. PhD Erasmus University Rotterdam The Netherlands
Leeuwenburgh Sander S. C. G. PhD Radboud University Nijmegen The Netherlands
Weinans Harrie H. PhD h.weinans@erasmusmc.nl Erasmus University Rotterdam The Netherlands
Amin Yavari Saber S. Delft University of Technology Delft The Netherlands
Zadpoor Amir A. A. PhD Delft University of Technology Delft The Netherlands
Jahr Holger H. PhD Erasmus University Rotterdam The Netherlands
van Lieshout Esther E.M.M. PhD Erasmus University Rotterdam The Netherlands
Patka Peter P. PhD Erasmus University Rotterdam The Netherlands

Submitted by:van der Stok, Johan MD

Porous titanium scaffolds that offer direct biomechanical support and an osteoconductive matrix were loaded with biodegradable gelatin nanosphere gels containing BMP-2 and FGF-2. This results in more bone formation after implantation in a segmental bone defect of a rat.

Introduction:

Treatment of large bone defects may be improved using porous titanium scaffolds, since they offer direct biomechanical support and function as an osteoconductive scaffold. To further enhance the regenerative capacity of the bone, strong osteoinductive and vasculoinductive stimuli are desired. Therefore, porous titanium scaffolds were loaded with biodegradable gelatin nanosphere-based colloidal gels capable of delivering osteogenic growth factor BMP-2 and vasculogenic growth factor FGF-2 in a controllable manner.

Materials & Methods:

Porous titanium scaffolds with a porosity of 88%, a pore size of 490µm and titanium struts of 120µm were produced by selective laser melting. Three different groups of injectable colloidal gels made of oppositely charged gelatin nanospheres were prepared and loaded with (1) BMP-2, (2) FGF-2, (3) BMP-2 and FGF-2 by diffusional loading. A further group was prepared as control, where the gel was left without any growth factors (GFs). The in vitro release kinetics of the GFs was determined in a previous study showing that the sequential release and diffusion kinetics of FGF-2 and BMP-2 is primarily controlled by gelatin degradation. Using a customized chamber connected to a conventional medical syringe, the gels can be easily placed in the titanium scaffold by injecting the gels to fill the chamber containing the porous scaffold.

The four different types of gel-loaded titanium scaffolds were implanted in critically (6 mm) sized segmental femur defects of four groups of rats. Each group consisted of ten skeletally mature male Wistar rats. The defect was stabilized using a 23 mm PEEK plate with three distal and proximal screws (AO RatFix). At four, eight, and twelve weeks after operation, in vivo micro-CT scans were acquired to monitor bone formation over time. Bone ingrowth was determined from the reconstructed micro-CT images at each timepoint. TBV was defined as the bone within the 6 mm defect segment, while BVp was defined as the bone within the porous volume of the titanium scaffolds.

Results:

Preliminary results show that more TBV is measured after implantation of the BMP and the BMP-FGF loaded titanium scaffolds (Table 1). At eight weeks, bone formation has almost bridged the defect in four animals receiving the BMP-FGF loaded scaffolds, two animals receiving the loaded BMP-scaffolds, one animal receiving the FGF-loaded scaffold and none of the animals receiving the empty gel (Fig. 1). The BVp is slightly increased for the BMP loaded titanium scaffolds, however this difference is not yet found to be statistically significant.

Discussion/conclusion:

Addition of the gelatin nanosphere gels that contained BMP-2 to the porous titanium scaffolds considerably enhanced bone regeneration during the first eight weeks after implantation. A synergistic effect of BMP-2 and FGF-2 was not seen within the first eight weeks.

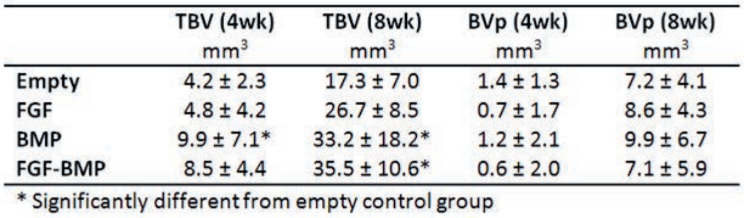

	TBV (4wk) mm^3	TBV (8wk) mm^3	BVp (4wk) mm^3	BVp (8wk) mm^3
Empty	4.2 ± 2.3	17.3 ± 7.0	1.4 ± 1.3	7.2 ± 4.1
FGF	4.8 ± 4.2	26.7 ± 8.5	0.7 ± 1.7	8.6 ± 4.3
BMP	9.9 ± 7.1*	33.2 ± 18.2*	1.2 ± 2.1	9.9 ± 6.7
FGF-BMP	8.5 ± 4.4	35.5 ± 10.6*	0.6 ± 2.0	7.1 ± 5.9

* Significantly different from empty control group

Table 1: micro-CT measurements

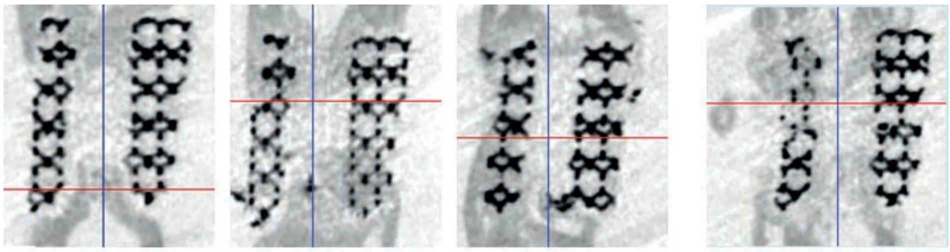

empty FGF-2 BMP-2 FGF-2 & BMP-2

Figure 1: micro-CT transversal images: Representative transversal images of in vivo micro-CT scans acquired of each treatment groups after eight weeks. Bone formation and incorporation of the porous titanium scaffold progresses from both cortical sites in and around the titanium structure.

BOTH N- AND C-TERMINAL PTHrP PEPTIDES IMPROVE THE OSTEOGENIC PROPERTIES OF HYBRID POLY-VINYL ALCOHOL/BIOACTIVE GLASS SCAFFOLDS IN VITRO IN OSTEOBLASTIC CELLS

Lozano Daniel Ph.D dlozano@fjd.es Laboratorio de Metabolismo Mineral y Óseo (IIS-FJD) and Instituto de Salud Carlos III-RETICEF Madrid Spain
Mortarino Pablo pablomortarino@hotmail.com Universidad de Rosario Rosario Argentina
Rocha Oliveira Agda Aline Universidade Federal de Minas Gerais Belo Horizonte Brasil
Portal-Núñez Sergio Ph.D sportal@fjd.es Laboratorio de Metabolismo Mineral y Óseo (IIS-FJD) and Instituto de Salud Carlos III-RETICEF Madrid Spain
Pereira Marivalda mpereira@demet.ufmg.br Universidade Federal de Minas Gerais Belo Horizonte Brasil
Feldman Sara saryfeldman@yahoo.com.ar Universidad de Rosario Rosario Argentina
Esbrit Pedro Ph.D pesbrit@fjd.es Laboratorio de Metabolismo Mineral y Óseo (IIS-FJD) and Instituto de Salud Carlos III-RETICEF Madrid Spain

Submitted by:Lozano, Daniel PhD

Both PTHrP (1-37) and PTHrP (107-111) coating onto hybrid poly-vinil alcohol/bioactive glass scaffolds exert similar osteogenic features in osteoblastic cells

Introduction.
Hybrid scaffolds of poly-vinyl alcohol/bioactive glass (PVA/BG) have been proposed as matrices for the controlled release of biofactors to improve bone regeneration following skeletal injuries like fractures. The N-terminal fragment of parathyroid hormone-related protein (PTHrP) is anabolic for bone. In addition, C-terminal parathyroid hormone-related protein (PTHrP) (107-111) peptide (osteostatin) has been shown to induce osteogenic features by directly acting on both osteoblasts and osteoclasts. We recently demonstrated that osteostatin confers osteoinductive properties to various bioceramics in vitro and as implants in a cavitary defect model in rabbits. In this study, we aimed to compare the effects of PTHrP (1-37) and osteostatin loading into PVA/BG scaffolds in vitro on osteoblastic cells.
Materials and methods.
PVA/BG scaffolds were prepared as described previously (Oliveira AAR et al. J Sol-Gel Sci Technol 2008; 47:335-46). Osteostatin and PTHrP (1-37) (a well characterized osteogenic factor) were adsorbed onto PVA/BG material by dipping into phosphate-buffered saline, pH 7.4, containing each peptide at 100 nM overnight at 4°C. Peptide release was assessed by using a radiotracer [¹²⁵I-[Tyr¹¹⁶] PTHrP (107-115)] or by spectrophotometry at A280 nm, following a standard protocol. Osteoblastic MC3T3-E1 cells were grown in differentiation medium (α-MEM with 10% FBS, 50 μg/ml ascorbic acid and 10 mM ß-glycerolphosphate), with or without (basal control) the tested materials containing or not the PTHrP peptides for 4-10 days. Cell proliferation and viability (assessed by AlamarBlue assay), alkaline phosphatase (ALP) activity, and matrix mineralization (alizarin red) were then determined.
Results.
First, we assesed the capacity of PVA/BG scaffolds to retain each PTHrP peptide. We found that mean uptake of osteostatin and PTHrP (1-37) by this material was 15 % and 30 %, equivalent to 0.2 μg and 0.1 μg peptide/g PVA/BG material, respectively, after 24 h of loading. These loaded scaffolds released (as mean %) 80 % of the loaded peptide to the surrounding medium at 1 h, and virtually 100 % at 48 h. PVA/BG scaffolds containing osteostatin increased cell proliferation and cell viability (by 75%) and also significantly increased ALP activity (by 10-15%) at day 4. Moreover, at day 10, matrix mineralization was 30% higher in the presence of this biomaterial in MC3T3-E1 cell cultures. Similar results bioactivities were observed with PTHrP (1-37) loaded onto PVA/BG material in these cells.
Conclusions.
These results indicate that either osteostatin or PTHrP (1-37) coating onto PVA/BG scaffolds exert similar osteogenic features in osteoblastic cells. Our in vitro findings also add credence to the notion that either PTHrP peptide might be useful to promote bone regeneration.
This work has been supported by a grant from Comunidad Autónoma de Madrid (S-2009/MAT/1472).

PARATHYROID HORMONE-RELATED PROTEIN (PTHrP) (1-37) OR PTHrP (107-111) LOADING INCREASES THE OSTEOGENIC CAPACITY OF BIOPOLYMER-COATED NANOCRYSTALLINE HYDROXYAPATITE (HAGlu) IN VITRO

Lozano Daniel Ph.D dlozano@fjd.es Laboratorio de Metabolismo Mineral y Óseo (IIS-FJD), Instituto de Salud Carlos III-RETICEF and Grupo de Investigación de Cirugía OsteoArticular, Instituto de Investigación Hospital Universitario La Paz (IdiPAZ) Madrid Spain
Vila Mercedes Ph.D Departamento de Química Inorgánica y Bioinorgánica, Facultad de Farmacia, Universidad Complutense Madrid Spain
Sánchez-Salcedo Sandra Ph.D Departamento de Química Inorgánica y Bioinorgánica, Facultad de Farmacia, Universidad Complutense Madrid Spain
Portal-Núñez Sergio Ph.D sportal@fjd.es Laboratorio de Metabolismo Mineral y Óseo (IIS-FJD), Instituto de Salud Carlos III-RETICEF Madrid Spain
Gómez-Barrena Enrique M.D egbarrena@telefonica.net Instituto de Investigación Hospital Universitario La Paz (IdiPAZ) Madrid Spain
Vallet-Regí María Ph.D Departamento de Química Inorgánica y Bioinorgánica, Facultad de Farmacia, Universidad Complutense Madrid Spain
Esbrit Pedro Ph.D pesbrit@fjd.es Laboratorio de Metabolismo Mineral y Óseo (IIS-FJD), Instituto de Salud Carlos III-RETICEF Madrid Spain

Submitted by:Lozano, Daniel PhD

PTHrP (1-37) and PTHrP (107-111) coating increases the bioactivity of biopolymer-coated nanocrystalline hydroxyapatite (HAGlu) in osteoblastic cell cultures.

Introduction.

Biopolymer-coated nanocrystalline hydroxyapatite (HA_{Glu}) made as macroporous foams are promising candidates as scaffolds for bone tissue regeneration. They exhibit an excellent cell (namely, osteoblast) internalization, proliferation and differentiation, with an adequate colonization over the entire scaffold surface. Parathyroid hormone-related protein (PTHrP) is an important modulator of bone formation. Its 107-111 epitope (osteostatin) can induce osteogenic features by directly acting on osteoblasts in vitro, and also as locally delivered into a cavitary defect in rabbits. The aim of this study was to evaluate whether osteostatin or PTHrP (1-37) loading might increase the osteogenic capacity of HA_{Glu} scaffolds in vitro in osteoblastic cells.

Materials and methods.

HA_{Glu} scaffolds were prepared as previously described (Sánchez-Salcedo S et al. J. Mater. Chem. 2010; 20:6956-61). Osteostatin and PTHrP (1-37) were adsorbed onto HA_{Glu} material by dipping into a 100 nM peptide solution (in saline at pH 7.4), following a standard protocol. The release of these peptides from the corresponding loaded material was assessed by using ¹²⁵I-[Tyr¹¹⁶]PTHrP (107-115) as tracer or by spectrophotometry at A280 nm. Mouse osteoblastic MC3T3-E1 cells were grown in differentiation medium (α-MEM with 10% FBS, 50 µg/ml ascorbic acid, and 10 mM ß-glycerolphosphate), in the presence or absence of the different tested materials with or without osteostatin for 2-10 days. Cell viability (assessed by trypan blue staining), alkaline phosphatase (ALP) activity, mineralization (alizarin red) and gene expression of osteoblast-related factors were then determined.

Results.

The capacity of HA_{Glu}scaffoldsto release these peptides was evaluated. We found that the mean uptake of osteostatin and PTHrP (1-37) by this material was 62 % and 70 %, respectively, after 24 h of loading. These scaffolds released (means): 80 % and 100 % of the loaded peptide to the surrounding medium at 1 and 24 h, respectively. Osteostatin-loaded onto HA_{Glu}significantly increased cell viability (by 40%) and ALP activity (by 20%) at day 4. In addition, at this time period, this biomaterial up-regulated (by 40%) osteoprotegerin gene expression and decreased the mRNA levels of receptor activator of nuclear factor kappa-B ligand. At day 10, matrix mineralization increased (by 50%) with osteostatin-coated HA_{Glu} scaffolds in MC3T3-E1 cells. PTHrP (1-37) loaded onto these scaffolds also improved the osteogenic properties of HA_{Glu}, but was in general less efficient than osteostatin in these cells.

Conclusions.

These results indicate that osteostatin or PTHrP (1-37) loading similarly increases the bioactivity of HA_{Glu} in osteoblastic cell cultures. Our findings suggest that these bioceramics might be envisioned as bone regeneration therapies.

This work has been supported by a grant from Comunidad Autónoma de Madrid (S-2009/MAT/1472).

Effect of Tricalcium Phosphate-Disilicate Calcium Ceramics on Human Bone Marrow Mesenchymal Stem Viability, Proliferation, Adhesion and Osteoblast Differentiation

Meseguer-Olmo Luis L. MD, PhD lmeseguer.doc@gmail.com Arrixaca University Hospital Murcia Spain
Garcia-Bernal David D. PhD redon@gmail.com CEIB Murcia Spain
Cragnolini Francesca F. Biotech dott.ssa_franci@hotmail.com Arrixaca University Hospital Murcia Spain
Martinez Isabel IM. Engineering martinez@upct.es Cartagena University Cartagena (Murcia) Spain
Velasquez Pablo P. Chemical PhD velasquez@umh.es Bioingineering Instutut Elche (Alicante) Spain
Aznar-Cervantes Salvador S. Biologist sdac1@um.es IMIDA Murcia Spain
Cenis-Anadon Jose Luis JL. Engineering PhD josel.cenis@carm.es IMIDA Murcia Spain
De Aza Piedad Nieves PN. Prof. Chemical piedad@umh.es Bioingineering Instutut Elche (Alicante) Spain

Submitted by:Meseguer-Olmo, Luis Prof, MD, PhD

In vitro culture of human bone marrow mesenchymal stem cells (hBMSCs) on bioceramics scaffolds prior to transplantation could improve their osteogenic properties and increase the bone formation efficacy when they are implanted for bone defect repair.

Introduction

Bone marrow Mesenchymal Stem Cells (hBMSCs) are characterized by their capacity to autorenew and differentiate into multiple mesenchymal cell lines such as adipocytes, chondrocytes and osteoblasts when the microenvironment in which they are located is optimal (presence of growth factors, cytokines, pressure of oxygen, pH, hormones, etc.). For this reason multipotent hBMSCs are an attractive cell source for bone regeneration due to their ability of self-renewal, high proliferative capacity and osteogenic differentiation potential. With the goal in mind of using Tricalcium Phosphate-Disilicate Calcium ceramics (TCP-C_2S) as bone substitutes or scaffold for bone tissue engineering, the aim of our work was to investigate if these biomaterials were no cytotoxic and provided a suitable niche for hBMSCs proliferation, adhesion and differentiation to cells with osteoblastic phenotype on the ceramics and to compare its behaviour with pure a-TCP.

Patient & Methods

The materials consisting of α-tricalcium phosphate doped with 1.5wt% and 3.0wt% of dicalcium silicate in the system Tricalcium Phosphate-Dicalcium Silicate (TCP-C_2S) were obtained by solid state reaction. Undifferentiated multipotent hBMSCs, which were $CD73^+$, $CD90^+$, $CD105^+$, $CD34^-$ and $CD45^-$were isolated from iliac crest marrow aspirates of human volunteers with their previous informed consent. hBMSCs were seeded onto the ceramics in 96- or 24-wells plates and incubated at 37°C, 5% CO_2 and 95% relative humidity atmosphere. The growth medium used was α-MEM supplemented with 10% FBS and antibiotics. Citotoxicity (Annexin-V/7-AAD staining), adhesion (ultrastructural SEM studies), proliferation (MTT assay) and osteogenic differentiation capacity (ALP activity, collagen-I expression, osteocalcin production and mineralization) and extracellular matrix synthesis (heparan-sulphate and osteopontin production), was investigated by seeding hBMSCs onto the 3 substrates for 30 days.

Results

Data obtained showed non-cytotoxic effect of the ceramics after applying an apoptosis test based on Annexin-V/7-AAD staining (see Fig. 1A). Furthermore hBMSCs proliferated (Fig. 1B), adhered and spread (see Fig. 2) and produced extracellular matrix (Heparan-sulphate proteoglycan and osteopontin) (see Fig. 3) on all the ceramics studied. Finally, cells lost the expression of CD73, CD90 and CD105, characteristic of hBMSCs and showed an osteoblastic phenotype, characterized by Alkaline phosphatase activity, Osteocalcin production, Collagen type-I expression and production of mineralization nodules (calcium deposit) on the extracellular matrix detected by Alizarin Red staining (see Fig 3). These observations were more evident in the TCP doped with 1.5 wt% C_2S, indicating osteoblastic differentiation as a result of the increased concentration of silicon in solid solution in TCP. Overall, these results suggest that the ceramics studied are cytocompatible and show osteoinductive properties.

Discussion

These experimental TCPss ceramics show appropiate biological properties providing a microenvironment optimal for the hBMSCs proliferation and osteoblastic differentiation. So, TCPss represents new potential bioactive materials for applications in orthopaedic surgery, dentistry and maxillofacial surgery when large bone defect filling is required, or to improve the osseointegration of implants. Also, TCPss could be considered as a promising scaffold for bone tissue engineering.

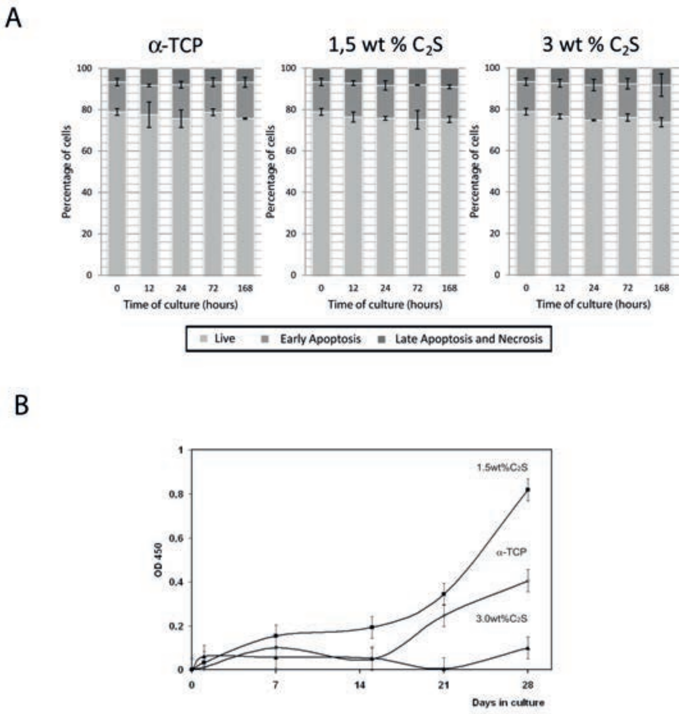

Figure 1. Effects of Ca_2SiO_4-$Ca_3(PO_4)_2$ ceramics on *h*BMSCs viability and proliferation. A) *h*BMSCs was cultivated in the absence (0) or presence of bioceramics for the indicated times. Mean percentages ± SD of live (Annexin-V^-/7-AAD^-), early apoptotic (Annexin-V^+/7-AAD^-) or late apoptotic/necrotic cells (Annexin-V^+/7-AAD^+) was measured by flow cytometry (N=3). **B)** Curves of growth of *h*BMSCs, measured by tetrazolium/formazan absorbance, on the α-TCP, 1.5 wt% and 3.0wt% C_2S ceramics at different times of study.

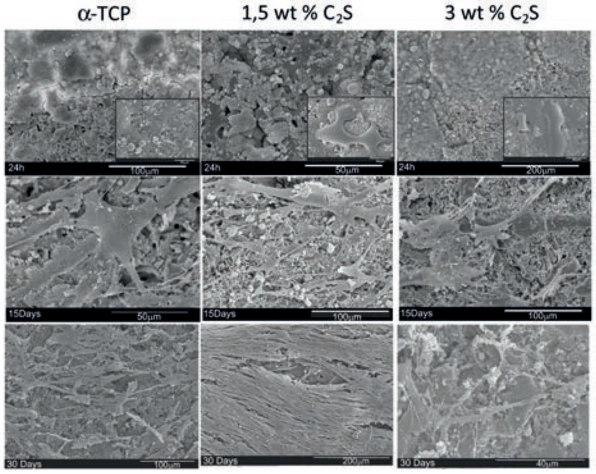

Figure 2. Effects of Ca_2SiO_4-$Ca_3(PO_4)_2$ ceramics on *h*BMSCs adhesion and cellular spreading. SEM micrographs of *h*BMSCs cultured on α-TCP and TCPss surfaces at 24 hours, 15 and 30 days.

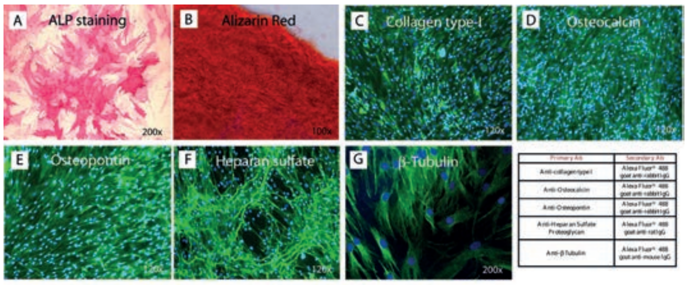

Primary Ab	Secondary Ab
Anti-collagen type I	Alexa Fluor® 488 goat anti-rabbit IgG
Anti-Osteocalcin	Alexa Fluor® 488 goat anti-rabbit IgG
Anti-Osteopontin	Alexa Fluor® 488 goat anti-rabbit IgG
Anti-Heparan Sulfate Proteoglycan	Alexa Fluor® 488 goat anti-rat IgG
Anti-β Tubulin	Alexa Fluor® 488 goat anti-mouse IgG

Figure 3. Effects of Ca_2SiO_4-$Ca_3(PO_4)_2$ ceramics on *h*BMSCs differentiation. (A) *h*BMSCs were positive for alkaline phosphatase staining; **(B)** Mineral deposits were stained bright red with the Alizarin Red Solution; **C),D),E),F),G)** Indirect immunofluorescence microscopy of *h*BMSCs using the indicated antibodies and summarized in table.

Submitted by:Leite Pereira, Catarina Msc

A new therapy for the treatment of Intervertebral Disc degeneration by the recruitment of MSCs through a biomaterial-based chemoattractant system, as an alternative to MSC-seeded scaffold transplantation.

Introduction

Human Mesenchymal stem cells (hMSCs) have an enormous potential for cell-based therapies due to their ability of differentiating into several cell types. Moreover, hMSCs are able to migrate to damaged tissues, regulated by different chemokines and growth factors[1]. hMSCs-chemoattractive factors may also be produced by the cells of a degenerating intervertebral disc (IVD)[2]. Therefore, MSCs recruitment towards the damaged IVD may be enhanced using a chemoattractant-delivery system. Poly(N-isopropylacrydamide) grafted hyaluronan (HA-PNIPAM) is an attractive delivery system due to its thermoreversible property, which allows this gel to be injected using a minimal invasive technique and its rapid gelling kinetics at 37ºC[3] . The present work aims to develop a HA-PNIPAM chemoattractant-delivery system for hMSCs recruitment in the degenerating IVD. For that, stromal-derived factor-1 (SDF-1) was incorporated in HA-PNIPAM as a model chemokine. SDF-1 is constitutively produced in the bone marrow, being strongly chemotactic to several cells, including hMSCs[4].

Methods

HA-PNIPAM (Mw 1.6 MDa) was synthesized as described previously[3] . For chemokine encapsulation, the gel powder was reconstituted at a concentration of 10% (w/v) in a 3000 ng/mL solution of SDF-1. To assess SDF-1 release kinetics, 50 µL HA-PNIPAM containing 150 ng of SDF-1, were casted in 2 mL tubes and gel formed at 37ºC. A control release system with alginate beads (1.2%) was used. Both gels were incubated in 1.5 mL of medium DMEM without serum at 37ºC, with orbital agitation at 225 rpm for 7 days. SDF-1 release kinetics was assessed by ELISA: at each time point (Fig 1.) 0.750 mL of medium was collected and replaced by fresh medium.

Results

Preliminary results show that the SDF-1 incorporation is successful and do not affect the thermo-reversibility of the HA-PNIPAM. The release of SDF-1 from both gels is similar, showing a continuous delivery of SDF-1 from in the first 48h (Fig. 1); after this period a steady-state is attained. The released amount of SDF-1 is approximately 40 ng, corresponding to a final concentration of 27 ng/mL after 48h, which can have already a chemoattractant effect[4].

Discussion

Herein we demonstrate the application of HA-PNIPAM gel as a suitable release platform for the delivery of chemokines, such as SDF-1. In this study, both systems were capable of delivering SDF-1 and contribute to the protein protection against proteolysis, increased life time and biological effectiveness. The results suggest that SDF-1 was mainly release by diffusion. HA-PNIPAM and alginate had shown a similar release profile, the thermoreversible gel is preferable due to its various properties but mainly because of it offers the possibility of injection and gelation in situ using minimal invasive strategies. Currently the bioactivity of released SDF-1 is being assessed by chemotaxis assay.

Conclusions

HA-PNIPAM gel incorporating chemokines such as SDF-1 represents a potential chemoattractant-delivery system, which can be used for tissue repair when injected in a degenerating IVD.

References

1 López Ponte et al. 2007. Stem Cells; 25:1737-1745
2 Illien-Jünger et al. 2012. Spine
3 Mortisen et al. 2010. Biomacromolecules, 11, 1261-1272.
4 Gonçalves et al. 2012. European Cells and Materials Vol.23, 249-261

Anatomic Risk of Anteroinferior shoulder portal in Comparison Between the Inside-out and Outside-in Techniques

Goto Hideyuki G H Nagoya City University Nagoya Japan
Takenaga Tetsuya T T Nagoya City University Nagoya Japan
Nishimori Yasuhiro N Y Nagoya City University Nagoya Japan
Nozaki Yasuhiro N M Nagoya City University Nagoya Japan
Otsuka Takanobu O T Nagoya City University Nagoya Japan

Submitted by:Yoshida, Masahito Anteroinferior Portal for Shoulder Arthroscopy at Anatomical Risk in Comparison Be

Neurovasculara structures are at the more risk of injury in the processes of inside-out technique of anteriorinferior portal for shoulder arthrosopy. The outside-to-inside technique could be safer in creation of that portal than inside-to-outside technique.

Introduction:
Arthroscopic repair techniques with a suture anchor have recently become common as a treatment for Bankart lesion. However, in some cases, it can be difficult to insert a suture anchor inside the glenoid bone at inferior position via anterosuperior portal depending on the angle and position of a the fixation device. The accessory portal, which is called anteroinferior portal (5 o'clock portal), can be needed for the approach of the inferior region of the glenoid rim at a right angle in these cases. However, the creation of that portal is at risk of neurovascular injury. The purpose of this study was to assess the neurovascluar structures at risk during establishment of 5 o'clock portals between inside-out and outside-in procedures.
Patients and Methods:
Ten embalmed cadaveric shoulder joints were dissected including 8 right and 2 left shoulders. The cadavers with shoulder scares and severe arthritis were excluded in this study. Cadavers were installed in a lateral decubitus position without traction. The arms were fixed at two positions: ①abduction 0° , internal rotation 30°(ADD) ②abduction 30°, internal rotation 30°(ABD). 2 mm Kirshner wires (K-w) were used to create anteroinferior portal, using established inside-to-outside (I-O) and outside-to-inside (O-I) techniques. At dissection, the shortest distances from K-w to the (1) axillary nerve, (2) axillary artery (3) musclocutaneous nerve, (4) cephalic vein, and (5) anterosuperior circumflex artery were measured by digital caliper. Each distance was measured three times and we recorded the average of those 3 measurements as the final distance.
Results:
The median distances with inside-out technique to the neurovascluar structures at ADD and ABD arm positions were (1) axillary nerve: 6.5 and 8.0, (2) axillary artery: 4.0 and 7.4, (3) musclocutaneous nerve: 1.8 and 5.1, (4) cephalic vein: 12.4 and 12.5 (5) anterosuperior circumflex artery: 9.4 and 7.4, respectively. On the other hand, the average distances at both arm positions were (1) axillary nerve: 8.3 and 9.6, (2) axillary artery: 7.8 and 10.7, (3) musclocutaneous nerve: 7.5 and 11.3, (4) cephalic vein: 8.0 and 8.3 (5) anterosuperior circumflex artery: 8.2 and 10.5, away from the K-w with outside-in technique, respectively (Fig1). The median distance with inside-out technique to all neurovascluar structures except cephalic vein at both positions is shorter than the distances with outside-to-inside technique. Furthermore, the musculocutaneous nerve, axillary artery and axillary nerve were pierced by or came intact with the K-w in the inside-to-outside procedure in 6 of 20 (30%), 2 of 20 (10%), and 2 of 20 (10%), respectively. On the other hand, the K-w did not injure these arteryand nerve in the outside-to-inside procedure at all.
Discussion/Conclusions:
This study showed the risk of injury in the creation of 5 o'clock portal using both inside-to-outside and outside-to-inside techniques in two arm positions. The axillary artery and the axillary nerve, and musculocutaneous nerve are at the more risk of injury in the processes of inside-out technique. In general, the outside-to-inside technique could be safer in creation of 5 o'clock portal than inside-to-outside technique.

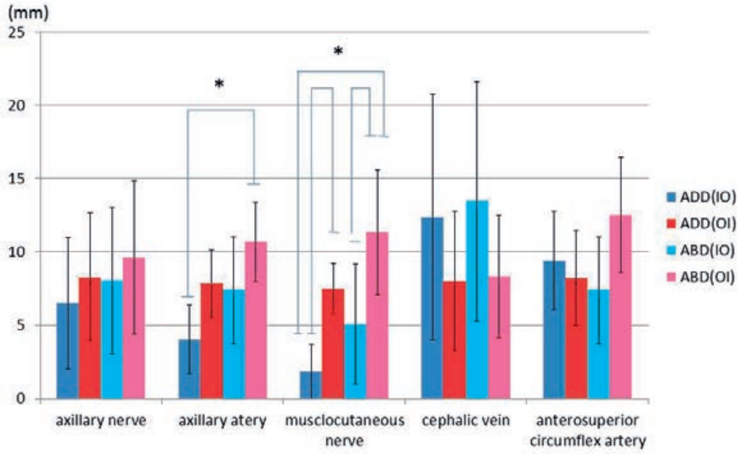

FIG1. Graphic representation of the mean distances from the K-wire to neurovascular structures
The specimen was fixed at two different arm positions (ADD: the arm was at adduction. ABD: the arm was at abduction of 30 degree). The anteroinferior portal was created with two methods(IO: Inside-out technique OI: Outside-in technique).

＊ : $P < .0.05$

Post operative Thigh pain in patients with Uncemeneted Hip Hemiarthroplasty : A retrospective outcome Study

Norton Ashlea Dr ashlea.norton@doctors.org.uk Fairfield Hospital Bury UK
Marappa Raghavendra Mr raghu.mg@gmail.com Fairfield Hospital Bury UK
Mamoowala Haider Mr nevsaj@aol.com Fairfield Hospital Bury UK
McGivney Ronan Mr ronan.mcgivney@pat.nhs.uk@ Fairfield Hospital Bury UK
Submitted by:Keerthi, Naveen Mr

Previous studies suggest that the incidence of significant thigh pain post procedure is 13 to 26%. However, in our study it is 8% (Albeit, the overall incidence is 31%). Assuming that the intermittent thigh pain in patients who are satisfied post procedure as clinically insignificant, the results seem to be convincing to continue with the current practice of Uncemented Hemiarthroplasty for this group of patients.

Objective:
To determine post operative thigh pain, patient satisfaction and change in mobility status in patients who had Uncemented Hip Hemiarthroplasty for Femoral neck fractures.
Design:
A retrospective study conducted using a standard set of questions posted to patients and answered either by patient or the immediate carer.
Setting:
Patients discharged from Trauma ward following a Hip Hemiarthroplasty for Fracture Neck of Femur.
Participants:
26 out of the 72 patients over the age of 65 who had Uncemented Hip Hemiarthroplasty between over 1 year period.
Method:
All the patients had Uncemented Hemiarthroplasty done more than 8 months ago to the least. A 6 item standard questionnaire is posted to everyone which assessed thigh pain on the side of operation using a visual analogue score, mobility status, patient satisfaction and functional outcome.
Conclusions:
Previous studies suggest that the incidence of significant thigh pain post procedure is 13 to 26%. However, in our study it is 8% (Albeit, the overall incidence is 31%). Assuming that the intermittent thigh pain in patients who are satisfied post procedure as clinically insignificant, the results seem to be convincing to continue with the current practice of Uncemented Hemiarthroplasty for this group of patients.
Recommendations:
A comparative study with Cemented arthroplasty and preferably in higher numbers and a study for longer term to identify the incidence of chronic pain.

Refixation of osteochondral fractures by ultrasound-activated, resorbable pins - an ovine in-vivo study

Neumann Hanjo HN Dr. Hanjo_Neumann@gmx.de BUK Hamburg Hamburg Germany
Schulz Arndt-Peter APS PD Dr. University of Lübeck Lübeck Germany
Gille Justus JG PD Dr. University of Lübeck Lübeck Germany
Jürgens Christian CJ Prof. Dr. BUK Hamburg Hamburg Germany
Kienast Benjamin BK Dr. BUK Hamburg Hamburg Germany

Submitted by:Neuman, H Dr.

The SonicPin™ system is suitable for the refixation of osteochondral fractures. The healing ratio is higher than with the Ethipin® system. A negative effect on the cartilage by the heat generated by the SonicPin™ system is not proven. No further surgery is necessary for removal of the implant. MRI imaging is not compromised

Introduction
Osteochondral injuries, if not treated adequately, often lead to sever osteoarthritis. Possible treatment options of these injuries include refixation of the fragment or replacement therapies like pridie drilling, microfracturing or osteochondral grafts. They all have certain disadvantages. Only refixation of the fragment can produce smooth and resilient joint surface.
Material and methods
Aim of this study was the evaluation of an ultrasound-activated bioresorbable pin (SonicPin™, Stryker) for the refixation of osteochondral fragments under physiological conditions. In 16 Merino sheep specific osteochondral fragments of the medial femoral condyle were produced and refixated with either SonicPins™, Ethipins® or conventional titanium microscrews. Macroscopic and microscopic scoring was accomplished after three months of full weight bearing.
Results
The SonicPin™ system is qualified for the refixation of osteochondral fractures. The healing ratio is higher than with the Ethipin®-group and lower than in the screw-group. A negative effect on cartilage from heat generated by the SonicPin™ system has not been shown. No further operation for the removal of the implant is necessary. MRI imaging is not compromised, as it is with implanted screws.

-SonicPin™ mounted on the ultrasound applicator and melted into cancellous bone.
-SonicPin™ mounted on the ultrasound applicator and melted into cancellous bone.
-Macroscopic view of SonicPin™ osteosynthesis </td></tr></tbody></table>

strain for cadaveric hip specimens when implanted with a novel Titanium foam acetabular shell

LOWRY CONOR J MR conor.lowry@coringroup.com Corin Cirencester U.K.
MORTON LEONA DR leona.morton@coringroup.com Corin Cirencester U.K.
SIMPSON DAVID J DR david.simpson@coringroup.com Corin Cirencester U.K.
COLLINS SIMON N DR simon.collins@coringroup.com Corin Cirencester U.K.
Submitted by:Lowry, Conor Mr

The aim of this work was to develop a robust method for characterising strain in the implanted cadaveric hip. The method, once verified on sawbones specimens, was applied to determine associated strain for a novel titanium foam acetabular cup design.

Introduction

Premature failure of orthopaedic implants is often a result of implant loosening. Factors such as bone integration and the ability of the implant to mimic the pre-operative state are critical to long term survival. Wolff's Law states that bone remodels in response to the mechanical stresses it experiences so as to produce a minimal-weight structure that is 'adapted' to its applied stresses[1]. The press-fit method of short term fixation and the relatively high elastic modulus of conventional implant materials such as Cobalt Chrome, Titanium and Stainless Steel, are factors known to contribute towards bone remodelling[2,3].

Cellular metals or 'foams' have recently gained interest from the medical device community. The potential to engineer and fabricate interconnecting porous structures with physical and mechanical characteristics similar to human bone opens a large spectrum of opportunities. Most cellular metal devices currently undergoing clinical trials have a pore size ranging from 100 to 500μm[4]. Depending on the desired mechanical properties, the porosity and elastic modulus can vary from 60 to 85% and 1.0 to 6.0 GPa[5] respectively; these ranges are known to be similar to that of bone[6].

Additive manufacturing (AM) facilitates the production of parts directly from CAD. This, unlike many counterpart technologies, enables parameters such as pore size, shape and porosity to be tailored to meet custom specification.

Corin has developed a novel Titanium foam acetabular device, fabricated using the latest AM technology. The objectives of this study were to develop and validate a robust method for characterising strain for the implanted adult hip, and apply this method to assess performance of a novel acetabular cup design in terms of strain.

Method

A protocol was devised, based on predicate work[79], to describe the experiment. This included a method for preparing the cadaveric specimens, marking anatomic landmarks and implant position, strain gauging, re-orientating and loading to simulate a physiological load scenario.

Three full pelvis specimens were prepared in an identical manner for the experiment. The pre and post operative states were recorded by means of a custom fixture and computed tomography (CT) scan. A collaborating surgeon performed the procedure, stripping soft tissue and implanting bi-lateral pelvises; one side with a clinically known Corin device; the other with a novel Titanium foam device. Physical markers for the Anterior Pelvic Plane (APP) were applied to each complete pelvis model before dividing into hemi-pelvises. A custom fixture was designed to reorientate the hemi-pelvis with 12° adduction and 36° rotation, relative to the APP, to accept a vertical load of 1.5kN and simulate walking¹⁰. Surface strain was assessed for the regions of interest using a photoelastic method.

Results

The method designed for this study has shown to be effective in characterising strain for implanted cadaveric models. Results indicated reduced strain in key regions for the novel titanium foam device when compared with the clinically known Corin device.

Discussion / Conclusion

The results of this study indicate Titanium foam to be a suitable technology for reducing undesirable bone remodelling, occurring as a product of the elastic mismatch between implant and bone.

Reference List

1. Callaghan JJ, Rosenberg AG, Rubash HE: The adult hip. Lippincott-Raven, 1998
2. Wright JM, Pellicci PM, Salvati EA, Ghelman B, Roberts MM, Koh JL: Bone density adjacent to press-fit acetabular components: a prospective analysis with quantitative computed tomography. J Bone Joint Surg 83A(4):529, 2001
3. Pitto RP, Bhargava A, Pandit S, Munro JT: Retroacetabular stress-shielding in THA. Clin Orthop Relat Res 466(2):353, 2008
4. Bobyn JD, Stackpool GJ, Hacking SA, Tanzer M, Krygier JJ: Characteristics of bone ingrowth and interface mechanics of a new porous tantalum biomaterial. J Bone Joint Surg Br 81(5):907, 1999
5. Balla VK, Bodhak S, Bose S, Bandyopadhyay A. Porous Tantalum Structures for bone implants: Fabrication, mechanical and in vitro biological properties. Acta Biomaterialia 6, 3349-3359. 2010.
6. Harrison A, Gioe T, Simonelli C, Tatman P, Schoeller M: Do Porous Tantalum Implants Help Preserve Bone?: Evaluation of Tibial Bone Density Surrounding Tantalum Tibial Implants in TKA. Clinical Orthopaedics and Related Research-« 468(10):2739, 2010
7. Dickinson AS, Taylor AC, Browne M. The influence of acetabular cup material on pelvis cortex surface strains, measured using digital image correlation. Journal of Biomechanics 45[4], 719-723. 23-2-2012.
8. Miles AW, McNamee PB. Strain gauge and photoelastic evaluation of the load transfer in the pelvis in THR. The effect of the position of the axis of rotation. Proc Instn Mech Eng [H] 203[2], 103-107. 18-1-1989.
9. Kroeber M, Ries MD, Suzuki Y, Renowitzky G, Ashford F, Lotz J. Impact biomechanics and pelvic deformation during insertion of press-fit acetabular cups. The journal of Arthroplasty 17[3], 349-354. 1-4-2002.
10. Bergmann G, Deuretzbacher G, Heller M, Graichen F, Rohlmann A, Strauss J, Duda GN: Hip contact forces and gait patterns from routine activities. J Biomech 34:859, 2001

Does the Secondary Structure of Collagen Determine which Regions of a Turkey Tendon Become Mineralised? An Investigation Using Raman Spectroscopy

Buckley Kevin Dr. kevin.buckley@stfc.ac.uk Science and Technology Facilities Council Harwell Oxford U.K.
Kerns Jemma G Dr. University College London London U.K.
Parker Anthony W Prof. Science and Technology Facilities Council Harwell Oxford U.K.
Matousek Pavel Prof. Science and Technology Facilities Council Harwell Oxford U.K.
Goodship Allen E Prof. University College London London U.K.

Submitted by:Buckley, Kevin Dr.

Calcified turkey leg tendons are a well characterised model system for studying the mineralisation process. Raman spectroscopy reveals the structure of the collagen differs between the mineralised and non-mineralised regions, and can be used to probe the micron-scale transition zones.

Calcified turkey leg tendons are a well characterised model system for studying the mineralisation process.[1] Electron-microscopy of turkey tendons has been used to show initialisation of mineralisation in the gap regions between the ends of the collagen molecules[1] and x-ray scattering has been used to elucidate the nature of the lateral packing of the collagen molecules.[2] Fourier Transform Infrared Microscopy has been used to study the alignment of both the mineral and protein components of the tissue[3] and the crystallinity of the hydroxyapatite across the mineralisation transition zone.[4] Biochemical analyses of turkey tendons have shown that the cross-linking in the mineralising regions and non-mineralising regions differ and that the differences are present in young animals even before the mineralisation commences.[5]

In the present study Raman spectroscopy is used to explore the hypothesis that the different crosslinking profiles associated with mineralisation manifest themselves in the intact turkey tendon tissue as changes in collagen structure. Raman is suited to this purpose because it allows non-destructive probing of the collagen phase[7] and its spatial resolution allows the probing of the micron-scale transition zone between the mineralised and non-mineralised regions.

he Raman measurements across the mineralisation transition zone (Figure 1) show that with increasing mineralisation (increasing phosphate bands), the amide III/amide I ratio increases and the amide III band changes shape; these spectral characteristics indicate that the less-mineralised tendon is preferentially orientated to a greater degree than the mineralised tendon[6] and its ratio of alpha-helical protein to random-coil protein is greater.[8] Work is now commencing to scan the pre-mineralised regions of tendons of young turkeys, this will confirm whether a collagen structure is already in place at certain anatomical sites which may control the process of mineralisation. These altered protein structures and their cause (the post-translational modifications reported by Knott et al.[5]) are interesting because they suggest a mechanism for controlling the mineral to collagen ratio, and thus the material properties, of bone.

References
1. W.J. Landis, J. Ultrastruc. Mol. Struct. Res. 94:217-238(1986)
2. P. Fratzl, N. Fratzl-Zelman & K. Klaushofer, Biophys. J. 64:260-266(1993)
3. S.J. Gadaleta, W.J. Landis, A.L. Boskey & R. Mendelsohn, Connective Tissue Research, 34(3):203-211(1996)
4. S.J. Gadaleta, N.P. Camacho, R. Mendelsohn & A.L. Boskey, Calcif. Tissue Int. 58:17023(1996)
5. L. Knott, J.F. Tarlton & A.J. Bailey, Biochem. J., 322:535-542(1997)
6. T. Lefevre, F. Paquet-Mercier, S. Lesage, M. Rousseau, S. Bedard & M. Pezolet, Vibrational Spectroscopy, 51(1):136-141(2008)
7. K. Buckley, P. Matousek, A.W. Parker & A.E. Goodship, J. Raman Spectrosc., in press
8. T. Buchwald, K. Niciejewski, M. Kozielski, M. Szybowicz, M. Siatkowski & H. Krauss, J. Biomed. Opt. 17:017007(2012)

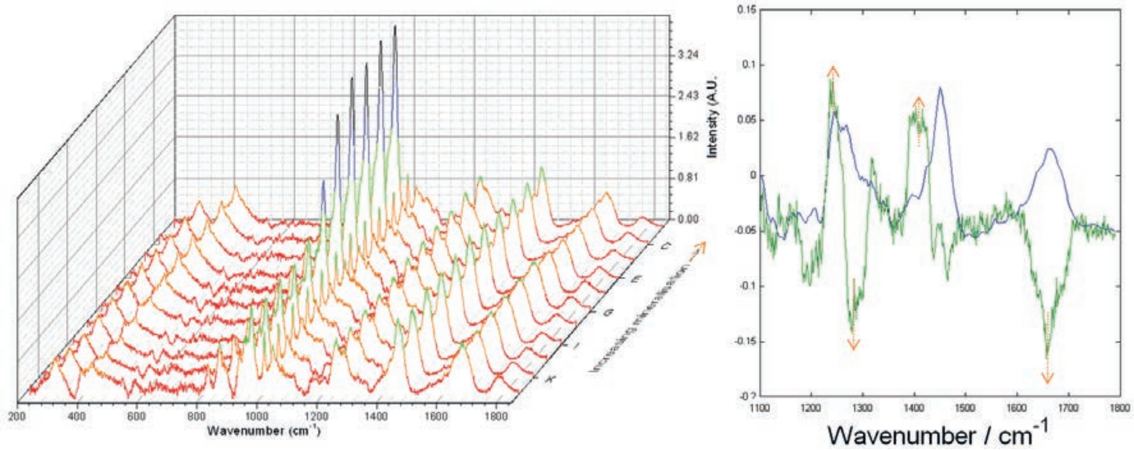

Raman spectra of turkey tendon showing the increasing phosphate band (960 cm-1) across the transition zone between mineralising and non-mineralising regions (Left, step: 30 m). The first two principal component eigenvectors show the changes in the collagen band profiles as mineralisation level increases (Right).

High-flexion Total Knee Arthroplasty is a safe alternative in selected patients: Similar migration during 5 year follow-up of a 4-arm randomized controlled clinical and Roentgen Stereophotogrammetric Analysis (RSA) Study

van der Voort Paul MD Leiden University Medical Center
Kaptein Bart L MSc, PhD Leiden University Medical Center
Valstar Edward R MSc, PhD Leiden University Medical Center
Nelissen Rob GHH MD, PhD Leiden University Medical Center
Submitted by:Nieuwenhuijse, Marc MD

The NexGen LPS high-flex TKA has comparable migration to its conventional counterpart and is expected to have similar (excellent) long-term survival. This high-flex TKA can safely be used in patients expected to benefit from this high flexion potential.

Introduction.

High-flexion Total Knee Arthroplasty (TKA) allows flexion up to 155^{○} in order to meet demands of increased flexion. Concerns have been raised regarding stability of high-flexion TKA due the required larger bone resection, possible higher wear and increased edge-loading. However, its migration, and thus fixation, has not been analyzed. In this 4-arm randomized clinical and Roentgen Stereophotogrammetric Analysis (RSA) trial, we evaluate the 5-year migration and functional results of the NexGen Legacy Posterior Stabilized high-flexion (LPS-Flex) TKA with either a mobile or fixed bearing and compare it to the conventional NexGen LPS TKA with either a mobile or fixed bearing.

Methods.

Seventy-four of 86 consecutive patients scheduled to receive 78 TKAs for end-stage osteoarthritis were randomized to receive one of four TKA designs as follows: I) 19 LPS-Flex mobile TKA, II) 20 LPS-Flex fixed TKA, III) 18 LPS mobile TKA and IV) 21 LPS fixed TKA. Patients were evaluated preoperatively and postoperatively at 6, 12, 26 and 52 weeks and annually thereafter. At each evaluation, the Knee Society Score (KSS) and RSA radiographs were obtained. Conventional radiographs were acquired at 6 weeks, 2 and 5 years postoperatively and on indication. At 5-year follow-up, 8 patients had died and 2 patients were lost-to-follow-up. Seventy-seven tibial but only 42 femoral components were suitable for RSA-measurements.

Results.

Overall 5-year migration of the 77 tibial components was not significantly different between the 4 TKA designs (Maximum Total Point Motion (MTPM) $p = 0.373$,figure 1) and values were comparable at the 2 and 5-year postoperative follow-up moments (MTPM $p=0.565$ and $p=0.604$). Migration stabilized in all but three components (2 LPS-Flex mobile, 1 LPS fixed); one of these components has already been revised and was confirmed to be (aseptically) loose.

Overall 5-year migration of the 42 femoral components was comparable between the 4 TKAs designs (MTPM $p=0.949$,figure 2) and similar at 2 and 5 years postoperatively (MTPM $p=0.971$ and $p=0.443$). One femoral component did not stabilize and is considered to be loose (LPS-flex mobile).

In patients who had I) mean postoperative flexion >125^{○} or II) maximum flexion >135^{○}during the 1 to 5 year follow-up period, migration of high-flexion tibial and femoral components was similar to conventional components ($p>0.05$).

Postoperative flexion, KSS and KSS-function were comparable during the 5-year follow-up period and at the 2 and 5-year follow-up moments ($p>0.05$). One TKA was revised for septic loosening and one TKA was revised for aseptic loosening of the tibial component (5-year survival 97.4%, 95%CI: 93.8:100).

Conclusion.

Migration, and thus fixation, of the NexGen LPS high-flexion TKA was comparable to that of the NexGen LPS conventional TKA. Even in the high-flexion segment, no difference in migration was found and appropriate stability was achieved. However, the high-flexion potential was on average not utilized more by patients with high-flexion TKAs. Nevertheless, for this TKA, the high-flexion design is expected to have similar (excellent) long-term survival as its conventional counterpart and can safely be used in selected patients expected to benefit from the high-flexion potential.

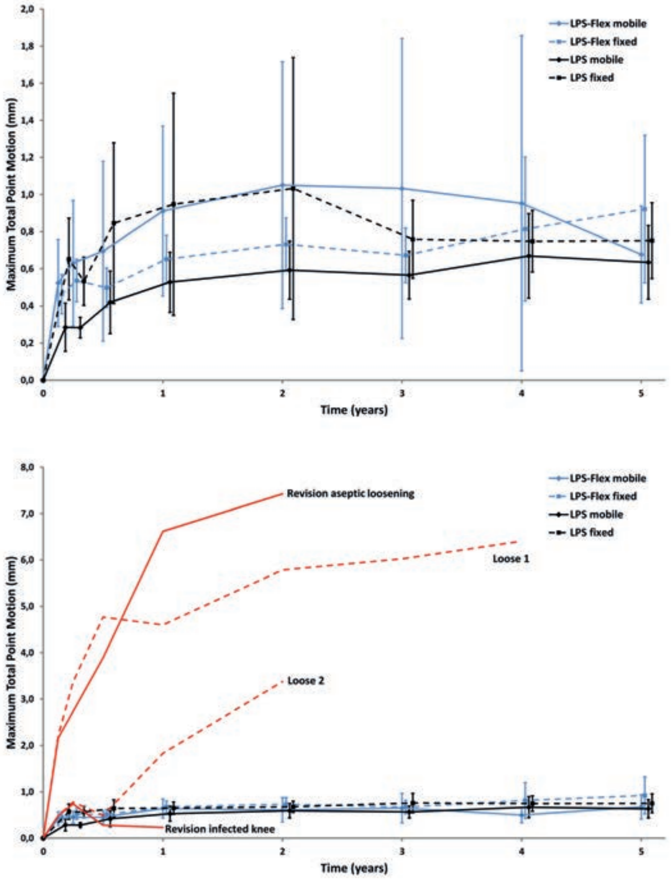

Mean with 95%CI of the Maximum Total Point Motion (MTPM) during 5 years of follow-up of the tibial components of the 4 different designs (upper) and with influential outliers separately (lower).

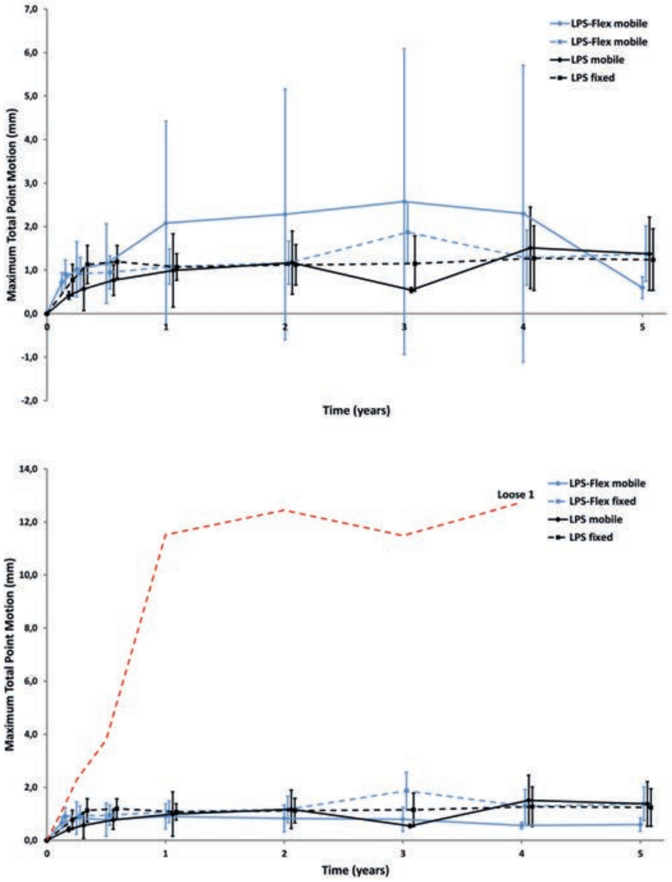

Mean with 95%CI of the Maximum Total Point Motion (MTPM) during 5 years of follow-up of the femoral components of the 4 different designs (upper) and with influential outliers separately (lower).

Submitted by:Pereira, Hélder MD

This study showed that silk-based scaffolds are non-cytotoxic and can support the adhesion, proliferation and viability of human meniscus cells, in vitro. Viable human meniscus cells increase biomechanical properties of silk-based constructs envisioning future clinical applications.

Introduction:

Advances in the field of meniscus tissue engineering (TE) are required and greatly depend on the improvement of biomaterials and cell culturing techniques. Silk fibroin scaffolds derived from Bombyx mori cocoon has been recognized as a versatile biomaterial for application in meniscus TE scaffolding [1]. In this work, we have developed a macro/micro porous silk fibroin scaffolds with suitable microstructure and superior mechanical properties by using highly concentrated aqueous silk fibroin solutions (10 and 12 wt%) and salt leaching/freeze-drying approaches. The biological performance of the silk scaffolds was in vitro evaluated using human meniscus cells (HMC's) up to 21 days of culturing.

Patients & Methods:

Different silk-based scaffolds (10 and 12 wt%) were produced using silk fibroin derived from Bombyx mori cocoon. The porous silk scaffolds were developed by combination of salt-leaching/freeze-drying methods. We evaluated 30 lateral and 14 medial menisci from 44 human donors, but only morphologically intact menisci were included [2]. HMC´s were isolated from human meniscus using enzymatic digestion and expanded using standard culture conditions. Then, HMC's (5 x 10^4cells/scaffold) were seeded onto the different silk scaffolds and cultured in static conditions, for times up to 21 days. HMC´s adhesion was investigated by scanning electron microscopy (SEM). Viability (calcein-AM assay) and proliferation (DNA quantification) tests were performed after each time point. Dynamic mechanical analysis (DMA) was carried out (at 37ºC and pH 7.4) for the silk scaffolds and cell-laden silk scaffolds (constructs) using a TRITEC8000B DMA (Triton Technology, UK).

Results:

SEM analysis revealed that the HMC´s adhered onto the surface of the silk scaffolds. The live/dead assay and DNA quantification showed that HMC´s were viable and proliferated well when cultured onto both silk-10 and silk-12 scaffolds, until 21 days. DMA analysis has shown that the moduli of the acellular scaffolds immersed in culture medium for 21 days were 25.6 ± 21.1 kPa and 77.9 ± 28.2 at 10 Hz, for silk-10 e silk-12, respectively. After 21 days of culturing, the moduli determined at 10 Hz of the constructs were 26.7 ± 19.4 and 84.6 ± 21.5 kPa, for silk-10 and silk-12, respectively. This data thus shows that HMC's produced viable, produced extracellular matrix, and increased the mechanical properties of the constructs.

Discussion/Conclusions:

This study showed that silk-based scaffolds are non-cytotoxic and can support the adhesion, proliferation and viability of human meniscus cells, in vitro. Viable human meniscus cells increase biomechanical properties of silk-based constructs. These results support that cell-based silk constructs have the capacity to mimic biological and biomechanical features of native human menisci envisioning future clinical application.

References

-LP. Yan, et al., Acta Biomater, 2012, 8(1):289-301.

-Pereira H , et al., 2011, 443 Cellular and Biomechanical Segmental Characterization of Human Meniscus, Osteoarthritis and Cartilage, 19 (S1) : S205

Submitted by:Borgwardt, Arne MD

A recently developed instrument for thromboelastography can be reliably and conveniently applied to measure the viscosity of synovial fluid. The inter-individual variability is large, and study of the relation between viscosity and longevity of hip or knee implants seems relevant.

Introduction

The longevity of hip or knee implants depends on reduction of wear through efficient lubrication. The adhesion between the cup and head of hip prostheses is stronger with higher viscosity of the fluid between the components, and this adhesion counteracts microseparation of the parts, which in turn would heavily increase wear. These conditions make the viscosity of the pseudosynovial fluid of prosthetic joints interesting and prompted us to measure it in samples of synovial fluid from arthritic patients who may be candidates for hip or knee arthroplasty. Initially we elucidated the usefulness of an instrument that was originally designed for measurement of blood coagulation variables, and validated a practicable method including storage, dilution and viscosity measurement of synovial fluid.

Patients & Methods

Synovial fluid was drawn from the joint cavity of the knee or a Baker cyst under ultrasound guidance, from patients where aspiration of the synovial fluid was indicated for relief of pain and improvement of function. The patients' diagnoses were rheumatoid arthritis (11 samples), osteoarthritis (2), psoriasis arthritis (1), and arthritis urica (1). Dilutions were prepared with an aqueous solution of sodium chloride 0.9% and sodium azide 0.065%, i.e. isotonic saline with an antibacterial preservative added, to make up 0.1x, 0.2x ……0.9x the concentration of the undiluted synovial fluid sample. Stable reference viscous samples were prepared by swelling and dilution of the polysaccharide xanthan gum in an aqueous solution of 0.065% sodium azide in the concentration range 0.05% to 0.20%.

The viscosity was determined by the principle 'free oscillation rheometry' at fixed shear rate (10.4 Hz) by a ReoRox, model Junior instrument (Medirox,Sweden). Calibration of the instrument was done with the manufacturer's calibrators, which are mixtures of glycerol and water. The viscosity of many synovial fluid samples exceeds that of the highest viscosity calibrator and the range where the instrument physically works, hence it is necessary to dilute most of the samples and know the algorithm for calculation of the viscosity of the original, undiluted sample from the data obtained by measurement of dilutions.

Results

Short term stability of synovial fluid samples was considered acceptable, since the difference was below +/- 20% in viscosity after storage for 7 days at 2-4^oC or after 3 freeze/thaw cycles. The measurement precision estimated using a high, medium and low concentration of xanthan gum was 13%, 12% and 3,5% CV %, respectively. The viscosity of individual synovial fluid samples varied greatly, from 2.7 mPa·s to 336 mPa·s.

Discussion & Conclusion

Determination of the viscosity of synovial fluid by the free oscillating rheometer ReoRox has been validated and works satisfactorily. We can not elucidate the possible relation between diagnosis and viscosity in the present material due to the uneven distribution of patient diagnoses. The correlation between measured viscosity and degree of dilution was exponential, as literature states, and must be determined for the individual sample if its viscosity exceeds the instrument calibration maximum 50 mPa·s in order to make proper calculation of the viscosity of the undiluted sample possible.

A NOVEL COATING TO RETARD FRETTING AND CORROSION OF TITANIUM ALLOY AGAINST COBALTCHROME TOTAL HIP ARTHROPLASTY TRUNION INTERFACES

Kinbrum Amy AK Dr amy.kinbrum@coringroup.com Corin Cirencester UK
Morton Leona LM Dr leona.morton@coringroup.com Corin Cirencester UK
Collins Simon SC Dr simon.collins@coringroup.com Corin Cirencester UK
Fox Andy AF Dr andy.fox@tecvac.com TecVac Cambridge UK
Housden Jonathon JH Dr jonathon.housden@tecvac.com TecVac Cambridge UK

Submitted by:Kinbrum, Amy Dr

This work aims to identify the key factors which cause the worst case fretting and corrosion for trunnion total hip arthroplasty interfaces. An electrochemical evaluation of the interface between femoral stems and heads with and without CrN coatings was completed.

Introduction

Evidence has been reported of fretting on the trunnion interface of modular hip prostheses (1). Previous work has shown that the titanium alloy-on-cobalt chrome pairing is the worst case metalurgically (2). Fretting, or relative displacements occurring at the taper interface, can cause corrosion products to migrate into the joint space and subsequently lead to osteloysis and host tissue inflammatory responses (3).

It is the author’s opinion that at least six potential variables can affect the extent of fretting and corrosion at the trunnions interface; the taper design (the contact area, the taper angle and interface roughness), the head/stem geometry (horizontal offset, head size), and finally the material used on either side of the taper junction. The relative importance of these variables in the wear of the taper has yet to be well described in the literature.

Surface coatings can increase the fretting and fretting corrosion resistance of modular implants (4). Chromium-Nitride (CrN) coatings are known for their wear, oxidation and corrosion resistance properties. It is proposed that CrN coatings will improve the fretting and corrosion properties of modular femoral components.

Method

To determine the effect of head offset and CrN coatings, four groups were tested. These are described in Table 1. For the coated groups, CrN coatings were deposited by Tecvac (Swavesey, Cambridge, UK) on the trunnions of the femoral stems (12/14 E) (Corin Ltd, Cirencester, UK), using the electron beam plasma vapour deposition technique. Testing was conducted by Endolab Mechanical Engineering GmbH (Rosenhiem,Germany).

The modular components were assembled according to ISO 7206-4:2002 (5), and fretting corrosion testing was performed in accordance with ASTM F1875-98 (2009) Method II (6). Features examined included surface area of the trunnion interface, offset of stem and material combination. Stems were compared with and without CrN coatings. Tests were performed in a temperature controlled saline lubricant, six tests were carried out in parallel, four different combinations of head and neck were studied, (n=3). Testing was completed as shown in Table 1.

Results

Results indicate that the head offset may have a large effect on the fretting and corrosion of the trunnion. The use of a CrN coating showed an improvement in the fretting and corrosion results indicated by the static and dynamic amplitudes at 0, 30, 360, 1000, 1800 and 3600 cycles

discussion / conclusion

At present, fretting and corrosion at the trunnion interface is hypothesised to increase with head diameter as the friction at the bearing surface can influence torque loads at this junction. These results support the use of CrN coatings to retard fretting and corrosion of the trunnion. It was noted, however, that this test does not produce torque on the trunnion and therefore is not entirely representative of the situation in vivo. It is suggested that further testing should be undertaken to verify that the coating can reduce fretting and corrosion in an experimental procedure which more closely simulates the in vivo situation.

Refereces

1) A multicentre retrieval study of the taper interfaces of modular hip prostheses, J.R Goldberg et al. Clin. Orthop. 104.
2) In Vitro assessment of strength, fatigue durability and disassembly of Ti6Al4V and CoCrMo necks in modular total hip replacements, M. Nganbe et al. J. Biomed. Mater. Res. B, 2 feb 11.
3) Concerns with modularity in total hip arthroplasty, J. D. Bobyn et al Clin. Orthop 298
4) Goldberg, J. R. & Gilbert, J. L. 2003, “In Vitro Corrosion Testing of Modular Hip Tapers”, J Biomed Mater Res B. 64, no. 2, pp. 78-93.

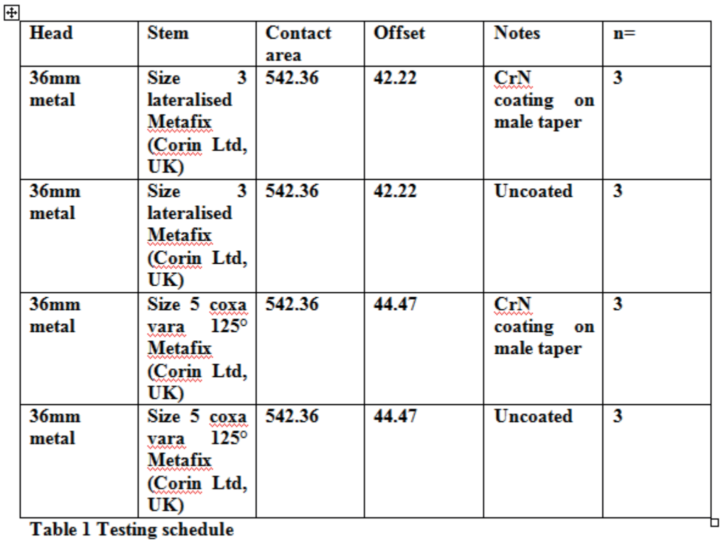

Head	Stem	Contact area	Offset	Notes	n=
36mm metal	Size 3 lateralised Metafix (Corin Ltd, UK)	542.36	42.22	CrN coating on male taper	3
36mm metal	Size 3 lateralised Metafix (Corin Ltd, UK)	542.36	42.22	Uncoated	3
36mm metal	Size 5 coxa vara 125° Metafix (Corin Ltd, UK)	542.36	44.47	CrN coating on male taper	3
36mm metal	Size 5 coxa vara 125° Metafix (Corin Ltd, UK)	542.36	44.47	Uncoated	3

Table 1 Testing schedule

Figure 1 - Testing Schedule

Ambulatory measurement of knee angles in the sagittal plane using inductive coil technology; a validation against 3D-motion analysis on healthy subjects.

Gransier Ruud R Drs ruud.gransier@maastrichtuniversity.nl Maastricht University Medical Centre Maastricht Netherlands
Dunias Par P Dr p.dunias@tno.nl TNO Eindhoven Netherlands
Emans Pieter P Dr Maastricht University Medical Centre Maastricht Netherlands
Arts Chris JJ Dr Maastricht University Medical Centre Maastricht Netherlands
Van Rhijn Lodewijk L Prof. Dr. l.vanrhijn@mumc.nl Maastricht University Medical Centre Maastricht Netherlands
Meijer Kenneth K Dr. kenneth.meijer@maastrichtuniversity.nl Maastricht University Medical Centre Maastricht Netherlands

Submitted by:Meijer, Kenneth Dr

In this study we were able to produce a validated ambulatory wireless system capable of gathering and analyzing ADL data concerning activity patterns and knee kinematics.

Introduction

Knee osteoarthritis (KNOA) is a common musculoskeletal condition causing pain, physical disability and reduced quality of life (1). To improve rehabilitation strategies and unravel the pathomechanics of KNOA, it is critical to monitor the kinematics of the affected joint during activities of daily living (ADL) which they are highly dependent upon (2,3). To our knowledge, no such ambulatory systems are currently available. Therefore, a smart knee brace quantifying flexion and extension angles and daily activity patterns was recently developed. This novel technology will enable to tailor treatment and rehabilitation strategies to the needs of the individual patient. The aim of our study was to validate the knee brace regarding knee angles in the sagittal plane by use of an inductance coil and accelerometry against 3D-motion analysis.

Methods

The study comprised of 10 healthy subjects. Exclusion criteria were pain, stiffness and any disability of the knee joint, former knee surgery, existing OA or inflammatory arthritis, obesity, injury of the upper and lower limb within 12 months prior to the start of the study. The knee brace comprises of two accelerometers and an inductance coil designed to gather and analyze data concerning (daily) activity and knee kinematics and comparing raw data.

The knee brace was validated, in a test-retest protocol, under ‘gold standard’ laboratory conditions by use of the 3D-motion analysis (Vicon Nexus MX3) system.

The Root Mean Square Error (RMSE) and Mean Absolute Error (MAE) were used as statistical analysis for accuracy in determining the knee angles.

Results

Our results show a Root Mean Square Error (RMSE) of 3,67 (SD 1,44) and a Mean Absolute Error (MAE) of 3,14 (SD 0,78) regarding knee angles in the sagittal plane. A Friedman test was done for estimation of trial similarity and comparability. The test showed a p-value of 0.066 (α=0.01) (Chi square 8.800).

Discussion

The present study aimed to validate the knee brace regarding knee angles in the sagittal plane in healthy subjects. Statistical analysis showed that the knee brace data were in accordance with the Vicon data regarding knee angle measurements. Our results show a RMSE of 3,67 (SD 1,44) and a MAE of 3,14 (SD 0,78) suggesting an accuracy within clinically acceptable standards. The clinical cut-off point was set at 5 degrees of deviation or more (3).

Research has shown the importance of measuring knee kinematics and kinetics during daily activity in relationship to the development of knee OA (2,3). Our technology enables ambulatory monitoring of knee angles during ADL, contributing to the further unraveling of the pathomechanics of knee OA and improvement of rehabilitation strategies. This was one of the first trials capable of gathering and analyzing data derived by a validated ambulatory wireless system.

References

Yelin EH et al. Arthritis Rheum. 1990;33:750-5.
Jordan KM et al. Ann Rheum Dis. 2003;62(12):1145-55.
Asay JL et al. J Orthop Res. 2009;27:325-329.

Smart Knee Brace showing the hardware configuration.

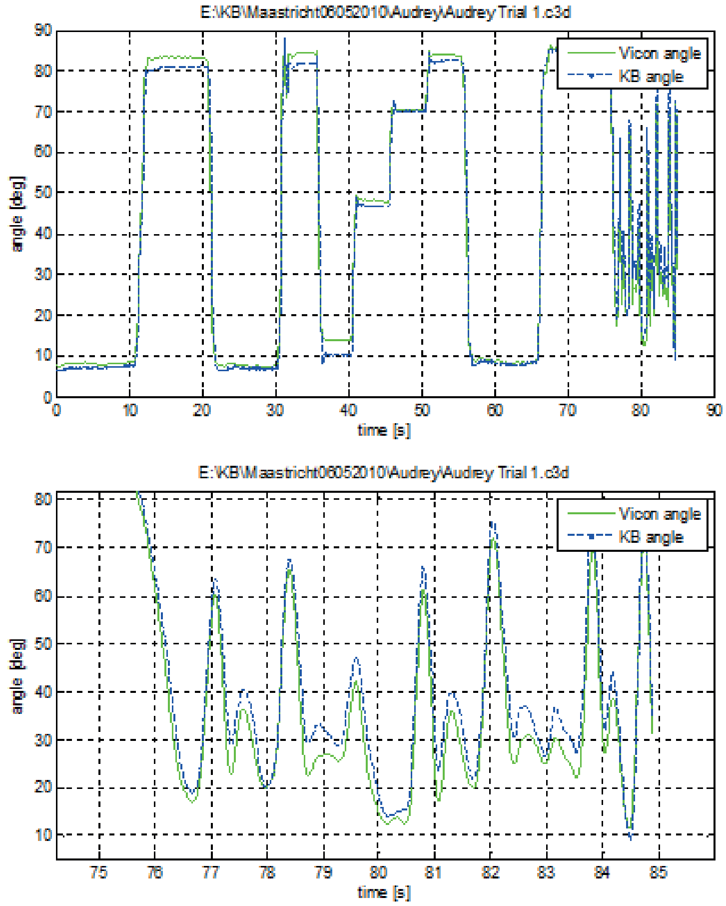

Knee angles in the sagittal plane measured by the knee brace (Blue) compared to the Vicon system (Green).
-</td></tr></tbody></table>

Submitted by:Kueny, Rebecca

The extensive fixation benefits of augmenting screws in osteoporotic bone shown in many prior pullout studies are yet to correlate with results from more physiologic fatigue testing. However, cement distribution patterns where cement contacts cortical bone provided greater fatigue stability.

Introduction

Pedicle screw fixation is the most often used intra-operative stabilization technique of the posterior spine and loosening at the bone-screw interface is the most prevalent complication. Many studies testing pedicle screw fixation have only reported pullout strength; even though pedicle screw pullout is not common clinically. The most efficient methods to increase pullout strength are to increase the screw diameter and to augment the screw with cement. Nevertheless, how an increase in diameter or the type of augmentation technique influences fatigue strength is still unclear. The aim of this study was to investigate how different diameters and augmentation techniques alter the motion, fatigue strength and pullout strength of pedicle screws.

Patients & Methods

Osteoporotic individual lumbar vertebrae (N=39, BMD= 93.7±42.4gHA/cm^3) were bi-laterally instrumented and augmented under fluoroscope guidance with pedicle screws (Ø=5.5 or 6.5mm, length=50mm, TangoRS^{TM}, ulrich medical, Ulm, Germany). Vertebrae were assigned to 4 groups to achieve comparable volumetric BMD and spine levels: 1) no cement, 2) big diameter (Ø=6.5) 3) vertebroplasty augmentation 4) augmentation through the screw (see Figure 1). Specimens first underwent sinusoidal fatigue loading at the screw head in the cranial and caudal directions (Bionix I, MTS, USA). Compressive, sinusoidal loading was increased step-wise starting with a range of 25N to 75N with an increase of the upper value by 25N every 250cycles (1Hz). The fatigue loading regime was based on in vivo loading ranges [1]. Fatigue testing was terminated when the screw head was displaced 5.4mm. A vicon motion capture system was used to monitor screw motion. Finally, the contralateral side was loaded in pure axial pullout using displacement control (5mm/min) until a peak force was reached.

Results

Volumetric BMD significantly affected pullout strength (r^2=0.17, p=0.036) and fatigue strength (r^2=0.44, p2=0.29, p=0.004). Both augmentation techniques exhibited a significant increase in pullout force from the no cement group (Figure 1) while increasing diameter caused a non-significant 24% increase. Augmentation through the screw yielded the best fatigue results; however, no groups significantly improved fatigue failure (p>0.48).

Discussion/Conclusion

Both augmentation methods increased pullout strength by over 65%; however, this fixation increase did not carry over to fatigue strength. Through screw augmentation exhibited a wider radial distribution of cement and greater cement contact with cortical bone directly outside the pedicle canal than vertebroplasty (Figure 1). The distinctive cement distribution patterns might be responsible for the tentatively better results for the through screw augmentation group (Figure 2).

Two distinctive motion patterns were exhibited (Figure 3). A widening of the screw hole along the screw axis (correlating to displacement creep at low forces and perhaps related to the crushing of trabecular as the screw loosens). As well as a distinct fulcrum correlating to where the screw exits the pedicle canal and enters the vertebral body.

Acknowledgements

Funding from the Marie Curie Action- SpineFX (238690) and the State of Hamburg is kindly acknowledged. The authors thank ulrich medical and TECRES medical for providing screws and cement.

References

[1]Rohlmann et al.,Spine,2000,25:2981-2986.

Submitted by:Russell, Serena Dr

Osteochondral allograft implantation may disrupt the local biotribology, causing increased wear and friction of the adjacent host tissue, the osteochondral allograft and the opposing bearing surface

Introduction

Osteochondral grafts are currently used to repair cartilage legions and, in turn help to restore joint function. There is limited understanding of the local biotribology post-implantation of these grafts and their interactions with host tissue environment. It is postulated that following implantation of an osteochondral graft changes in biotribological and biomechanical function of the natural joint system may lead to degradation and wear on the opposing bearing surface, the osteochondral grafts and the cartilage adjacent to the grafts. The aim of this study was to establish whether osteochondral allografts had an effect on the local biotribology post-implantation, in a simple tribological model of the natural joint.

Materials and methods

A simple geometry single station multidirectional tribological simulator was used to determine the coefficient of friction and degradation of bovine osteochondral plates (45 mm x 19 mm x 7mm) sliding against 9 mm diameter bovine osteochondral pins. The osteochondral pins and plates were harvested from the patella groove of skeletally mature bovine (18-24 months). Intact osteochondral plates (n=6) represented the negative control. The positive control and test samples (n=6) had a 6 mm diameter osteochondral defect drilled in the centre of the plates. Stainless steel plugs inserted in the defects were used as positive control. The experimental model investigated bovine (allograft) osteochondral plugs which were implanted into the 6 mm diameter defects in the bovine osteochondral plates. Tests were performed in phosphate buffered saline plus 25% (v/v) newborn calf serum. A stroke length of 20 mm was used with a velocity of 4 mm/s. A load of 160 N was applied to represent a physiological contact pressure of 2.5 MPa for a period of 6 h. A Form Talysurf Profilometer was used to measure the surface roughness of the cartilage samples after the test to determine damage degradation and wear.

Results

The negative control exhibited a friction coefficient below 0.2 throughout the 6 h test period (Figure 1). The positive control and bovine allografts showed a significantly higher coefficient of friction compared to the negative control. Moreover, the friction of the bovine allografts reached and surpassed that of the positive control, but the difference was not significant. Visual observations and surface roughness measurements showed that high friction resulted in increased wear of the opposing reciprocating osteochondral plug. Cartilage damage was also evident on the bovine plates (adjacent to the grafts) and osteochondral grafts in tests which exhibited higher friction.

Conclusion

This study indicated that post-implantation of the osteochondral graft, the local biotribology was altered, possibly due to ‘edge effects’. There was a relationship between increased cartilage wear/damage with increased friction. The increased wear/damage was identified on the reciprocating osteochondral plugs, the osteochondral grafts and the cartilage on the bovine plates adjacent to the grafts in tests which exhibited a high coefficient of friction.

APPLICATION OF COMPUTATIONAL ULTRASOUND FOR DETECTION OF CARTILAGE DEFECTS

Koomen Teun T.J. teun.koomen@gmail.com Delft University of Technology Delft The Netherland
Mores Giovanni G. giovannimores@gmail.com Delft University of Technology Delft The Netherland
Vennema Björn B. bjornvennema@gmail.com Delft University of Technology Delft The Netherland
Wessels Jan J. jwessels90@gmail.com Delft University of Technology Delft The Netherland
Tuijthof Gabrielle G.J.M. Dr.ir. G.J.M.Tuijthof@tudelft.nl Delft University of Technology/Academic Medical Center Delft/Amsterdam The Netherlands
Zadpoor Amir A.A. Dr. A.A.Zadpoor@tudelft.nl Delft University of Technology Delft The Netherlands
Submitted by:Koomen, Teun -

This pilot study presents a concept to detect defects in the articular cartilage of an ankle joint. Using 2D-simulations on a modeled ankle, a good indication is given that a defect in articular cartilage of a joint can be confirmed.

Introduction

Ultrasound is a non-invasive, dynamic and relatively cheap imaging modality. Several studies have shown that ultrasound is able to discriminate damaged from healthy cartilage tissue, which makes it a candidate alternative to the rather expensive MRI imaging. The drawback of ultrasound is that not all cartilage surfaces can be visualized due to the surrounding bones. This pilot study presents a concept to overcome this drawback. Ultrasound waves are transmitted through the articular joint space, which is altered when the joint space morphology is changed due to the presence of a cartilage defect. This research focuses on the joint space between the tibia and talus. The expectations were that a defect of 0.8 mm width and 1.4 mm depth in the articular cartilage would result in a lower magnitude of the output signal in the frequency domain.

Method

A 2D wave propagation computer model was constructed using geometric contours derived from a radiograph of a human ankle joint (Fig. 1). The three most important material properties were implemented in this geometric model; bone, cartilage and synovial fluid. Preliminary tests with a simplified model were performed to determine the thickness of the materials, frequency of the LIPUS and the effects of the curvature. The simulated transducer sends out a low-intensity pulsed ultrasound (LIPUS) at a frequency of 1.3 MHz, which is observed by a virtual receiver on the other side of the joint (Fig. 1). A total of 18 conditions were evaluated where a virtual defect was created on nine different locations on each of both articular surfaces (Fig. 1). Per condition, two separate 2D-simulations were performed where the transducer pulse was sent from left to right and from right to left. The output signals were compared, at the peak value in the frequency domain, with the intact model. These magnitudes were normalized to the magnitude of the intact condition (no defect). The wave propagation concept was indicated to be a feasible concept if the 95% confidence interval of the mean of all normalized magnitudes of the output peaks did not include the value of 1.

Results

The conditions with defects show a change in magnitude with respect to the undamaged model (Figs. 2 & 3). The mean of the normalized peaks for each condition was 0.864 and the 95% confidence interval was 0.834 : 0.895. The confidence interval indicates that the presence of a defect of 0.8 mm in width and 1.4 mm in depth in the cartilage of the investigated joint space can successfully be determined with 95% certainty.

Conclusion & Discussion

The confidence interval is significantly lower than the normalized magnitude of the undamaged condition. Based on these findings, this pilot study provides a good indication that a defect in the articular cartilage of the ankle joint can be detected. Further research of the applicability of the concept is required. Also decisive conclusions about the location and the size of the defect have yet to be found.

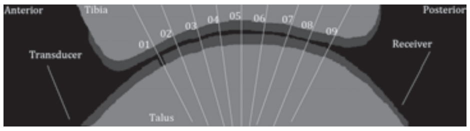

X-ray model of the ankle joint

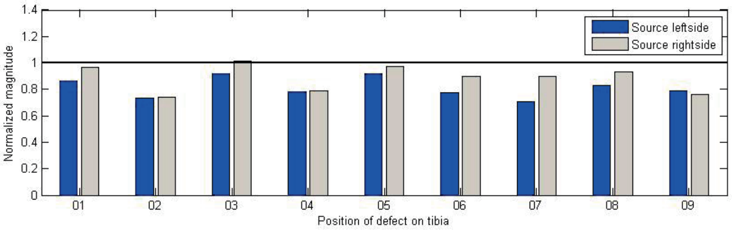

Magnitude graph with defects on upper layer of cartilage

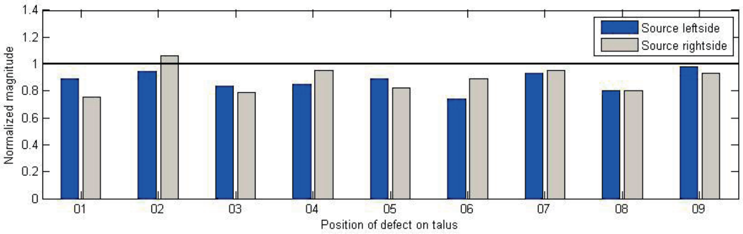

Magnitude graph with defects on lower layer of cartilage</td></tr></tbody></table>

MANAGEMENT OF LARGE BONE DEFECT : A STUDY OF 40 CASES USING MECHANICAL PRINCIPLES OF ILIZAROV CIRCULAR FIXATOR

Submitted by:Chandrasekaran, Annamalai Professor

Ilizarov external fixators mechanical stability factors are utilised to regererate bone

There are various methods to treat a bone defect more than 3 cm. This study of 40 cases, in 37 procedures of different aetiology is treated by using mechanical principles of Ilizarov Circular fixator. 1 amputated patient, 1 bad compliance, 2 under progress excluded, 33 are followed.

Large bone defects of bone are difficult to treat for the reason, the regenerated bone has to restore its anatomical structure, able to withstand for the routine daily activity and physiologically restore the normal functions.

This work was done in Sri Ramachandra Medical University, Chennai; India from June 1995 to April 2012. The age group was between 3years to 70 years, Males 34 and females 8, 30 on right and 10 on left leg. The gap measured from 3 am to 20 cm, mean 5.08 cm.3 of them had their opposite limb amputated. The distraction time and consolidation time is very prolonged between 8 months to 33 months with mean 14.03 months.

The patient comes for follow up when it is possible for him to come to the hospital. Patient education for a proper follow up does not work. The desired length may not be achieved due to different causes. But finally it is a rewarding procedure as it gives back a sensitive feet by preventing amputation.

MANAGEMENT OF INFECTED NON UNION OF TIBIA BY ILIZAROV CIRCULAR FIXATOR- a study of 41 cases.

Submitted by:Chandrasekaran, Annamalai Professor

Infected non union of both bones legs are successfully managed by applying Ilizarov external fixator percutaneous method withou disturbing the fracture site and bony union is achieved

To study the outcome of infected non union of both bones of leg treated with Ilizarov circular fixator system.

By Ilizarov methodology an infected non union is treated percutaneous way, using tensioned wires mounted on a circular frame.

This is a retrospective study was done in Sri Ramachandra Medical University between May 1995- April 2012. 41 cases were treated in a single unit and followed up periodically. There were 5 females, 36 males; between the ages of 14 : 60 years with a mean of 37.21 years. 22 patients had the right leg and 19 left side affected.

All the cases are of trauma origin and infected during the course of treatment elsewhere presented to us with an intra medullary device and screws, external fixators :tubular/ring, plaster of paris casts or native bandages. Invariably they had discharging sinus or healed ones during the course of treatment. Few discharges from sinuses grew organism. Blood investigations occasionally normal, few with raised ESR and CRP.

When a culture is positive appropriate antibiotics were given for 3 days, and when no organism was grown routine prophylactic antibiotics were given. The patient was ambulated next day with maximal weight bearing. All the fractures healed between 3- 15 months with a mean period of 5.9 months.

This study proves the circular external fixator has a biomechanical advantage, single procedure, percutaneous and no bone graft was used when the techniques improved. 100% union was achieved.

Submitted by:Arts, Jacobus Dr

With high resolution peripheral quantitative computed tomography (HR-pQCT) scanners it is possible to follow changes in bone density, stiffness and bone microarchitecture over time in patients with distal radius fractures.

Background

To quantify bone strength, information regarding both bone density and bone microarchitecture is necessary. High resolution peripheral quantitative computed tomography (HR-pQCT) scanners with a resolution of 82 µm offer the opportunity to assess in-vivo 3-D bone density and bone micro-architecture changes over time in patients. Furthermore, 3D-models representing the cortical and trabecular architecture can be created and used for finite element analysis (FEA) and assessment of morphological changes. The purpose of this pilot study was to study the feasibility of HR-pQCT for longitudinal studies of distal radius fracture healing in vivo at the micro-scale in patients.

Methods

In a prospective longitudinal cohort study 7 post-menopausal and 1 pre-menopausal woman (mean age 60.9 ± 7.9 years), with a stable distal radius fracture were included. The fracture of each patient was treated conservatively without reduction.

To assess changes in bone density, micro-architecture and biomechanics, all patients underwent HR-pQCT scanning at the fracture side at 1-2 weeks post fracture (baseline) and 3-4 weeks, 6-8 weeks and 12 weeks post fracture (follow-up). The following bone density parameters were assessed: volumetric bone mineral density [mgHA/cm^3] for the total region (D₁₀₀) and for the trabecular (D_{trab}) and cortical region (D_{cort}) separately. Furthermore bone volume fraction BV/TV [-] of the trabecular region was derived by dividing D_{trab} by 1200 mgHA/cm^3 . The micro-architectural parameters assessed were: trabecular number (Tb.N) [mm⁻¹], trabecular thickness (Tb.Th) [mm] and trabecular spacing (Tb.Sp) [mm] as well as cortical thickness (Ct.Th) [mm].

Based on HR-pQCT images µFEA models were created to calculate stiffness in compression, torsion and bending of the bone structure. Furthermore follow-up HR-pQCT images were registered to the baseline images to calculate and visualize locations of bone resorption and apposition.

The Maastricht University Medical Ethical Committee approved the study and informed consent was obtained from all patients.

Results

Total bone density increased significantly by 14% compared to baseline during the first six weeks post-fracture and then decreased again reaching a final value 6.5% higher than baseline at 12 weeks post-fracture. The micro-architecture as expressed by trabecular number showed a slight increase during the first six weeks post-fracture. At 12 weeks post-fracture, the trabecular number was 3.6% less than at baseline. The cortical thickness increased during the first six weeks post-fracture and then remained stable 12% above baseline value until 12 weeks post-fracture.

At 12 weeks post-fracture, bone stiffness in compression, bending and torsion were increased by approximately 40% compared to baseline. The increase in compression and bending stiffness was significant (p-value < 0.05).

Locations of bone resorption and apposition and its changes over time could be adequately visualized. (Figure 1).

While bone resorption mainly occurred in the trabecular region, bone apposition was primarily observed in the endo-cortical area and close to the fracture line.

Discussion

This pilot study showed that HR-pQCT in combination with µFEA and image registration is able to study the healing process of distal radius fractures over time in patients in great detail. Future research will focus on correlation with histological and blood marker test results.

The predictive value of RSA on different stem designs. A systematic review.

de Vries Lieke LMA MSc ldvries@fzr.nl Franciscus Hospital Roosendaal The Netherlands
van der Weegen Walter W MSc w.vander.weegen@st-anna.nl St. Anna Hospital Geldrop The Netherlands
Stolarczyk Piotr PA MD pstolarczyk@fzr.nl Franciscus Hospital Roosendaal The Netherlands
Sijbesma Thea T dr. t.sybesma@st-anna.nl St. Anna Hospital Geldrop The Netherlands
Hoffman Erik EL MD ehoffman@fzr.nl Franciscus Hospital Roosendaal The Netherlands

Submitted by:de Vries, Lieke MSc

Even though roentgen stereophotogrammetric analysis (RSA) is a highly accurate tool to predict implant failure requiring a short follow up, some hip stems are designed to subside and can tolerate such a migration pattern without clinical relevance.

Introduction

Due to the high precision of roentgen stereophotogrammetric analysis (RSA), excessively migrating prostheses can be discriminated and it is used to predict implant failure, requiring only a small sample size of 15-25 patients and short follow up (Valstar et al., 2005). RSA is therefore recommended for the introduction of new implant designs. However, there is no clear data on the predictive value of RSA for different stem designs. The purpose of our systematic review was to investigate if two year RSA results could accurately predict the 10 year survival rate of different total hip arthroplasty stem designs as reported in national joint registries.

Patients and methods

We systematically reviewed literature to determine the maximum total point motion (MTPM) (i.e. translation vector) or distal migration of stem designs in total hip arthroplasty two years postoperative and correlated these values to the survival rates of these specific stems in the Swedish, Australian and New Zealand hip registries. RSA-studies had to report on at least 20 patients with a minimum follow up of two years. There were no language restrictions and two independent observers checked inclusion and exclusion criteria in all studies. A detailed match between stem design reported in the RSA study and in the arthroplasty registry was compulsory. Acceptable two years postoperative stem migration was defined as < 1.2 mm.

Results

We included 19 studies describing the distal stem migration of 11 different stem designs. Three stems (Exeter, CLS and C-stem) showed distal migration >1.2 mm in the RSA studies. The Exeter and C-stem are designed to subside and still showed excellent results in the arthroplasty registries (10 year survival rate >93%).

In 5 of the 19 studies the MTPM was described, involving five different stem types (ABG-II, Spectron EF, Charnley, Charnley Elite Plus and Omnifit). All five stems showed acceptable migration values below the threshold of 1.2 mm and had sufficient or excellent 10 year survival rates in the arthroplasty registries (>91%).

Discussion/conclusion

Overall, distal migration is consistent with arthroplasty registry results. However, unacceptable distal stem migration measured with RSA does not always predict implant failure consistently. Polished hip stems are designed to subside and can tolerate such a migration pattern without clinical relevance.

{mso-style-name:"Table Normal";

Our study shows that plate fixation is an effective way of managing high-energy bicondylar proximal tibial fractures. Single plate fixation with contralateral screws is sufficient depending on the fracture configuration. Double plating is not required for these fractures.

A prospective randomized clinical trial with radiostereometric analysis comparing the Taperloc® and Mallory-Head Porous® uncemented femoral stem designs

van der Voort Paul MD p.van_der_voort@lumc.nl Leiden University Medical Center Leiden The Netherlands
Wolkenfelt Julius MD Sint Lucas Adreas Hospital Amsterdam The Netherlands
Valstar Edward R MSc, PhD Leiden University Medical Center Leiden The Netherlands
Nelissen Rob GHH MD, PhD Leiden University Medical Center Leiden The Netherlands
Submitted by:van der Voort, Paul Drs

A flat and wedge-shaped femoral stem contributes to better early rotational stability and an anatomical bi-planar wedged shaped femoral stem contributes to better early vertical stability.

Introduction

Development in uncemented hip arthroplasty has led to several stem designs in order to reduce the incidence of osteolysis and aseptic loosening. Excellent clinical results have been reported on both the Taperloc and the Mallory-Head Porous prosthesis. The Taperloc hip prosthesis is a flat, wedged-shaped and collarless design, allowing for gradual self-settling of the implant and achievement of optimal rotational fixation. The Mallory-Head Porous hip prosthesis on the other hand has a bi-planar wedged anatomical design providing a three-point fixation for immediate stem stability. But is the different design rationale between both prostheses really of influence on migration stability?

Patients & methods

40 consecutive patients with a mean age of 60 years receiving an uncemented total hip arthroplasty for primary or secondary end-stage osteoarthritis were evaluated in a prospective double-blinded randomized clinical trial with Roentgen Stereophotogrammetric Analysis (RSA) combined with clinical and radiographic evaluation. Migration measured with RSA, Harris Hip Scores (HHS) and signs of osteolysis on plain X-ray were assessed and compared preoperatively and at six weeks, 3 ,6 ,12 and 24 months postoperatively. The main objective of this study was to observe and compare the micro-motion after 24 months between the Taperloc hip prosthesis and the Mallory-Head Porous hip prosthesis. The secondary objective is to predict the long-term differences based on the two year prosthetic migration together with clinical and radiographic assessment.

Results

RSA showed no significant differences in mean migration, subsidence and rotation in both groups. There was a mean subsidence of 0.9 mm in the first two months for both designs (Figure 1). After the self-settling period, there was a smaller variability in subsidence in the Mallory Head Porous group. There was an axial rotational movement in retroversion with a mean of 0,8 degrees in both designs (Figure 2). The Taperloc design showed less initial axial rotation within the self-settling period and less variability in rotational movement after 24 months. Both groups had excellent clinical results at 24 months follow-up. The mean HHS improved significantly for both groups, with a score of 38 (±11.3) preoperatively and 89 (±9.5) postoperatively for the Taperloc group and a score of 36 (±15.2) preoperatively and 84(±9.5) postoperatively for the Mallory-Head Porous group. There was no significant difference in pre- and postoperative HHS between both designs. Postoperative routine X-rays of both designs revealed no signs of osteolysis in all Gruen zones.

Conclusion

This study confirms the rotational stability of the flat and wedge-shaped Taperloc prosthesis and the vertical stability of the anatomical shaped Mallory-Head Porous prosthesis. The initial fixation of the flat and wedge-shape of the Taperloc prosthesis seems to be more sufficient in stabilizing the prosthesis and withstanding immediate postoperative loadings. But apparently the anatomic shape of the Mallory Head Porous prosthesis offers just enough rotational stability to stabilize after the settling period. Morevover, the stability obtained after 24 months measured with RSA suggest good long term performance of both designs.

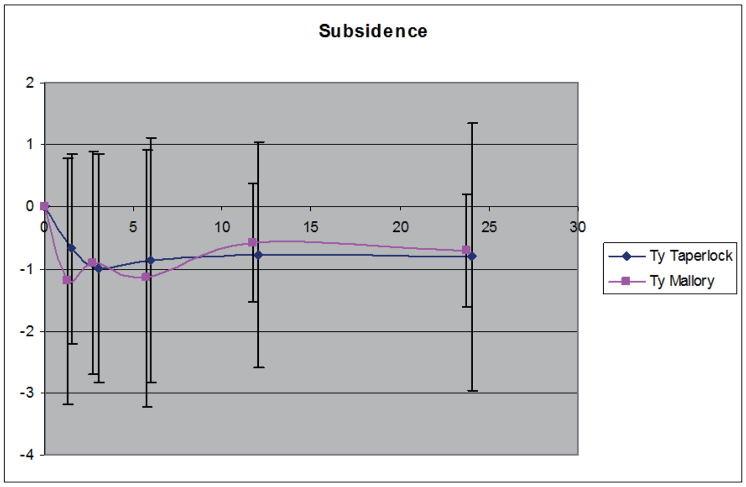

Figure 1

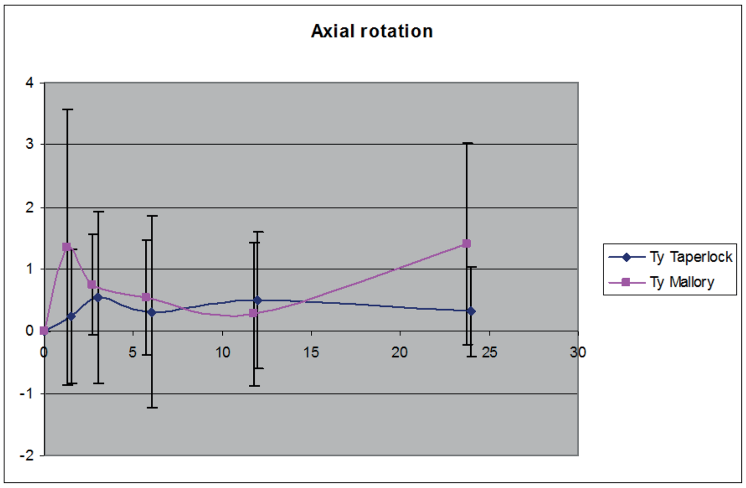

Figure 2

A comparison of mesenchymal stem cell incorporation and growth in 3 dimensional scaffolds with potential for osteochondral tissue repair

KOHLI NUPUR NK Miss Kohlin@aston.ac.uk School of Life & Health Sciences, Aston University Birmingham United Kingdom
SNOW MARTYN Mr snowmartyn@gmail.com 2The Royal Orthopaedic Hospital Birmingham United Kingdom
JOHNSON EUSTACE Dr. w.e.johnson@aston.ac.uk School of Life & Health Sciences, Aston University Birmingham United Kingdom

Submitted by:KOHLI, NUPUR MISS

Chondro-Gide® shows better mesenchymal stem cell incorporation and viability as compared to Alpha Chondro shield® and Hyalofast™.

Introduction:
Osteoarthritis is a multifactorial disease, which is characterised by the destruction of the articular cartilage and occasionally the underlying bone in hip and knee joints. This study is focussed on cell based therapies for repairing osteochondral defects using commercially available cell scaffolds to deliver mesenchymal stem cells (MSCs). MSCs were assessed for their incorporation and viability in three different scaffolds, i.e. Chondro-Gide®, Alpha Chondro Shield® and Hyalofast™. Chondro-Gide® is composed of type I/III collagen and has a bilayer structure consisting of one compact non porous side and one porous side with a honeycomb structure. Alpha Chondro shield® is a synthetic scaffold composed of fibres of polyglycolic acid (PGA) and Hyalofast™ is similarly fibrous in nature and made of a semi-synthetic derivative of hyaluronic acid (HA). Each of these scaffolds is used clinically in the treatment of cartilage defects.
Methods:
Bone marrow-derived human MSCs were seeded at a density of 50,000 cells per scaffold. The scaffolds were then assessed for MSCs incorporation and viability using fluorescent Live/Dead cell imaging and confocal microscopy.
Results:
There was a greater initial incorporation of MSCs into Chondro-Gide® and Hyalofast™ than Alpha Chondro Shield®. With time in culture the proliferation of MSCs became significantly greater in Chondro-Gide® than the other two scaffolds (p value = 0.0041, one way ANOVA). In all cases, the viability of cells by Live/Dead scoring remained greater than 90%. The appearance of MSCs in Chondro-Gide® and Alpha Chondro Shield® was fibroblast-like, with clear adhesion to the scaffolds, whereas the cells were frequently more rounded in shape with fewer adhesions in the fibrous Hyalofast™ scaffold.
Discussion/Conclusions:
These preliminary findings suggest that human MSCs incorporate, adhere and proliferate best in Chondro-Gide®, compared to the more fibrous scaffolds. This increased growth may be due to differences in the scaffold structure and/or composition, e.g. in the relative areas available for direct cell contact or because collagen types I/III may be pro-adhesive compared with HA. Further studies will extend this analysis to examine and compare the differentiation potential of human MSCs into cartilage and bone within these scaffolds, in comparison with other cell types/sources.

Treatment of stable intertrochantric fractures : A comparison between 2hole and 4 hole Dynamic Hip Screw. A prospective Randomized Clinical Trial.

Younesi Darab Dr Jundishapur university of medical sciences ahvaz IRAN

Submitted by:Tabatabaei, Saeid

To compare the results of internal fixation of stable intertrochantric hip fractures with 2-hole and 4- hole dynamic hip screw

Objective:
The incidence of intertrochantric fractures is expected to increase because of increase in the number of elderly population around the world.
Dynamic hip screws are used widely in stable intertrochantric fractures with high success rate.
The purpose of this randomized clinical trial was comparison between the results of surgical fixation of these fractures by 2 hole and 4 hole intertrochantric fractures.
Methodology:
between April 2009 until March 2011 a number of 80 stable intertrochantric fractures were treated in two university hospitals of Jundishapur university of medical sciences in Ahvaz .
We treated the patients intermittently by 2 hole and 4 hole DHS , groups were compared and the data analyzed using SPSS 16 and T-test and the P value of less than 0.05 considered as significant difference.
The inclusion criteria consisted of the patients with stable intertrochantric fractures between the age of 30 to 80 years and all of the patients with unstable or pathologic fractures or patients with other medical conditions were excluded from the study.
The patients were followed up until complete union and during the follow up time the complications like surgical wound problems or screw cutout, breakage, delayed or non-union or any other complication recorded in the follow up sheath of the patient.
results: eighty patients with stable intertrochantric hip fracturs were treated intermittently by 2 hole and 4 hole DHS and in each group consisted of 40 patients.
Eight patients in 2-hole group and seven patients in 4-hole group lost follow up and at the end of study there were 32 patients in 2-hole and 33 patients in 4-hole DHS groups.
In 40% of the patients in 2-hole DHS group, the time of operation was under 40 minutes , in 45% between 40-65 minutes and in 15% more than 65 minutes(65-90 minutes).
In 50% of the patients in 4-hole DHS group, the time of operation was between 40-65 minutes and in 50% it was between 65 to 90 minutes.
There was significant difference between respective groups regarding the length of operation ($P<0.05$).
In 2-hole DHS group patients, the amount of intraoperative bleeding in 45% of the patients was less than 100 cc, in 20% was between 100-200 cc and in 35% the amount of bleeding was between 300-500 cc.
In 4-hole DHS group, the amount of intraoperative bleeding was less than 100 cc in 5% of the patients, in 15% between 100-200 cc in 60% between 300-500 cc and in 20% it was more than 500 cc bleeding.
There was significant difference in intraoperative bleeding . ($P<0.05$)
There was no significant difference in union, weight bearing time and screw cutout.
Conclusion:
Both devices can be used in stable intertrochantric fractures but, according to our study one can conclude that 2-hole DHS can be used in these fractures with less bleeding and shorter operation time.
Keywords:
intertrochantric fractures, 2-hole DHS, 4-hole DHS, hip fracture

Clinical Results and Prognostic Factors of Primary Osteosarcoma of Extremities with Pulmonary Metastasis: CCHE Experience

Abou-Elnaga Sherif Pediatric Oncology Consultant snaga@57357.com Children Pediatric Oncology/Haematology Department Egypt
Sidhom Iman Pediatric Oncology Consultant iman.sidhom@57357.com Children Pediatric Oncology/Haematology Department Egypt
Mahmoud Sonia Pediatric Oncology Consultant sonia.mahmoud@57357.com Children Pediatric Oncology/Haematology Department Egypt
El-Ghoneimy Ahmed Orthopaedic Oncology Consultant aghoneimy@me.com Children Orthopaedic Surgery Department Egypt
El-Sherbiny Magdy Orthopaedic Oncology Consultant magdy.elsherbiny@57357.com Children Orthopaedic Surgery Department Egypt
El-Shafeiy Maged Surgical Oncology Consultant majed.elshafiey@57357.com Children Surgical Oncology Department Egypt
Soliman Ranin Clinical Research Specialist ranin.magdi@57357.com Children Research Department Egypt
Gouda Iman Pathology Consultant eman.gouda@57357.com Children Pathology Department Egypt
Taha Hala Pathology Consultant Hala.taha@57357.com Children Pathology Department Egypt
Zaky Iman Radiology Consultant iman.zaky@57357.com Children Radiology Department Egypt

Submitted by:Zamzam, Manal Pediatric Oncology Consultant

Pediatric patients with Osteosarcoma of the extremities that were initially presented with pulmonary metastases showed shorter survival duration than the non-metastatic ones. Factors affecting patients' outcomes included number of pulmonary metastases and incomplete surgical resection of all lesions.

Introduction:
Clinically detectable metastatic disease at initial diagnosis occurs in less than 20% of patients with high-grade osteosarcoma and predicts a poor outcome. More precise risk assessment, for definition of treatment regimes based on reliable stratification criteria is necessary. To date, neither prognostic factors nor optimal management are well established in patients with metastatic osteosarcoma.
Purpose:
To identify the potential prognostic factors in patients presenting with osteosarcoma of extremities with clinically detectable pulmonary metastases at initial presentation, to study their survival, and to evaluate the results of the treatment protocol.
Patients and methods:
One hundred and thirteen patients with newly diagnosed, previously untreated high-grade osteosarcomas of bone were registered in our hospital between July 2007 and December 2010. Thirty three patients (29.2%) had proven pulmonary metastases at diagnosis and were enrolled into an analysis of demographic-, tumor-, and treatment-related variables, response, and survival. The intended therapeutic strategy included pre- and post-operative multi-agent chemotherapy as well as aggressive surgery of all resectable lesions.
Results:
With a median follow-up of 20 months (12-54 months), fifteen patients were alive, seven of whom were in continuously complete remission. The 2-year event-free survival (EFS) and overall survival (OS) were 36.1% and 54.6%, respectively. These results are significantly poorer than those achieved in 57 patients with non-metastatic disease at presentation, treated in our hospital with the same chemotherapy protocol at the same period (2-year EFS and OS of 70.5% and 89 %, respectively). Several potential prognostic factors were investigated in univariate analysis, prognostic factors that were associated significantly with a shorter survival duration were the number of pulmonary nodules (> 5 nodules) ($P= 0.001$), bilateral lung metastases ($P= 0.015$), high serum level of alkaline phosphatase ($P= 0.026$) and incomplete surgical resection of all tumor sites ($P= 0.001$). Factors that remained significantly associated withpoor outcomes after multivariate Cox regression analysis were incomplete surgical remission (RHR=7.75), > 5 pulmonary nodules (RHR=6.89) and high serum level of alkaline phsphatase (RHR=3.94).
Conclusions:

The results of our study confirm the poor prognosis of patients with osteosarcoma of the extremity with pulmonary metastases at presentation despite the use of aggressive treatment. The number of metastases at diagnosis, serum level of alkaline phosphatase and the completeness of surgical resection of all clinically detected tumor sites are independent prognostic factors. To improve the prognosis for this group of patients new therapeutic approaches are needed.

-Overall Survival of Metastatic Osteosarcoma in Pediatrics
-Event-free Survival of Metastatic Osteosarcoma in Pediatrics

A study to predict transverse fracture strength of long bones in an infant by development of an in-vitro animal model of immature porcine metacarpal bones and using three-point bending.

Malik Shahbaz S Mr Shahb.malik@gmail.com Cardiff School of Engineering Cardiff UK
Malik Sheraz S Mr smalik888@gmail.com Cardiff School of Engineering Cardiff UK
Theobald Peter S Dr TheobaldPS@cardiff.ac.uk Cardiff School of EngineeringCardiff School of Engineering Cardiff UK
Jones Mike D Dr JonesMD@cardiff.ac.uk Cardiff School of Engineering Cardiff UK
Submitted by:Malik, Shahbaz Mr

This study is of immature porcine model to estimate the forces required to sustain a transverse fracture in long bones of an infant. Results provide an estimate of the fracture threshold, which can be used to assess non-accidental injury.

Fractures constitute approximately 10-25% of all paediatric trauma cases and are the second most common presentation of child abuse. Fractures from non-accidental injury comprise a very small proportion of all fractures in children but identifying these can often be challenging for the clinicians. When a child presents to casualty, a clinician must judge if the child's fracture matches the account of injury. An objective tool is needed to aid the assessment of injury credibility, and predicting the fracture strength is the key to developing such a tool.

This study investigated immature porcine metacarpal fracture load and stiffness in three-point bending at two different displacement rates: 1mm/second (Group A) and 15mm/min (Group B). The objective of this study was to develop an animal bone model to understand infant long bone fracture mechanics and threshold in bending and to highlight the methodology for calculating bone strength from Dual Energy X-ray Absorptiometry (DEXA) measurements.

The results indicate that the fracture threshold of immature porcine metacarpal in bending is 1892.93N (SD +/- 291.55N) at the loading rate of 1mm/sec and 1875.10N (SD +/- 226.64N) at the loading rate of 15mm/min. This information provides an estimate of the fracture threshold of long bones in bending in an infant, which can be used to assess injury potential from the supplied history. The study also shows that a correlation exists between measures of internal bone structure and the bone strength. For both groups of displacement linear bone mineral composition (BMC_L), section modulus (Z) and whole bone strength index (S_B) were highly correlated with bone strength. This study found that at both loading rates Z (Group A: r^2= 0.715; Group B: r^2=0.878) and S_B (Group A: r^2= 0.684; Group B: r^2=0.850) were found to be the best predictors of bone strength. These findings are consistent with the bone strength models based on the engineering beam theory.

Introduction

Foot orthotics are prescribed for a broad range of foot and ankle pathologies. Due to inter subject variations the prediction of the effect of such orthotics is difficult. In clinical practice it is impossible to evaluate many different designs to provide the patient with the best solution. Alternatively, biomechanical, in silico, models offer the potential to predict a-priori the functional outcome for a particular footshape and motion. Existing FE models of foot and ankle are of high detail, however there computational complexity renders them unsuitable for simulation of realistic dynamic loading conditions. Recently, a new foot and ankle model has been developed, which can be used efficiently in a dynamic situation to predict the effects of an insole on a highly detailed plantar surface [1]. The outcome of this model is highly influenced by the anatomical structures and mechanical properties of the foot and ankle. The aim of this study was to develop a method to characterise these properties for an individual patient. Therefore, the geometry of anatomical structures are directly derived from CT scans, while the mechanical properties are estimated from optimal correspondence between model and a series of weight bearing CT scans.

Patients & Methods

Ten healthy subjects, seven patients with a flexible flatfoot deformity and seven patients suffering on metatarsalgia have been measured. [2] Three loaded CT scans of the subjects right foot and 1 unloaded CT scan of the right lower leg have been made (figure 1). During scanning, plantar pressure has been measured with a pedar insole (Novel gmbh, Munich, Germany). These images were segmented with MIMICS (Materialise, Leuven, Belgium) and a finite element mesh has been generated with 3-matic (Materialise, Leuven, Belgium). Tissue parameters were adjusted to optimize the agreement between FE mesh and CT data. The final outcome of the finite element simulation is validated with the plantar pressure measurement obtained during CT-measurement.

Results

Complete CT datasets were obtained for all subjects and all CT data has been segmented. A 2.5D mesh has been defined that accurately captures the foot geometry (figure 2). Additional thresholding was required to define the boundary between bones and soft tissue. Preliminary results show that the mechanical properties of the plantar tissue can be estimated using this optimisation procedure.

Discussion/Conclusion

A method has been developed that determines the anatomy of the foot and ankle from the segmented CT images and allows direct implementation in a patient specific model. Mechanical properties of the plantar tissue can be derived via finite element simulation and implemented to estimate the effect of an insole.

References

1. Oosterwaal M, Telfer S, Carbes S, Torholm S, Meijer K, Woodburn J, Rhijn Lv: Generation of a dataset to develop a subject-specific, multibody, finite element, dynamic foot model. In EUROMECH Colloquium 511. Ponta Delgada, Azores, Portugal; 2011.

2. Oosterwaal M, Telfer S, Torholm S, Carbes S, van Rhijn LW, Macduff R, Meijer K, Woodburn J: Generation of subject-specific, dynamic, multisegment ankle and foot models to improve orthotic design: a feasibility study. BMC Musculoskelet Disord 2011, 12:256.

Category: Foot & Ankle

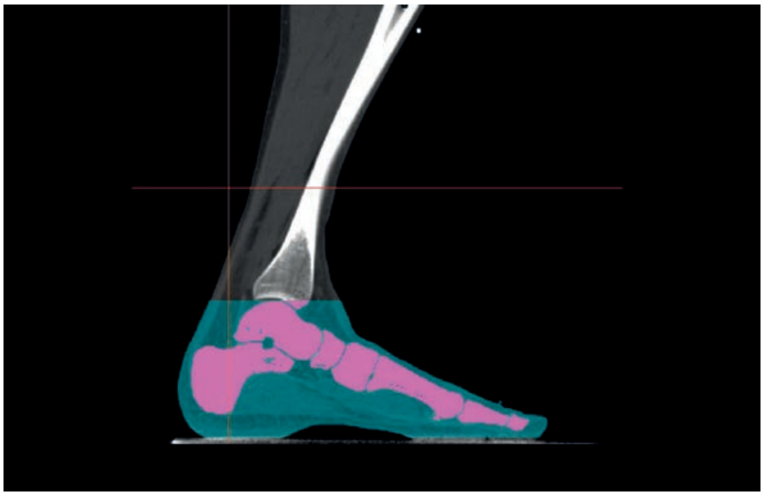

CT Image of the foot

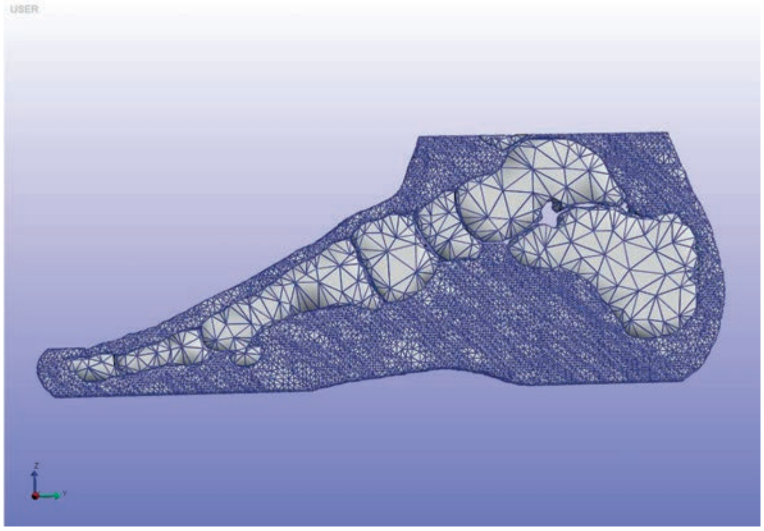

FE mesh for assement of plantar tissue mechanical characteristics

ghj

Submitted by:jani, priyanka Ms

Submitted by:Smola, Hans Prof. Dr. med.

Stort-term negative pressure wound therapy (NPWT) followed by polyacrylate superabsorber wound dressings is more efficient in stimulating granulation tissue, higher scores for fibroblasts and neo-vascularization in histology compared with standard NPWT alone.

Introduction:

Negative pressure wound therapy (NPWT) stimulates granulation tissue formation in complex wounds. While highly effective, NPWT is expensive and therapy algorithms to shorten NPWT are needed. We compared the efficacy of a modified treatment protocol consisting of stort-term NPWT followed by polyacrylate superabsorber wound dressings (polyacrylate dressings) versus NPWT alone on granulation tissue formation.

Methods:

Twenty full thickness porcine wounds each were treated with i. NPWT for 8d (VivanoMed, HARTMANN), ii. NPWT for 4d followed by polyacrylate dressings for 4d (TenderWet, HARTMANN) and iii. NPWT for 6d plus polyacrylate dressings for 2d. Dressing changes were every 48 hours. Wounds were evaluated macroscopically and in histology.

Results:

After 8d a continuous granulation tissue was observed in 70% and 45% of short-term NPWT protocol wounds (4d NPWT + 4d polyacrylate dressings; 6d + 2d polyacrylate dressings respectively) while only in 5% of standard NPWT wounds. Granulation tissue thickness was significantly thicker in both short-term NPWT protocols (2.1+0.6 mm 4d NPWT + 4d polyacrylate dressings; 2.3+0.6 mm 6d NPWT + 2d polyacrylate dressings) compared with the standard NPWT protocol (1.8+0.5 mm). Semi-quantitative grading of histology sections revealed higher scores for neo-vascularization and fibroblast density in short-term NPWT protocol wounds while the scores for macrophages and foreign body giant cells were similar.

Discussion:

These results demonstrate that short-term NPWT protocols in combination with polyacrylate wound dressings are highly effective. In our experiments the switch from NPWT to polyacrylate wound dressings was safe after the inflammatory phase subsided and before the granulation tissue became apparent macroscopically.

Submitted by:Walsh, Pauline

Preconditioned myotubes showed greater cell viability after exposure to 4 hours of ischaemia. This increase in cell viability was associated with an increase in Nrf2 signalling.

Introduction

Ischaemic preconditioning is a powerful protective stimulus capable of protecting a tissue against the effects of prolonged ischaemia and reperfusion. While much is known about its ability to protect myocardial tissue against ischaemia-reperfusion injury, its potential to confer benefit in an orthopaedic setting remains relatively unexplored. One mechanism by which ischaemic preconditioning may induce thisprotection is through a reduction in oxidative stress. ROS are generated both during prolonged ischaemia and also upon reperfusion by infiltrating neutrophils, thereby leading to an increase in oxidative stress. An important mechanism by which cellsrespond to oxidative stress is to increase the expression of an array of genes involved in the detoxification and elimination of reactive oxidants. The transcription factor, Nrf2, is a key regulator of the cells response to oxidative stress as it regulates the expression of a network of anti-oxidant/detoxifying enzymes. Nrf2 signalling has recently been shown to protect against ischaemia-reperfusion injury in both a kidney cell line and in liver biopsies, thus indicating that this transcription factor may play a key role in the protection provided by ischaemic preconditioning. The aim of this study was to investigate the ability of ischaemic preconditioning to protect skeletal myotubes against ischaemia-reperfusion, and also to determine the role of Nrf2 signalling in this protection.

Materials & Methods

C2C12 mouse myoblasts were maintained at 37^oC in a humidified atmosphere of 95% air and 5% CO_2 in DMEM containing 20% FBS. When cultures were approximately 90% confluent, myoblasts were differentiated to myotubes by changing to DMEM supplemented with 2% horse serum and culturing for 7-10 days. Differentiated myotubes were then exposed to simulated ischaemia for 4h (1% O_2) followed by 2h reoxygenation (21% O_2). To precondition myotubes, cells were subjected to 30 min of simulated ischaemia followed by 1 hour reoxygenation prior to the prolonged ischaemic event. Cell survival was assessed by lactate dehydrogenase release. Changes in gene expression (Nrf2, catalase, GSTT1, SQSTM1) were assessed by real-time PCR.

Results

Exposure of myotubes to 4 hours of simulated ischaemia resulted in a decrease in cell viability. However, preconditioned myotubes showed greater cell viability both after 4h of ischaemia, and after 4h ischaemia followed by 2h of reoxygenation. This increase in cell viability was associated with an increase in the mRNA expression of Nrf2. In addition, increased expression of SQSTM1, andtwo antioxidant genes, catalase and GSTT1, was found in preconditioned cultures.

Discussion

Our findings indicate that IPC can protect skeletal myotubes against the effects of ischaemia-reperfusion in vitro. This protection is associated with increased Nrf2 signalling indicating that this transcription factor may play a role in mediating the cytoprotection induced by IPC.

Submitted by:Keijsers, Renee

LIA might be able to decrease the postoperative pain and the use of opioids following a TKA.

Introduction

Following total knee arthroplasty (TKA) many patients experience postoperative pain. This pain may result in to delayed mobilization leading to stiffness of the joint, an increased risk of deep venous thrombosis and pulmonary embolism, a higher chance of developing chronic pain and a prolonged hospitalization resulting in higher health care costs.

Local infiltration analgesia is an, especially in Scandinavia, popular method for decreasing postoperative pain.

The goal of this literature study is to compare LIA with a placebo on the intensity of postoperative pain and the consumption of opioids.

Patients & Methods

A meta-analysis has been performed, studying the effect of LIA on pain and opioid consumption in the first two days following TKA. Seven placebo-controlled RCT's were included based on peroperative infiltration of at least one analgesic component. Review Manager 5.1 of the Cochrane Collaboration was used for analyzing the results of the RCT's following the random effect model.

Results

Postoperative pain was an outcome measure in all seven RCT's. Six of them studied the need for opioids in patients following TKA. The statistic heterogenity between the studies turned out to be 71% for pain and 39% for opioid consumption (p=0,002 and p=0,0005). On the first postoperative day LIA provides a reduction in pain of 0,6 points on a 10-point VAS-scale, equivalent to an average decrease of 12,3%. Besides, there was a decrease in opioid consumption of 14,8% compared to the placebo group. On the second postoperative day the effect on both outcome measures is diminished and no longer significant.

Discussion/Conclusion

LIA might be able to decrease the postoperative pain and the use of opioids following a TKA. However, the high level of heterogenity between the studies makes especially more homogenous research necessary.

Continuous Local Infiltration Analgesia; the effect of an intra- articular catheter on pain management after TKA, a meta-analysis.

van den Bekerom Michel MPJ MD bekerom@gmail.com Spaarne Hospital Hoofddorp The Netherlands
van Delft Rogier R MD rogiervandelft@gmail.com Spaarne Hospital Hoofddorp The Netherlands
van Lotten Manon ML MD MvanLotten@spaarneziekenhuis.nl Spaarne Hospital Hoofddorp The Netherlands
Rademakers Maarten MV MD, PhD mrademakers@spaarneziekenhuis.nl Spaarne Hospital Hoofddorp The Netherlands
Nolte Peter PA MD, PhD pnolte@spaarneziekenhuis.nl Spaarne Hospital Hoofddorp The Netherlands

Submitted by:Keijsers, Renee

Continuous Local Infiltration Analgesia (CLIA) for postoperative pain management after TKA can achieve prolonged analgesia for 48 hours. This is associated with a reduction of opiate use.

Introduction

Many patients still have severe pain after Total Knee Arthroplasty (TKA). This pain leads to a delayed mobilization which may cause increased incidence of venous thrombosis, pulmonal embolus and a prolonged hospital stay.
In the last few years, several studies have been conducted on Local Infiltration Analgesia (LIA), often involving a single-shot intra-articular injection (SLIA). The injection usually contains a mixture of an anesthetic drug, a NSAID and sometimes epinephrine. LIA is easy to use, is relatively cheap to perform and many authors conclude that it will be reducing pain and opioid consumption. However, the effect of postoperative analgesia lasted for only a short time in SLIA. Therefore the concept of Continuous Local Infiltration Analgesia (CLIA) through an intra-operative placed intra-articular catheter arose. In this manner it would be possible to achieve prolonged analgesia through bolus injections or pump infusion of analgesics. The purpose of this meta-analysis is to assess the effect of CLIA versus placebo on pain after TKA.

Patients & Methods

A systematic search was performed in multiple databases to identify all RCT's comparing intraarticular CLIA with placebo for TKA. In this study, CLIA is defined as followed; local infiltration analgesia through an intra-articular placed catheter, through which analgesia is provided postoperative by a pump or with multiple bolus injections.
All trials were assessed for eligibility. The primary outcome measures were VAS- scores after 24, 48 and 72 hours. Secondary outcome measures were ROM and opioid consumption. Data were pooled using Cochrane software.

Results

The initial search resulted in 326 trials. Ten RCT's were included. Four articles were eligible for meta-analysis, involving 193 Total Knee Arthroplasties. Others were excluded due to lack of reporting relevant data.
Postoperative VAS scores in rest after 24 hours were in favor of CLIA (WMD -16.2 (95% CI -19.2 to -13.1)) and also after 48 hours (WMD -10.6 (95% CI -19.4 to -1.8)). During activity VAS scores were also in favor of CLIA after 24 hours (WMD -19.1 (95% CI -31.7 to -6.6)) and 48 hours (WMD -13.9 (95% CI -24.6 to -3.2)). After 72 hours there was no difference anymore (WMD -8.9 (95% CI -18.8 to 1.0)).
The lower VAS scores in the CLIA- group are also supported by a lower opioid intake over the first 48 hours postoperative (WMD -117.97 (95% CI -181.98 to : 53.95)).
In one study 2 patients in the treatment group developed a postoperative infection, However, the sample sizes are too small to draw meaningful conclusions. One study has been prematurely discontinued due to potentially toxic serum levels of bupivacaine (1.2 μg/mL), no other study confirmed this. No other major complications were mentioned.

Discussion/Conclusion

We conclude that CLIA provides adequate pain relief, in rest and during activity, up till 48 hours after performing a TKA with reduction of opiate use. Some serious complications occurred after CLIA, so the beneficial effect of CLIA should be seen in this light.

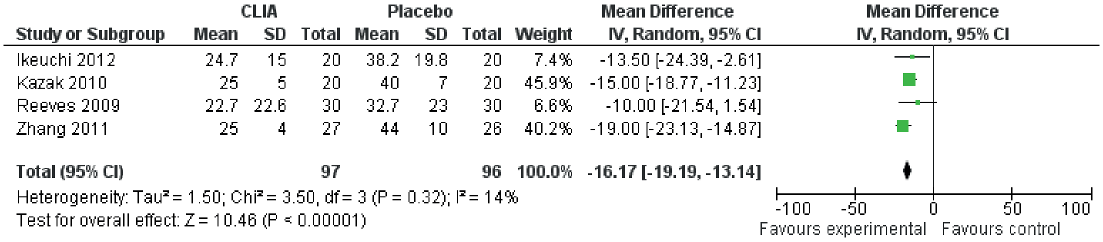

Study or Subgroup	CLIA Mean	CLIA SD	CLIA Total	Placebo Mean	Placebo SD	Placebo Total	Weight	Mean Difference IV, Random, 95% CI
Ikeuchi 2012	24.7	15	20	38.2	19.8	20	7.4%	-13.50 [-24.39, -2.61]
Kazak 2010	25	5	20	40	7	20	45.9%	-15.00 [-18.77, -11.23]
Reeves 2009	22.7	22.6	30	32.7	23	30	6.6%	-10.00 [-21.54, 1.54]
Zhang 2011	25	4	27	44	10	26	40.2%	-19.00 [-23.13, -14.87]
Total (95% CI)			**97**			**96**	**100.0%**	**-16.17 [-19.19, -13.14]**

Heterogeneity: Tau² = 1.50; Chi² = 3.50, df = 3 (P = 0.32); I² = 14%
Test for overall effect: Z = 10.46 (P < 0.00001)

CLIA vs. Placebo after 24 hours in rest.

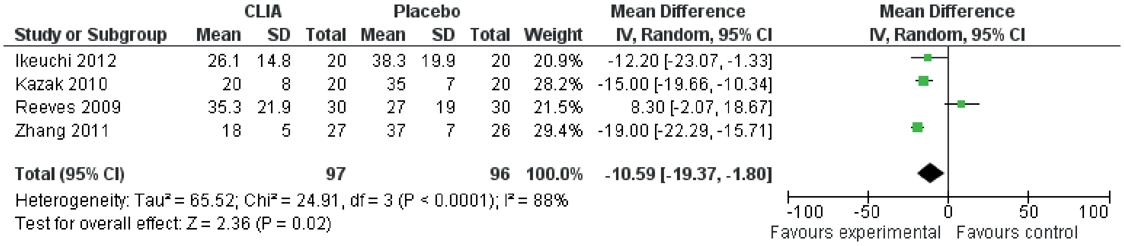

Study or Subgroup	CLIA Mean	CLIA SD	CLIA Total	Placebo Mean	Placebo SD	Placebo Total	Weight	Mean Difference IV, Random, 95% CI
Ikeuchi 2012	26.1	14.8	20	38.3	19.9	20	20.9%	-12.20 [-23.07, -1.33]
Kazak 2010	20	8	20	35	7	20	28.2%	-15.00 [-19.66, -10.34]
Reeves 2009	35.3	21.9	30	27	19	30	21.5%	8.30 [-2.07, 18.67]
Zhang 2011	18	5	27	37	7	26	29.4%	-19.00 [-22.29, -15.71]
Total (95% CI)			**97**			**96**	**100.0%**	**-10.59 [-19.37, -1.80]**

Heterogeneity: Tau² = 65.52; Chi² = 24.91, df = 3 (P < 0.0001); I² = 88%
Test for overall effect: Z = 2.36 (P = 0.02)

CLIA vs. Placebo after 48 hours in rest.

Physical activity monitoring in knee arthroplasty patients using a body-fixed sensor: Reference data and comparison with clinical scores.

Senden Rachel rach_senden@yahoo.com AHORSE Research Institute, Atrium Medical Center, Dept Orthopaedics Heerlen the Netherlands
van Laarhoven Simon AHORSE Research Institute, Atrium Medical Center, Dept Orthopaedics Heerlen the Netherlands
Lipperts Matthijs AHORSE Research Institute, Atrium Medical Center, Dept Orthopaedics Heerlen the Netherlands
Heyligers Ide AHORSE Research Institute, Atrium Medical Center, Dept Orthopaedics Heerlen the Netherlands
Grimm Bernd b.grimm@atriummc.nl AHORSE Research Institute, Atrium Medical Center, Dept Orthopaedics Heerlen the Netherlands

Submitted by:Senden, Rachel

In clinical practice sensor-based activity monitoring showed equal or better completion rates than questionnaires and provided objective, unbiased data about real-life physical activity and function. It is feasible to add this independent outcome dimension in routine clinical follow-up.

Introduction
Physical activity is an important outcome dimension related to general health, social participation and patient satisfaction while being largely independent of functional capacity. This is particularly true in orthopaedics where the movement apparatus is electively treated. To use physical activity (PA) as a clinical outcome measure in orthopaedics, this study measures PA using a body-fixed accelerometer and patient reported outcome measures (PROMs) in patients with end-stage OA to establish reference data for the new sensor technology and compare the outcome to clinical scores.
Method
Eighteen patients (avg. 65±9yrs, 13F/5M) indicated for TKA wore a 3D-accelerometer (64x25x13mm, 18g, Fig 1) at the nonaffected upper leg (lateral) for 7 successive days to monitor activity in real life. In addition, patients completed an activity questionnaire (SQUASH), a functional questionnaire (KOOS-PS) and the function scale of the New-KSS score which was completed by the surgeon-administered clinical scale. Sensor data was analysed using self-designed, previously validated algorithms producing duration of activities (walking, sitting, resting), number of activities (sit-stand transfers, bouts walking, bouts stair climbing (up& down)) and cadence (steps/min).
Results
The sensors and PROMs were mailed back by all patients. Completion rate of PROMs were 88% SQUASH, 72% KOOS-PS and 55% New-KSS. Four sensor measurements failed (78% completed) due to technical issues (e.g. overnight charging failed). In total 89 days (avg. 12.8±2.6h/day, 6±1 days/week) were measured.
On average, preoperative TKA patients rest 64% ±18%, walk 9% ±5% and stand 27% ±15% of the day. On average 37±14 sit-stand transfers, 137±76 bouts walking and 36±54 bouts stair climbing were performed a day (Table 1). Patients walked on average 3644±2808 steps/day showing an average cadence of 76±10 steps/min. A moderate correlation was found between bouts walking and the new-KSS discretional subscale (r=0.7) and between age and amount sit-stand transfers (r = -0.6).
Discussion/conclusion
The activity monitor (AM) had a comparable or better completion rate than popular PROMs proofing its dependability in routine clinical use. The lack of correlations between AM output and the functional PROM's confirms the independence of physical activity (PA) as an outcome measure. The absent correlations with the SQUASH activity questionnaire prove the poor link between subjectively reported and objectively measured PA as previously published (Wagenmakers et.al.).
Step counts were comparable to Tonelli et. al who recorded 4726 steps/day in younger preoperative TKA patients (avg. 61.8yrs) with both values well below the WHO target for obtaining health benefits (10.000 steps/day).
Also the amount of sit-stand transfers was lower than literature values by the Groot et al. (46.2±13.7). They only measured two successive days using less comfortable equipment and thus were more affected by the known first-day observation bias. In addition patients were younger (61.8±11.2yrs) and this study showed the correlatiof between age and sit-stand transfers.

Real-life cadence was lower than measured under lab-based conditions (Senden et al.) for preoperative TKA patients (avg. 105 steps/min) and age-matched healthy controls (avg. 109 steps/min). This confirms a strong observation bias with patients performing infront of an observer and further highlights the value of real-life, sensor based activity monitoring.

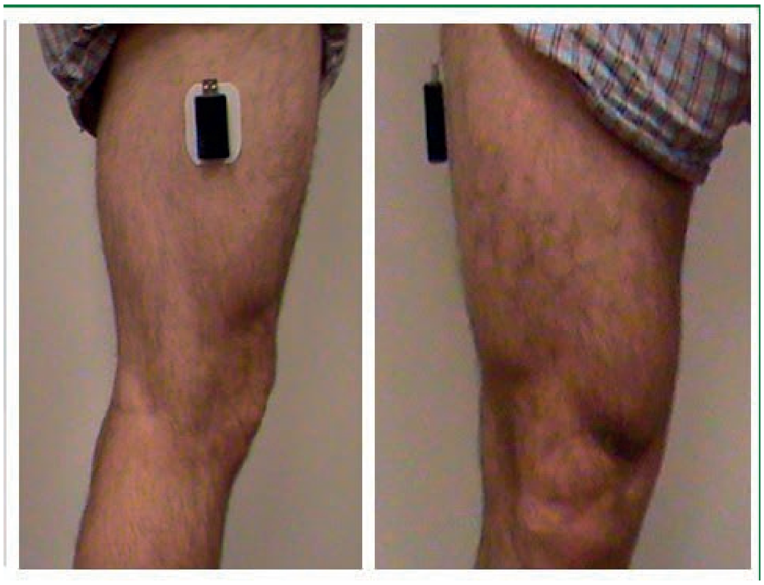

Body-fixed 3D-accelerometer sensor to monitor patient activity.

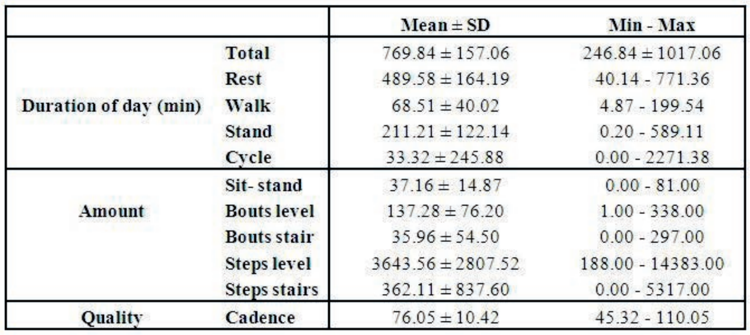

		Mean ± SD	Min - Max
Duration of day (min)	**Total**	769.84 ± 157.06	246.84 ± 1017.06
	Rest	489.58 ± 164.19	40.14 - 771.36
	Walk	68.51 ± 40.02	4.87 - 199.54
	Stand	211.21 ± 122.14	0.20 - 589.11
	Cycle	33.32 ± 245.88	0.00 - 2271.38
Amount	**Sit- stand**	37.16 ± 14.87	0.00 - 81.00
	Bouts level	137.28 ± 76.20	1.00 - 338.00
	Bouts stair	35.96 ± 54.50	0.00 - 297.00
	Steps level	3643.56 ± 2807.52	188.00 - 14383.00
	Steps stairs	362.11 ± 837.60	0.00 - 5317.00
Quality	**Cadence**	76.05 ± 10.42	45.32 - 110.05

See you in Venice!

CORS 2013
VENICE
8th COMBINED MEETING
OF ORTHOPAEDIC
RESEARCH SOCIETIES
13-16 OCTOBER 2013
SAN SERVOLO
VENICE, ITALY
www.cors2013.org

EUROPEAN ORTHOPAEDIC
RESEARCH SOCIETY